

**DEVELOPMENT OF AN OBJECTIVE  
METHOD FOR THE COMPARISON OF  
FIRED PROJECTILES USING AN AIR  
PISTOL AS A TEMPLATE**

**NOOR HAZFALINDA HAMZAH**

**CENTRE FOR FORENSIC SCIENCE**

**DEPARTMENT OF PURE AND APPLIED CHEMISTRY**

**UNIVERSITY OF STRATHCLYDE**

**A thesis presented in fulfilment of the requirements for the degree of  
Doctor of Philosophy**

**2017**

**CENTRE FOR FORENSIC SCIENCE  
DEPARTMENT OF PURE AND APPLIED CHEMISTRY  
UNIVERSITY OF STRATHCLYDE**

**DEVELOPMENT OF AN OBJECTIVE  
METHOD FOR THE COMPARISON OF  
FIRED PROJECTILES USING AN AIR  
PISTOL AS A TEMPLATE**

**PhD Thesis**

**NOOR HAZFALINDA HAMZAH**

**2017**

**This thesis is the result of the author's original research. It has been composed by the author and has not yet been previously submitted for examination which has led to the award of a degree. The copyright of this thesis belongs to the author under the terms of the United Kingdom Copyright Acts as qualified by the University of Strathclyde Regulation 3.50. Due acknowledgement must always be made of the use of any material contained in, or derived from, this thesis.**

**Signed: \_\_\_\_\_**

**Date: \_\_\_\_\_**

## **Abstract**

The ability to objectify ballistic evidence is a challenge faced by firearms examiners around the world. A number of researchers are trying to improve bullet-identification systems to address the deficiencies in this regard and which were detailed within the National Academy of Sciences report (2009).

Bullet to bullet comparisons have largely relied on the supposition that the rifling marks within the barrel of a weapon have class characteristics that identify a weapon type and individual characteristics that identify a specific weapon. Such characteristics are impressed onto projectiles when they are fired through a particular weapon and an examination of specific regions displaying striated marks on the projectiles allows for identification and comparison to be undertaken. This premise has been the foundation for comparative firearms examination for many decades. In many cases only small portions of striated regions of the projectile are examined and the process is essentially subjective. More recently focus has turned to making use of more sophisticated imaging modalities to view entire regions of the projectile and the development of automated systems for the comparison of the topographical surfaces recorded.

Projectiles from a fired series of 609 pellets were examined using an Alicona infinite focus microscope. A mathematical methodology was developed to pre-process the resultant topographical maps generating point data for comparison. Comparisons between different data sets were undertaken using chemometric techniques (principal component analysis, hierarchical cluster analysis and linear discriminant analysis) to

assess (1) the repeatability and reproducibility of the method, (2) the variability of land engraved areas (LEAs) in repetitively fired projectiles over a series of test fires, (3) the ability of the developed method to distinguish between different classes of weapons (pistols and rifles) and weapons within the same class (rifles) and (4) the ability of the method to correctly associate distorted projectiles to the weapon that fired them.

The developed objective method still requires an operator to identify the LEAs to be scanned; however the mathematical alignments were objectively achieved. The discrimination of weapons by class was achieved although weapons within the same class could not be easily separated from each other. The LEAs on a single projectile varied in terms of distinction from each other and, while there was some variation with use of the same weapon over time, this was not pronounced. Generally the LEAs with more distinguishing features across the entire region created a better discriminating surface and in particular facilitated the correct association for distorted projectiles.

## **Acknowledgements**

To my supervisors, Prof Niamh Nic Daéid and Dr Alison Nordon, thank you for giving me the opportunity to take on this PhD and for your continued support and advice.

To Mr Martin Connolly and Mr Colin Murphy, from the Ballistic Department, Forensic Services Glasgow Laboratory, Strathclyde Police Headquarters, Glasgow, thank you for providing valuable advice especially in firearms.

To The Ministry of Education, Malaysia, thank you for the funding of this research and to the Universiti Kebangsaan Malaysia for allowing me to take study leave in pursuing my PhD.

To the research colleagues and employees of the Centre for Forensic Science, Department of Pure and Applied Chemistry, thank you for supporting me in finishing the research.

To my beloved husband and my sons, my sister and my mum, love you all so much for the patience and care you have given me in finishing this research.

## **Publications and Presentations Related to this Research**

### **Journal Publications:**

1. Noor Hazfalinda Hamzah, *Development of an objective method for the comparison of fired projectiles using an air pistol as a template*, Forensic Science International, 2016. 264: 106-112

### **Oral Presentations:**

1. Noor Hazfalinda Hamzah, N. Nic Daéid, *Air Weapons and Automated Comparison of Pellets Identification*, University of Dundee, Dundee, July 2014
2. Noor Hazfalinda Hamzah, N. Nic Daéid, *Air Weapons and Automated Bullet-Identification System Using Pellets as a Template*, 7<sup>th</sup> European Academy of Forensic Science Conference, Prague, 6-11 September 2015

### **Poster Presentations:**

1. Noor Hazfalinda Hamzah, K. Savage, N. Nic Daéid, *Investigation of toolmarks from repetitively fired bullets*, 6<sup>th</sup> European Academy of Forensic Science Conference, The Hague, 20-24 August 2012
2. Noor Hazfalinda Hamzah, A. Nordon, N. Nic Daéid, *Airgun and automated comparison of pellets identification*, Scottish Student Forensic Research Symposium, University of Strathclyde, Glasgow, 14 March 2014
3. Noor Hazfalinda Hamzah, N. Nic Daéid, *Investigation of pellet marks from fired air weapons*, University Research Day, University of Strathclyde, Glasgow, 19 June 2014

### **Images of Research Competition**

1. Noor Hazfalinda Hamzah, N. Nic Daéid, *Pellet of Destiny*, Images of Research Competition, University of Strathclyde, April 2014

## List of Abbreviations

ACP	Automatic Colt Pistol
AFTE	Association of Firearm and Toolmark Examiners
ANN	Artificial Neural Networks
ATF	Bureau of Alcohol, Tobacco, Firearms and Explosives
CCD	Charge-coupled device
CCF	Cross Correlation Function
CCF <sub>max</sub>	Cross Correlation Function Maximum
CMS	Consecutive Matching Striae
Ds	Signature Differences
ENFSI	European Network of Forensic Science Institutes
FFT	Fast Fourier Transform
FBI	Federal Bureau of Investigation
GEA	Groove Engraved Area
HCA	Hierarchical Cluster Analysis
IAFIS	Integrated Automated Fingerprint Identification System
IBIS	Integrated Ballistics Identification System
LEA	Land Engraved Area
LDA	Linear Discriminant Analysis
LD	Linear Discriminant
NAS	National Academy of Sciences
NBIC	National Ballistics Imaging Comparison
NIBIN	National Integrated Ballistic Information Network
NIST	National Institute of Standards and Technology



PCA	Principal Component Analysis
PC	Principal Component
ROI	Region of Interest
RSS	Residual Sum of Squares
SNP	Spain National Police
SRM	Standard Reference Materials
US	United States

## Table of Contents

<b>Abstract.....</b>	<b>i</b>
<b>Acknowledgements.....</b>	<b>iii</b>
<b>Publications and Presentations Related to this Research.....</b>	<b>iv</b>
<b>List of Abbreviations .....</b>	<b>vi</b>
<b>Table of Contents .....</b>	<b>viii</b>
<b>Outline of Thesis.....</b>	<b>xix</b>
<b>Chapter 1: Introduction .....</b>	<b>1</b>
<b>1.1 General Introduction .....</b>	<b>1</b>
<b>1.2 Toolmark Identification Criteria Used in Firearms Analysis .....</b>	<b>8</b>
<b>1.2.1 Empirical Studies .....</b>	<b>9</b>
<b>1.2.2 The Development of Mathematical Models .....</b>	<b>12</b>
<b>1.2.3 Consecutive Matching Striae (CMS) Theory .....</b>	<b>13</b>
<b>1.3 Air Weapons .....</b>	<b>32</b>
<b>1.4 Principal Component Analysis (PCA).....</b>	<b>36</b>
<b>1.5 Hierarchical Cluster Analysis (HCA).....</b>	<b>41</b>
<b>1.6 Linear Discriminant Analysis (LDA) .....</b>	<b>42</b>
<b>1.7 Conclusions .....</b>	<b>46</b>
<b>1.8 References .....</b>	<b>49</b>

<b>Chapter 2: Materials and Methods .....</b>	<b>54</b>
<b>2.1 Introduction.....</b>	<b>54</b>
<b>2.2 Materials .....</b>	<b>56</b>
<b>2.2.1 Air pistol .....</b>	<b>56</b>
<b>2.2.2 Air rifles .....</b>	<b>57</b>
<b>2.2.3 Pellets .....</b>	<b>59</b>
<b>2.3 Test Firings .....</b>	<b>60</b>
<b>2.4 Generation of test sets - Pellet firing and collection.....</b>	<b>62</b>
<b>2.4.1 Velocity studies.....</b>	<b>63</b>
<b>2.4.2 Within and between pellet comparison.....</b>	<b>65</b>
<b>2.4.3 Longitudinal study .....</b>	<b>65</b>
<b>2.4.4 Comparison of pellets fired from different weapons.....</b>	<b>65</b>
<b>2.4.5 Pellet distortion study .....</b>	<b>65</b>
<b>2.5 Alicona® Infinite Focus G4, 3D optical microscope .....</b>	<b>66</b>
<b>2.5.1 Image acquisition .....</b>	<b>67</b>
<b>2.5.2 Measurement repeatability .....</b>	<b>71</b>
<b>2.5.3 Data transformation and image alignment .....</b>	<b>82</b>
<b>2.5.4 Curve flattening .....</b>	<b>82</b>
<b>2.6 Analysis data.....</b>	<b>88</b>
<b>2.7 Chronograph Studies – calculation of kinetic energy .....</b>	<b>88</b>

<b>2.8</b>	<b>Conclusions .....</b>	<b>90</b>
<b>2.9</b>	<b>References .....</b>	<b>91</b>
<b>Chapter 3: Variation of striation marks on projectiles repetitively fired from the same weapon..... 94</b>		
<b>3.1</b>	<b>Introduction.....</b>	<b>94</b>
<b>3.2</b>	<b>Selection of pellets and data collection .....</b>	<b>94</b>
<b>3.3</b>	<b>Data analysis – alignment.....</b>	<b>97</b>
	<b>3.3.1 LEA A.....</b>	<b>97</b>
	<b>3.3.2 LEA B.....</b>	<b>100</b>
	<b>3.3.3 LEA C.....</b>	<b>101</b>
	<b>3.3.4 LEA D.....</b>	<b>102</b>
	<b>3.3.5 LEA E.....</b>	<b>102</b>
	<b>3.3.6 LEA F .....</b>	<b>103</b>
	<b>3.3.7 LEA G .....</b>	<b>104</b>
	<b>3.3.8 LEA I.....</b>	<b>105</b>
	<b>3.3.9 LEA K .....</b>	<b>106</b>
	<b>3.3.10 LEA L.....</b>	<b>107</b>
	<b>3.3.11 LEA H and J.....</b>	<b>108</b>
	<b>3.3.12 Data summary .....</b>	<b>108</b>
<b>3.4</b>	<b>Principal Component Analysis (PCA), Hierarchical Cluster Analysis (HCA) and Linear Discriminant Analysis (LDA) .....</b>	<b>109</b>

<b>3.5</b>	<b>Conclusions .....</b>	<b>120</b>
<b>3.6</b>	<b>References .....</b>	<b>122</b>
	<b>Chapter 4: Variation of striation marks across 600 pellets fired from the same weapon.....</b>	<b>124</b>
<b>4.1</b>	<b>Introduction .....</b>	<b>124</b>
<b>4.2</b>	<b>Selection of pellets .....</b>	<b>125</b>
<b>4.3</b>	<b>Specific regions examined .....</b>	<b>128</b>
<b>4.4</b>	<b>Data alignment .....</b>	<b>132</b>
<b>4.4.1</b>	<b>LEA A.....</b>	<b>132</b>
<b>4.4.2</b>	<b>LEA B.....</b>	<b>136</b>
<b>4.4.3</b>	<b>LEA C.....</b>	<b>139</b>
<b>4.4.4</b>	<b>LEA D.....</b>	<b>142</b>
<b>4.4.5</b>	<b>LEA E.....</b>	<b>144</b>
<b>4.4.6</b>	<b>LEA F .....</b>	<b>145</b>
<b>4.4.7</b>	<b>LEA G .....</b>	<b>147</b>
<b>4.4.8</b>	<b>LEA H .....</b>	<b>149</b>
<b>4.4.9</b>	<b>LEA I.....</b>	<b>151</b>
<b>4.4.10</b>	<b>LEA J .....</b>	<b>152</b>
<b>4.4.11</b>	<b>LEA K.....</b>	<b>154</b>
<b>4.4.12</b>	<b>LEA L.....</b>	<b>155</b>
<b>4.4.13</b>	<b>Summary of data .....</b>	<b>157</b>

<b>4.5</b>	<b>PCA, HCA and LDA results .....</b>	<b>159</b>
<b>4.5.1</b>	<b>Analysis of LEAs with more than 90% aligned measurements.....</b>	<b>181</b>
<b>4.6</b>	<b>Conclusions .....</b>	<b>186</b>
<b>4.7</b>	<b>References .....</b>	<b>187</b>
<b>Chapter 5: Comparison and evaluation of striated marks on projectiles fired from different weapons.....</b>		
<b>189</b>		
<b>5.1</b>	<b>Introduction .....</b>	<b>189</b>
<b>5.2</b>	<b>Alignment results .....</b>	<b>192</b>
<b>5.2.1</b>	<b>Edgar Brother Model 35 .....</b>	<b>192</b>
<b>5.2.2</b>	<b>Baikal 90042234 ИЖ-35.....</b>	<b>199</b>
<b>5.3</b>	<b>PCA, HCA and LDA analysis .....</b>	<b>201</b>
<b>5.3.1</b>	<b>Edgar Brother Model 35 .....</b>	<b>202</b>
<b>5.3.2</b>	<b>Baikal 90042234 ИЖ-35.....</b>	<b>205</b>
<b>5.3.3</b>	<b>Differentiation between pellets fired from different weapons.....</b>	<b>209</b>
<b>5.3.3.1</b>	<b>Air pistol and Edgar Brother Model 35 air rifle.....</b>	<b>209</b>
<b>5.3.3.2</b>	<b>Air pistol and Baikal 90042234 ИЖ-35 air rifle.....</b>	<b>212</b>
<b>5.3.3.3</b>	<b>All three weapons .....</b>	<b>216</b>
<b>5.4</b>	<b>Conclusions .....</b>	<b>219</b>
<b>5.5</b>	<b>References .....</b>	<b>220</b>

<b>Chapter 6: Matching the striations on damaged pellets shot from an air pistol through a target at different distances .....</b>	<b>222</b>
<b>6.1 Introduction.....</b>	<b>222</b>
<b>6.2 Selection of the pellets for testing .....</b>	<b>222</b>
<b>6.3 Distance Measurement.....</b>	<b>226</b>
<b>6.4 Results .....</b>	<b>228</b>
<b>6.4.1 LEA A .....</b>	<b>232</b>
<b>6.4.2 LEA D .....</b>	<b>236</b>
<b>6.4.3 LEA H.....</b>	<b>239</b>
<b>6.4.4 LEA J.....</b>	<b>242</b>
<b>6.4.5 LEA K.....</b>	<b>246</b>
<b>6.4.6 All aligned LEAs from the air rifles and LEAs from the damaged pellets.....</b>	<b>250</b>
<b>6.5 Conclusions .....</b>	<b>262</b>
<b>6.6 References .....</b>	<b>263</b>
<b>Chapter 7: Conclusion and Future Works .....</b>	<b>265</b>
<b>7.1 Conclusions.....</b>	<b>265</b>
<b>7.2 Recommendations Future Work .....</b>	<b>269</b>
<b>Appendix 1.....</b>	<b>270</b>
<b>Appendix 2.....</b>	<b>271</b>

<b>Appendix 3</b> .....	<b>272</b>
<b>Appendix 4</b> .....	<b>273</b>
<b>Appendix 5</b> .....	<b>282</b>
<b>Appendix 6</b> .....	<b>292</b>
<b>Appendix 7</b> .....	<b>302</b>
<b>Appendix 8</b> .....	<b>312</b>
<b>Appendix 9</b> .....	<b>322</b>
<b>Appendix 10</b> .....	<b>332</b>
<b>Appendix 11</b> .....	<b>342</b>
<b>Appendix 12</b> .....	<b>352</b>
<b>Appendix 13</b> .....	<b>362</b>
<b>Appendix 14</b> .....	<b>372</b>
<b>Appendix 15</b> .....	<b>382</b>
<b>Appendix 16</b> .....	<b>392</b>
<b>Appendix 17</b> .....	<b>394</b>
<b>Appendix 18</b> .....	<b>396</b>
<b>Appendix 19</b> .....	<b>398</b>
<b>Appendix 20</b> .....	<b>400</b>
<b>Appendix 21</b> .....	<b>402</b>
<b>Appendix 22</b> .....	<b>404</b>
<b>Appendix 23</b> .....	<b>406</b>



<b>Appendix 24</b> .....	<b>408</b>
<b>Appendix 25</b> .....	<b>410</b>
<b>Appendix 26</b> .....	<b>412</b>
<b>Appendix 27</b> .....	<b>414</b>
<b>Appendix 28</b> .....	<b>416</b>
<b>Appendix 29</b> .....	<b>418</b>
<b>Appendix 30</b> .....	<b>420</b>
<b>Appendix 31</b> .....	<b>422</b>
<b>Appendix 32</b> .....	<b>424</b>
<b>Appendix 33</b> .....	<b>426</b>
<b>Appendix 34</b> .....	<b>428</b>
<b>Appendix 35</b> .....	<b>430</b>
<b>Appendix 36</b> .....	<b>432</b>
<b>Appendix 37</b> .....	<b>434</b>
<b>Appendix 38</b> .....	<b>436</b>
<b>Appendix 39</b> .....	<b>438</b>
<b>Appendix 40</b> .....	<b>440</b>
<b>Appendix 41</b> .....	<b>442</b>
<b>Appendix 42</b> .....	<b>444</b>
<b>Appendix 43</b> .....	<b>446</b>
<b>Appendix 44</b> .....	<b>448</b>

<b>Appendix 45</b> .....	<b>450</b>
<b>Appendix 46</b> .....	<b>452</b>
<b>Appendix 47</b> .....	<b>454</b>
<b>Appendix 48</b> .....	<b>456</b>
<b>Appendix 49</b> .....	<b>458</b>
<b>Appendix 50</b> .....	<b>460</b>
<b>Appendix 51</b> .....	<b>462</b>
<b>Appendix 52</b> .....	<b>464</b>
<b>Appendix 53</b> .....	<b>466</b>
<b>Appendix 54</b> .....	<b>468</b>
<b>Appendix 55</b> .....	<b>470</b>
<b>Appendix 56</b> .....	<b>472</b>
<b>Appendix 57</b> .....	<b>474</b>
<b>Appendix 58</b> .....	<b>476</b>
<b>Appendix 59</b> .....	<b>478</b>
<b>Appendix 60</b> .....	<b>480</b>
<b>Appendix 61</b> .....	<b>482</b>
<b>Appendix 62</b> .....	<b>484</b>
<b>Appendix 63</b> .....	<b>486</b>
<b>Appendix 64</b> .....	<b>488</b>
<b>Appendix 65</b> .....	<b>490</b>

<b>Appendix 66 .....</b>	<b>492</b>
<b>Appendix 67 .....</b>	<b>494</b>
<b>Appendix 68 .....</b>	<b>496</b>
<b>Appendix 69 .....</b>	<b>498</b>
<b>Appendix 70 .....</b>	<b>500</b>
<b>Appendix 71 .....</b>	<b>502</b>
<b>Appendix 72 .....</b>	<b>504</b>
<b>Appendix 73 .....</b>	<b>506</b>
<b>Appendix 74 .....</b>	<b>508</b>
<b>Appendix 75 .....</b>	<b>510</b>
<b>Appendix 76 .....</b>	<b>511</b>
<b>Appendix 77 .....</b>	<b>512</b>
<b>Appendix 78 .....</b>	<b>513</b>
<b>Appendix 79 .....</b>	<b>514</b>
<b>Appendix 80 .....</b>	<b>515</b>
<b>Appendix 81 .....</b>	<b>516</b>
<b>Appendix 82 .....</b>	<b>517</b>
<b>Appendix 83 .....</b>	<b>518</b>
<b>Appendix 84 .....</b>	<b>519</b>
<b>Appendix 85 .....</b>	<b>520</b>
<b>Appendix 86 .....</b>	<b>521</b>

<b>Appendix 87 .....</b>	<b>522</b>
<b>Appendix 88 .....</b>	<b>523</b>
<b>Appendix 89 .....</b>	<b>524</b>
<b>Appendix 90 .....</b>	<b>525</b>
<b>Appendix 91 .....</b>	<b>526</b>
<b>Appendix 92 .....</b>	<b>527</b>
<b>Appendix 93 .....</b>	<b>528</b>
<b>Appendix 94 .....</b>	<b>529</b>
<b>Appendix 95 .....</b>	<b>530</b>
<b>Appendix 96 .....</b>	<b>531</b>

## **Outline of Thesis**

**Chapter 1** introduces and reviews the literature relevant to the comparison of bullets through the examination of striated marks along regions of their surface. In particular the use of surface topography imaging techniques is explored. A high velocity air pistol and two air rifles were used in this research and the operation of such weapons is briefly introduced. Finally the research aims are presented at the end of the chapter.

**Chapter 2** presents the research methodology including how the images of the air pistol pellets were acquired and the means by which these were mathematically analysed. A validation of the research methodology is also presented to demonstrate repeatability of measurements across individual projectiles.

**Chapter 3** contains analysis data of the first 50 pellets shot from the air pistol. The objective of this part of the research was to determine whether a method could be established to objectively measure the striation marks impressed on the pellets as they were fired, and it establishes the reproducibility of the method. Whether the striated marks present within each land engraved area (LEA) on different pellets fired by the same air pistol could be associated with each other using objective mathematical methods was explored. The analysis includes detail relating to data handling and pre-processing and the analysis results for each LEA. The results obtained suggest that the developed methodology could, in most cases, objectively differentiate between the LEAs but only in cases where 90% alignment of the striated marks on the pellets was observed.

**Chapter 4** focuses on analysis of groups of pellets selected from amongst 590 pellets sequentially fired from the air pistol. The purpose was to assess whether the striated marks within an LEA change as the weapon is used. The air pistol was not cleaned during the test fires. The results obtained illustrated that in some cases the LEAs did not demonstrate any appreciable differences, but this was not universally the case.

**Chapter 5** reveals the comparison between pellets shot with the air pistol and pellets shot with two air rifles. The results show that the air pistol and air rifles' pellets could be differentiated; however there was some convolution of the LEAs from the pellets fired by the air pistol, suggesting that their separation was more problematic.

**Chapter 6** concentrates on the comparison of a series of progressively distorted pellets with pellets where only marks acquired through the firing process were visualised. The analysis revealed that in some cases the damaged pellets could be associated with the undistorted fired pellets; however this was dependent on the level of distortion.

**Chapter 7** presents a short overall conclusion of the research work and areas for further work.

## **Chapter 1: Introduction**

### **1.1 General Introduction**

Firearms identification has been undertaken as part of criminal investigations for centuries. Indeed Emperor Maximilian was noted to discuss firearms rifling when he ruled Germany from 1486 to 1519 [1] and, over 300 years later in 1835, Mr Henry Goddard used only physical evidence to show a linkage between a projectile and the weapon that fired it [1]. In 1835, a servant was accused of shooting his master. Mr Henry Goddard examined the paper patch which sealed the projectile and the gunpowder of the suspected weapon used in the crime. The paper patch came from a torn newspaper found in the servant's room; therefore the servant was found guilty of murdering his master based on the physical evidence.

In 1915, in New York, the first microscopic examination of bullets fired from a revolver was undertaken by Dr Max Poser in a murder case [1]. In 1932, the Federal Bureau of Identification (FBI) was established and part of its repertoire was the microscopic examination of striated marks on projectiles. The continued development of firearms examination as a discipline saw the establishment of the Association of Firearm and Toolmark Examiners (AFTE) in 1969 in Chicago [1]. AFTE continues to have a remit to discover new procedures, produce scientific papers and organise annual training seminars in regards to firearms and toolmark examination. The European Network of Forensic Science Institutes (ENFSI) [2] facilitates a European firearms working group which has a similar remit in terms of development of the field.

In the 1990s the US Bureau of Alcohol, Tobacco, Firearms and Explosives (ATF) [3] introduced a National Integrated Ballistic Information Network (NIBIN) [4] which aims to provide an automated ballistic imaging network for US laboratories to facilitate cross referencing of samples and cases, where examiners use the automated integrated ballistic imaging system (IBIS) for data entry [4].

In 2009, firearms and ballistic examination came under specific scrutiny in the National Academy of Sciences report published by the American Academy of Sciences [5]. In particular the following were highlighted:

1. The AFTE principles and theory of identification were not mandatory and in particular it was considered difficult to achieve the ‘sufficient agreement’ suggested in the methodology because, even though NIBIN and IBIS were available to assist the examiners, the final decision whether two samples were matched or excluded relied upon the specific ability of the examiners. This decision remained subjective in nature with no statistical method to determine error rates [5].
2. There was no standard operating protocol to follow which explains what is meant by ‘sufficient agreement’. AFTE suggested that sufficient agreement should be defined as ‘when it exceeds the best agreement demonstrated between tool marks known to have been produced by different tools and is consistent with the agreement demonstrated by tool marks known to have been produced by the same tool’ [5]; however there are very few statistical studies which address this issue.



3. The National Academy of Sciences noted that marks from tools and guns were subject to variability; however there was not enough information to objectify this variability. The committee agreed that class and individual characteristics were helpful in firearms identification; however more studies were needed to grasp the concept of reliability and repeatability of the method of firearms identification. A recent *Ballistic Imaging* report typified the situation [6] stating that ‘the validity of the fundamental assumptions of uniqueness and reproducibility of firearms-related toolmarks has not yet been fully demonstrated. Although they are subject to numerous sources of variability, firearms-related toolmarks are not completely random and volatile; one can find similar marks on bullets and cartridge cases from the same gun. A significant amount of research would be needed to scientifically determine the degree to which firearms-related toolmarks are unique and reproducible or even to quantitatively characterise the probability of uniqueness’ [6]. Empirical studies to date have generally been subjective in approach [7-10].

The term ‘cognitive bias’ was recognised as one of the negative influences in the forensic world [11, 12]. As humans, decisions are made based on perception, experience or influence by others, especially in processes which involve subjective interpretations [13, 14], as in fingerprints, glass comparisons, shoe print comparisons, document analyses, hair comparisons and firearms and tool mark analyses [15, 16]. Cognitive bias is determined by multifactorial risks. Risks of bias are lower when the results are clear; standard operating procedures are well defined, tested and validated; and practitioners

are well trained. The risks are higher if the results are ambiguous, the research is personal to the practitioner (who is inexperienced and unmonitored) and ungrounded, and where the validation and repeatability of the results are questionable. There are six categories of cognitive bias, as described in detail by *Kassin et al.* [17]: expectation bias, confirmation bias, anchoring effects, contextual bias, role effects and reconstructive effects. Expectation bias happens when researchers only see what they want to see, and they tend to manipulate data to get the desired results. It is also known as experimenter's bias. Confirmation bias is closely related to expectation bias. This is when the researchers tend to confirm the evidence and overlook the conflicting elements which present from the evidence, as mentioned by *Charlton et al.* [18], in relation to the famous Madrid bombing case [19]. In 2004, several commuter trains in Spain were bombed by terrorists, killing 200 people with more than a thousand injured. The Spanish National Police (SNP) found latent fingerprints on a bag of detonators and asked the FBI to help in identifying suspects. The FBI used the Integrated Automated Fingerprint Identification System (IAFIS) to process the fingerprints. The software generated 20 potential fingerprints based on the evidence provided. Examiner Brandon Mayfield was then identified as the owner of the fingerprints. This result was verified by two other examiners; hence Brandon Mayfield was arrested as a suspect. A couple of months later, the SNP informed the FBI that they had identified, positively, the fingerprints found on said bag belonged to an Algerian. After extensive review of the new finding, the FBI released Mr Mayfield. An international panel of fingerprint experts concluded that the initial examiner relied too much on the

result from IAFIS and pressure working on a high-profile case clouded his judgement [19]. This is an example of confirmation bias where the examiners' experience contributed to errors in fingerprint identification. The next bias is called anchoring effects, which is closely related to the other two biases. This occurs when the examiners are fixed on the initial evidence from the case and try to work around it, using it as an anchor, while neglecting other evidence that may contribute to solving the case. Contextual bias occurs when the examiner has other information regarding the case which influences him/her, either consciously or subconsciously. This is also known as 'psychological contamination' or 'cognitive contamination'. Role effects are when the examiners 'pick a team'; that is, they decide to side with either the prosecution or the defence. The examiners can make a conscious decision toward one side when the desire for that side to win is high. Reconstructive effects occur when the gaps are filled with a memory rather than looking at the evidence. An examiner thinks about what he/she believes should happen, influenced by a previous memory of a similar event. In order to minimise unintended bias, especially in firearms and toolmark examination, several suggestions have been recommended [5, 14]. An independent review and the use of a 'blind' checker should be introduced to evaluate the evidence processed by the initial examiner. For the 'blind' checker, contextual information should not be supplied, in order to minimise the cognitive bias. An independent reviewer should evaluate the initial examiner as to whether the standard operating procedures were followed while examining the evidence, and the method used by the initial examiner should also be validated. Training and education of staff

regarding risk of cognitive bias in interpreting evidence should be conducted in order to minimise errors. The most important suggestion is to actively do research in obtaining objective measurements and interpretation of evidence to replace the subjective approach which has been used for decades. This suggestion is the key concept for this research: to develop an objective method for the comparison of fired projectiles using an air pistol as template.

4. The Daubert ruling [20] established a set of criteria for the evaluation of scientific evidence which includes that:
  1. the principle upon which the evaluation was made must be tested,
  2. potential errors of the method should be known,
  3. research relating to the method should be published and peer reviewed,
  4. the methods should be generally accepted by the relevant scientific community.

Scientific evidence being presented in the US courts where the Daubert tests were accepted can be challenged against these criteria in relation to their admissibility. This refers to the US courts introducing a standard where an expert is permitted to testify in court. In 1993, there was a case brought up to the federal court in the US, *Daubert vs Dow Pharmaceuticals* [20]. The parents of Jason Daubert and Eric Schuller sued Dow Pharmaceuticals for causing birth defects in their children after both mothers took Bendectin during pregnancy. The parents presented *in vivo* and *in vitro* animal studies of Bendectin teratogenicity; however the pharmaceutical company proved that there was no published scientific study of the said drug. The court ruled in favour of the

pharmaceutical company and this is when the US court decided to demand that only reliable scientific evidence be presented. In January 2002, Judge Louis Pollack made a controversial decision in *United States v. Llera Plaza* when he dismissed the fingerprint evidence in court [21, 22]. According to him, fingerprint identification techniques had never been tested and verified scientifically, even though fingerprints were used as evidence for more than 100 years in court. He made his decision based on the Daubert recommendation of the admissibility of scientific evidence. This is one of the examples of how the Daubert recommendation affected the presentation of forensic evidence in court [23]. Page *et al.* [24, 25] reviewed 541 cases related to forensic science where the expert witnesses were challenged in US court, mainly due to fingerprint analysis, firearm and toolmark analysis, handwriting analysis (document analysis) and forensic odontology. The results showed that the highest exclusion of forensic identification of evidence came from document analysis and firearm and toolmark analysis, followed by forensic odontology and fingerprint analysis. Reliability (that is, the ability to provide scientific information from a trustworthy source), education and qualifications of the expert witness, as well as methodology or scientific basis used by the expert witness, were the main reasons why the evidence was excluded. The Daubert test affects so much in forensic science identification of evidence, resulting in inadmissibility of expert witness testimony in US courts. In order to overcome cognitive bias, to meet with the Daubert test and to comply with the suggestions from the NAS, this study aimed to develop an objective method of forensic

identification of evidence in toolmarks analysis, with validated and tested methodology which is scientifically proven.

## **1.2 Toolmark Identification Criteria Used in Firearms Analysis**

Schwartz, in 2008 [26], challenged the methodology used in firearms and toolmark identification suggesting that the ballistic and toolmark identification system had no statistical and foundational support. Evidence was presented subjectively and, as a consequence, was open to errors in judgement and interpretation, and could be affected by cognitive bias [11, 12].

In response to these challenges, Nichols defended the foundation of the identification system [27, 28] based on the AFTE Theory and Methodology of Identification which was written in 1985 by the Criteria for Identification Committee. This methodology was based on three principles of identification: '1 – two toolmarks are identical when the surface contours are in sufficient agreement, 2 – the sufficient agreement is determined by the similarity of height or depth, width, curvature and spatial relationship of ridges, peaks, furrows between two toolmarks and it is beyond reasonable doubt that these two toolmarks can be made by other different tools, 3 – the current identification process is subjective and based on scientific research and examiner's training and experience' [29].

### 1.2.1 Empirical Studies

#### Bullets and Barrels

Ballistic samples – bullets and cartridges – can provide evidential material related to alleged criminal activities involving firearms. Both bullets and cartridge cases can be characterised through the examination of the striation marks on their surfaces which occur as a result of contact with the rifling of the barrel or other areas of the firing mechanism (in the case of cartridge cases).

A rifled barrel consists of a number of grooves and lands as shown in Figure 1.1 [30]. Lands are the raised areas within the weapon's barrel and grooves are the depressions in between the lands.

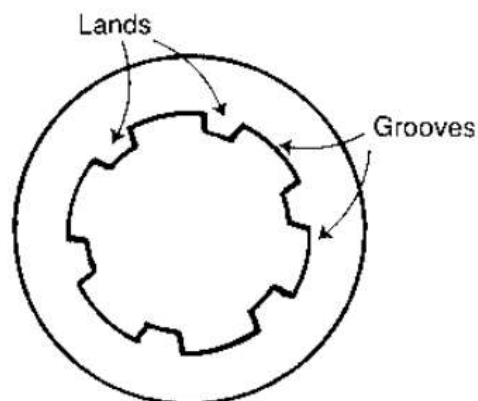


Figure 1.1: Cross-section of a barrelled weapon with lands and grooves [30]

Projectiles are normally made of a soft metal such as lead or lead with a copper coating. When a projectile (such as a pellet or bullet) is propelled out of the steel barrel of a rifled weapon, the projectile comes into contact with the lands and the grooves within

the barrel during flight. As a result a set of impressed striation marks is left on the projectile through contact with the harder steel surface of the barrel.

Rifling is designed to stabilise the projectile in flight and will cause the pellet to spin when it is fired out of the muzzle of the weapon [31]. The land engraved area (LEA) on the projectile corresponds to the lands within the barrel, and the groove engraved area (GEA) corresponds to the grooves within the barrel. For firearms, the LEA and the GEA (number of lands and grooves, direction of twist and widths of the lands and grooves) can indicate class characteristics, which can give information relating to the type and the manufacturer of the weapon that propelled the ammunition [32]. Individual characteristic marks are more refined and in the context of bullet examination are the striated marks which appear within the LEA and GEA regions of the projectile. It has been assumed that these striated marks provide a 'fingerprint' of the weapon that fires the ammunition [33].

Imperfections of the lands and grooves of the barrel may introduce individual characteristics onto the surface of the bullet. Unlike class characteristics, which are non-specific to the firearm that fired the bullet, it has been suggested that the individual characteristics act almost like a 'fingerprint' of the particular firearm that fired the bullet. The assumption has been made that no two barrels will produce the same markings on a bullet even if they are made by same manufacturer [30].

In the early 1960s Biasotti defined the terms 'line' and 'consecutiveness' where 'line' (striation) was defined as 'an engraving or striation appearing on the bullet as a result



of being engraved by the individual irregularities and characteristics of the barrel plus any foreign material present in the barrel capable of engraving the bullet' [34, 35]. 'Consecutiveness' was defined as an 'accumulation of a number of individual characteristics'. As stated by Di Maio [30], striations can be changed due to any imperfection on the barrel. These imperfections can be caused by wear and tear as well as presence of build-up lead.

Biasotti evaluated the objectivity and subjectivity of firearm examination using jacketed bullets. He found that while 15-20% of striations could be 'matched' between bullets fired from different weapons, only 21-24% of striations could be matched between bullets fired from same weapon. He concluded that the percentage of matching striations is not the only indication for identification [34, 35]. His findings suggested that the percentage of matching striations for the jacketed bullet is low, which contradicted Di Maio [30], who suggested that land marks are most prominent in jacketed bullets; hence the percentage of matching striations should be higher in jacketed bullets. Biasotti's findings are based on his experience, which can be influenced by confirmation bias. However, this is considered a step in objectifying the striation marks in forensic science.

Biasotti's work concentrated on the comparison of bullets with each other. In 1970, Lutz [7, 34] suggested that the barrel of the weapon which fires a projectile could also be identified using striated marks and presented a series of photomicrographs to underpin the subjective observations. Matty undertook similar work [10] performing comparisons of Mikrosil casts of a rifled barrel. Mikrosil is a silicone casting material

which is designed to recover latent fingerprints or toolmarks. It can give fine details of the recovered items for microscopic examination. A new rifled barrel was cut into three sections to produce three barrels. The casts were taken before firing any bullets from each of the three barrels. The three barrels were used in test firings; however there was no mention of number of test firings carried out. The casts from the three barrels were then taken after test firings and these casts (before and after test firings) were compared microscopically. He noticed that the striations from new barrels showed an initial rapid change in characteristics on the land impressions after a settling-in period, supporting the statement that no two firearms, even those of the same make and model, would produce the same marks on fired bullets [10]. This suggests that striation marks can change over a period of time and identification of the firearm which fired the bullet may not actually be possible. Furthermore, the authors did not investigate if or when the striation marks stop changing over time.

### **1.2.2 The Development of Mathematical Models**

In 1970 Brackett discussed a set of theoretical models with the potential to deliver an objective means of assessing the matching of striation marks. These were capable of describing individual sets of striations and comparing these sets against each other [36]. There were four models included in the approach: geometric models, number-based models, random number outcome models and random number replica models. Brackett also developed an ideal distribution equation demonstrating the independence of the striae examined, suggesting that the presence of one striation was independent of the presence of its neighbours [34]. The theoretical model was quite tedious to

implement but did suggest that consecutiveness of striations was a reliable measure for comparative purposes.

In 1980 Blackwell and Framan applied Brackett's formulas and models to develop an automated firearms identification system [37]. In 1988, Uchiyama discussed the formulation of examiners' identification criteria and noted that 'there were no definitive or objective explanations to support the conclusions of identity reached by the examiner and no clear explanation about what is meant by the word identified, likely, not identified or no correspondence' [38]. He also developed a significance level of identification for test fired bullets and noted that the total number of matching striae and the percentage of matching striae were not exclusive in terms of matching criteria but that the consecutiveness of the striation marks should also be taken into account. Indeed, he suggested that consecutive striation marks acted as the principle indicator in identification of bullets fired from the same gun.

### **1.2.3 Consecutive Matching Striae (CMS) Theory**

The basis of consecutive matching striae theory is that there are at least three striations which match between projectiles fired from the same weapon. The theory was based on observations by Biasotti [35] and further developed by Tulleners, Giusto and Hamiel [39] in 1998. They removed six one-inch sections out of a gun barrel. Test fires were done before and after sectioning, generating 464 land and groove impressions. They concluded that the percentage of matching striations is not the only indicator for bullet identification. Furthermore, no more than three CMS were found for known non-matching samples [35, 40].

Miller [41] published a number of studies related to CMS. Initially he analysed fifty pairs of .38 calibre full metal-jacketed bullets test fired from Smith & Wesson revolvers using the IBIS system. In total 2,000,000 land-to-land impression comparisons involving a total of 1600 test bullets from the database were undertaken using two-dimensional and three-dimensional data comparisons. The top five scoring land impressions for each bullet were used in the comparison processes [41]; however no further explanation was given regarding the definition of the scoring. From this work Miller concluded that, while there was an extremely low probability of having two different firearms produce the same marks, it was still difficult, if not impossible, to establish specific criteria for firearms identification [41]. In further work, Miller extended his studies following the same methodology and examining three different calibres of jacketed bullets, including .25 ACP (Automatic Colt Pistol), .380 ACP and 9-mm Luger [42]. In total 60 land-to-land impression comparisons were undertaken using the IBIS system and Miller concluded for projectiles which were known not to match each other, the .25 and .380 ACP weapons did not produce more than four CMS in any of the regions examined using 2D visualisation, and this reduced to three CMS for 3D visualisation of the .380 ACP weapon and for both the 2D and 3D visualisation of the projectiles fired by the 9-mm Luger. In a further examination of two consecutively manufactured .44 calibre barrels, Miller concluded that 'there were no CMS exceeding a run of two in the known non-matches while the known matches had nine incidences of three CMS, eight of four, one of five and five of six' [43].

Not all researchers agreed with the CMS approach. In 2000, Bunch criticised the CMS theory, taking instead a Bayesian perspective [44] and arguing that CMS had 'no

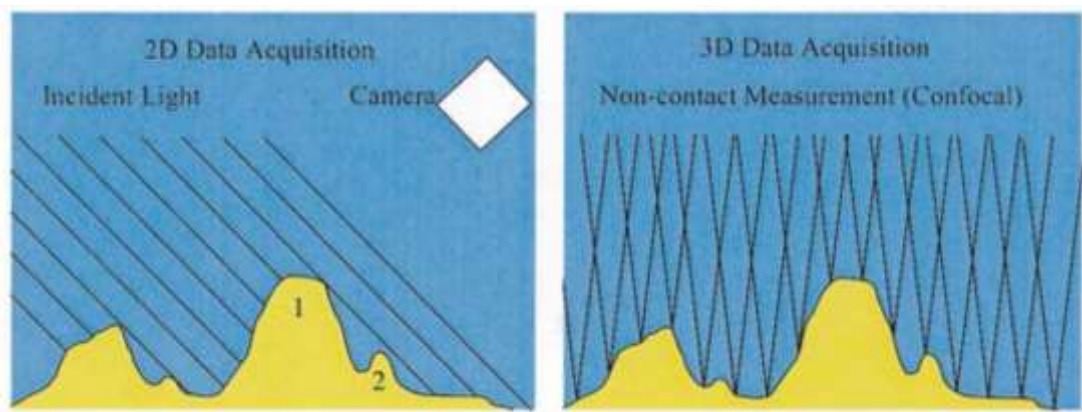
rational or scientific ground for making claims of absolute certainty in any of the traditional identification sciences'. Research into the various limiting factors relating to the potential to produce striated marks, such as the barrel manufacturing method, barrel length, barrel hardness, bullet hardness and bullet surface materials, was required in order to better understand the repeatability of the production of the striation marks. Bunch in particular was critical of the CMS theory due to the scientific status of such a subjective examination [44].

More recently, Howitt *et al.* [45] used comparison microscopy in the examination of land impressions and suggested that the number of striae in a land impression could vary depending on the size of the bullet and the characteristics of the barrel. They suggested mathematical formulae to identify the matching striae, noting that the probabilities of consecutively matching striae 'are not all equivalent and depend upon the width of the striae', and they suggested that certain individual measurements including the 'width of the land, the magnification used and the number and width of striae on the bullets could provide a reliable likelihood of finding a match by chance' [45].

Recently, there have been increasing efforts to use 3D microscopy coupled with computerised methods of capture of the striation marks to facilitate comparison. Commercial systems include the Fireball system in Australia [46], the Balistika system from Turkey [47], SCICLOPS<sup>TM</sup> [32] and BulletTRAX<sup>TM</sup>-3D [48]. Even though these advanced systems may improve image capture [49], research is still on-going to

improve the comparative methods, such as that being undertaken currently by the NIST [50, 51].

Conventional comparison microscopy is still useful in visualising, simultaneously, 2D striation marks on the bullet using a split view [52]. However, 3D visualisation of the marks is now also available. Bachrach [32] suggested that 3D imaging of the marks provided a better measure of the surface topography, as illustrated in Figure 1.2.



**Figure 1.2: Feature 2 is not captured in 2D view (left) because in 2D view side lighting is used to examine samples. The 3D view (right) with a confocal microscope with laser beam is better able to capture surface topography [32]**

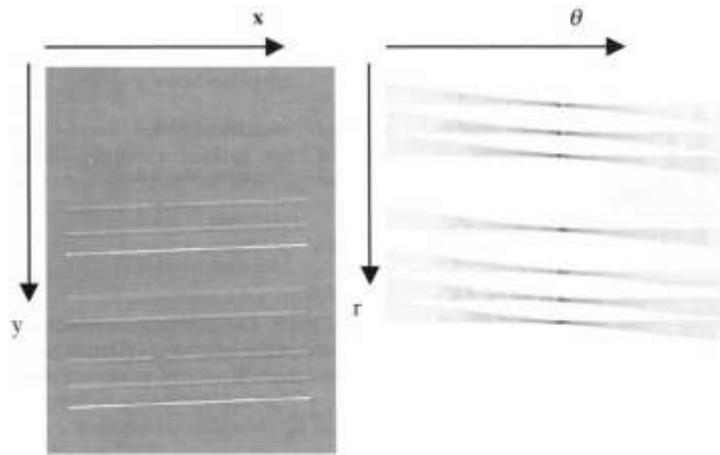
The current trend in ballistic identification systems is to attempt to capture the surface topography rather than simply examining the striations [46, 47, 53-59]. This is undertaken using either a 2D or 3D microscope (optical or confocal) [60], followed by transformation of the resultant images into numerical data for objective comparison.

De Kinder *et al.* [33, 61] published two papers on the transformation of 3D images to produce feature vectors in order to measure the correlation of the striations automatically using a simple correlation algorithm with LabVIEW® software. Based

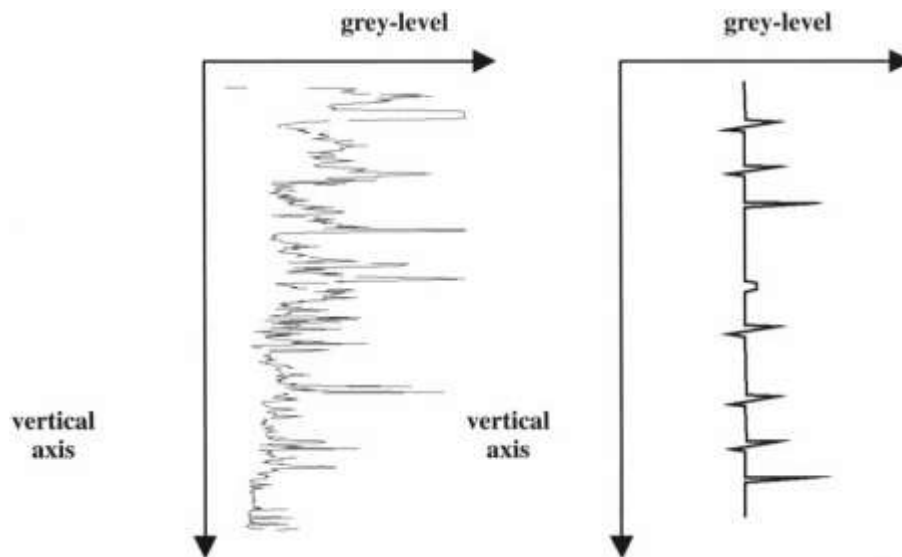
on the 3D images generated from the microscope, a specific region of interest (ROI) on the bullet was chosen as containing characteristic striation marks by an experienced operator as illustrated in Figure 1.3. An algorithm was created, based on the Hough transformation, which is a feature extraction technique focusing on the identification and extraction of imperfections within images. The algorithm transformed the striation marks on the selected ROI into straight lines as depicted in Figure 1.4 and Figure 1.5. Figure 1.4 shows a Hough transformation of the chosen ROI. This transformation changed the striation marks in the ROI into a straight line, using the constant  $\Theta$  value, which rotated the striation marks into horizontal lines. Then the software used the Hough transformation to produce a feature vector (Figure 1.5) which enabled two striations to be compared automatically using a classical correlation algorithm [33]. The results demonstrated that the automated comparison of striations can be achieved depending on the quality of the images produced. Higher resolution images produce better image comparison than lower resolution images. The authors also proposed the automated identification of the ROI rather than relying on operator choice.



**Figure 1.3: Region of interest (ROI) on the bullet as chosen by the experienced operator. The selected area was near the base of the bullet [61]**



**Figure 1.4: On the left is the synthetic image from the ROI and on the right is its corresponding Hough ( $\theta$ ,  $r$ ) transformed image [61]**

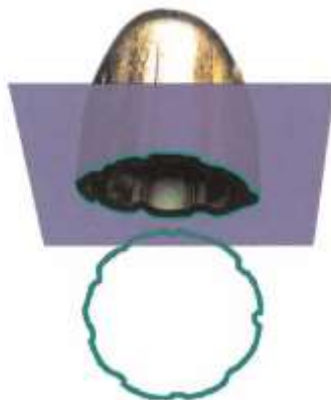


**Figure 1.5: The synthetic image is on the right and its feature vector image on the left [61]**

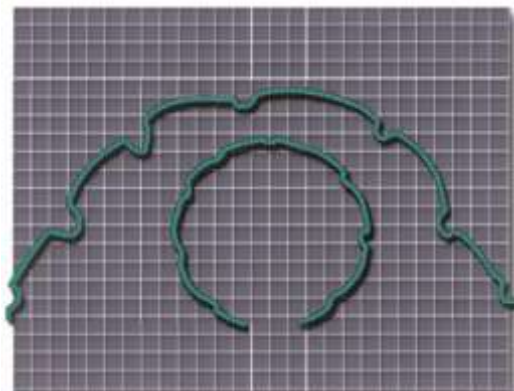
Bachrach [32] investigated the use of SCICLOPS<sup>TM</sup>, a commercially available 3D based automated firearms evidence comparison system which uses a confocal autofocus microscope for image acquisition. SCICLOPS<sup>TM</sup>, developed by Intelligent Automation Inc, is an automated system for microscopic comparison of ballistic



evidence. Using the confocal microscope, Bachrach examined two bullets fired from the same gun. Five cross-sectional images were taken from the bullet at 250  $\mu\text{m}$  intervals, starting from 1 mm from the base of the bullet, along the longitudinal axis as shown in Figure 1.6; Figure 1.7 reveals the groove and land impression of the bullet.

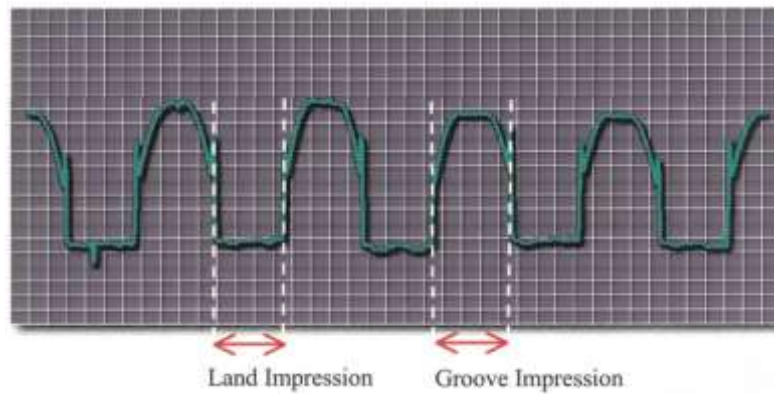


**Figure 1.6: A cross-sectional measurement taken 1 mm from the base of the bullet and subsequently at 250  $\mu\text{m}$  intervals, along the longitudinal axis [32]**



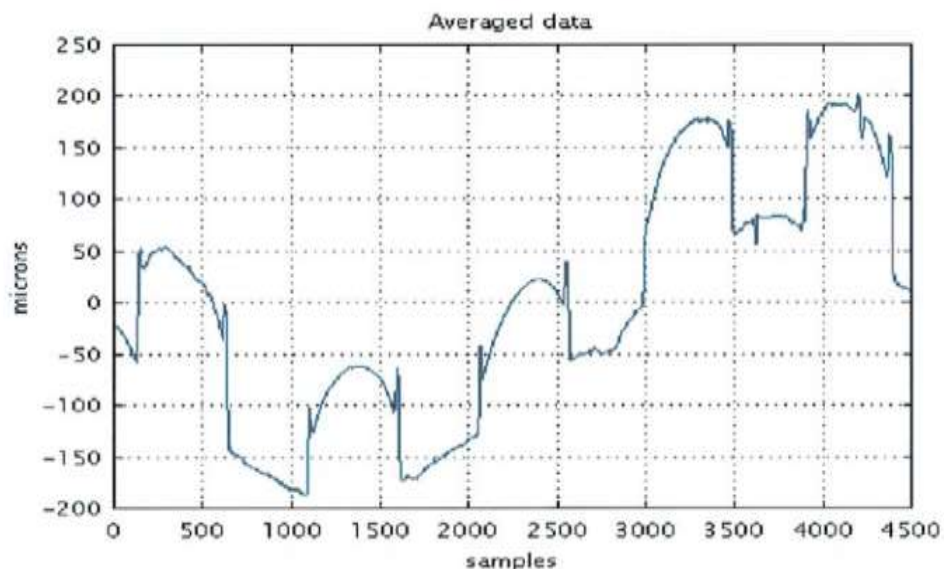
**Figure 1.7: The process of unfolding the bullet surface using SCICLOPS™ [32]**

In order to measure the width of each groove and land impression, the cross-sectional image need to be unfolded and this is illustrated in Figure 1.8.



**Figure 1.8: Unfolded bullet surface with clear view of land and groove impression [32]**

A view of the unfolded bullet surface, Figure 1.8, clearly illustrates the distinction between the land impressions and the groove impressions which are characteristic of the manufacturer of the weapon [32]. The unfolded bullet surface was transformed into numerical data using SCICLOPS™. The author used two bullets in the project. Five images of each bullet surface were acquired and processed to produce a set of average numerical data, as shown in Figure 1.9, which was normalised using a correlation function.



**Figure 1.9: An average bullet surface measurement. The y-axis is the measurement of the bullet surface and the x-axis is the sample points [32]**

Figure 1.10 illustrates the superimposed normalised data from both bullets which can be seen to have similar land engraved areas (LEA) and groove engraved areas (GEA).

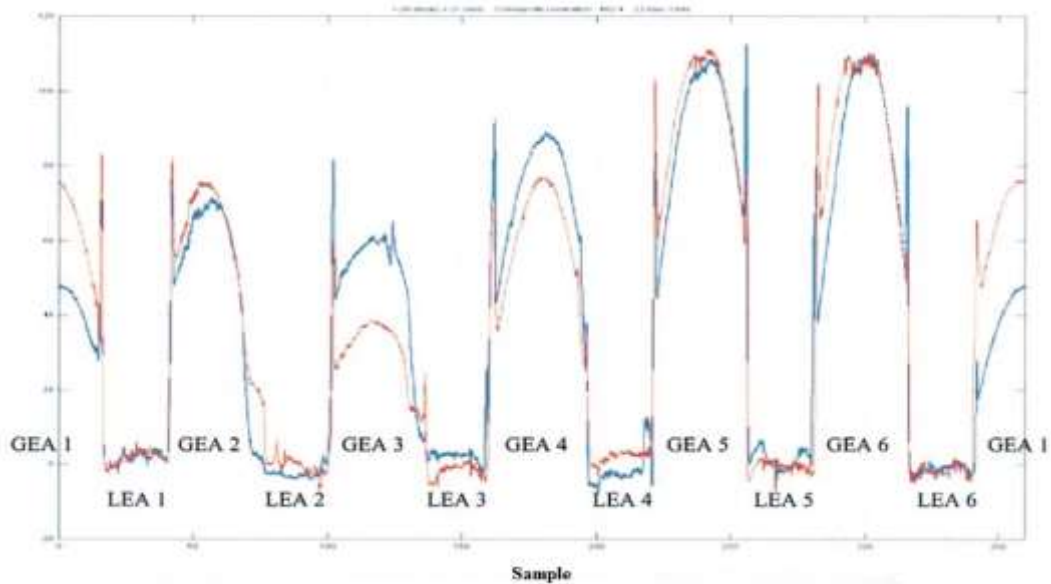


Figure 1.10: Blue and red colours represent two different bullets fired from the same weapon. This is the normalised data of two bullet surfaces showing LEA and GEA [32]

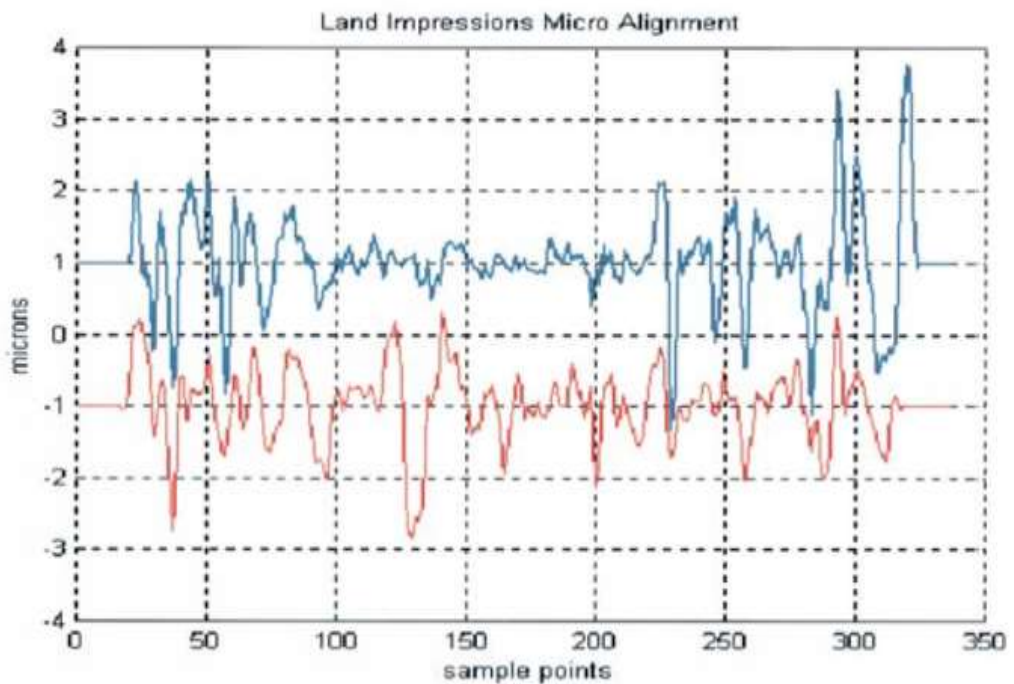


Figure 1.11: Blue and red colours represent LEA 6 on bullets a and b. The region between 0 and 100 and between 200 and 300 sample points show the similarity between the two bullets. The middle region was slightly different [32]

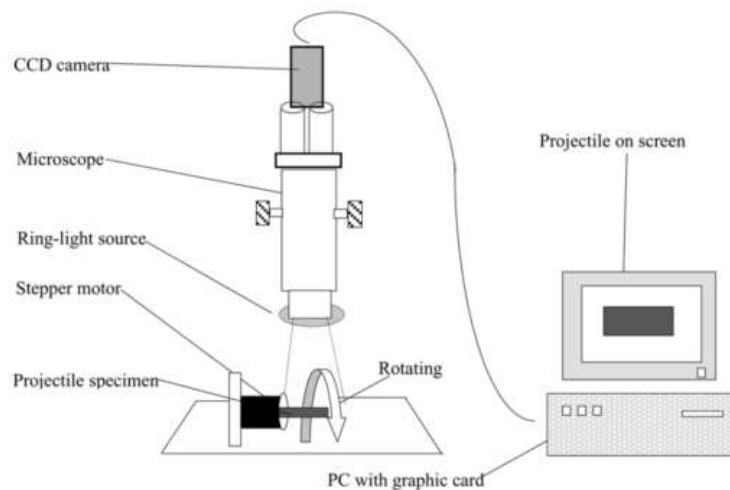
Figure 1.11 shows the comparison of LEA 6 on bullets a and b. There are similarities between sample points 0 and 100 and between 200 and 300. The middle region was different. This is because the barrel of the weapon has better contact with the sides of the LEA as compared to the middle. Macro and micro correlation functions define the similarity of the width (class characteristics) of the LEAs and the GEAs and the micro similarity (individual characteristics) on the LEAs and the GEAs respectively. A composite correlation function was used to reveal the overall similarities between the macro correlation and micro correlation. The similarity index suggested that the lands of the barrel produced impressions which were more consistent. The maximum similarity measure for a false match was divided by the minimum similarity measure for a true match to generate a discrimination ratio  $d(x)$  [32]. This was used to assess the discrimination of the method using six bullets fired from three different weapons and the results obtained are illustrated in Table 1.1.

**Table 1.1: The discrimination evaluation of six bullets fired from three different guns where the matching bullets are in italics [32]**

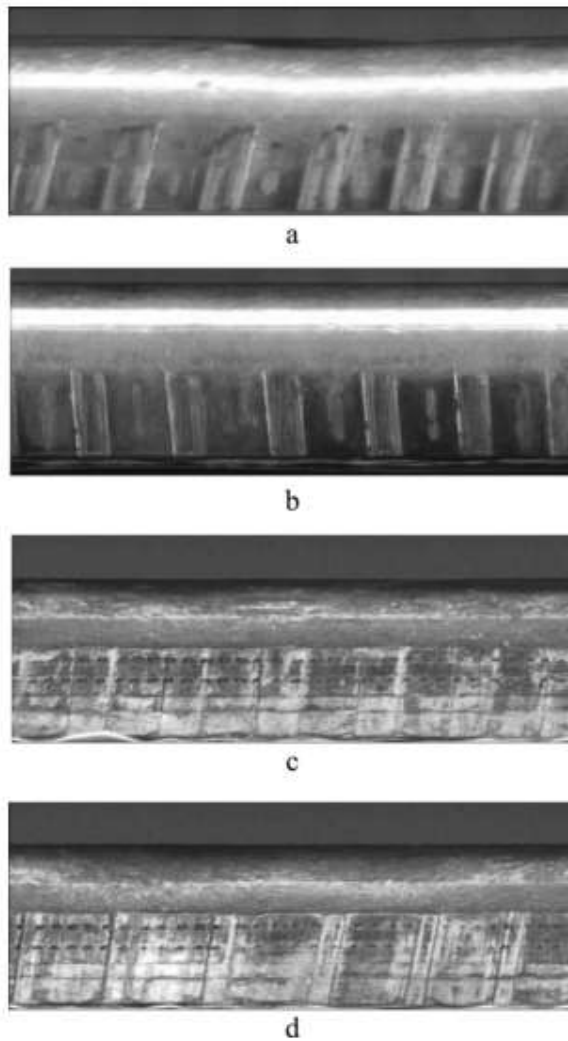
	Gun 1		Gun 2		Gun 3	
	r-10	r-11	r-20	r-21	r-30	r-31
Gun 1						
r-10	100.00	<i>35.20</i>	22.70	27.96	30.86	24.36
r-11	<i>35.20</i>	100.00	22.29	23.69	24.50	23.65
Gun 2						
r-20	22.70	22.29	100.00	<i>50.67</i>	27.24	22.04
r-21	27.96	23.69	<i>50.67</i>	100.00	24.76	23.08
Gun 3						
r-30	30.86	24.50	27.24	24.76	100.00	<i>35.46</i>
r-31	24.36	23.65	22.04	23.08	<i>35.46</i>	100.00

Based on Table 1.1, a discrimination ratio  $d(x)$  was calculated. Min  $d(x)$  is 0.54, max  $d(x)$  is 0.88 and average  $d(x)$  is 0.70. The  $d(x)$  demonstrates a high false positive result (88%); however, the author found that it was possible to identify similarities between bullets fired from the same gun. This work demonstrated that examining the full striated topography across the land engraved area of the bullets was viable and could be used as a means of comparison.

Dongguang Li [46] introduced a line-scan imaging technique to capture the image of striations and a new analytic system using fast Fourier transform (FFT) for bullet identification. Figure 1.12 illustrates the experimental set up where the camera captures 2D images of the striations from the projectile as it rotates and the images are ultimately re-combined to produce a complete image of the striation, as seen in Figure 1.13.

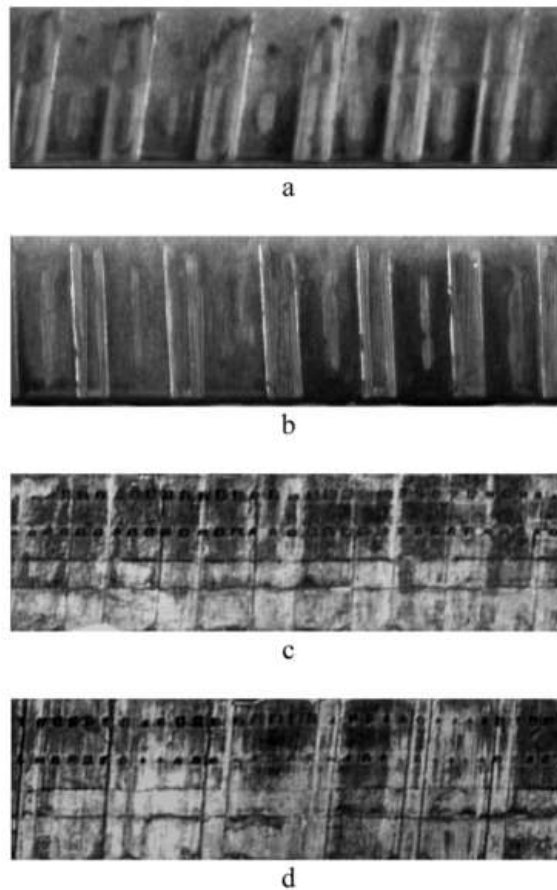


**Figure 1.12: The proposed line-scan imaging system [46]**



**Figure 1.13: The combined 2D image processed by the optical microscope from four different bullets shot with four different guns [46]**

Each image was then transformed to produce a contrast version (Figure 1.14) using a charge-coupled device (CCD) within the camera's software where the darkest pixel is set to black, the brightest value set to white, and each of the others to linearly interpolated shades of grey [46].

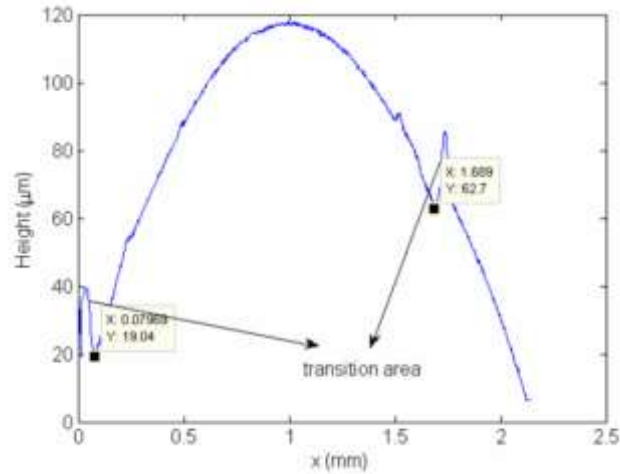


**Figure 1.14:** These images are the contrast enhancement version of images from Figure 1.13 [46]

The purpose of the study was to introduce a new scanning technique and fast Fourier transform (FFT) in image processing of the striations. Therefore, the new scanning method using an edge detector and a FFT were used to determine the edge of the striations to differentiate the LEA and the GEA, to reduce the image noise and to quantify characteristics on the bullet surface.

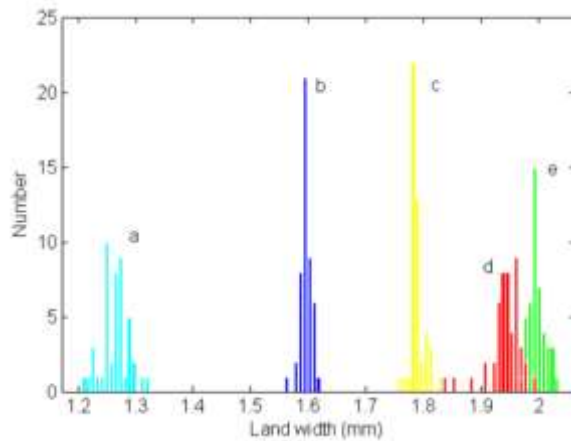
Chu *et al.* [62] proposed a new method of matching striations for automated bullet identification and examined 48 bullets of two different brands fired using six different weapons. The LEA width measurement was captured using a confocal microscope and Figure 1.15 depicts the calculation of the LEA width where the blue line indicates a

measurement of the LEA and the two square dots mark the border points of the LEA. The LEA width is derived from the abscissa difference (the perpendicular distance of a point from the vertical axis) between the border points [62].



**Figure 1.15: The border points of the LEA (the minima points of the transition area) are marked as two square dots. The LEA width is the abscissa difference between the border points [62]**

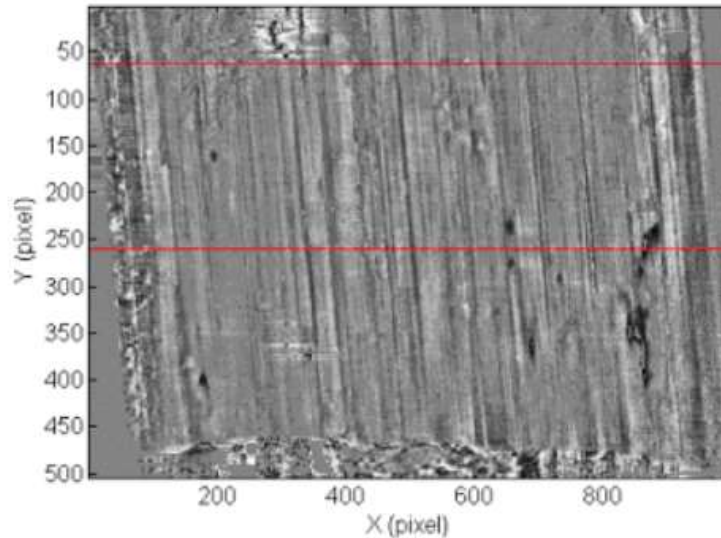
A histogram of the distributions of the LEA width for the various weapon types are presented in Figure 1.16 and could be differentiated.



**Figure 1.16: Histogram of the LEA width of five different firearms: a) Taurus, b) SIG Sauer, c) Browning, d) Beretta and e) Ruger. The y-axis represents the total number of bullets (48 bullets) for each firearm [62]**

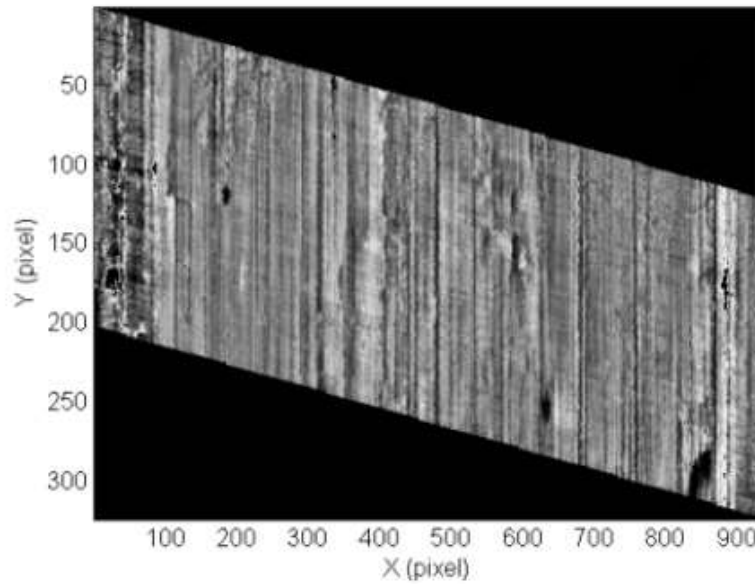


Interpolation and noise reduction across the LEA surface was undertaken using a Gaussian filter and an example of the resultant flattened image is shown in Figure 1.17 which was corrected for any twist obvious in the image using a cross correlation function (CCF). A CCF of two digitised profiles indicates where the striations are related or correlated to each other.

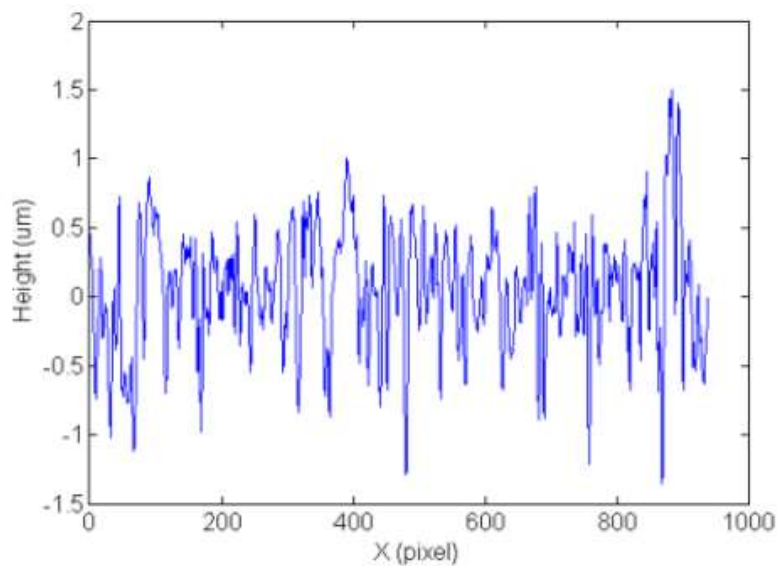


**Figure 1.17: This is the flattened image of the LEA post removal of groove width, outliers and dropout of data, interpolation of data and filtering with a Gaussian filter. The selected area of LEA is in between the red lines [62]**

The authors chose about 0.31 mm of the area on the LEA, consisting of 200 horizontal profiles across the striated region, and calculated the average profile. The selection of the area was based on the authors' experience; Figure 1.18 shows the selected area originating from Figure 1.17. Figure 1.19 is the average profile of the striation.



**Figure 1.18:** This is twisted image of the selected LEA originally from Figure 1.17. In order to straighten the striation, the authors used CCF to correct the twisted angle of the image [62]



**Figure 1.19:** This is the average profile from Figure 1.18, calculated using the residual sum of squares (RSS) formula. ‘The RSS is the sum of squares of residuals between a segment of the step curve and its corresponding fitting line’ [62]

Once the average profile of the striation was calculated, the correlation between the two bullets could be computed and is presented in Table 1.2.

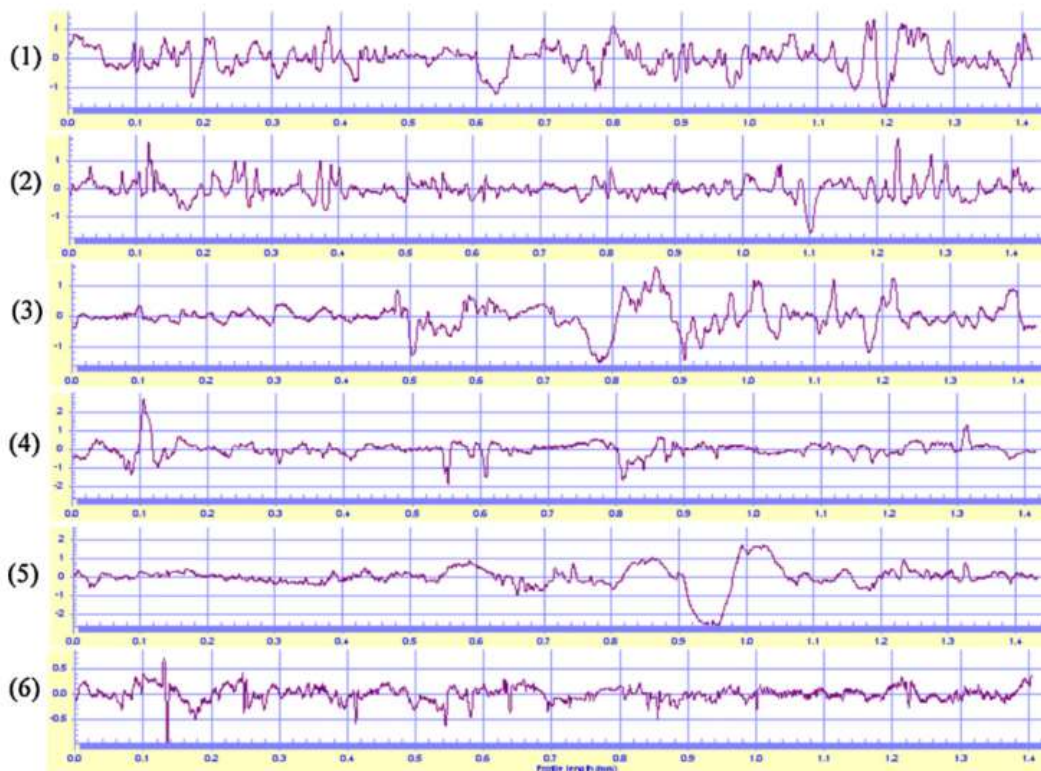
**Table 1.2: This is the average of cross correlation function values of eight bullets fired from Ruger barrels, and nonmatching correlation [62]**

Matching		Nonmatching			
Bullets Being Correlated	Average CCF for 6 LEAs	Bullets Being Correlated	Average CCF for 6 LEAs	Bullets Being Correlated	Average CCF for 6 LEAs
1 vs. 2	0.593	1 vs. 5	0.250	3 vs. 5	0.245
1 vs. 3	0.528	1 vs. 6	0.250	3 vs. 6	0.266
1 vs. 4	0.501	1 vs. 7	0.255	3 vs. 7	0.258
2 vs. 3	0.467	1 vs. 8	0.236	3 vs. 8	0.244
2 vs. 4	0.447	2 vs. 5	0.232	4 vs. 5	0.261
3 vs. 4	0.533	2 vs. 6	0.246	4 vs. 6	0.266
5 vs. 6	0.392	2 vs. 7	0.244	4 vs. 7	0.264
5 vs. 7	0.312	2 vs. 8	0.239	4 vs. 8	0.237
5 vs. 8	0.332				
6 vs. 7	0.517				
6 vs. 8	0.496				
7 vs. 8	0.582				

Based on Table 1.2, the average CCF of matching bullets is more than 0.3 while that for the nonmatching bullets is less than 0.3. This study managed to quantify and correlate the striations from bullets shot from different weapons for class characteristic differentiation. Despite the successful automatic transformation of images using the algorithm and correlation function, the image acquisition and area selection of the striations were still manually chosen and largely dependent on the experience and skill of the operator. However, the method did suggest a means of undertaking the automatic correlation of the striation marks on the bullets and generated a quantifiable matching criterion.

An extension of this concept led to the National Ballistics Imaging Comparison (NBIC) project in 2012 [51] established by the National Institute of Standards and Technology (NIST) in collaboration with the Bureau of Alcohol, Tobacco, Firearms

and Explosives (ATF). Six master bullets, each fired from a different handgun (types of handguns were not mentioned), were collected and processed. One selected land engraved area on each bullet was used to generate the profile signature as shown in Figure 1.20. These profiles were then used to create a total of 2460 bullets to be used as a set of Standard Reference Materials (SRM).



**Figure 1.20: These are the six modified (after removal of curvature and Gaussian filtering) digitised bullet profile signatures for the master bullets used for the NBIC project [51]**

The goal of the NBIC project was to assure that the assessment processes carried out by firearms examiners were robust and that examiners could be tested in their abilities to match the SRM bullets to the master set. In this way the variability of examiners' opinions could be quantified and an understanding of measurement uncertainty could be achieved.

During the preparation of the SRM, NIST suggested using signature differences (Ds) and a cross correlation function maximum (CCF<sub>max</sub>) in order to identify any differences between the SRM bullet's striations and those of the master bullets from which they were generated as shown in Figure 1.21.



Figure 1.21: Profile signature from the actual bullet and the SRM [51]

The top most box displays two almost identical striation profiles. The actual bullet, signature A, is on the top and the SRM bullet, signature B, is below it. The profile signatures were very similar to each other generating a CCF value of 99.55% and a calculated Ds value of 0.92%. This shows that both CCF and Ds values can be used to quantify the ballistic samples and improve accuracy of ballistic evidence.

### 1.3 Air Weapons

Air rifles and air pistols are widely used in sport, target shooting and firearms training [30]. Air weapons are different from firearms because of the type of propellant used. Firearms need gunpowder as the explosive propellant [63], whereas air weapons have three types of propellant, depending on the weapon, which are pneumatic, spring-piston and carbon dioxide [30, 64].

Pneumatic air weapons use compressed air pumped into a gas reservoir which is used to propel the pellet out of the weapon. All pneumatic air weapons are recoilless as compared to other types of air weapons. There are three types of pneumatic air weapons: multi-stroke or 'pump-up', single-stroke and pre-charge. Multi-stroke refers to the number of strokes needed to pump the lever to get the desired pressure in order to fire the weapon. These weapons are accurate, light weight and compact. Unlike multi-stroke air weapons, single-stroke weapons, as the name suggests, only need one stroke of the lever to maximise the pressure and are more accurate than the multi-stroke type. Pre-charged air weapons are used mostly for sport and training because they are more accurate than multi-stroke and single-stroke weapons. The air is pumped up from a scuba tank and, unlike single and multi-stroke weapons which fire single shots only, multiple shots can be fired.

Spring-piston weapons use a powerful spring mechanism and recoil [30]. The spring is compressed manually and the air is released when the trigger is pulled, pushing the piston forward and launching the projectile. Figure 1.22 below depicts a diagram for further understanding [65].

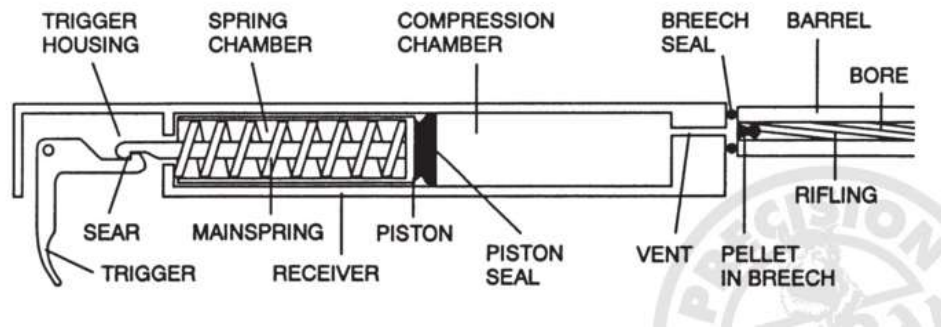


Figure 1.22: Spring-piston airgun [65]

When the airgun is cocked, the piston compresses the spring in the chamber until the sear hooks with the trigger. This creates air pressure within the compression chamber. Pulling the trigger causes the spring to uncoil, moving and pushing the piston forward. The pellet is then propelled out of the muzzle when the air pressure in the compression chamber is higher than the friction which holds the pellet in the barrel. All these movements take place in just seconds, with formation of heat over several hundred degrees Celsius and cooling down of air as it expands. This type of weapon is user friendly and easy to maintain; however, the spring is subject to wear and tear and, if it is fired without any pellet in the barrel, the piston may break because it will smash directly into the vent tube. The spring and the piston are replaceable.

The third type of air weapon uses carbon dioxide from disposable cartridges as the propellant. They are highly temperature dependent, easy to cock and recoilless. The weapons can stabilise at ambient temperature, usually in the field, and produce consistent and accurate results [64].

Air weapons, like other firearms, are categorised by calibre where the calibre refers to the internal diameter of the barrel of the weapon in relation to the diameter of the projectile/bullet used. It is a numerical value which is included in the cartridge name as an indication of the approximate diameter of the projectile/bullet [66]. In a rifled barrel, the diameter is measured from land to land or from groove to groove. The abbreviation 'cal' is used with 'inches' when the barrel diameter is given in inches; for example, a .338 Winchester Magnum with a diameter of 0.338 inches is a .338 cal. The decimal point is silent when spoken, making it 'three-three-eight calibre'. Within Europe, measurements are always quoted in millimetres, for example, 9 mm. In modern cartridge nomenclature, the cartridge firearms are generally referred to by the cartridge name such as .38 cal with the metric equivalent of 9 mm. The most common cartridges are .38 Special, .380 ACP, .357 Magnum, 9x19 mm Parabelum and 9x18 mm Makarov [66].

In the United Kingdom, according to the Firearms Act 1968 [67], any air weapon with kinetic energy of less than 6 foot pounds (handgun) or less than 12 foot pounds (rifle) do not require an Firearm Certificate. The make and model of the air weapons used in this study are further explained in Chapter 2.

For air weapons, most airguns use .177 calibre pellets, which are also known as 4.5 mm calibre pellets, and this is the pellet of choice for target shooting or 'plinking' [30, 64]. Other calibres which are available are .20, .22 and .25. There are also two types of ammunition that are commonly used with air weapons. The first is a steel ball, with



‘an average diameter of 0.175 inches and a weight of 5.5 grains’ although this is not that popular [30].

The second is known as a waisted Diabolo pellet which is a soft lead ammunition used for most air rifles [30] and air pistols. These pellets look like a shuttle cock. The bottom part of the pellet, which looks like a skirt, sits in the breech of the air weapon’s barrel as in Figure 1.23 and seals the breech.



**Figure 1.23: Four different types of pellets: (from bottom to top) RWS® Superpoint, RWS® Super H-Point, RWS® Superdome and RWS® Supermag’ [68]. The striation marks are left on the skirt of the pellet**

As shown in Figure 1.23, there are four types of pellets offered by Umarex USA® [68]. The RWS® Supermag has a flat head. This type of pellet will make a well-defined round mark on paper and is used mainly in target shooting. The RWS® Superdome has a round head, and it is good for hunting because it provides better accuracy even at long distances and has good retention of energy when shooting at a moving target. The RWS® Super H-Point is a hollow point pellet which causes the

pellet to smash upon impact, resulting in more damage. It is usually used in hunting larger animals. The RWS® Superpoint has a pointed tip and is designed for hunting and outdoor field target shooting [69]. The choice of pellet depends on the purpose of the shooting. Most of these pellets are sold in tins to prevent damage to the pellets.

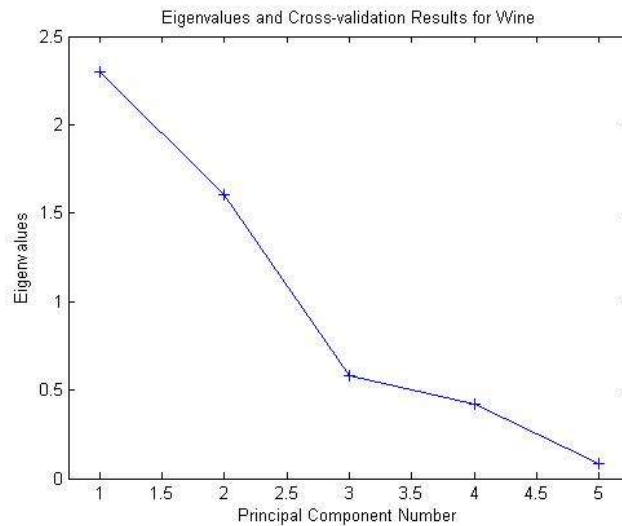
#### **1.4 Principal Component Analysis (PCA)**

Data from this study is analysed by supervised and unsupervised analysis. Supervised analysis ‘uses the information about the class membership of the samples to a certain group in order to classify new unknown samples in one of the known classes. It consists of training set selection (objects of known class membership), building a model from the training set and validation of the model using independent test set of samples for evaluation of the classification achieved’ [70]. Unsupervised analysis is when the software classifies the data without sample classes input from the user. PCA and HCA are two examples of unsupervised analysis tools while LDA is an example of supervised analysis. PCA ‘provides a direct mapping of high-dimensional data into lower-dimensional space showing most of the information in the original data’ [71]. ‘PCA reduces the data dimensionality and retains as much as possible the information present in the original data’ [70]. This study used principal component analysis (PCA) for exploratory data of the striation marks. PCA is used for data compression. A data matrix, such as that in Table 1.3 (in this case for alcohol consumption) [72], is described by new and reduced variables called principal components (PCs).

**Table 1.3: The alcohol data set [72]**

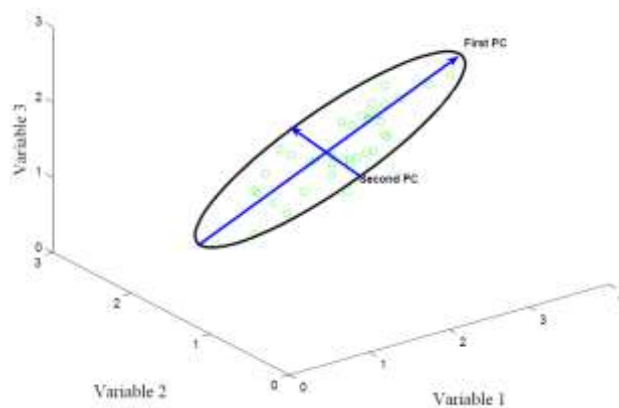
	<b>liquor consumption <u>liter/year</u></b>	<b>wine consumption <u>liter/year</u></b>	<b>beer consumption <u>liter/year</u></b>	<b>life expectancy <u>years</u></b>	<b>heart disease rate <u>cases/10e5/yr</u></b>
<b>France</b>	2.5	63.5	40.1	78	61.1
<b>Italy</b>	0.9	58.0	25.1	78	94.1
<b>Switzerland</b>	1.7	46.0	65.0	78	106.4
<b>Australia</b>	1.2	15.7	102.1	78	173.0
<b>Great Britain</b>	1.5	12.2	100.0	77	199.7
<b>United States</b>	2.0	8.9	87.8	76	176.0
<b>Russia</b>	3.8	2.7	17.1	69	373.6
<b>Czech Republic</b>	1.0	1.7	140.0	73	283.7
<b>Japan</b>	2.1	1.0	55.0	79	34.7
<b>Mexico</b>	0.8	0.2	50.4	73	36.4

‘Each PC is a linear combination of original measured variables’ [70] and associated with a value called an eigenvalue. Larger eigenvalues correspond with more significant PCs. The first few eigenvalues account for almost 80% or more variation for the data set, and this is sufficient for data interpretation [73]. How many principal components are required to adequately describe a data set is indicated by the eigenvalue, as shown in Figure 1.24.



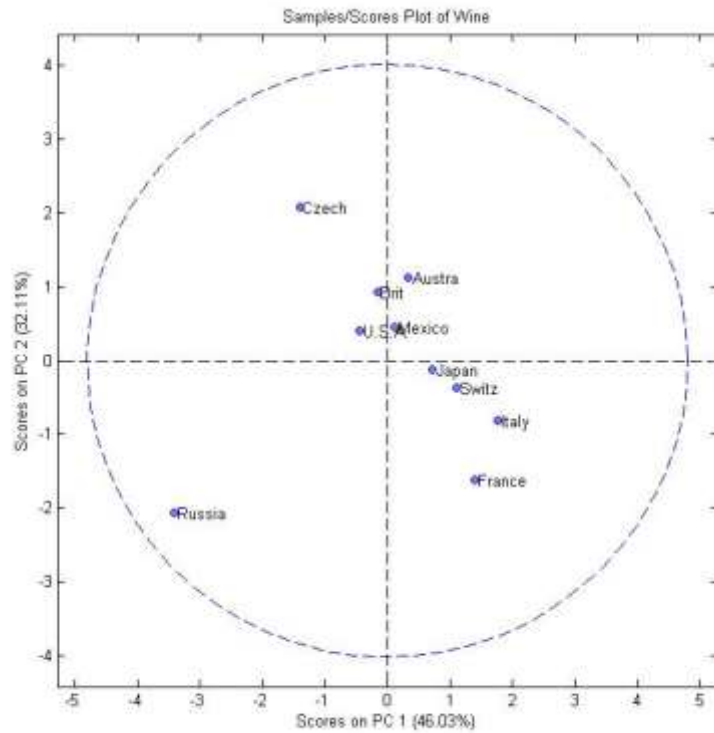
**Figure 1.24: This is an eigenvalue plot for the alcohol data from Table 1.3. PC1 and PC2 adequately represent the data set because they have the higher eigenvalues as compared to PC3, PC4 and PC5 [72]**

Principal components are drawn through the centroid of the data and through the direction of maximum variation of the data (the first PC or PC1), shown in Figure 1.25, the major axis for the ellipse, with less distribution along PC2, the minor axis for the ellipse.



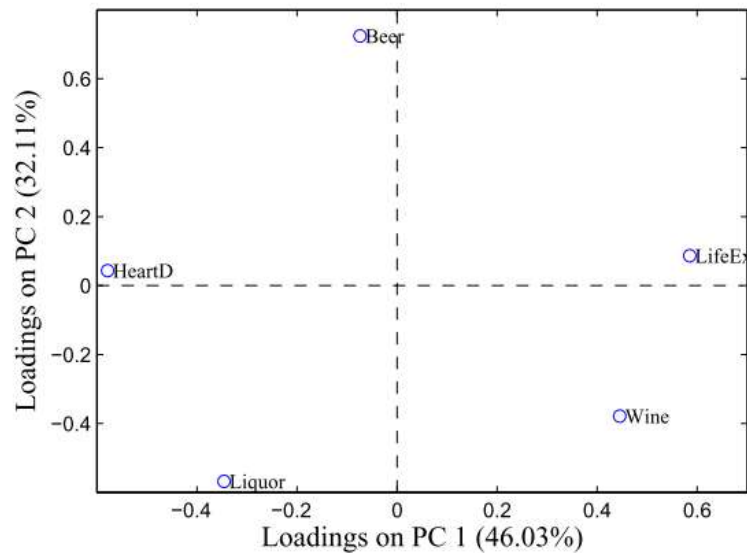
**Figure 1.25: A 3D graphical presentation of PCA. The first PC, or PC1, is a line drawn through the centroid of the data and along the maximum variation of the data. The second PC, or PC2, is drawn through the centroid and along the next maximum variation of the data; however, it must be perpendicular to PC1 [72]**

Scores and loadings are the outputs of PCA. PC scores show the relationship between samples in the data and describe the pattern of the data set. Samples with similar scores will be plotted in the same area, as shown in Figure 1.26.



**Figure 1.26: The scores plot for the alcohol data. Russia is a bit further away than other countries. The circle represents the confidence level of the data [72]**

Based on Figure 1.26, Russia is clearly separated from the other countries. Figure 1.27 shows the loading plot from the alcohol data for further explanation.



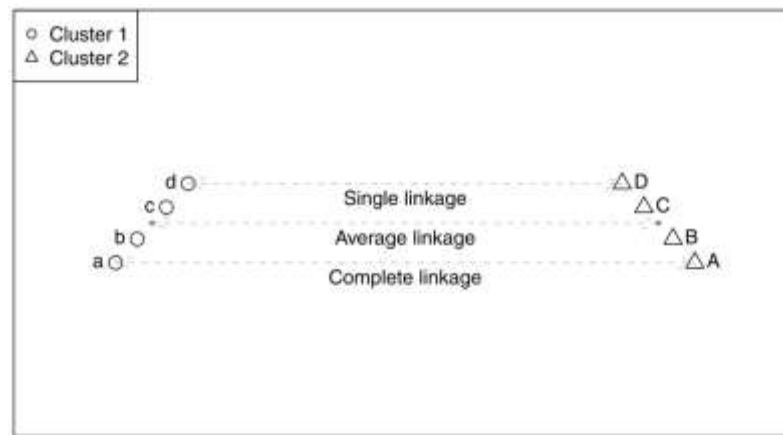
**Figure 1.27: Loading plot from the alcohol data [72]**

Life expectancy and wine load on PC1 with positive values and heart disease and liquor load with negative values. This shows that wine is positively correlated with life expectancy and liquor is positively correlated with heart disease. Anti-correlated means the variables load with opposite signs, for example, ‘life expectancy is altered with the presence of heart disease, or varies inversely with heart disease rate’ [72]. For PC2, beer loads with positive values and wine and liquor load with negative values. These loadings can be connected with the scores plot from Figure 1.26. Russia has negative scores for both PC1 and PC2 (Figure 1.26). Based on the loading plot, an increase in liquor consumption will move the sample down and to the left, an increase heart disease rate and a reduction in life expectancy will move the sample to the left, a reduction in beer consumption will move the sample down and increase in wine consumption will move the sample towards the lower right. These loadings explain which variables cause Russia to be different to the other countries. The interpretation of the scores and loadings plots can be observed in the original data set, as in Table

1.3 where Russia has the highest liquor consumption per year, is among the lowest consumers of wine and beer, has the highest heart disease rate and thus the lowest life expectancy, as compared to other countries in the table. This interpretation is subjective in nature. There are many factors that can contribute to an increase in life expectancy, such as exercise and a healthy diet, availability of healthcare facilities, genetic factors, socioeconomic status and psychosocial factors [74, 75]; therefore drinking less liquor and more wine or beer is not the only factor in living longer.

### **1.5 Hierarchical Cluster Analysis (HCA)**

Hierarchical cluster analysis (HCA) is often used to interrogate data which may consist of groups and sub-groups [71, 76] to show the hierarchical structure of the data. Distances between groups of data are important in clustering. There are four types of distance measurement available: Euclidean, Canberra, Mahalanobis (quadratic) and Manhattan (city-block) [76]. Euclidean distance is most widely used because of its simplicity and is applicable to this study. It is measured with a straight line distance between two points that exist in the clusters. Figure 1.28 explains the possibility of distance link between two clusters of data, clusters 1 and 2. Single linkage is when the distance between clusters 1 and 2 is measured by the shortest distance or the closest objects in the group, objects d and D. If any members of both groups are close together, they are joined together; this is often referred to as friends-of-friends [71]. Complete linkage means the distance between two groups is determined by the objects that are furthest apart, objects a and A. Average linkage is joining two clusters using average distances between objects in two groups.



**Figure 1.28** Single linkage uses the distance between the two closest points in cluster 1 and 2. Average linkage uses the average points between the two clusters and complete linkage uses the distance between the two the farthest points [71]

A dendrogram, a tree-like structure, is used to visualise the hierarchical structure: the y-axis shows the distance between groups and the x-axis shows the successful splits of groups. Objects that are similar are positioned and linked together. The interpretation of HCA might be straightforward; however, one of the drawbacks of HCA is when the cluster is not fully determined. When this happens, loss of information is unavoidable and interpretation of the HCA result is difficult. In order to overcome this, the method of clustering should be explored, such as determination of type of measurement for the data.

## 1.6 Linear Discriminant Analysis (LDA)

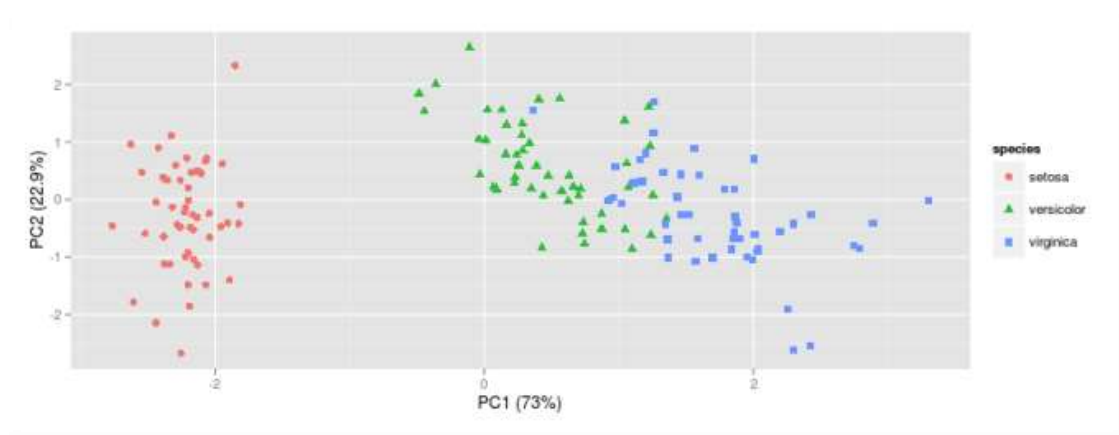
Linear discriminant analysis is an example of supervised analysis. LDA is known as a classifier; it reduces the dimensionality of data and preserves as much of the class information as possible [71, 76]. ‘LDA is based on the determination of linear discriminant functions, which maximise inter-class and minimise intra-class ratio’ [70]. LDA finds the boundaries around clusters of class and discriminates data. It



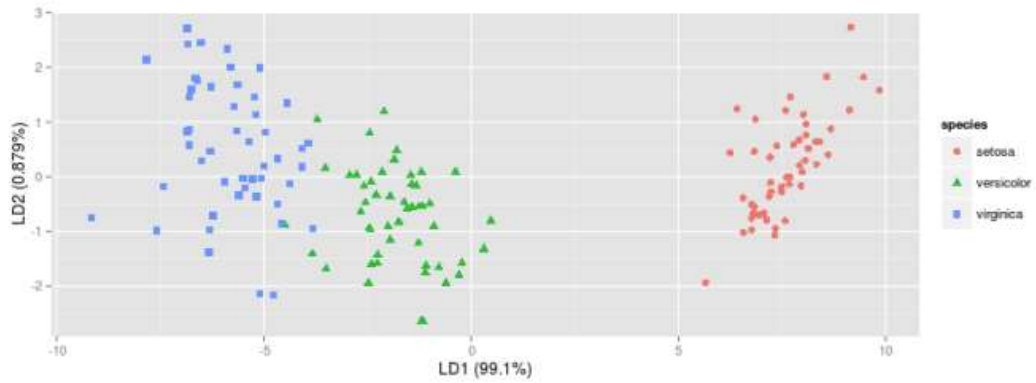
reduces dimension of input variables to new variables called linear discriminants (LD). An example of how LDA works is detailed below. Table 1.4 is taken from an iris data set [77] which contains measurements of 150 iris flowers from three different species: Iris-setosa, s, (n=50), Iris-virginica, c, (n=50) and Iris-versicolor, v, (n=50). Not all data from the 150 measurements is shown in Table 1.4; the full data set is available from the UCI Machine Learning Repository [77]. There are four types of measurements of the iris flowers in the data set (all are measured in cm): sepal length, sepal width, petal length and petal width. The 150 iris flowers were measured and categorised into three different classes (species) based on the sepal and petal length and width measurements. With LDA, a model is built using training samples that relates the data known to known groups. In this example, 150 measurements are grouped into three different classes of species and the discrimination is slightly better than that achieved with PCA. With the PCA results (Figure 1.29), there is still some overlapping between versicolor species and virginia species while setosa species can be separated. The LDA results (Figure 1.30) show better separation between versicolor and virginia species as compared to the PCA results. LDA and PCA can be calculated automatically using the PLS\_Toolbox software from Matlab® [72].

**Table 1.4:** An excerpt of the iris data set containing measurements of 150 iris flowers from three different species: *Iris-setosa*, s, (n=50), *Iris-virginica*, c, (n=50) and *Iris-versicolor*, v, (n=50). Sp denotes species of the iris flowers measured. Not all 150 measurements are shown here. The full data set can be accessed at UCI Machine Learning Repository [77]

	Sepal.L. ↕	Sepal.W. ↕	Petal.L. ↕	Petal.W. ↕	Sp ↕
37	5.0	3.3	1.5	0.2	s
38	4.9	3.6	1.4	0.1	s
39	4.4	3.0	1.3	0.2	s
40	5.1	3.4	1.5	0.2	s
41	5.0	3.5	1.3	0.3	s
42	4.5	2.3	1.3	0.3	s
43	4.4	3.2	1.3	0.2	s
44	5.0	3.5	1.6	0.6	s
45	5.1	3.8	1.9	0.4	s
46	4.8	3.0	1.4	0.3	s
47	5.1	3.8	1.6	0.2	s
48	4.6	3.2	1.4	0.2	s
49	5.3	3.7	1.5	0.2	s
50	5.0	3.3	1.4	0.2	s
51	7.0	3.2	4.7	1.4	c
52	6.4	3.2	4.5	1.5	c
53	6.9	3.1	4.9	1.5	c
54	5.5	2.3	4.0	1.3	c
55	6.5	2.8	4.6	1.5	c

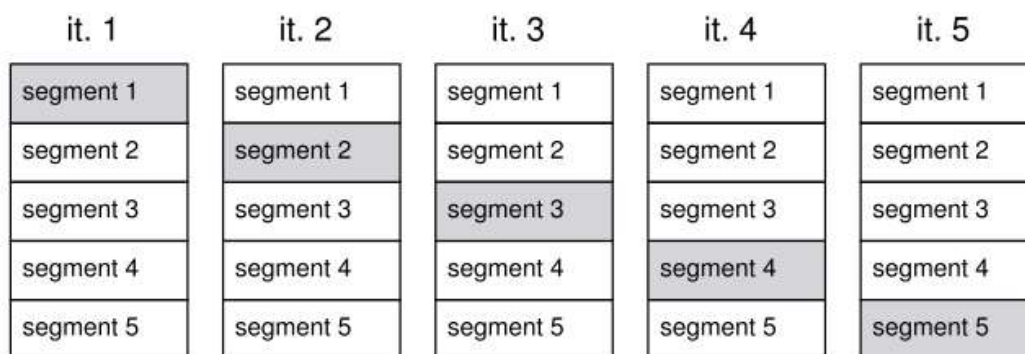


**Figure 1.29:** The PCA results for the iris data set. There is still some overlapping between versicolor species and virginia species while setosa species can be separated [77]



**Figure 1.30: The LDA results for the iris data set. The LDA results show better separation between versicolor and virginica species as compared to the PCA results [77]**

Both PCA and LDA reduce dimensionality of the iris data set; however PCA retains more variability of the data while LDA retains more of the class information of the data. The PCA results explain only 95.9% (PC1 and PC2) of the data while LDA results explain 99.9% (LD1 and LD2) of the data. This shows that LDA discriminates and separates data better than PCA, based on class input from the user. The LDA results can be tested for accuracy of class prediction, using a leave-one-out cross validation. Cross validation is needed for assessing whether the predictive model built from the data is accurate enough for an independent dataset. The process is illustrated in Figure 1.31. The first segment from iteration 1, segment 1 is left out during training/calculation and acts as a test set. Subsequently, one segment from each iteration is left out. These left out samples provide the prediction errors which give the estimation of the cross validated error for the model built [71].



**Figure 1.281: The cross validation process. The first segment from the first iteration (it.1), segment 1, is left out during training and is used as a test set. Subsequently, one segment from each iteration is left out. The overall cross validated error estimation is calculated from the prediction errors of the left out samples [71]**

For this study, the aligned measurements were explored using PCA and HCA. The PCs' values were used as input variables for LDA because this study produced large number of variables. 'PCA is needed for data compression to transform the original data set of large number into a reduced new set of variables' [78], only then the data were analysed using LDA to maximise the separation among the given classes.

## 1.7 Conclusions

Table 1.5 summarises the previous research in objectifying ballistic evidence.

**Table 1.5: Summary of previous research in objectification**

<b>Year</b>	<b>Author</b>	<b>Method</b>	<b>Achievement</b>
1965	Brackett	Theoretical model and mechanical model	Consecutiveness of striation marks is very reliable in firearms identification
1999	Kinder <i>et al.</i>	Labview®, 3D images	Automated comparison of striations can be achieved depending on the quality of the images produced and the speed of taking the images; authors proposed to use automated identification of ROI instead of relying on experienced operator to select the ROI
2002	Bachrach	SCICLOPS™ 3D images	Method suggested was able to objectify and match bullets shot from the same gun, although with a high false positive value
2006	Dongguang Li	Line-scanning 2D image capture, Sobel operator for edge detector, FFT	FFT provided numerical values of spectra, corresponds to the striations from the projectiles, but not the individual characteristics of the weapons
2010	Chu <i>et al.</i>	Automated bullet signature comparison based on correlation function	The algorithm managed to process the images and provide feature profiles of bullet striations; striae comparison was improved based on correlation function maximum
2011	Song <i>et al.</i>	CCFmax	Using cross correlation function to determine the matching bullets fired by different guns; this led to the NBIC project which successfully replicated the SRM bullets and used CCF in objectifying the striation marks on the SRM bullets for identification

The evolution of the methodology for ballistic comparisons has in recent years been heavily influenced by technological advances in imaging. In particular the application of three-dimensional microscopy coupled with an implementation of mathematical tools has allowed firearms examiners the opportunity to move forward from the methods heavily criticised by the National Academy of Sciences report.

Examination of the full surface topography across the land engraved areas rather than a subjective subset of striation marks selected by an examiner allows an evaluation of the validity of using LEA regions for such comparisons. Furthermore, establishing a mathematical method for pre-processing the LEA surface topographical profiles, through a process of curve fitting and normalisation, facilitates an objective means of

aligning and comparing LEAs from projectile to projectile and interpreting how individualising these regions may be.

This research takes forward these approaches. There are five aims in this research.

1. To develop a robust methodology of imaging projectiles using a three-dimensional optical microscope. This would be coupled with the development of a mathematical methodology which would facilitate the alignment and comparison of the surface topology across a land engraved area (LEA).
2. Using the developed methodology (image scanning and data analysis) to explore whether the LEAs across repetitively fired projectiles from the same weapon are independent of each other and if they are, what threshold of alignment is required to describe such independence.
3. To evaluate any variations in aligned LEAs across 600 repetitively fired projectiles from the same weapon and, in particular, to test the hypothesis that alterations are minimal and that projectiles can be linked back to the weapon that fired them.
4. To evaluate the ability of the proposed methodology to link damaged projectiles where the LEAs may have been distorted as a result of impact to the weapon that fired them.

5. To evaluate the ability of the proposed methodology to differentiate between projectiles fired from different weapons.

## 1.8 References

1. Hamby, J.E. and Thorpe, J.W. *The History Of Firearm And Toolmark Identification*. AFTE 2008 [cited 2013; 30th Anniversary Issue, Volume 31 Number 3, Summer 1999:[Available from: [http://www.firearmsid.com/A\\_historyoffirearmsID.htm](http://www.firearmsid.com/A_historyoffirearmsID.htm)].
2. ENFSI. *European Network of Forensic Science Institutes*. 2013 [cited 2015; Available from: <http://www.enfsi.eu/>].
3. Justice, U.S.D.o. *Bureau of Alcohol, Tobacco, Firearms and Explosives* [cited 2015; Available from: <https://www.atf.gov/>].
4. Justice, U.S.D.o. *National Integrated Ballistic Information Network* [cited 2015; Available from: <https://www.atf.gov/firearms/national-integrated-ballistic-information-network-nibin>].
5. Committee on Identifying the Needs of the Forensic Sciences Community, N.R.C., *Strengthening Forensic Science in the United States: A Path Forward*. 2009: National Academies Press.
6. Cork, D.L., Rolph, J.E. and Meieran, E.S., *Ballistic Imaging*. 2008, Washington, DC: The National Academies Press. 344.
7. Lutz, M., *Consecutive Revolver Barrels*. AFTE Newsletter, 1970. Aug: p. 8.
8. Matty, W.R., *.25 automatic pistol breech face toolmarks*. AFTE, 1984. Jul 16(3): p. 57-60.
9. Matty, W., Johnson T., *A comparison of manufacturing marks on Smith & Wesson firing pins*. AFTE, 1984. Jul 16(3): p. 51-6.
10. Matty, W., *A Comparison Of Three Individual Barrels Produced From One Button Rifled Barrel Blank*. AFTE, 1985. 17(3): p. 64-69.
11. Kantner, J. and Lindsay, D.S., *Response bias in recognition memory as a cognitive trait*. *Memory & Cognition*, 2012. 40(8): p. 1163-1177.
12. Mata, R., *Cognitive Bias*. *The Encyclopedia of Human Behavior*, 2012. 1: p. 531-535.
13. Haselton, M.G., Nettle, Daniel., Andrews, Paul W., *The Evolution of Cognitive Bias*, in *The Handbook of Evolutionary Psychology*. 2015, John Wiley & Sons, Inc. p. 724-746.
14. Regulator, F.S. *Cognitive Bias Effects Relevant to Forensic Science Examinations*. 2015 [cited 2016; Available from: [https://www.gov.uk/government/uploads/system/uploads/attachment\\_data/file/510147/217\\_FSR-G-217\\_Cognitive\\_bias\\_appendix.pdf](https://www.gov.uk/government/uploads/system/uploads/attachment_data/file/510147/217_FSR-G-217_Cognitive_bias_appendix.pdf)].
15. Budowle, B., Bottrell, M. C., Bunch, S. G., Fram, R., Harrison, D., Meagher, S., Oien, C. T., Peterson, P. E., Seiger, D. P., Smith, M. B., Smrz, M. A., Soltis, G. L., Stacey, R. B., *A perspective on errors, bias, and interpretation in the forensic sciences and direction for continuing advancement*. *J Forensic Sci*, 2009. 54(4): p. 798-809.

16. Kerstholt, J., Eikelboom, A., Dijkman, T., Stoel, R., Hermsen, R., van Leuven, B., *Does suggestive information cause a confirmation bias in bullet comparisons?* *Forensic Science International*, 2010. 198(1–3): p. 138-142.
17. Kassin, S.M., Dror, Itiel E., Kukucka, Jeff, *The forensic confirmation bias: Problems, perspectives, and proposed solutions.* *Journal of Applied Research in Memory and Cognition*, 2013. 2(1): p. 42-52.
18. Charlton, D., Fraser-Mackenzie, Peter A. F., Dror, Itiel E., *Emotional Experiences and Motivating Factors Associated with Fingerprint Analysis.* *Journal of Forensic Sciences*, 2010. 55(2): p. 385-393.
19. U.S. D.o.J. *A Review of the FBI's Handling of the Brandon Mayfield Case.* 2006 [cited 2016; Available from: <https://oig.justice.gov/special/s0601/exec.pdf>.
20. Grzybowski, R.A. and Murdock, J.E., *Firearm and Toolmark Identification - Meeting The Daubert Challenge.* *AFTE*, 1998. 30(1): p. 3-14.
21. Moenssens, A.A. *The Reliability of Fingerprint Identification - A Case Report.* 2002 [cited 2016; Available from: [http://onin.com/fp/reliability\\_of\\_fp\\_ident.html](http://onin.com/fp/reliability_of_fp_ident.html).
22. Mnookin, J.L. *Fingerprints: Not a Gold Standard.* *Issues in Science and Technology* 20 2003 [cited 2016; No 1 (Fall 2003):[Available from: <http://issues.org/20-1/mnookin/>.
23. Fradella, H.F., O'Neill, Lauren., Fogarty, Adam, *The impact of Daubert in forensic science.* *Pepperdine Law Review*, 2004. 31(2): p. 323-361.
24. Page, M., Taylor, J., Blenkin, M., *Forensic Identification Science Evidence Since Daubert: Part I-A Quantitative Analysis of the Exclusion of Forensic Identification Science Evidence.* *Journal of Forensic Sciences*, 2011. 56(5): p. 1180-1184.
25. Page, M., Taylor, J., Blenkin, M., *Forensic identification science evidence since Daubert: Part II-judicial reasoning in decisions to exclude forensic identification evidence on grounds of reliability.* *Journal of Forensic Sciences*, 2011. 56(4): p. 913-917.
26. Schwartz, A. *Challenging Firearms and Toolmark Identification.* 2008 [cited 2013; Available from: <http://www.nacdl.org/Champion.aspx?id=1612&terms=adina+champion>.
27. Nichols, R. *The Scientific Foundations of Firearms and Tool Mark Identification – A Response to Recent Challenges.* 2006 [cited 2006 9]; Available from: <http://www.firearmsid.com/Feature%20Articles/nichols060915/nicholsASreview.htm>.
28. Nichols, R.G., *Defending the Scientific Foundations of the Firearms and Tool Mark Identification Discipline: Responding to Recent Challenges.* *Journal of Forensic Sciences*, 2007. 52(3): p. 586-594.
29. Justice, N.I.O. *Firearm Examiner Training.* [web page] 2012 [cited 2012; Available from: [http://www.nij.gov/training/firearms-training/module01/fir\\_m01.htm](http://www.nij.gov/training/firearms-training/module01/fir_m01.htm).
30. Di Maio, V.J.M., *Gunshot wounds : practical aspects of firearms, ballistics, and forensic techniques.* 1999: Boca Raton : CRC Press.



31. Gerules, G., Bhatia, S.K. and Jackson, D.E., *A survey of image processing techniques and statistics for ballistic specimens in forensic science*. Science & Justice, 2013. 53(2): p. 236-250.
32. Bachrach, B., *Development of a 3D-based automated firearms evidence comparison system*. J. Forensic Sci., 2002. 47(6): p. 1253-64.
33. De Kinder, J. and Bonfanti, M., *Automated comparisons of bullet striations based on 3D topography*. Forensic Science International, 1999. 101(2): p. 85-93.
34. Nichols, R.G., *Firearm and toolmark identification criteria: A review of the literature*. J. Forensic Sci, 1997. 42(3): p. 466-474.
35. Biasotti, A., *A Statistical Study of The Individual Characteristics Of Fired Bullets*. Forensic Sci, 1959. 4(1): p. 34-50.
36. Brackett Jr, J.W., *A Study of Idealized Striated Marks and their Comparisons using Models*. Journal of the Forensic Science Society, 1970. 10(1): p. 27-56.
37. Blackwell, R.J. and Framan, E.P., *Automated Firearms Identification System (AFIDS): Phase I*. AFTE, 1980. 12(4): p. 11-37.
38. Uchiyama, T., *A Criterion For Land Mark Identification*. AFTE, 1988. 20(3): p. 236-51.
39. Tulleners F., Giusto M. and Hamiel J., *Striae Reproducibility of Sectional Cuts of One Thompson Contender Barrel*. AFTE, 1998. 30(1): p. 62-81.
40. Nichols, R.G., *Firearm and toolmark identification criteria: A review of the literature, part II*. J Forensic Sci, 2003. 48(2): p. 1-10.
41. Miller, J., *Criteria for identification of tollmarks*. AFTE, 1998. 30(1): p. 15-61.
42. Miller, J., *Criteria for identification of toolmarks. Part II: Single land impression comparisons*. AFTE, 2000. 32(2): p. 116-31.
43. Miller, J., *An examination of two consecutively rifled barrels and a review of the literature*. AFTE, 2000. 32(3): p. 259-70.
44. Bunch, S.G., *Consecutive matching striation criteria: A general critique*. J. Forensic Sci, 2000. 45(5): p. 955-962.
45. Howitt, D., Tulleners, F., Cebra, K. and Chen, S., *A Calculation of the Theoretical Significance of Matched Bullets*. Journal of Forensic Sciences, 2008. 53(4): p. 868-875.
46. Li, D., *Ballistics Projectile Image Analysis for Firearm Identification*. IEEE Transactions On Image Processing, 2006. 15(10): p. 2857-2865.
47. Sakarya, U., Leloğlu, U.M. and Tunali, E., *Three-dimensional surface reconstruction for cartridge cases using photometric stereo*. Forensic Science International, 2008. 175(2-3): p. 209-217.
48. IBIS. *IBIS TRAX-HD3D*. 2013 [cited 2013; Available from: <http://www.forensictechnology.com/>].
49. Brinck, T.B., *Comparing the performance of IBIS and BulletTRAX-3D technology using bullets fired through 10 consecutively rifled barrels*. J Forensic Sci, 2008. 53(3): p. 677-682.
50. Ma, L., Song, J., Whitenton, E., Zheng, A., Vorburger, T. and Zhou, J., *NIST bullet signature measurement system for RM (Reference Material) 8240 standard bullets*. J Forensic Sci, 2004. 49(4): p. 649-59

51. Song, J., Vorburger, T.V., Ballou, S., Thompson, R.M., Yen, J., Renegar, T.B., Zheng, A., Silver, R.M. and Ols, M., *The National Ballistics Imaging Comparison (NBIC) project*. *Forensic Sci Int*, 2012. 216(1-3): p. 168-82.
52. Lamagna, D., *Advances In Microscopy and Microanalysis in the Field of Forensic Firearm Examination and Identification*. *Microscopy and Microanalysis*, 2011. 17(S2): p. 622-623.
53. Breitmeier, U. and Schmid, H., *Lasercomp: A surface measurement system for forensic applications*. *Forensic Science International*, 1997. 89(1): p. 1-13.
54. Senin, N., Groppetti, R., Garofano, L., Fratini, P. and Pierni, M., *Three-dimensional surface topography acquisition and analysis for firearm identification*. *J. Forensic Sci.*, 2006. 51(2): p. 282-295.
55. Xie, F., Xiao, S., Blunt, L., Zeng, W. and Jiang, X., *Automated bullet-identification system based on surface topography techniques*. *Wear*, 2009. 266(5): p. 518–522.
56. Gambino, C., McLaughlin, P., Kuo, L., Kammerman, F., Shenkin, P., Diaczuk, P., Petraco, N., Hamby, J. and Petraco, N.D.K., *Forensic Surface Metrology: Tool Mark Evidence*. *Scanning*, 2011. 33(5): p. 272–278.
57. Mathia, T.G., Pawlus, P. and Wieczorowski, M., *Recent trends in surface metrology*. *Wear*, 2011. 271(3–4): p. 494-508.
58. Song, J., Chu, W., Vorburger, T.V., Thompson, R., Renegar, T.B., Zheng, A., Yen, J., Silver, R. and Ols, M., *Development of ballistics identification-from image comparison to topography measurement in surface metrology*. *Meas. Sci. Technol.*, 2012. 23(5): p. 1-6.
59. Zheng, X., Soons, J., Vorburger, T., Song, J., Renegar, T. and Thompson, R., *Applications of surface metrology in firearm identification*. *Surface Topography: Metrology and Properties*, 2014. 2(1): p. 1-10.
60. Bonfanti, M.S. and Ghauharali, R.I., *Visualisation by confocal microscopy of traces on bullets and cartridge cases*. *Science & Justice*, 2000. 40(4): p. 241-256.
61. Pirlot, M., Chabottier, A., Celens, E., De Kinder, J. and Van Ham, P., *Feature extraction of optical projectiles images*. *Science & Justice*, 1999. 39(1): p. 53-56.
62. Chu, W., Song, J., Vorburger, T., Yen, J., Ballou, S. and Bachrach, B., *Pilot study of automated bullet signature identification based on topography measurements and correlations*. *J Forensic Sci*, 2010. 55(2): p. 341-347.
63. Wallace, J.S., *Chemical analysis of firearms, ammunition, and gunshot residue*. 2008: Boca Raton : CRC Press.
64. Saltzman, B. *American Airguns*. 2006 [cited 2014; Available from: [http://www.airguns.net/general\\_airgun\\_types.php](http://www.airguns.net/general_airgun_types.php).
65. Airgun, B.P. *Beeman precision airguns spring-piston manual pellets and pistons*. 2004 [cited 2013; Available from: [http://www.afpmb.org/sites/default/files/pubs/standardlists/equipment/pdfs/1005-01-544-1044\\_manual.pdf](http://www.afpmb.org/sites/default/files/pubs/standardlists/equipment/pdfs/1005-01-544-1044_manual.pdf).
66. Heard, B.J., *Handbook of firearms and ballistics [internet resource] examining and interpreting forensic evidence*, ed. P.D.A. Dawsonera. 2008: Oxford : Wiley-Blackwell.
67. Parliament, U., *Firearms Act 1968*. 1968.

68. Mitchell, R. *Best Airgun Pellet for Hunting*. 2013 [cited 2014; Available from: <http://blog.umarexusa.com/category/airguns/>].
69. Gaylor, T., *The right pellet makes a difference*. Airgun Revue #1. Vol. #1. 1997: GAPP, Inc.
70. Berrueta, L.A., Alonso-Salces, R. M., Héberger, K., *Supervised pattern recognition in food analysis*. Journal of Chromatography A, 2007. 1158(1–2): p. 196-214.
71. Wehrens, R., *Chemometrics with R: Multivariate Data Analysis in the Natural Sciences and Life Sciences*. 2011: Springer Berlin Heidelberg.
72. Eigenvector Research, I. *PLS\_Toolbox*. 2006 [cited 2015; Available from: [http://www.eigenvector.com/software/pls\\_toolbox.htm](http://www.eigenvector.com/software/pls_toolbox.htm)].
73. Gardiner, W.P., *Statistical analysis methods for chemists : a software-based approach*. 1997: United Kingdom: Royal Society Of Chemistry.
74. Gremeaux, V., Gayda, M., Lepers, R., Sosner, P., Juneau, M., Nigam, A., *Exercise and longevity*. Maturitas, 2012. 73(4): p. 312-317.
75. Griffin, B., Loh, V., Hesketh, B., *A mental model of factors associated with subjective life expectancy*. Social Science & Medicine, 2013. 82: p. 79-86.
76. Brereton, R.G., *Chemometrics : data analysis for the laboratory and chemical plant*. 2002: New York : J. Wiley.
77. Bache, K., Lichman, M. *UCI Machine Learning Repository*. 2013 [cited 2016; Available from: <https://archive.ics.uci.edu/ml/datasets/Iris>].
78. Kumar, N., Bansal, A., Sarma, G. S., Rawal, R. K., *Chemometrics tools used in analytical chemistry: An overview*. Talanta, 2014. 123: p. 186-199.

## **Chapter 2: Materials and Methods**

### **2.1 Introduction**

Air pellets were repetitively fired from the same weapon over time in order to produce striation marks on the pellets could be imaged and compared objectively. An air pistol was chosen because it generated a sample set which contained the desired striation marks. Two air rifles were also used to generate two further sample sets both originating from different weapons. This study used lead pellets (unjacketed pellets) and air weapons while other researchers used jacketed bullets with firearms [1-4]. Jacketed bullets (either full metal-jacketed or partial metal-jacketed) are bullets coated with copper or steel alloy as compared to unjacketed bullets [5, 6]. The coating helps in prevention of build-up lead in the barrel after repetitive shooting. Di Maio [6] suggested that striations are more prominent on jacketed bullets than unjacketed bullets. This study explored the behaviour of unjacketed pellets and showed that striations on unjacketed pellets are in fact prominent. They could be identified and scanned using the microscope. The possible explanation of this is when the unjacketed pellets were fired from the air weapons, the pellets were directly in contact with the barrels, with no coating, and hence striation marks could be seen on the pellets. This shows that the striations marks imparted on the unjacketed pellets can be used for identification, as long as they were shot using barrelled air weapons. This study also used air weapons with kinetic energy less than 6 foot pounds (air pistol) and air rifles with kinetic energy of less than 12 foot pounds [7], as compared to higher kinetic energy firearms, such as .25 Auto, .38 Special or .44 Magnum with kinetic energy ranging from 64 to 971 foot pounds and rifles with kinetic energy of more than 1000 foot pounds [6, 8]. Even

though air weapons has lower kinetic energy from firearm,unjacketed pellets shot from these air weapons can acquire striation marks from the barrelled air weapon. These striation marks are sufficient for identification. Oxidation is another important factor affecting the striations on the pellets, regardless jacketed or unjacketed. In jacketed bullets, a research [9] showed that complete corrosion of bullets found in putrefied bodies. This study also noted that oxidation and corrosion occurred on pellets which interfere with striation identification. Based on all these reasons, air weapons with unjacketed pellets were chosen as a template for development of an objective method for the comparison of fired projectiles because striation marks can still be obtained from these pellets and the developed method can be applied for jacketed bullets.

Pellets were fired to generate a number of sample sets, which is further explained in its respective chapters;

- (1) A set of samples fired from air pistol which were essentially undamaged by impact
- (2) A set of samples fired from air pistol over 17 months which were essentially undamaged by impact
- (3) A set of pellets fired from different air weapons which were essentially undamaged by impact
- (4) A set of pellets which were fired from air pistol into a metal trap and distorted through impact

Digital images of the striated regions of the lead pellets fired from the weapons were obtained using an optical 3D microscope. The images were subjected to data

processing using a number of mathematical methods to facilitate effective interpretation of the data. Data was analysed using PCA, HCA and LDA.

## 2.2 Materials

### 2.2.1 Air pistol

A Weihrauch model HW 45, 12 right rifling, .177 calibre, air pistol, (Crocketts retailers, Glasgow) was purchased new and had only been fired as part of the manufacturers tests during production accounting for less than 10 fired pellets. The air pistol was 278mm in length, with barrel length of 170mm [10, 11] and weighed 1.15kg. The Weihrauch model HW 45 has two velocity settings depending on how the cocking mechanism is used. These are listed by the manufacturer as 125 m/s and 170 m/s. The cocking mechanism is shown in Figure 2.1.

This Pistol can be operated at two different velocity levels:  
Position 1: Low velocity  
Position 2: High velocity

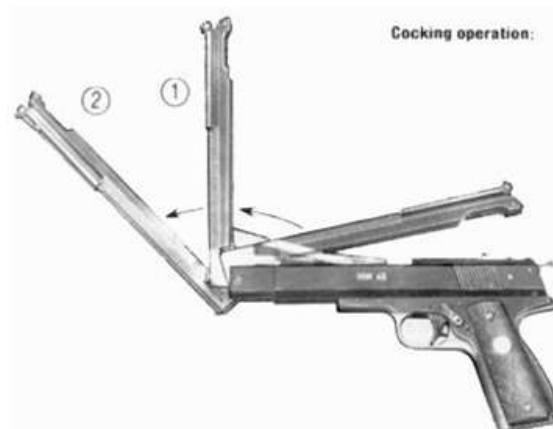


Figure 2.1: The different types of cocking mechanism of HW 45 Weihrauch [10]

The HW 45 Weihrauch air pistol was chosen because it was listed as one of the most powerful air pistols available in the marketplace [11]. The weapon uses a spring-piston mechanism firing one pellet at a time. Spring-piston weapons use a powerful spring mechanism and recoil to project the lead pellet out of the weapon barrel [6]. The spring is compressed manually and the air is released when the trigger is pulled, pushing the piston forward and launching the projectile [12].

The air pistol was not cleaned during the research work, internally and externally.

### **2.2.2 Air rifles**

An Edgar Brother Model 35 and a Baikal 90042234 ИЖ-35 illustrated in Figures 2.2 and 2.3 respectively were also used to produce fired pellets. These air rifles were a number of years old and there was no record of the number of air pellets the weapons may have fired, the purchase invoice or a cleaning log available prior to their use. Both air rifles had 12 right rifling, and were .177 calibre, break barrel design with spring-piston mechanisms. The breech of the rifles was opened in order to feed the pellet into the barrel and one pellet was loaded into the chamber one at a time.



**Figure 2.2: Edgar Brother Model 35 in breech position**



**Figure 2.3: Baikal 90042234 ИЖ-35 in breech position**

Both air rifles are .177 calibre which can fire pellets used in this study, the RWS® Superdome 4.5mm (.177cal).



### 2.2.3 Pellets

RWS® Superdome 4.5mm (.177 cal), round nosed pellets, were used throughout the project (2 boxes). Pellets were purposely bought from similar manufacturer with similar weight, size and shape. Each pellet weighed 8.3 grains, and examples are presented in Figure 2.4. These were waisted Diabolo pellets which are described as a soft-lead ammunition and are noted as the pellet of choice for air pistols [6] and for target shooting [13, 14]. The fanned out bottom part of the pellet (Figure 2.5), sits in the breech of the air weapon's barrel. This skirt is the part of the pellet that makes contact with the barrel of the air pistol as the projectile moves through the weapon and as such is the portion of the pellet upon which the striation marks are impressed.



**Figure 2.4: RWS® Superdome 4.5 mm (.177 cal), round nosed pellets, weight 8.3 grains**



**Figure 2.5: A used pellet bearing striation marks, indicated by the red rectangle on the skirt area, which were important in this research**

### **2.3 Test Firings**

A series of pellets were fired over time using the HW 45 Weihrauch air pistol. In some cases the shooting was undertaken through a chronograph so that the velocity of the pellet could be recorded. Test firings were mostly carried out into water tanks where the pellet was recovered post firing, dried using tissue paper and packaged into small individually labelled polythene bags for storage prior to analysis.

Table 2.1 shows the chronology of the test firings undertaken.

**Table 2.1: Chronology of shooting for the research**

Date of test	Pellet Number	Test Done	Weapon	Total Pellets fired	Pellets Collected	Purpose	Number of pellets analysed using the Alicona Microscope
April 2012	1-50	Low Velocity	HW 45	50	50	Method development	0
April 2012	51-100	High Velocity	HW 45	50	50		10/50
April 2012	101-122	Chronograph: low and high velocity	HW 45	22	0	Velocity measurement	0
January 2013	123-158	Bones & Gelatine	HW 45	36	36	Distorted pellet study	22/22
April 2013	159-208	High Velocity	HW 45	50	50	Inter and intra pellet study	50/50
April 2013	209-219	Chronograph: high velocity	HW 45	11	0	Velocity measurement check	0
May 2013	220-319	High Velocity	HW 45	100	100	Longitudinal study	10/100
May 2013	320-341	Chronograph: high velocity	HW 45	22	0	Velocity measurement check	0
June 2013	342-441	High Velocity	HW 45	100	100	Longitudinal study	10/100
July 2013	442-465	Low Velocity Distance	HW 45	24	24	Distorted pellet and distance study	0
July 2013	466-489	High Velocity Distance	HW 45	24	24		24/24
July 2013	490-499	Rifle 1	Edgar Brother Model 35	10	10	Inter weapon study	5/10
July 2013	500-509	Rifle 2	Baikal 90042234 ИЖ-35	10	10		5/10
September 2013	510-559	Chronograph: low velocity	HW 45	50	50	Velocity measurement check	0
September 2013	560-609	Chronograph: high velocity	HW 45	50	50	Velocity measurement check, Longitudinal study	10/50
<b>Total number of pellets</b>				<b>609</b>	<b>554</b>		<b>146 (24%)</b>

## **2.4 Generation of test sets - Pellet firing and collection**

A total of 100 pellets fired from the air pistol were used to refine the method of pellet collection and storage and for the initial velocity measurements. These pellets were fired in a ballistic test facility to define the safe parameters for discharging the weapon and assess the safety requirements for subsequent tests.

All of the first 100 pellets fired were examined using a conventional comparison microscope. In almost all cases, corrosion of the surface of the metal occurred very quickly and this affected the quality of the striation marks visible on the surface. As a consequence, the collection methodology was modified so that the pellets were immediately dried once removed from the collection tank and placed in individually labelled small polythene bags. This resulted in much less corrosion of the pellet surfaces although some minor corrosion did still occur.

Comparison microscopy also demonstrated that the striation marks observed on the fired pellets were better defined on those fired at high velocity rather than those fired at low velocity. As such only the high velocity pellets were examined using infinite focus microscopy. A total of 10 pellets from the first 100 pellets were subsequently analysed using the Alicona® infinite focus microscope to determine the abilities of the instrument and develop the measurement parameters (section 2.5).

### 2.4.1 Velocity studies

The kinetic energy was calculated using data derived from a chronograph and Equation 2.1:

$$\mathbf{KE = \frac{1}{2}MV^2 \dots \dots \dots \mathbf{Equation 2.1}}$$

where KE is kinetic energy in joules (J), M is mass in kilograms (kg), and V is velocity in meters per second (m/s).

The repeatability of the velocities of the pellets fired at a given time and the reproducibility of these velocities over a time span of a year was assessed using two different chronograph systems. Four sets of measurements were taken over different time frames and of both low and high velocity test firings.

The first chronograph consisted of four optical sensors and a stopper at the end of the chronograph into which the pellet was fired. When the pellet was fired, the muzzle of the air pistol was set within a maximum and the minimum line so that the projectile passed across all four cameras (Figure 2.6). The time taken for the pellet to travel between the cameras was measured electronically and the data was stored in a computer attached to the chronograph system. This chronograph was used to assess the velocity of the projectiles fired in April 2012 till May 2013.

The second chronograph was a CED M2 Optical Chronograph [15] purchased from Recreational Software, Inc. and is presented in Figure 2.7. It is an easy-to-use, portable chronograph system. This chronograph was used to assess the velocity of the projectiles fired in September 2013.



**Figure 2.6:** The chronograph consisted of four optical sensors. The muzzle of the air pistol is fired between the minimum and the maximum lines as labelled in the picture



**Figure 2.7:** CED M2 Optical Chronograph [15]

#### **2.4.2 Within and between pellet comparison**

50 pellets (numbered 159 to 208), collected in April 2013 were analysed using the Alicona® infinite focus microscope. In each case the 12 LEA regions, labelled A through to L, were landscaped and scrutinised to develop the mathematical processing tools using Matlab® R2014a with PLS\_Toolbox® software. The results are presented and discussed in Chapter 3.

#### **2.4.3 Longitudinal study**

Pellets (n=10 in each group, a total of 50 pellets) were chosen from the April 2013, May 2013, June 2013 and September 2013 pellet sets. These were compared with the pellets from April 2012 using the Alicona® infinite focus microscope and derived mathematical processing methods to explore the variation within each LEA over usage of the weapon. The results are presented and discussed in Chapter 4.

#### **2.4.4 Comparison of pellets fired from different weapons**

10 pellets were fired from each of the two air rifles. In each case five pellets from each air rifle were chosen for further analysis using the Alicona® infinite focus microscope and derived mathematical processing methods to explore the variation within each LEA across the three weapons used in the study. The results are presented and discussed in Chapter 5.

#### **2.4.5 Pellet distortion study**

Two sets of pellets were fired into a metal collection trap (shown in Chapter 6) across a variety of distances. In each cases 6 pellets were fired at distances of 1, 2, 3

and 4 meters from the metal collection trap and at high and low velocities resulting in 24 pellets associated with each velocity. Only the high velocity pellets were subjected to further analysis. The results are presented and discussed in Chapter 6.

## **2.5 Alicona® Infinite Focus G4, 3D optical microscope**

The Alicona® Infinite Focus G4 is an optical microscope capable of producing a 3D image, and is illustrated in Figure 2.8 [16]. It is highly accurate for automatic 3D micro coordinated and surface roughness measurements. The speed of measurement is 1.7 million measure points per second. All scanned and measurement data was stored in an encrypted portable data storage device which was password protected.



**Figure 2.8: Alicona® Infinite Focus G4 optical microscope [16]**

The microscope has five objective lenses, ranging from 2.5x to 50x. For this research, only the 10x objective lens was used to capture the images. Lenses with 2.5 and 5 times magnification were not suitable because the striations were not visible.



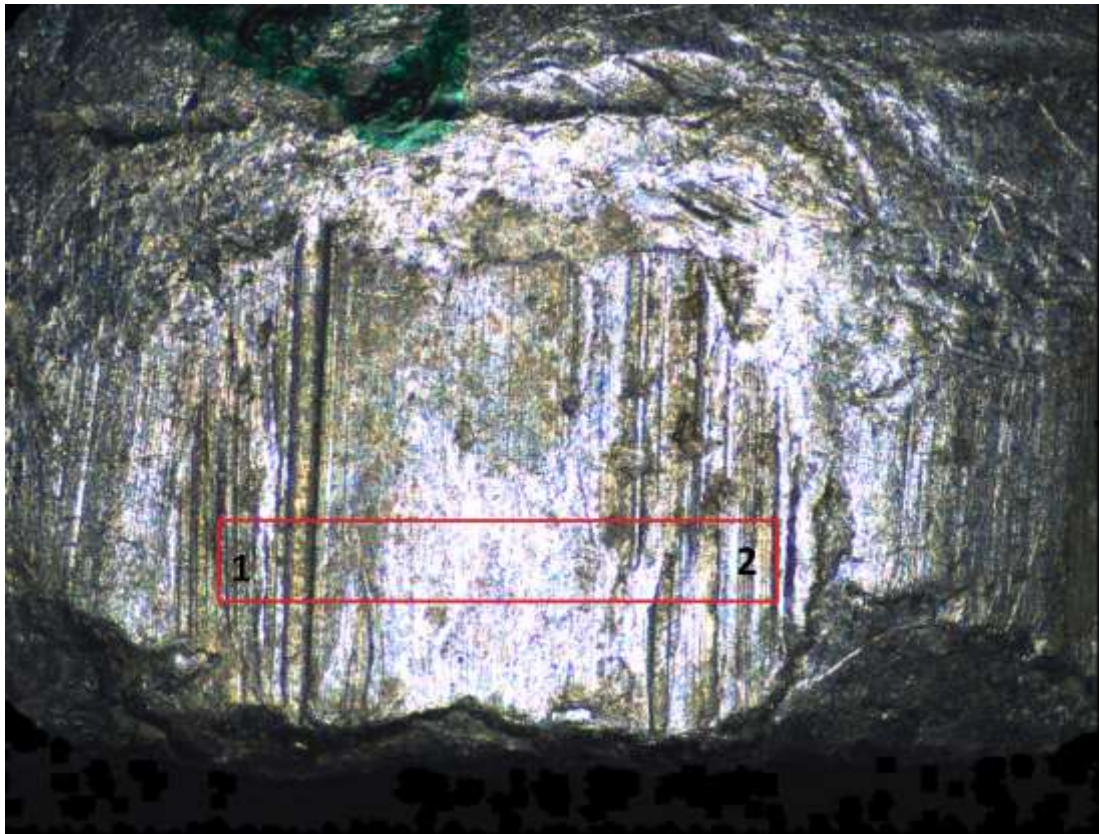
Lenses with 20 and 50 times magnification produced images which were too magnified for the whole length of the LEA to be captured. The x10 magnification lens generated the most useful images of the striations. The Alicona® microscope was calibrated by the specialist technician prior to use.

### **2.5.1 Image acquisition**

The head of the pellet was placed in the holder and attached using Blu-Tac™ so that the skirt area or the bottom most part of the pellet was oriented to face the microscope. The pellet was positioned so that the target LEA was directly below the lighting source and perpendicular to the lens of the microscope. The identification of the LEAs was initially undertaken under the supervision of an experienced ballistics expert so that these regions could be identified with confidence.

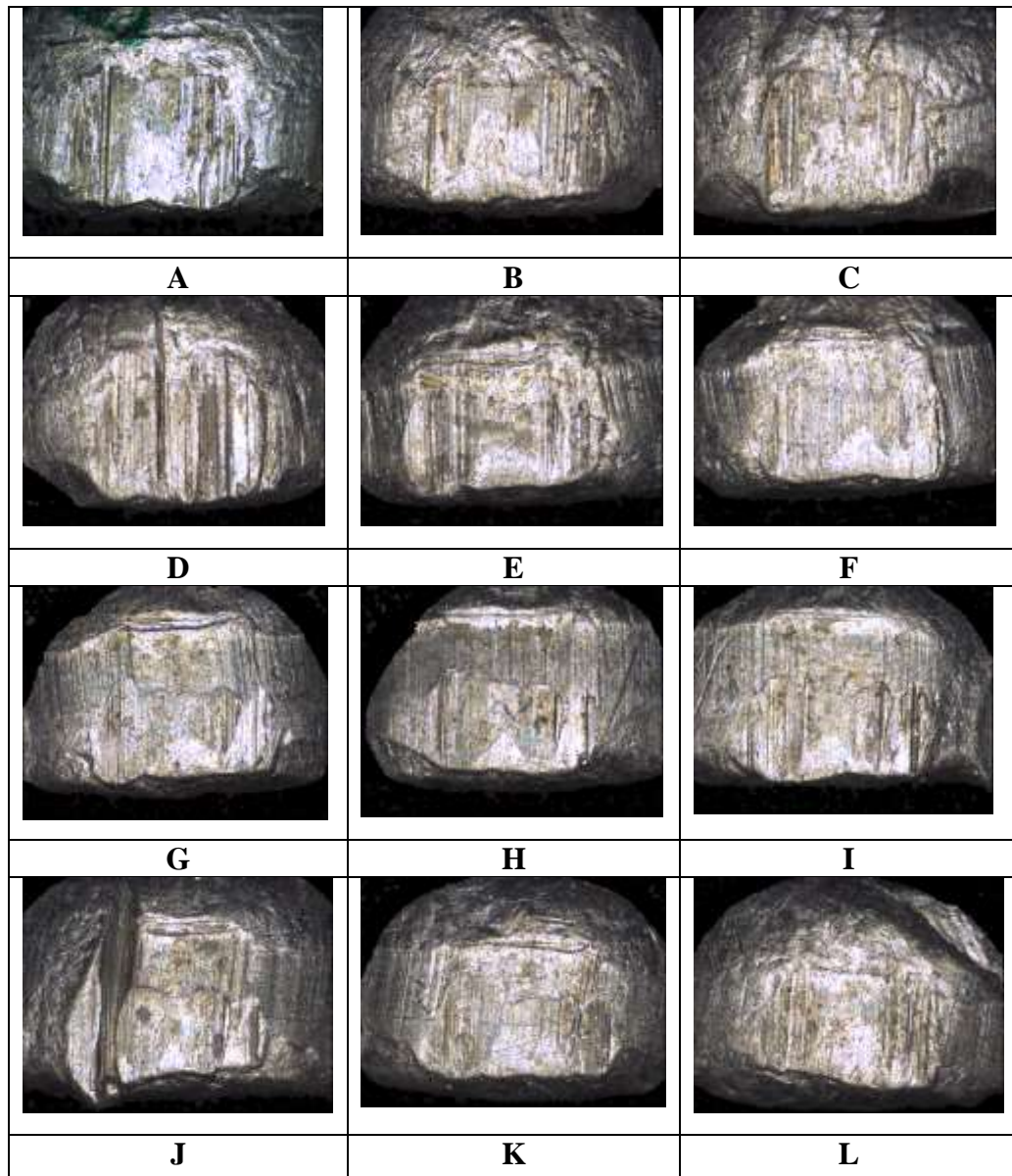
The platform holding the pellet could be moved along the x, y and z axis in order for the microscope to scan and measure the surface of the regions of interest. The image produced was in 3D format. These images were evaluated by the experienced ballistic examiner to determine the best-captured surface which contained details of the striations on the surface of the pellet. Those images were then selected to be processed and analysed.

Once the image of the striated region was captured using the microscope, a line was drawn across the LEA using the software associated with the instrument (Figure 2.9). The red box from point 1 to point 2 represents the distance of one LEA from a pellet drawn onto the image using the software.



**Figure 2.9: A 2D image generated from the Alicona® showing a LEA on a pellet. The length of the LEA is measured from 1 to 2. The green colour is from a green marker pen, as a way to mark the LEA for identification**

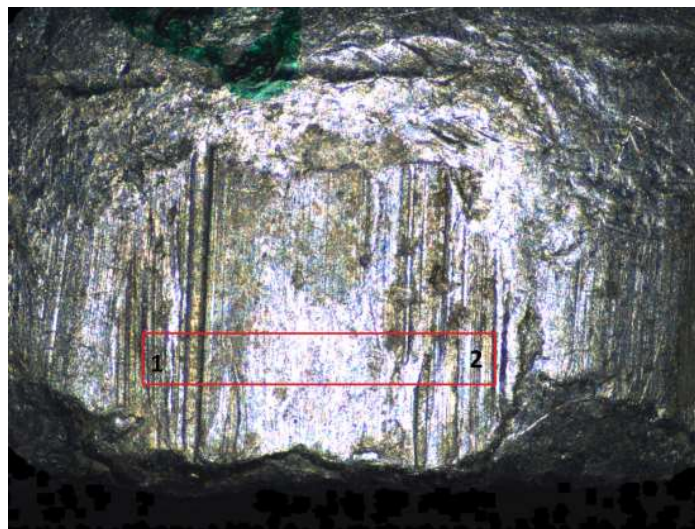
All weapons used in this study have similar class characteristics (12 lands and grooves). The LEAs are labelled A to L as suggested by the ballistic examiner, Mr Martin Connolly, a senior ballistic examiner from the Ballistic Department, Forensic Services Glasgow Laboratory, Strathclyde Police Headquarters, Glasgow, as a way to differentiate them. There is no specific nomenclature for naming the LEA. This is based on the examiner's experience. Images of the striation marks within each of the 12 LEA regions taken from pellet number 159 are presented in Figure 2.10 as an example.



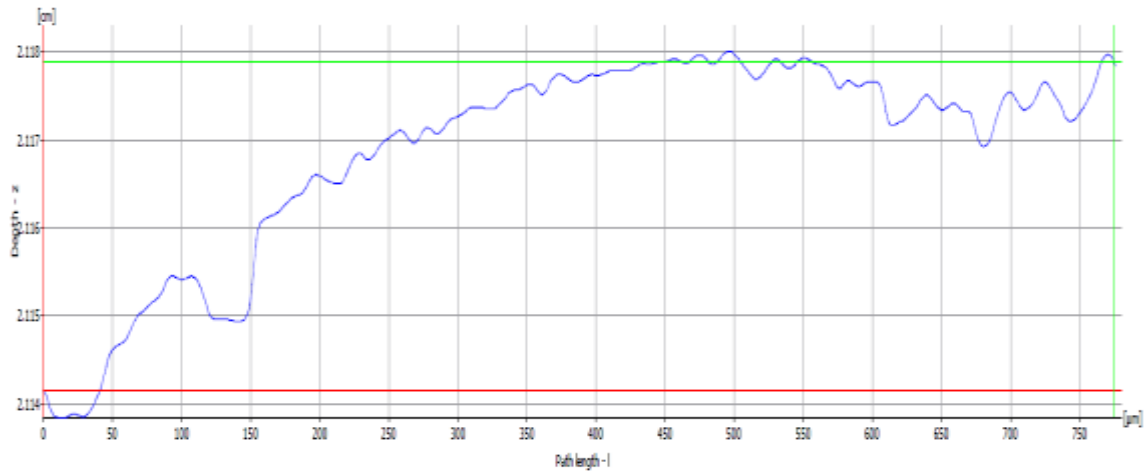
**Figure 2.10: Images of the 12 LEA regions taken from pellet number 159**

After scanning, the image of the LEA was displayed on the computer monitor. The Alicona® comes with its own software for length measurement. Primary profile measurement was selected, as recommended by the British Standards Institution [17-20]. Primary profile gives the measurement of length and depth of the LEA, as shown in Figure 2.12.

The borders of the LEA were selected and the Alicona® software transformed the LEA striation image such that the surface topography of the pellet was displayed as a graph post measurement, as shown in Figures 2.11 and 2.12. This surface measurement graph contains numerical values which indicate the depth or the surface topography of the striation. Each point in the graph corresponds to a valley or peak of the pellet surface. The numerical values were then selected for image transformation using Matlab® R2014a with PLS\_Toolbox® software.



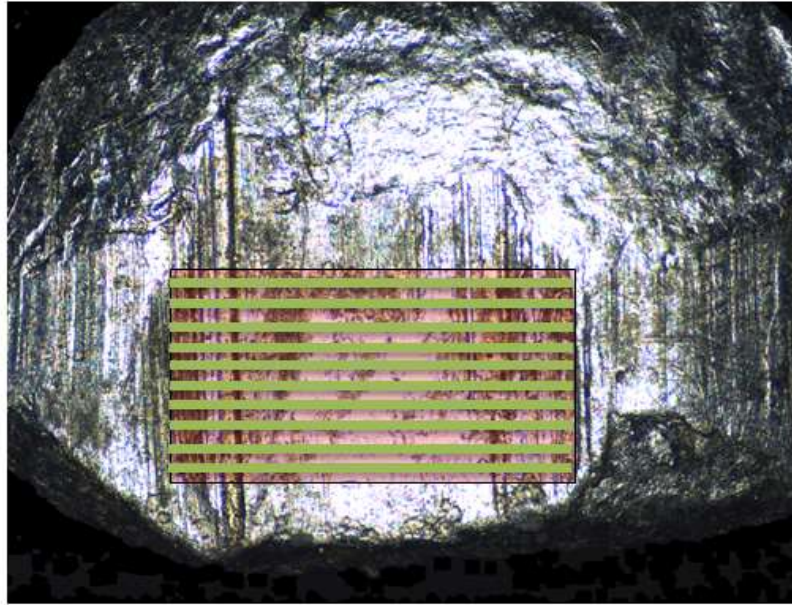
**Figure 2.11: Surface topography measurement of LEA A using Alicona® software from point 1 to point 2**



**Figure 2.12: Example graph of surface topography of LEA A, along the length of the LEA**

### **2.5.2 Measurement repeatability**

The repeatability of the topography of the striation marks within the LEA and that of the mathematical data processing was assessed by taking 10 measurements across each of the 12 LEAs across a range of pellets (1 pellet was chosen for 1 LEA) as illustrated in Figure 2.13. Table 2.2 shows the chosen pellet for the repeatability measurement.



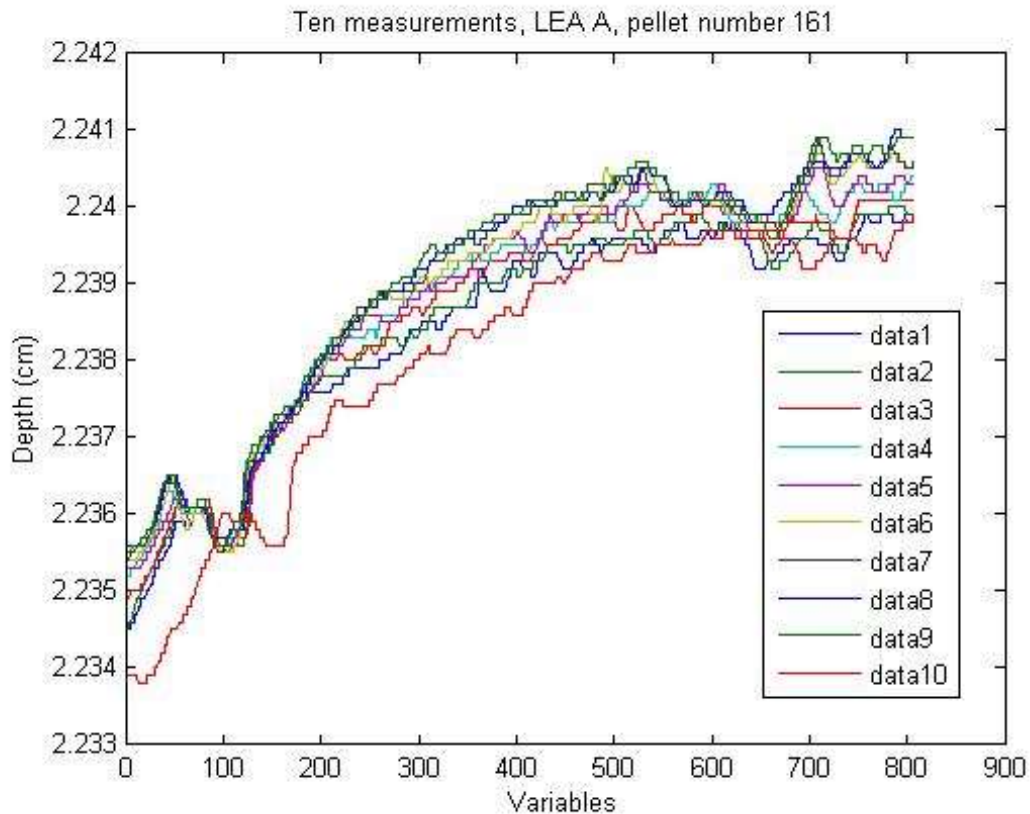
**Figure 2.13: Ten measurements of the LEA length were taken at different levels, from one border to the other, as depicted with the green lines. The red boxes indicate the borders of the LEAs. This is LEA A from pellet number 161**

**Table 2.2: Pellets chosen for repetitive LEA analysis for measurement validation**

LEA	Pellet examined	LEA	Pellet examined
A	161	G	198
B	161	H	161
C	185	I	163
D	186	J	192
E	181	K	198
F	190	L	195

In each case the 2D LEA topographical maps were generated and compared. Matlab® R2014a with PLS\_Toolbox® (MathWork Inc.) was used to create algorithms and produce the numerical data for data analysis and visualization of the contour maps produced from the LEAs [21, 22]. PLS\_Toolbox® is a software package for Matlab® developed by Eigenvector Research Inc. [23] and provides

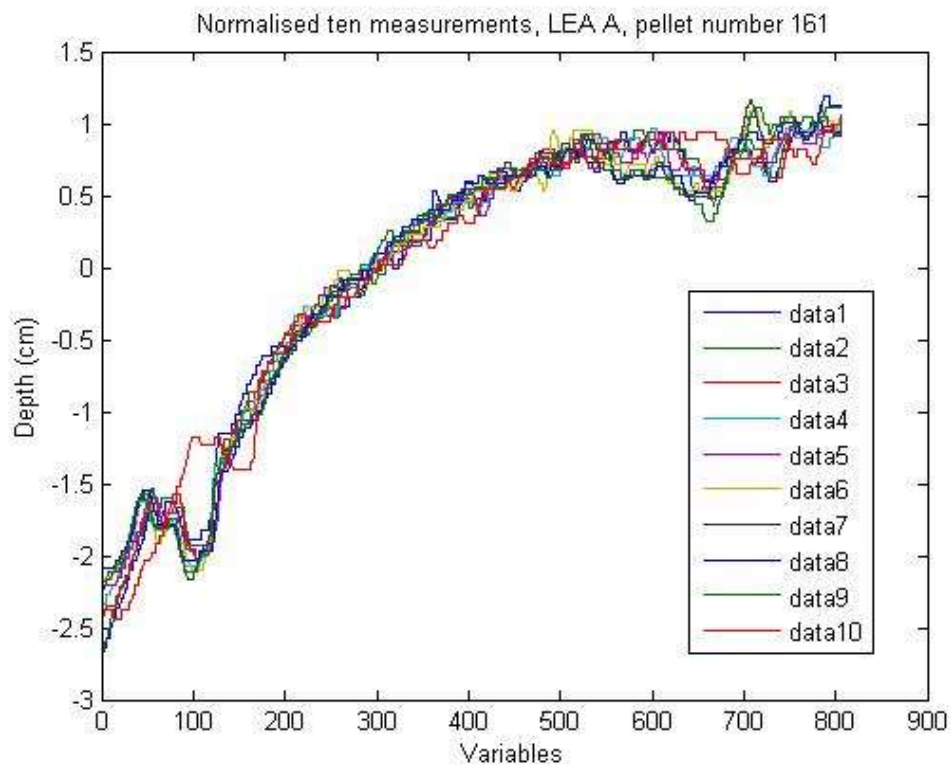
advanced analysis tools for use with Matlab® to present data in graphic form. PLS\_Toolbox® contains data exploration and pattern recognition techniques such as the PCA, HCA and LDA which was used in the interpretation of the data. Figure 2.14 shows the overlaid ten surface measurements made at different levels of LEA A, on pellet 161.



**Figure 2.14: Ten surface measurements made at different levels of LEA A from pellet number 161. The graph shows that all the measurements are similar to each other irrespective of where across the LEA they were taken from. Variables are the points measured automatically by Alicona®. For example, at variable 100, the Alicona® measures the depth of the striation of the LEA**

These numerical values were then mean-centered and normalised. The data is stored in a standard form, an  $n \times p$  array, where  $p$  is the number of dimensions in the data set and  $n$  is the number of data points in the array. The data has mean value. Mean-

centered value is from subtracting off the mean from each column. The normalised data is depicted in Figure 2.15.



**Figure 2.15: This is the normalised and mean centered data from Figure 2.14. All of the curves except measurement 10 are similar to each other. This shows that length of the LEA can be measured on any level and it shows repeatability of the measurement**

Figures 2.16 to 2.26 illustrate the normalised data for the remaining eleven striation regions, n=10 measurements in each case.



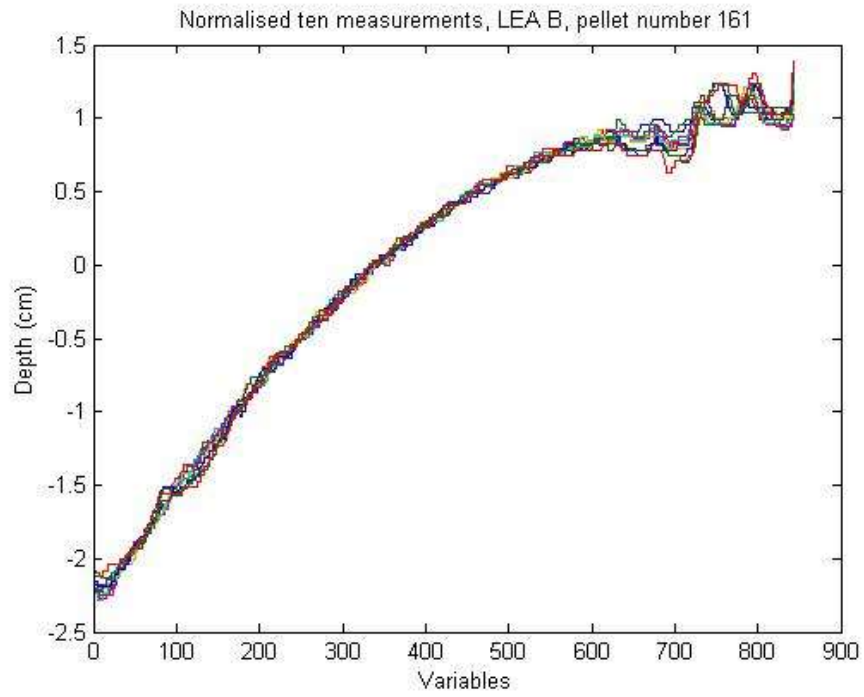


Figure 2.16: Normalised data of ten surface measurements for LEA B from pellet number 161

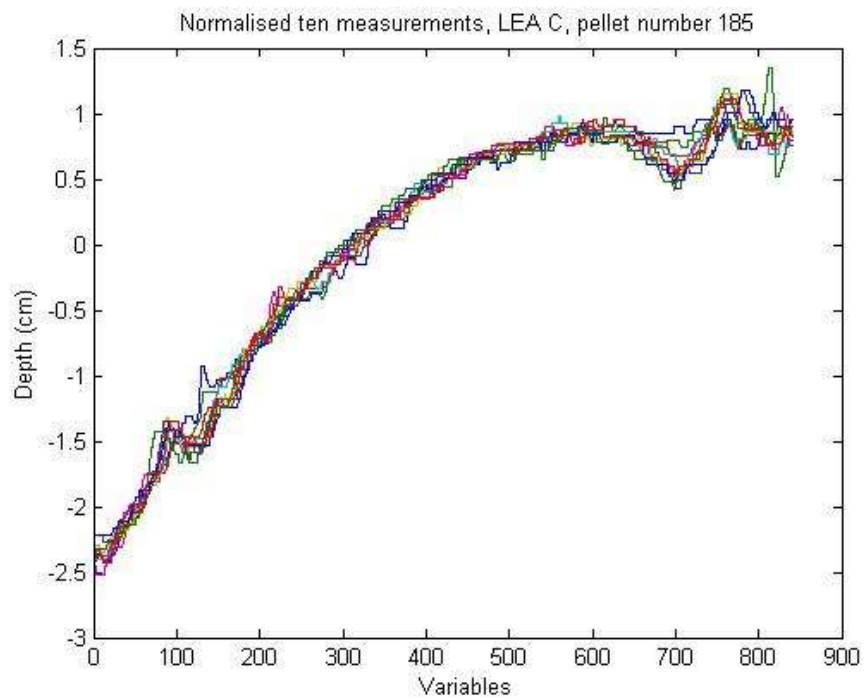
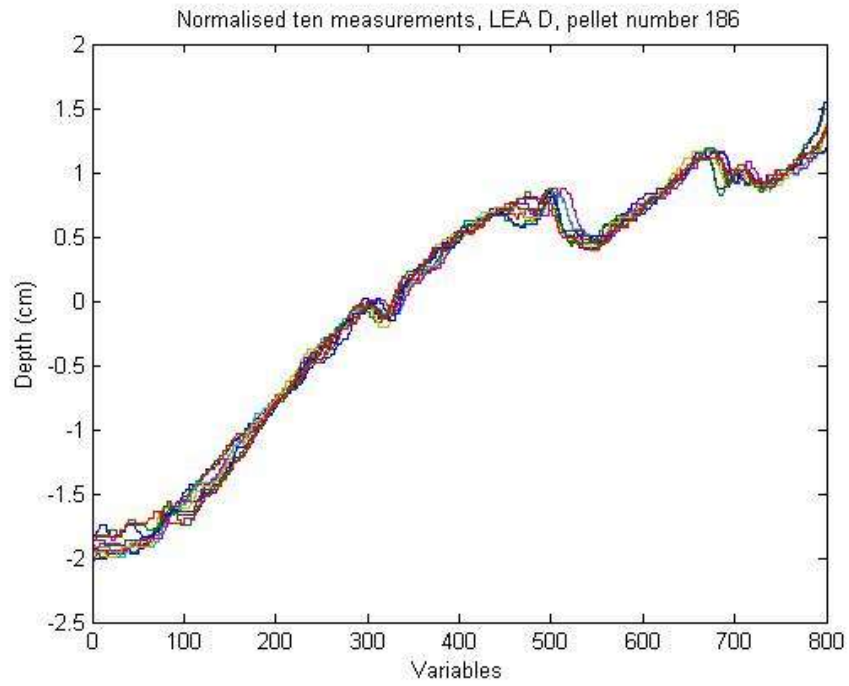
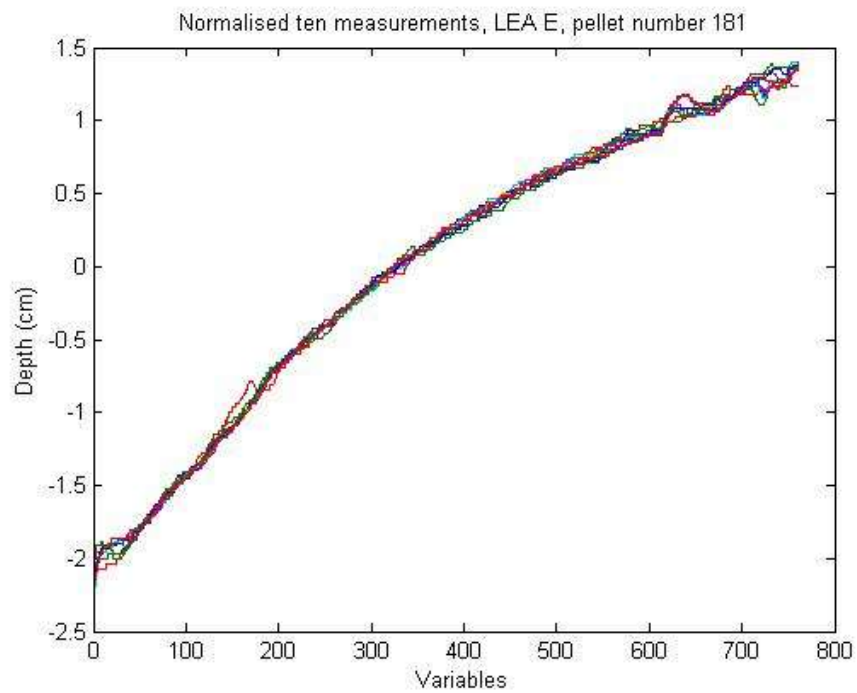


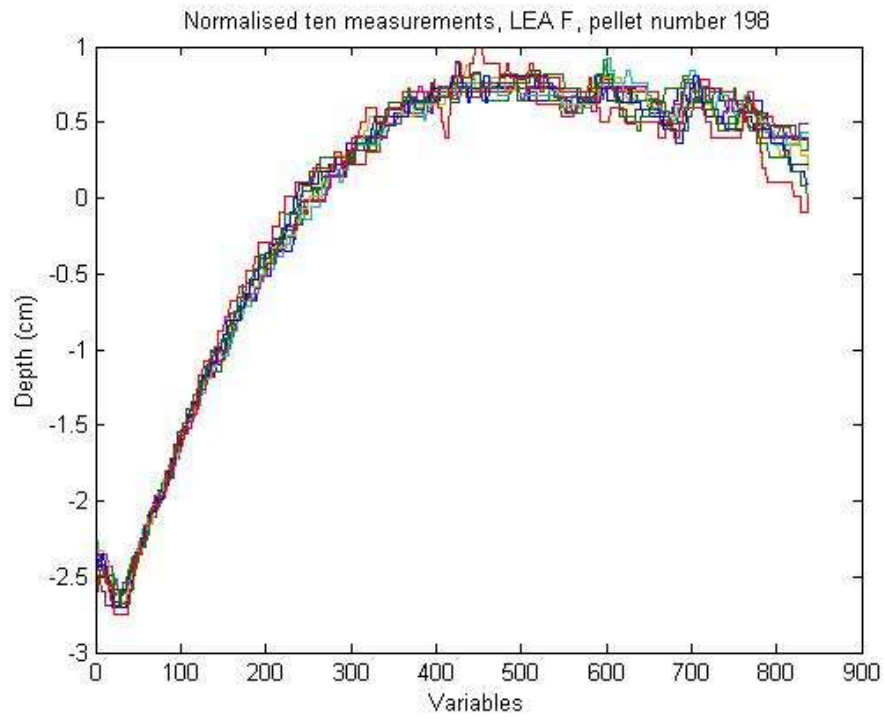
Figure 2.17: Normalised data of ten surface measurements for LEA C from pellet number 185



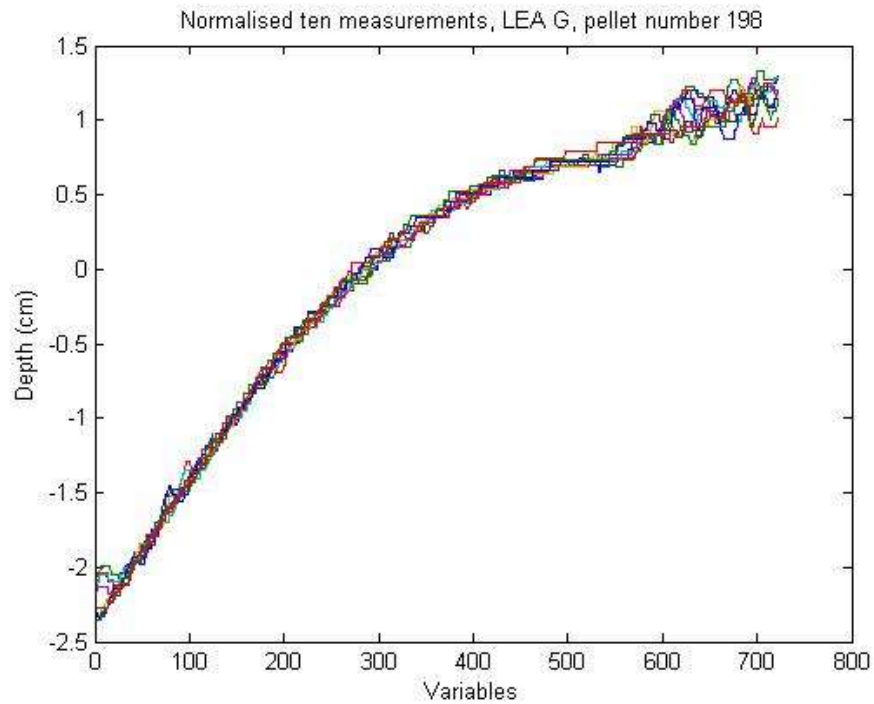
**Figure 2.18:** Normalised data of ten surface measurements for LEA D from pellet number 186



**Figure 2.19:** Normalised data of ten surface measurements for LEA E from pellet number 181



**Figure 2.20: Normalised data of ten surface measurements for LEA F from pellet number 190**



**Figure 2.21: Normalised data of ten surface measurements for LEA G from pellet number 198**

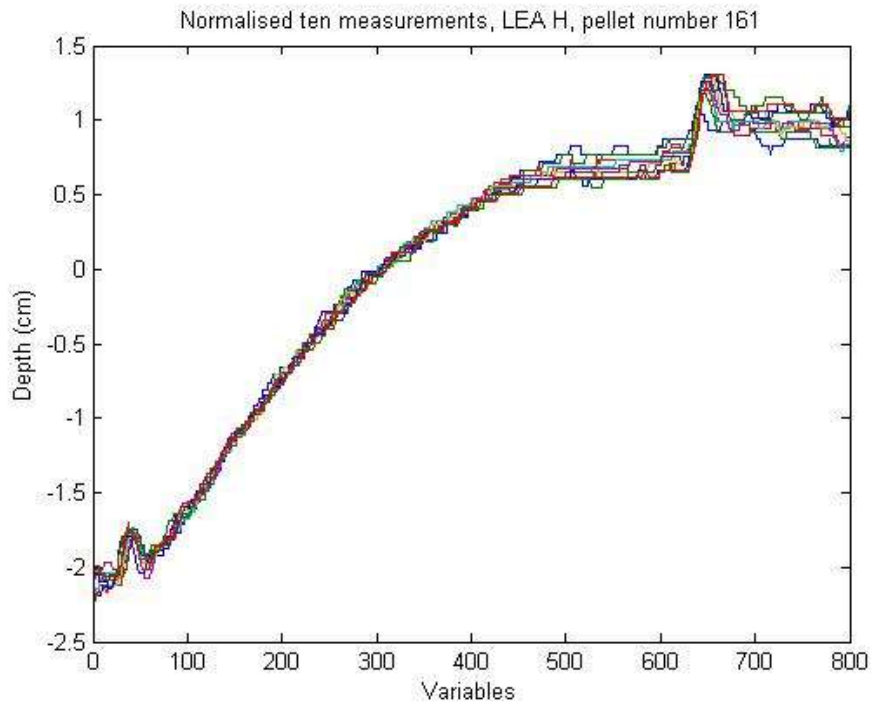


Figure 2.22: Normalised data of ten surface measurements for LEA H from pellet number 161

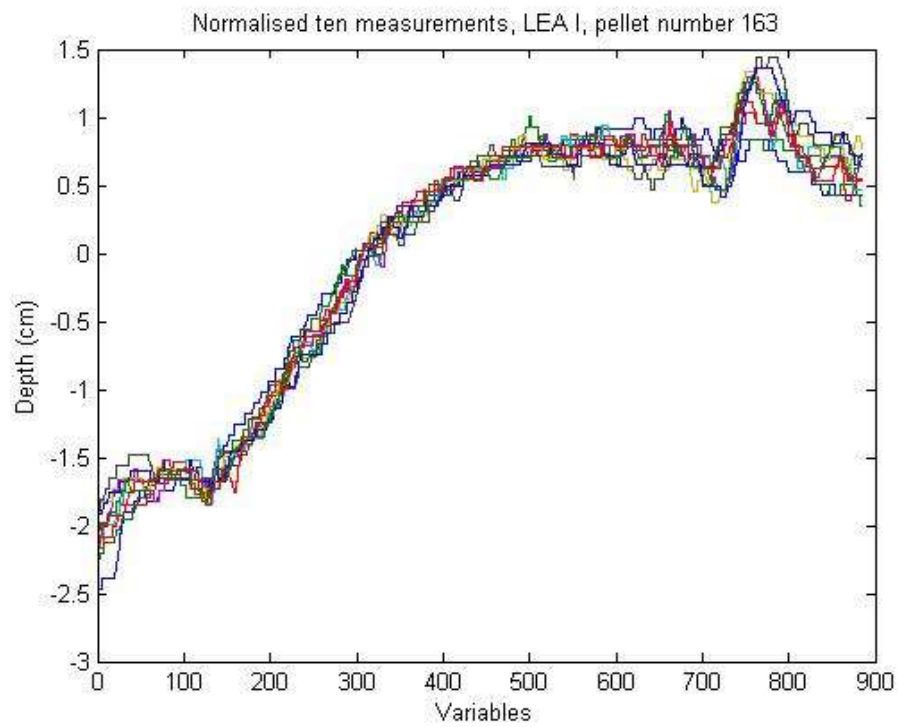
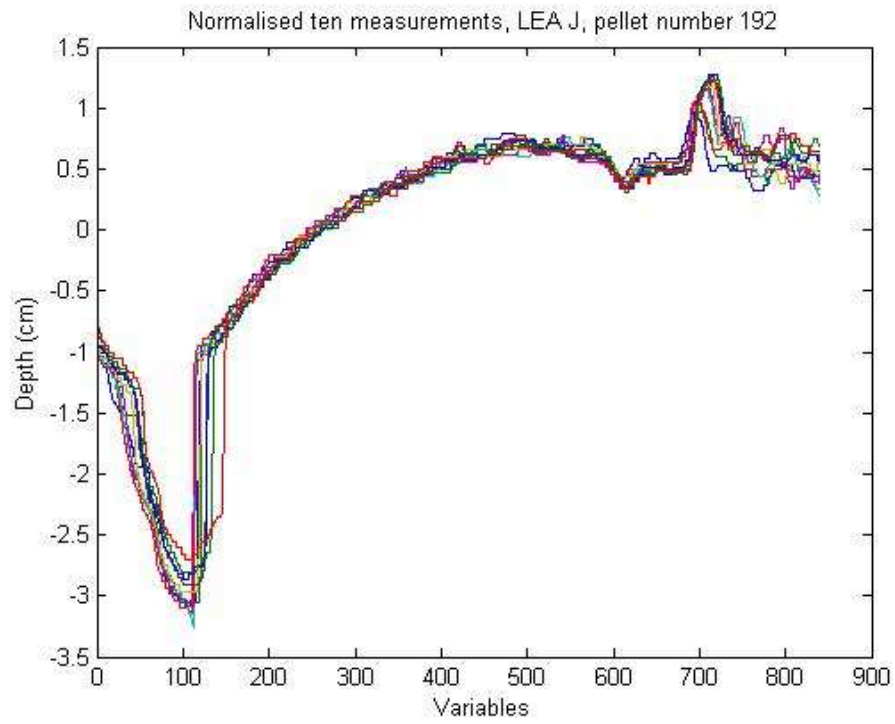
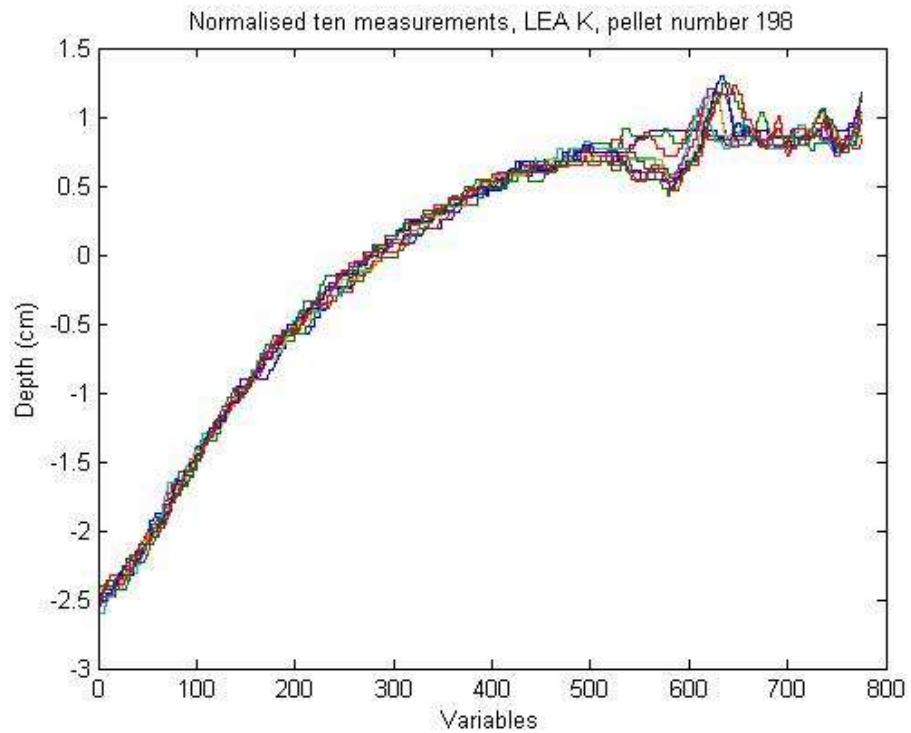


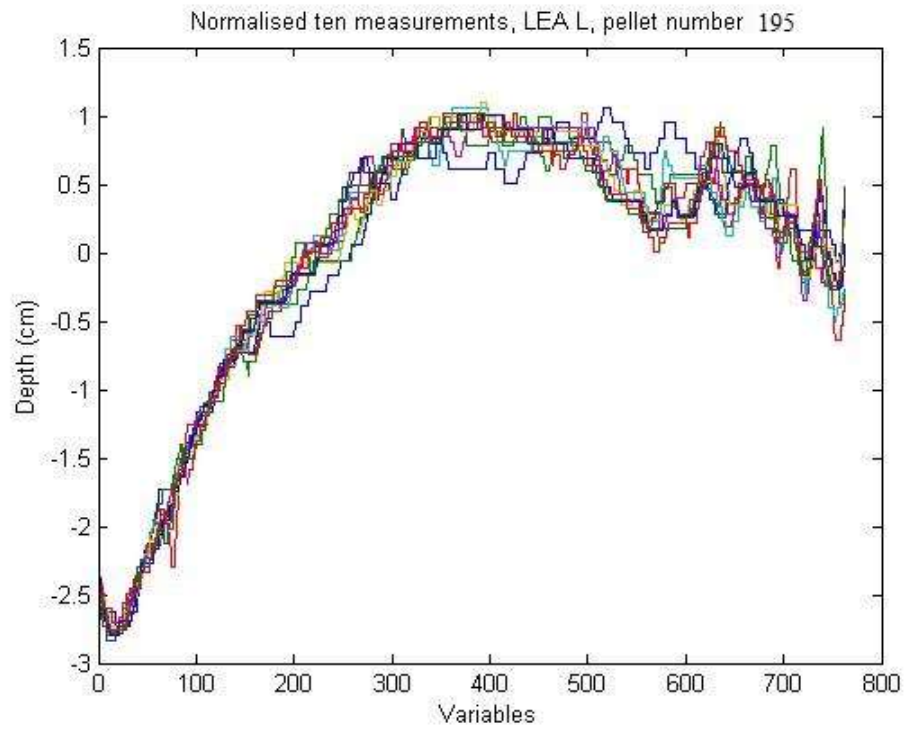
Figure 2.23: Normalised data of ten surface measurements for LEA I from pellet number 163



**Figure 2.24: Normalised data of ten surface measurements for LEA J from pellet number 192**



**Figure 2.25: Normalised data of ten surface measurements for LEA K from pellet number 198**



**Figure 2.26: Normalised data of ten surface measurements for LEA L from pellet number 195**

These results have demonstrated that the method of image acquisition and normalisation of data produces repeatable results across the same region on the same pellet. The analysis furthermore, demonstrates that the LEAs are different across the 12 regions of the pellet and this is presented in Figure 2.27.

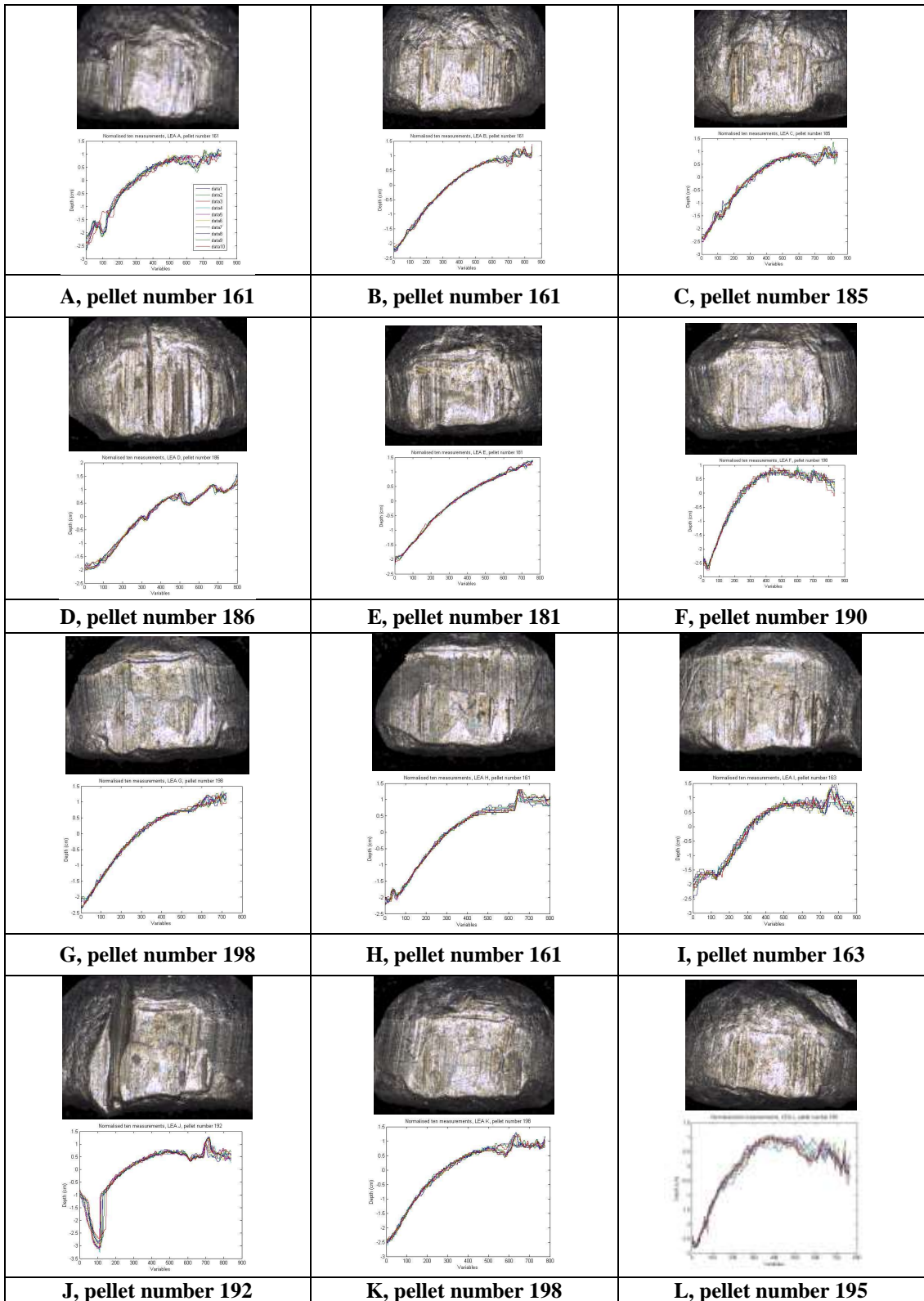


Figure 2.27: Normalised data of ten surface measurements for LEA A-L

As a consequence of this measurement validation exercise which demonstrated the repeatability of measurement across the LEA, three measurements across each LEA of each pellet were taken for all subsequent measurements which reflected each LEA examined.

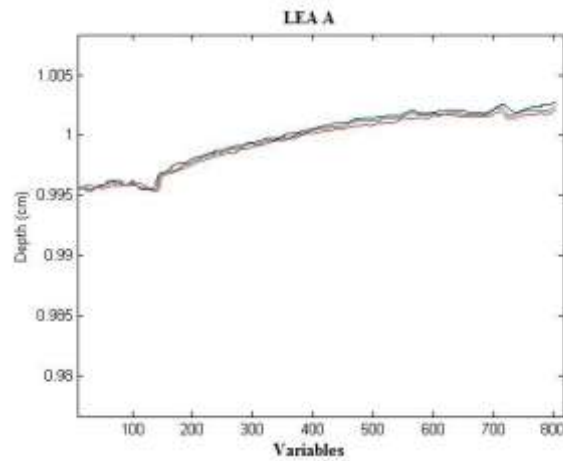
### **2.5.3 Data transformation and image alignment**

All numerical data selected from the topographical graphs required further data processing so that analysis and comparisons could be undertaken. This was carried out using a curve flattening script followed by an image alignment script. The resultant data set was then subjected to the PCA, HCA and LDA.

### **2.5.4 Curve flattening**

Pre-processing data is required for this study to remove inaccuracy or noisy (from measurement error) and inconsistency (due to variation instrumental artefacts), in order to have higher data quality [24-27]. Raw data from this study is pre-processed using polynomial curve fit to remove the curve and a cross correlation function for data alignment to smooth the noisy data and resolve the inconsistencies. The process is explained in details from Figure 2.28 to Figure 2.33. It starts with Figure 2.28, a close up graph for a set of three measurements of LEA A on the same pellet where the topographical maps are aligned.

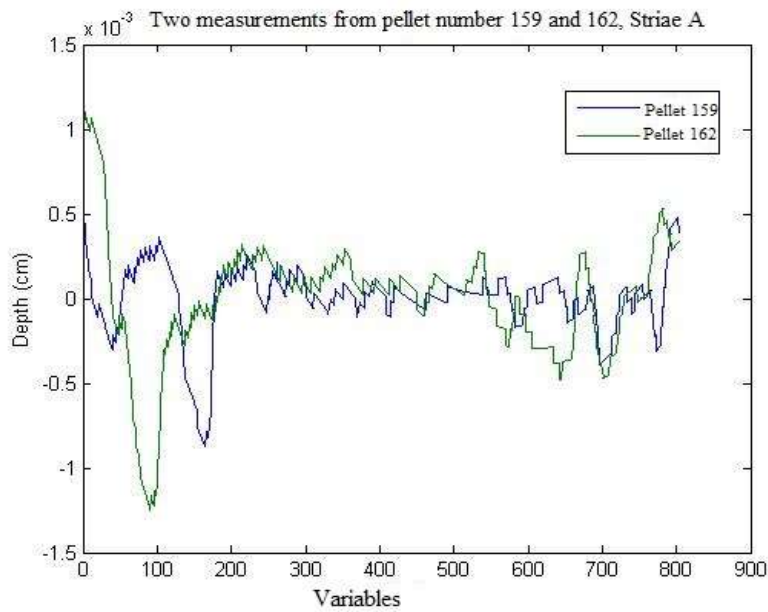




**Figure 2.28:** This is a close up of one of the three repeat surface measurements for LEA A

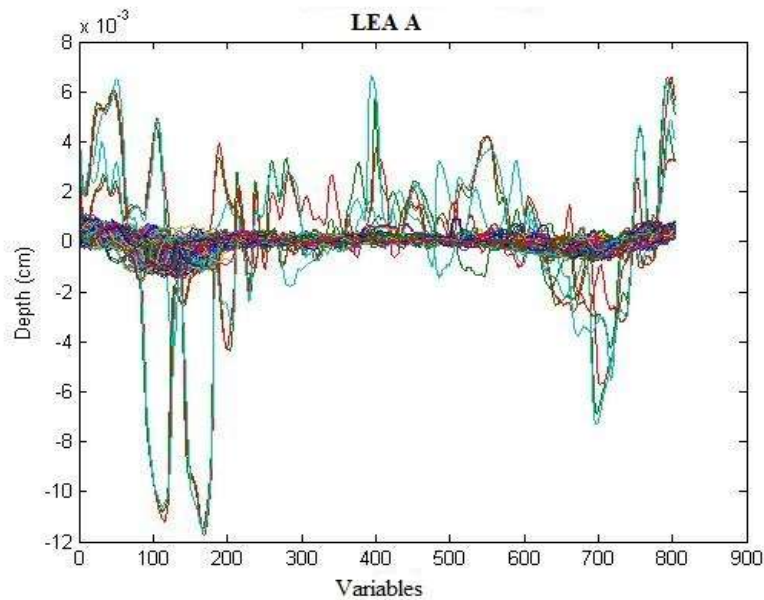
A curve removal script from Matlab® was used to flatten the curve so that all of the data from repetitive measurements ( $n=3$ ) across each LEA on each pellet could be aligned.

Figure 2.29 is the close up of two measurements from two pellets after the curve was removed. There are two sharp features from pellet 159 and pellet 162. For pellet 159, the valley feature is between variable number 100 and 200; for pellet 162, the valley feature is just before variable number 100. These sharp features are similar but mismatched. A cross correlation function was used to align both features. The scripts from Matlab® for data loading, curve removal and data alignment are included as Appendix 1 to 3.



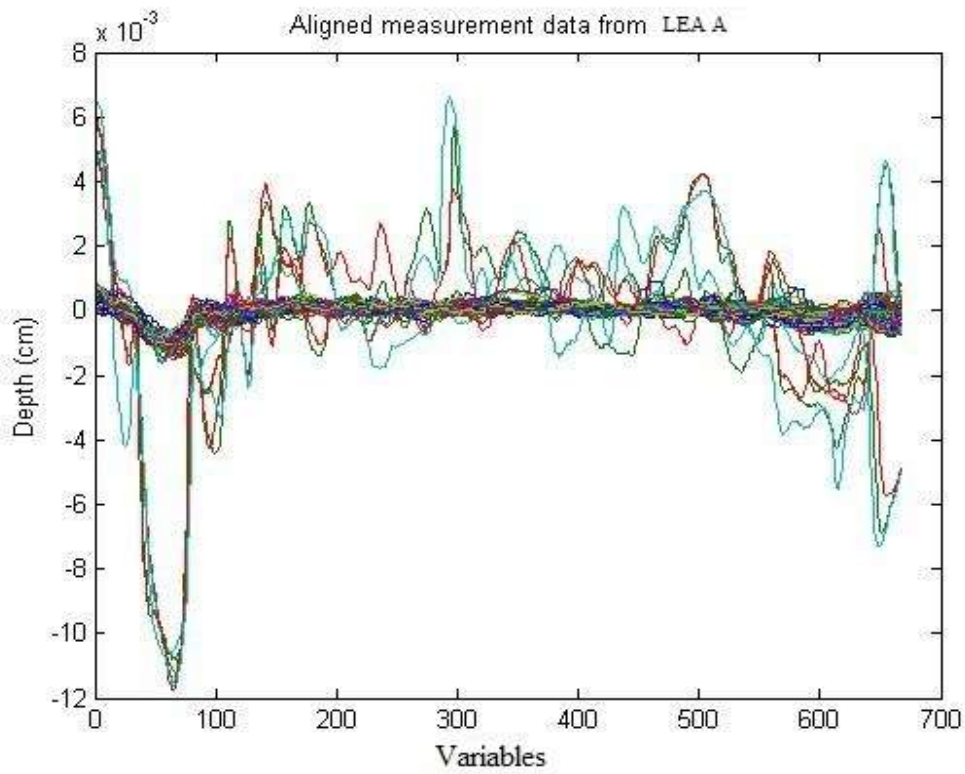
**Figure 2.29:** This is an example of polynomial curve fitting of measurements of LEAs from two pellets (pellet 159 and pellet 162), LEA A. Both graphs are similar; however, alignment is needed before comparison of the striated marks is effective

Figure 2.30 illustrate this process applied across 3 repetitive measurements of LEA A measured for 50 pellets.



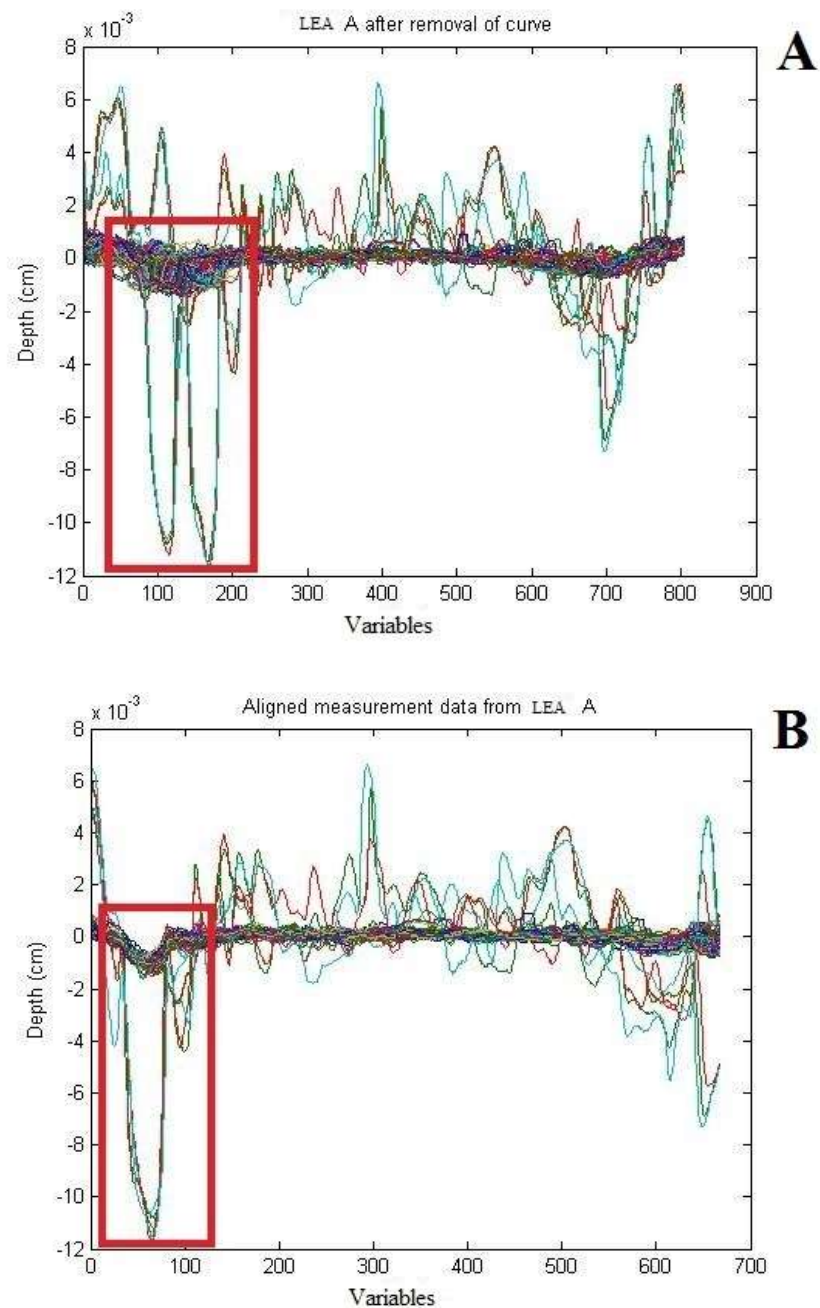
**Figure 2.30:** This is an example of removal of curve from LEA A (150 measurements of striations – three repetitive measurements of the region across 50 pellets). The original surface topography, as in Figure 2.12, was fitted with a polynomial curve before alignment

Figure 2.31 shows the alignment of all 150 measurements for LEA A (3 repetitive measurements of LEA A across 50 separate pellets) after the alignment script was applied to data in Figure 2.30.



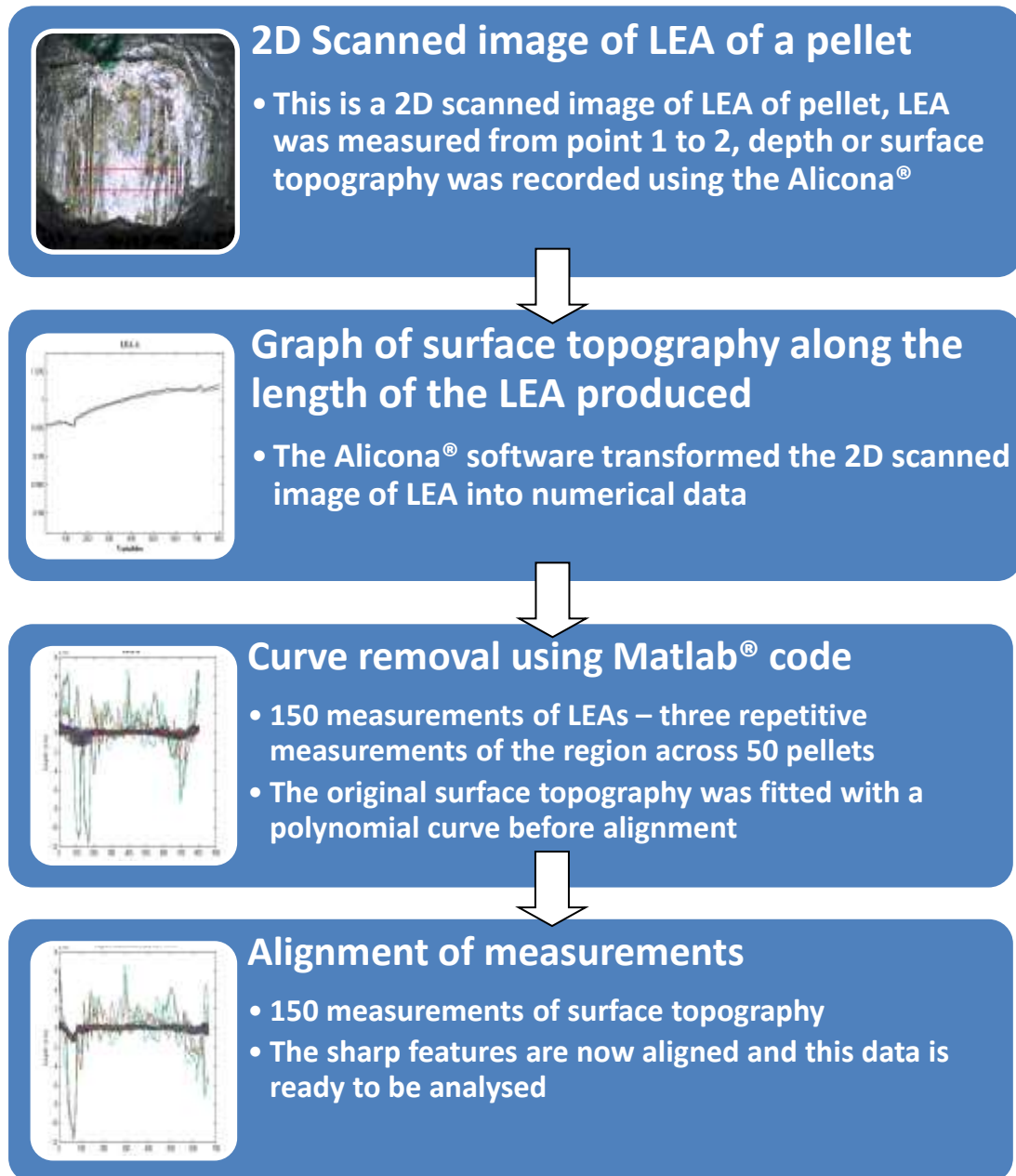
**Figure 2.31: Aligned measurements of LEA A (150 measurements of surface topography). The sharp features are now aligned and this data is ready to be analysed**

The difference between the unaligned data in Figure 2.30 and aligned data in Figure 2.31 are highlighted in Figure 2.32 with the misaligned graph labelled (A) and the aligned one (B). The cross correlation function moves the signals on top of each other facilitating the analysis of correlation between groups of data.



**Figure 2.32: The sharp features highlighted by the red rectangle before (A) and after (B) alignment using the cross correlation function from Matlab®**

In summary, the scanned images of the LEAs from the pellets were transformed into a set of numerical data. This data were then pre-processed by removing the curve followed by data aligning using Matlab®. The aligned data were then analysed using the PCA, HCA and LDA. Figure 2.33 presents a flowchart of the whole process.



**Figure 2.33: Flowchart of data acquisition and pre-processed data with curve removal and data alignment**

## 2.6 Analysis of data

Principal Component Analysis was used to further analyse the correlation of each set of striations, as suggested by previous researchers [28, 29]. After the alignment process, the data was mean-centred by subtracting the mean from the processed data. The data was then analysed using the PCA, HCA and LDA options in Matlab®.

## 2.7 Chronograph Studies – calculation of kinetic energy

The kinetic energy of the air pistol was measured using the chronograph system as described in section 2.4.1. The results are derived from the series of test shootings at the high velocity setting and are presented in Table 2.3.

**Table 2.3: Kinetic energy of air pistol, HW 45 Weihrauch, with high velocity setting**

Date	Average KE (foot pounds)	Mean Velocity(ft/s)	Std Dev	RSD (%)
April 2012	4.855	518.015	5.216	1.01
April 2013	4.269	481.518	6.501	1.35
May 2013	4.188	477.272	8.170	1.71
September 2013	4.115	472.722	7.018	1.48

The HW 45 Weihrauch has a kinetic energy of less than 6 foot pounds which is the value at which a Firearms Certificate is not required.

The kinetic energy of the air pistol was calculated using two different chronographic system. The first chronograph was used from April 2012 to May 2013 and the

portable chronograph was used for the September 2013 firing tests. Based on Table 2.3, the difference between the average kinetic energy in May 2013 and September 2013 was 0.073 foot pounds and the mean velocity decreased gradually from 518.015 ft/s to 472.722 ft/s.

The kinetic energy was noticed to have reduced gradually during use over a period of 17 months and this can be as a result of a number of contributing factors.

- (1) The air pistol is a spring-piston air weapon and the kinetic energy may reduce as a result of wear and tear of the spring.
- (2) The HW 45 was deliberately not cleaned during the study as this was one of the aspects which was of interest. Pellets are made of mainly lead, and normal wear and tear may contribute to lead build up in the barrel. Lead debris increases the friction experienced by subsequent pellets in their interaction with the barrel on firing slowing the pellets down and decreasing kinetic energy. A build-up of dirt on the piston surface may also reduce the air pressure pushed towards the pellet held in the barrel during firing. Di Maio suggested that low-powered springs made of cheaper material may reduce the performance of air weapon [6].

All these factors can contribute to reducing the kinetic energy of the air pistol over time. The air pistol was bought new for this study and record of every shootings was available. As stated before, the air rifles used for this study were a number of years old and there was no record of the number of air pellets the weapons may have fired,

the purchase invoice or a cleaning log available prior to their use. The reference (initial) kinetic energy when the rifles were first bought was not available hence the kinetic energy for them are not measured. However, the manufacturers stated that, the air rifles 'are set to between 10.5-11.6 foot pounds in the .177 version' [7]. The kinetic energy of the air rifles is less than 12 foot pounds however it is larger than the kinetic energy of the air pistol. The effect of larger kinetic energy and longer barrel of the air rifles is discussed in Chapter 5.

## **2.8 Conclusions**

The purpose of this study is to explore the potential to generate an objective method of assessing the striated marks generated when a projectile is fired from a weapon. Methods of examination of surface topography, adapted from [30-37] were used. A 3D optical microscope capable of scanning and transforming the image data into numerical value for further pre-processing was used. Mathematical processing was undertaken using Matlab® [28].

The method of scanning the pellets, image transformation and data alignment were demonstrated to be repeatable across 10 measurements within each of the 12 striated regions generated on the fired projectiles.

The air pistol and air rifles used in this study were deliberately not cleaned during the research work to explore whether this factor would have an effect on the final striated marks produced. Firing an air pistol repetitively without cleaning of the



weapon appears to reduce the kinetic energy of the air pistol gradually over a period of time.

## 2.9 References

1. Biasotti, A., *A Statistical Study of The Individual Characteristics Of Fired Bullets*. Forensic Sci, 1959. 4(1): p. 34-50.
2. Nichols, R.G., *Firearm and toolmark identification criteria: A review of the literature*. J. Forensic Sci, 1997. 42(3): p. 466-474.
3. Miller, J., *Criteria for identification of tollmarks*. AFTE, 1998. 30(1): p. 15-61.
4. Biasotti, A.A., *The Principles Of Evidence Evaluation As Applied To Firearms And Tool Mark Identification*. 1964. 9(4).
5. Wallace, J.S., *Chemical analysis of firearms, ammunition, and gunshot residue*. 2008: Boca Raton : CRC Press.
6. Di Maio, V.J.M., *Gunshot wounds : practical aspects of firearms, ballistics, and forensic techniques*. 1999: Boca Raton : CRC Press.
7. Heapy, T., *Average Kinetic Energy for Air Rifle*. 2016: Email to Author.
8. Warlow, T.A., *Firearms, the law, and forensic ballistics*, ed. MyiLibrary. 2005: Boca Raton, Fla. : CRC Press.
9. Rao, D., Singh, H., Mowatt, J., *Effects of human decomposition on test fired bullet – An experimental research*. Egyptian Journal of Forensic Sciences, 2016. 6(1): p. 17-21.
10. Air, P. *Weihrauch Guns*. 2012 [cited 2014; Available from: <http://www.pyramydair.com/manual/hw45>].
11. Weihrauch, H.-H. and Weihrauch, S. *Weihrauch Sport - Air Pistols*. 2012 [cited [2014]; Available from: [http://www.weihrauch-sport.de/seiten/englisch/luftpistolen/e\\_luftpistolen.html#TD\\_Luftpistolen\\_d](http://www.weihrauch-sport.de/seiten/englisch/luftpistolen/e_luftpistolen.html#TD_Luftpistolen_d)].
12. Airgun, B.P. *Beeman precision airguns spring-piston manual pellets and pistons*. 2004 [cited 2013; Available from: [http://www.afpmb.org/sites/default/files/pubs/standardlists/equipment/pdfs/1005-01-544-1044\\_manual.pdf](http://www.afpmb.org/sites/default/files/pubs/standardlists/equipment/pdfs/1005-01-544-1044_manual.pdf)].
13. Saltzman, B. *American Airguns*. 2006 [cited 2014; Available from: [http://www.airguns.net/general\\_airgun\\_types.php](http://www.airguns.net/general_airgun_types.php)].
14. Gaylor, T., *The right pellet makes a difference*. Airgun Revue #1. Vol. #1. 1997: GAPP, Inc.
15. Recreational Software, I. *CED M2 Optical Chronograph*. 2013 [cited 2013; Available from: <http://www.shootingsoftware.com/chronographs.htm>].
16. Alicona. *Alicona Infinite Focus*. 2013 [cited 2014; Available from: <http://www.aliconaco.uk/home/products/infinitefocus.html>].
17. Tdw, *Geometrical product specification (GPS). Surface texture. Profile method. Motif parameters*. Geometrische Produktspezifikationen (GPS).

- Oberflächenbeschaffenheit. Tastschnittverfahren. Motifkenngrößen. 1997.
18. Tdw, *Geometric product specification (GPS). Surface texture. Profile method: Rules and procedures for the assessment of surface texture.* Geometrische Produktspezifikation (GPS). Oberflaechenbeschaffenheit. Tastschnittverfahren. Regeln und Verfahren fuer die Beurteilung der Oberflaechenbeschaffenheit. 1997.
  19. Tdw, *Geometrical product specification (GPS). Surface texture: Profile method. Terms, definitions and surface texture parameters.* Geometrische Produktspezifikation (GPS). Oberflächenbeschaffenheit. Tastschnittverfahren. Benennungen, Definitionen und Kenngrößen der Oberflächenbeschaffenheit. 2000.
  20. Tdw, *Geometrical product specifications (GPS). Surface texture. Areal. Terms, definitions and surface texture parameters.* Geometrische Produktspezifikation (GPS). Oberflächenbeschaffenheit. Flächenhaft. Begriffe und Oberflächen-Kenngrößen. 2012.
  21. MathWorks. *Getting Started with MATLAB.* 2011 [cited 2014; Available from: <https://moss.strath.ac.uk/developmentandtraining/resourcecentre/Resource%20Library/Getting%20Started%20with%20MATLAB.pdf>.
  22. MathWorks. *MATLAB, The Language of Technical Computing.* 2013 [cited 2014; Available from: <http://www.mathworks.co.uk/products/matlab/>.
  23. Eigenvector Research, I. *PLS\_Toolbox.* 2006 [cited 2015; Available from: [http://www.eigenvector.com/software/pls\\_toolbox.htm](http://www.eigenvector.com/software/pls_toolbox.htm).
  24. Rinnan, Å., Berg, Frans van den., Engelsen, S. B., *Review of the most common pre-processing techniques for near-infrared spectra.* TrAC Trends in Analytical Chemistry, 2009. 28(10): p. 1201-1222.
  25. Bertinetto, C.G., Vuorinen, T., *Influence of pre-processing and distance on spectral classification: A simulation study.* Vibrational Spectroscopy, 2014. 74: p. 110-119.
  26. Han, J., Kamber, M., Pei, J., 3 - *Data Preprocessing*, in *Data Mining (Third Edition)*. 2012, Morgan Kaufmann: Boston. p. 83-124.
  27. Rodionova, O.Y., Pomerantsev, A. L., *Chemometrics: achievements and prospects.* Russian Chemical Reviews, 2006. 75(4): p. 271.
  28. Riva, F. and Champod, C., *Automatic Comparison and Evaluation of Impressions Left by a Firearm on Fired Cartridge Cases.* Journal of Forensic Sciences, 2014. 59(3): p. 637-647.
  29. Brereton, R.G., *Chemometrics : data analysis for the laboratory and chemical plant.* 2002: New York : J. Wiley.
  30. Breitmeier, U. and Schmid, H., *Lasercomp: A surface measurement system for forensic applications.* Forensic Science International, 1997. 89(1): p. 1-13.
  31. Bonfanti, M.S. and Ghauharali, R.I., *Visualisation by confocal microscopy of traces on bullets and cartridge cases.* Science & Justice, 2000. 40(4): p. 241-256.
  32. Li, D., *Ballistics Projectile Image Analysis for Firearm Identification.* IEEE Transactions On Image Processing, 2006. 15(10): p. 2857-2865.

33. Senin, N., Groppetti, R., Garofano, L., Fratini, P. and Pierni, M., *Three-dimensional surface topography acquisition and analysis for firearm identification*. J. Forensic Sci., 2006. 51(2): p. 282-295.
34. Xie, F., Xiao, S., Blunt, L., Zeng, W. and Jiang, X., *Automated bullet-identification system based on surface topography techniques*. Wear, 2009. 266(5): p. 518–522.
35. Gambino, C., McLaughlin, P., Kuo, L., Kammerman, F., Shenkin, P., Diaczuk, P., Petraco, N., Hamby, J. and Petraco, N.D.K., *Forensic Surface Metrology: Tool Mark Evidence*. Scanning, 2011. 33(5): p. 272–278.
36. Song, J., Chu, W., Vorburger, T.V., Thompson, R., Renegar, T.B., Zheng, A., Yen, J., Silver, R. and Ols, M., *Development of ballistics identification-from image comparison to topography measurement in surface metrology*. Meas. Sci. Technol., 2012. 23(5): p. 1-6.
37. Zheng, X., Soons, J., Vorburger, T., Song, J., Renegar, T. and Thompson, R., *Applications of surface metrology in firearm identification*. Surface Topography: Metrology and Properties, 2014. 2(1): p. 1-10.

## **Chapter 3: Variation of striation marks on projectiles repetitively fired from the same weapon.**

### **3.1 Introduction**

Within firearms examination there is a need to address the subjective approach to the observation and interpretation of a limited number of striation marks and move to more objective methods where the whole striated region is examined and compared. Firearm identification appears to be evolving from simple visual comparative methods [1] to the use of more sophisticated confocal microscopy [2] coupled with the introduction of automated and computerised striation evaluation of the surface topography measurements [3-16]. This more objective approach would also provide a means of addressing challenges to the robustness and scientific basis of comparative firearms evidence highlighted in the NAS report [17].

This chapter explores the use of infinite focus microscopy and mathematical pre-processing of the resultant data. PCA, HCA and LDA were used to examine whether the striated marks present on each land engraved area (LEA) could be used to demonstrate the reproducibility of the approach across 50 projectiles.

### **3.2 Selection of pellets and data collection**

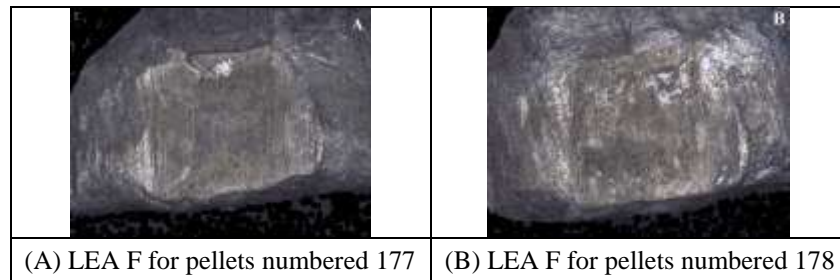
A set of 50 pellets was selected as highlighted in Table 3.1. These pellets were fired into a water tank and carefully retrieved post firing. Each land engraved area on each pellet was scanned with the Alicona® infinite focus microscope and the data was

processed as described in Chapter 2 including image acquisition, pre-processing 2D images of the striations and analysis of the data using Matlab®.

**Table 3.1: The group of pellets used in this study is highlighted in grey**

Date of test	Pellet Number	Test Done	Weapon	Total Pellets fired	Pellets Collected	Purpose	Number of pellets analysed using the Alicona Microscope
April 2012	1-50	Low Velocity	HW 45	50	50	Method development	0
April 2012	51-100	High Velocity	HW 45	50	50		10/50
April 2012	101-122	Chronograph: low and high velocity	HW 45	22	0	Velocity measurement	0
January 2013	123-158	Bones & Gelatine	HW 45	36	36	Distorted pellet study	22/22
April 2013	159-208	High Velocity	HW 45	50	50	Inter and intra pellet study	50/50
April 2013	209-219	Chronograph: high velocity	HW 45	11	0	Velocity measurement check	0
May 2013	220-319	High Velocity	HW 45	100	100	Time study	10/100
May 2013	320-341	Chronograph: high velocity	HW 45	22	0	Velocity measurement check	0
June 2013	342-441	High Velocity	HW 45	100	100	Time study	10/100
July 2013	442-465	Low Velocity Distance	HW 45	24	24	Distorted pellet and distance study	0
July 2013	466-489	High Velocity Distance	HW 45	24	24		24/24
July 2013	490-499	Rifle 1	Edgar Brother Model 35	10	10	Inter weapon study	5/10
July 2013	500-509	Rifle 2	Baikal 90042234 ИЖ-35	10	10		5/10
September 2013	510-559	Chronograph: low velocity	HW 45	50	50	Velocity measurement check	0
September 2013	560-609	Chronograph: high velocity	HW 45	50	50	Velocity measurement check, Time study	10/50
<b>Total number of pellets</b>				<b>609</b>	<b>554</b>		<b>146 (24%)</b>

All 12 LEAs for each of the 50 pellets were scanned, with the exception of the surface area of LEA F on pellets numbered 177 and 178, illustrated in Figure 3.1 (A) and (B), where the degree of surface corrosion meant that imaging would not yield results of sufficient quality for comparison and LEA L on pellet number 161 which bore an additional mark as illustrated in Figure 3.2.



**Figure 3.1: LEA measurements could not be taken from LEA F for pellets numbered 177 (A) and 178 (B) due to corrosion**



**Figure 3.2: LEA L of pellet number 161 with an additional mark highlighted in the red box and oxidation which meant the LEA measurements could not be taken**

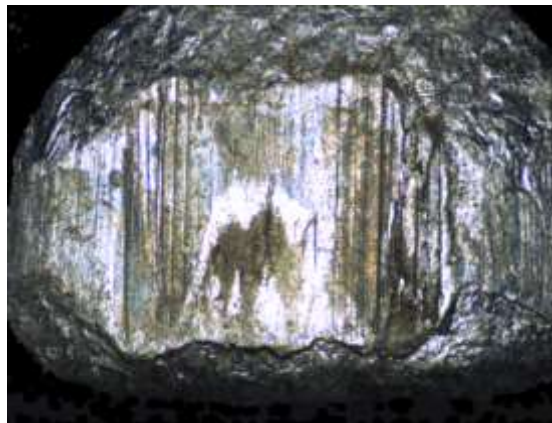
In total, 597 images were scanned and 1791 LEA measurements were recorded where three LEA measurements were for taken for each image.

### 3.3 Data analysis – alignment

A Matlab® script was used to align the measurements taken from the pellets. The alignment used a cross-correlation function to estimate the correlation between the variables [17]. All measurements were aligned to the first measurement of pellet (number 159) in the sequence.

#### 3.3.1 LEA A

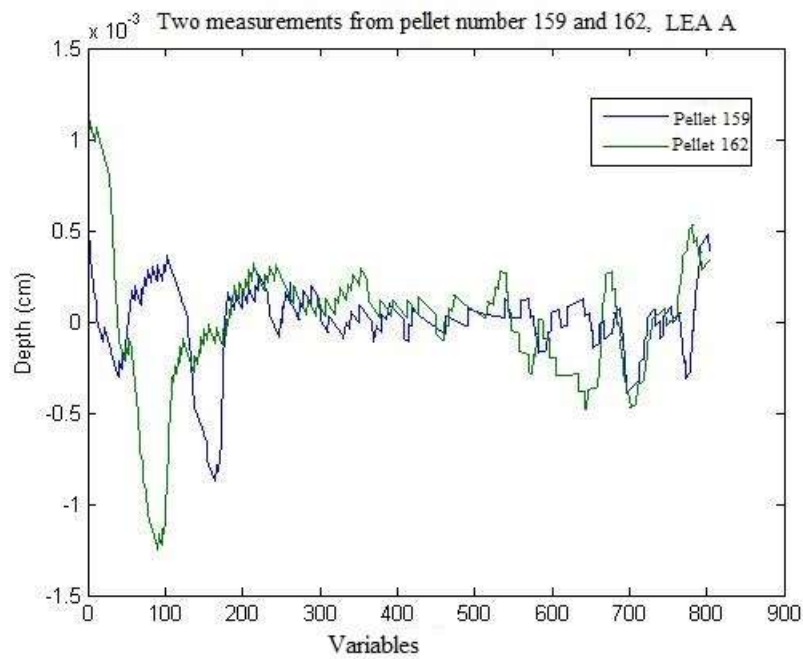
For LEA A, 147 of 150 (98%) measurements were aligned; only those from pellet number 201 were not aligned, and this was most likely due to some limited corrosion of the surface of the LEA, as shown in Figure 3.3.



**Figure 3.3: Oxidised pellet number 201, LEA A**

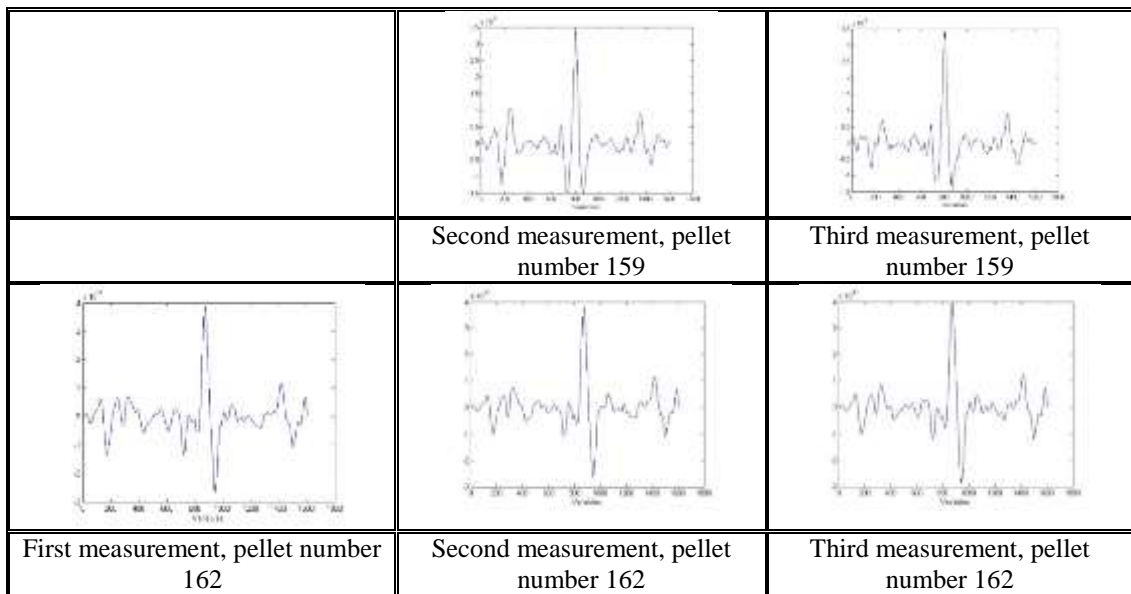
Figure 3.4 shows the surface topography (representing the variables examined) from pellet number 159 and 162, at LEA A. During alignment, the cross-correlation function determines the maximum correlation between the two sets of variables.





**Figure 3.4: Two surface topography from pellet number 159 and 162, before alignment**

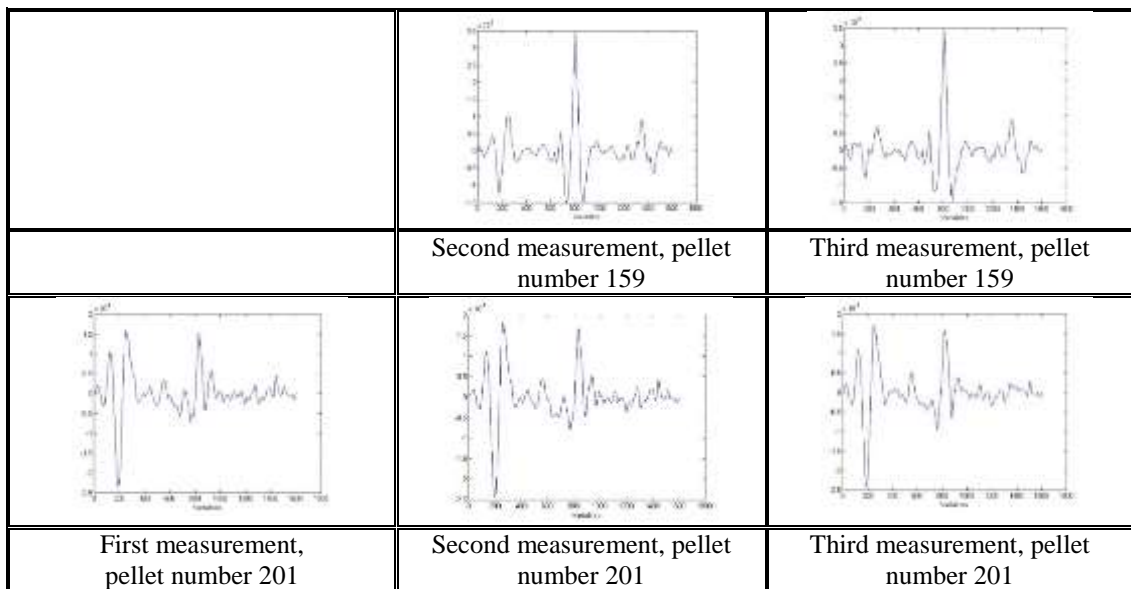
When the two sets of variables mapping out the sample topography correlate with each other, the alignment reveals a single maximum peak as illustrated in Figure 3.5.



**Figure 3.5: The alignment result of pellet number 159 and 162, LEA A. The maximum peak that present in second and third measurements, pellet numbered 159 and 162 is well aligned with the first measurement of pellet numbered 159 (i.e. the reference)**

In this case, alignment with the first measurement of pellet 159 is revealed across the three repetitive scans of both pellets 159 and 162 and one main peak is aligned with all other features being closely mirrored on each diagram.

Pellet number 201, Figure 3.3, revealed some limited corrosion on the surface of the LEA and this affected the alignment across the pellets within the region as revealed in Figure 3.6. In this case there was a clear mismatch between the alignment of pellet 159 and 201.













**Figure 3.6: The alignment result of pellet number 159 and 201, LEA A. The maximum peak were absent in first, second and third measurement of pellet numbered 201**

The full set of alignment for LEA A are presented in Appendix 4.

### 3.3.2 LEA B

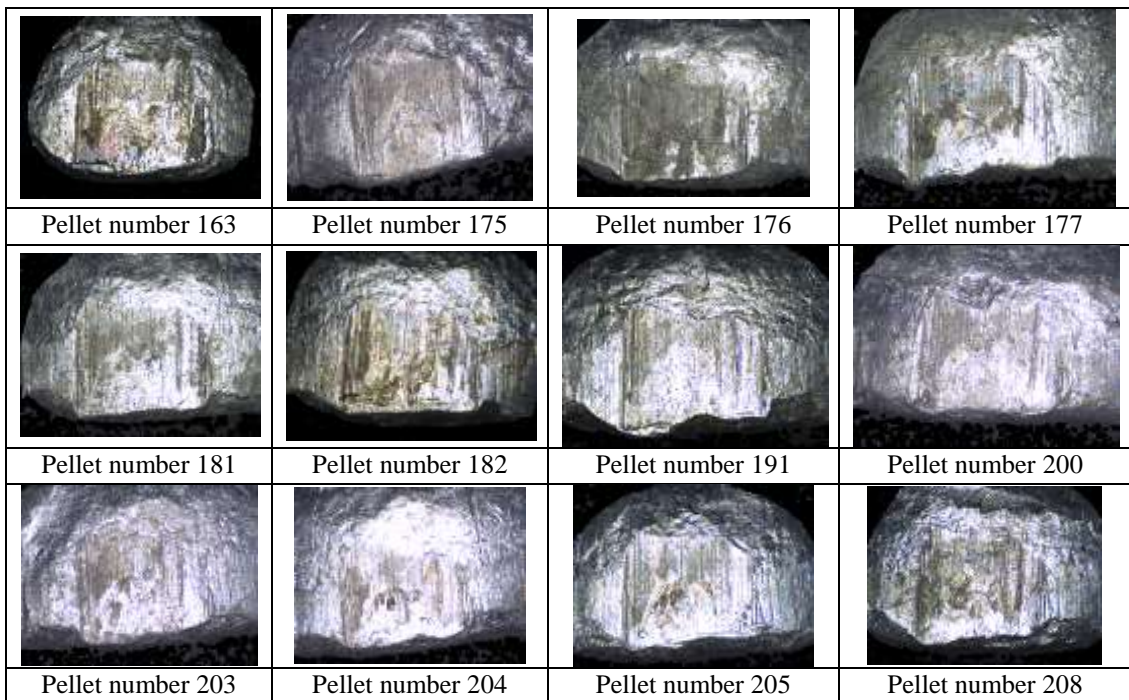
A total of 150 measurements were taken for alignment for LEA B; however, only 120 (80%) measurements were aligned. Measurements from 10 pellets (pellets numbered 163, 166, 171, 177, 181, 189, 198, 200, 203 and 208) could not be aligned, due to corrosion, see Figure 3.7. The alignment are presented in Appendix 5.

			
Pellet number 163	Pellet number 166	Pellet number 171	Pellet number 177
			
Pellet number 181	Pellet number 189	Pellet number 198	Pellet number 200
			
	Pellet number 203	Pellet number 208	

**Figure 3.7: Misaligned pellets for LEA B**

### 3.3.3 LEA C

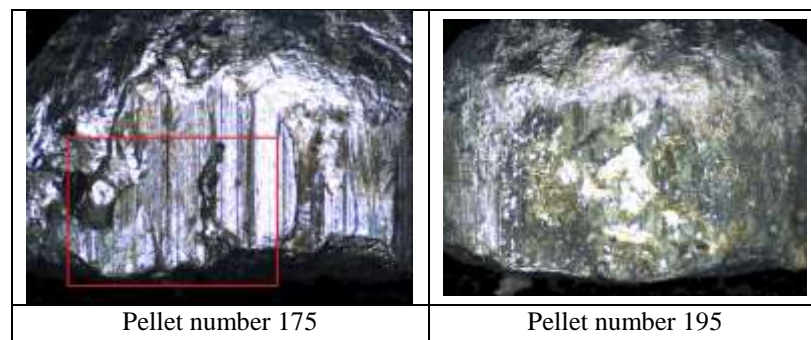
A total of 150 measurements were taken for LEA C; however, only 114 (76%) measurements were successfully aligned. Measurements from 12 pellets could not be aligned due to corrosion, see Figure 3.8. They were pellets numbered 163, 175 to 177, 181, 182, 191, 200, 203 to 205 and 208. The alignments are presented in Appendix 6.



**Figure 3.8: Misaligned pellets for LEA C**

### 3.3.4 LEA D

The percentage of successfully aligned measurements for LEA D was 96% (144) of the total measured striations. Only six of 150 measurements were misaligned, and all of these came from pellets numbered 175 and 195. There was an additional mark on the surface of pellets numbered 175, as in Figure 3.9 (left). Pellet number 195 showed some corrosion, as illustrated in Figure 3.9 (right). The alignments are presented in Appendix 7.



**Figure 3.9: Misaligned pellets for LEA D. Pellet number 175, left, had an additional mark on the surface which interfered with the alignment process**

### 3.3.5 LEA E

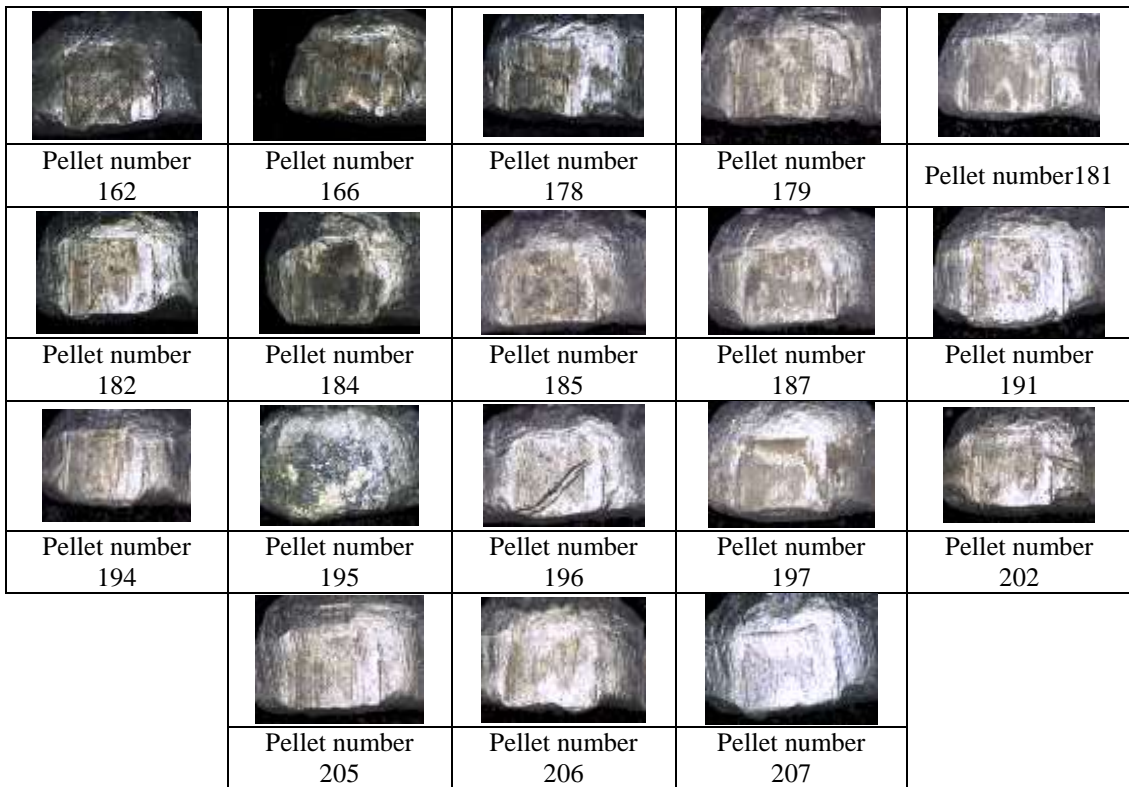
For LEA E, only 78 of 150 (52%) measurements were aligned. The misaligned measurements came from 24 pellets (160, 162, 166, 171, 172, 176, 177, 179 to 183, 186, 187, 191, 195, 197, 200 and 203 to 208). Most of the excluded pellets were corroded; however, for pellet number 205, there was presence of an additional mark on the surface and pellet number 180 was flattened, as shown in Figure 3.10. The alignments are presented in Appendix 8.

				
Pellet number 160	Pellet number 162	Pellet number 166	Pellet number 171	Pellet number 172
				
Pellet number 176	Pellet number 177	Pellet number 179	Pellet number 180	Pellet number 181
				
Pellet number 182	Pellet number 183	Pellet number 186	Pellet number 187	Pellet number 191
				
Pellet number 195	Pellet number 197	Pellet number 200	Pellet number 203	Pellet number 204
				
Pellet number 205	Pellet number 206	Pellet number 207	Pellet number 208	

**Figure 3.10: Misaligned pellets for LEA E. Pellet number 180 was flattened. Pellet number 205 bore additional mark on its surface**

### 3.3.6 LEA F
















For LEA F, 90 of 144 (60%) measurements were aligned. The misaligned measurements came from 18 pellets (162, 166, 178, 179, 181, 182, 184, 185, 187, 191, 194 to 197, 202, 205 to 207). Corrosion was the main reason for misalignment, however, pellet number 196, bore an additional mark on the surface which interfered with the alignment, see Figure 3.11. The alignments are presented in Appendix 9.



**Figure 3.11: Misaligned pellets for LEA F. Pellet number 196 bore an additional mark on its surface which interfered with the alignment process**

### 3.3.7 LEA G

The percentage of aligned measurements for LEA G was only 70%: with 105 of 150 measurements aligned. 15 misaligned pellets (162, 164, 169, 173, 175, 177, 179, 187, 189 to 191, 194, 197, 199 and 207) were not aligned, mainly because of corrosion, as in Figure 3.12. The alignments are presented in Appendix 10.

				
Pellet number 162	Pellet number 164	Pellet number 169	Pellet number 173	Pellet number 175
				
Pellet number 177	Pellet number 179	Pellet number 187	Pellet number 189	Pellet number 190
				
Pellet number 191	Pellet number 194	Pellet number 197	Pellet number 199	Pellet number 207

**Figure 3.12: Misaligned pellets for LEA G**

### 3.3.8 LEA I

LEA I had the lowest percentage of successful alignments, where only 72 measurements aligned out of 150 (48%). The 78 misaligned measurements came from pellets numbered 162, 164, 166, 168, 177, 180 to 182, 186, 187, 189 to 193, 196 to 204, 206 and 207 and again corrosion was the main reason for failed alignment, as in Figure 3.13. The alignments are presented in Appendix 12.

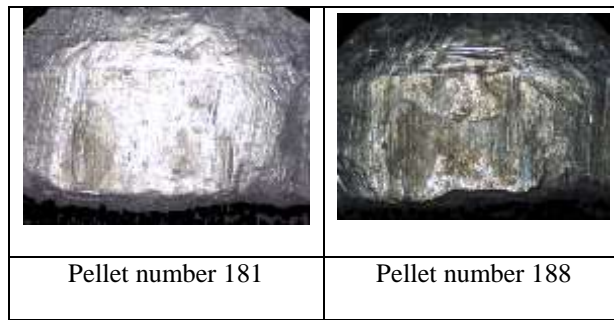


					
Pellet number 162	Pellet number 164	Pellet number 166	Pellet number 168	Pellet number 177	Pellet number 180
					
Pellet number 181	Pellet number 182	Pellet number 186	Pellet number 187	Pellet number 189	Pellet number 190
					
Pellet number 191	Pellet number 192	Pellet number 193	Pellet number 196	Pellet number 197	Pellet number 198
					
Pellet number 199	Pellet number 200	Pellet number 201	Pellet number 202	Pellet number 203	Pellet number 204
					
Pellet number 206	Pellet number 207				

**Figure 3.13: Misaligned pellets for LEA I**

### 3.3.9 LEA K

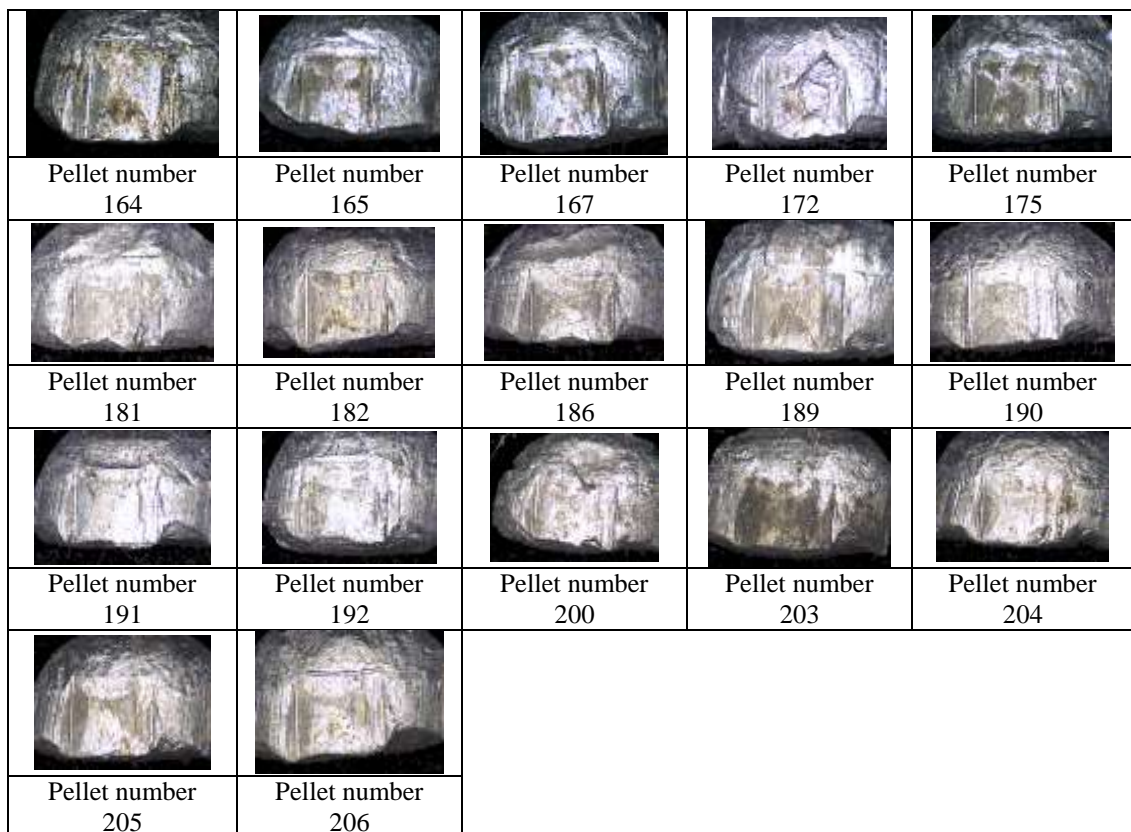
For LEA K, 144 of 150 (96%) measurements were aligned. The two misaligned measurements came from pellets numbered 181 and 188, which were mostly corroded as in Figure 3.14. The alignments are presented in Appendix 14.



**Figure 3.14: Misaligned pellets for LEA K**

### 3.3.10 LEA L

96 out of 147 (65%) measurements were aligned with 51 misaligned measurements (164, 165, 167, 172, 175, 181, 182, 186, 189 to 192, 200 and 203 to 206) and these are presented in Figure 3.15. The alignments are presented in Appendix 15.



**Figure 3.15: Misaligned pellets for LEA L**

### 3.3.11 LEA H and J

For LEA H and J, all measurements were aligned and the alignments are presented in Appendix 11 and 13 respectively.

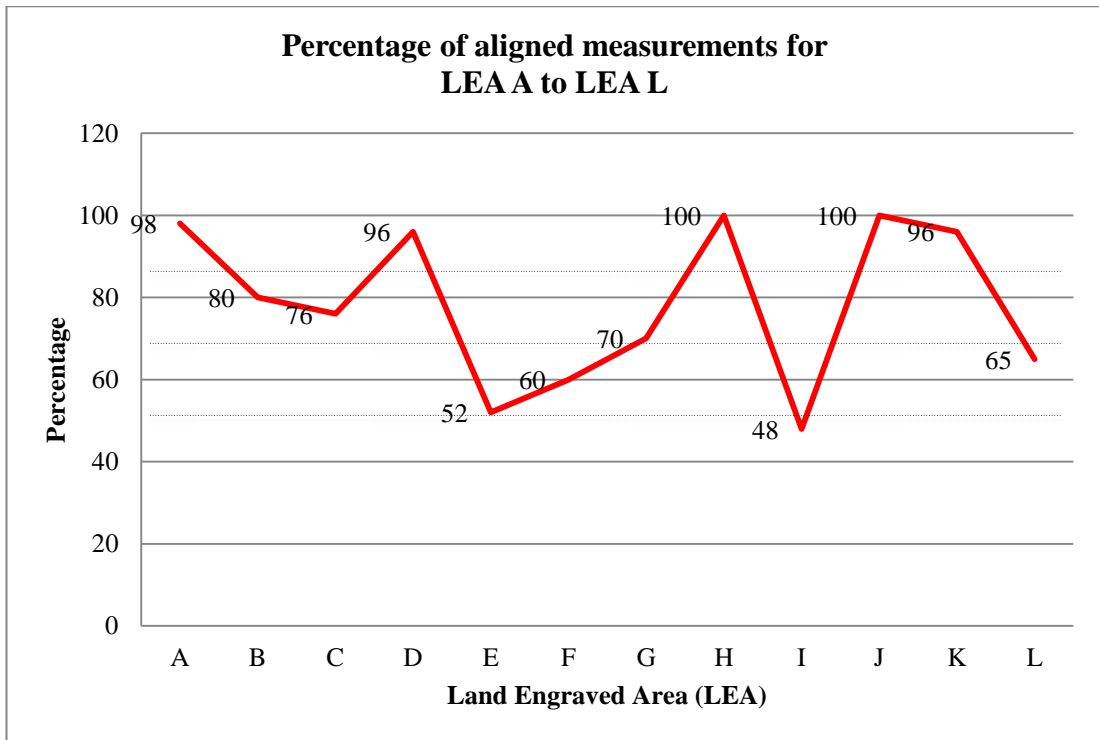
### 3.3.12 Data summary

In total, 1410 measurements were aligned out of a possible 1791 taken from 597 scanned images. Corrosion of the LEA surface resulting in obscuring or distorting the striation marks was the main reason for misalignment; however, other factors contributed, such as the presence of additional marks on the surface of the pellet or some flattening of the pellets also affected alignment.

A summary of this data is presented in Table 3.2 and Figure 3.16.

**Table 3.2: Summary of aligned measurements for LEA A to LEA L**

LEA	Number of pellets scanned	Number of measurements for alignment	Number of aligned measurements	Percentage of aligned measurements (%)
A	50	150	147	98
B	50	150	120	80
C	50	150	114	76
D	50	150	144	96
E	50	150	78	52
F	48	144	90	60
G	50	150	105	70
H	50	150	150	100
I	50	150	72	48
J	50	150	150	100
K	50	150	144	96
L	49	147	96	65
<b>Total</b>	<b>597</b>	<b>1791</b>	<b>1410</b>	<b>78</b>



**Figure 3.16: Percentage of aligned measurements for LEA A to LEA L**

### **3.4 Principal Component Analysis (PCA), Hierarchical Cluster Analysis (HCA) and Linear Discriminant Analysis (LDA)**

The data derived from the aligned topographical maps presented a set of variables for each striated region which could be subject to mathematical methods in order that pattern matching could be undertaken. This provides an objective mathematical method to evaluate the linkage between the different striated regions of interest (the LEA regions) on bullets of known origin.

The PCA, HCA and LDA were undertaken using Matlab® and three data sets were originally chosen depending on the percentage of aligned measurements within the

data representing the various LEA at 50%, 70% and 90% alignment. The reason for choosing these categories is an arbitrary decision.

Based on Table 3.2, below are the groupings of LEAs which were considered;

- more than 50% of measurements aligned - LEA A, B, C, D, E, F, G, H, J, K, L
- more than 70% of measurements aligned - LEA A, B, C, D, G, H, J, K
- more than 90% of measurements aligned - LEA A, D, H, J, K

LEA I was not included in the analysis because of the lower than 50% of aligned measurements.

Figures 3.17 and 3.18 reveal the PCA and HCA results for all LEAs except for LEA I. These LEAs are presented at 50% alignment or greater across the striated regions. For the PCA results, LEA D is the only region that remains well defined and differentiated from all others. Based on the HCA results of more than 50%, 11 different LEAs clusters can be seen.

Scores for LEA A, B, C, D, E, F, G, H, J, K and L

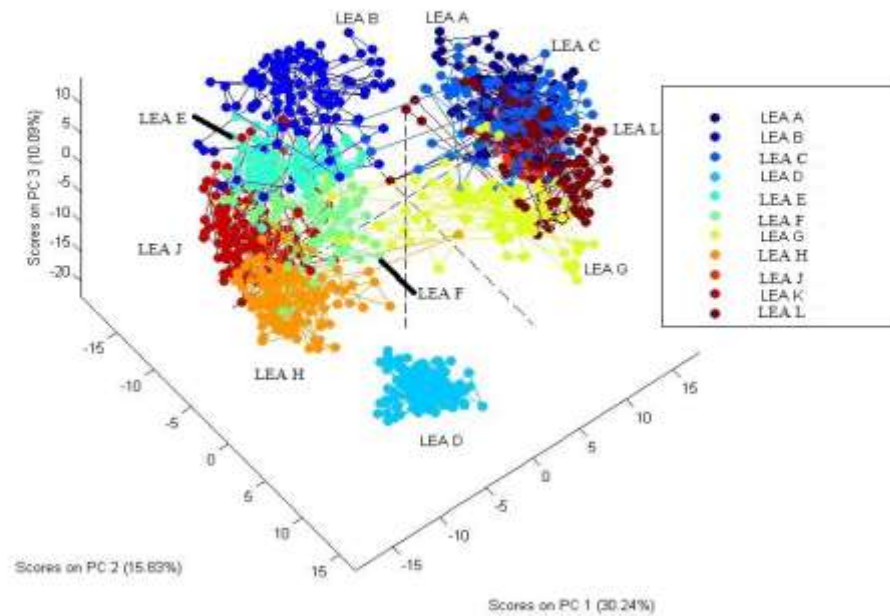


Figure 3.17: The PCA results for the more than 50% aligned measurements of LEAs

### Cluster Dendrogram

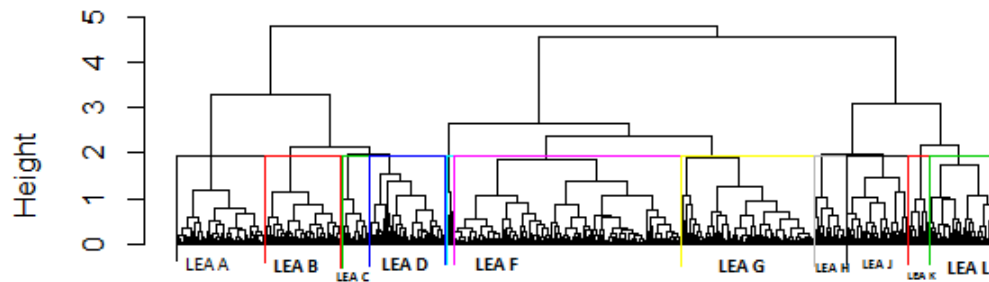
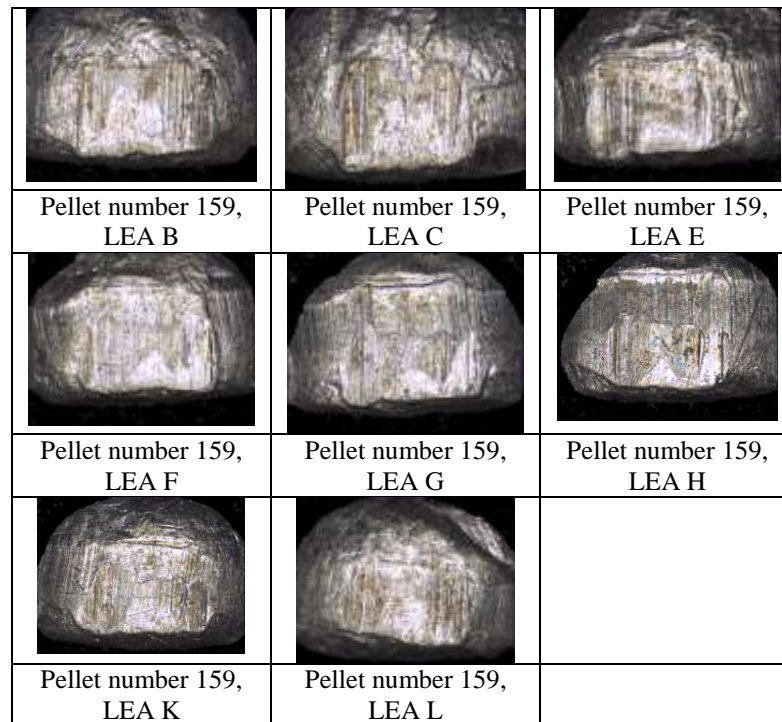


Figure 3.18: The HCA results for the more than 50% aligned measurements of LEAs

Table 3.3 shows the LDA classification table of more than 50% aligned measurements of LEAs. The diagonal values represent correctly classified LEAs. Based on the classification table, LEA D and LEA J are well separated from the other LEAs. All 144 measurements for LEA D and 150 measurements for LEA J can be classified into its respective LEAs. The other LEAs were not separated as well as LEA D and J because visually, LEA B, C, E, F, G, H, K and L all look similar with no individual characteristic marks on their surface. Figure 3.19 illustrates all these LEAs.

**Table 3.3: The LDA classification table of more than 50% aligned measurements of LEAs. The diagonal values (in bold) represent correctly classified LEAs**

LEA	A	B	C	D	E	F	G	H	J	K	L	Percentage of classification
A	<b>133</b>	0	6	0	0	0	0	0	0	0	8	90.5
B	0	<b>106</b>	0	0	14	0	0	0	0	0	0	88.3
C	4	3	<b>95</b>	0	0	0	0	0	6	0	6	83.3
D	0	0	0	<b>144</b>	0	0	0	0	0	0	0	100
E	0	2	0	0	<b>76</b>	0	0	0	0	0	0	97.4
F	0	1	0	0	3	<b>67</b>	0	9	0	10	0	74.4
G	0	0	0	0	0	9	<b>82</b>	0	0	0	14	78.1
H	0	0	0	0	0	4	0	<b>133</b>	0	13	0	88.7
J	0	0	0	0	0	0	0	0	<b>150</b>	0	0	100
K	0	2	0	0	1	11	0	11	0	<b>119</b>	0	82.6
L	9	1	3	0	0	1	15	0	0	0	<b>67</b>	69.8



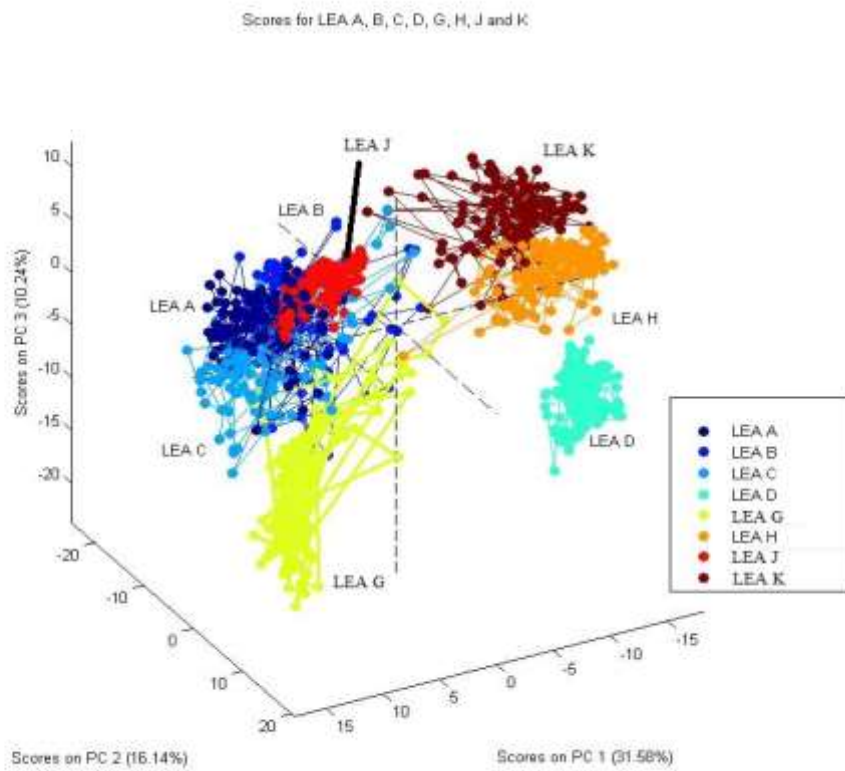
**Figure 3.19: The scanned image of pellet number 159, LEAB, C, E, F, G, H, K and L. These pellets have no individual characteristic marks on their surface therefore these LEAs were not separated well**

The PCA, HCA and LDA results illustrate quite clearly that at the lower threshold for alignment the LEAs convolute providing little discrimination across these regions of interest. The model built for this group is 86.7% accurate. This is expected because there are 8 LEAs (LEA B, C, E, F, G, H, K and L) with no individual characteristic marks on their surface which can be difficult to differentiate. Next is the analysis for the more than 70% aligned measurements of LEAs.

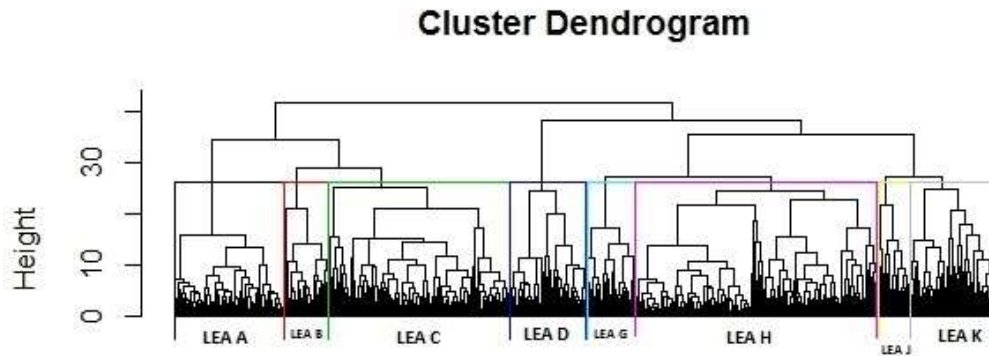
Figures 3.20 and 3.21 reveal the PCA and HCA analysis results of more than 70% aligned measurements of LEAs A, B, C, D, G, H, J and K. All LEAs are poorly



differentiated from each other except for LEA D. Based on the HCA results of more than 70%, 8 different LEAs clusters can be seen.



**Figure 3.20: The PCA results for the more than 70% aligned measurements of LEAs**



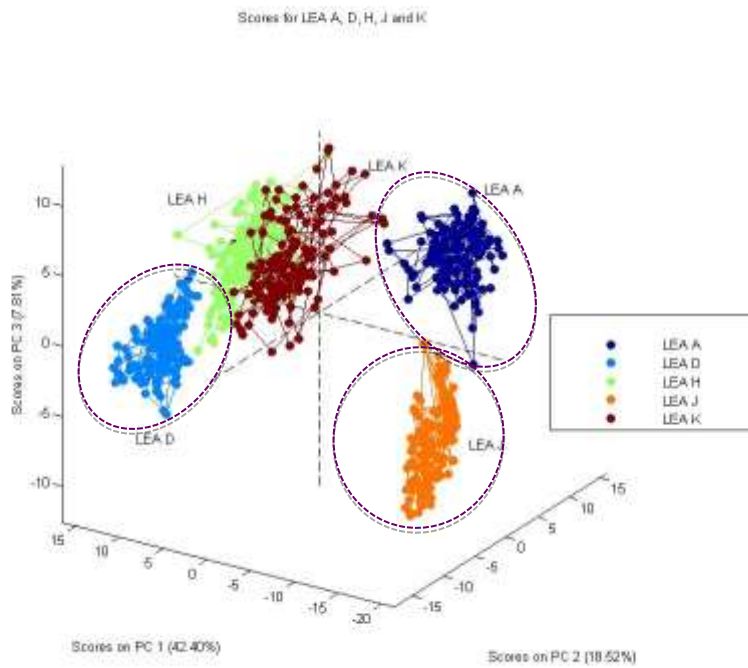
**Figure 3.21: The HCA results for the more than 70% aligned measurements of LEAs**

Table 3.4 shows the LDA classification table of more than 70% aligned measurements of LEAs. The diagonal values represent correctly classified LEAs. Based on the classification table, LEA D and LEA J are well separated from the other LEAs. All 144 measurements for LEA D and 150 measurements for LEA J can be classified into its respective LEAs. The other LEAs were not separated as well as LEA D and J, however, the percentage of classification of all LEAs reaches more than 90%. This group is less convoluted as compared to the 50% group, therefore the LEAs can be discriminated slightly better. The model built for this group is 94.6% accurate. This is expected because there are 5 LEAs (LEA B, C, G, H and K) with no individual characteristic marks on their surface which can be difficult to differentiate.

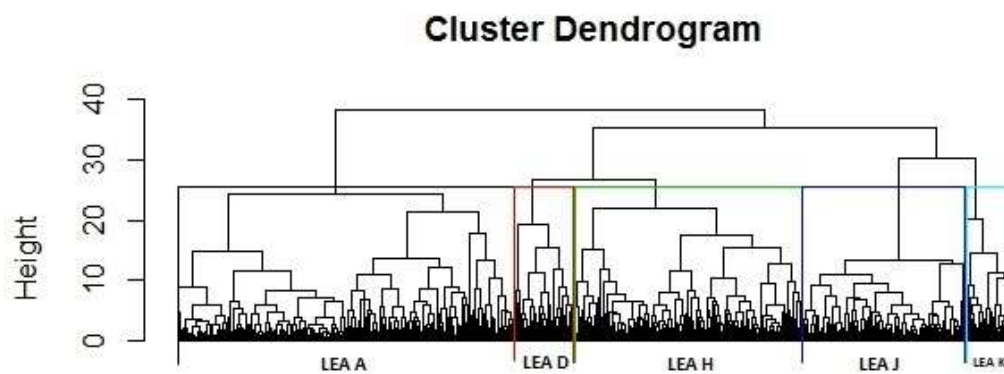
**Table 3.4: The LDA classification table of more than 70% aligned measurements of LEAs. The diagonal values (in bold) represent correctly classified LEAs**

LEA	A	B	C	D	G	H	J	K	Percentage of classification
<b>A</b>	<b>142</b>	0	2	0	0	0	0	0	98.6
<b>B</b>	0	<b>118</b>	0	0	1	0	0	1	98.3
<b>C</b>	6	3	<b>100</b>	0	0	0	5	0	87.7
<b>D</b>	0	0	0	<b>144</b>	0	0	0	0	100.0
<b>G</b>	2	0	0	0	<b>98</b>	3	0	2	93.3
<b>H</b>	0	0	0	1	0	<b>138</b>	0	11	92.0
<b>J</b>	0	0	0	0	0	0	<b>150</b>	0	100.0
<b>K</b>	0	3	0	0	0	16	0	<b>125</b>	86.8

Next is the analysis for the more than 90% aligned measurements of LEAs. Figures 3.22 and 3.23 show the PCA and HCA analysis results derived from the LEA where 90% or better alignment of the topographical maps was achieved. At 90% alignment of the striation marks, LEA A, D and J are well defined and separated from the convoluted group of LEA K and H (Figure 3.22). Based on the HCA results of more than 90%, 5 different LEAs clusters can be seen.



**Figure 3.22:** The PCA results for the more than 90% aligned measurements of LEAs




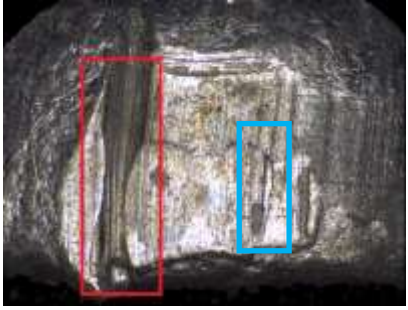



**Figure 3.23:** The HCA results for the more than 90% aligned measurements of LEAs

Table 3.5 shows the LDA classification table of more than 90% aligned measurements of LEAs. The diagonal values represent correctly classified LEAs. Based on the classification table, all but one LEA can be separated well. Visually, LEA A, D and J contain a set of individual characteristic marks different from LEA H and K (Figure 3.24). This is probably the reason for the separation of these three LEAs. 7 measurements from LEA K was misclassified as LEA H. LEA H and LEA K contains no individual characteristic marks, however, for more than 90% aligned measurements, this group is less convoluted as compared to the previous two groups. Visually, between LEA H and LEA K, LEA H has a mark (in red rectangle, as in Figure 3.24, LEA H) which is different from LEA K. This mark is not exclusive for LEA H only because LEA J has similar mark, as shown in blue rectangle (Figure 3.24, LEA J), but LEA J has a very distinctive individual characteristic mark on its surface (in red rectangle, as in Figure 3.24, LEA J), therefore LEA J can be differentiated very well. The mark on LEA H is possibly shallow hence it is not distinguishable well, especially when the measurements are convoluted as in two previous groups but this mark can differentiate between LEA H and LEA K when the group is less convoluted. This is probably the explanation of well classification for LEA H and not LEA K. The model built for this group is 99.0% accurate.

**Table 3.5: The LDA classification table of more than 90% aligned measurements of LEAs. The diagonal values (in bold) represent correctly classified LEAs**

LEA	A	D	H	J	K	Percentage of classification
A	<b>147</b>	0	0	0	0	100
D	0	<b>144</b>	0	0	0	100
H	0	0	<b>150</b>	0	0	100
J	0	0	0	<b>150</b>	0	100
K	0	0	7	0	<b>137</b>	95.1

	
Pellet number 159, LEA A	Pellet number 159, LEA D
	
Pellet number 159, LEA H	Pellet number 159, LEA J
	
Pellet number 159, LEA K	

**Figure 3.24: The scanned image of pellet number 159, LEA A, D, H, J and K. Visually, LEA A, D and J have distinct individual characteristic marks on its surface which make them different from LEA H and K, as shown in the red rectangle for LEA A, D and J. LEA H has a mark (in red rectangle) that is absent in LEA K, however the same mark presents in LEA J (blue rectangle). This is possibly the reason of all LEAs are well differentiated, except for LEA K**

### **3.5 Conclusions**

Burd and Kirk's [1] suggestion that a single weapon does not necessarily leave identical marks on projectiles is corroborated by this study. Through the use of a 3D microscope, 2D images were pre-processed and aligned for further analysis, as suggested by Dongguang Li [14]. This facilitated accurate measurement of the surface of each pellet and the outputted surface topography was used for a comparison in line with previous studies and approaches [3, 6, 8, 9, 12, 14, 18-21].

As mentioned in Chapter 2, section 2.5.1 Image Acquisition, the selection of the LEAs required some experience, however the instrument delivered reproducible results across the chosen region and once the numerical data had been retrieved using the Alicona® software, the pre-processing, alignment and analysis of the data were all done automatically in line with the approach suggested by Riva and Champod [13]. While other researchers have created new algorithms, software or tools for the purpose of objectifying ballistic evidence, such as De Kinder and Bonfanti with Labview® [5], Bachrach [16] and SCICLOPS™ and this research suggests that using an optical microscope with software which can measure the surface topography of the projectiles then Matlab® with PLS\_Toolbox® can be used to objectify the striation marks.

Corrosion of the pellet surface was a limiting factor in terms of choice of LEA available for alignment measurements. In occasional circumstances, additional marks were also in evidence on the projectile surfaces.

The analysis results for eleven of the twelve LEAs illustrated that the striation marks were neither exclusive nor specific to the LEA regions but rather crossed over regions. As the degree of alignment of the striation marks is increased the convolution of the LEA regions decreases however it is not completely resolved. Given that such discrimination is critical to the process, only LEAs where 90% or better alignment across repetitive measurements is achieved can be recommended for comparative purposes.

It was evident that as the percentage alignment was increased to 90%, the best discrimination of LEAs was achieved, nevertheless, only 5 out of 12 LEAs (42%) could be aligned at this level and even at 90%, one of the five LEAs was still convoluted suggesting that only four out of 12 LEAs were differentiable (33.3%). The implication of this result is profound. It suggests that the assumption that any specific striated region of a projectile is discriminatory is in fact incorrect and that such discrimination is only achieved in a small proportion of such regions. Moreover in the regions where discrimination was objectively achieved, this occurred because of the presence of very specific marks (groves) rather than a specific series of striations.

**Table 3.6: Percentage of aligned measurement and accuracy of the model built using the LDA results. The higher the percentage of alignment, the higher the level of accuracy**

<b>Percentage of aligned measurement</b>	<b>Model accuracy (%)</b>
More than 50	86.7
More than 70	97.8
More than 90	99.0

Models built for these 3 groups show that the accuracy percentage correlates with the percentage of alignment, where the accuracy increases with better alignment of the



LEAs, as shown in Table 3.6. The value of the accuracy percentage can be used to objectify the striation marks, which is the core for the study.

### 3.6 References

1. Burd, D.Q. and Kirk, P.L., *Tool Marks. Factors Involved in Their Comparison and Use as Evidence*. *Journal of Criminal Law and Criminology* (1931-1951), 1942. 32(6): p. 679-686.
2. Banno, A., Masuda, T. and Ikeuchi, K., *Three dimensional visualization and comparison of impressions on fired bullets*. *Forensic Science International*, 2004. 140(2-3): p. 233-240.
3. Breitmeier, U. and Schmid, H., *Lasercomp: A surface measurement system for forensic applications*. *Forensic Science International*, 1997. 89(1): p. 1-13.
4. Pirlot, M., Chabottier, A., Celens, E., De Kinder, J. and Van Ham, P., *Feature extraction of optical projectiles images*. *Science & Justice*, 1999. 39(1): p. 53-56.
5. De Kinder, J. and Bonfanti, M., *Automated comparisons of bullet striations based on 3D topography*. *Forensic Science International*, 1999. 101(2): p. 85-93.
6. Senin, N., Groppetti, R., Garofano, L., Fratini, P. and Pierni, M., *Three-dimensional surface topography acquisition and analysis for firearm identification*. *J. Forensic Sci.*, 2006. 51(2): p. 282-295.
7. Puente León, F., *Automated comparison of firearm bullets*. *Forensic Science International*, 2006. 156(1): p. 40-50.
8. Xie, F., Xiao, S., Blunt, L., Zeng, W. and Jiang, X., *Automated bullet-identification system based on surface topography techniques*. *Wear*, 2009. 266(5): p. 518-522.
9. Sakarya, U., Leloğlu, U.M. and Tunali, E., *Three-dimensional surface reconstruction for cartridge cases using photometric stereo*. *Forensic Science International*, 2008. 175(2-3): p. 209-217.
10. Chu, W., Song, J., Vorburger, T., Yen, J., Ballou, S. and Bachrach, B., *Pilot study of automated bullet signature identification based on topography measurements and correlations*. *J Forensic Sci*, 2010. 55(2): p. 341-347.
11. Chu, W., Song, J., Vorburger, T.V., Thompson, R. and Silver, R., *Selecting Valid Correlation Areas for Automated Bullet Identification System Based on Striation Detection*. *J. Res. Natl. Inst. Stand. Technol.*, 2011. 116(3): p. 647-653.
12. Song, J., Chu, W., Vorburger, T.V., Thompson, R., Renegar, T.B., Zheng, A., Yen, J., Silver, R. and Ols, M., *Development of ballistics identification-from image comparison to topography measurement in surface metrology*. *Meas. Sci. Technol.*, 2012. 23(5): p. 1-6.

13. Riva, F. and Champod, C., *Automatic Comparison and Evaluation of Impressions Left by a Firearm on Fired Cartridge Cases*. *Journal of Forensic Sciences*, 2014. 59(3): p. 637-647.
14. Li, D., *Ballistics Projectile Image Analysis for Firearm Identification*. *IEEE Transactions On Image Processing*, 2006. 15(10): p. 2857-2865.
15. Li, D. *A Novel Ballistics Imaging System for Firearm Identification in Technological Developments in Networking, Education and Automation*. 2010. Springer Netherlands.
16. Bachrach, B., *Development of a 3D-based automated firearms evidence comparison system*. *J. Forensic Sci.*, 2002. 47(6): p. 1253-64.
17. MathWorks. *MATLAB, The Language of Technical Computing*. 2013 [cited 2014; Available from: <http://www.mathworks.co.uk/products/matlab/>].
18. Bonfanti, M.S. and Ghauharali, R.I., *Visualisation by confocal microscopy of traces on bullets and cartridge cases*. *Science & Justice*, 2000. 40(4): p. 241-256.
19. Gambino, C., McLaughlin, P., Kuo, L., Kammerman, F., Shenkin, P., Diaczuk, P., Petraco, N., Hamby, J. and Petraco, N.D.K., *Forensic Surface Metrology: Tool Mark Evidence*. *Scanning*, 2011. 33(5): p. 272–278.
20. Mathia, T.G., Pawlus, P. and Wieczorowski, M., *Recent trends in surface metrology*. *Wear*, 2011. 271(3–4): p. 494-508.
21. Zheng, X., Soons, J., Vorburger, T., Song, J., Renegar, T. and Thompson, R., *Applications of surface metrology in firearm identification*. *Surface Topography: Metrology and Properties*, 2014. 2(1): p. 1-10.

## **Chapter 4: Variation of striation marks across 600 pellets fired from the same weapon**

### **4.1 Introduction**

There are three principles stated by the AFTE Theory of Identification [1] relating to tool marks:

- (1) two tool marks are identical when the surface contours are in sufficient agreement,
- (2) the sufficient agreement is determined by the similarity of height or depth, width, curvature and spatial relationship of ridges, peaks, furrows between two tool marks and it is beyond reasonable doubt that these two toolmarks can be made by other different tools,
- (3) the current identification process is subjective and based on scientific research and; examiner's training and experience.

This theory is not considered to be absolute, but rather more of a guideline [2] for tool marks identification. There are other researchers who have implied that changes may occur to tool marks over time. Di Maio [3] suggested that any changes that occur to the barrel of the weapon, such as rust, corrosion or after repetitive firing, will result in changes on the striation marks on the bullets fired from that weapon over a period of time. Heard [4] also mentioned that if the barrel of the weapon was poorly maintain or not cleaned regularly, there was a possibility of alteration of the striation marks after firing bullets over a period of time. Burd and Kirk [5] also suggested that no two tools can leave identical marks. However, a single tool is possible to produce similar mark over a period of time unless major changes occur to

the tool to produce different markings and alter its originality. This study is still relevant given the mass production of tools because recent publications (in 2015) used fifty sequentially manufactured tools in their studies and they agreed that ‘manufactured tools are unique due to the machining processes used in the production of tools’ [6, 7]. The tools are mass produced within manufacturing tolerance, metal would rust or accumulate debris and repeated usage would cause wear and tear to the manufacturing machine. These can affect the surface topography of tools produced by the machining processes. Therefore the initial study from 1942 is still relevant.

Castro *et al.* [8] and Nichols [9, 10] wrote extensively regarding tool mark identification and as imaging technology advances [11, 12], surface topography is playing an increasingly important role in tool mark identification [11, 13-18].

The ability to establish how striation marks on land engraved areas either LEAs change or remain static over repetitive firing of projectiles through a weapon is of obvious importance and this is particularly the case at LEAs with strong alignments (strong reproducibility).

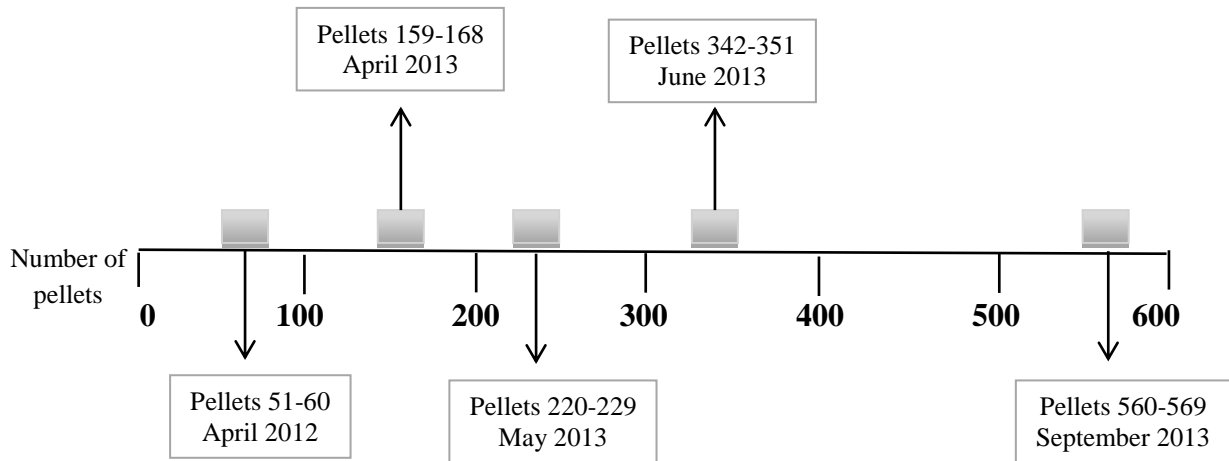
#### **4.2 Selection of pellets**

A set of pellets fired across a 17 months period was chosen for examination. Across this time frame a total of 609 pellets were fired from the air pistol. The weapon was not cleaned during the test firing period. The time line for the selected pellets is provided in Table 4.1 and Figure 4.1. Over all five sets of ten pellets (50 in total)

were selected. The pellets were consecutively numbered and 41 of the 50 selected pellets were scanned using the Alicona® microscope as described in Chapter 2. 9 pellets could not be scanned because of corrosion to their surfaces. The scanned images were processed, aligned and analysed with Matlab® as previously described.

**Table 4.1: Pellets used in this study were selected from the shootings highlighted in grey**

<b>Date of test</b>	<b>Pellet Number</b>	<b>Test Done</b>	<b>Weapon</b>	<b>Total Pellets fired</b>	<b>Pellets Collected</b>	<b>Pellet number selected for this study</b>
April 2012	1-50	Low Velocity	HW 45	50	50	
April 2012	51-100	High Velocity	HW 45	50	50	51-60
April 2012	101-122	Chronograph: low and high velocity	HW 45	22	0	
January 2013	123-158	Bones & Gelatine	HW 45	36	36	
April 2013	159-208	High Velocity	HW 45	50	50	159-168
April 2013	209-219	Chronograph: high velocity	HW 45	11	0	
May 2013	220-319	High Velocity	HW 45	100	100	220-229
May 2013	320-341	Chronograph: high velocity	HW 45	22	0	
June 2013	342-441	High Velocity	HW 45	100	100	342-351
July 2013	442-465	Low Velocity Distance	HW 45	24	24	
July 2013	466-489	High Velocity Distance	HW 45	24	24	
July 2013	490-499	Rifle 1	Edgar Brother Model 35	10	10	
July 2013	500-509	Rifle 2	Baikal 90042234 ИЖ-35	10	10	
September 2013	510-559	Chronograph: low velocity	HW 45	50	50	
September 2013	560-609	Chronograph: high velocity	HW 45	50	50	560-569
<b>Total number of pellets</b>				<b>609</b>	<b>554</b>	



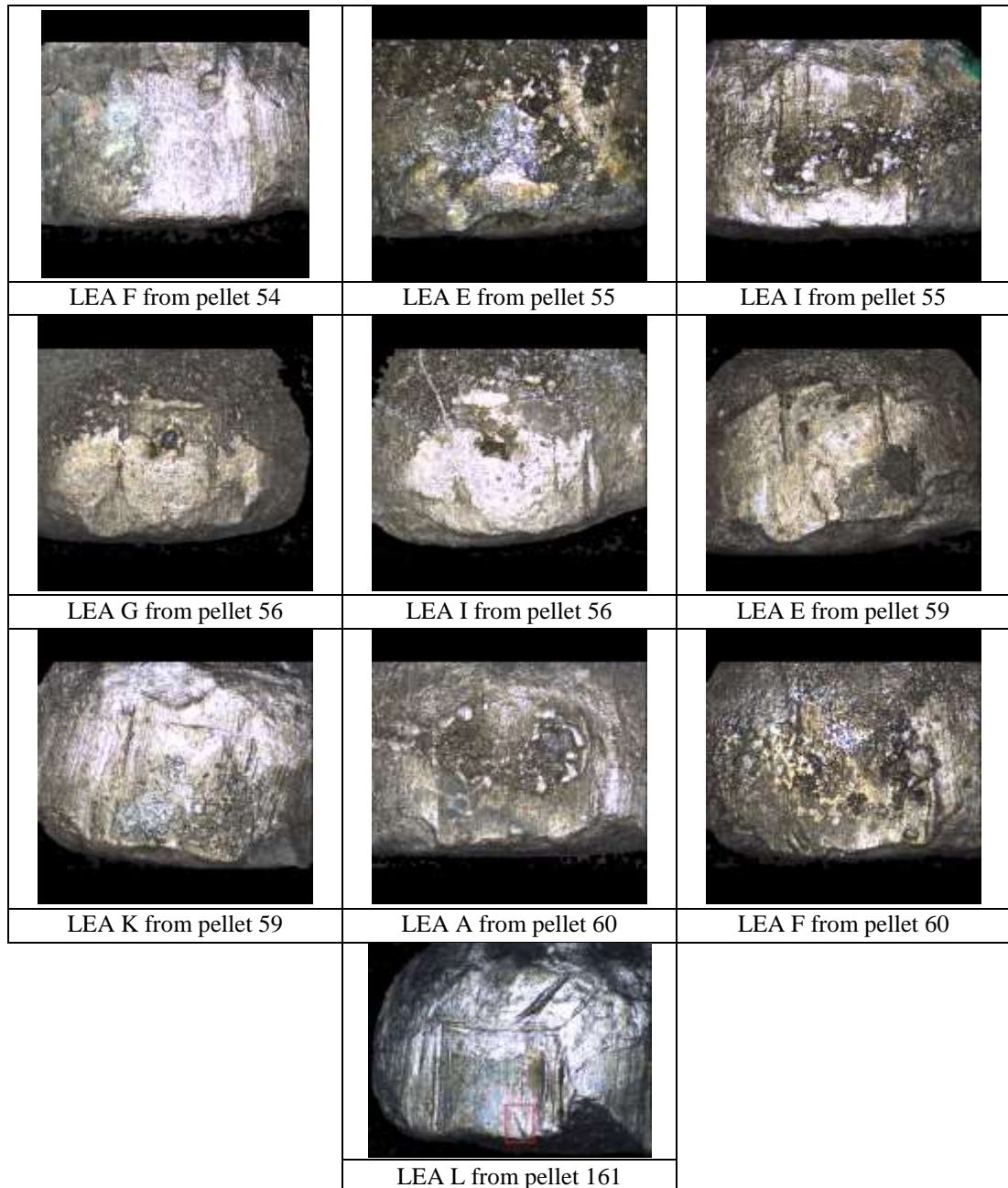
**Figure 4.1: Pellets examined in the longitudinal study**

### 4.3 Specific regions examined

All 12 of the LEAs previously described were examined across all of the pellets. A number of the pellets displayed evidence of corrosion, although this was much less prevalent than observed on earlier samples. For the samples fired in September 2013, a different collection method involving the use of a stopper rather than water was used and it appears to have resulted in additional marks appearing within some of the LEAs. The stopper was made of a piece of cardboard layered with cotton cloths. When the pellet came into contact with the stopper, there would have been an energy loss due to the presence of the cloth [19] and cardboard. The impact with cloth and cardboard might have contributed to disfiguration of the striation and, hence, the misalignment of the striation.

Five of the 10 pellets fired in April 2012 had at least one LEA where the microscopic measurements could not be performed because of surface corrosion, and these are

presented in Figure 4.2. In all but one case, two LEAs were affected. These pellets were fired in the early stages of the project, and in total corrosion affected nine out of 120 LEAs measured (7.5%). Triplicate measurements were made of each of the three measured region providing 333 measurements in total.



**Figure 4.2: Corroded land engraved areas on pellets fired in April 2012 (pellets numbered 54, 55, 56, 59 and 60). Pellet number 161 fired in April 2013 bore an additional mark as in the red box**



One LEA from pellet number 161 fired in April 2013 bore an additional mark and illustrated in Figure 4.2 producing 357 LEAs measured for the April 2013 set.

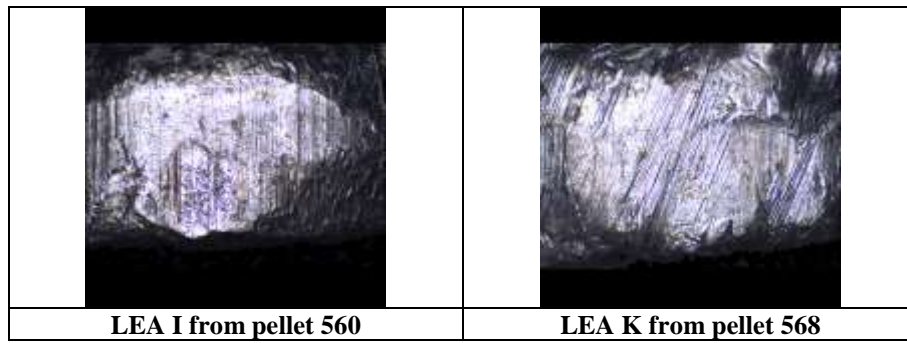
All 12 of the LEAs on the May 2013 were successfully scanned in triplicate producing 360 measurements.

For the set of pellets recovered from the June 2013 experiments, pellet number 348 was corroded in two LEAs and pellet number 347 was corroded in one LEA as shown in Figure 4.3. The remaining 117 LEAs in the June 2013 set produced 351 measurements.



**Figure 4.3: Corroded land engraved areas on pellets fired in June 2013**

Finally, in the September 2013 pellets, LEA I on pellet number 560 and LEA K on pellet number 568 (Figure 4.4) were incomplete and disfigured, respectively, resulting in the analysis of a total of 118 striated regions across the 10 pellets, generating 354 LEA measurements.



**Figure 4.4: Disfigured land engraved areas on pellets fired in September 2013**

In total 585 LEAs were scanned in triplicate for the study producing 1755 measurements. Each set of triplicate measurements across the LEAs were curve fitted and aligned as previously described. The measurements are summarised in Tables 4.2 and 4.3.

**Table 4.2: Summary of scanned results and LEA measurements for pellets used for this study based on date of firing**

<b>Pellet number</b>	<b>Date Pellets fired</b>	<b>Number of scanned images</b>	<b>Number of LEA measurements</b>
51-60	April 2012	111	333
159-168	April 2013	119	357
220-229	May 2013	120	360
342-351	June 2013	117	351
560-569	September 2013	118	354
<b>Total</b>		<b>585</b>	<b>1755</b>

**Table 4.3: Summary of scanned results and LEA measurements for pellets used for this study based on LEA**

<b>Striations (A to L)</b>	<b>Number of scanned images</b>	<b>Number of LEA measurements</b>
A	49	147
B	50	150
C	50	150
D	49	147
E	47	141
F	47	141
G	49	147
H	50	150
I	47	141
J	50	150
K	48	144
L	49	147
<b>Total</b>	<b>585</b>	<b>1755</b>

#### 4.4 Data alignment

Before the LEA measurements could be analysed, the data had to be aligned as described in Chapter 2. Alignment was undertaken across the LEA regions on each set of pellets within each time frame that the pellets were fired. This was so that differences in the individual LEAs could be evaluated across the total numbers of pellets fired as illustrated in Figure 4.5.

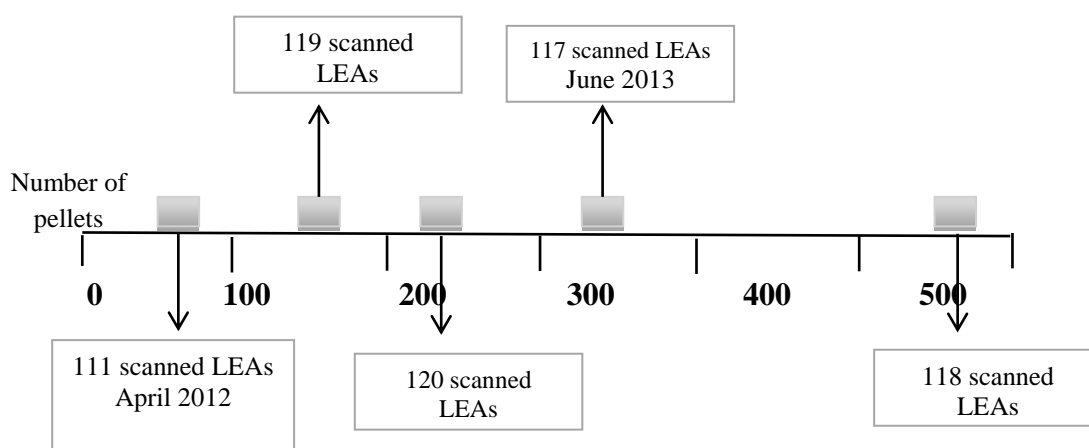


Figure 4.5: numbers of LEAs scanned and examined in the longitudinal study

##### 4.4.1 LEA A

A total of 147 LEA scanned images of the striated marks in region A were examined across the pellets and these are presented in Table 4.4.

Table 4.4: Pellets in the longitudinal study where LEA A was examined

Pellet number	Date Pellets fired	Pellet number where LEA A was imaged	Number of LEA measurements
51- 60	April 2012	51- 59	27
159-168	April 2013	159-168	30
220-229	May 2013	220-229	30
342-351	June 2013	342-351	30
560-569	September 2013	560-569	30
<b>Total number of pellets</b>		<b>49</b>	<b>147</b>

In each case three repetitive measurements were made as previously described in Chapter 2. Factors which contribute to misalignment of striation measurements included corrosion and flattening of the striations. Examples of these complicating factors can be seen in the scanned image for pellet number 55, Figure 4.6.



**Figure 4.6: LEA A of pellet 55 showing corrosion on the top left of the striated region and flattening of the striation, as shown in the red rectangle are**

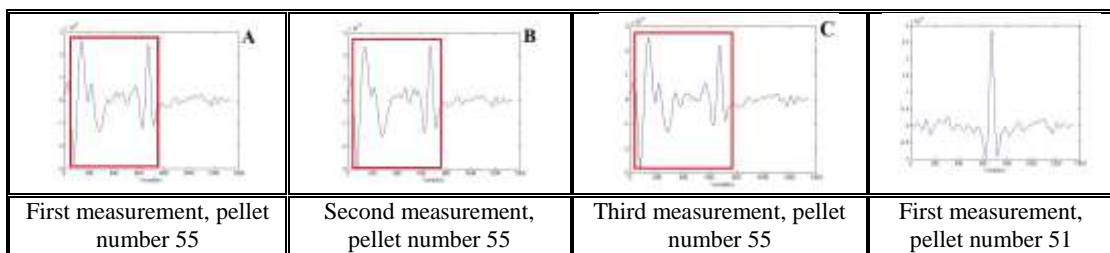
Figure 4.7 illustrates the topographical profiles obtained from the microscopic measurements for samples 51-59, LEA A. These profiles were aligned with the first measurement from pellet number 51.



**Figure 4.7: Topographical profiles obtained from the microscopic measurements for samples 51-59, LEA A**

The April 2012 sequence of pellets was among the first fired from the air pistol into the water tank. Oxidative corrosion, potentially a consequence of the pellets not being fully dried after collection, was noted on these pellets using conventional microscopy. Pellets fired after April 2012 was dried more carefully to minimise the occurrence of oxidative corrosion.

During the alignment process using Matlab®, each sample measurement (the measurement across the LEA) was assessed to examine how close the correlation was to the first measurement from the reference pellet (pellet 51 in this case) across all of the variables (where the variables are the striations mapped by the microscope in the LEA). The cross-correlation function locates the maximum correlation between two sets of variables, as previously discussed. The alignment displays a single maximum peak in the graph, as shown in Figure 4.8, if the two sets of variables correlate very well with each other. Based on Figure 4.7, all measurements were aligned with the reference measurement except for pellet number 55. Figure 4.8 shows the differences observed from the region on pellet 51 where there were two peaks present in between the variables. This pellet was excluded from PCA for LEA A.

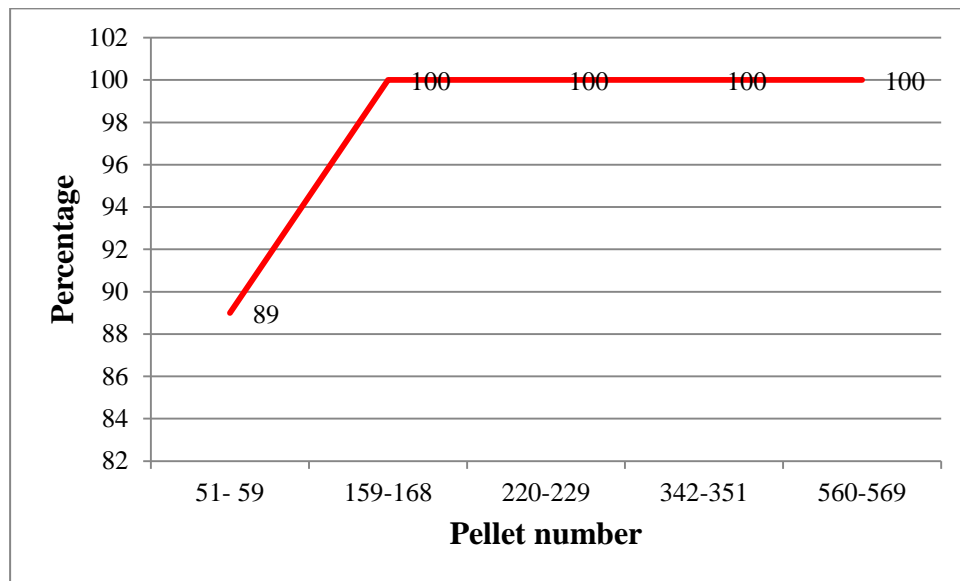


**Figure 4.8: First (A), second (B) and third (C) measurements of pellet number 55. These measurements display the presence of two peaks in between variables during alignment with the reference pellet, pellet number 51, as displayed on the last box on the right**

All 30 measurements from pellets fired at each sampling interval were aligned with each other within their groups; see Appendices 16 to 19. Table 4.5 and Figure 4.9 reveal the degree of alignment at LEA A in the repetitively fired pellets within the groups of pellets examined.

**Table 4.5: Pellets in the longitudinal study where LEA A was examined**

Pellet number	Pellet number where LEA A was imaged	Number of LEA measurements	Number of LEA measurements which were aligned
51- 60	51- 59	27	24 (89%)
159-168	159-168	30	30 (100%)
220-229	220-229	30	30 (100%)
342-351	342-351	30	30 (100%)
560-569	560-569	30	30 (100%)
<b>Total number of pellets</b>	<b>49</b>	<b>147</b>	<b>144 (98%)</b>



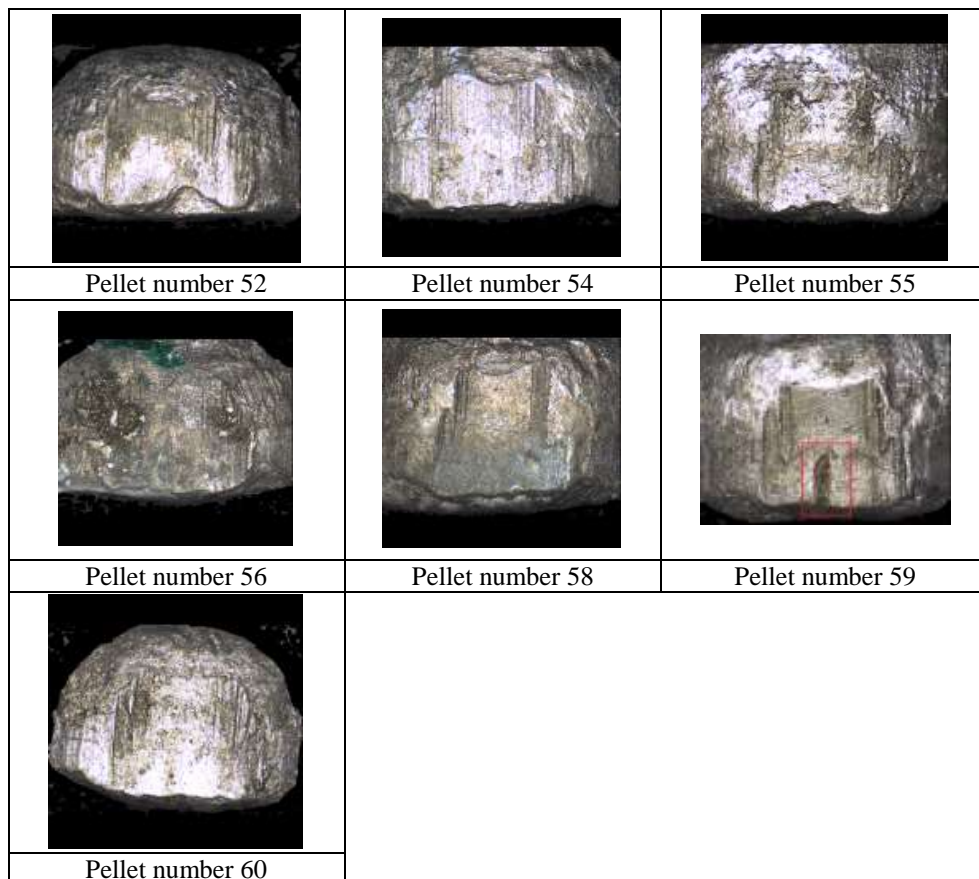
**Figure 4.9: Percentage of pellets in the longitudinal study where LEA A aligned within groups of repetitively fired pellets**

#### **4.4.2 LEA B**

A total of 150 LEA scanned images of the striated marks in region B were examined across the pellets. However the alignment within this region was quite poor overall with only 93 out of 150 measurements, or 62%, aligned.

Pellets numbered 52, 54 to 56, 58 to 60 (April 2012) are misaligned, shown in Figure 4.10, where corrosion of the surface was the main reason for misalignment.

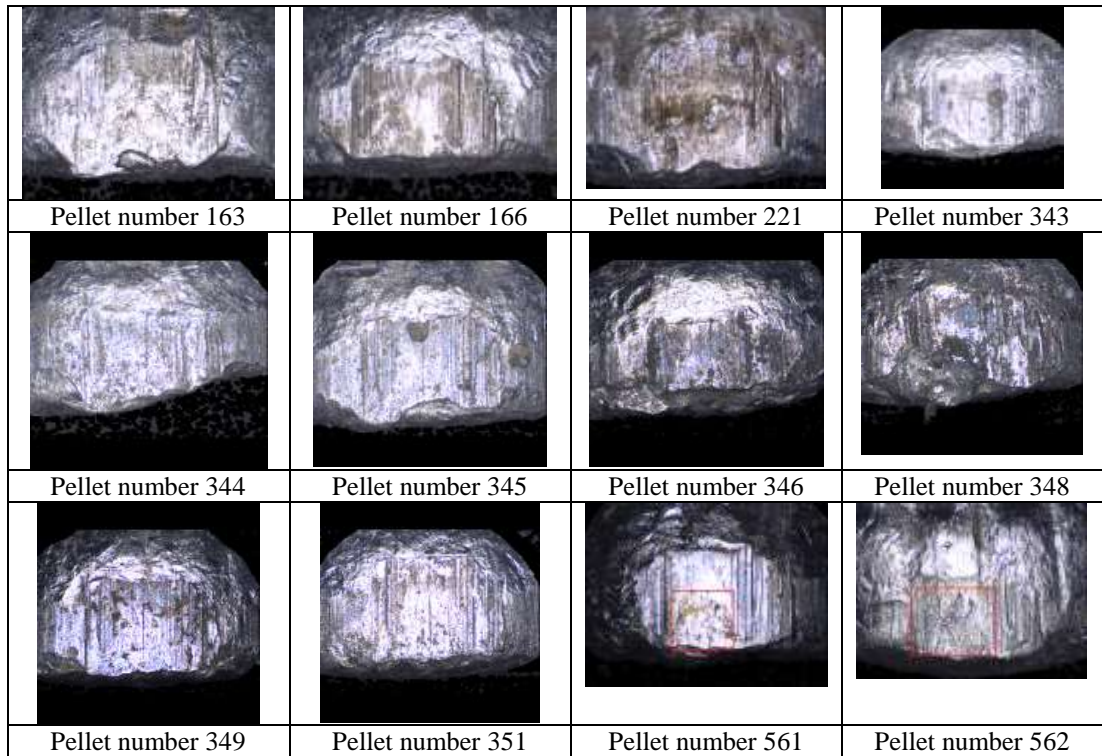
Pellet number 59 bore an additional mark which interfered with the alignment process. This mark did not appear on pellet 60. A possible explanation for this additional mark was the presence of build-up debris inside the barrel, which was then dislodged before pellet number 60 was fired.



**Figure 4.10: Misaligned pellets for LEA B from those fired in April 2012. Corrosion was the main reason for misalignment. Pellet number 59 bore an additional mark on its surface which interfered with the alignment process, as shown in the ref rectangle**

The remaining misaligned pellets are shown in Figure 4.11, numbered 163 and 166 (fired in April 2013), 221 (fired in May 2013), 343 to 346, 348, 349 and 351 (fired in June 2013) and numbered 561 and 562 which were fired in September 2013. Appendices 20 to 24 show the alignment results.



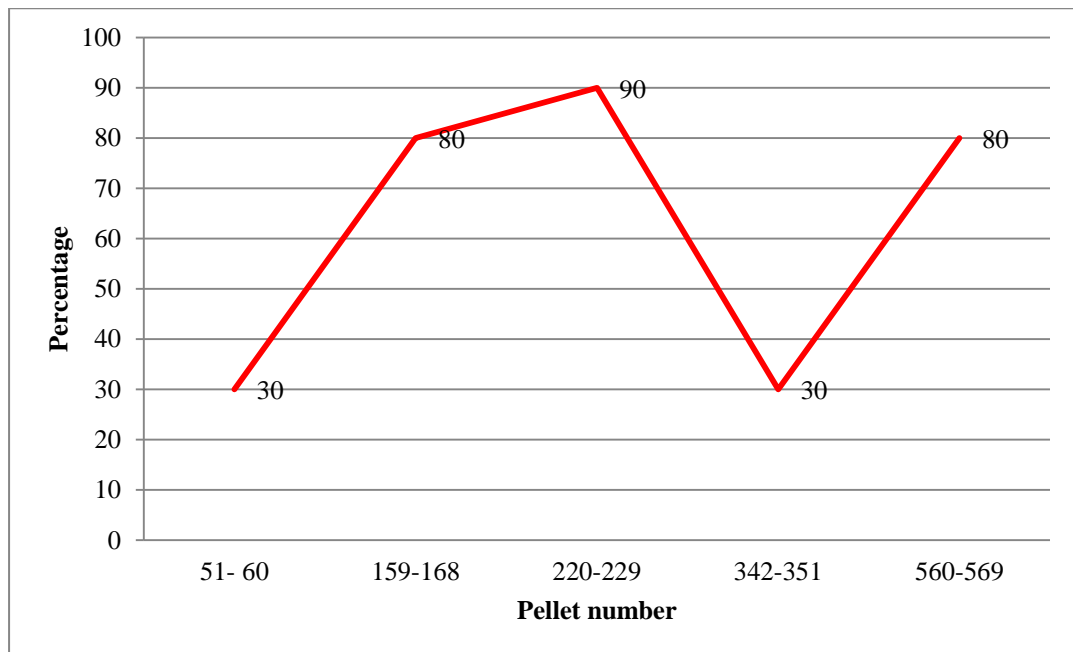


**Figure 4.11: Misaligned pellets for LEA B from those fired in April 2013. Corrosion was the main reason for misalignment however for pellets numbered 561 and 562, these pellets had additional marks (as shown in the red rectangle), most likely caused by impact with the stopper, as discussed previously**

Table 4.6 and Figure 4.12 summarised the alignment result for LEA B.

**Table 4.6: Pellets in the longitudinal study where LEA B was examined**

Pellet number	Pellet number where LEA B was imaged	Number of LEA measurements	Number of LEA measurements which were aligned
51- 60	51- 60	30	9 (30%)
159-168	159-168	30	24 (80%)
220-229	220-229	30	27 (90%)
342-351	342-351	30	9 (30%)
560-569	560-569	30	24 (80%)
<b>Total</b>	<b>50</b>	<b>150</b>	<b>93 (62%)</b>



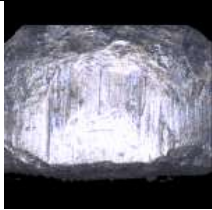


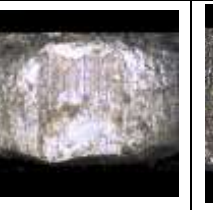









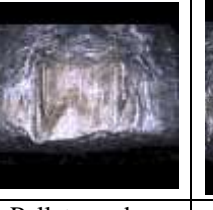







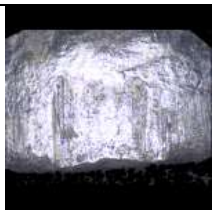


**Figure 4.12: Percentage of pellets in the longitudinal study where LEA B aligned within groups of repetitively fired pellets**

Percentage of aligned LEA B is lower than LEA A but it is not the lowest of all LEAs. Unlike LEA A with individual characteristic, as mentioned in Chapter 3, LEA B has no individual characteristic on its surface. This contributed to more pellets misalignment, as well as corrosion and additional marks, hence the lower percentage of aligned measurements.

#### **4.4.3 LEA C**

78 measurements (52%) of LEA C were aligned out of 150 measurements. Pellets numbered 51 to 60 (fired in April 2012), pellet number 163 (fired in April 2013), pellets numbered 220 to 229 (fired in May 2013) and pellets numbered 343, 348 and 351 (fired in June 2013) could not be aligned: Pellets numbered 53 to 58, 163, 220 to 229 and 343, 348 and 351 were corroded, illustrated in Figure 4.13. The rest of the pellets in the group were difficult to align because of lack of individual

characteristics in the striated regions. All measurements from the September 2013 set were aligned (Appendices 25-29 show the alignment result). There are factors which can contribute to the lack of individual characteristics on projectiles such as property of the pellet and uncleaned barrel. These pellets are made of lead, unjacketed. Lead pellets can deposit fragments of lead on the barrel. Hence, it may obscure or cause less contact between pellets and barrel [3]. When this occurs, pellets shot with the same barrel which was not cleaned since it was newly acquired, may have lack of individual characteristics on its surface.

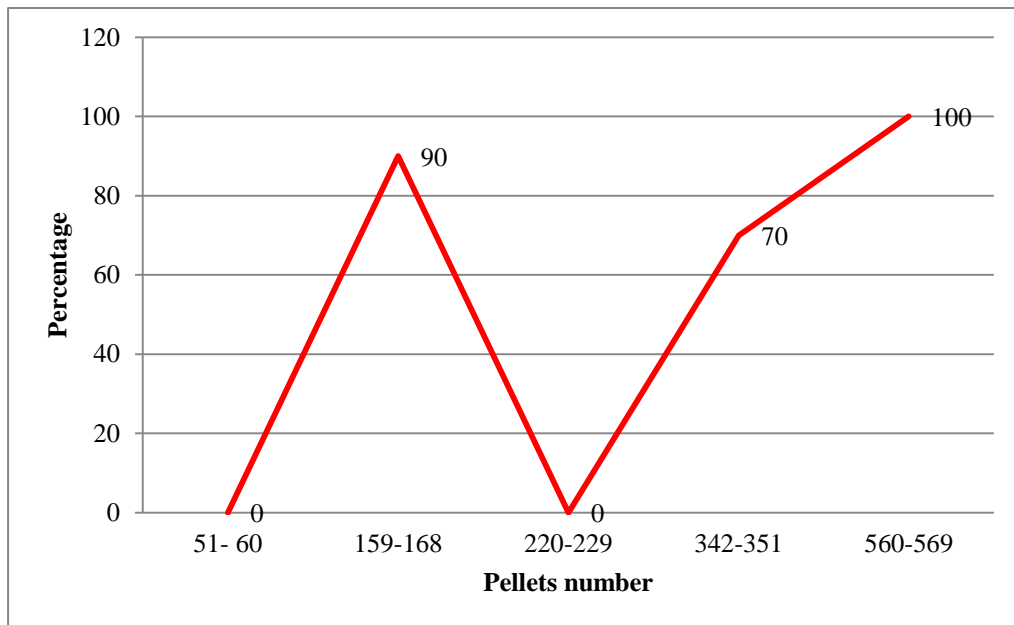
				
Pellet number 51	Pellet number 52	Pellet number 53	Pellet number 54	Pellet number 55
				
Pellet number 56	Pellet number 57	Pellet number 58	Pellet number 59	Pellet number 60
				
Pellet number 163	Pellet number 220	Pellet number 221	Pellet number 222	Pellet number 223
				
Pellet number 224	Pellet number 225	Pellet number 226	Pellet number 227	Pellet number 228
				
Pellet number 229	Pellet number 343	Pellet number 348	Pellet number 351	

**Figure 4.13: Misaligned pellets for LEA C. Pellets numbered 53 to 58, 163, 220 to 229 and 343, 348, 351 were corroded. The other pellets were misaligned because of lack of individual characteristics in striations**

Table 4.7 and Figure 4.14 show the percentage of aligned measurements.

**Table 4.7: Pellets in the longitudinal study where LEA C was examined**

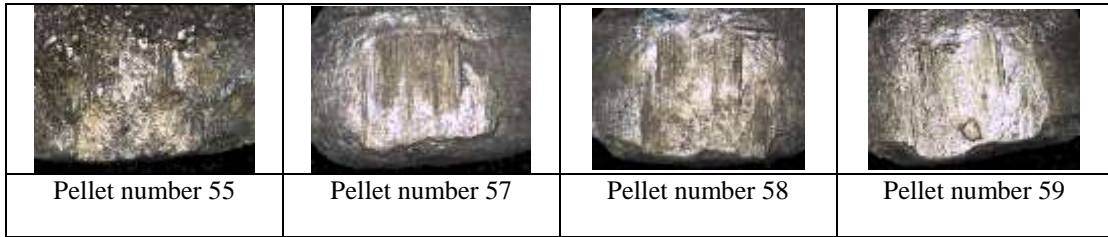
Pellet number	Pellet number where LEA C was imaged	Number of LEA measurements	Number of LEA measurements which were aligned
51- 60	51- 60	30	0 (0%)
159-168	159-168	30	27 (90%)
220-229	220-229	30	0 (0%)
342-351	342-351	30	21 (70%)
560-569	560-569	30	30 (100%)
<b>Total number of pellets</b>	<b>50</b>	<b>150</b>	<b>78 (52%)</b>



**Figure 4.14: Percentage of pellets in the longitudinal study where LEA C aligned within groups of repetitively fired pellets**

#### 4.4.4 LEA D

92% of measurements of LEA D across 49 pellets could be aligned. For the April 2012 set, four pellets (pellets numbered 55, 57, 58 and 59) were corroded and shown in Figure 4.15. All measurements for the other pellets were aligned. Appendices 30 to 34 show the alignment results.

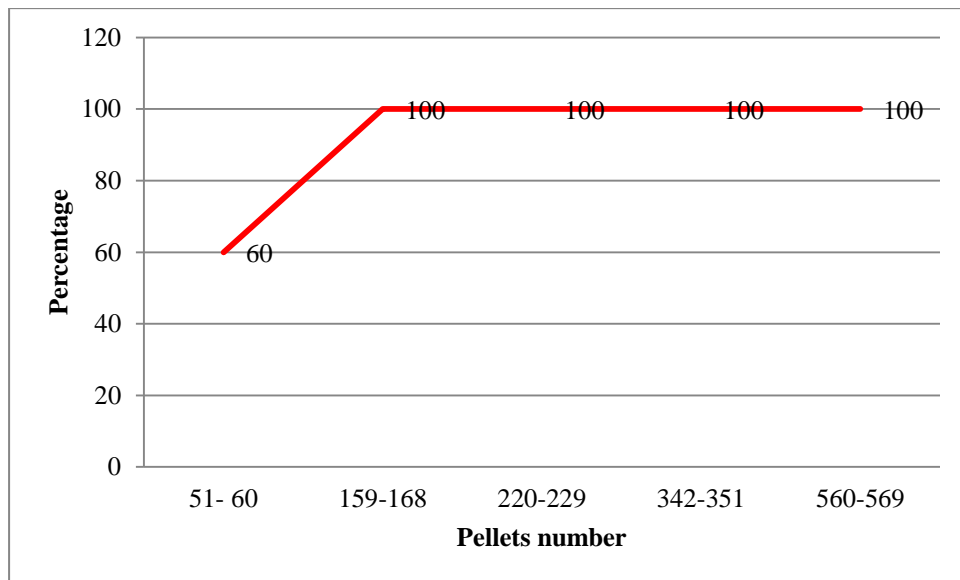


**Figure 4.15: Misaligned pellets for LEA D, shot in April 2012, due to corrosion**

Table 4.8 and Figure 4.16 show the percentage of aligned measurements for LEA D.

**Table 4.8: Pellets in the longitudinal study where LEA D was examined**

Pellet number	Pellet number where LEA D was imaged	Number of LEA measurements	Number of LEA measurements which were aligned
51- 60	51- 60	30	18 (60%)
159-168	159-168	30	30 (100%)
220-229	220-229	30	30 (100%)
342-351	342-351	27	27 (100%)
560-569	560-569	30	30 (100%)
<b>Total number of pellets</b>	<b>49</b>	<b>147</b>	<b>135 (92%)</b>



**Figure 4.16: Percentage of pellets in the longitudinal study where LEA D aligned within groups of repetitively fired pellets**

#### 4.4.5 LEA E

68% of measurements of LEA E were aligned across 47 pellets (141 measurements). Pellets numbered 53, 57 and 58 (fired in April 2012), pellets numbered 160, 162 and 166 (fired in April 2013) and all pellets from the June 2013, could not be aligned due to corrosion, presented in Figure 4.17. All measurements from the May and September 2013 set were aligned. Appendices 35 to 39 show the alignment result.

Table 4.9 and Figure 4.18 show the percentage of aligned measurements for LEA E.

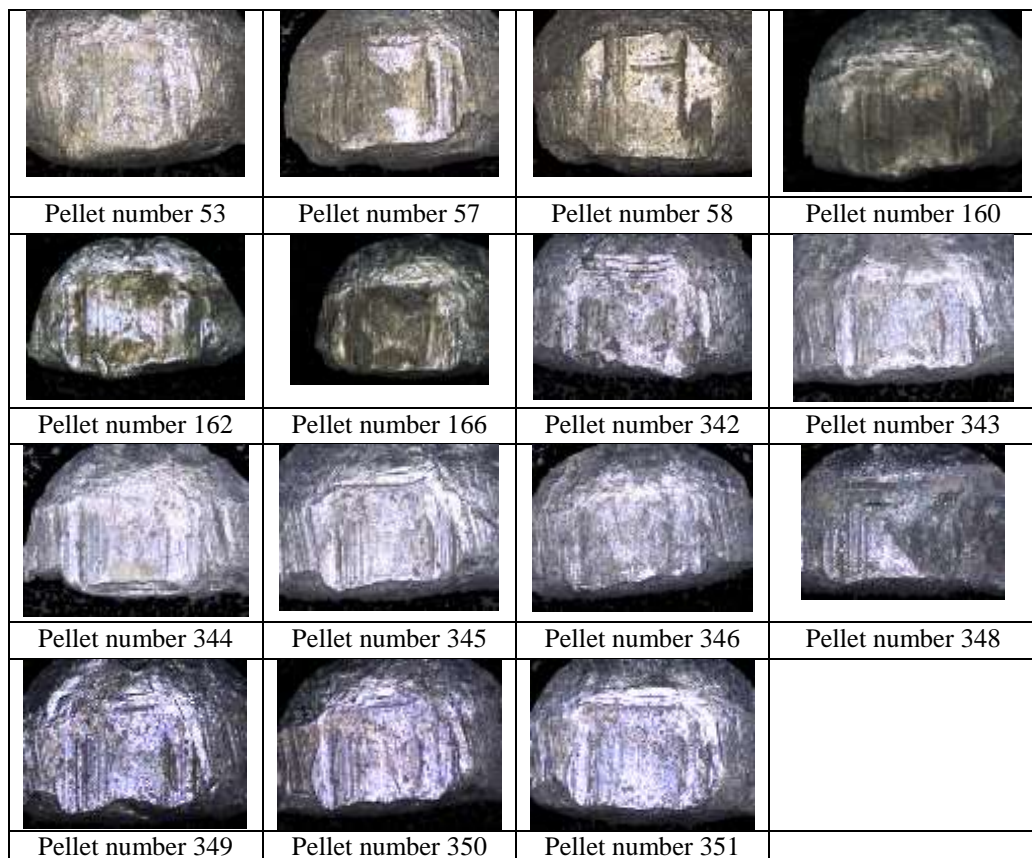
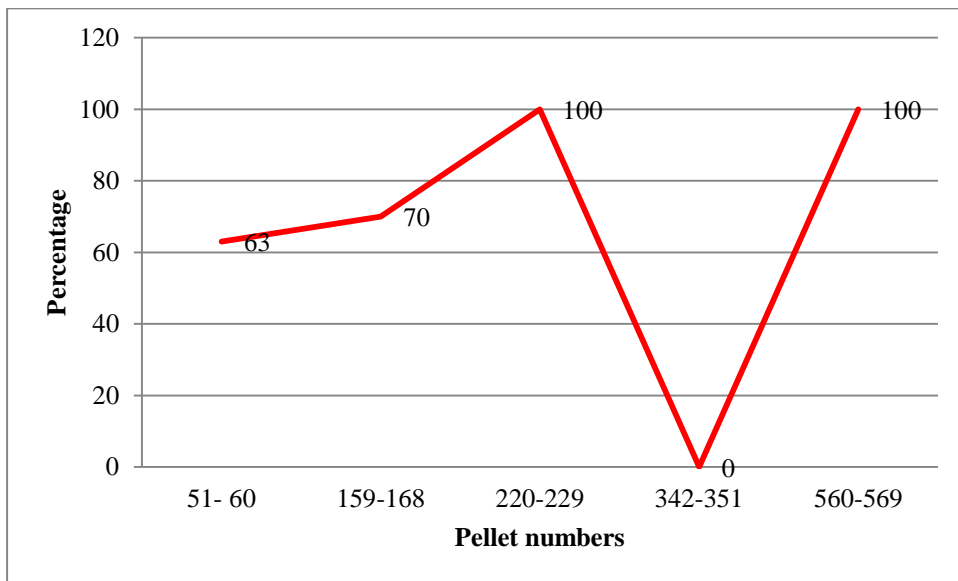


Figure 4.17: Misaligned pellets for LEA E due to corrosion

**Table 4.9: Pellets in the longitudinal study where LEA E was examined**

Pellet number	Pellet number where LEA E was imaged	Number of LEA measurements	Number of LEA measurements which were aligned
51- 60	51- 60	24	15 (63%)
159-168	159-168	30	21 (70%)
220-229	220-229	30	30 (100%)
342-351	342-351	27	0 (0%)
560-569	560-569	30	30 (100%)
<b>Total number of pellets</b>	<b>47</b>	<b>141</b>	<b>96 (68%)</b>


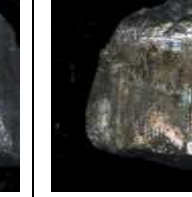


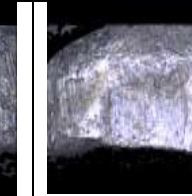

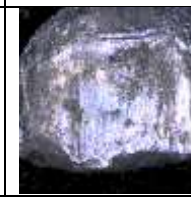

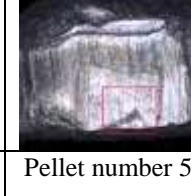


**Figure 4.18: Percentage of pellets in the longitudinal study where LEA E aligned within groups of repetitively fired pellets**

#### **4.4.6 LEA F**

81 measurements for LEA F were aligned (57%). Figure 4.19 presents the pellets which were misaligned, numbered 52, 53 and 59 (fired in April 2012), pellets numbered 162 and 166 (fired in April 2013), all of the pellets fired in June 2013 and pellets numbered 561 to 564, 566 and 569 (fired in September 2013). All measurements from the May 2013 set were aligned. Appendices 40 to 44 show the result of alignment.



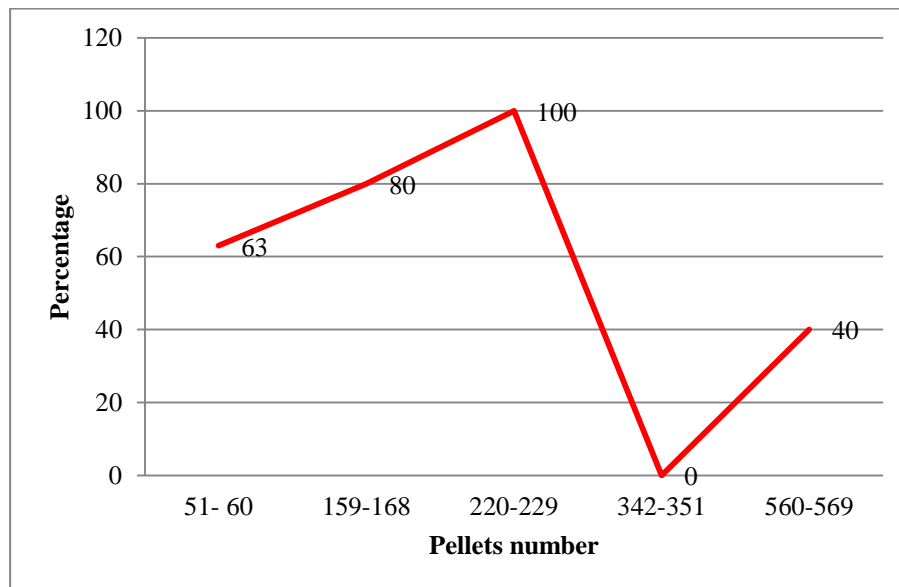
				
Pellet number 52	Pellet number 53	Pellet number 59	Pellet number 162	Pellet number 166
				
Pellet number 342	Pellet number 343	Pellet number 344	Pellet number 345	Pellet number 346
				
Pellet number 347	Pellet number 348	Pellet number 349	Pellet number 350	Pellet number 351
				
Pellet number 561	Pellet number 562	Pellet number 563	Pellet number 564	Pellet number 566
				
		Pellet number 569		

**Figure 4.19: Misaligned pellets for LEA F because of corrosion, except for pellets numbered 561 to 569 due to additional marks on their surfaces**

Table 4.10 and Figure 4.20 show the percentage of aligned measurements for LEA F.

**Table 4.10: Pellets in the longitudinal study where LEA F was examined**

Pellet number	Pellet number where LEA F was imaged	Number of LEA measurements	Number of LEA measurements which were aligned
51- 60	51- 60	24	15 (63%)
159-168	159-168	30	24 (80%)
220-229	220-229	30	30 (100%)
342-351	342-351	27	0 (0%)
560-569	560-569	30	12 (40%)
<b>Total number of pellets</b>	<b>47</b>	<b>141</b>	<b>81 (57%)</b>

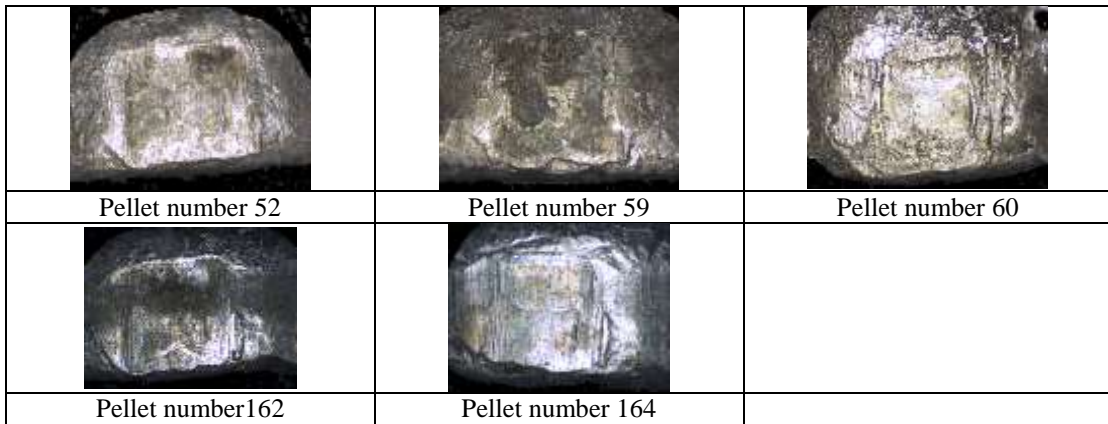


**Figure 4.20: Percentage of pellets in the longitudinal study where LEA F aligned within groups of repetitively fired pellets**

#### 4.4.7 LEA G

90% of the 49 pellets were aligned for LEA G. Figure 4.21 presents the misaligned pellets which were numbers 52, 59 and 60 (fired in April 2012) and pellets numbered 162 and 164 (fired in April 2013). All measurements from the May, June

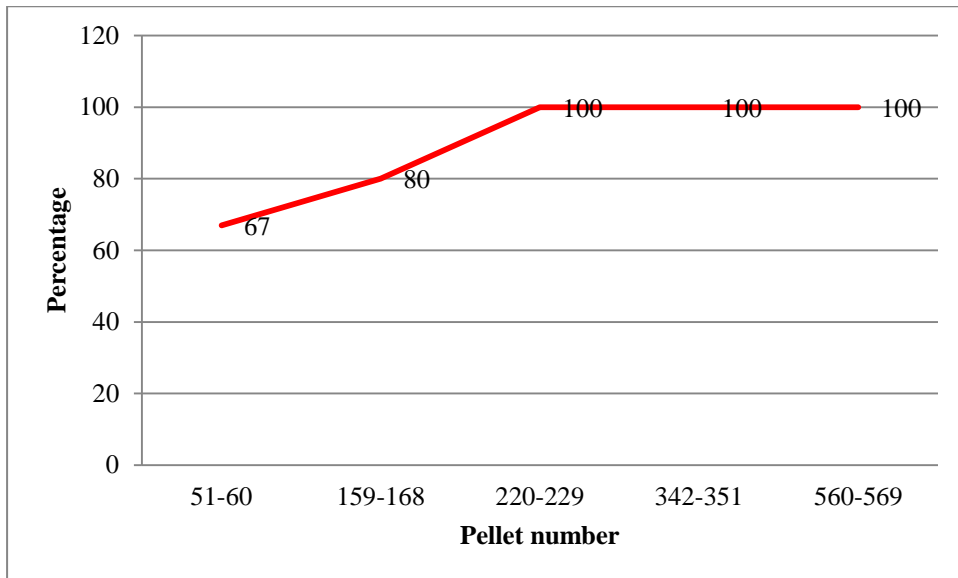
and September 2013 sets were aligned. Appendices 45 to 49 show the alignment results. The results are summarised in Table 4.11 and Figure 4.22.



**Figure 4.21: Misaligned pellets for LEA G due to corrosion**

**Table 4.11: Pellets in the longitudinal study where LEA G was examined**

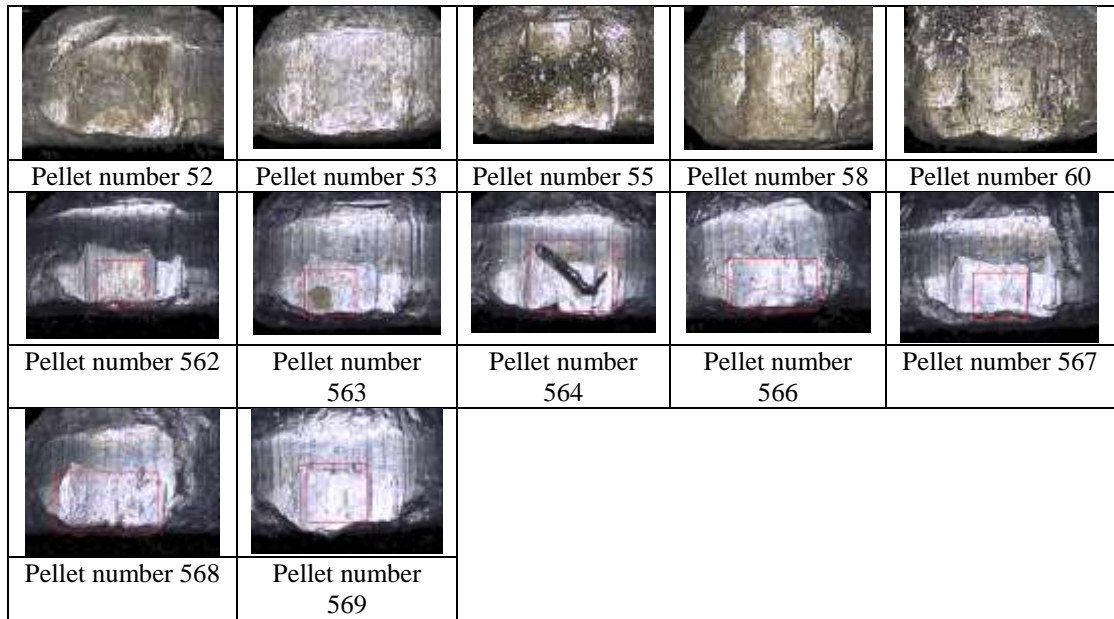
Pellet number	Pellet number where LEA G was imaged	Number of LEA measurements	Number of LEA measurements which were aligned
51- 60	51- 60	27	18 (67%)
159-168	159-168	30	24 (80%)
220-229	220-229	30	30 (100%)
342-351	342-351	30	30 (100%)
560-569	560-569	30	30 (100%)
<b>Total number of pellets</b>	<b>49</b>	<b>147</b>	<b>132 (90%)</b>



**Figure 4.22: Percentage of pellets in the longitudinal study where LEA G aligned within groups of repetitively fired pellets**

#### **4.4.8 LEA H**

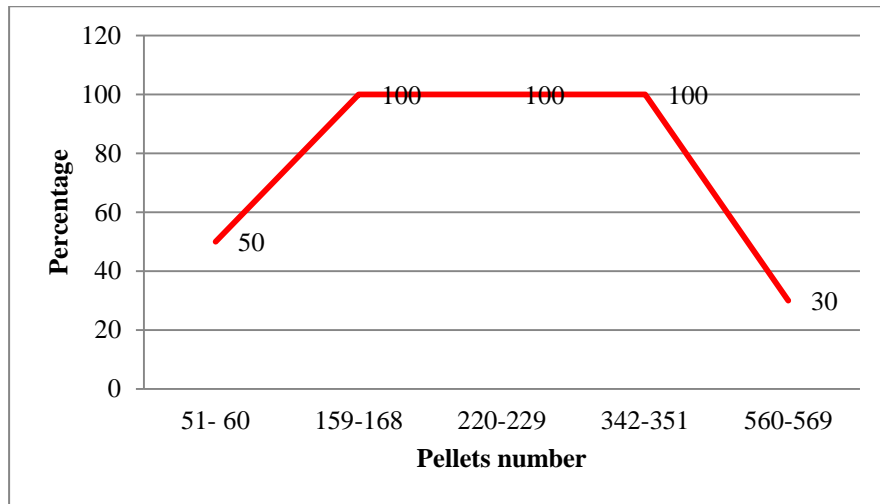
For LEA H, 150 measurements were analysed and 76% were aligned across the different groups. Figure 4.23 presents the misaligned pellets numbered 52, 53, 55, 58 and 60 (fired in April 2012), and pellets numbered 562, 563, 564 and 566 to 569 (fired in September 2013). All measurements from the April, May and June 2013 were aligned. Appendices 50 to 54 show the alignment results and summarised in Table 4.12 and Figure 4.24.



**Figure 4.23: Misaligned pellets for LEA H. Pellets shot in April 2012 were oxidised. Pellets numbered 562 to 564 and 566 to 569 bore additional marks on their surfaces as shown in the red rectangle**

**Table 4.12: Pellets in the longitudinal study where LEA H was examined**

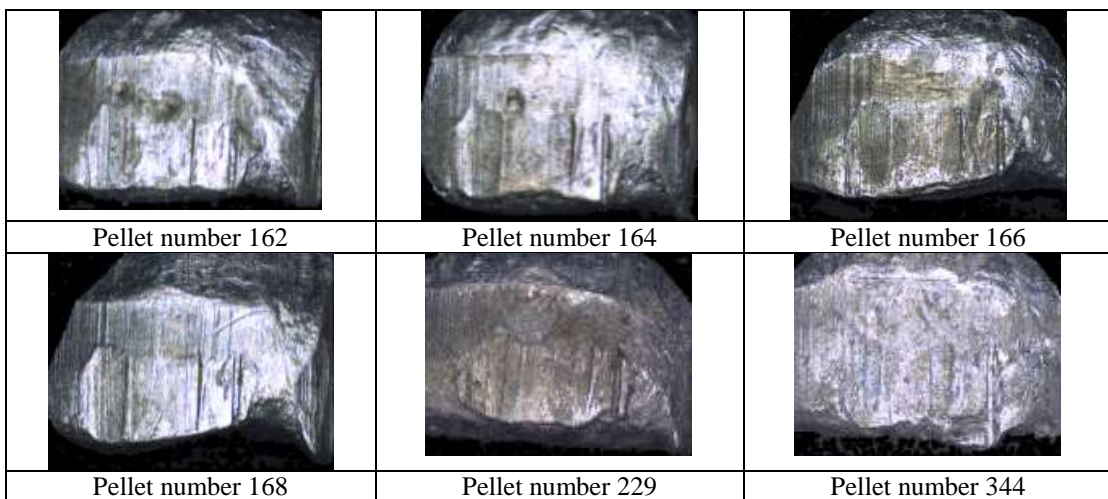
Pellet number	Pellet number where LEA H was imaged	Number of LEA measurements	Number of LEA measurements which were aligned
51- 60	51- 60	30	15 (50%)
159-168	159-168	30	30 (100%)
220-229	220-229	30	30 (100%)
342-351	342-351	30	30 (100%)
560-569	560-569	30	9 (30%)
<b>Total number of pellets</b>	<b>50</b>	<b>150</b>	<b>114 (76%)</b>



**Figure 4.24: Percentage of pellets in the longitudinal study where LEA H aligned within groups of repetitively fired pellets**

#### 4.4.9 LEA I

87% of 47 pellets were aligned at LEA I. Misaligned pellets (Figure 4.25) were numbered 162, 164, 166 and 168 (fired in April 2013), number 229 (fired in May 2013) and number 344 (fired in June 2013). For the April 2012 and September 2013 sets of pellets, all measurements were aligned.

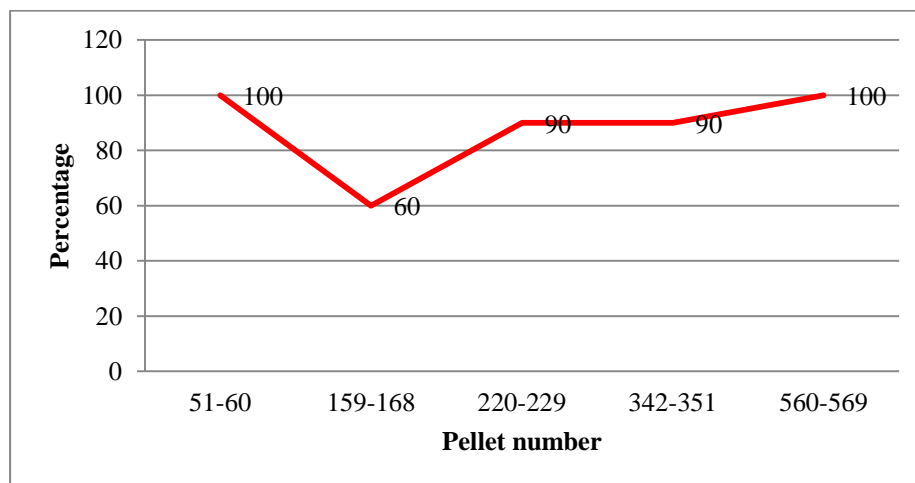


**Figure 4.25: Misaligned pellets for LEA I due to corrosion**

Appendices 55 to 59 show the alignment results and Table 4.13 and Figure 4.26 summarise the data.

**Table 4.13: Pellets in the longitudinal study where LEA I was examined**

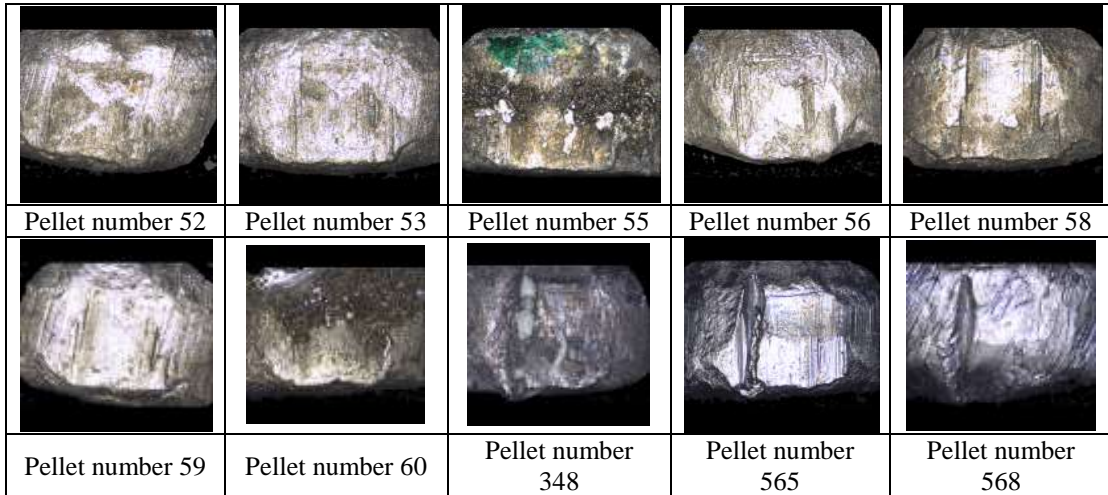
Pellet number	Pellet number where LEA I was imaged	Number of LEA measurements	Number of LEA measurements which were aligned
51- 60	51- 60	24	24 (100%)
159-168	159-168	30	18 (60%)
220-229	220-229	30	27 (90%)
342-351	342-351	30	27 (90%)
560-569	560-569	27	27 (100%)
<b>Total number of pellets</b>	<b>47</b>	<b>141</b>	<b>123 (87%)</b>



**Figure 4.26: Percentage of pellets in the longitudinal study where LEA I aligned within groups of repetitively fired pellets**

#### 4.4.10 LEA J

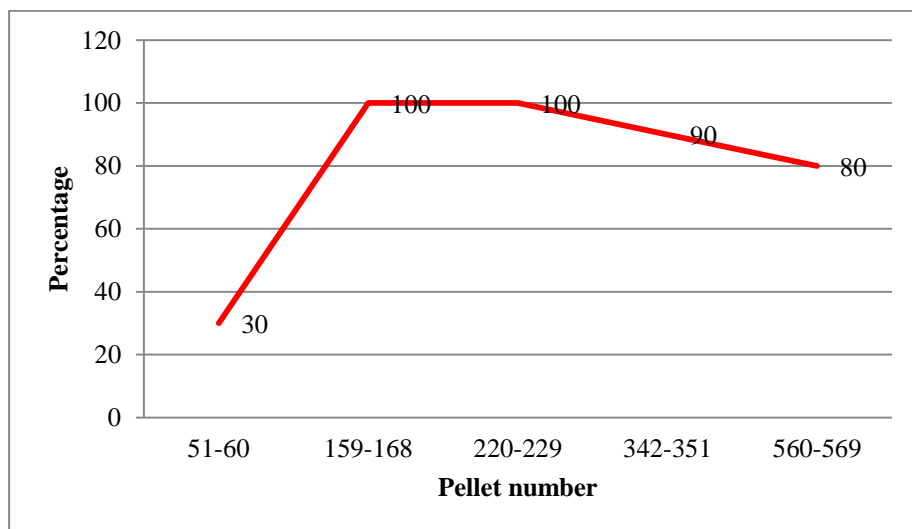
50 pellets were scanned at LEA J resulting in 80% alignment. Figure 4.27 presents the misaligned pellets numbered 52, 53, 55, 56 and 58 to 60 (fired in April 2012), number 348 (fired in June 2013) and numbered 565 and 568 (fired in September 2013). All measurements from the April and May 2013 pellets were aligned. Appendices 60 to 64 show the alignment results which are summarised in Table 4.14 and Figure 4.28.



**Figure 4.27: Misaligned pellets for LEA J. Pellets shot in April 2012 and June 2013 were corroded**

**Table 4.14: Pellets in the longitudinal study where LEA J was examined**

Pellet number	Pellet number where LEA J was imaged	Number of LEA measurements	Number of LEA measurements which were aligned
51- 60	51- 60	30	9 (30%)
159-168	159-168	30	30 (100%)
220-229	220-229	30	30 (100%)
342-351	342-351	30	27 (90%)
560-569	560-569	30	24 (80%)
<b>Total number of pellets</b>	<b>50</b>	<b>150</b>	<b>120 (80%)</b>

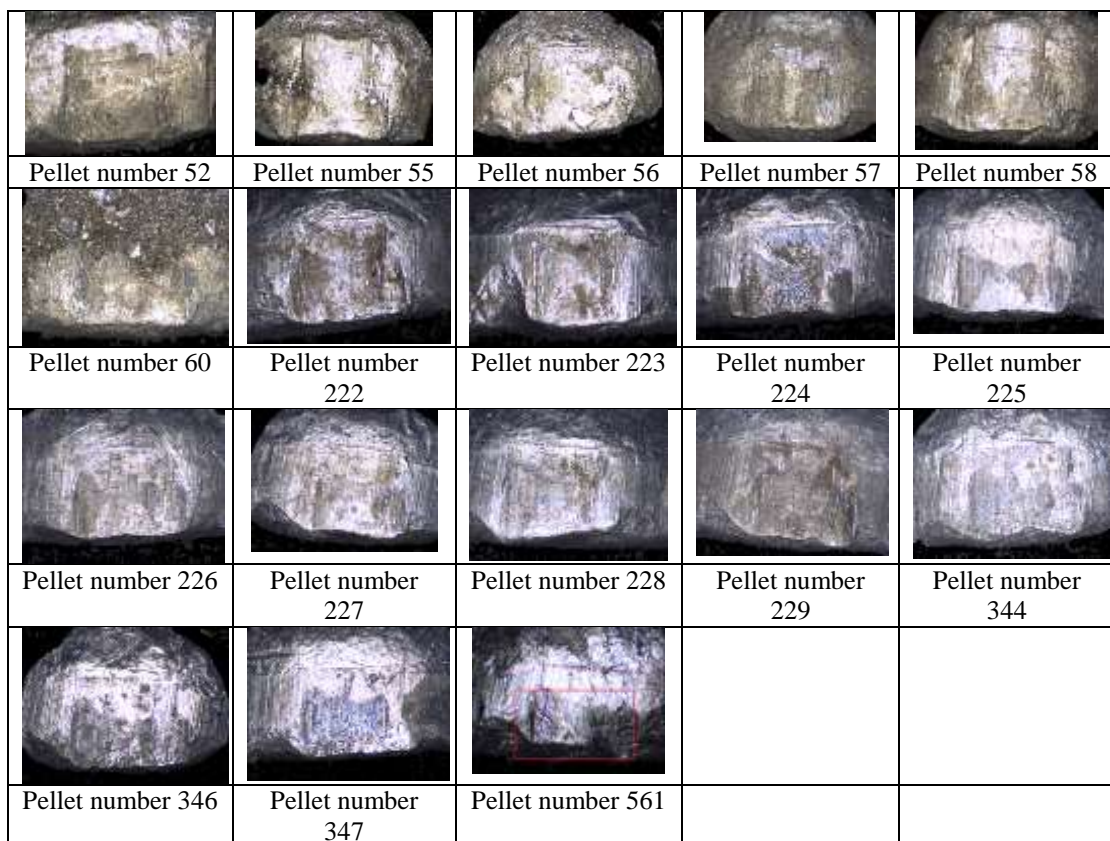


**Figure 4.28: Percentage of pellets in the longitudinal study where LEA J aligned within groups of repetitively fired pellets**



#### 4.4.11 LEA K

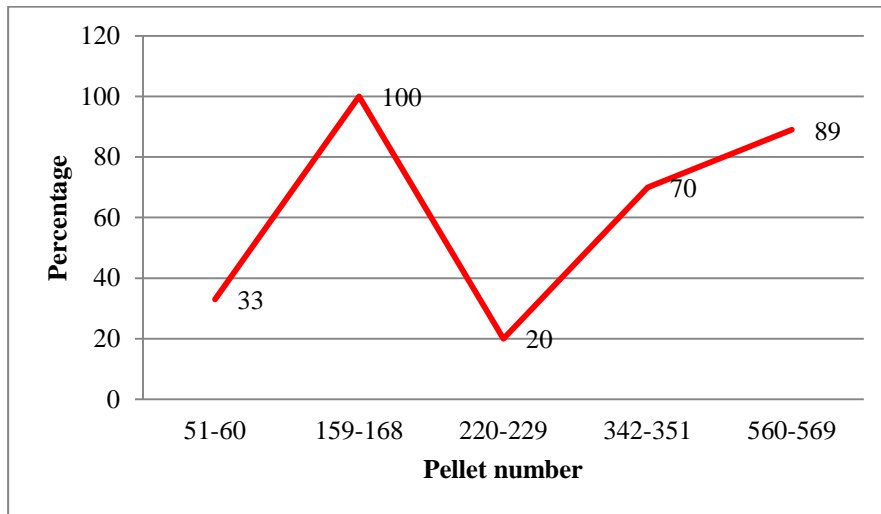
A total of 144 measurements of LEA K were analysed. Misaligned pellets (Figure 4.29) were numbered 52 and 55 to 60 (fired in April 2012), numbered 222 to 229 (fired in May 2013), numbered 344, 346 and 347 (fired in June 2013) and pellet number 561 (fired in September 2013). All measurements for the April 2013 set were aligned. Appendices 65 to 69 illustrate the alignment results. In summary, as shown in Table 4.15 and Figure 4.30, 63% of measurements of LEA K were aligned.



**Figure 4.29: Misaligned pellets for LEA K due to corrosion, except for pellet number 561 which bore additional marks on its surface as in the red rectangle**

**Table 4.15: Pellets in the longitudinal study where LEA K was examined**

Pellet number	Pellet number where LEA K was imaged	Number of LEA measurements	Number of LEA measurements which were aligned
51- 60	51- 60	27	9 (33%)
159-168	159-168	30	30 (100%)
220-229	220-229	30	6 (20%)
342-351	342-351	30	21 (70%)
560-569	560-569	27	24 (89%)
<b>Total number of pellets</b>	<b>48</b>	<b>144</b>	<b>90 (63%)</b>



**Figure 4.30: Percentage of pellets in the longitudinal study where LEA K aligned within groups of repetitively fired pellets**

#### **4.4.12 LEA L**

A total of 147 measurements were analysed for LEA L but only 45% alignment was achieved. Misaligned (Figure 4.31) pellets were those numbered 52 to 60 (fired in April 2012), numbered 164, 165 and 167 (fired in April 2013), numbered 223 to 228 (fired in May 2013), numbered 346 to 351 (fired in June 2015) and pellets numbered 561, 563 and 568 (fired in September 2015) are summarised in Appendices 70 to 74, Table 4.16 and Figure 4.32.

				
Pellet number 52	Pellet number 53	Pellet number 54	Pellet number 55	Pellet number 56
				
Pellet number 57	Pellet number 58	Pellet number 59	Pellet number 60	Pellet number 164
				
Pellet number 165	Pellet number 167	Pellet number 223	Pellet number 224	Pellet number 225
				
Pellet number 226	Pellet number 227	Pellet number 228	Pellet number 346	Pellet number 347
				
Pellet number 348	Pellet number 349	Pellet number 350	Pellet number 351	Pellet number 561
				
Pellet number 563	Pellet number 568			

**Figure 4.31: Misaligned pellets for LEA L. Corrosion were the main reason except for pellets numbered 561, 563 and 568 with additional marks on their surface. The green mark on pellet number 228 is because of marking done for identification purpose, as explained in previous chapter**

**Table 4.16: Pellets in the longitudinal study where LEA L was examined**

Pellet number	Pellet number where LEA L was imaged	Number of LEA measurements	Number of LEA measurements which were aligned
51- 60	51- 60	30	3 (10%)
159-168	159-168	27	18 (67%)
220-229	220-229	30	12 (40%)
342-351	342-351	30	12 (40%)
560-569	560-569	30	21 (70%)
<b>Total number of pellets</b>	<b>49</b>	<b>147</b>	<b>66 (45%)</b>



**Figure 4.32: Percentage of pellets in the longitudinal study where LEA L aligned within groups of repetitively fired pellets**

#### 4.4.13 Summary of data

A total of 50 pellets across a 17 month time frame were analysed. Out of a possible 1755 scanned images, alignment was achieved for 1272 measurements as presented in Table 4.17.

**Table 4.17: Summary of the number of aligned measurements according to LEAs**

LEAs (A to L)	Number of scanned images	Number of LEA measurements	Number of aligned measurements	Percentage of aligned measurements (%)
A	49	147	144	98
B	50	150	93	62
C	50	150	78	52
D	49	147	135	92
E	47	141	96	68
F	47	141	81	57
G	49	147	132	90
H	50	150	114	76
I	47	141	123	87
J	50	150	120	87
K	48	144	90	63
L	50	150	66	45
<b>Total</b>	<b>585</b>	<b>1755</b>	<b>1272</b>	<b>Average: 73%</b>

Corrosion of the LEA was the main reason why measurements could not be aligned, however in some cases additional marks on the surface of the pellets were observed which also affected the outcome of the alignment process. Research suggests that such added marks could occur as a result of the material that the projectiles may have been fired through, such as clothing [19], ballistic gel or skin [3, 20, 21] or through the accumulation of lead deposits from projectiles within the barrel or general wear and tear [3-5].

**Table 4.18: Summary of the percentage of aligned measurements according to months of shooting**

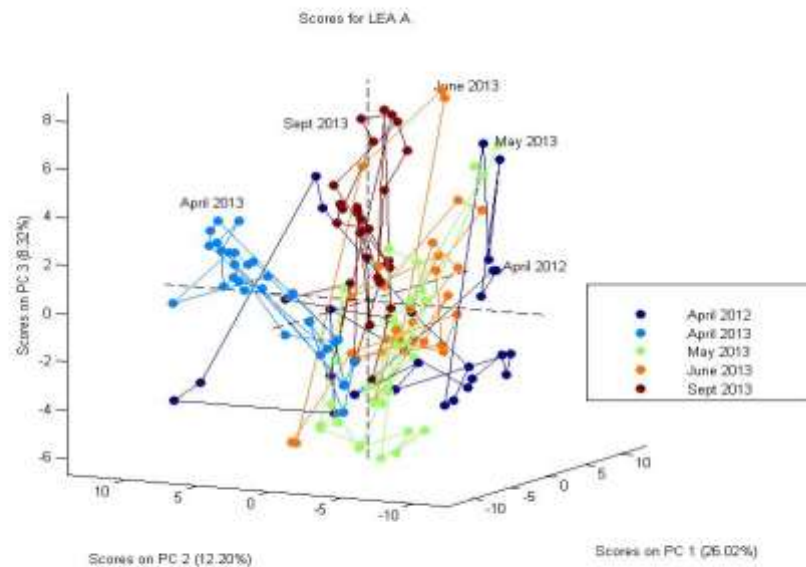
LEA/ Percentage of aligned measurements in months	April 2012	April 2013	May 2013	June 2013	September 2013	Total aligned percentage
A	89	100	100	100	100	98
B	30	80	90	30	80	62
C	0	90	0	70	100	52
D	60	100	100	100	100	92
E	63	70	100	0	100	68
F	63	80	100	0	40	57
G	67	80	100	100	100	90
H	50	100	100	100	30	76
I	100	60	90	90	100	87
J	30	100	100	90	80	80
K	33	100	20	70	89	63
L	10	67	40	40	70	45
<b>Average aligned percentage</b>	50%	86%	78%	66%	82%	73%

Table 4.18 summarises the percentage of aligned measurements according to when in the sequence the pellets were fired. The April 2012 set has the lowest average of successful alignment because of corrosion of the pellets and this is most likely due to the methodology used to dry and store the pellets. Pellets gathered after this period generally aligned much better across the test fire sequence, with more than 50% of aligned measurements.

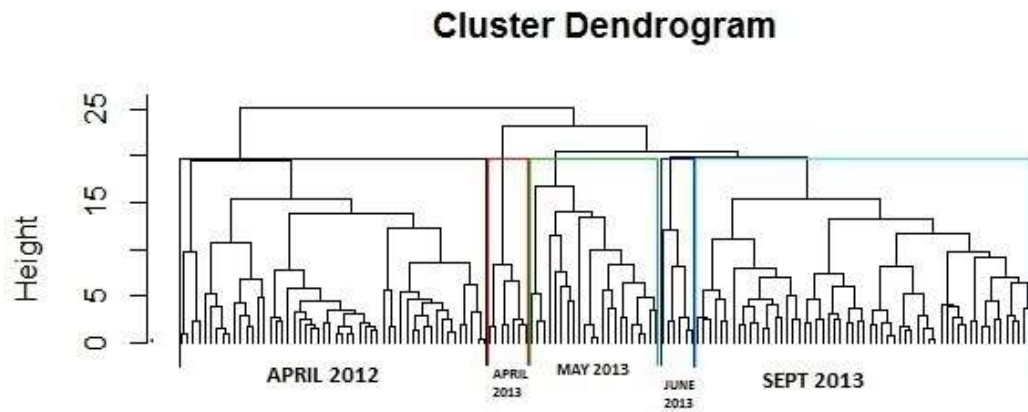
#### 4.5 PCA, HCA and LDA results

The analysis was undertaken using Matlab® and PLS\_Toolbox® as discussed in Chapter 2. In each case, for the PCA results, the colour represents a group of pellets fired at the same time, and each dot represents the triplicate measurements.

The analysis of the data presents the changes in the topography of the striation marks within the various LEAs that have occurred as the projectiles were fired through the weapon. Initially all of the data was included in the analysis for each LEA, followed by the LEAs where only 90% alignment was achieved.



**Figure 4.33: The PCA results for LEA A where 144 measurements were evaluated**



**Figure 4.34: The HCA results for LEA A**

**Table 4.19: The LDA classification table of LEA A. The diagonal values (in bold) represent correctly classified LEAs**

Months of shooting	April 2012	April 2013	May 2013	June 2013	Sept 2013	Percentage of classification
April 2012	<b>14</b>	1	5	4	0	58.3
April 2013	0	<b>29</b>	1	0	0	96.7
May 2013	2	2	<b>23</b>	3	0	76.7
June 2013	1	0	6	<b>23</b>	0	76.7
Sept 2013	2	0	0	4	<b>24</b>	80.0

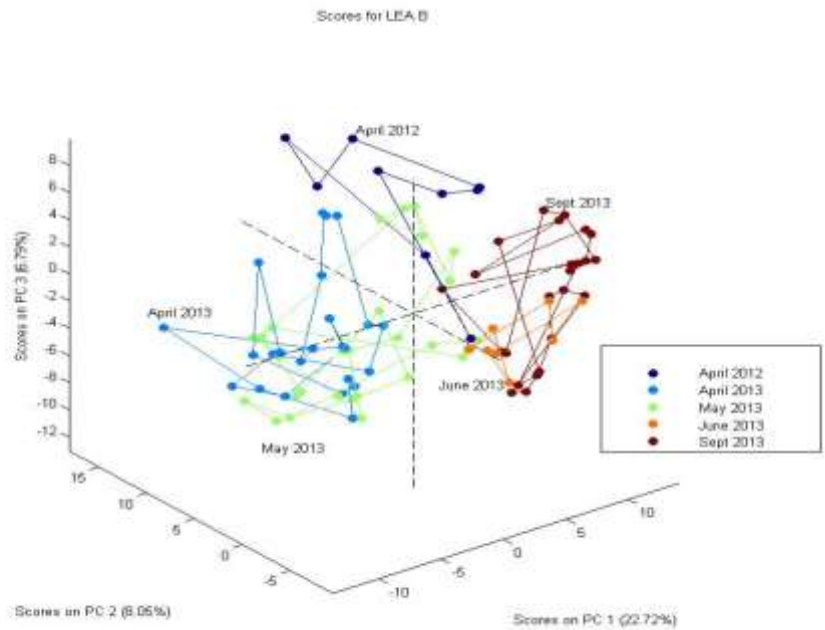


Figure 4.35: The PCA results for LEA B where 93 measurements were evaluated

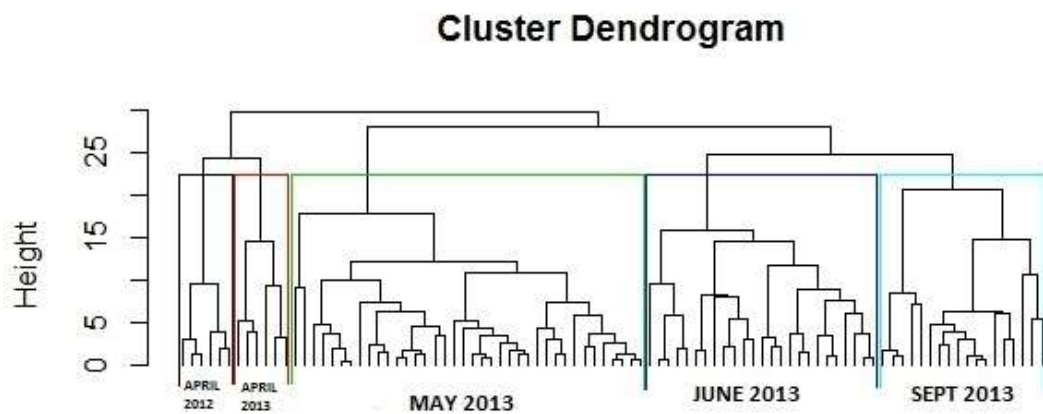


Figure 4.36: The HCA results for LEA B



Table 4.20: The LDA classification table of LEA B. The diagonal values (in bold) represent correctly classified LEAs

Months of shooting	April 2012	April 2013	May 2013	June 2013	Sept 2013	Percentage of classification
April 2012	7	0	0	0	2	77.8
April 2013	1	<b>14</b>	9	0	0	58.3
May 2013	0	6	<b>20</b>	1	0	74.1
June 2013	0	0	1	<b>8</b>	0	88.9
Sept 2013	1	0	0	0	<b>23</b>	95.8

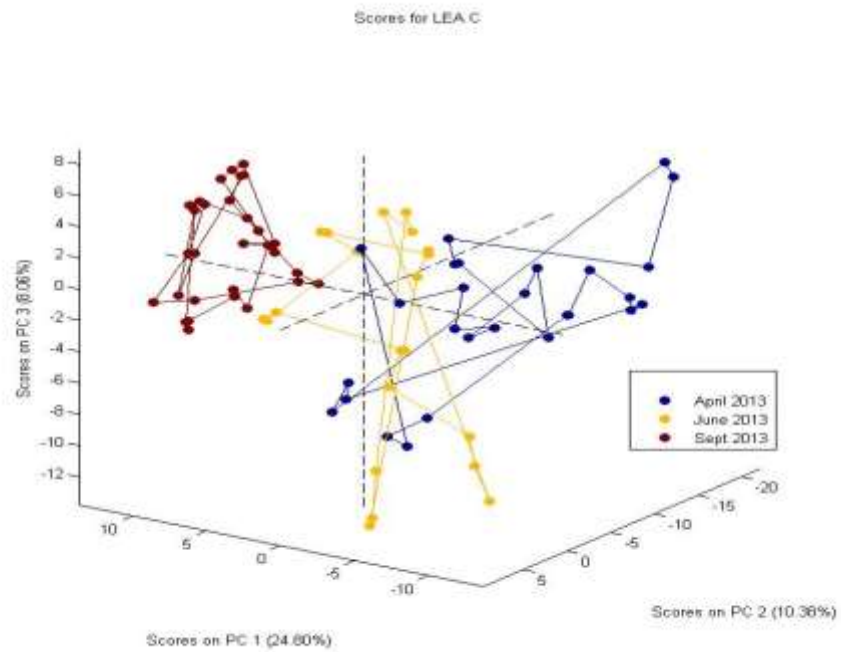
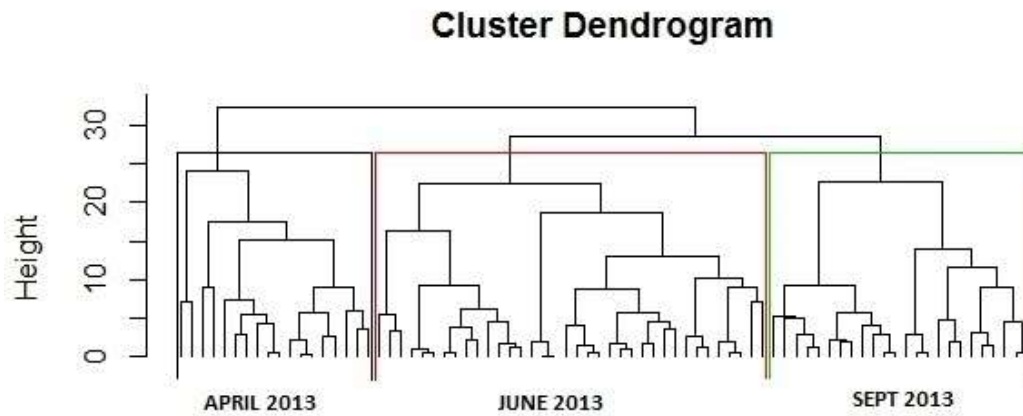


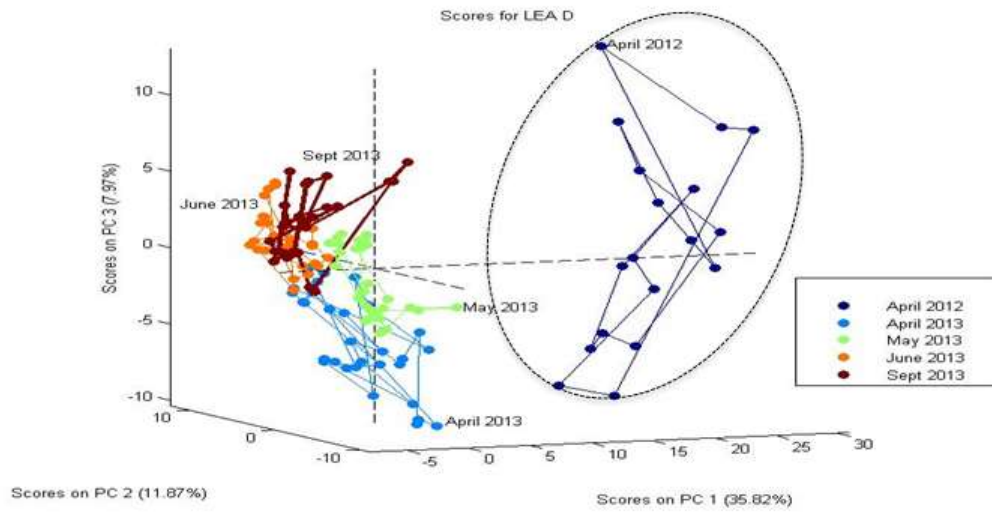
Figure 4.37: The PCA results for LEA C where 78 measurements were evaluated



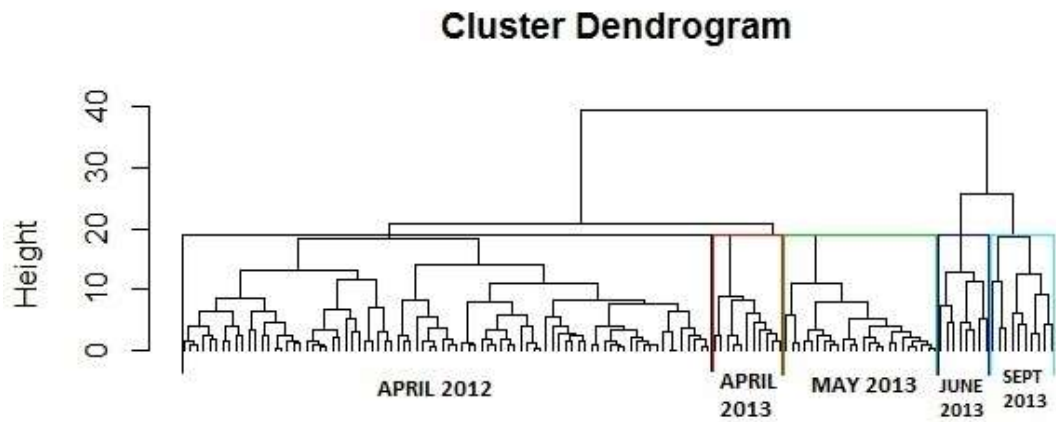
**Figure 4.38: The HCA results for LEA C**

**Table 4.21: The LDA classification table of LEA C. The diagonal values (in bold) represent correctly classified LEAs**

Months of shooting	April 2013	June 2013	Sept 2013	Percentage of classification
<b>April 2013</b>	<b>20</b>	6	1	74.1
<b>June 2013</b>	3	<b>18</b>	0	85.7
<b>Sept 2013</b>	0	0	<b>30</b>	100.0



**Figure 4.39: The PCA results for LEA D where 135 measurements were evaluated. The April 2012 striated marks in this region were distinguishable from all others**



**Figure 4.40: The HCA result for LEA D**

Table 4.22: The LDA classification table of LEA D. The diagonal values (in bold) represent correctly classified LEAs

Months of shooting	April 2012	April 2013	May 2013	June 2013	Sept 2013	Percentage of classification
April 2012	<b>18</b>	0	0	0	0	100.0
April 2013	0	<b>28</b>	0	0	2	93.3
May 2013	0	0	<b>30</b>	0	0	100.0
June 2013	0	2	0	<b>25</b>	0	92.6
Sept 2013	0	0	0	0	<b>30</b>	100.0

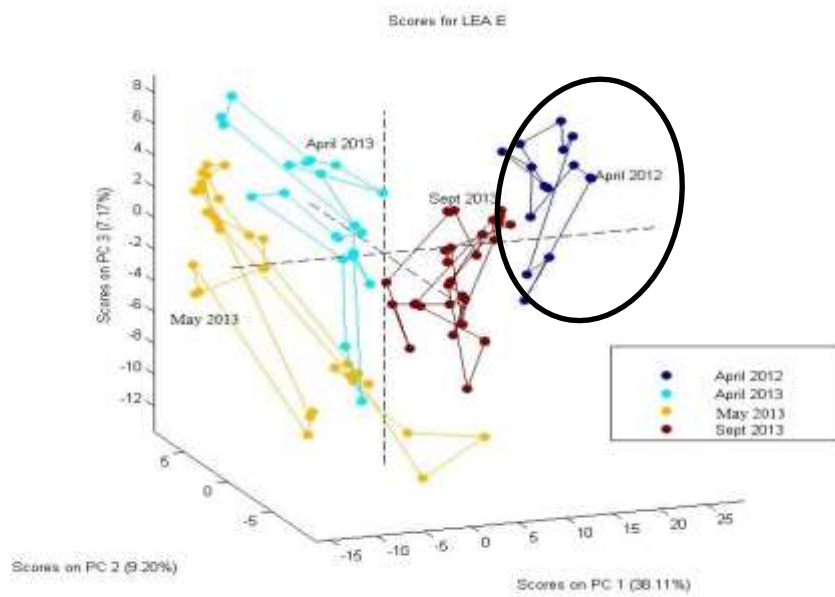
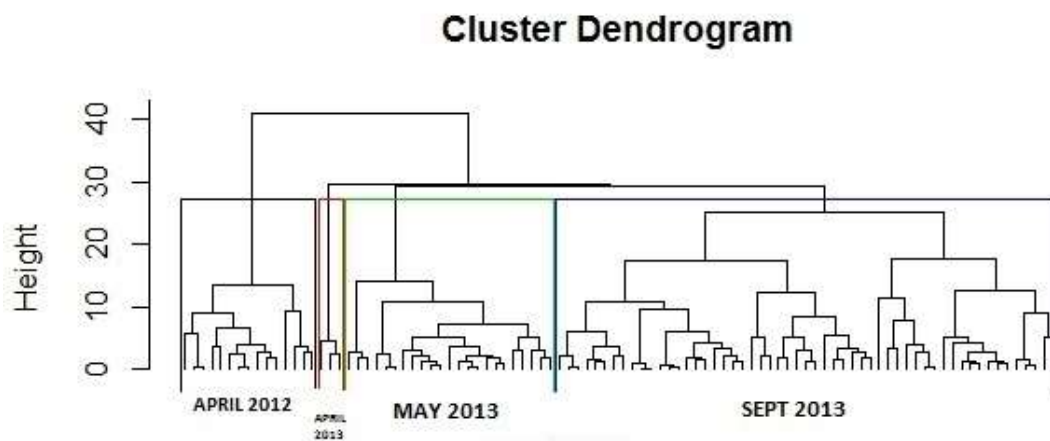


Figure 4.41: The PCA results for LEA E where 96 measurements were evaluated. The April 2012 striated marks in this region were distinguishable from all others



**Figure 4.42: The HCA result for LEA E**

**Table 4.23: The LDA classification table of LEA E. The diagonal values (in bold) represent correctly classified LEAs**

Months of shooting	April 2012	April 2013	May 2013	Sept 2013	Percentage of classification
April 2012	<b>15</b>	0	0	0	100.0
April 2013	0	<b>20</b>	0	1	95.2
May 2013	0	2	<b>28</b>	0	93.3
Sept 2013	0	0	0	<b>30</b>	100.0

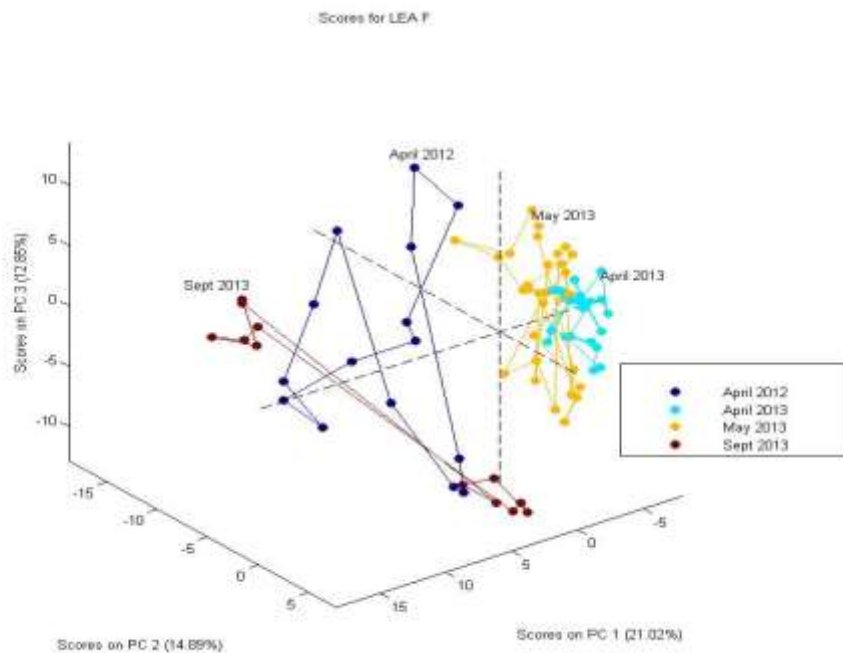


Figure 4.43: The PCA results for LEA F where 81 measurements were evaluated

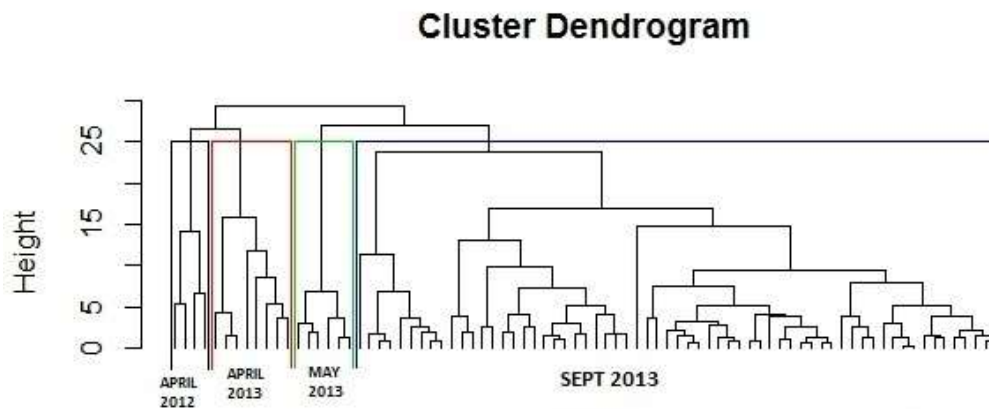
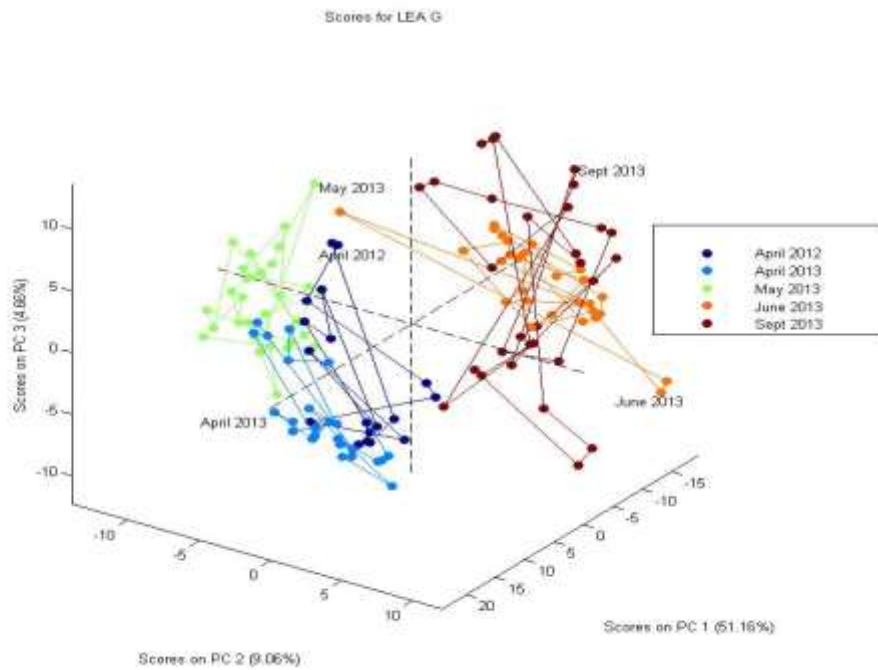


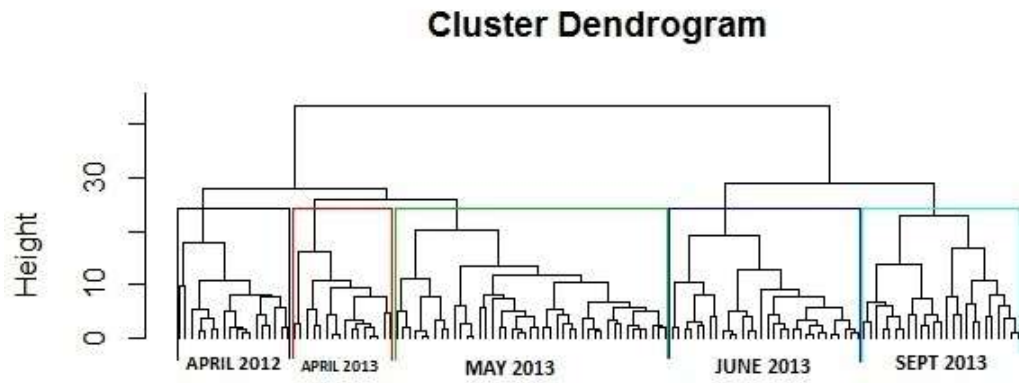
Figure 4.44: The HCA result for LEA F

**Table 4.24: The LDA classification table of LEA F. The diagonal values (in bold) represent correctly classified LEAs**

Months of shooting	April 2012	April 2013	May 2013	Sept 2013	Percentage of classification
April 2012	<b>13</b>	0	0	2	86.7
April 2013	0	<b>23</b>	1	0	95.8
May 2013	0	4	<b>26</b>	0	86.7
Sept 2013	0	0	0	<b>12</b>	100.0



**Figure 4.45: The PCA results for LEA G where 132 measurements were evaluated**

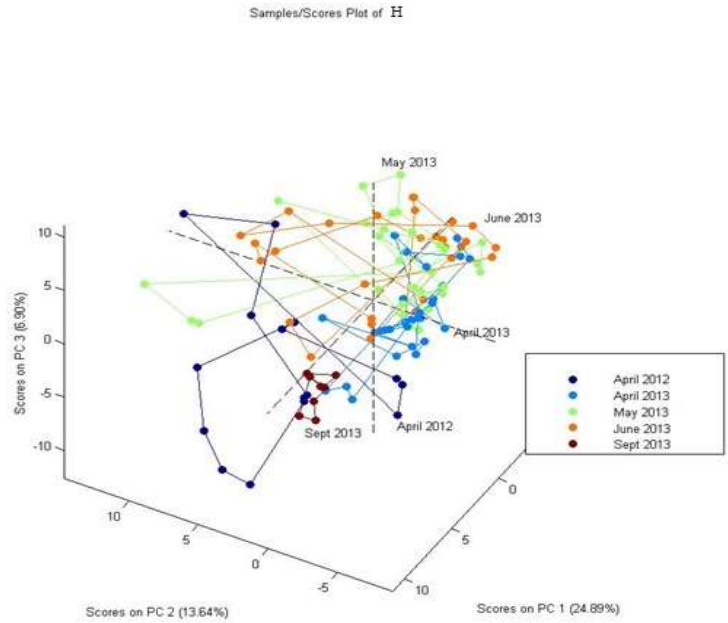


**Figure 4.46: The HCA result for LEA G**

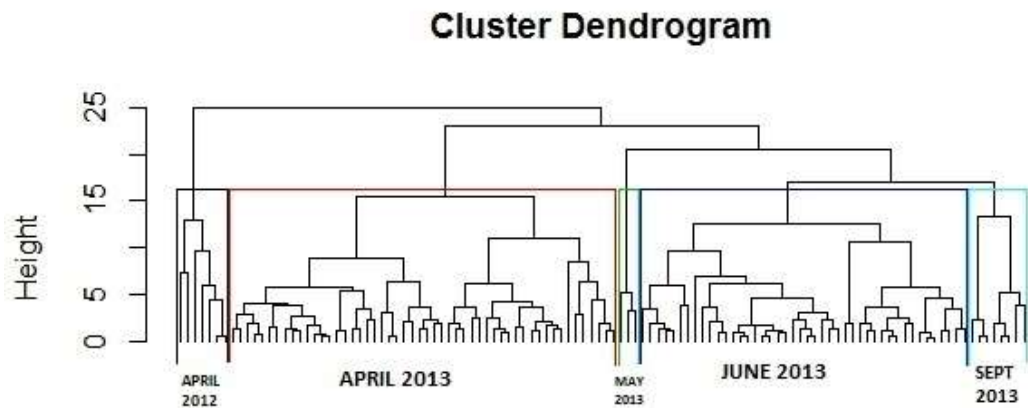
**Table 4.25: The LDA classification table of LEA G. The diagonal values (in bold) represent correctly classified LEAs**

Months of shooting	April 2012	April 2013	May 2013	June 2013	Sept 2013	Percentage of classification
April 2012	14	4	0	0	0	77.8
April 2013	0	<b>24</b>	0	0	0	100.0
May 2013	1	1	<b>28</b>	0	0	93.3
June 2013	0	0	1	<b>29</b>	0	96.7
Sept 2013	1	0	0	0	<b>29</b>	96.7





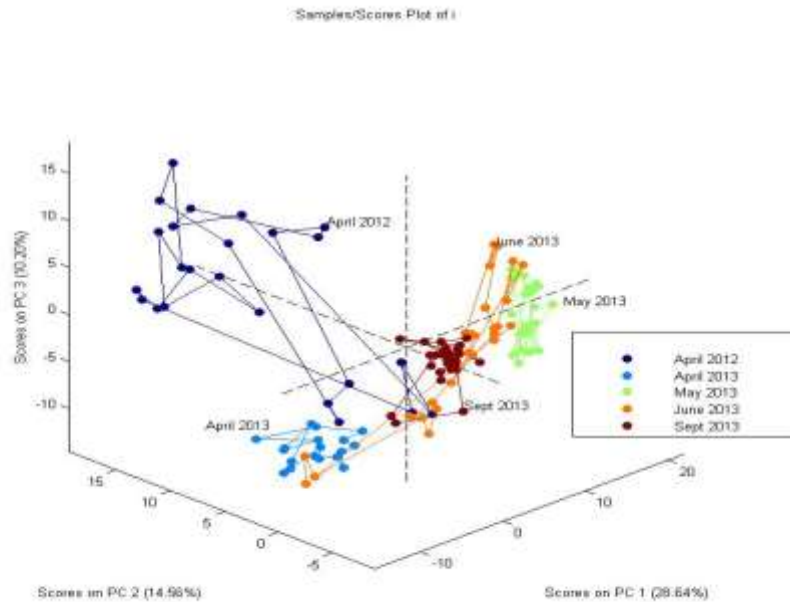
**Figure 4.47: The PCA results for LEA H where 114 measurements were evaluated**



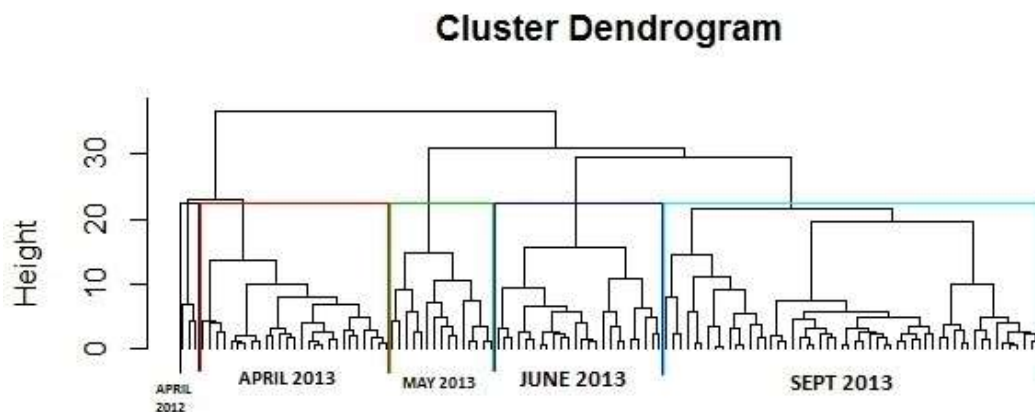
**Figure 4.48: The HCA result for LEA H**

**Table 4.26: The LDA classification table of LEA H. The diagonal values (in bold) represent correctly classified LEAs**

Months of shooting	April 2012	April 2013	May 2013	June 2013	Sept 2013	Percentage of classification
April 2012	<b>13</b>	0	0	0	2	86.7
April 2013	0	<b>21</b>	4	3	2	70.0
May 2013	1	7	<b>15</b>	6	1	50.0
June 2013	0	4	5	<b>20</b>	1	66.7
Sept 2013	0	1	0	0	<b>8</b>	88.9



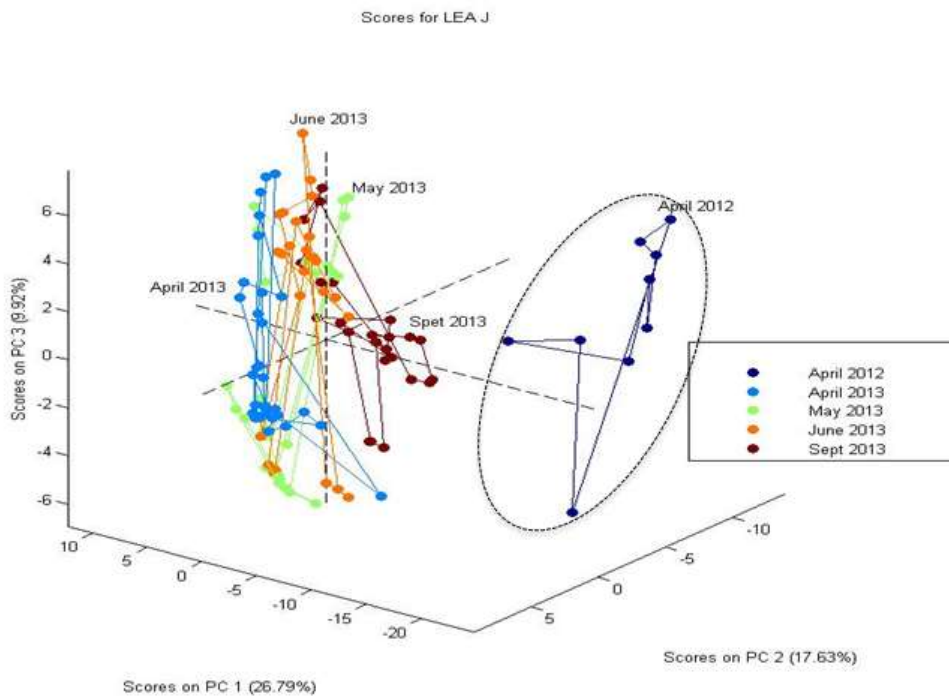
**Figure 4.49: The PCA results for LEA I where 123 measurements were evaluated**



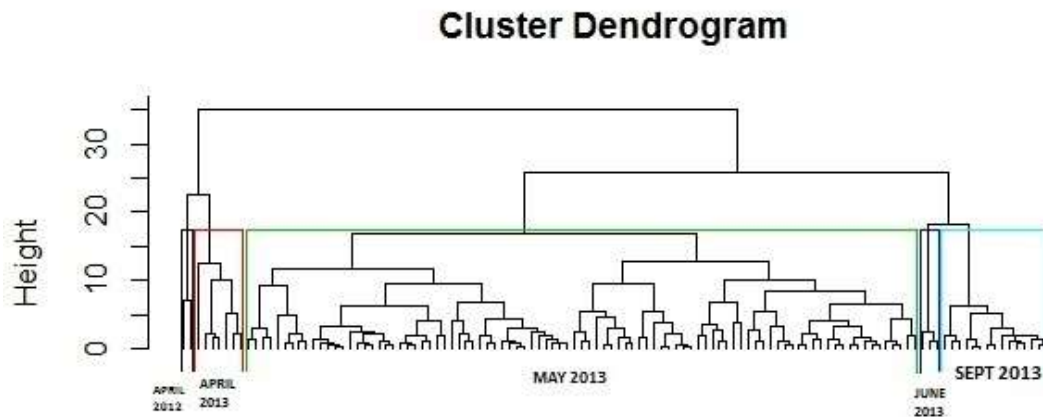
**Figure 4.50: The HCA result for LEA I**

**Table 4.27: The LDA classification table of LEA I. The diagonal values (in bold) represent correctly classified LEAs**

Months of shooting	April 2012	April 2013	May 2013	June 2013	Sept 2013	Percentage of classification
April 2012	<b>23</b>	1	0	0	0	95.8
April 2013	0	<b>18</b>	0	0	0	100.0
May 2013	0	0	<b>27</b>	0	0	100.0
June 2013	0	1	0	<b>26</b>	0	96.3
Sept 2013	0	0	0	1	<b>26</b>	96.3



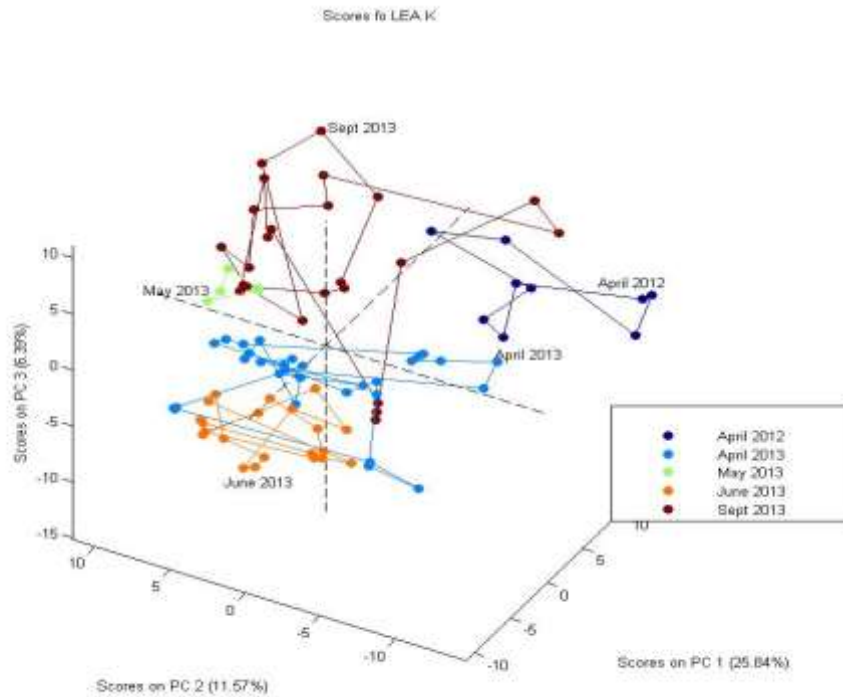
**Figure 4.51: The PCA results for LEA J where 120 measurements were evaluated. The April 2012 striated marks in this region were distinguishable from all others**



**Figure 4.52: The HCA result for LEA J**

**Table 4.28: The LDA classification table of LEA J. The diagonal values (in bold) represent correctly classified LEAs**

Months of shooting	April 2012	April 2013	May 2013	June 2013	Sept 2013	Percentage of classification
April 2012	<b>9</b>	0	0	0	0	100.0
April 2013	0	<b>26</b>	0	4	0	86.7
May 2013	0	0	<b>24</b>	6	0	80.0
June 2013	0	3	5	<b>19</b>	0	70.4
Sept 2013	0	0	3	0	<b>21</b>	87.5



**Figure 4.53: The PCA results for LEA K where 90 measurements were evaluated**

### Cluster Dendrogram

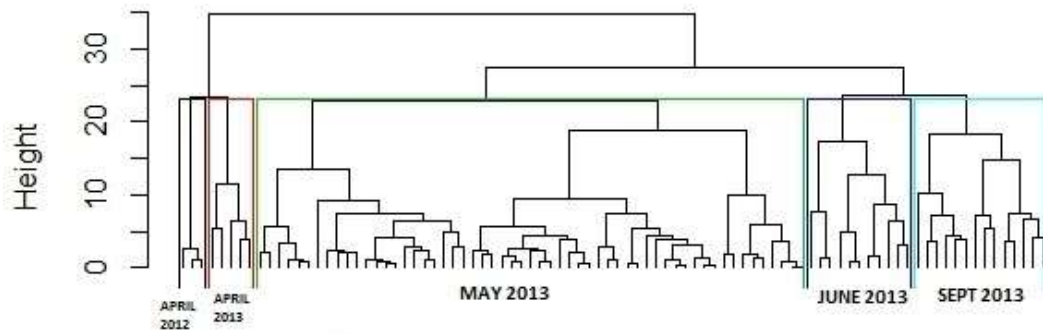


Figure 4.54: The HCA result for LEA K

Table 4.29: The LDA classification table of LEA K. The diagonal values (in bold) represent correctly classified LEAs

Months of shooting	April 2012	April 2013	May 2013	June 2013	Sept 2013	Percentage of classification
April 2012	7	0	0	0	2	77.8
April 2013	0	<b>24</b>	0	6	0	80.0
May 2013	0	0	<b>6</b>	0	0	100.0
June 2013	0	3	0	<b>18</b>	0	85.7
Sept 2013	2	0	0	0	<b>22</b>	91.7

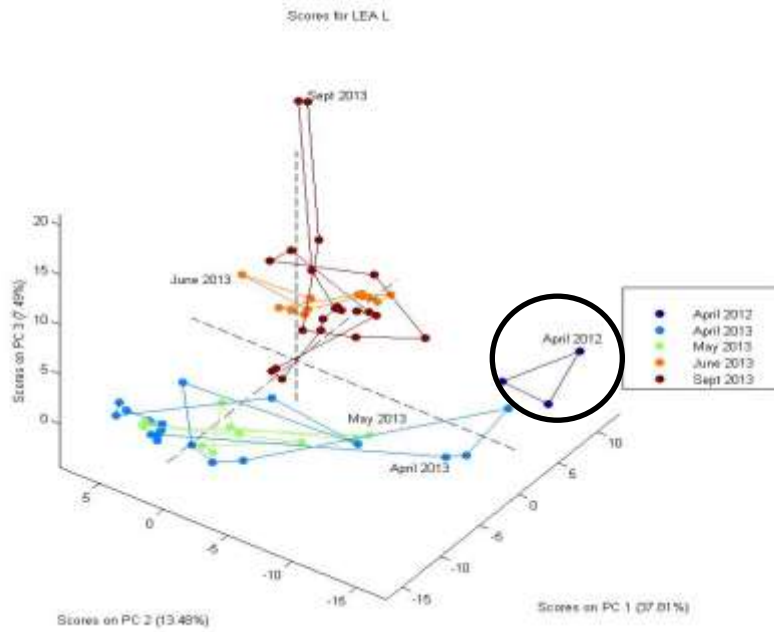


Figure 4.55: The PCA results for LEA L where 66 measurements were evaluated. The April 2012 striated marks in this region were distinguishable from all others

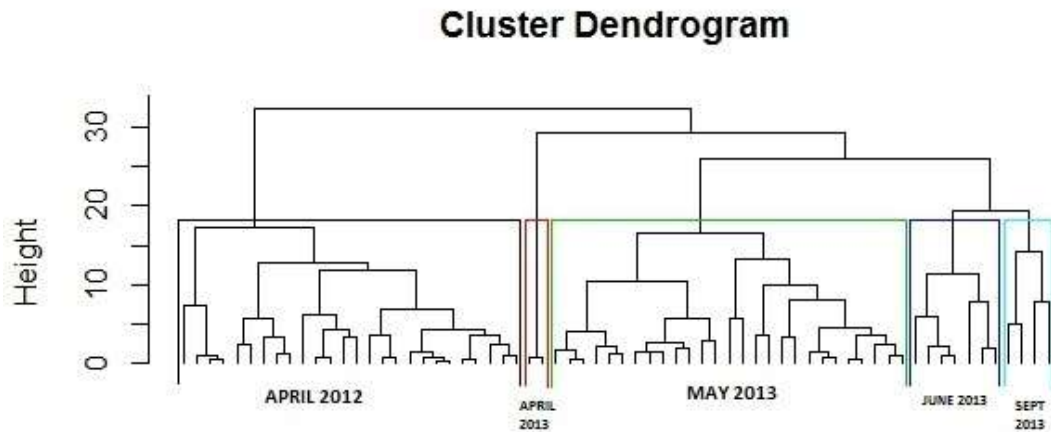


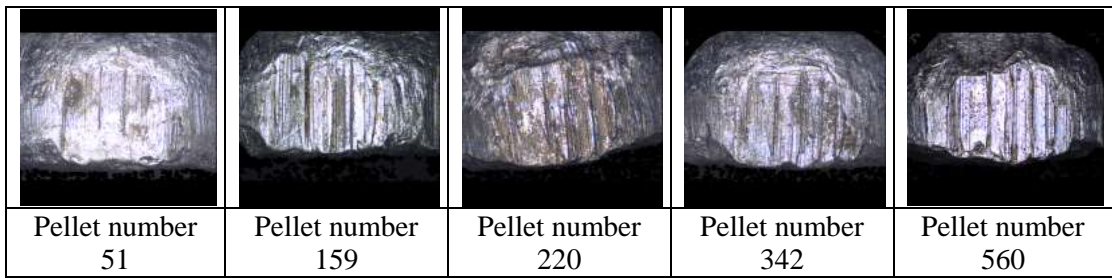
Figure 4.56: The HCA result for LEA L

**Table 4.30: The LDA classification table of LEA L. The diagonal values (in bold) represent correctly classified LEAs**

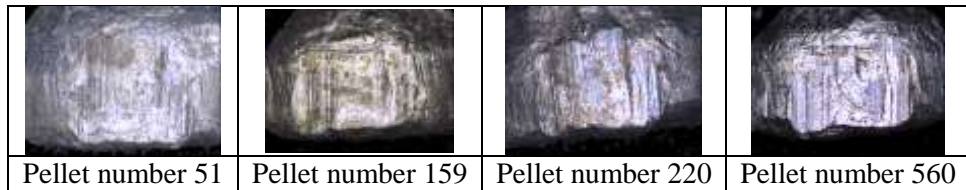
<b>Months of shooting</b>	<b>April 2012</b>	<b>April 2013</b>	<b>May 2013</b>	<b>June 2013</b>	<b>Sept 2013</b>	<b>Percentage of classification</b>
<b>April 2012</b>	<b>3</b>	0	0	0	0	100.0
<b>April 2013</b>	1	<b>12</b>	5	0	0	66.7
<b>May 2013</b>	0	12	<b>0</b>	0	0	0.0
<b>June 2013</b>	0	0	0	<b>12</b>	0	100.0
<b>Sept 2013</b>	0	0	0	1	<b>20</b>	95.2

The PCA and HCA results for each of the LEAs are presented in Figures 4.33 to 4.56. The LDA results are presented in Table 4.19 to 4.30. Based on the analysis results, there are four LEAs that show separation of data, LEA D, E, J and L, where all these LEAs demonstrate that the April 2012 group is separated from the other group. Figures 4.57 to 4.60 show the scanned images of LEA D, E, J and L pellets spanning April 2012 to September 2013. Figures 4.57, 4.58 and 4.60 illustrate that the striation marks on LEA D, E and L became more prominent and more defined as more pellets are fired from the weapon and this is particularly evident in the comparison of the 51<sup>st</sup> and 560<sup>th</sup> pellet. And for this reason, the LDA can separate more than one group for LEA D (May and September 2013 groups), a group for LEA E (September 2013 group) and L (June 2013 group), where all these groups can be classified to month of shooting. For LEA J, pellets shot in April 2012 can be separated from the other groups. Based on Figure 4.59, this group is different (a well define mark is absent on the 51<sup>st</sup> pellet as compared to other pellets from different group).

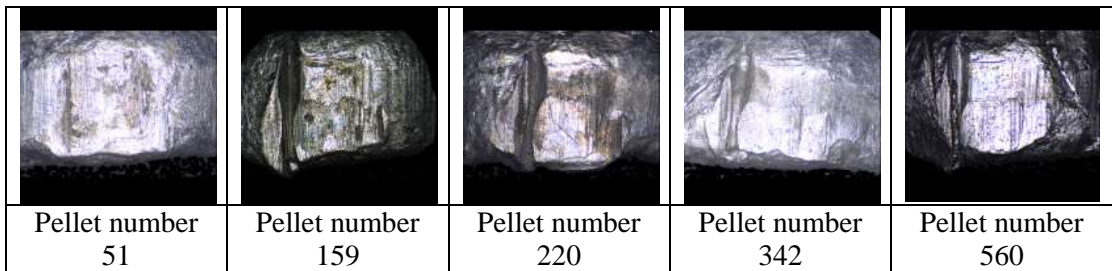




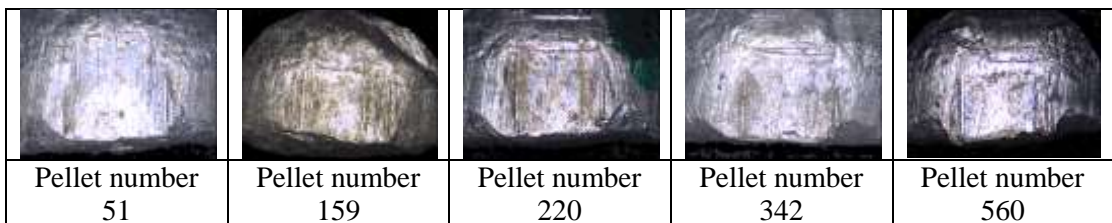
**Figure 4.57: Pellets fired in each of the five groups for LEA D. The striation became more prominent and much clearer after repetitive firing**



**Figure 4.58: Pellets fired in each of the four groups for LEA E. The striation became more prominent and much clearer after repetitive firing**

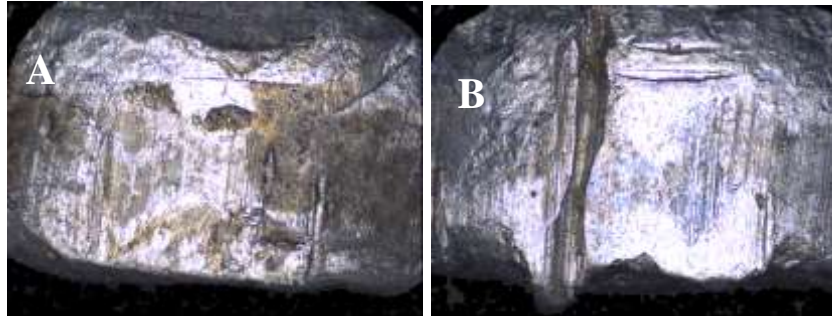


**Figure 4.59: Pellets fired in each of the five groups for LEA J. A very well-defined mark appeared on LEA J as the firing history of the pellet developed**



**Figure 4.60: Pellets fired in each of the five groups for LEA L. The striation became more prominent and much clearer after repetitive firing. The green colour on pellet number 220 is for identification purpose**

Based on Figure 4.59, a very well-defined mark appeared on LEA J as the firing history of the pellet developed. This new mark appeared first on pellet 123 which is presented in Figure 4.61 beside pellet 100 where the difference can be clearly observed.



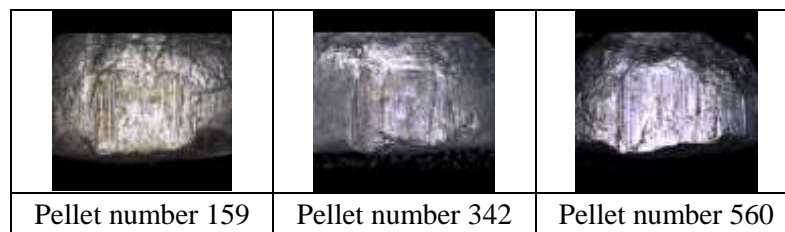
**Figure 4.61: LEA J on pellet 100 (A) and pellet 123 (B)**

Observation of other LEAs (for example LEA K, pellet number 100) reveal that the lower portion of the pellet was missing (Figure 4.62) and it may be postulated that such fragmentation may have left residues within the weapons barrel that affected subsequently fired pellets. Such a residue build up and its subsequent affect on striation marks was previously suggested by Di Maio and Burd and Kirk [3-5].

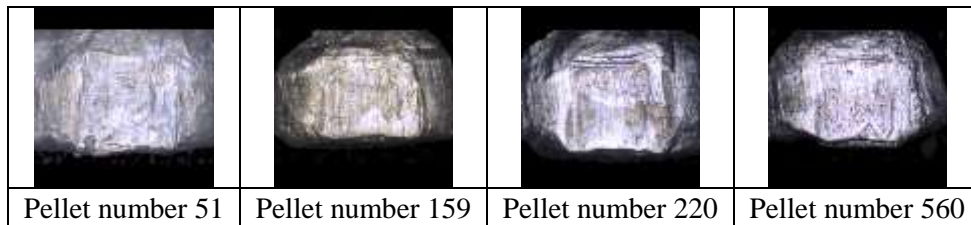


**Figure 4.62: Pellet number 100, LEA K. Note the missing lower part of the pellet**

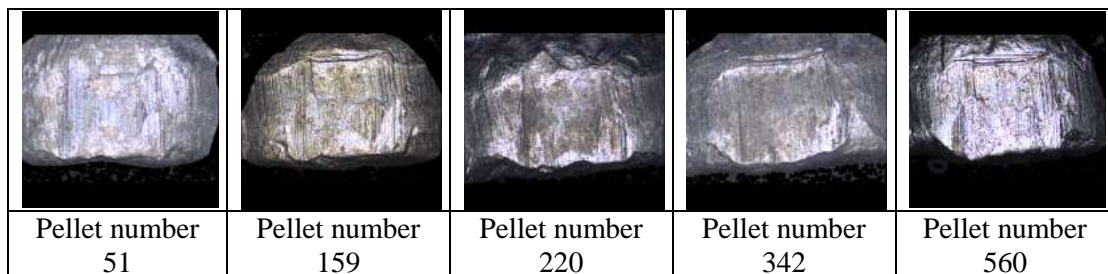
The LDA classification tables for five LEAs (LEA C, F, G, I and K) produce better separation as compared to the PCA results. For these LEAs, the PCA results are unable to separate the pellets according to months of shooting. However the LDA can classify one to two LEAs according to months of shooting. Figures 4.63 to 4.67 illustrate the scanned images of LEA C, F, G, I and K pellets spanning April 2012 to September 2013. The LDA can classify pellets with more prominent and much clearer striation to its group of month of shooting such as LEA C and F (September 2013), LEA G (April 2013), LEA I (April and May 2013) and LEA K (May 2013).



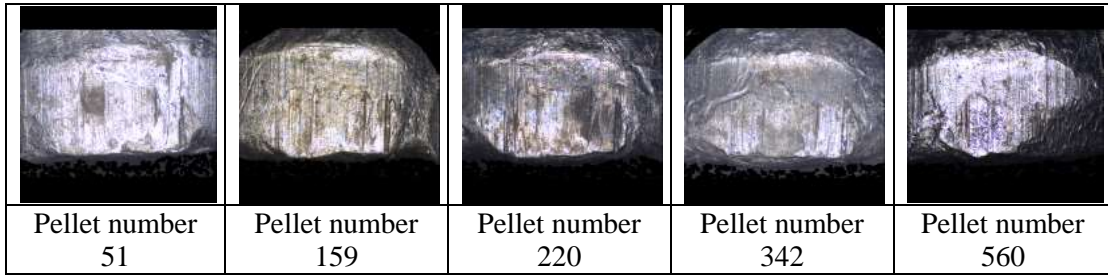
**Figure 4.63: Pellets fired in each of the three groups for LEA C. The striation on pellet number 560 (September 2013 group) is more prominent and much clearer as compared to other pellets**



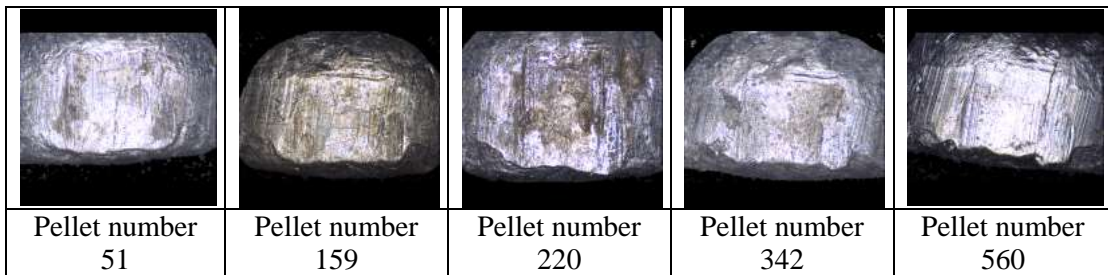
**Figure 4.64: Pellets fired in each of the four groups for LEA F. The striation on pellet number 560 (September 2013 group) is more prominent and much clearer as compared to other pellets**



**Figure 4.65: Pellets fired in each of the five groups for LEA G. The striation on pellet number 159 (April 2013 group) is more prominent and much clearer as compared to other pellets**



**Figure 4.66: Pellets fired in each of the five groups for LEA I. The striation mark on pellet number 159 and 220 (April and May 2013 group) is more prominent and much clearer as compared to other pellets**

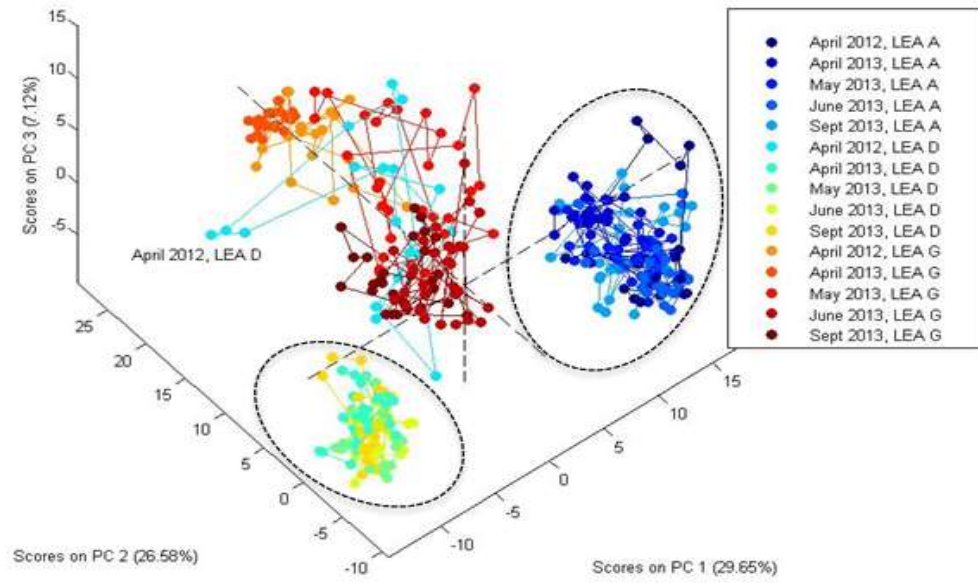


**Figure 4.67: Pellets fired in each of the five groups for LEA K. The striation mark on pellet number 220 (May 2013 group) is more prominent and much clearer as compared to other pellets**

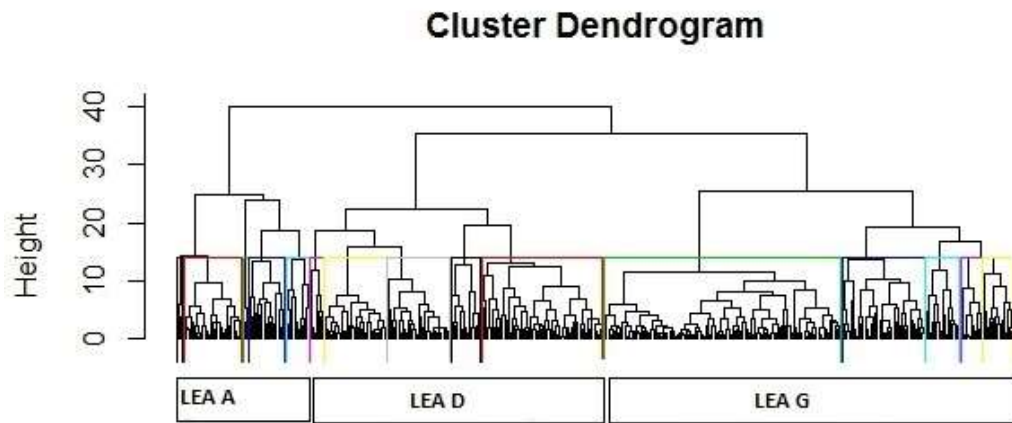
The analysis results support the previous researchers' assertion that a single tool is able to produce different markings and alter its originality over a period of time.

#### **4.5.1 Analysis of LEAs with more than 90% aligned measurements**

LEA A, D and G, all of which had 90% or greater alignment across all sample sets and thus good reproducibility, were explored to investigate whether given the consistency of measurement, the LEAs would remain clustered as individual LEAs across the repetitively fired pellets. Figure 4.68 and 4.69 show the PCA and HCA results, respectively. The PCA results show that LEA A, D and G can be differentiated except for the April 2012, LEA D which convolutes with LEA G.



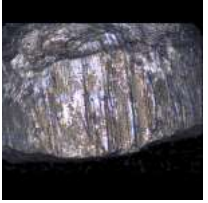
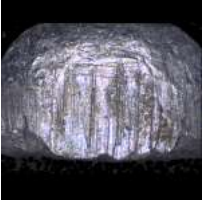


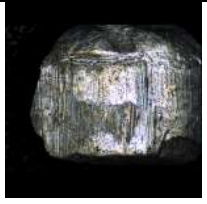





**Figure 4.68: The PCA results for LEA A, D and G all of which have demonstrated 90% alignment. These LEAs can be differentiated, except for the April 2012, LEA D which convolutes with LEA G**



**Figure 4.69: The HCA result for LEA A, D and G**

Figure 4.70 illustrates pellets from LEA D and LEA G. Pellets fired in April 2013 onwards for LEA D are clearly visually different from the LEA G pellets. However, the initial LEA D pellet has less prominent striations as compared to the other pellets in the same group. This is the possible reason of why the April 2012, LEA D group convoluted with LEA G.

				
Pellet number 51, LEA D	Pellet number 159, LEA D	Pellet number 220, LEA D	Pellet number 342, LEA D	Pellet number 560, LEA D
				
Pellet number 51, LEA G	Pellet number 159, LEA G	Pellet number 220, LEA G	Pellet number 342, LEA G	Pellet number 560, LEA G

**Figure 4.70: Scanned images of pellets from LEA D and pellets from LEA G. Visually, pellets numbered 159 to 560, LEA D are different from the LEA G pellets. This difference is shown in the analysis result**

Table 4.31: The LDA classification table with more than 90% aligned measurements. The diagonal values (in bold) represent correctly classified LEAs

LEA	Months of shooting	A	A	A	A	A	D	D	D	D	D	G	G	G	G	G	Percentage of classification
		April 2012	April 2013	May 2013	June 2013	Sept 2013	April 2012	April 2013	May 2013	June 2013	Sept 2013	April 2012	April 2013	May 2013	June 2013	Sept 2013	
A	April 2012	<b>14</b>	2	4	3	1	0	0	0	0	0	0	0	0	0	0	58.3
A	April 2013	0	<b>28</b>	2	0	0	0	0	0	0	0	0	0	0	0	0	93.3
A	May 2013	4	1	<b>23</b>	2	0	0	0	0	0	0	0	0	0	0	0	76.7
A	June 2013	1	0	5	<b>23</b>	1	0	0	0	0	0	0	0	0	0	0	76.7
A	Sept 2013	0	1	1	2	<b>26</b>	0	0	0	0	0	0	0	0	0	0	86.7
D	April 2012	0	0	0	0	0	<b>15</b>	0	0	0	0	0	0	0	1	2	83.3
D	April 2013	0	0	0	0	0	0	<b>23</b>	1	3	3	0	0	0	0	0	76.7
D	May 2013	0	0	0	0	0	0	0	<b>30</b>	0	0	0	0	0	0	0	100.0
D	June 2013	0	0	0	0	0	0	6	2	<b>17</b>	2	0	0	0	0	0	63.0
D	Sept 2013	0	0	0	0	0	0	0	0	0	<b>30</b>	0	0	0	0	0	100.0
G	April 2012	0	0	0	0	0	0	0	0	0	0	<b>11</b>	7	0	0	0	61.1
G	April 2013	0	0	0	0	0	0	0	0	0	0	5	<b>19</b>	0	0	0	79.2
G	May 2013	0	0	0	0	0	0	0	0	0	0	3	0	<b>27</b>	0	0	90.0
G	June 2013	0	0	0	0	0	0	0	0	0	0	0	0	1	<b>29</b>	0	96.7
G	Sept 2013	0	0	0	0	0	1	0	0	0	0	0	0	0	4	<b>25</b>	83.3



Table 4.31 shows the LDA classification table for LEA A, D and G. Two groups from LEA D, May and September 2013 groups are well differentiated from the other groups. For LEA A, no measurements are misclassified as other LEAs. For LEA D, only the April 2012 group is misclassified as LEA G, the June and September 2013 group and for LEA G, only the September 2013 group is misclassified as LEA D, the April 2012 group. Both LEA D April 2012 group and LEA G September 2013 group have more than 80% accuracy of classification. This result supports the PCA analysis which shows LEA D, the April 2012 group is convoluted with LEA G (Figure 4.68). The reason is, as explained in Figure 4.70 LEA D, the striation marks on the April 2012 group (pellet number 51) is less prominent as compared to the other groups from LEA D. This is why the April 2012 group is misclassified. The accuracy of classification for this model is 82.7%. The value of the accuracy percentage can be used to objectify the striation marks, which is the core for the study.

#### **4.6 Conclusions**

The analysis results illustrate that the suggestion of the LEA's surface topography remains the same on projectiles from the same weapon irrespective of the sequence of firing is not always the case. Where alterations do occur they can be both permanent (as observed for LEA J) and/or transient. The condition of the surface of the LEA and whether corrosion has occurred presumably as a result of storage appears a critical factor and influences the degree of misalignment within the regions.

The investigation into the marks observable within LEAs certainly suggests a change can occur as more projectiles are fired from the weapon. In particular, it is quite conceivable that portions of a projectile may break off and accumulate in the weapons

barrel which in turn may give rise to the alteration of the surface topography of LEAs in subsequently fired pellets. This can be seen in LEA J where the initial fired pellets from the April 2012 set are different from the pellets fired after that date.

Changes in the LEA surface topography can affect the identification of striations for pellets after a period of time with obvious implications for both projectile to projectile comparisons if there are long periods of time between the firing of the projectiles and for exploring the links to projectiles and specific weapons again where sufficient time may have passed. This study used pellets which are non-jacketed ammunition. The result supports that striation marks can change over a period of time due to wear and tear of the barrel, with one of the reasons being built up lead in the barrel. According to Di Maio, land marks are prominent in jacketed bullet. If the barrel is uncleaned, wear and tear of the barrel can happen and because there's a possibility of lead build up in the barrel, hence, change of striation to the jacketed bullet can occur. A study to verify this hypothesis should be conducted for future research.

#### 4.7 References

1. Justice, N.I.O. *Firearm Examiner Training*. [web page] 2012 [cited 2012; Available from: [http://www.nij.gov/training/firearms-training/module01/fir\\_m01.htm](http://www.nij.gov/training/firearms-training/module01/fir_m01.htm)].
2. Tobin, W.A. and Blau, P.J., *Hypothesis testing of the critical underlying premise of discernible uniqueness in firearms-toolmarks forensic practice*. *Jurimetrics Journal of Law, Science and Technology*, 2013. 53(2): p. 121-142.
3. Di Maio, V.J.M., *Gunshot wounds : practical aspects of firearms, ballistics, and forensic techniques*. 1999: Boca Raton : CRC Press.
4. Heard, B.J., *Handbook of firearms and ballistics [internet resource] examining and interpreting forensic evidence*, ed. P.D.A. Dawsonera. 2008: Oxford : Wiley-Blackwell.
5. Burd, D.Q. and Kirk, P.L., *Tool Marks. Factors Involved in Their Comparison and Use as Evidence*. *Journal of Criminal Law and Criminology (1931-1951)*, 1942. 32(6): p. 679-686.

6. Spotts, R., Chumbley, L. S., Ekstrand, L., Zhang, S., Kreiser, J., *Optimization of a Statistical Algorithm for Objective Comparison of Toolmarks*. *Journal of Forensic Sciences*, 2015. 60(2): p. 303-314.
7. Spotts, R. and Chumbley, L.S., *Objective Analysis of Impressed Chisel Toolmarks*. *Journal of Forensic Sciences*, 2015. 60(6): p. 1436-1440.
8. Castro, C.E., Norris, S.A., Setume, B.K. and Hamby, J.E., *The examination, evaluation, and identification of 40 S&W calibre cartridge cases fired from 1079 different GLOCK semiautomatic pistols manufactured over a six-year period*. 2014. 47(2): p. 65-73.
9. Nichols, R.G., *Firearm and toolmark identification criteria: A review of the literature*. *J. Forensic Sci*, 1997. 42(3): p. 466-474.
10. Nichols, R.G., *Firearm and toolmark identification criteria: A review of the literature, part II*. *J Forensic Sci*, 2003. 48(2): p. 1-10.
11. Senin, N., Groppetti, R., Garofano, L., Fratini, P. and Pierni, M., *Three-dimensional surface topography acquisition and analysis for firearm identification*. *J. Forensic Sci.*, 2006. 51(2): p. 282-295.
12. Bonfanti, M.S. and Ghauharali, R.I., *Visualisation by confocal microscopy of traces on bullets and cartridge cases*. *Science & Justice*, 2000. 40(4): p. 241-256.
13. Breitmeier, U. and Schmid, H., *Lasercomp: A surface measurement system for forensic applications*. *Forensic Science International*, 1997. 89(1): p. 1-13.
14. Xie, F., Xiao, S., Blunt, L., Zeng, W. and Jiang, X., *Automated bullet-identification system based on surface topography techniques*. *Wear*, 2009. 266(5): p. 518–522.
15. Gambino, C., McLaughlin, P., Kuo, L., Kammerman, F., Shenkin, P., Diaczuk, P., Petraco, N., Hamby, J. and Petraco, N.D.K., *Forensic Surface Metrology: Tool Mark Evidence*. *Scanning*, 2011. 33(5): p. 272–278.
16. Sakarya, U., Leloğlu, U.M. and Tunalı, E., *Three-dimensional surface reconstruction for cartridge cases using photometric stereo*. *Forensic Science International*, 2008. 175(2–3): p. 209-217.
17. Song, J., Chu, W., Vorburger, T.V., Thompson, R., Renegar, T.B., Zheng, A., Yen, J., Silver, R. and Ols, M., *Development of ballistics identification-from image comparison to topography measurement in surface metrology*. *Meas. Sci. Technol.*, 2012. 23(5): p. 1-6.
18. Zheng, X., Soons, J., Vorburger, T., Song, J., Renegar, T. and Thompson, R., *Applications of surface metrology in firearm identification*. *Surface Topography: Metrology and Properties*, 2014. 2(1): p. 1-10.
19. Wightman, G., Wark, K. and Thomson, J., *The interaction between clothing and air weapon pellets*. *Forensic Science International*, 2105. 246: p. 6-16.
20. DiMaio, V.J., Copeland, A.R., Besant-Matthews, P.E., Fletcher, L.A. and Jones, A., *Minimal velocities necessary for perforation of skin by air gun pellets and bullets*. *J Forensic Sci*, 1982. 27(4): p. 894-8.
21. MacPherson, D., *Bullet penetration: Modeling the dynamics and the incapacitation resulting from wound trauma*. 1994: Ballistic Publications (El Segundo, CA)

## **Chapter 5: Comparison and evaluation of striated marks on projectiles fired from different weapons.**

### **5.1 Introduction**

The premise upon which ballistic comparison of bullets is based on that different weapons will impart different striated marks on a projectile while the same weapon will impart the same striated marks on every projectile fired from that weapon with little variation. These striated marks possess ‘class characteristics’, which indicate the make and model of the weapon that fired the projectile and ‘individual characteristics’ which are suggested as being exclusive to a specific weapon [1-5].

Three different air weapons were investigated to examine the variation in class characteristics and individual characteristics that the projectiles fired from these weapons may reveal. The ability of the developed objective mathematical approach to assess and separate these projectiles from each other using the striated marks within the Land Engraved Areas (LEAs) was explored. The HW 45 Weihrauch air pistol used for this project was made in Germany [6], the Edgar Brother Model 35 air rifle was made in Turkey by Hatsan [7] and the Baikal 90042234 ИЖ-35 is a Russian-made air rifle. Further information regarding all three air weapons was discussed in Chapter 2.2. All three weapons are .177 calibres therefore capable of firing the pellets used in this study, the RWS® Superdome 4.5mm (.177 calibre). The testing and comparison method has been described in Chapter 2 relating to image acquisition, pre-processing 2D images of the striated marks and analysis of the data using Matlab®.

60 pellets were examined in total, 50 from the air pistol and 5 from each of the air rifles as highlighted in Table 5.1. A total of 10 first pellets were chosen from each air rifles. The previous chapter used first 10 pellets from each month of shooting, hence this chapter used the same method to choose the pellets. However, only 10 pellets were chosen out of 20 pellets fired from the air rifles. This is because the non-selected pellets will be used for future study which will involve comparison with other type of air weapons, and if possible, bullets from firearms.

**Table 5.1: The pellets examined for weapon comparison were from the groups highlighted in grey**

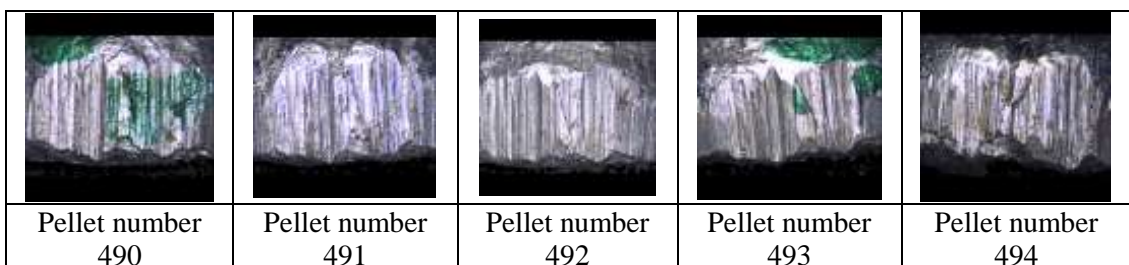
<b>Date of test</b>	<b>Pellet Number</b>	<b>Test Done</b>	<b>Weapon</b>	<b>Total Pellets fired</b>	<b>Pellets Collected</b>	<b>Selected pellets</b>
April 2012	1-50	Low Velocity	HW 45	50	50	
April 2012	51-100	High Velocity	HW 45	50	50	
April 2012	101-122	Chronograph: low and high velocity	HW 45	22	0	
January 2013	123-158	Bones & Gelatine	HW 45	36	36	
April 2013	159-208	High Velocity	HW 45	50	50	159-208
April 2013	209-219	Chronograph: high velocity	HW 45	11	0	
May 2013	220-319	High Velocity	HW 45	100	100	
May 2013	320-341	Chronograph: high velocity	HW 45	22	0	
June 2013	342-441	High Velocity	HW 45	100	100	
July 2013	442-465	Low Velocity Distance	HW 45	24	24	
July 2013	466-489	High Velocity Distance	HW 45	24	24	
July 2013	490-499	Rifle 1	Edgar Brother Model 35	10	10	490-494
July 2013	500-509	Rifle 2	Baikal 90042234 ИЖ-35	10	10	500-504
September 2013	510-559	Chronograph: low velocity	HW 45	50	50	
September 2013	560-609	Chronograph: high velocity	HW 45	50	50	
<b>Total number of pellets</b>				<b>609</b>	<b>554</b>	

## 5.2 Alignment results

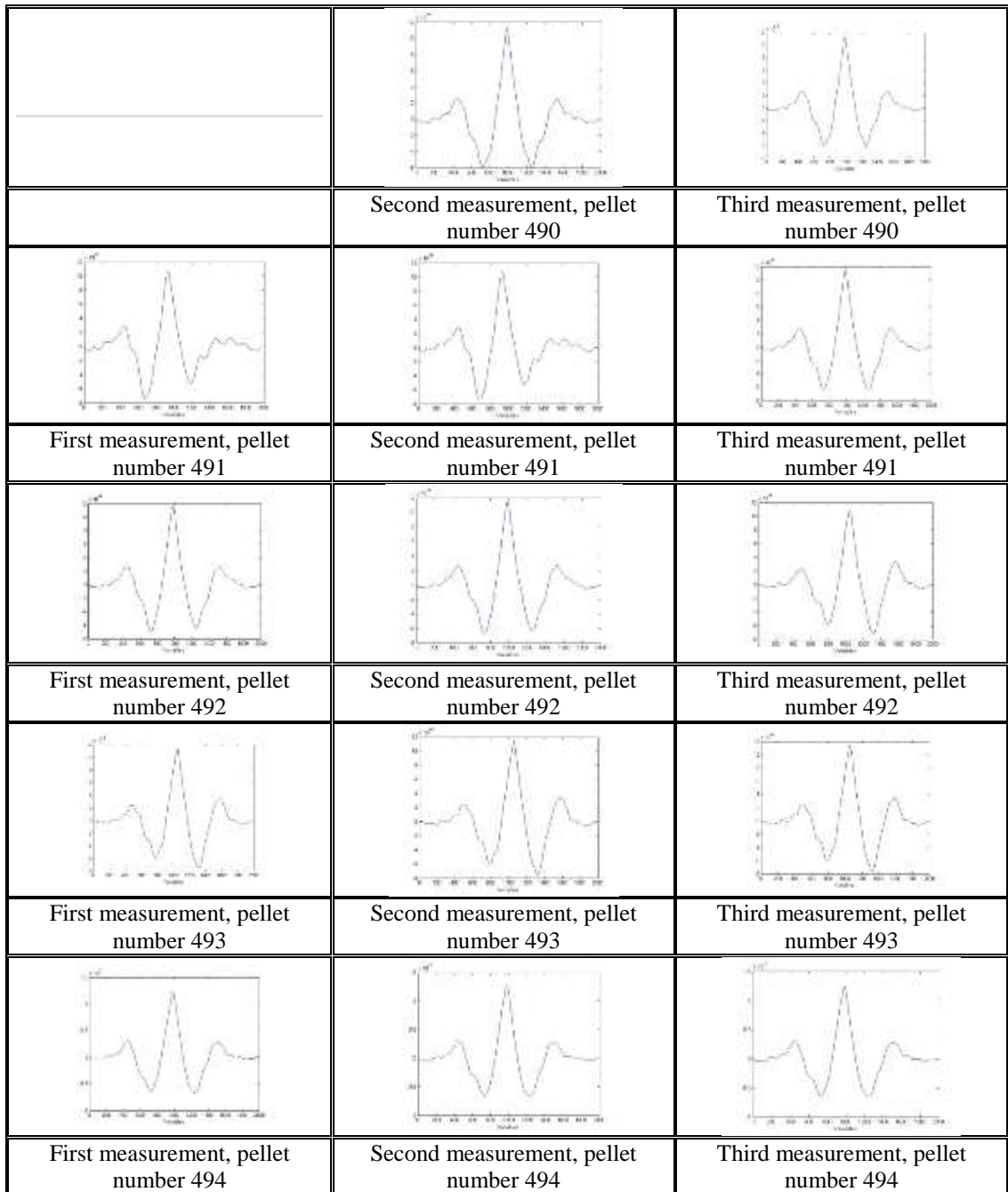
A total of 60 pellets were chosen for comparison and evaluation (five pellets from each of the air rifles and 50 pellets from the air pistol). All pellets were scanned using the Alicona® microscope and aligned using Matlab® as outlined in Chapter 2. The LEAs which generated 90% or better alignment across the various sample sets were chosen for comparison as this threshold had demonstrated the greatest potential for sample clustering across the LEAs. Pellets shot from all three weapons revealed 12 striated regions in each case. These LEAs were labelled BA to BL for pellets fired from the Baikal 90042234 ИЖ-35, and EA to EL for pellets fired from the Edgar Brother Model 35. The LEAs of pellets shot from the air pistol were labelled A to L as previously described.

### 5.2.1 Edgar Brother Model 35

Each of the twelve LEAs was scanned in triplicate using the Alicona® microscope and the data was subjected to curve smoothing and alignment as previously described. The scanned images and alignment results for LEA EA are presented as an exemplar in Figures 5.1 and 5.2. All measurements from LEA EA were fully aligned. The green marks on the pellets are for identification purpose in this study.



**Figure 5.1: LEA EA of the five pellets shot with the Edgar Brother Model 35 were visually similar. The green marks are for identification purpose for this study**



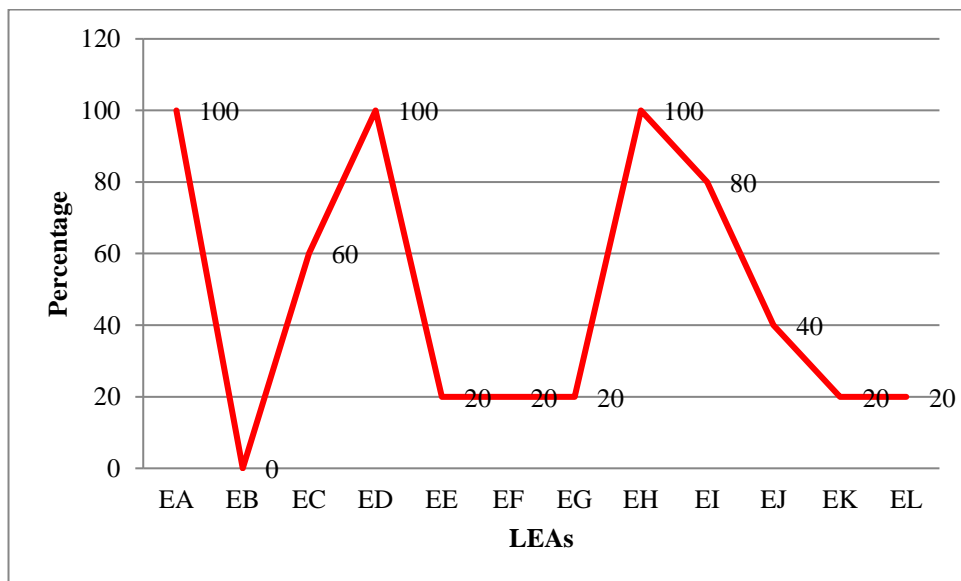
**Figure 5.2: Topographical profiles obtained from the microscopic measurements of LEA EA of pellets shot with the Edgar Brother Model 35**

In addition to LEA EA, all measurements for LEA ED and EH were fully aligned. All of the other regions of interest were aligned to lesser degrees and the percentage of its alignment is presented in Table 5.2 and Figure 5.3.



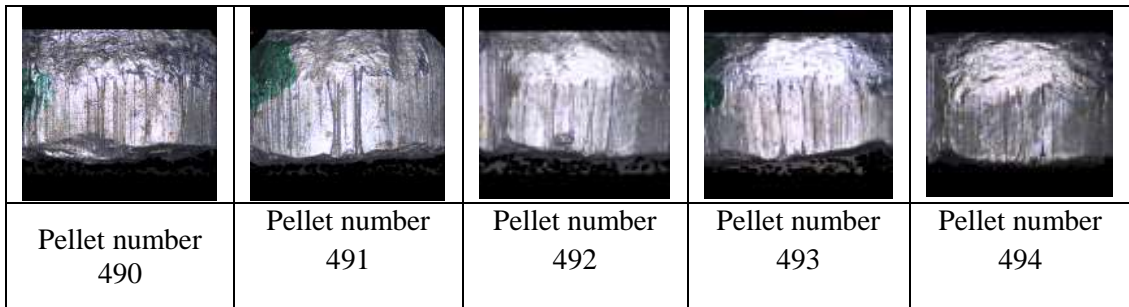
**Table 5.2: Summary of scanned results and measurements for pellets shot with the Edgar Brother Model 35**

Striations	Number of pellets scanned	Number of measurements for alignment	Number of aligned measurements	Percentage of aligned measurements (%)
EA	5	15	15	100
EB	5	15	0	0
EC	5	15	9	60
ED	5	15	15	100
EE	5	15	3	20
EF	5	15	3	20
EG	5	15	3	20
EH	5	15	15	100
EI	5	15	12	80
EJ	5	15	6	40
EK	5	15	3	20
EL	5	15	3	20
Total	5	180	87	48

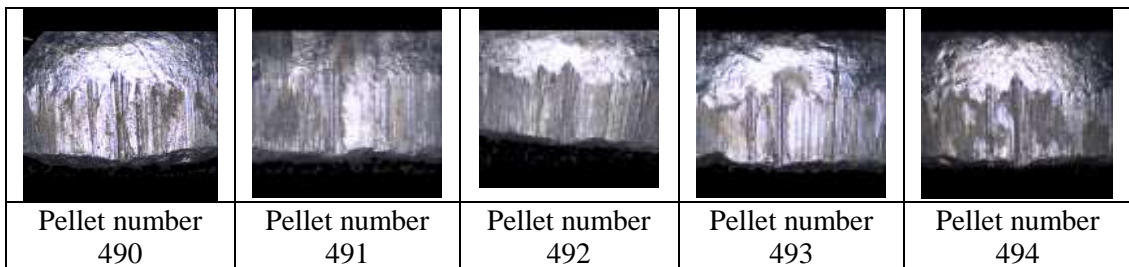


**Figure 5.3: Percentage of aligned measurements for LEA EA to EL, pellets numbered 490-494, Edgar Brother Model 35**

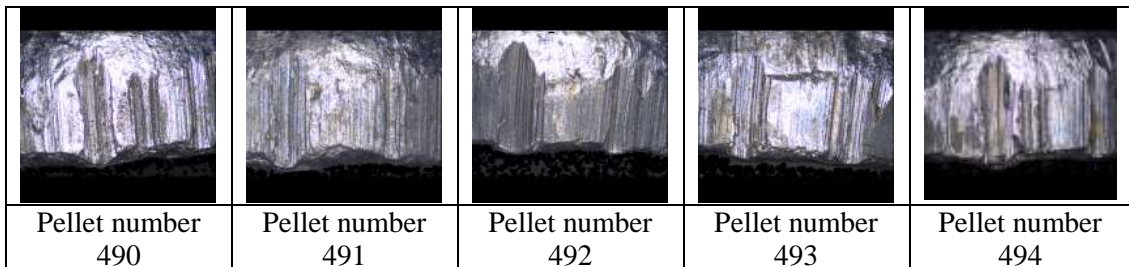
Figures 5.4 to 5.14 illustrate the various LEAs for each region on each of the five repetitively fired pellets.



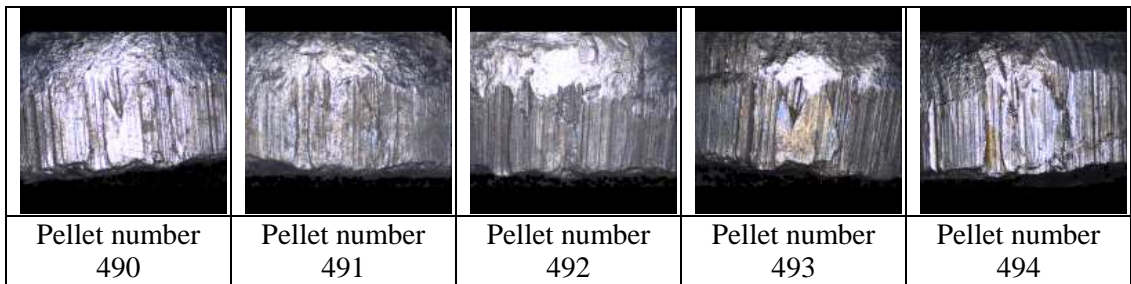
**Figure 5.4: LEA EB for the five pellets shot with the Brother Edgar Model 35. No alignment was possible. Green marks on pellets are for the purpose of identification**



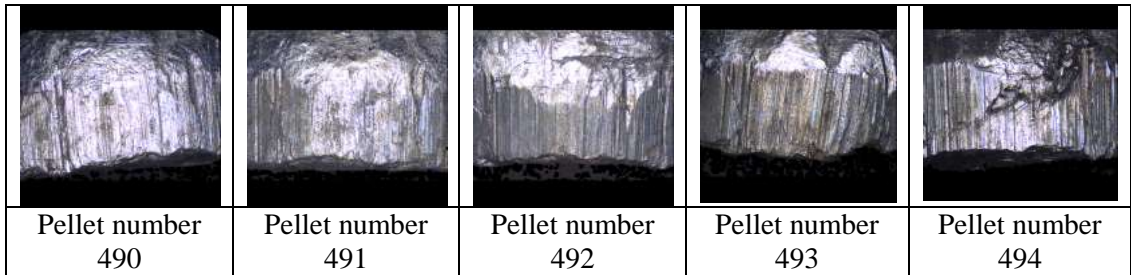
**Figure 5.5: LEA EC for the five pellets shot with the Brother Edgar Model 35. 60% of the pellets could be aligned. The misaligned pellets were 491 and 493**



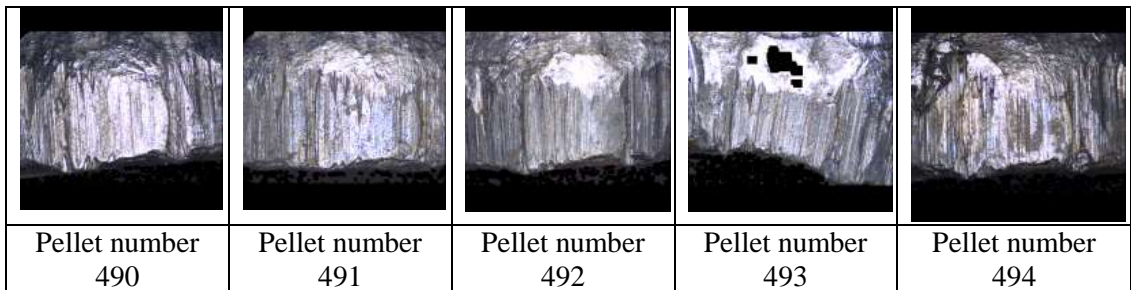
**Figure 5.6: LEA ED for the five pellets shot with the Brother Edgar Model 35. All pellets were aligned**



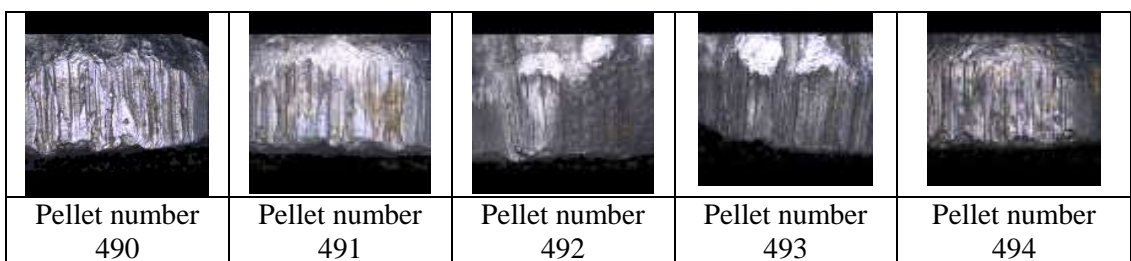
**Figure 5.7: LEA EE for the five pellets shot with the Brother Edgar Model 35. 20% of the pellets could be aligned. Only pellet number 490 was aligned**



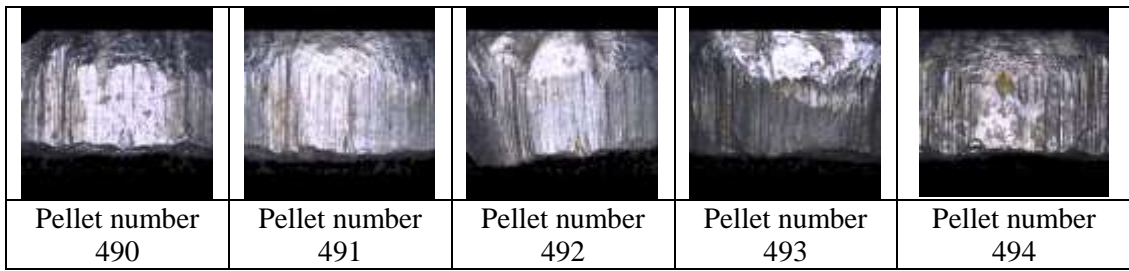
**Figure 5.8: LEA EF for the five pellets shot with the Brother Edgar Model 35. 20% of the pellets could be aligned. Only pellet number 490 was aligned**



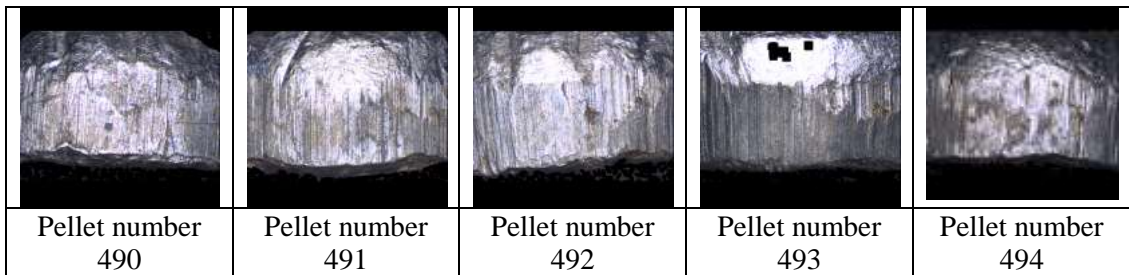
**Figure 5.9: LEA EG for the five pellets shot with the Brother Edgar Model 35. 20% of the pellets could be aligned. Only pellet number 490 was aligned**



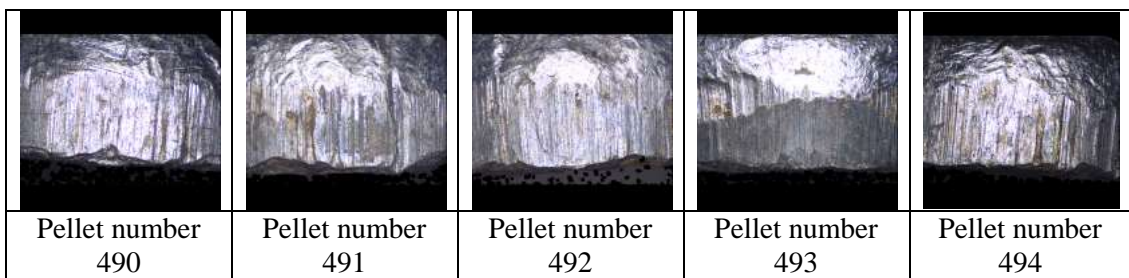
**Figure 5.10: LEA EH for the five pellets shot with the Brother Edgar Model 35. All pellets were aligned**



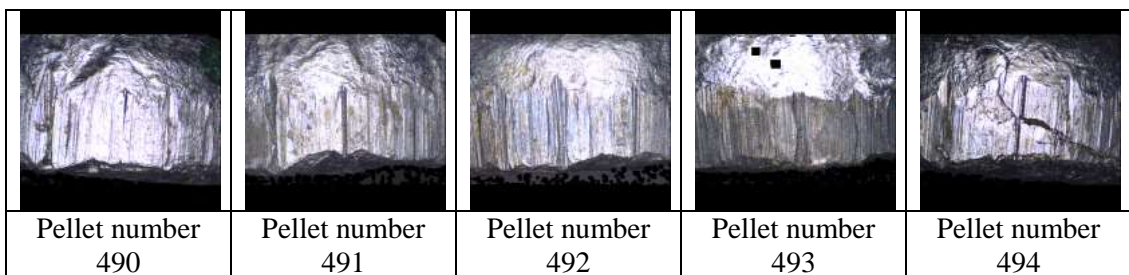
**Figure 5.11: LEA EI for the five pellets shot with the Brother Edgar Model 35. 80% of the pellets could be aligned. Pellet number 493 was misaligned**



**Figure 5.12: LEA EJ for the five pellets shot with the Brother Edgar Model 35. 40% of the pellets could be aligned. The misaligned pellets were 491 to 493**



**Figure 5.13: LEA EK for the five pellets shot with the Brother Edgar Model 35. 20% of the pellets could be aligned. Only pellet number 490 was aligned**



**Figure 5.14: LEA EL for the five pellets shot with the Brother Edgar Model 35. 20% of the pellets could be aligned. Only pellet number 490 was aligned**

Only LEA EA, ED and EH revealed more than 90% successful alignment. This is in general agreement with the results obtained from the observational studies with the air pistol, where greater than 90% alignment was revealed across only 5 striated regions (LEA A, D, J, H and K).

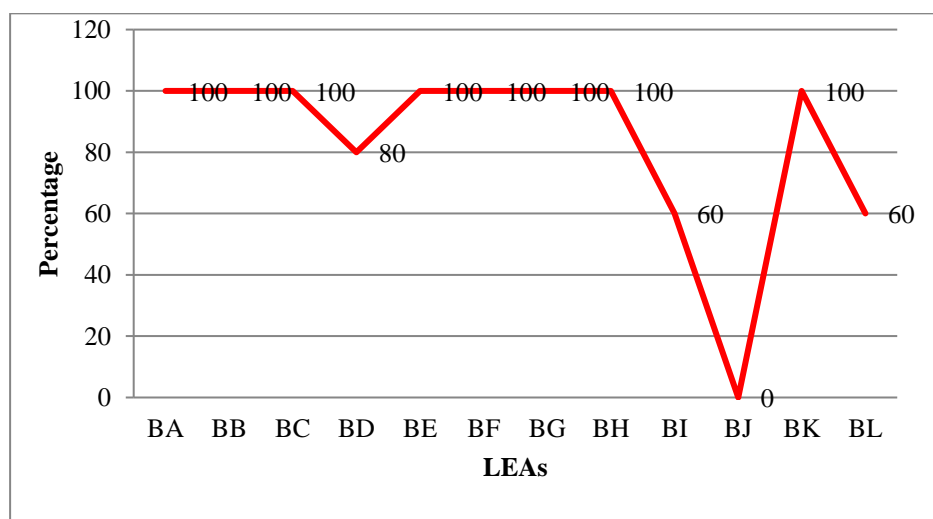
The Edgar Brother Model 35 used for this study was an old weapon, unavailable to purchase on the market and no research data is available for it. It uses spring-piston mechanism as described in Chapter 1, section 1.3, which requires air pressure to propel the pellets from its muzzle. The spring is subject to wear and tear, and when this occurs, less air pressure acts on the pellet. Lock and Morris [8] suggested that pressure exerted on the tools can affect the striation mark on it. Less pressure may cause some of the striation marks to be less imparted on the pellets resulting in only three LEAs being successfully aligned. Appendices 75 to 85 show the alignment results of LEA EB to EL.

## 5.2.2 Baikal 90042234 ИЖ-35

Table 5.3 and Figure 5.15 summarise the alignment results for the Baikal 90042234 ИЖ-35air rifle. In this case all but four of the LEAs (BD, BI, BJ and BL) revealed full alignment of the relevant striated marks.

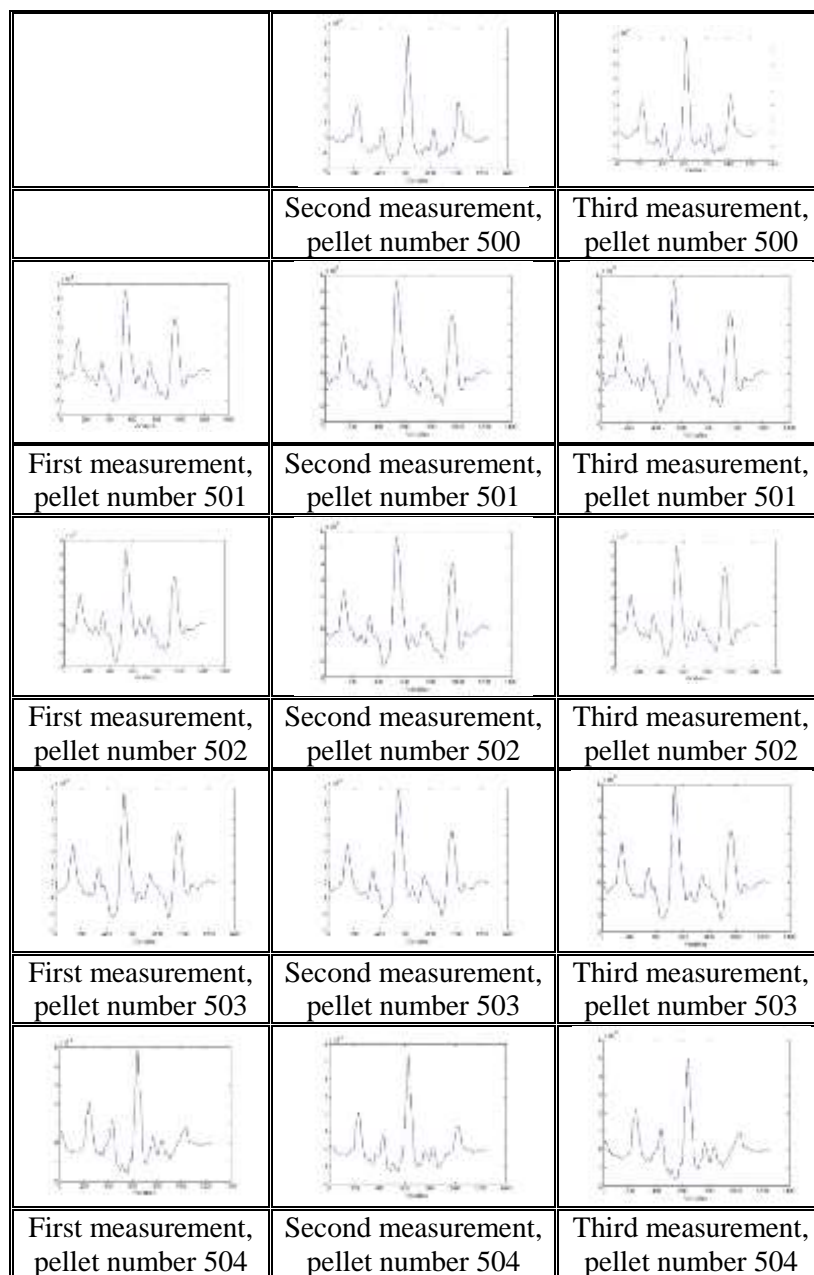
**Table 5.3: Summary of scanned results and measurements for pellets shot with the Baikal 90042234 ИЖ-35**

Striations	Number of pellets scanned	Number of measurements for alignment	Number of aligned measurements	Percentage of aligned measurements (%)
BA	5	15	15	100
BB	5	15	15	100
BC	5	15	15	100
BD	5	15	12	80
BE	5	15	15	100
BF	5	15	15	100
BG	5	15	15	100
BH	5	15	15	100
BI	5	15	9	60
BJ	5	15	0	0
BK	5	15	15	100
BL	5	15	9	60
Total	5	180	150	83



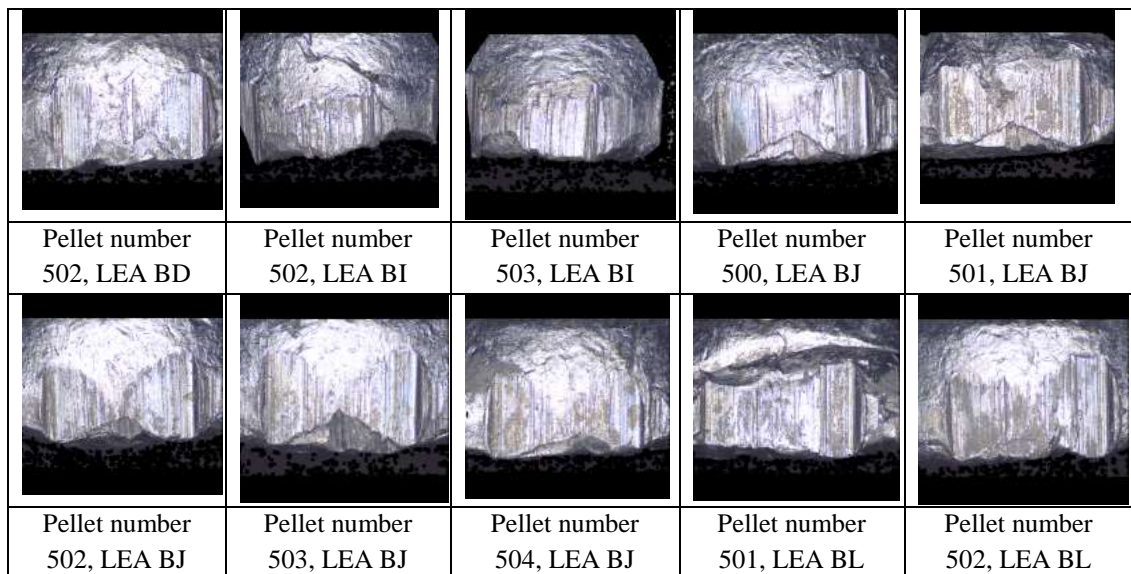
**Figure 5.15: Percentage of aligned measurements for LEA BA to BL, pellets numbered 500-504, Baikal 90042234 ИЖ-35**

The alignment result for LEA BA is shown in Figure 5.16 by way of an example. All measurements for LEA BA were aligned.



**Figure 5.16: Topographical profiles obtained from the microscopic measurements of LEA BA for pellets fired with the Baikal 90042234 ИЖ-35**

For LEA BD, 12 measurements (80%) were aligned. Pellet number 502 was misaligned due to corrosion. Similar corrosion was observed at LEA BI with 60% alignment, LEA BJ, where none of the pellets were aligned and LEA BL with 60% alignment. Figure 5.17 displays the misaligned pellets. Appendices 86 to 96 show the alignment results of LEA BB to BL.



**Figure 5.17: Misaligned pellets fired with the Baikal 90042234 ИЖ-35. All these pellets were corroded**

A total of 83% of striated regions were successfully aligned for pellets fired with the Baikal 90042234 ИЖ-35. Only measurements which were aligned at 90% were used for analysis which excluded LEA BD, BI, BJ and BL.

### 5.3 PCA, HCA and LDA analysis

The analysis was undertaken using Matlab® and PLS\_Toolbox® as discussed in Chapter 2. Only the data from the LEAs where greater than 90 % alignment was obtained were compared with each other as this threshold was demonstrated (in

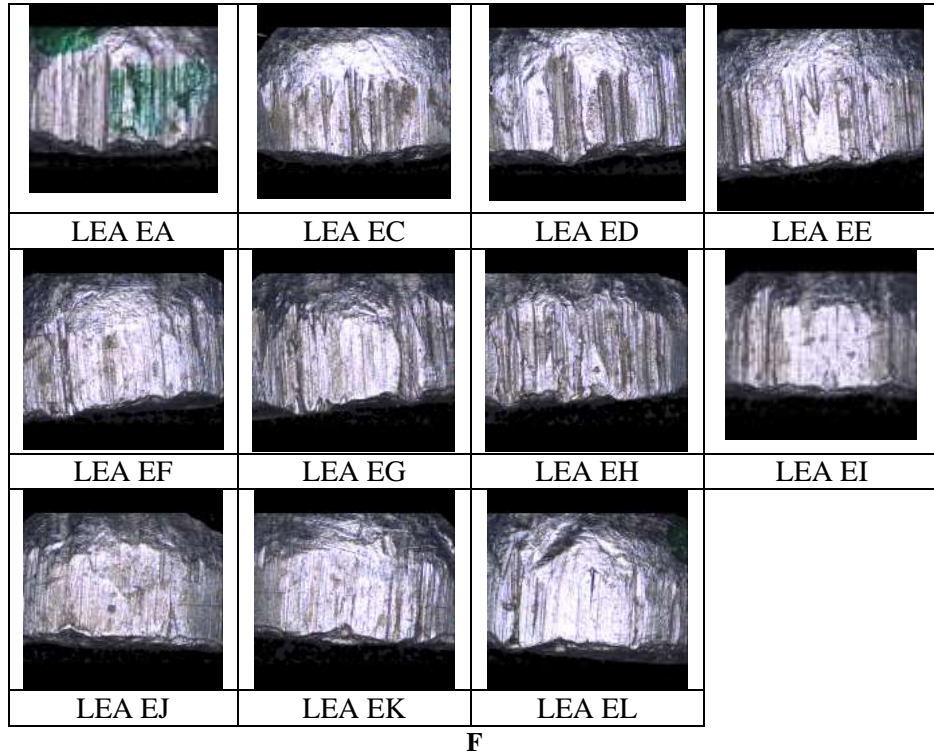


Chapter 3) to be required to provide the best opportunity for correct assignment of the striated marks to their respective LEAs.

Initially the results from each rifle were examined on their own and later, in combination with each other to explore whether differentiation could be achieved across all three weapons using the developed mathematical method. In each PCA graph, the colours represent the different LEAs and each dot provides the aligned measurements for a given pellet.

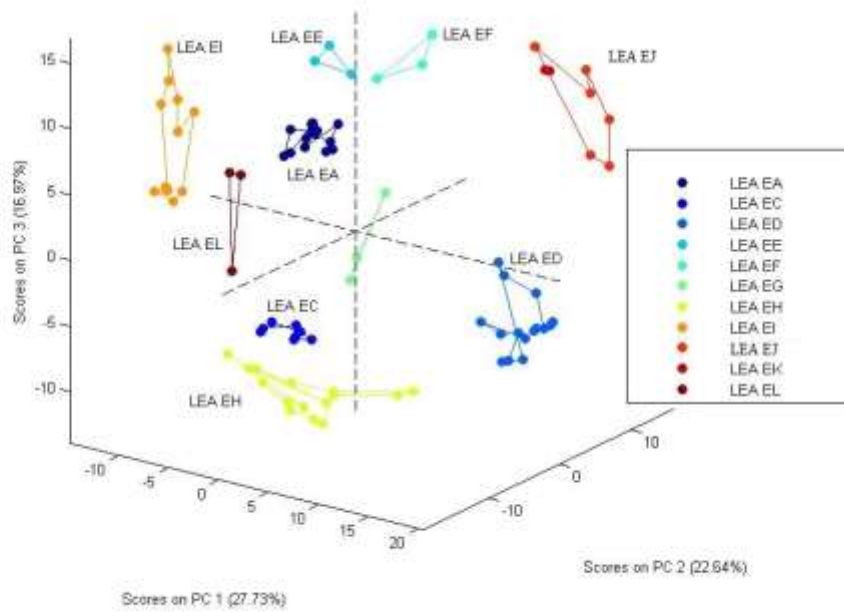
### **5.3.1 Edgar Brother Model 35**

All aligned LEA regions were analysed. The number of data points associated with each LEA varied because in some cases only a small number of pellets were analysed due to corrosion of the surface of the region of interest. Figure 5.18 illustrates the scanned images from all aligned LEAs on the pellets fired from the Edgar Brother Model 35 rifle.

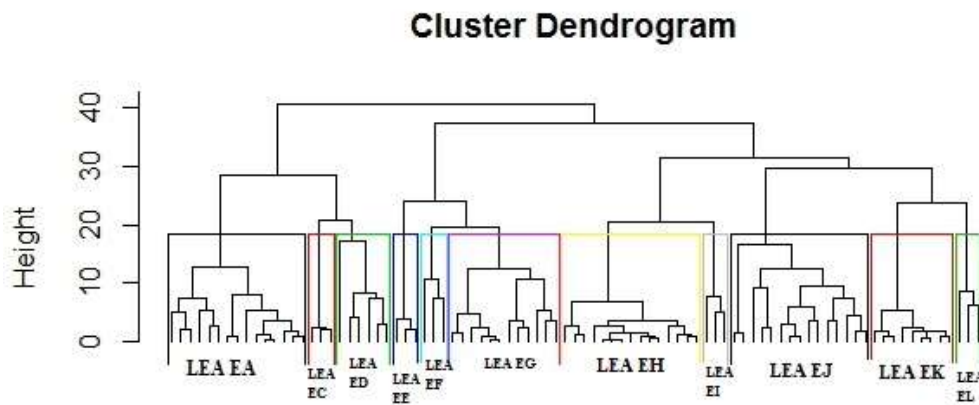


**Figure 5.18: Scanned images of all aligned LEAs from the Edgar Brother Model 35 air rifle. This is from pellet number 490. Based on these images, all LEAs are visually different. Green mark on LEA EA is for the purpose of identification, as previously stated in earlier chapters**

Figures 5.19 and 5.20 show the PCA and HCA results of all aligned LEAs and the results suggested that all LEAs can be differentiated from each other even though 90% alignment was achieved at only three of the 12 possible regions of interest across the five pellets fired from the Edgar Brother Model 35 air rifle. Table 5.4 shows the LDA classification results with 100% accuracy. All LEAs are well differentiated.



**Figure 5.19: The PCA results of all aligned LEAs from Edgar Brother Model 35 air rifle. All LEAs are differentiated from each other**



**Figure 5.20: The HCA result for all aligned LEAs from Edgar Brother Model 35 air rifle**

**Table 5.4: The LDA classification table of all aligned LEAs from Edgar Brother Model 35 air rifle. The diagonal values (in bold) represent correctly classified LEAs**

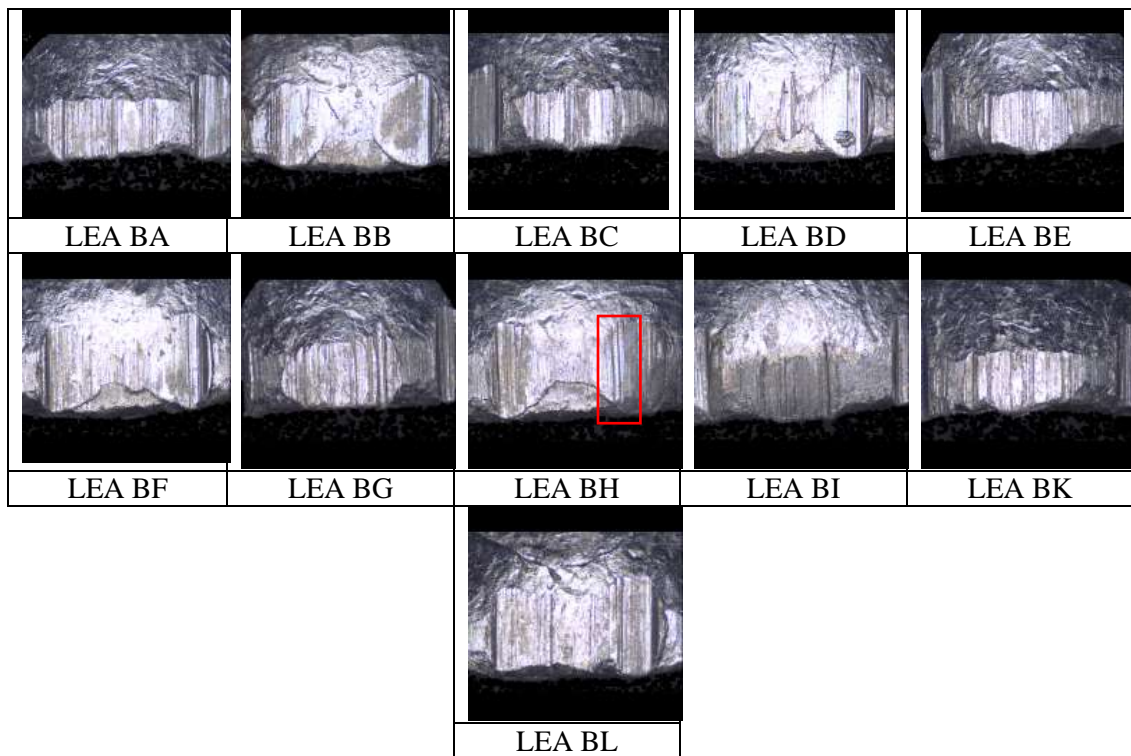
LEA	EA	EC	ED	EE	EF	EG	EH	EI	EJ	EK	EL	Percentage of classification
<b>EA</b>	<b>15</b>	0	0	0	0	0	0	0	0	0	0	100
<b>EC</b>	0	<b>9</b>	0	0	0	0	0	0	0	0	0	100
<b>ED</b>	0	0	<b>15</b>	0	0	0	0	0	0	0	0	100
<b>EE</b>	0	0	0	<b>3</b>	0	0	0	0	0	0	0	100
<b>EF</b>	0	0	0	0	<b>3</b>	0	0	0	0	0	0	100
<b>EG</b>	0	0	0	0	0	<b>3</b>	0	0	0	0	0	100
<b>EH</b>	0	0	0	0	0	0	<b>15</b>	0	0	0	0	100
<b>EI</b>	0	0	0	0	0	0	0	<b>12</b>	0	0	0	100
<b>EJ</b>	0	0	0	0	0	0	0	0	<b>6</b>	0	0	100
<b>EK</b>	0	0	0	0	0	0	0	0	0	<b>3</b>	0	100
<b>EL</b>	0	0	0	0	0	0	0	0	0	0	<b>3</b>	100

The analysis results show that these LEAs can be clustered according to its own LEAs, based on the PCA, HCA and LDA results. The model built for this group is 100% accurate, with no misclassification.

### 5.3.2 Baikal 90042234 ИЖ-35

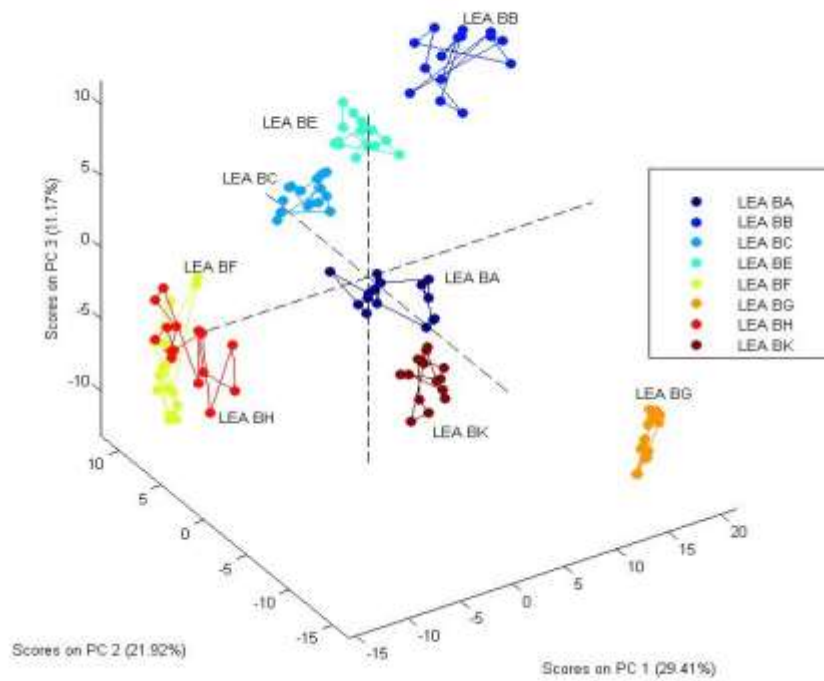
All aligned LEA regions were analysed. The number of data points associated with each LEA varied because in some cases only a small number of pellets were analysed due to corrosion of the surface of the region of interest.

Figure 5.21 illustrates the scanned images from all aligned LEAs on the pellets fired from the Baikal 90042234 ИЖ-35rifle.

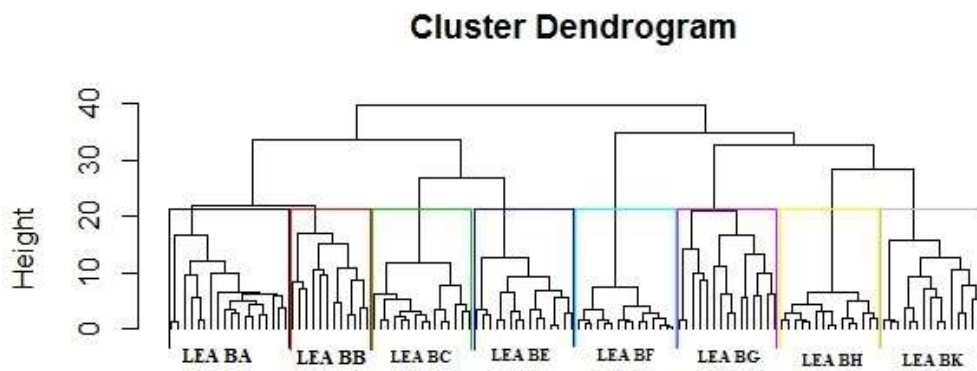


**Figure 5.21: The scanned images of all aligned LEAs from the Baikal 90042234 ИЖ-35 air rifle. This is pellet number 500. Visually, all LEAs are different except for LEA BF and BH which appear almost similar to each other. LEA BH has a striation mark as in the red rectangle. This is probably the reason it is differentiated from LEA BF based on the LDA results**

Figures 5.22 and 5.23 show the PCA and HCA results of all aligned LEAs. Table 5.5 shows the LDA classification table of all aligned LEAs.



**Figure 5.22:** The scores plot for PCA results for LEA BA, BB, BC, BE, BF, BG, BH and BK. All LEAs can be separated except for LEA BF and BH



**Figure 5.23:** The HCA result for all aligned LEAs from Baikal 90042234 ИЖ-35

**Table 5.5: The LDA classification table of all aligned LEAs from Baikal 90042234 ИЖ-35air rifle. The diagonal values (in bold) represent correctly classified LEAs**

LEA	BA	BB	BC	BE	BF	BG	BH	BK	Percentage of classification
<b>BA</b>	<b>15</b>	0	0	0	0	0	0	0	100
<b>BB</b>	0	<b>15</b>	0	0	0	0	0	0	100
<b>BC</b>	0	0	<b>15</b>	0	0	0	0	0	100
<b>BE</b>	0	0	0	<b>15</b>	0	0	0	0	100
<b>BF</b>	0	0	0	0	<b>15</b>	0	0	0	100
<b>BG</b>	0	0	0	0	0	<b>15</b>	0	0	100
<b>BH</b>	0	0	0	0	0	0	<b>15</b>	0	100
<b>BK</b>	0	0	0	0	0	0	0	<b>15</b>	100

The analysis shows that all aligned LEAs from Baikal 90042234 ИЖ-35 can be differentiated except for LEA BF and BH, based on the PCA results. However, the LDA can classify all LEAs very well. As explained in Figure 5.21, LEA BH has a striation mark (as in the red rectangle) which is absent in LEA BF. This is probably the reason LDA can differentiate both LEAs. The model built for this group is 100% accurate.

Based on the analysis results for both air rifles, models built for these groups show 100% accuracy. In Chapter 3, the accuracy percentage for more than 90% successful alignment for the newly bought air pistol is 98.9%. Both air rifles have the accuracy percentage of 100%. These show that models built using the methodology suggested, image scanning, data aligning and mathematical analysis can be utilised to objectify the striation marks on the pellets. The kinetic energy and the length of the barrel of the air rifles [1, 9] may have contributed to the accuracy of built model. The kinetic energy for the air pistol is between 4.1 to 4.9 foot pounds and based on manufacturer's email to author [10], the kinetic energy of air rifles is set between

10.5-11.6 foot pounds. The kinetic energy of air rifles is higher than the air pistol and air rifles has longer barrels than air pistol. Higher kinetic energy is needed to propel the pellets along the longer barrel. While the pellets were travelling along the rifled barrel, striation marks were imparted on the pellets. Given that air rifles have longer barrels, it allowed the pellets to acquire more marks from the rifled barrel [11]. Therefore the striation marks on the pellets shot by the air rifles can be differentiated well.

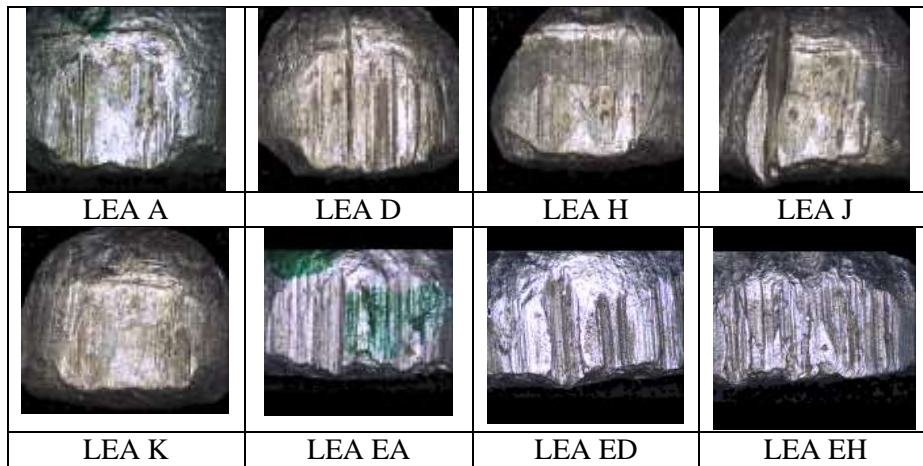
### **5.3.3 Differentiation between pellets fired from different weapons**

All LEAs aligned at 90% or greater were compared across the pellets fired from the air pistol (LEA A, D, H, J and K), the Edgar Brother Model 35 air rifle (LEA EA, ED and EH) and the Baikal 90042234 ИЖ-35 (LEA BA, BB, BC, BE, BF, BG, BH and BK).

#### **5.3.3.1 Air pistol and Edgar Brother Model 35 air rifle**

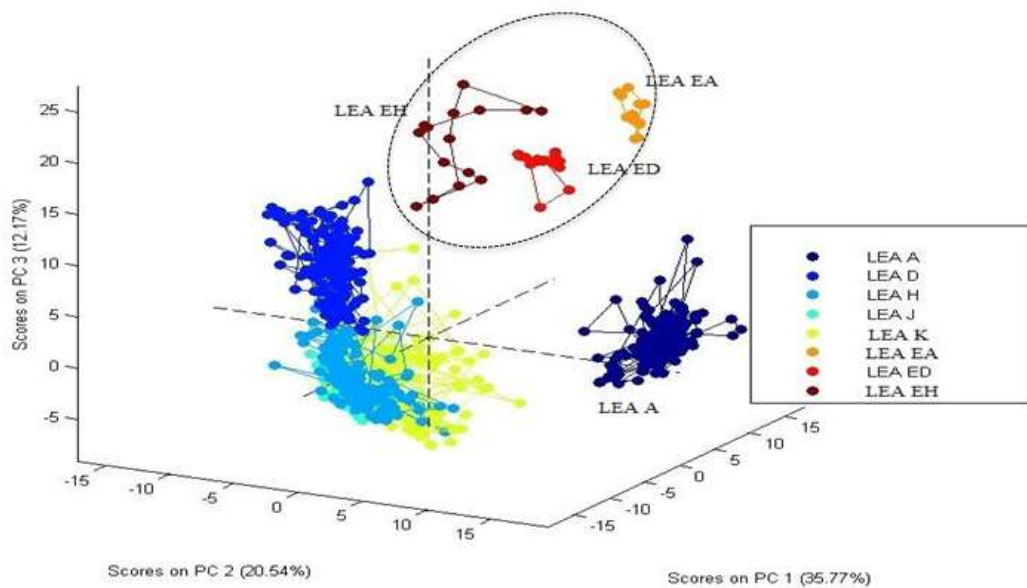
The LEA A, D, J, H, EA, ED and EH appear visually different from each other. LEA K from the air pistol has subtle differences in some cases (Figure 5.24).



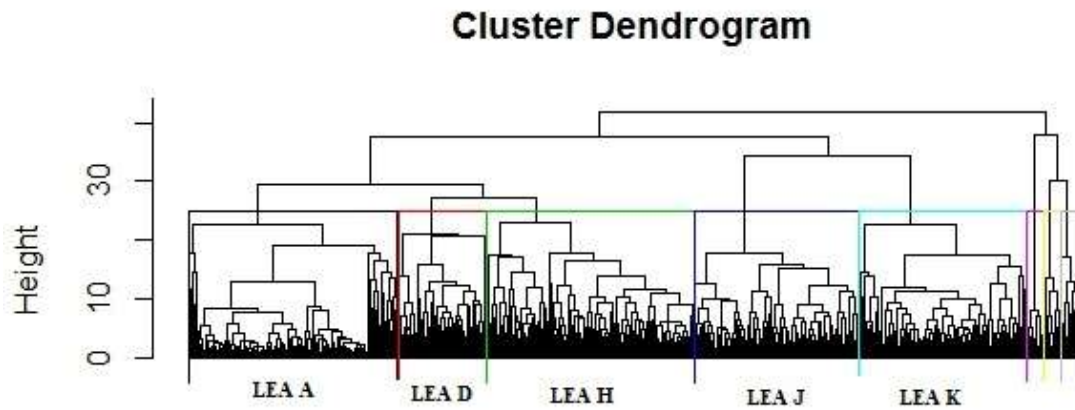


**Figure 5.24: Scanned images of pellet number 159 from the air pistol (LEA A, D, H, J and K) and pellet number 490 from the Edgar Brother Model 35 air rifle (LEA EA, ED and EH)**

Figures 5.25 to 5.26 and Table 5.6 present the analysis results of all aligned LEAs from the air pistol and the Edgar Brother Model 35 air rifle.



**Figure 5.25: The PCA results for air pistol and the Edgar Brother Model 35 air rifle pellets. This clearly shows a separation between the two weapons. LEA EA, ED and EH are clearly separated from the other striated regions of the air pistol, as shown in the circle**



**Figure 5.26: The HCA results for air pistol and the Edgar Brother Model 35 air rifle pellets. The last 3 LEAs are not labelled to avoid crowding. The pink colour is LEA EA, followed by yellow for LEA ED and grey for LEA EH**

**Table 5.6: The LDA classification table of all aligned LEAs from the air pistol and the Edgar Brother Model 35 air rifle. The diagonal values (in bold) represent correctly classified LEAs**

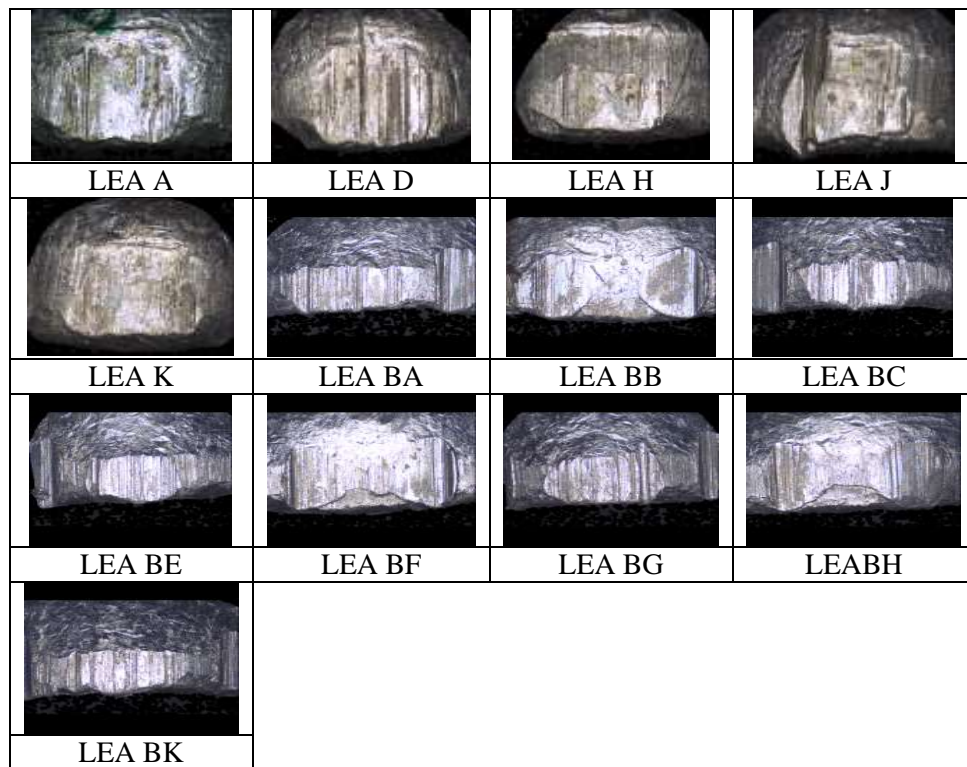
LEA	A	D	H	J	K	EA	ED	EH	Percentage of classification
<b>A</b>	<b>147</b>	0	0	0	0	0	0	0	100.0
<b>D</b>	0	<b>144</b>	0	0	0	0	0	0	100.0
<b>H</b>	0	0	<b>150</b>	0	0	0	0	0	100.0
<b>J</b>	0	0	0	<b>150</b>	0	0	0	0	100.0
<b>K</b>	0	0	7	0	<b>137</b>	0	0	0	95.1
<b>EA</b>	0	0	0	0	0	<b>15</b>	0	0	100.0
<b>ED</b>	0	0	0	0	0	0	<b>15</b>	0	100.0
<b>EH</b>	0	0	0	0	0	0	0	<b>15</b>	100.0

Based on the analysis results, the LEAs from the air rifles can be separated from LEAs of the air pistol. The model built for this group is 99.4% accurate. The accuracy is more than 90% because as shown in Figure 5.24, LEAs from both weapons are visually different and it is proven in the analysis result, especially in the

LDA classification table. The pellets fired from both weapons can be distinguished from each other, although there is clearly convolution of LEA K from the air pistol (which was explained in Chapter 3).

### 5.3.3.2 Air pistol and Baikal 90042234 ИЖ-35 air rifle

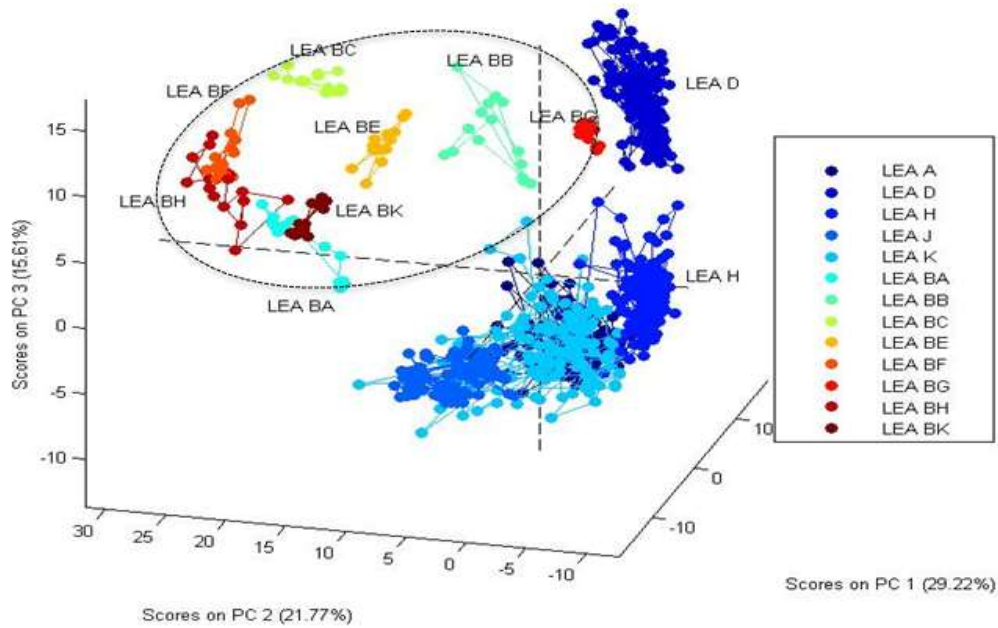
The LEA A, D, H, J and K from the air pistol and LEA BA, BB, BC, BE, BF, BG, BH and BK were analysed and Figure 5.27 shows the scanned images of these pellets.



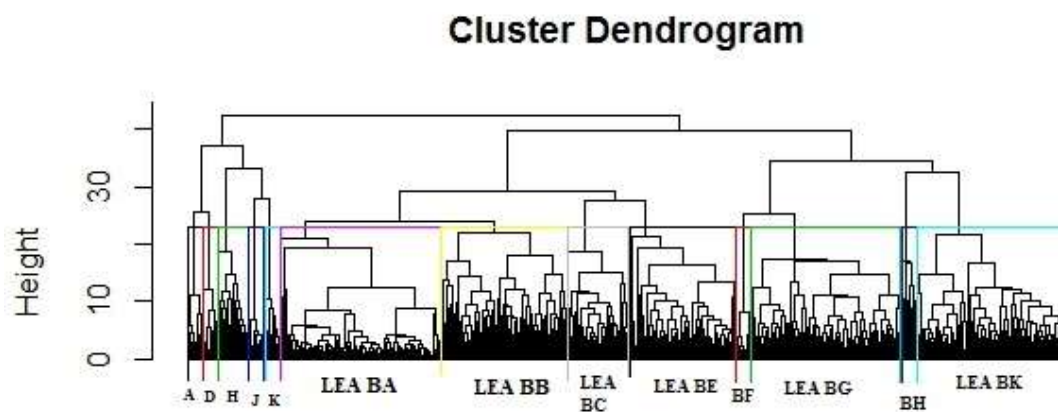
**Figure 5.27: The scanned images of the air pistol pellet number 159 (LEA A, D, H, J and K) and the Baikal 90042234 ИЖ-35 air rifle pellet number 500 (LEA BA, BB, BC, BE, BF, BG, BH and BK)**

Visually, the air pistol pellets and the air rifle pellets appear different. The analysis results are presented in Figures 5.28 and 5.29 and Table 5.7. The model built for this

group is 99.6% accurate. The accuracy is more than 90% because as shown in Figure 5.27, LEAs from both weapons are visually different and it is proven in the analysis result. The pellets fired from both weapons can be distinguished from each other, although there is clearly convolution of LEA K from the air pistol.



**Figure 5.28: The PCA results for air pistol and Baikal 90042234 ИЖ-35 air rifle. LEAs from the air pistol are separated from LEAs from the air rifle, as in the circle**



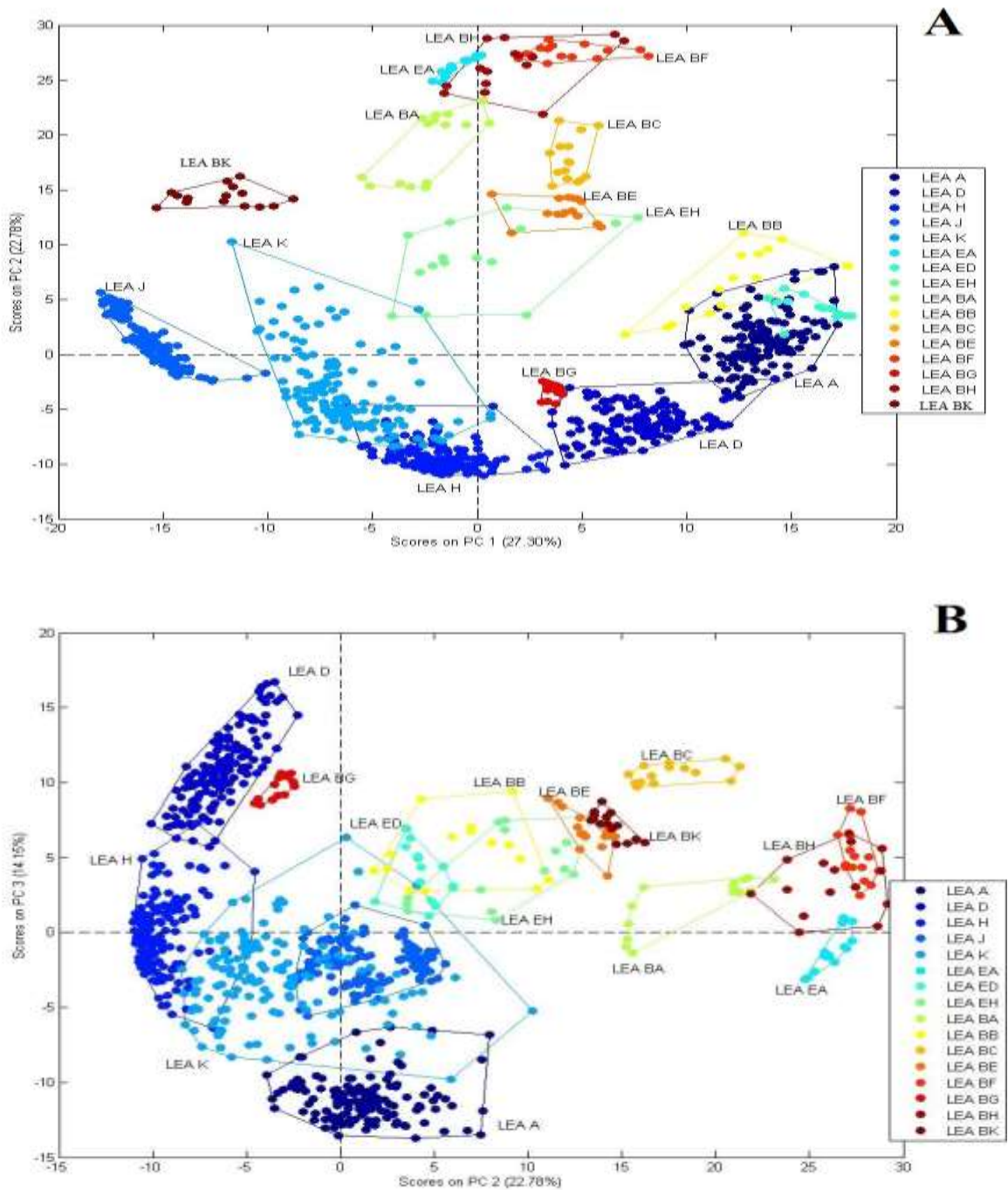
**Figure 5.29: The HCA results for air pistol and Baikal 90042234 ИЖ-35 air rifle**

**Table 5.7: The LDA classification table of all aligned LEAs from the air pistol and Baikal 90042234 ИЖ-35 air rifle. The diagonal values (in bold) represent correctly classified LEAs**

LEA	A	D	H	J	K	BA	BB	BC	BE	BF	BG	BH	BK	Percentage of classification
<b>A</b>	<b>147</b>	0	0	0	0	0	0	0	0	0	0	0	0	100.0
<b>D</b>	0	<b>144</b>	0	0	0	0	0	0	0	0	0	0	0	100.0
<b>H</b>	0	0	<b>150</b>	0	0	0	0	0	0	0	0	0	0	100.0
<b>J</b>	0	0	0	<b>150</b>	0	0	0	0	0	0	0	0	0	100.0
<b>K</b>	0	0	7	0	<b>137</b>	0	0	0	0	0	0	0	0	95.1
<b>BA</b>	0	0	0	0	0	<b>15</b>	0	0	0	0	0	0	0	100.0
<b>BB</b>	0	0	0	0	0	0	<b>15</b>	0	0	0	0	0	0	100.0
<b>BC</b>	0	0	0	0	0	0	0	<b>15</b>	0	0	0	0	0	100.0
<b>BE</b>	0	0	0	0	0	0	0	0	<b>15</b>	0	0	0	0	100.0
<b>BF</b>	0	0	0	0	0	0	0	0	0	<b>15</b>	0	0	0	100.0
<b>BG</b>	0	0	0	0	0	0	0	0	0	0	<b>15</b>	0	0	100.0
<b>BH</b>	0	0	0	0	0	0	0	0	0	0	0	<b>15</b>	0	100.0
<b>BK</b>	0	0	0	0	0	0	0	0	0	0	0	0	<b>15</b>	100.0

### 5.3.3.3 All three weapons

The relationship between all aligned LEAs from the air pistol and both air rifles are shown in Figures 5.30 and 5.31 and Table 5.8.



**Figure 5.30: The PCA results for all aligned LEAs from the air pistol and the air rifles in 2D. In both (A) and (B), LEAs from the air pistol can be differentiated from most LEAs from the air rifles**

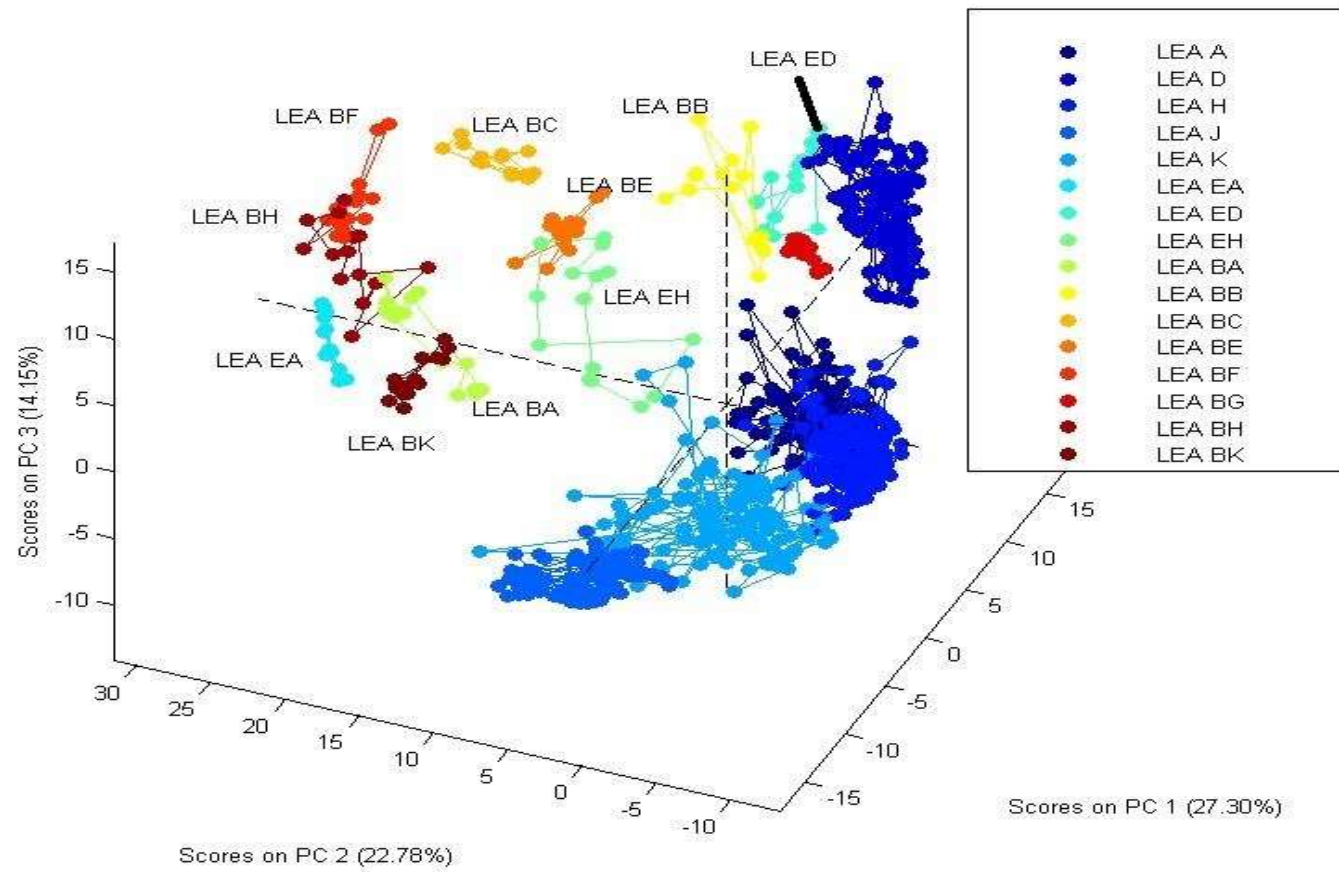


Figure 5.31: 3D PCA incorporating all three PCs



**Table 5.8: The LDA classification table of all aligned LEAs from the air pistol and the air rifles. The diagonal values (in bold) represent correctly classified LEAs**

LEA	A	D	H	J	K	EA	ED	EH	BA	BB	BC	BE	BF	BG	BH	BK	Percentage of classification
<b>A</b>	<b>147</b>	0	0	0	0	0	0	0	0	0	0	0	0	0	0	0	100.0
<b>D</b>	0	<b>144</b>	0	0	0	0	0	0	0	0	0	0	0	0	0	0	100.0
<b>H</b>	0	0	<b>150</b>	0	0	0	0	0	0	0	0	0	0	0	0	0	100.0
<b>J</b>	0	0	0	<b>150</b>	0	0	0	0	0	0	0	0	0	0	0	0	100.0
<b>K</b>	0	0	7	0	<b>137</b>	0	0	0	0	0	0	0	0	0	0	0	95.1
<b>EA</b>	0	0	0	0	0	<b>15</b>	0	0	0	0	0	0	0	0	0	0	100.0
<b>ED</b>	0	0	0	0	0	0	<b>15</b>	0	0	0	0	0	0	0	0	0	100.0
<b>EH</b>	0	0	0	0	0	0	0	<b>15</b>	0	0	0	0	0	0	0	0	100.0
<b>BA</b>	0	0	0	0	0	0	0	0	<b>15</b>	0	0	0	0	0	0	0	100.0
<b>BB</b>	0	0	0	0	0	0	0	0	0	<b>15</b>	0	0	0	0	0	0	100.0
<b>BC</b>	0	0	0	0	0	0	0	0	0	0	<b>15</b>	0	0	0	0	0	100.0
<b>BE</b>	0	0	0	0	0	0	0	0	0	0	0	<b>15</b>	0	0	0	0	100.0
<b>BF</b>	0	0	0	0	0	0	0	0	0	0	0	0	<b>15</b>	0	0	0	100.0
<b>BG</b>	0	0	0	0	0	0	0	0	0	0	0	0	0	<b>15</b>	0	0	100.0
<b>BH</b>	0	0	0	0	0	0	0	0	0	0	0	0	0	0	<b>15</b>	0	100.0
<b>BK</b>	0	0	0	0	0	0	0	0	0	0	0	0	0	0	0	<b>15</b>	100.0

The PCA results show that some of the LEAs, LEA ED and EH are convoluted with LEAs from the air pistol. However, based on the LDA classification table, Table 5.8, all LEAs from both air rifles can be separated well from LEAs from the air pistol. The model built for this group is 99.7% accurate. The accuracy is more than 90% because all three weapons produce different surface topography on the pellets (Figures 5.24 and 5.27). The higher kinetic energy and longer air rifles' barrels may have contributed to well separated LEAs from the air rifles as compared to LEAs from the air pistol, as discussed earlier.

#### **5.4 Conclusions**

Class characteristics of the bullet, which include the number of lands and grooves and direction of rifling twist, indicate the make and model of the gun. However, it is not specific. All three weapons used in this study has similar class characteristics: 12 lands and grooves with right rifling, as mentioned in Chapter 2. Therefore individual characteristics can be used for identification. In this study, when comparing LEAs from the air pistol with LEAs from the air rifles separately, LEAs from the air rifles can be differentiated from the LEAs from the air pistol. This is where the class characteristic plays its role to differentiate LEAs from pellets fired from the air pistol and LEAs from pellets fired with the air rifles. When comparing the LEAs from all three weapons, all LEAs from the two air rifles could be correctly assigned to the air rifle while separation from the air pistol pellets was more convincing. The analysis results suggest that the LEAs on projectiles from different weapons may be differentiated from each other according to the weapon that fired them. All aligned LEAs from the air rifles are well differentiated from each other.

The results reaffirm that the older a weapon gets, the more unique it becomes due to damage, build up lead and uncleaned barrels. Higher kinetic energy and longer barrels may contribute to well differentiated LEAs from the air rifles.

Based on the analysis results from Chapter 3 to 5, it is proven that the LDA produced better results for objectivity as compared to the PCA and HCA. PCA and HCA are unsupervised analysis, as mentioned in Chapter 1, while LDA is a supervised analysis. Therefore for Chapter 6, only PCA and LDA were used for data analysis, because LDA shows better discriminant of data and that is the core for this study. Models built for these groups show that the accuracy percentage are more than 90%. The value of the accuracy percentage can be used to objectify the accuracy of objectifying the striation marks. The model built can be used to predict the accuracy percentage of striation marks on ammunition, to be tested on firearms bullet, for future studies.

## 5.5 References

1. Di Maio, V.J.M., *Gunshot wounds : practical aspects of firearms, ballistics, and forensic techniques*. 1999: Boca Raton : CRC Press.
2. Chu, W., Song, J., Vorburger, T., Yen, J., Ballou, S. and Bachrach, B., *Pilot study of automated bullet signature identification based on topography measurements and correlations*. J Forensic Sci, 2010. 55(2): p. 341-347.
3. Nichols, R.G., *Defending the Scientific Foundations of the Firearms and Tool Mark Identification Discipline: Responding to Recent Challenges*. Journal of Forensic Sciences, 2007. 52(3): p. 586-594.
4. Nichols, R.G., *Firearm and toolmark identification criteria: A review of the literature, part II*. J Forensic Sci, 2003. 48(2): p. 1-10.
5. Churchman, J., *The Reproduction of Characteristics in Signatures of Cooney Rifles*. RCMP Gaz, 1949. 11(5): p. 133-40.
6. Air, P. *Weihrauch Guns*. 2012 [cited 2014; Available from: <http://www.pyramydair.com/manual/hw45>.

7. Company, H.A. *Hatsan Arms Company*. 1976 [cited 2015; Available from: [http://www.hatsan.com.tr/en\\_company.html](http://www.hatsan.com.tr/en_company.html)].
8. Lock, A.B., Morris, M. D., *Significance of Angle in the Statistical Comparison of Forensic Tool Marks*. *Technometrics*, 2013. 55(4): p. 548-561.
9. Heard, B.J., *Handbook of firearms and ballistics [internet resource] examining and interpreting forensic evidence*, ed. P.D.A. Dawsonera. 2008: Oxford : Wiley-Blackwell.
10. Heapy, T., *Average Kinetic Energy for Air Rifle*. 2016: Email to Author.
11. Cork, D.L., Nair, V.N. and Rolph, J.E., *Some forensic aspects of ballistic imaging*. 2010. 38(2).

## **Chapter 6: Matching the striations on damaged pellets shot from an air pistol through a target at different distances**

### **6.1 Introduction**

When a projectile impact on a hard surface, a compression of the projectile can occur, rendering the visualisation of the striated marks difficult. As a consequence, it may be equally difficult to compare the marks, either with other projectiles or with exemplars fired from a questioned weapon for comparison purposes. Exploring the potential evidential links between a weapon and projectiles that have been damaged as a result of impact is of particular significance and importance. Booker [1] suggested that the examination of damaged pellets are challenging to the firearms examiners. He also suggested that damaged bullets must be compared with the test-fired bullet from the suspected weapon. Any similar mark on both bullets should be marked as the best-matched orientation or alignment. Several different test-fired bullets should be collected to check for reproducibility. When reproducibility is confirmed for the test-fired bullets, these test-fired bullets must be compared against the evidence bullet for striation similarity.

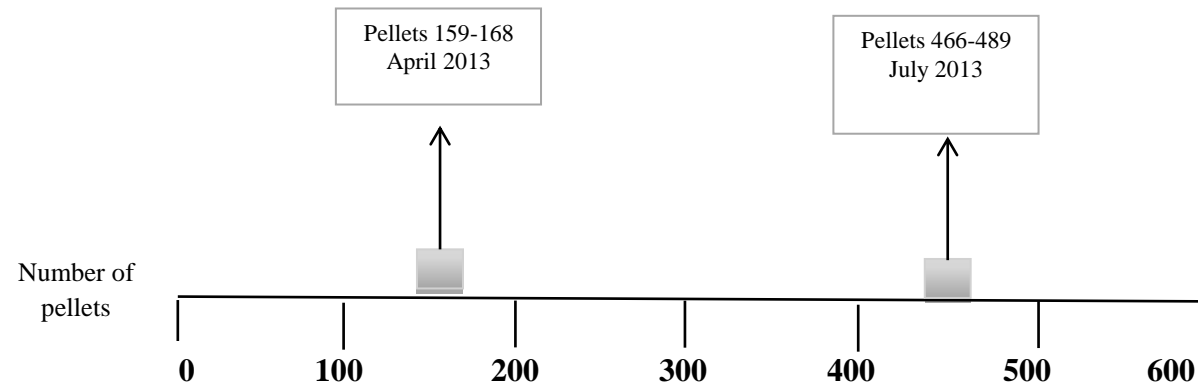
### **6.2 Selection of the pellets for testing**

The methodology used was as described in Chapter 2 regarding image acquisition, pre-processing and data analysis using Matlab®. Based on Table 6.1 and Figure 6.1, a set of 24 pellets was used from the firings undertaken in July 2013. These pellets were purposely damaged by being fired into a target which was placed sequentially at 1 metre, 2 metres, 3 metres and 4 metres distances from the muzzle. The

methodology of shooting is discussed in detail below. These damaged pellets were compared with pristine pellets shot in April 2013.

**Table 6.1: Group of pellets used in this objective are highlighted in grey**

<b>Date of test</b>	<b>Pellet Number</b>	<b>Test Done</b>	<b>Weapon</b>	<b>Total Pellets fired</b>	<b>Pellets Collected</b>	<b>Pellets selected for this study</b>
April 2012	1-50	Low Velocity	HW 45	50	50	
April 2012	51-100	High Velocity	HW 45	50	50	
April 2012	101-122	Chronograph: low and high velocity	HW 45	22	0	
January 2013	123-158	Bones & Gelatine	HW 45	36	36	
April 2013	159-208	High Velocity	HW 45	50	50	159-208
April 2013	209-219	Chronograph: high velocity	HW 45	11	0	
May 2013	220-319	High Velocity	HW 45	100	100	
May 2013	320-341	Chronograph: high velocity	HW 45	22	0	
June 2013	342-441	High Velocity	HW 45	100	100	
July 2013	442-465	Low Velocity Distance	HW 45	24	24	
July 2013	466-489	High Velocity Distance	HW 45	24	24	466-489
July 2013	490-499	Rifle 1	Edgar Brother Model 35	10	10	
July 2013	500-509	Rifle 2	Baikal 90042234 ИЖ-35	10	10	
September 2013	510-559	Chronograph: low velocity	HW 45	50	50	
September 2013	560-609	Chronograph: high velocity	HW 45	50	50	
<b>Total number of pellets</b>				<b>609</b>	<b>554</b>	<b>74</b>

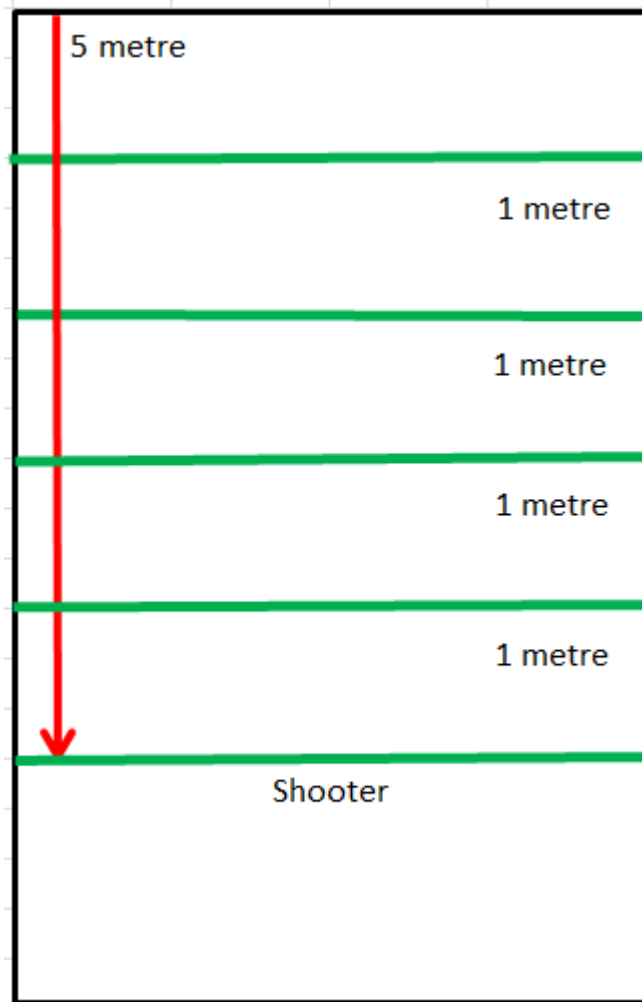


**Figure 6.1: Pellets examined in the distortion study**



### 6.3 Distance Measurement

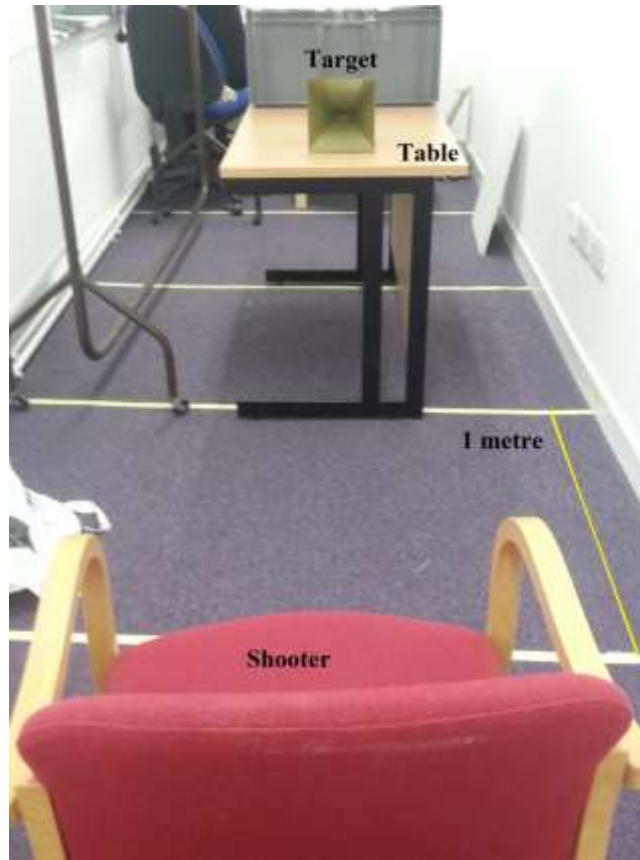
The schematic diagram of the laboratory and the distance measurements are presented in Figure 6.2.



**Figure 6.2:** The schematic view of distance measuring in the lab. The red line indicates the distance between the shooter and the wall. The target was placed on each green line as the samples were generated

Initially, the shooter line was measured 5 metres from the wall of the laboratory as shown in Figure 6.2. Then four green lines in the schematic were measured at 4 metres, 3 metres, 2 metres and 1 metre from the wall and marked with tape. For

shooting, a table with the target at its edge was placed on the appropriate line, as in Figure 6.3.

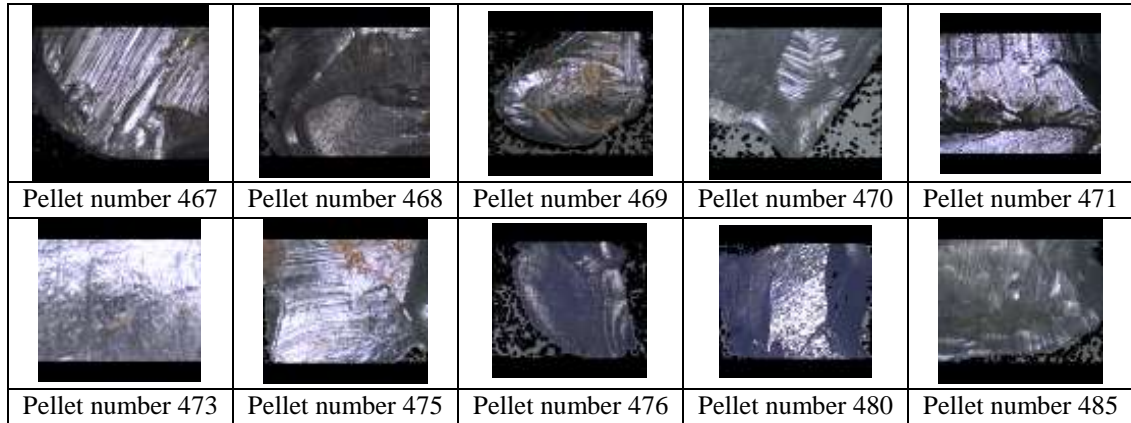


**Figure 6.3: The shooting process. The shooter sat on the chair. The target was placed on the edge of the table on the marked line which was 1 metre from the shooter**

The shooter sat on the chair so that he/ she was at the same level as the target. In each case 6 pellets were fired one after another into the target for each distance. Each pellet was collected after firing and individually packaged and labelled. All 24 pellets were scanned with the Alicona® for further analysis.

## 6.4 Results

Figure 6.4 provide examples of severely deformed pellets. In these cases it was not possible to scan the pellets successfully.



**Figure 6.4: Examples of severely deformed pellets**

Table 6.2 indicates the number of pellets scanned. Boxes with an ‘x’ and highlighted in grey indicate pellets that are not possible to be successfully scanned by the LEA because of the damage to the pellet in that region. Based on Table 6.2, a total of 93 LEA measurements were possible. These measurements were pre-processed with Matlab® for curve removal and alignment as previously described.

Table 6.3 and Figure 6.5 show the percentage of LEAs scanned according to distance of shooting.

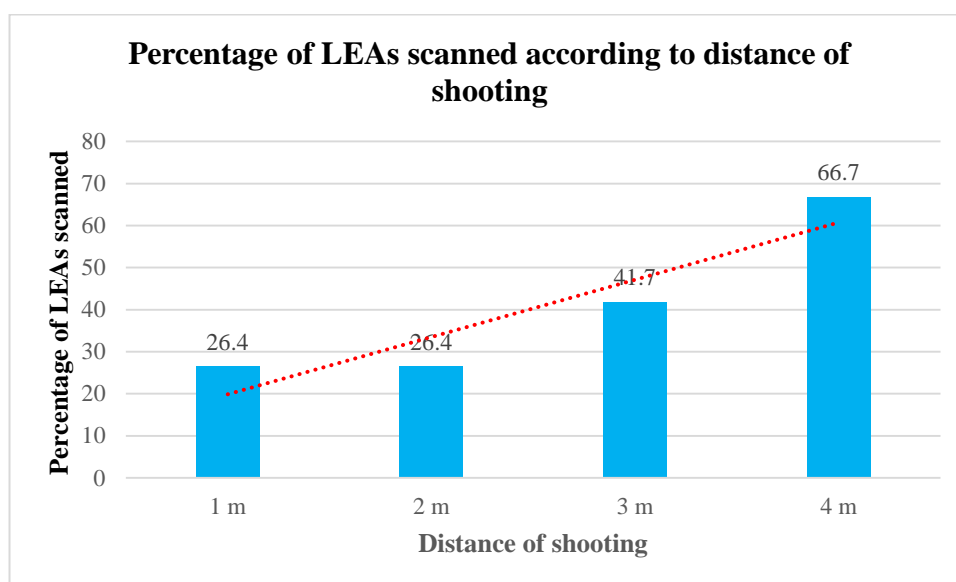
**Table 6.2: Total LEAs scanned for this study. Boxes with an ‘x’ and highlighted in grey indicate LEAs that could not be scanned due to severe deformation**

Distance	LEA/ Pellet number	A	B	C	D	E	F	G	H	I	J	K	L	Total LEAs scanned
1 m	466	/	/	/	x	x	x	/	/	/	/	/	/	9
	467	x	x	x	x	x	x	x	x	/	/	x	x	2
	468	x	x	x	x	x	x	x	x	x	/	x	x	1
	469	x	x	x	x	x	x	x	x	x	/	/	x	2
	470	/	x	x	x	x	x	x	x	/	/	x	x	3
2 m	471	x	x	x	x	x	x	x	x	/	/	x	x	2
	472	x	x	x	x	x	x	/	/	/	/	x	x	4
	473	/	x	x	x	x	x	x	x	x	X	x	x	1
	474	x	x	x	x	x	x	/	/	/	/	/	/	6
	475	x	x	x	x	x	x	x	x	x	/	/	x	2
	476	/	/	x	x	x	x	x	x	/	/	x	x	4
	477	/	x	x	x	x	x	x	x	x	X	x	/	2
3 m	478	x	x	x	x	x	x	/	/	x	/	/	/	5
	479	x	x	x	/	/	/	/	/	/	X	x	x	6
	480	x	x	x	x	x	x	x	x	x	/	x	x	1
	481	x	x	x	x	x	x	x	x	x	X	x	x	0
	482	x	x	x	/	/	/	/	x	x	x	X	x	x
4 m	483	/	/	/	/	/	/	/	/	/	/	x	x	10
	484	/	/	/	/	/	/	/	/	/	/	/	/	12
	485	x	x	x	x	x	x	x	x	x	X	x	x	0
	486	/	/	x	/	/	/	/	/	x	/	/	/	10

	487	/	x	x	x	x	x	x	x	x	X	/	/	3
	488	x	x	x	x	x	x	x	x	x	X	x	x	0
	489	x	x	x	/	x	x	x	/	/	/	/	x	5
<b>Total pellets scanned</b>		<b>9</b>	<b>5</b>	<b>3</b>	<b>6</b>	<b>5</b>	<b>5</b>	<b>8</b>	<b>8</b>	<b>12</b>	<b>16</b>	<b>9</b>	<b>7</b>	<b>93</b>

**Table 6.3: Percentage of LEAs scanned according to distance of shooting**

Distance of shooting	Total pellets fired	Total number of available LEAs (before scanning)	Total pellets useable for scanning	Total number of LEAs supposedly available for scanning	Total LEAs scanned from useable pellets	Percentage of LEAs scanned (%)
1 m	6	72	6	72	19	26.4
2 m	6	72	6	72	19	26.4
3 m	6	72	5	60	25	41.7
4 m	6	72	4	48	32	66.7
Total	24	288	21	252	93	36.9



**Figure 6.5: A total of 24 pellets were fired according to distance, 1m to 4m however only 21 pellets were used for LEA scanning. 3 pellets were badly damaged (pellets number 481, 485 and 488) therefore no LEAs can be obtained from them. A total of 93 LEAs can be scanned from these 21 pellets. Percentage of LEAs that was able to be scanned from these 21 pellets are shown here. These LEAs were then compared to the LEAs from the April 2013 group with more than 90% aligned measurements, LEA A, D, H, J and K**






A total of 24 pellets were fired according to distance. However, 3 pellets were badly damaged (pellets number 481, 485 and 488). Therefore only 21 pellets were useable for further analysis. These 21 pellets produced 93 LEAs that can be scanned. These LEAs were then compared to the LEA regions of the previously generated pellets

where 90% alignment was obtained, from the pellets shot in April 2013. These were LEAs A, D, H, J and K. All data was treated as previously described and subjected to analysis using Matlab.

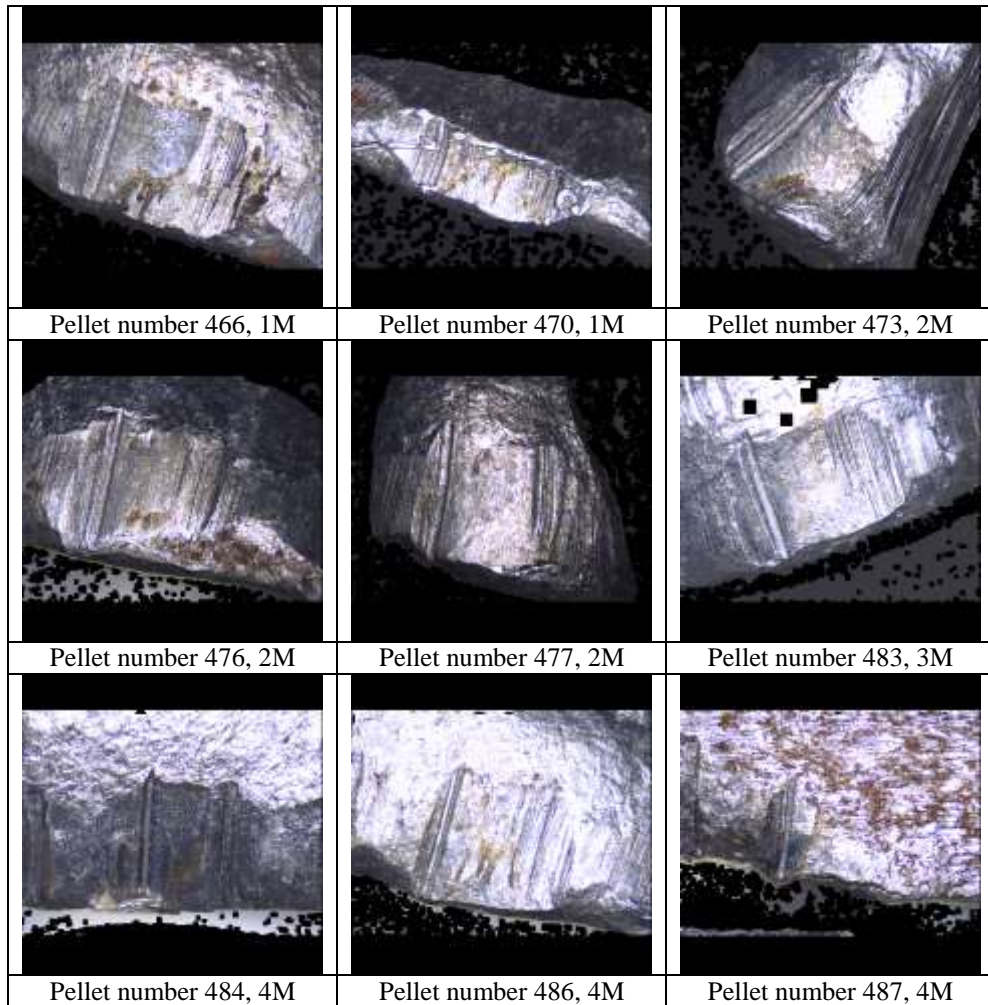
Based on Figure 6.5, it is noted that the percentage of successful scanned LEAs increased when the distance of shooting increased. The percentage were calculated based on total LEAs scanned from useable pellets over total number of LEAs which are supposedly available for scanning from 21 useable pellets.

#### 6.4.1 LEA A

Figures 6.6 and 6.7 illustrate the LEA A of the scanned images of the undamaged and damaged pellets.

		
Pellet number 159, LEA A	Pellet number 159, LEA D	Pellet number 159, LEA H
		
Pellet number 159, LEA J	Pellet number 159, LEA K	

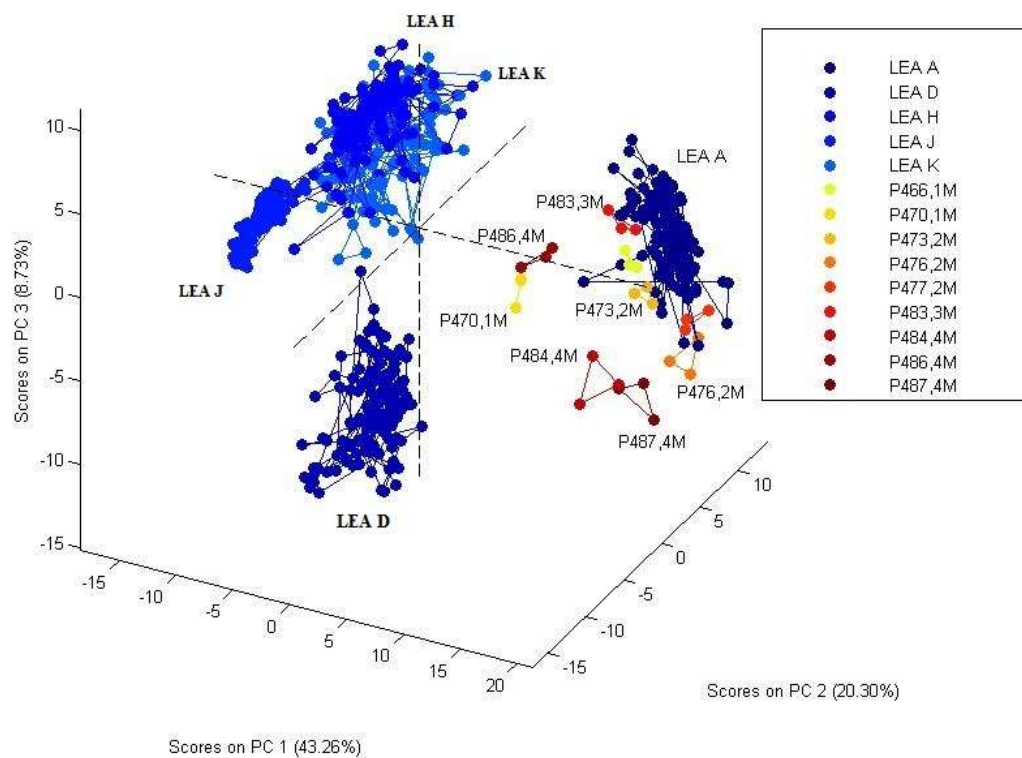
**Figure 6.6: The scanned images of LEA A, D, H, J and K for pellet number 159. Visually, LEA A, D and J have distinct individual characteristic marks on their surfaces differentiating them from LEA H and K. For LEA H, as explained in Chapter 3, can be differentiated from LEA K**



**Figure 6.7: Scanned images of the damaged pellets for LEA A. Rust on P487 4M interferes with classification of this pellet to its pristine LEA. P470 1M, P484 and P486 4M have flattened surface measurement which can interfere with classification of these pellets**

All pellets in Figure 6.7 were damaged after being fired into the metal target. Scanned image of Pellet 487 shows some of the colour and rust, removed from the target upon contact but notwithstanding, this LEA A could still be recognised and scanned. All pellets exhibited similar marks to LEA A observed on the undamaged pellet.





**Figure 6.8: The PCA results of LEA A, D, H, J and K from pristine pellets numbered 159-208 and LEA A from the nine damaged pellets are shown together. The damaged pellets are closer to LEA A than the other LEAs**

**Table 6.4: The LDA classification table of LEA A, D, H, J and K from pristine pellets numbered 159-208 and LEA A from the nine damaged pellets. The values represent correctly classified damaged pellets to LEAs**

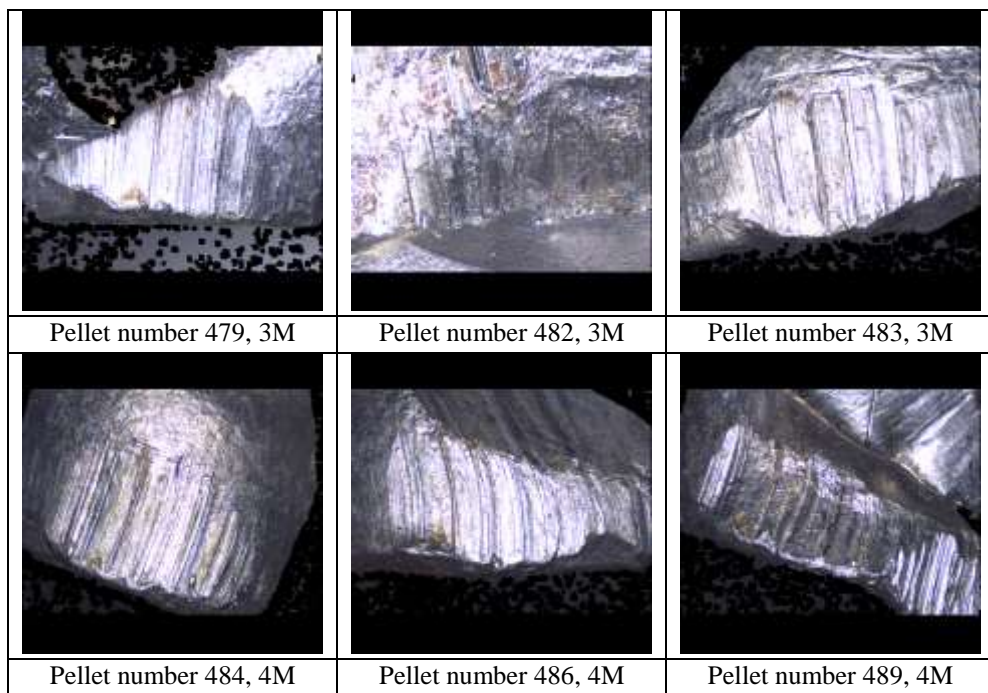
The damaged pellets	The pristine LEAs				
	A	D	H	J	K
P466 1M	3	0	0	0	0
P470 1M	0	0	0	0	3
P473 2M	3	0	0	0	0
P476 2M	3	0	0	0	0
P477 2M	3	0	0	0	0
P483 3M	3	0	0	0	0
P484 4M	0	0	0	0	3
P486 4M	0	0	2	0	1
P487 4M	0	0	0	0	3

The PCA results (Figure 6.8) show that LEA A of the damaged pellets clustered around the equivalent LEA of the undamaged pellet allowing an association to be suggested. 4 pellets, P470, P484, P486 and P487 however, are a little bit further than the rest of other damaged pellets which clustered well with LEA A from the pristine pellets. This result is supported by the LDA classification table (Table 6.4) which shows these four pellets are misclassified. Only five damaged pellets can be associated well with its pristine LEA, LEA A (P466 1M, P473 2M, P476 2M, P477 2M and P483 3M). This result is generated using the prediction from the model based on the LDA classification, as mentioned in Chapter 1. The results show that the firing distance had no tangible effect on the clustering of pellets, as long as the marks were identifiable. Damaged pellets shot at 2 to 3 metres can still be identified to its pristine pellets, as long as the striation marks can be scanned and not badly damaged. Damaged pellets shot at 4 metres however, show poor classification with

its pristine LEA, as compared to damaged pellets shot at less than 4 metres. The presence of rust on P487 4M (Figure 6.7) can interfere with the surface measurement. For P470 1M, P484 4M and P486 4M, the surface measurements are flattened. This is the possible reason for misclassification of these pellets.

#### 6.4.2 LEA D

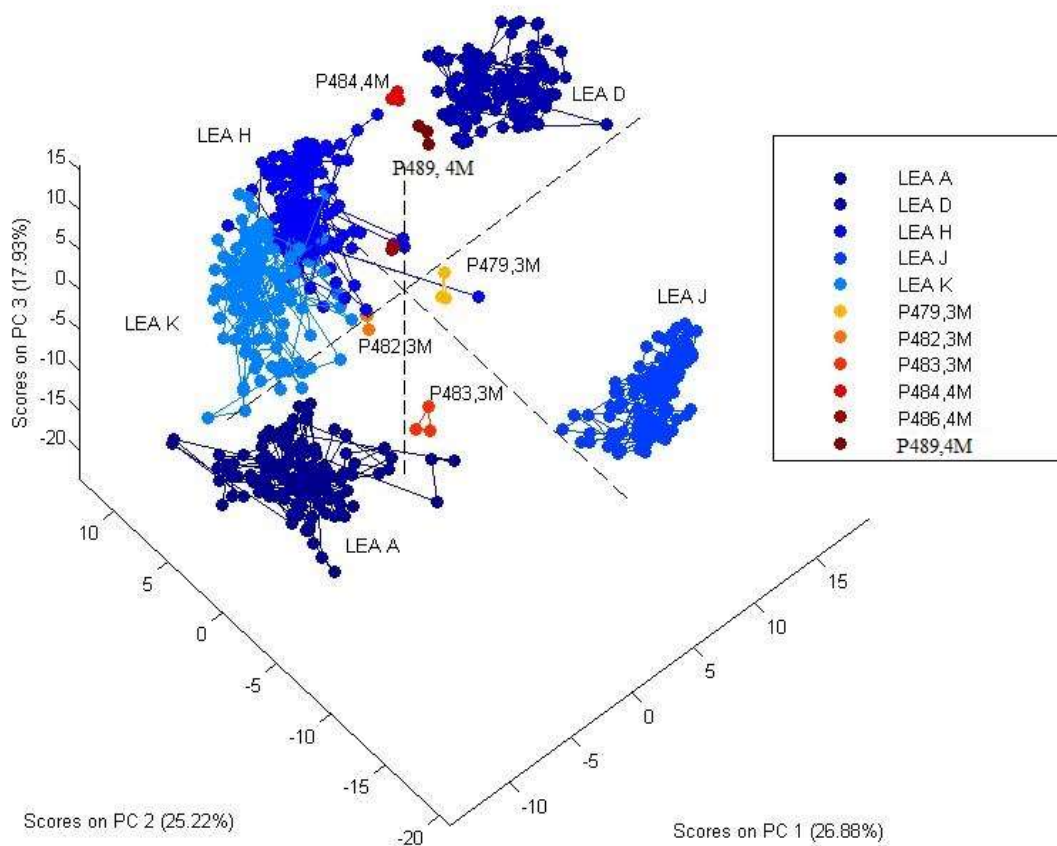
The LEA D regions for the damaged pellets are presented in Figure 6.9.



**Figure 6.9: Scanned images of the six damaged pellets for LEA D**

The LEA D from the damaged pellets was more challenging to scan and in particular for pellets numbered 482 and 486. The region was badly deformed where the surface topography of the pellet was flattened.

The analysis results for LEA D are shown in Figure 6.10 and Table 6.5. All aligned measurements of LEA A, D, H, J and K from undamaged pellets numbered 159-208 and LEA D from the six damaged pellets were included for analysis.



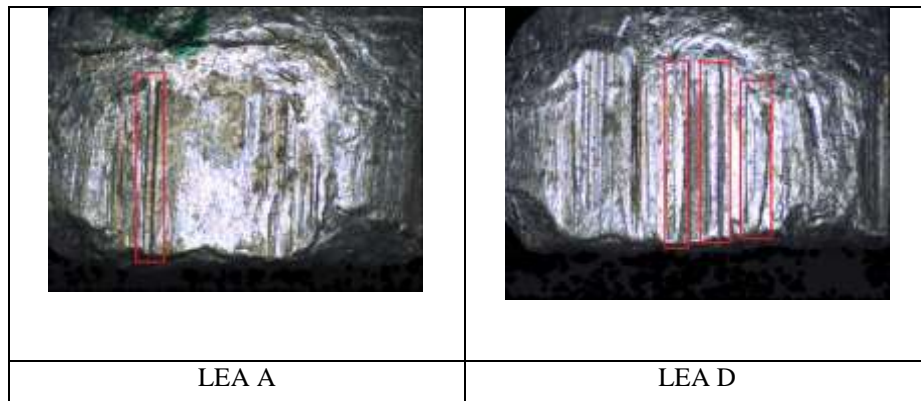
**Figure 6.10: The PCA separate LEA A, D and J from LEA H and K within the undamaged pellets; however, the damaged pellets do not cluster well with LEA D**

**Table 6.5: The LDA classification table of LEA A, D, H, J and K from pristine pellets numbered 159-208 and LEA D from the damaged pellets. The values represent correctly classified damaged pellets to LEAs**

The damaged pellets	The pristine LEAs				
	A	D	H	J	K
P479 3M	0	0	3	0	0
P482 3M	0	0	0	0	3
P483 3M	0	3	0	0	0
P484 4M	0	0	0	0	3
P486 4M	3	0	0	0	0
P489 4M	0	0	0	0	3

As shown in Figure 6.9, damaged pellets for LEA D were more challenging to scan. The analysis results show that only one damaged pellet, P483 shot at 3 metres, can be classified to its pristine LEA, LEA D. This result supports that distance does not affect whether the damaged pellet can be identified to its pristine LEA or not, but depends on how bad the damaged pellets are. Both LEA A and D had individual characteristics. LEA A from damaged pellets however, shows slightly better classification as compared to LEA D.

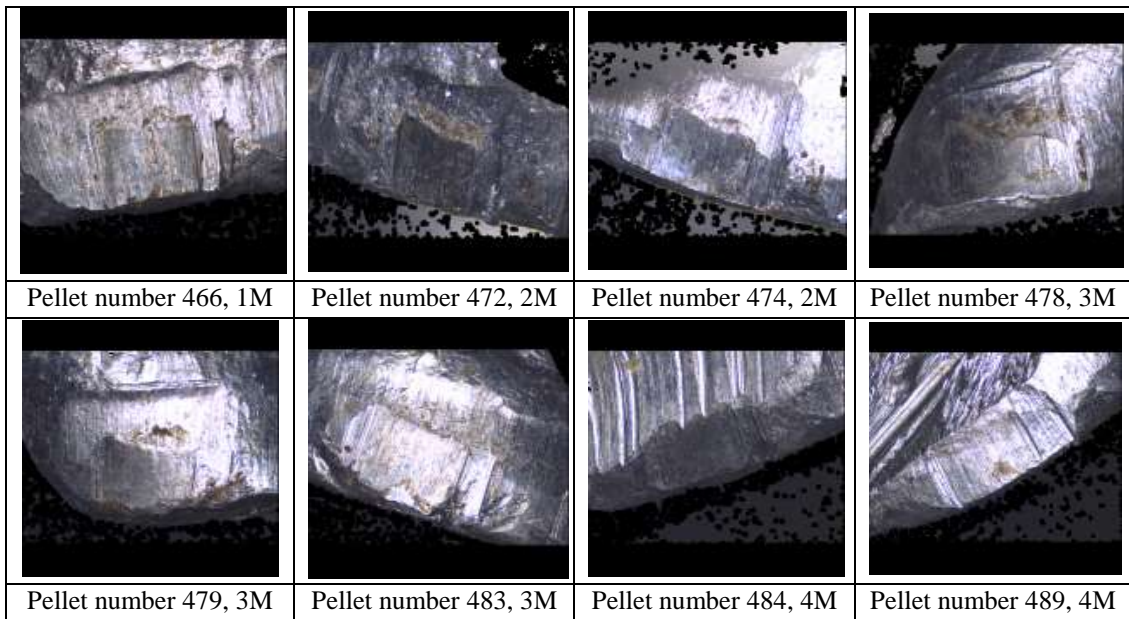
LEA A and LEA D contained identified individual characteristics; LEA A had a deep valley feature and LEA D had a peak feature. These are illustrated in Figure 6.11 highlighted in the red regions. It appears that the peak feature of LEA D was more easily altered through deformation than the deep valley of LEA A and this may be part of the reason for the poorer clustering observed in the results.



**Figure 6.11: The difference in individual characteristics in LEA A and LEA D. LEA A had a deep valley feature while LEA D had a peak feature, illustrated by the red boxes. It may be suggested that upon impact with the target, the peak feature was more easily altered than the valley feature leading to poor clustering of the damages and undamaged pellets**

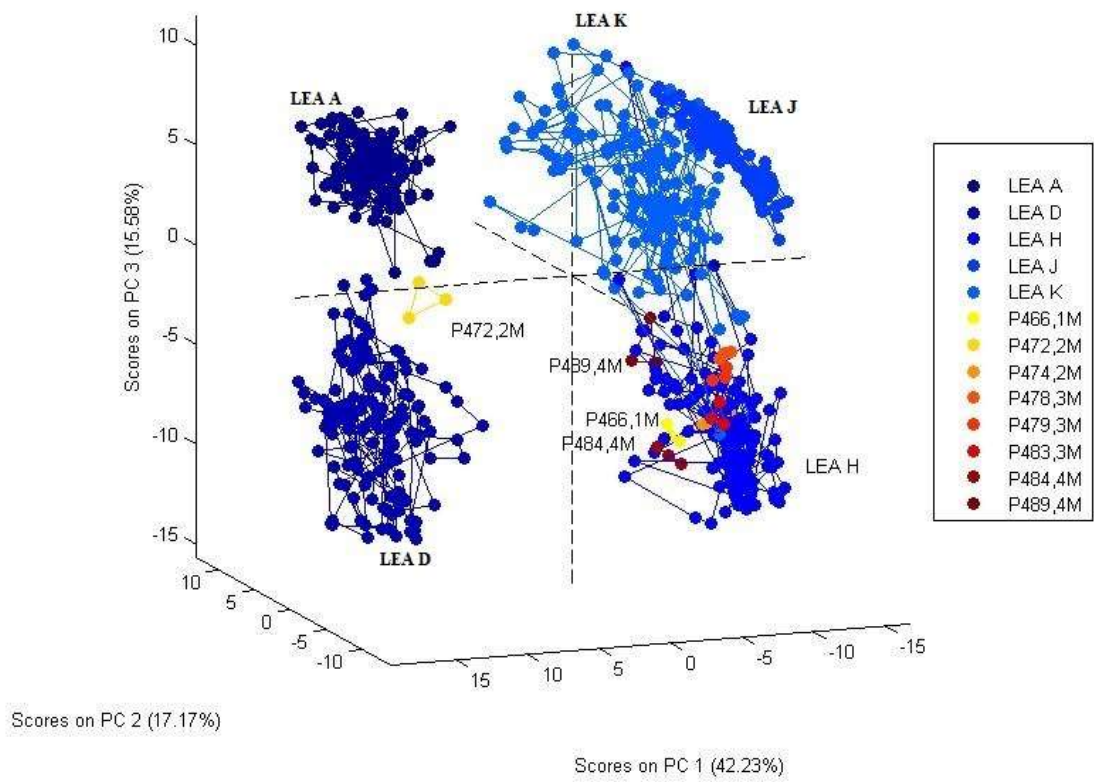
### 6.4.3 LEA H

All aligned measurements of LEA A, D, H, J and K from the undamaged pellets and LEA H from the damaged pellets (in this case 8) were included for analysis and are presented in Figure 6.12. These pellets are damaged, hence the appearance of uneven surfaces. These images are taken at the angle where LEA can be measured. They look different but, as long as the LEA can be measured, alignment is possible.



**Figure 6.12: Scanned images of LEA H for the eight damaged pellets**

All but one of the damaged pellets clustered with LEA H of the undamaged pellets, with the exception of pellet number 472 as presented in Figure 6.12. This pellet was badly distorted and flattened as compared to the other damaged pellets and this may account for the observation on the analysis (Figure 6.13 and Table 6.6).



**Figure 6.13: The PCA results of LEA A, D, H, J and K from undamaged pellets and LEA H from the eight damaged pellets**

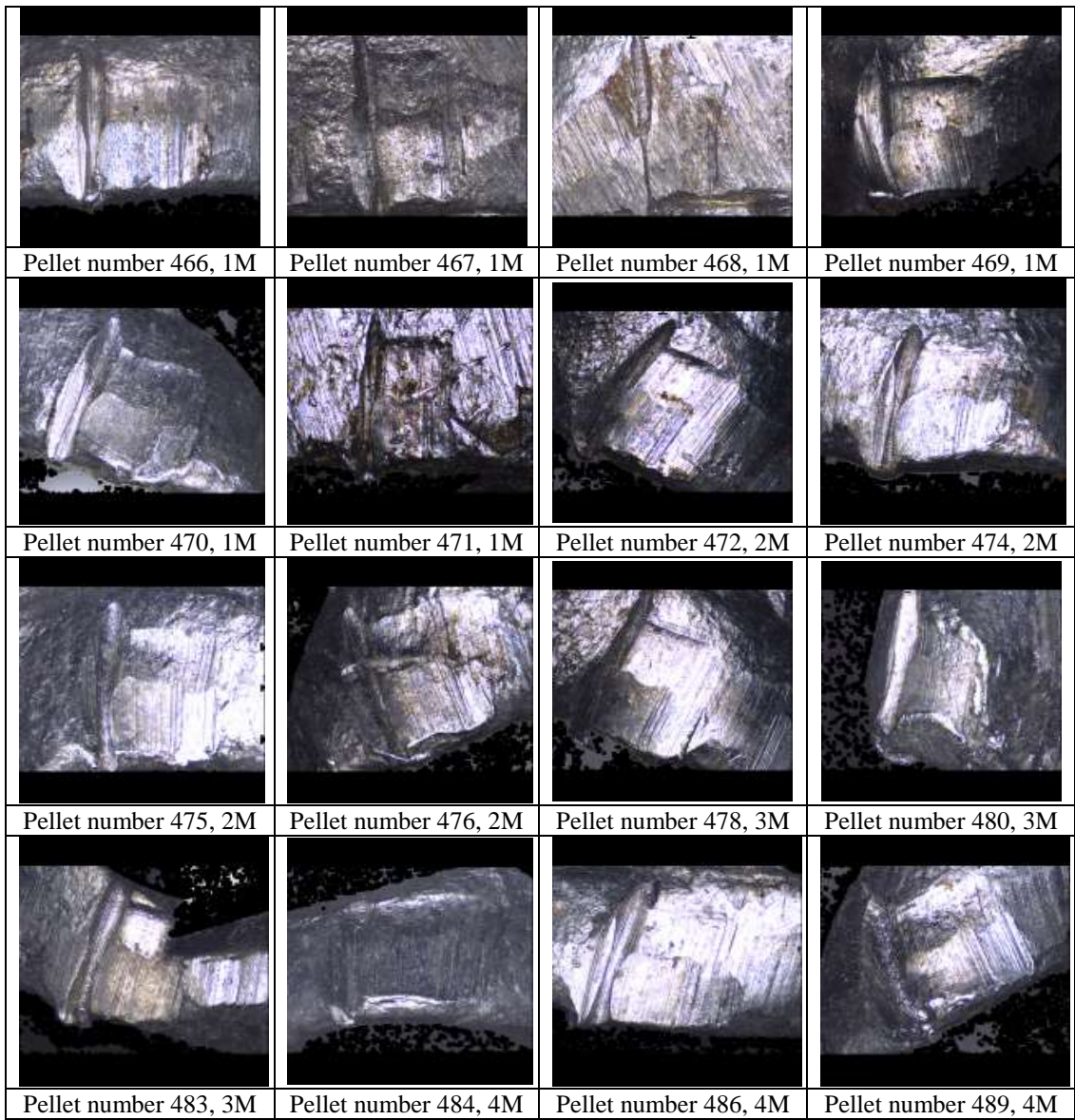


**Table 6.6: The LDA classification table of LEA A, D, H, J and K from pristine pellets numbered 159-208 and LEA H from the damaged pellets. The values represent correctly classified damaged pellets to LEAs**

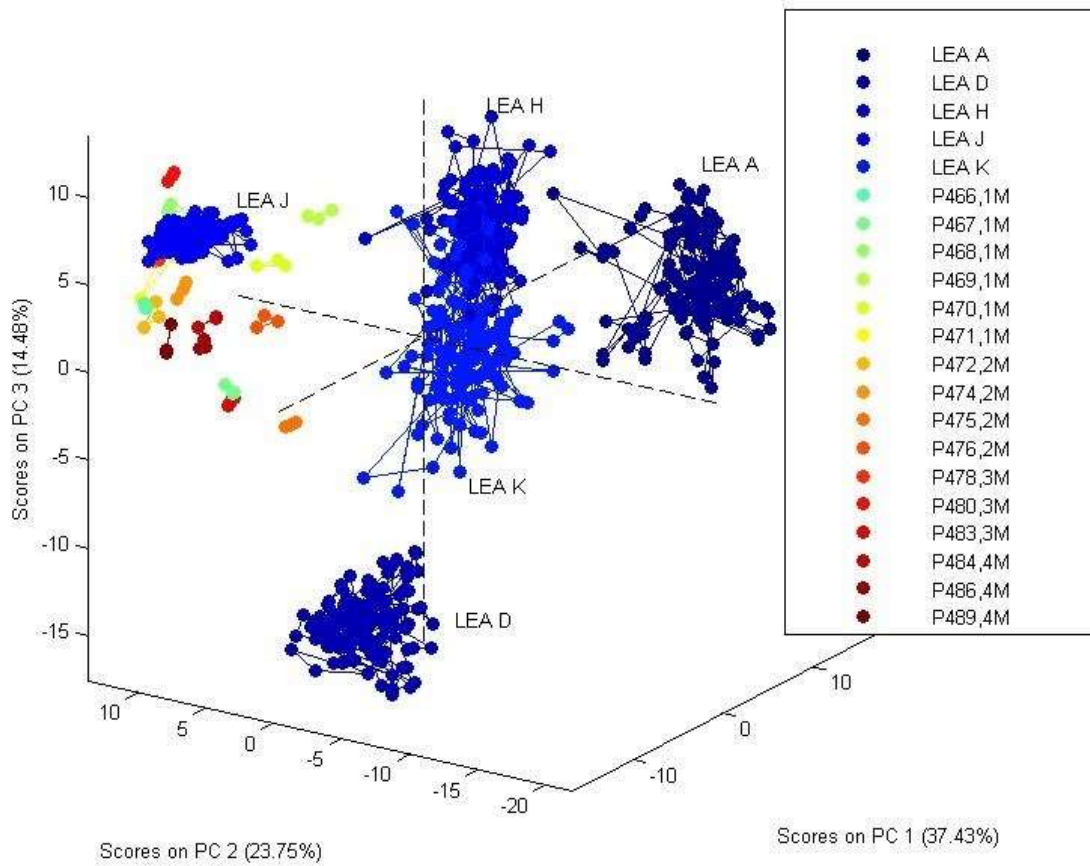
The damaged pellets	The pristine LEAs				
	A	D	H	J	K
P466 1M	0	0	3	0	0
P4722M	0	3	0	0	0
P474 2M	0	0	3	0	0
P4783M	0	0	3	0	0
P4793M	0	0	3	0	0
P483 3M	0	0	3	0	0
P484 4M	0	0	3	0	0
P489 4M	0	0	3	0	0

#### 6.4.4 LEA J

All aligned measurements of LEA A, D, H, J and K from the undamaged pellets and LEA J from the damaged pellets (in this case 16) were included for analysis and are presented Figure 6.14.



**Figure 6.14: Scanned images of LEA J for the sixteen damaged pellets**



**Figure 6.15: The PCA results of LEA A, D, H, J and K from undamaged pellets and LEA J from the sixteen damaged pellets (the labels were omitted to avoid overcrowding)**

**Table 6.7: The LDA classification table of LEA A, D, H, J and K from pristine pellets numbered 159-208 and LEA J from the damaged pellets. The values represent correctly classified damaged pellets to LEAs**

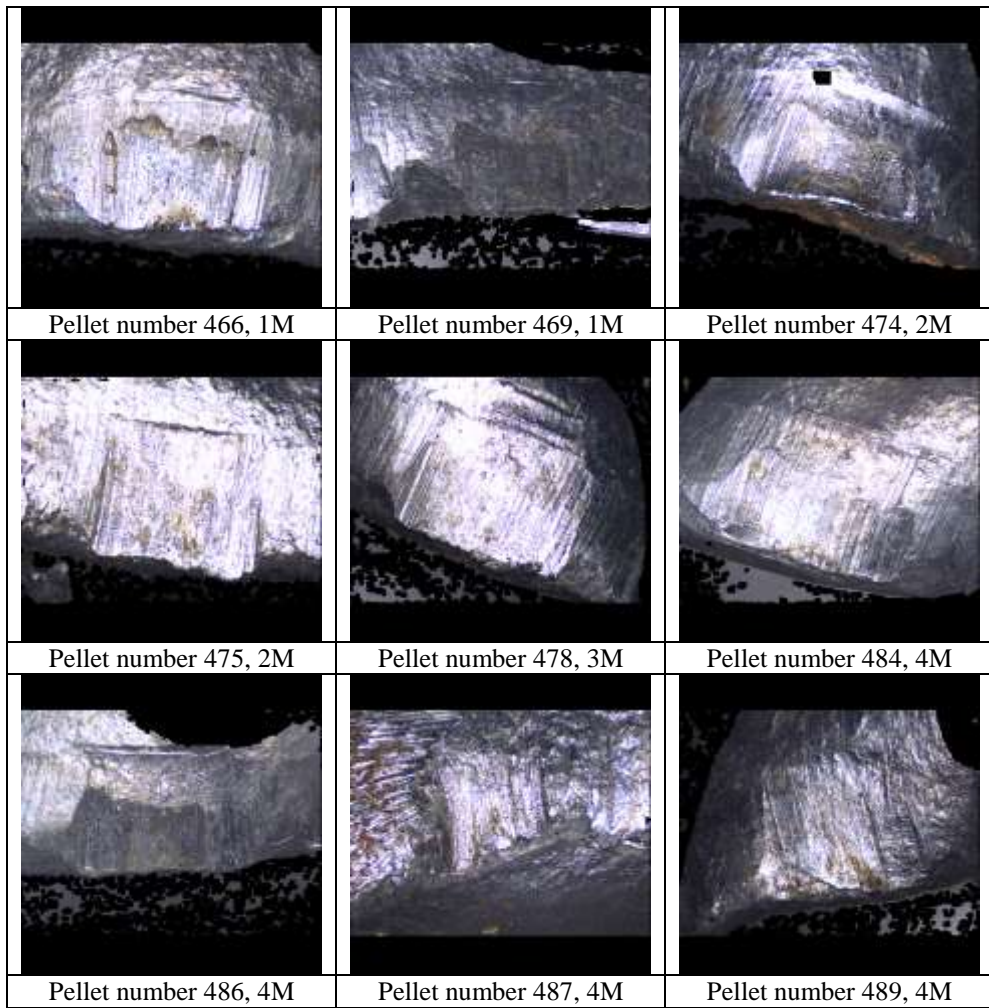
The damaged pellets	The pristine LEAs				
	A	D	H	J	K
P466 1M	0	0	0	3	0
P467 1M	0	0	0	3	0
P468 1M	0	0	0	3	0
P469 1M	0	0	0	3	0
P470 1M	0	0	0	3	0
P471 1M	0	0	0	3	0
P472 2M	0	1	0	2	0
P474 2M	0	3	0	0	0
P475 2M	0	0	3	0	0
P476 2M	0	0	0	3	0
P478 3M	0	0	0	3	0
P480 3M	0	0	0	3	0
P483 3M	2	0	0	1	0
P484 4M	0	0	0	3	0
P486 4M	0	0	0	3	0
P489 4M	0	0	0	3	0

The analysis results revealed that most of the damaged pellets clustered to the LEA J from the undamaged pellets and the LDA results show that four damaged pellets

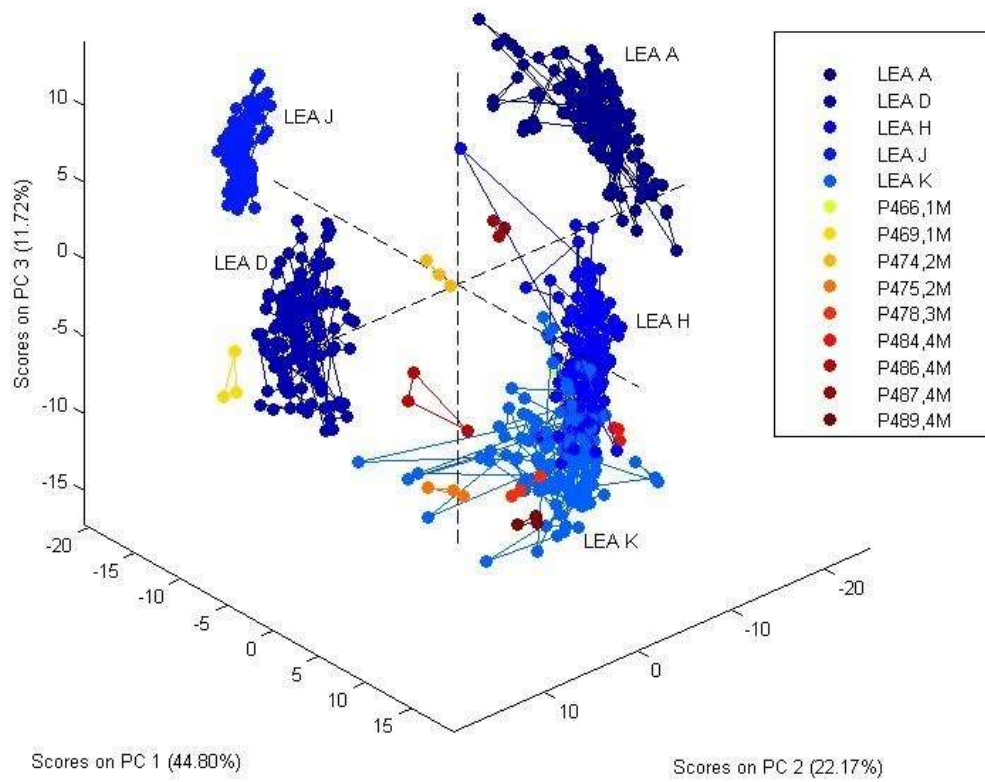
were misclassified (P472, P474, P475 and P483). LEA J had an individual characteristic mark that was different from the other LEAs. Even though this mark can be seen and scanned, it is not guaranteed that it can be classified to its pristine LEA, especially if the surface of the damaged pellets is flattened or damaged. For LEA J, only 12 out of 16 LEAs from the damaged pellets can be classified to its pristine LEA, LEA J.

#### **6.4.5 LEA K**

All aligned measurements of LEA A, D, H, J and K from the undamaged pellets and LEA K from nine of the damaged pellets were included for the PCA. The damaged pellets are shown in Figure 6.16 and the analysis in Figure 6.17 and Table 6.8.



**Figure 6.16: Scanned images of LEA K for nine damaged pellets**



**Figure 6.17: The PCA results of LEA A, D, H, J and K on undamaged pellets and LEA K from the nine damaged pellets showing poor clustering**

**Table 6.8: The LDA classification table of LEA A, D, H, J and K from pristine pellets numbered 159-208 and LEA K from the damaged pellets. The values represent correctly classified damaged pellets to LEAs**

The damaged pellets	The pristine LEAs				
	A	D	H	J	K
P466 1M	0	0	3	0	0
P4691M	0	3	0	0	0
P474 2M	1	2	0	0	0
P4752M	0	1	0	0	2
P4783M	0	0	0	0	3
P4844M	0	0	0	0	3
P486 4M	0	3	0	0	0
P487 4M	0	0	2	0	1
P489 4M	0	0	0	0	3

LEA K did not have individual characteristic and this has been reflected in relatively poor clustering of the damaged pellets to the correct LEA. However, the LDA results can separate three LEAs from the damaged pellets to its pristine LEA, LEA K, out of the nine damaged pellets. Table 6.9 shows the percentage of correctly classified LEAs from the damaged pellets to its pristine pellets.

**Table 6.9: The percentage of correctly classified damaged pellets to its pristine pellets**

LEAs	Number of the damaged pellets analysed	Number of the damaged pellets correctly classified to its pristine pellets	Percentage of correctly classified pellets
A	9	5	55.6
D	6	1	16.7
H	8	7	87.5
J	16	12	75.0
K	9	3	33.3



Based on Table 6.9, LEA A, H and J show more than half of the damaged pellets can be classified to its own pristine pellets. LEA A and J have individual characteristic marks on their surfaces, hence assisting in classifying the damaged pellets. Even though LEA H has no individual characteristic mark, as explained in Chapter 3, LEA H has a mark which is different from LEA K. This may explain the reason of better classification of the damaged pellets for LEA H as compared to LEA K. The analysis results also show that firing distance had no effect on clustering the pellets, as long as the marks were identifiable for scanning and the pellets are not badly damaged.

#### **6.4.6 All aligned LEAs from the air rifles and LEAs from the damaged pellets**

The aligned LEAs from the air rifles, the undamaged LEAs from the air pistol and LEAs from the damaged pellets were included for the analysis, Figures 6.18 to 6.22 and Table 6.10 to 6.14.

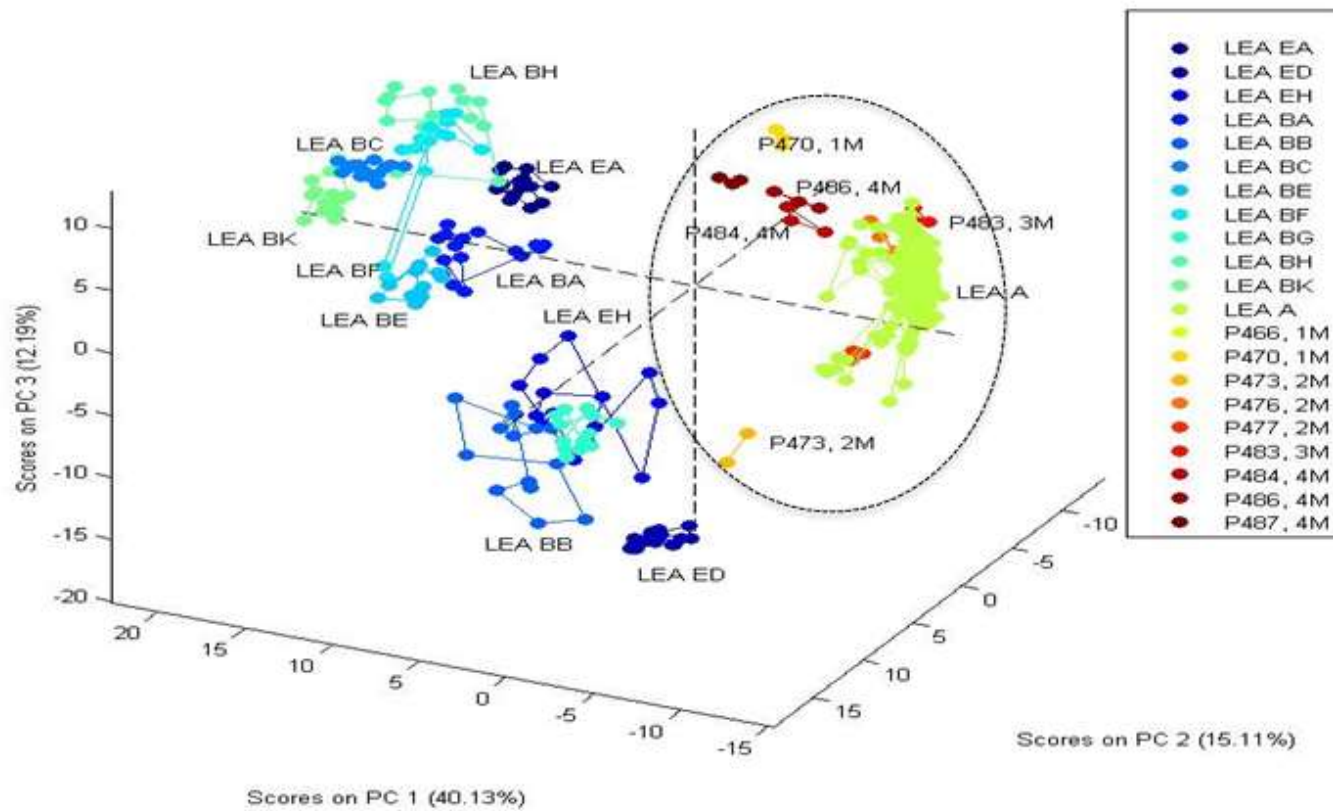


Figure 6.18: All aligned LEAs from the air rifles and LEA A from the undamaged and damaged pellets

**Table 6.10: The LDA classification table of all aligned LEAs from the air rifles and LEA A from the undamaged and damaged pellets. The values represent correctly classified damaged pellets to LEAs from the pristine pellets**

The damaged pellets	The pristine LEAs from the air pistol and the air rifles											
	A	BA	BB	BC	BE	BF	BG	BH	BK	EA	ED	EH
P466 1M	3	0	0	0	0	0	0	0	0	0	0	0
P470 1M	2	0	0	0	0	0	1	0	0	0	0	0
P473 2M	0	0	0	0	0	0	0	0	0	0	3	0
P476 2M	3	0	0	0	0	0	0	0	0	0	0	0
P477 2M	3	0	0	0	0	0	0	0	0	0	0	0
P483 3M	3	0	0	0	0	0	0	0	0	0	0	0
P484 4M	2	0	0	0	0	0	0	0	0	0	1	0
P486 4M	2	0	1	0	0	0	0	0	0	0	0	0
P487 4M	0	0	3	0	0	0	0	0	0	0	0	0

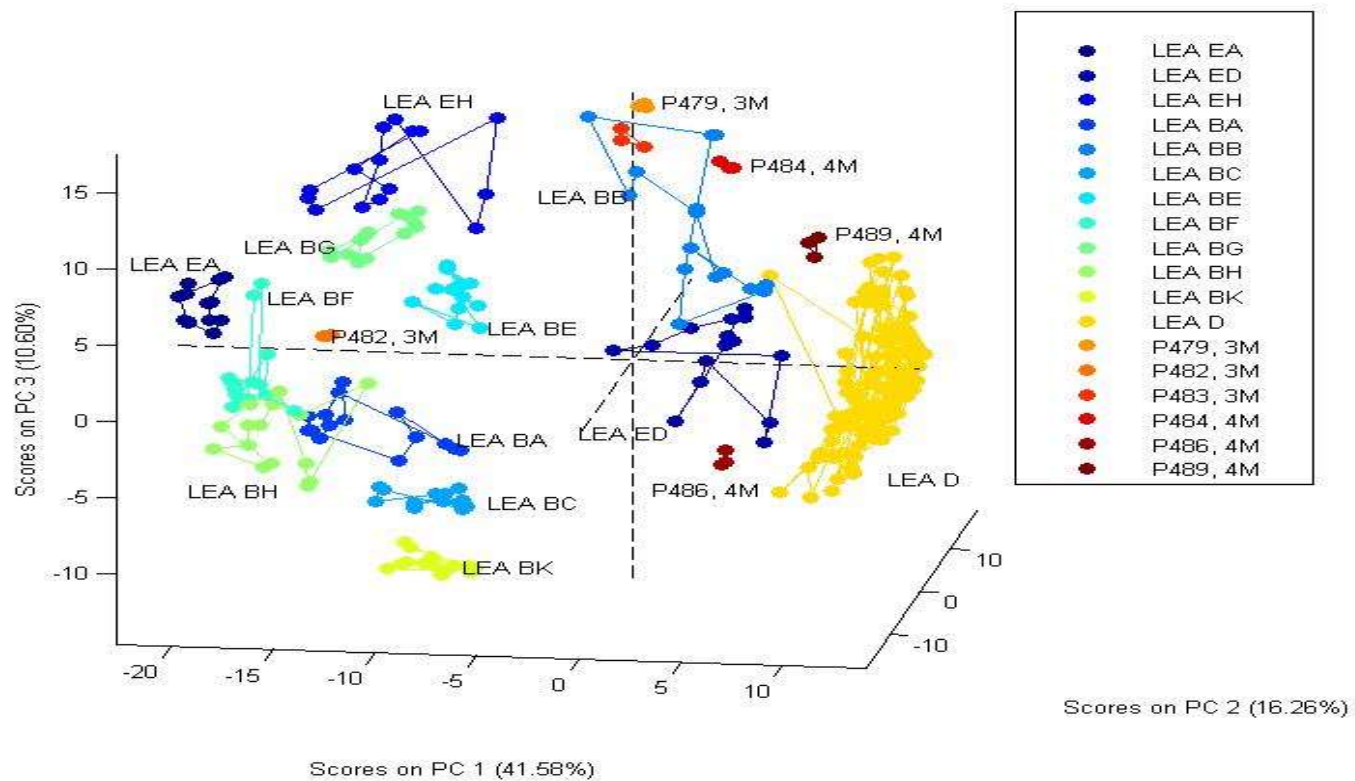


Figure 6.19: All aligned LEAs from the air rifles and LEA D from the undamaged and damaged pellets. Alignment to the correct LEA was not possible

**Table 6.11: The LDA classification table of all aligned LEAs from the air rifles and LEA D from the undamaged and damaged pellets. The values represent correctly classified damaged pellets to LEAs from the pristine pellets**

The damaged pellets	The pristine LEAs from the air pistol and the air rifles											
	D	BA	BB	BC	BE	BF	BG	BH	BK	EA	ED	EH
P479 3M	0	0	3	0	0	0	0	0	0	0	0	0
P482 3M	0	0	0	0	0	3	0	0	0	0	0	0
P483 3M	0	0	3	0	0	0	0	0	0	0	0	0
P484 4M	1	0	2	0	0	0	0	0	0	0	0	0
P486 4M	0	0	0	0	0	0	0	0	0	0	3	0
P489 4M	1	0	0	0	0	0	0	0	0	0	2	0

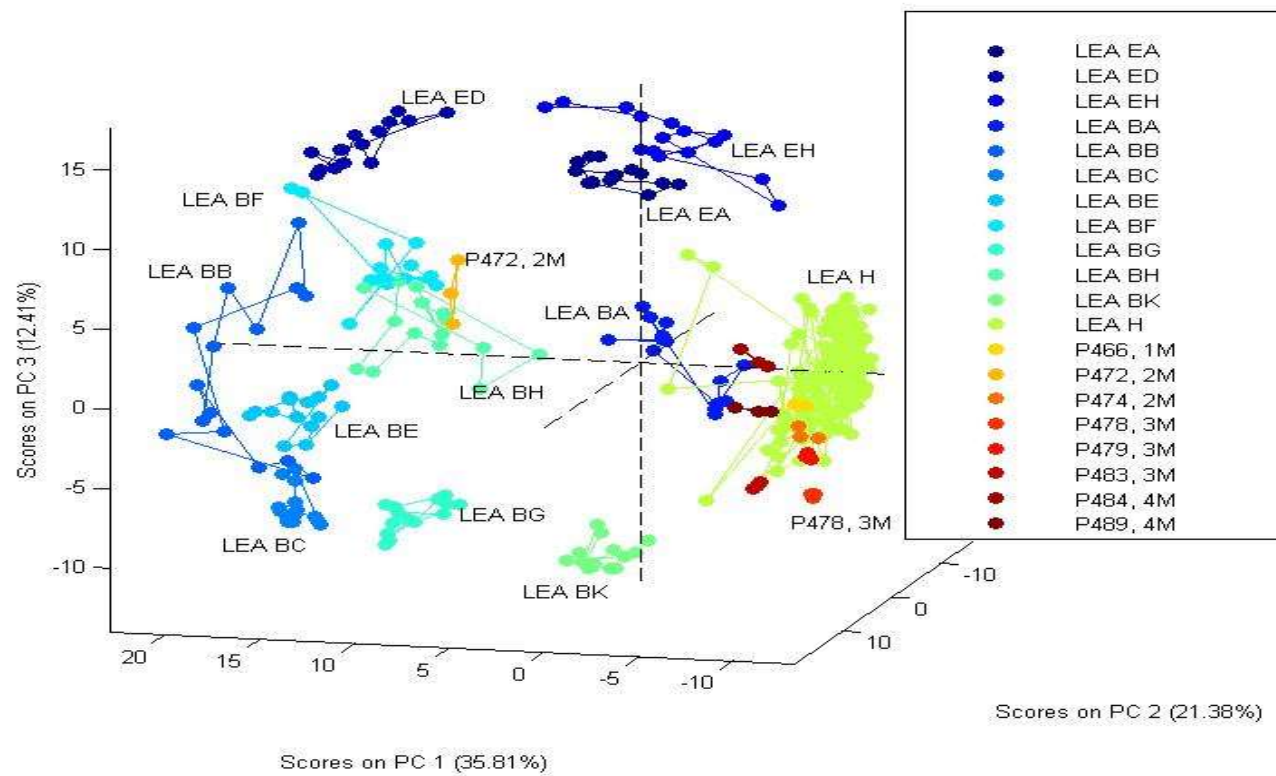


Figure 6.20: All aligned LEAs from the air rifles and LEA H from the undamaged and damaged pellets

**Table 6.12: The LDA classification table of all aligned LEAs from the air rifles and LEA H from the undamaged and damaged pellets. The values represent correctly classified damaged pellets to LEAs from the pristine pellets**

The damaged pellets	The pristine LEAs from the air pistol and the air rifles											
	H	BA	BB	BC	BE	BF	BG	BH	BK	EA	ED	EH
P466 1M	3	0	0	0	0	0	0	0	0	0	0	0
P472 2M	0	0	0	0	0	0	0	0	0	0	3	0
P474 2M	3	0	0	0	0	0	0	0	0	0	0	0
P478 3M	3	0	0	0	0	0	0	0	0	0	0	0
P479 3M	3	0	0	0	0	0	0	0	0	0	0	0
P483 3M	3	0	0	0	0	0	0	0	0	0	0	0
P484 4M	3	0	0	0	0	0	0	0	0	0	0	0
P489 4M	3	0	0	0	0	0	0	0	0	0	0	0

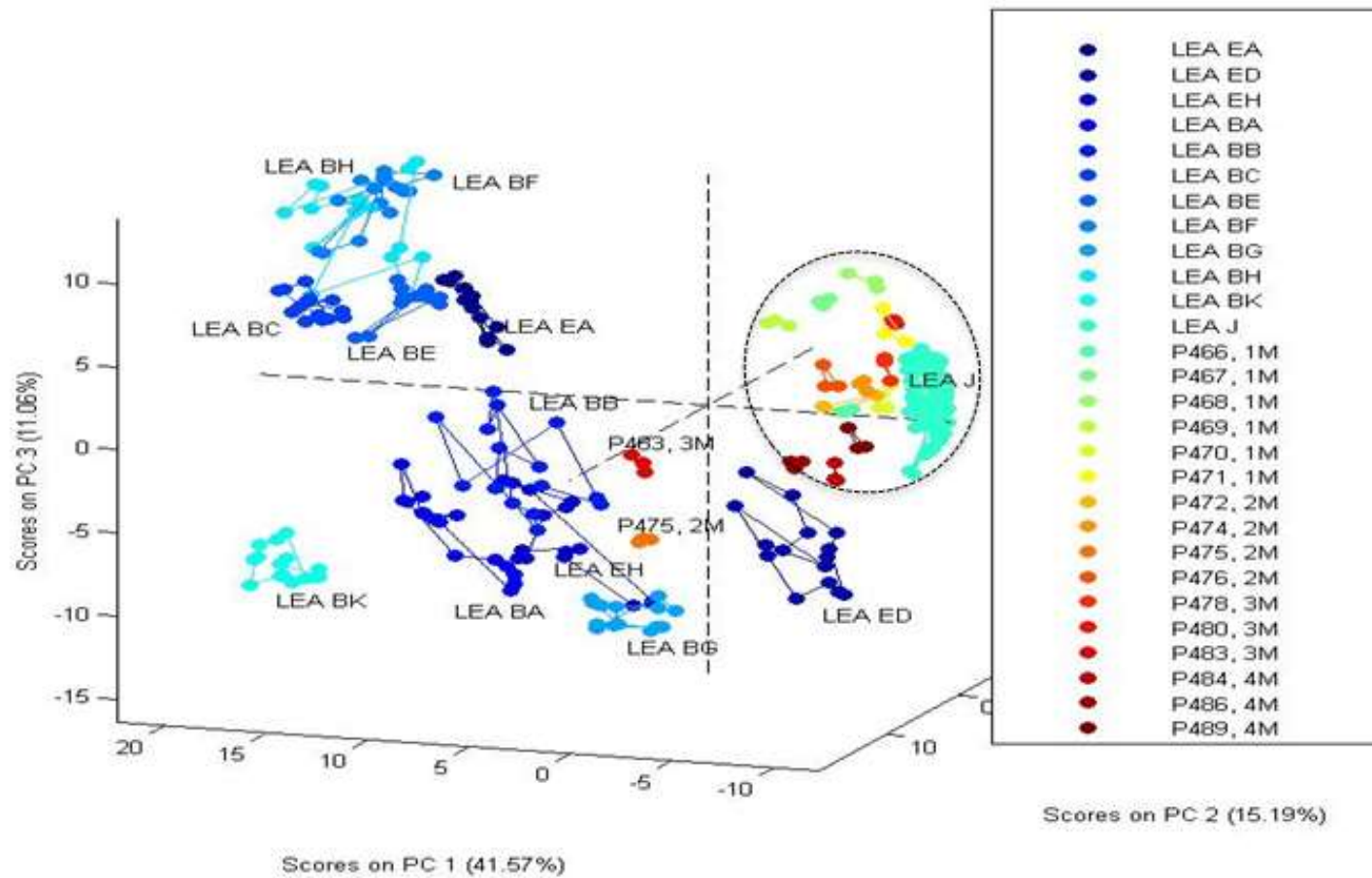


Figure 6.21: All aligned LEAs from the air rifles and LEA J from the undamaged and damaged pellets. Most of the damaged pellets clustered with the correct LEA



**Table 6.13: The LDA classification table of all aligned LEAs from the air rifles and LEA J from the undamaged and damaged pellets. The values represent correctly classified damaged pellets to LEAs from the pristine pellets**

The damaged pellets	The pristine LEAs from the air pistol and the air rifles											
	J	BA	BB	BC	BE	BF	BG	BH	BK	EA	ED	EH
<b>P466 1M</b>	3	0	0	0	0	0	0	0	0	0	0	0
<b>P467 1M</b>	3	0	0	0	0	0	0	0	0	0	0	0
<b>P468 1M</b>	3	0	0	0	0	0	0	0	0	0	0	0
<b>P469 1M</b>	3	0	0	0	0	0	0	0	0	0	0	0
<b>P470 1M</b>	3	0	0	0	0	0	0	0	0	0	0	0
<b>P471 1M</b>	3	0	0	0	0	0	0	0	0	0	0	0
<b>P472 2M</b>	3	0	0	0	0	0	0	0	0	0	0	0
<b>P474 2M</b>	3	0	0	0	0	0	0	0	0	0	0	0
<b>P475 2M</b>	0	0	0	0	0	0	3	0	0	0	0	0
<b>P476 2M</b>	3	0	0	0	0	0	0	0	0	0	0	0
<b>P478 3M</b>	3	0	0	0	0	0	0	0	0	0	0	0
<b>P480 3M</b>	3	0	0	0	0	0	0	0	0	0	0	0
<b>P483 3M</b>	0	0	3	0	0	0	0	0	0	0	0	0
<b>P484 4M</b>	3	0	0	0	0	0	0	0	0	0	0	0
<b>P486 4M</b>	3	0	0	0	0	0	0	0	0	0	0	0
<b>P489 4M</b>	3	0	0	0	0	0	0	0	0	0	0	0

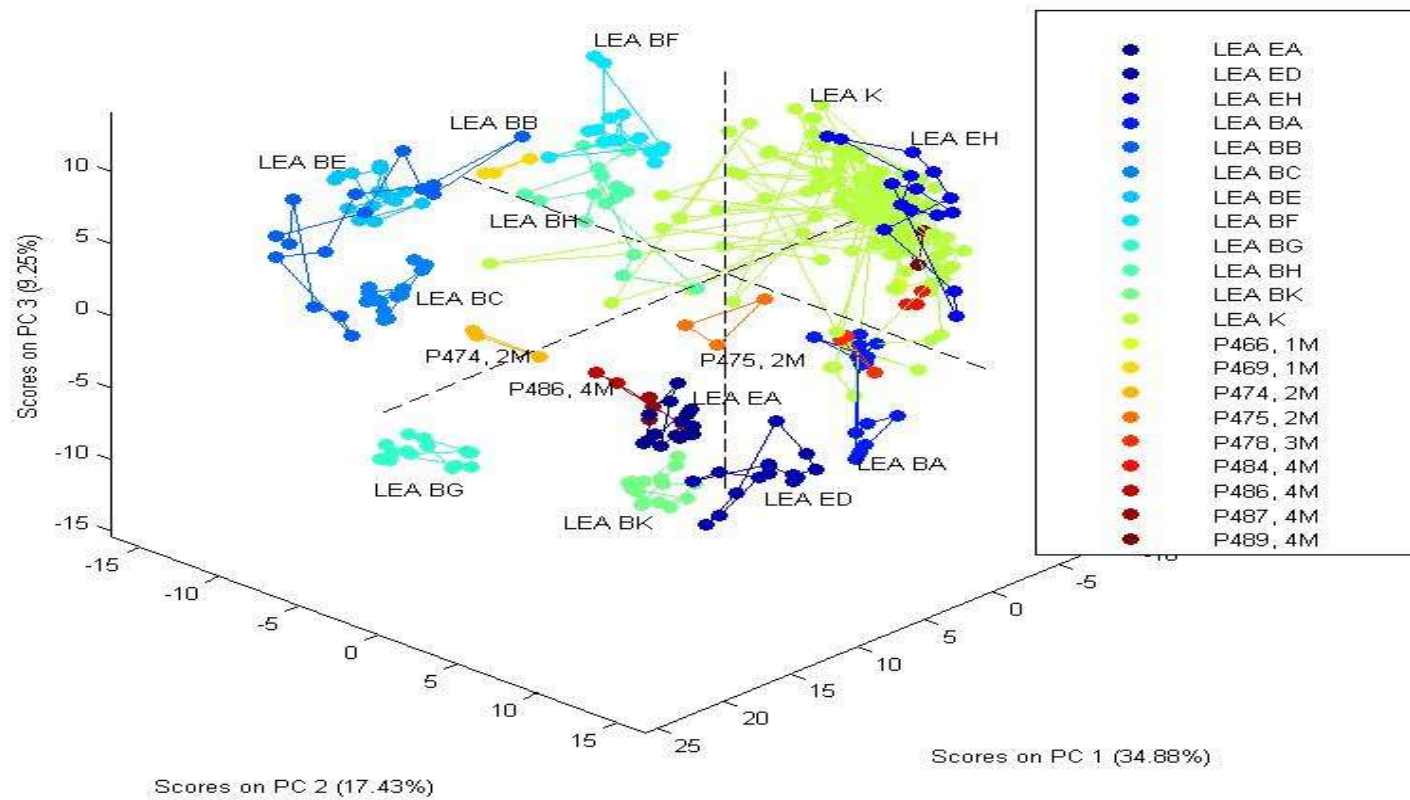


Figure 6.22: All aligned LEAs from the air rifles and LEA K from the undamaged and damaged pellets. Clustering to the correct LEA was not possible

**Table 6.14: The LDA classification table of all aligned LEAs from the air rifles and LEA K from the undamaged and damaged pellets. The values represent correctly classified damaged pellets to LEAs from the pristine pellets**

The damaged pellets	The pristine LEAs from the air pistol and the air rifles											
	K	BA	BB	BC	BE	BF	BG	BH	BK	EA	ED	EH
P466 1M	3	0	0	0	0	0	0	0	0	0	0	0
P469 1M	0	0	3	0	0	0	0	0	0	0	0	0
P474 2M	0	0	0	0	0	0	0	3	0	0	0	0
P475 2M	2	1	0	0	0	0	0	0	0	0	0	0
P478 3M	2	1	0	0	0	0	0	0	0	0	0	0
P484 4M	3	0	0	0	0	0	0	0	0	0	0	0
P486 4M	0	0	0	0	0	0	0	2	0	0	1	0
P487 4M	0	0	0	0	0	0	0	0	0	0	3	0
P489 4M	3	0	0	0	0	0	0	0	0	0	0	0

Based on the analysis results (Figures 6.18 to 6.22 and Table 6.10 to 6.14), only the LEAs which had very distinctive individual characteristics could be grouped correctly to the LEA on the exemplar pellets fired from the air pistol. This occurred for LEA A and to a large extent, LEA J. LEA H has no distinctive individual characteristic, nevertheless, as described in Chapter 3, there is a mark present on LEA H that can be differentiated, as compared to LEAs from the air rifles. This could explain better grouping between the pristine and the damaged pellets for LEA H.

Researchers have suggested that individual characteristics are specific to the weapon that fired the bullet [2] but this work has demonstrated that only in a small number of cases does this objectively distinguish the projectiles and group them correctly. While the firing distance is important in crime scene reconstruction, especially for the detection of gunshot residue [3-5] the results obtained suggested that defining features with LEAs were present on the damaged pellets even when the distance of firing is altered. In fact more LEAs were able to be scanned for pellets which were fired at further distances.

The measurement of the surface topography and the use of automated bullet-identification systems combined with mathematical tools and software [6-20] can be used in the comparison of undamaged fired pellets. This work has extended the application of the developed methodology to investigate the ability to link damaged pellets to undamaged pellets for a set of known samples. Based on the analysis, 28 out of 48 damaged pellets were successfully classified to its pristine pellets (LEA A

– 4 pellets, LEA H – 7 pellets, LEA J – 14 pellets, LEA K – 3 pellets). The developed methodology was able to classify 58.3% of damaged pellets to its pristine pellets. Booker [1], in his work explained that the examination of damaged pellets are tedious and challenging to firearms examiners and often not conducted. Although the percentage of correct classification is not at 100%, the tested method in this study was able to successfully group more than 50% of damaged pellets to its known samples. This percentage can be considered as a successful breakthrough considering the novel work conducted in classifying damaged pellets to its pristine pellets.

## **6.5 Conclusions**

Surface topography is suggested as having the potential to provide an objective or semi objective method for bullet-identification. The work presented in this chapter reflects a set of tests used to explore the technique's ability to identify land engraved areas on projectiles and whether they can be used to potentially provide a link between undamaged fired projectiles and projectiles fired from the same weapon but which have impacted on a surface so as to cause damage and distortion of the LEA.

The results obtained indicated that some of the LEAs from the damaged pellets, where marked individual characteristics were present could be clustered and as a consequence, they could be associated with the same LEA region on a test fired projectile. When comparing pellets fired from the air pistol, results displayed that, by using all available LEAs from the damaged pellets (all identifiable and measurable LEAs), and with the presence of individual characteristic from LEAs, some of the damaged LEAs can be classified to its pristine LEA. For the analysis of pellets fired

from different air weapons, results demonstrated that more than 50% of damaged pellets fired from the air pistol could be correctly classified to its pristine pellets (fired from the similar air pistol) and could be differentiated from pellets fired from air rifles. The developed methodology for this study has proven to be functional and acceptable to objectively identify damaged pellets.

## 6.6 References

1. Booker, J.L., *Examination of the Badly Damaged Bullet*. Journal of the Forensic Science Society, 1980. 20(3): p. 153-162.
2. Di Maio, V.J.M., *Gunshot wounds : practical aspects of firearms, ballistics, and forensic techniques*. 1999: Boca Raton : CRC Press.
3. Cecchetto, G., Giraud, C., Amagliani, A., Viel, G., Fais, P., Cavarzeran, F., Feltrin, G., Ferrara, S.D. and Montisci, M., *Estimation of the firing distance through micro-CT analysis of gunshot wounds*. Int. J. Legal Med., 2011. 125(2): p. 245–251.
4. Brown, H., Cauchi, D.M., Holden, J.L., Wrobel, H. and Cordner, S., *Image analysis of gunshot residue on entry wounds: I – The technique and preliminary study*. Forensic Science International, 1999. 100(3): p. 163-177.
5. Brown, H., Cauchi, D.M., Holden, J.L., Allen, F.C.L., Cordner, S. and Thatcher, P., *Image analysis of gunshot residue on entry wounds: II – A statistical estimation of firing range*. Forensic Science International, 1999. 100(3): p. 179-186.
6. Xie, F., Xiao, S., Blunt, L., Zeng, W. and Jiang, X., *Automated bullet-identification system based on surface topography techniques*. Wear, 2009. 266(5): p. 518–522.
7. Ma, L., Song, J., Whinterton, E., Zheng, A., Vorburger, T. and Zhou, J., *NIST bullet signature measurement system for RM (Reference Material) 8240 standard bullets*. J Forensic Sci, 2004. 49(4): p. 649-59
8. Huang, Z. and Leng, J. *An online ballistics imaging system for firearm identification*. in *Signal Processing Systems (ICSPS), 2010 2nd International Conference on*. 2010.
9. Chu, W., Song, J., Vorburger, T., Yen, J., Ballou, S. and Bachrach, B., *Pilot study of automated bullet signature identification based on topography measurements and correlations*. J Forensic Sci, 2010. 55(2): p. 341-347.
10. Chu, W., Song, J., Vorburger, T.V., Thompson, R. and Silver, R., *Selecting Valid Correlation Areas for Automated Bullet Identification System Based on Striation Detection*. J. Res. Natl. Inst. Stand. Technol., 2011. 116(3): p. 647-653.

11. Song, J., Vorburger, T.V., Ballou, S., Thompson, R.M., Yen, J., Renegar, T.B., Zheng, A., Silver, R.M. and Ols, M., *The National Ballistics Imaging Comparison (NBIC) project*. *Forensic Sci Int*, 2012. 216(1-3): p. 168-82.
12. Song, J., Chu, W., Vorburger, T.V., Thompson, R., Renegar, T.B., Zheng, A., Yen, J., Silver, R. and Ols, M., *Development of ballistics identification-from image comparison to topography measurement in surface metrology*. *Meas. Sci. Technol.*, 2012. 23(5): p. 1-6.
13. Zheng, X., Soons, J., Vorburger, T., Song, J., Renegar, T. and Thompson, R., *Applications of surface metrology in firearm identification*. *Surface Topography: Metrology and Properties*, 2014. 2(1): p. 1-10.
14. John, S., Wei, C., Mingsi, T. and Johannes, S., *3D topography measurements on correlation cells—a new approach to forensic ballistics identifications*. *Measurement Science and Technology*, 2014. 25(6): p. 064005.
15. Senin, N., Groppetti, R., Garofano, L., Fratini, P. and Pierni, M., *Three-dimensional surface topography acquisition and analysis for firearm identification*. *J. Forensic Sci.*, 2006. 51(2): p. 282-295.
16. Sakarya, U., Leloğlu, U.M. and Tunali, E., *Three-dimensional surface reconstruction for cartridge cases using photometric stereo*. *Forensic Science International*, 2008. 175(2–3): p. 209-217.
17. Puente León, F., *Automated comparison of firearm bullets*. *Forensic Science International*, 2006. 156(1): p. 40-50.
18. De Kinder, J. and Bonfanti, M., *Automated comparisons of bullet striations based on 3D topography*. *Forensic Science International*, 1999. 101(2): p. 85–93.
19. Pirlot, M., Chabottier, A., Celens, E., De Kinder, J. and Van Ham, P., *Feature extraction of optical projectiles images*. *Science & Justice*, 1999. 39(1): p. 53-56.
20. Bachrach, B., *Development of a 3D-based automated firearms evidence comparison system*. *J. Forensic Sci.*, 2002. 47(6): p. 1253-64.

## **Chapter 7: Conclusion and Future Works**

### **7.1 Conclusions**

Methods to develop an objective means for the comparison of striation marks impressed onto projectiles are an ongoing challenge within the firearms examination domain in the field of forensic science. The recommendations of the US National Academy of Sciences made in 2009 were clear and the requirement for objective assessments was compelling. Notwithstanding this, the use of a conventional comparison microscope approach where individual striation marks are identified and a subjective comparison of the number of matching striations is interpreted is still the normal mechanism utilised within forensic science laboratories for the comparison of projectiles recovered in firearm cases. The need for a change to objectify methods of comparison is technologically viable and achievable but is culturally challenging. This work follows on from the initial studies emerging within the current literature and attempts to add to the body of knowledge in advocating the abovementioned objective approach.

Using pellets fired from a set of air weapons as templates, the full surface topography of all land engraved areas (LEAs) present on projectiles fired from three different weapons were investigated. The research included a study into the potential alteration of LEAs over repetitively fired projectiles for the same weapon, the ability to differentiate weapons based on the evaluation and comparison of the LEAs of the resultant projectiles and the ability to link damaged projectiles correctly to the weapon that fired them.



The LEAs were initially scanned using an infinite focus 3D microscope. This allowed the surface of the LEAs to be imaged in three dimensions. These images were then converted into two dimensional topographical maps. Finally the data was transformed into a numerical value suitable for further pre-processing using the PLS\_Toolbox® of Matlab®.

A total of 609 pellets were fired using an air pistol and two air rifles. Pellets were collected and analysed to assess the following:

- (1) the repeatability and reproducibility of the imaging and mathematical method
- (2) the variability of land engraved areas in repetitively fired projectiles over a series of test fires
- (3) the ability of the developed method to distinguish between different classes of weapons (air pistols and air rifles) and weapons within the same class (air rifles)
- (4) the ability of the method to correctly associate distorted projectiles to the weapon that fired them

Data analysis has demonstrated that the method developed in this study was both repeatable and reproducible. The initial analysis examined the LEA regions repetitively on the same sample (fired pellet). This allowed an assessment of the repeatability of measurement across a single region of the pellet. In each case, the topographical scan revealed strong repeatability across ten scans taken across different areas of each LEA. This served to validate measurements of the inter LEA variation on the same region of the same pellet using the experimental methods.

In order to assess intra LEA variability between fired pellets, the experimental methodology was further developed to examine each of the twelve LEAs across fifty repetitively fired pellets. The hypothesis was that each LEA would exhibit some variability but that the variability within a LEA would be minimal. A second hypothesis was that each striated region would be in itself differentiated from all others. This was a premise upheld by firearms experts as they suggested that the LEAs contained 'individual' striated regions.

The mathematical analysis demonstrated that the individualisation of LEAs could, in part, be achieved depending on the percentage alignment of the topographical surface maps. In Chapter 3, the pellets used were taken from those fired in April 2013 where oxidation was less pronounced and five LEAs (A, D, H, J and K) demonstrated 90% successful alignment. In Chapter 4, the selected pellets were taken from amongst those fired in April 2012 where a greater number of pellets were corroded and as a consequence only three LEAs (A, D and G) revealed alignment of 90% or better.

In Chapter 3, models built were tested for accuracy percentage of all aligned LEAs measurement. The results showed that, the accuracy percentage correlates with the percentage of alignment, where the accuracy increases with better alignment of the LEAs. As the percentage alignment was increased to 90%, the best discrimination of LEAs was achieved where four out of five LEAs can be accurately classified. The model was tested and proven useful in terms of the accuracy of clustering of the aligned LEAs. This method can potentially be applied to provide percentage of matching values of LEAs from air weapons.

One of the other important goals within firearm examination is to demonstrate that the discriminating marks impressed onto a projectile by a weapon remain static over time. This was shown to be largely a valid assumption. Based on the analysis results, four out of 12 LEAs (LEA D, E, J and L) suggested that changes to striation marks within a LEA after repetitive firing over a period of time could occur. Build-up of lead residues within the barrel may possibly account for these changes.

One of the objectives of firearm comparison is in the ability for any method to be able to differentiate conclusively between projectiles fired by different weapons as well as the ability to connect a damaged projectile to a potential source weapon. This involves both a class differentiation (to weapon classification) and a potential individualisation to a specific weapon.

The combination of the imaging and mathematical analysis suggested that when a threshold is set (in this case 90% topographical alignment) then the discrimination of weapon type was possible. All LEAs from both air rifles can be separated well from LEAs from that of air pistol. When it came to the association of damaged projectiles with the known source, the developed imaging and mathematical methods worked well where there were more obvious morphological features in evidence.

This study used barrelled air weapons withunjacketed lead pellets. Previous studies mostly utilised jacketed bullet where land marks are more prominent, however the matching percentage of the jacketed bullets were low. This study is different (using unjacketed pellets) and it showed the matching percentage for unjacketed pellets, with

more than 90% of matching percentage of aligned LEAs. The method used in this study can potentially be applied to those of jacketed bullets. Air weapons used were barrelled, and similar to barrel firearms, they can leave striation marks on the surface of projectiles. Hence, the scanning method and data analysis on the pellets used in this study can definitely be applied to jacketed bullets fired by barrelled firearms.

The method used in this study can be applied to differentiate pellets fired from different weapons with similar class characteristics. Class characteristics provides information of make and model of the weapon, however, three different air weapons used in this study possessed similar class characteristics. Only individual characteristic can be used to differentiate pellets fired from different weapons, scanned and analysed using the method proposed in this study. This can help in the bullets and firearms identification process.

## **7.2 Recommendations for future work**

This work has developed a ground truth database for three air weapons. The study should be developed further to incorporate more weapons so that the developed methodology could be applied to a wider range of samples. Future work should also incorporate firearms that have fired jacketed bullets as samples. Previous researchers suggested that the percentage of matching are low for jacketed bullets despite having more prominent land markings when shot from barrelled firearms. Methods used in this study can be applied to jacketed bullets, to predict the matching percentage of the bullets based on models built from analysis data.

## Appendix 1

Matlab® script for data loading

```
filestem=input('striation? ','s');
file1=input('number of first file? ');
no_pellets=input('number of pellets? ');
no_repeats=input('number of repeats per pellet? ');
i=file1;
data=zeros(1500,no_pellets*no_repeats);    % if any files contain more than 1500
points, set this value to e.g. 2000

for i=file1:file1+no_pellets-1
    j=1;
    for j=1:no_repeats
        fname=['p',int2str(i),filestem,int2str(j),'.txt']
        f=dlmread(fname,'\t',2,3);
        f=f(:,2);
        [no_rows,no_cols]=size(f);
        nr(1,j+(no_repeats*(i-file1)))=no_rows;
        data(1:no_rows,j+(no_repeats*(i-file1)))=f;
    end
end
min_rows=min(nr);
final_data=data(1:min_rows,:);

% disp('-----');
% disp('signals are contained in data variable and are arranged in columns');
% disp('-----');

clear filestem no_pellets no_repeats data fname i j f no_rows no_cols nr min_rows
file1    % clean-up of redundant variables
```

## Appendix 2

Matlab® script for curve removing

```
orig_data=input('enter name of variable containing raw data ');
orient1=input('are signals in rows or columns? (rows=1, columns=0) ');
poly_order=input('enter polynomial order of curve ');
if orient1==0
    orig_data=orig_data';
elseif orient1==1
end

[no_rows,no_cols]=size(orig_data);
fit_data=zeros(no_rows,no_cols);
diff_data=zeros(no_rows,no_cols);

i=1;
for i=1:no_rows
    [P,S,MU]=polyfit(1:no_cols,orig_data(i,:),poly_order);
    Y=polyval(P,1:no_cols,[],MU);
    fit_data(i,:)=Y;
end

diff_data=orig_data-fit_data;

% clear I c c_first i k lags max_time min_time no_cols no_rows orient1 time
```

### Appendix 3

Matlab® script for data aligning

```
orig_data=input('enter name of variable containing raw data ');
orient1=input('are signals in rows or columns? (rows=1, columns=0) ');
if orient1==0
    orig_data=orig_data';
elseif orient1==1
end

[no_rows,no_cols]=size(orig_data);
c=zeros((2*no_cols)-1,no_rows-1);
i=1;
for i=1:no_rows-1
    c(:,i)=xcorr((orig_data(1,:)),(orig_data(i+1,:)));
end
[c_first,lags]=xcorr((orig_data(1,:)),(orig_data(1,:)));

[~,I]=max(c);
time=lags(I)';
time=[0;time];

min_time=min(time);
max_time=max(time);

% min_time=-40;
% time(129)=-40;

new_orig_data=zeros(no_rows,abs(min_time)+max_time+no_cols);

k=1;
for k=1:no_rows

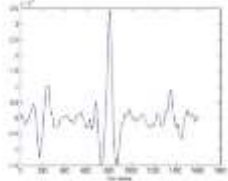
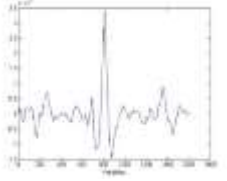
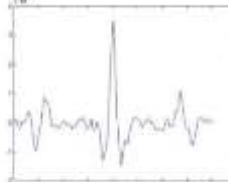
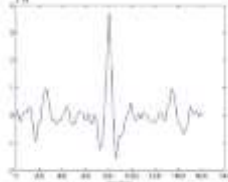
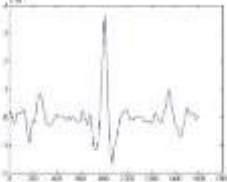
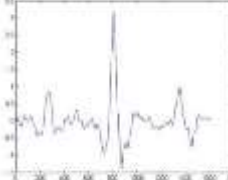

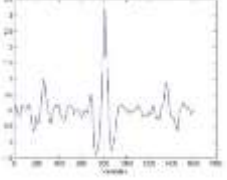
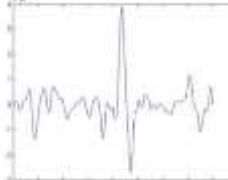

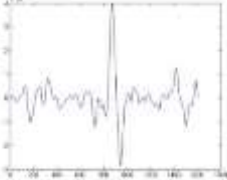


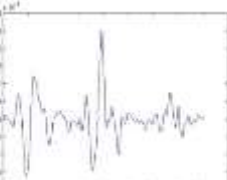
new_orig_data(k,abs(min_time)+time(k)+1:abs(min_time)+no_cols+time(k))=orig_data(k,:);
end

new_orig_data_trimmed=new_orig_data(:,abs(min_time)+max_time+1:no_cols);

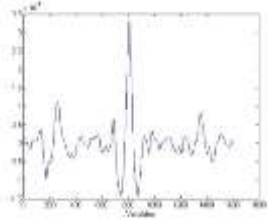
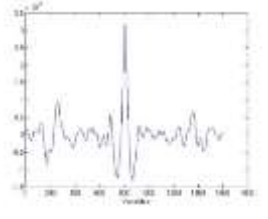
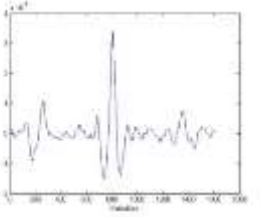
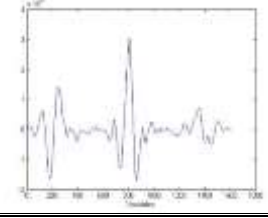
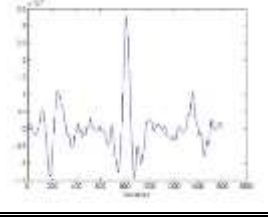
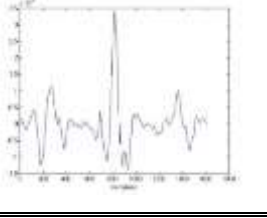
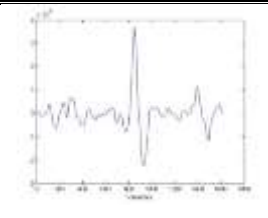
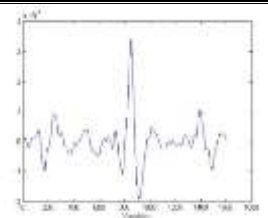
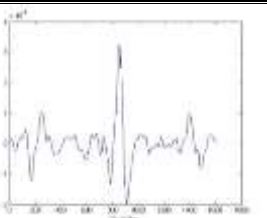
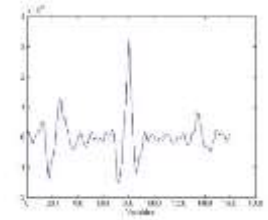
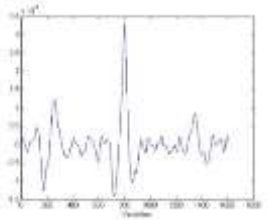
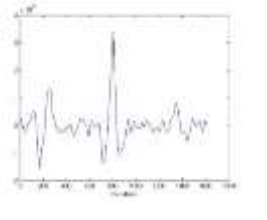
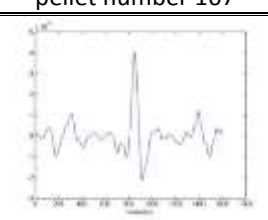
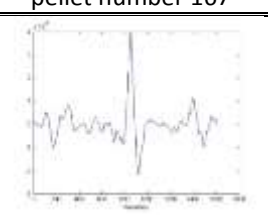
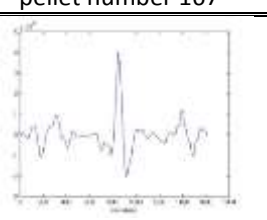
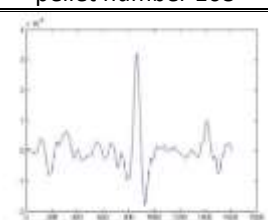
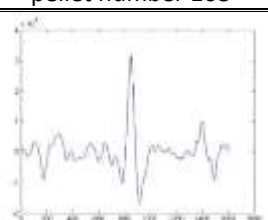
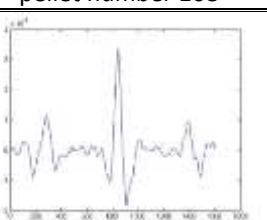
% clear I c c_first i k lags max_time min_time no_cols no_rows orient1 time
```

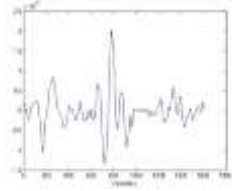
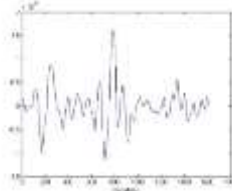
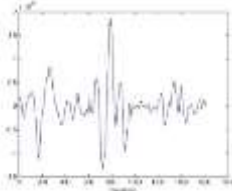
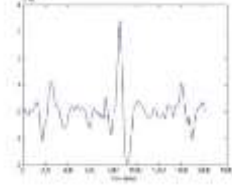
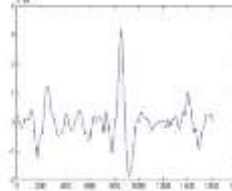
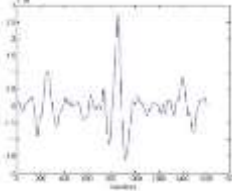
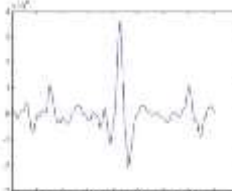
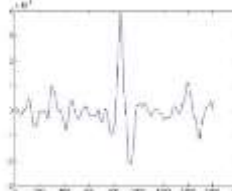
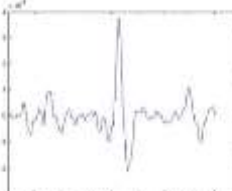



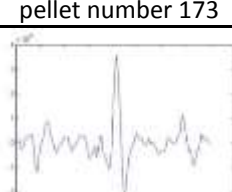
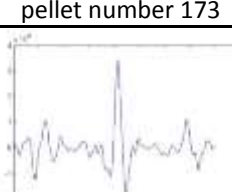

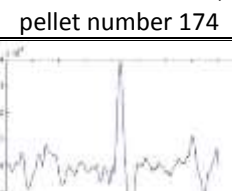
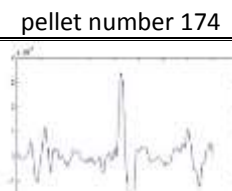
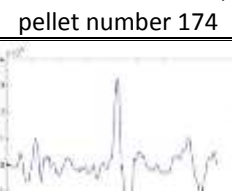
## Appendix 4

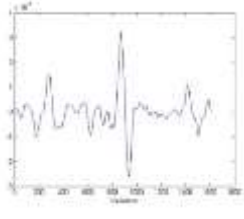
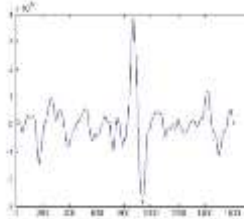
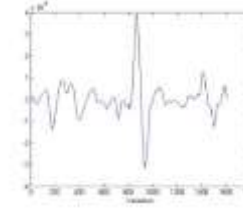
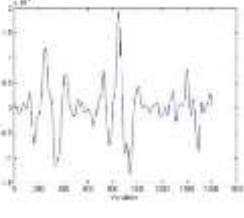
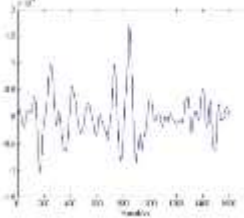
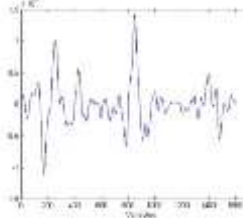
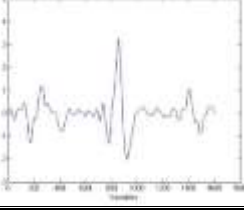
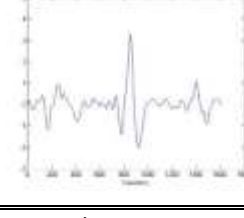
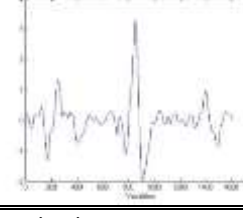
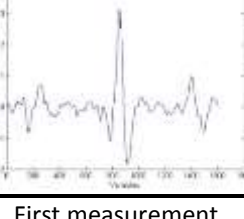
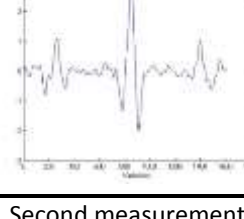
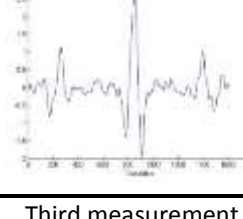
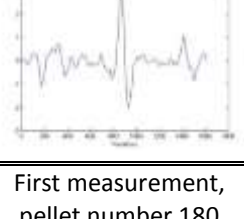
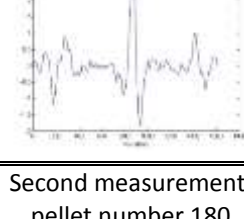
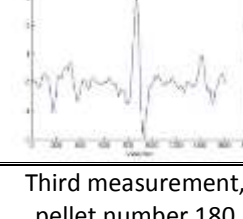
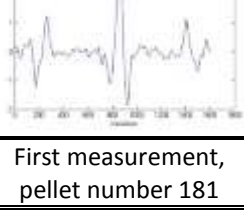
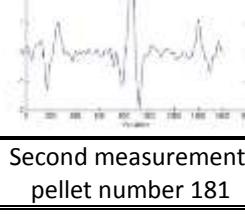
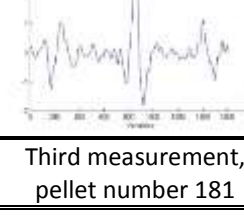
Alignment result for LEA A, pellet number 159 – 208

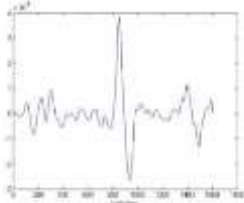
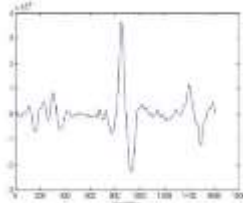
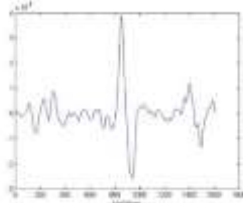
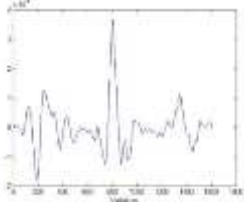
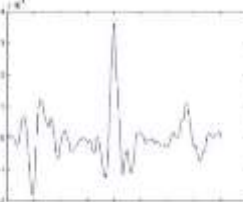
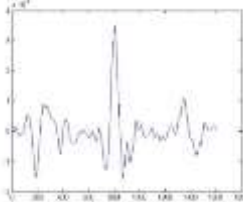

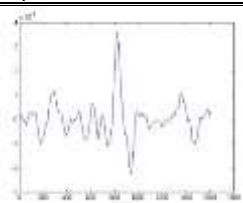

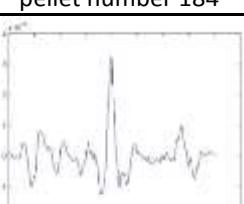
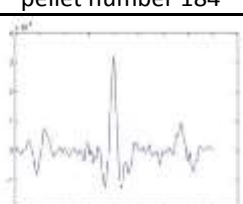
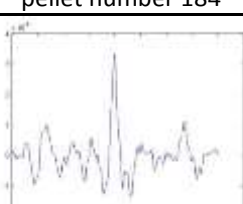
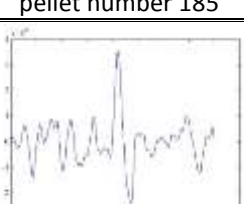
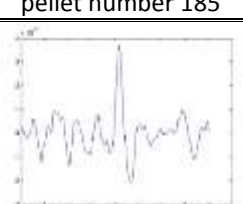
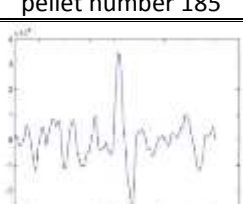

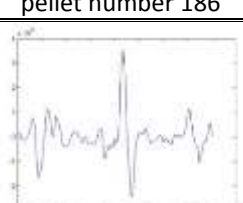
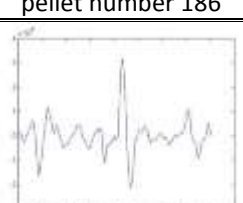
		
	Second measurement, pellet number 159	Third measurement, pellet number 159
		
First measurement, pellet number 160	Second measurement, pellet number 160	Third measurement, pellet number 160
		
First measurement, pellet number 161	Second measurement, pellet number 161	Third measurement, pellet number 161
		
First measurement, pellet number 162	Second measurement, pellet number 162	Third measurement, pellet number 162
		
First measurement, pellet number 163	Second measurement, pellet number 163	Third measurement, pellet number 163

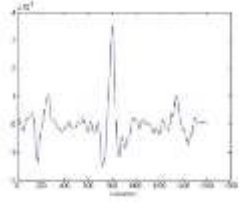
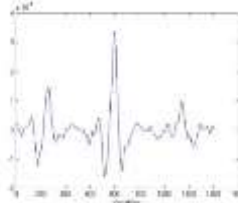
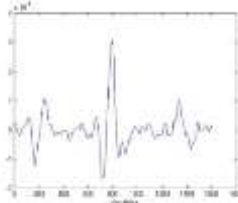
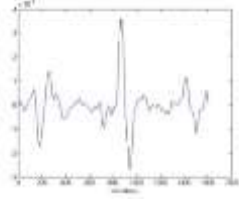
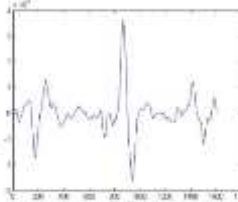
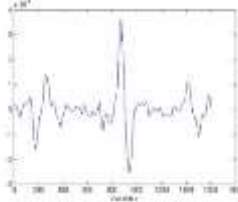
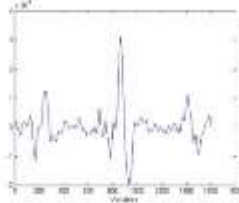
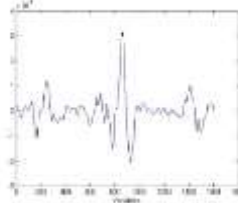
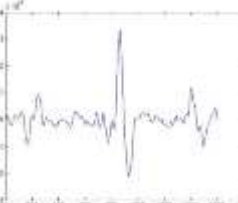

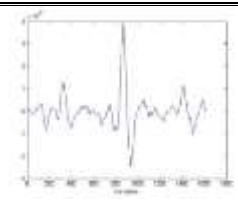
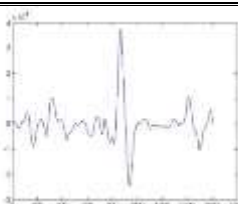
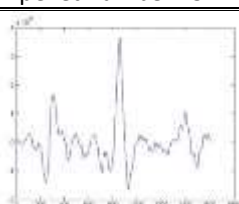
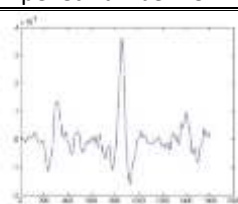
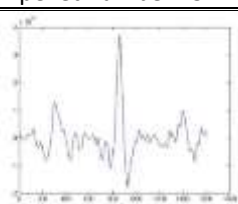
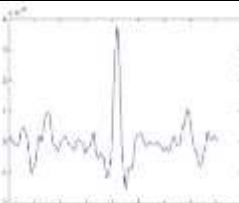
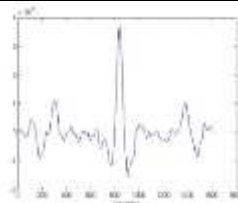
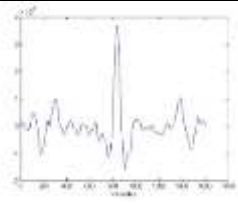


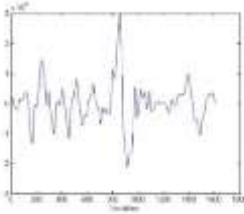
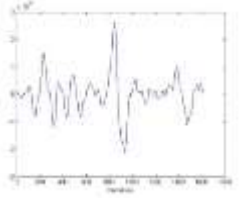
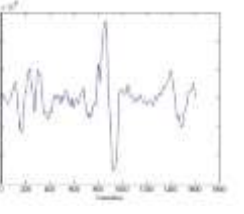
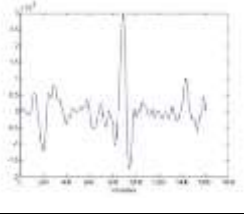
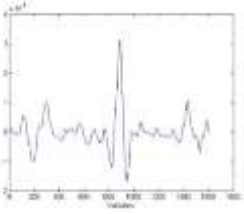
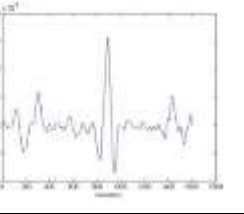
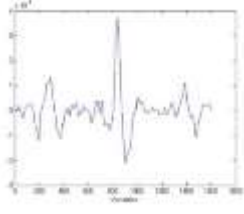
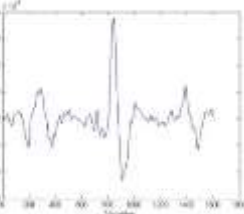
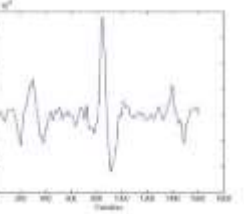
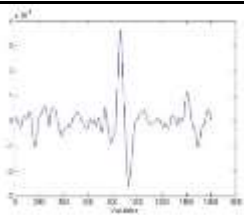
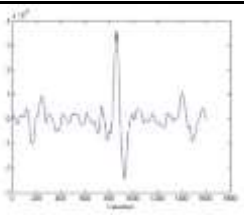
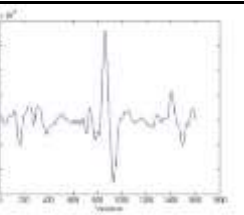
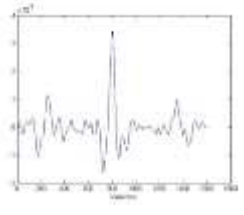
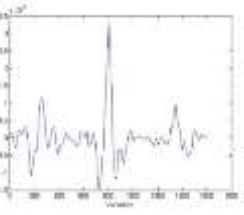
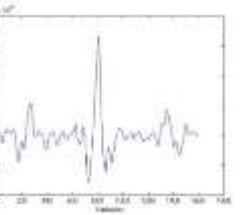
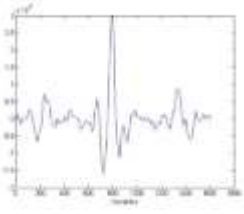
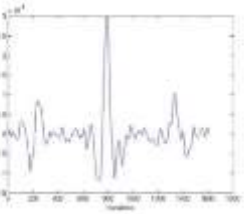
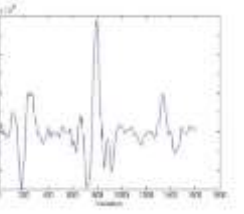
		
First measurement, pellet number 164	Second measurement, pellet number 164	Third measurement, pellet number 164
		
First measurement, pellet number 165	Second measurement, pellet number 165	Third measurement, pellet number 165
		
First measurement, pellet number 166	Second measurement, pellet number 166	Third measurement, pellet number 166
		
First measurement, pellet number 167	Second measurement, pellet number 167	Third measurement, pellet number 167
		
First measurement, pellet number 168	Second measurement, pellet number 168	Third measurement, pellet number 168
		
First measurement, pellet number 169	Second measurement, pellet number 169	Third measurement, pellet number 169

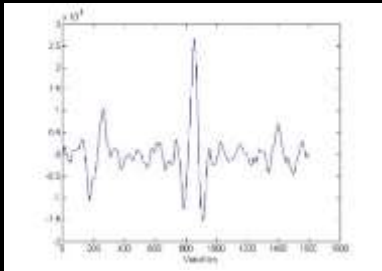
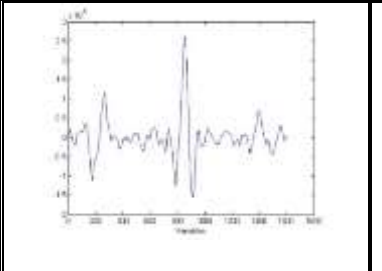
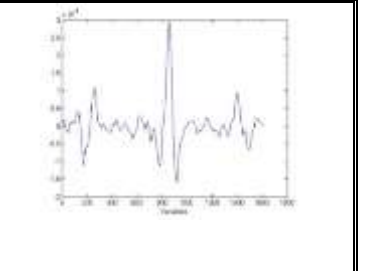
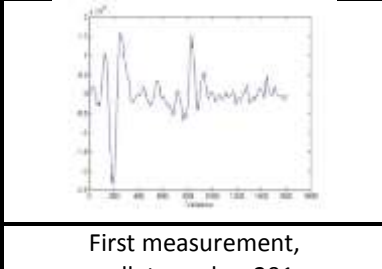
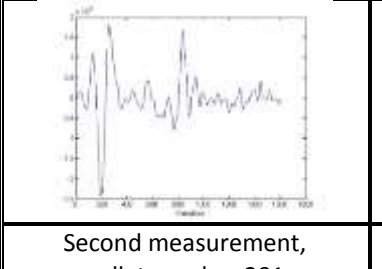
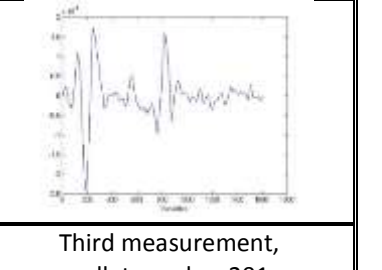
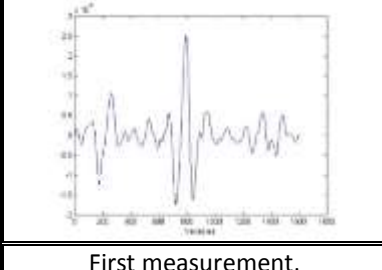
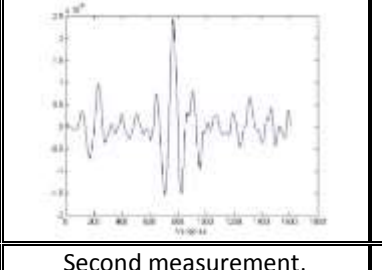
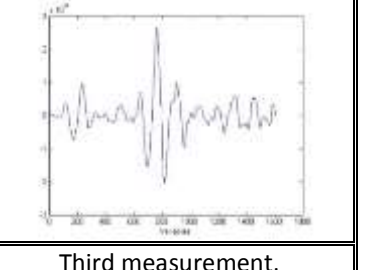
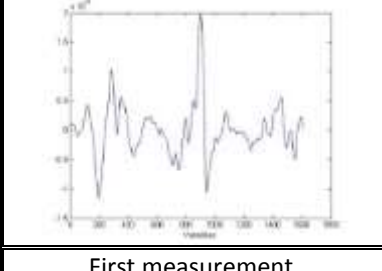
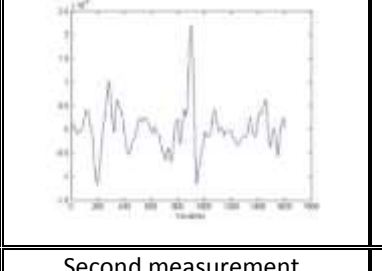
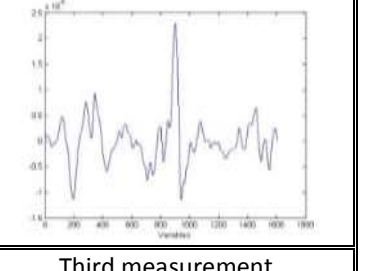
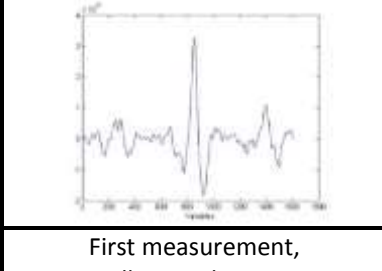
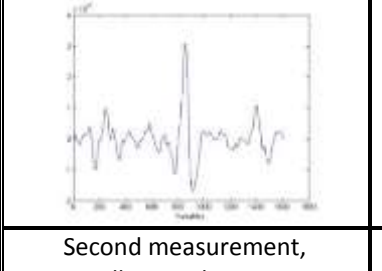
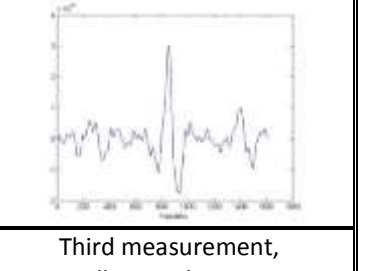
		
First measurement, pellet number 170	Second measurement, pellet number 170	Third measurement, pellet number 170
		
First measurement, pellet number 171	Second measurement, pellet number 171	Third measurement, pellet number 171
		
First measurement, pellet number 172	Second measurement, pellet number 172	Third measurement, pellet number 172
		
First measurement, pellet number 173	Second measurement, pellet number 173	Third measurement, pellet number 173
		
First measurement, pellet number 174	Second measurement, pellet number 174	Third measurement, pellet number 174
		
First measurement, pellet number 175	Second measurement, pellet number 175	Third measurement, pellet number 175

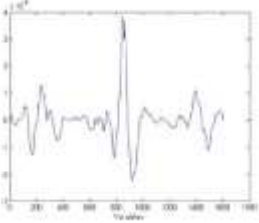
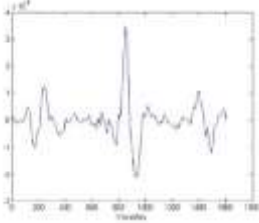
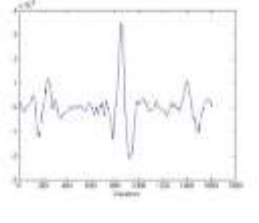
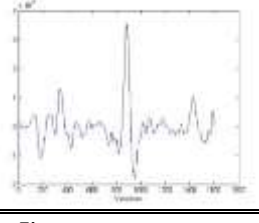
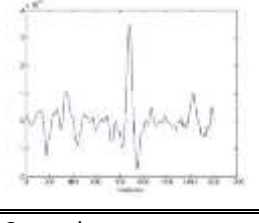
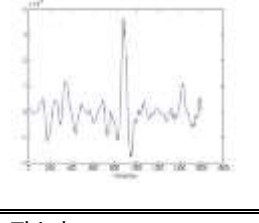
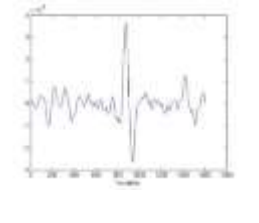
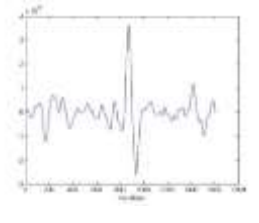
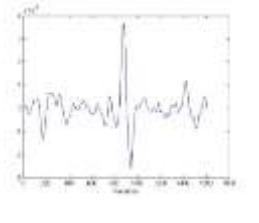
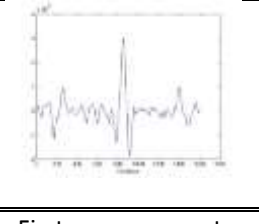
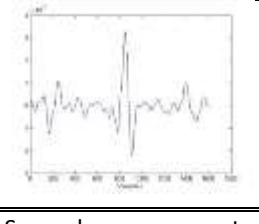
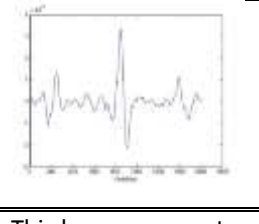
		
First measurement, pellet number 176	Second measurement, pellet number 176	Third measurement, pellet number 176
		
First measurement, pellet number 177	Second measurement, pellet number 177	Third measurement, pellet number 177
		
First measurement, pellet number 178	Second measurement, pellet number 178	Third measurement, pellet number 178
		
First measurement, pellet number 179	Second measurement, pellet number 179	Third measurement, pellet number 179
		
First measurement, pellet number 180	Second measurement, pellet number 180	Third measurement, pellet number 180
		
First measurement, pellet number 181	Second measurement, pellet number 181	Third measurement, pellet number 181

		
First measurement, pellet number 182	Second measurement, pellet number 182	Third measurement, pellet number 182
		
First measurement, pellet number 183	Second measurement, pellet number 183	Third measurement, pellet number 183
		
First measurement, pellet number 184	Second measurement, pellet number 184	Third measurement, pellet number 184
		
First measurement, pellet number 185	Second measurement, pellet number 185	Third measurement, pellet number 185
		
First measurement, pellet number 186	Second measurement, pellet number 186	Third measurement, pellet number 186
		
First measurement, pellet number 187	Second measurement, pellet number 187	Third measurement, pellet number 187

		
First measurement, pellet number 188	Second measurement, pellet number 188	Third measurement, pellet number 188
		
First measurement, pellet number 189	Second measurement, pellet number 189	Third measurement, pellet number 189
		
First measurement, pellet number 190	Second measurement, pellet number 190	Third measurement, pellet number 190
		
First measurement, pellet number 191	Second measurement, pellet number 191	Third measurement, pellet number 191
		
First measurement, pellet number 192	Second measurement, pellet number 192	Third measurement, pellet number 192
		
First measurement, pellet number 193	Second measurement, pellet number 193	Third measurement, pellet number 193

		
First measurement, pellet number 194	Second measurement, pellet number 194	Third measurement, pellet number 194
		
First measurement, pellet number 195	Second measurement, pellet number 195	Third measurement, pellet number 195
		
First measurement, pellet number 196	Second measurement, pellet number 196	Third measurement, pellet number 196
		
First measurement, pellet number 197	Second measurement, pellet number 197	Third measurement, pellet number 197
		
First measurement, pellet number 198	Second measurement, pellet number 198	Third measurement, pellet number 198
		
First measurement, pellet number 199	Second measurement, pellet number 199	Third measurement, pellet number 199

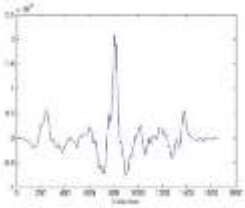
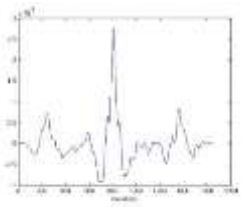
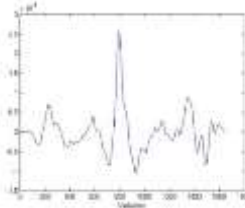
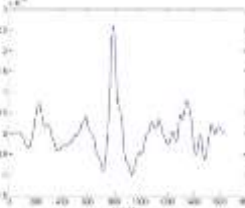
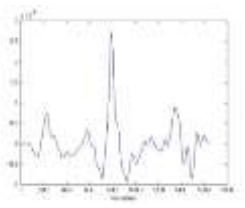

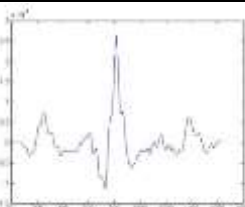
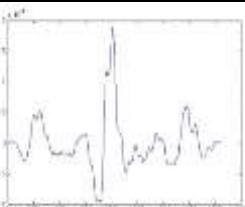

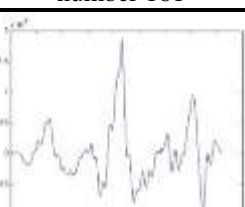



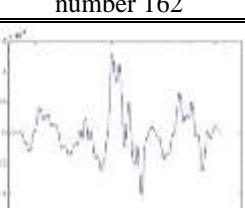
		
First measurement, pellet number 200	Second measurement, pellet number 200	Third measurement, pellet number 200
		
First measurement, pellet number 201	Second measurement, pellet number 201	Third measurement, pellet number 201
		
First measurement, pellet number 202	Second measurement, pellet number 202	Third measurement, pellet number 202
		
First measurement, pellet number 203	Second measurement, pellet number 203	Third measurement, pellet number 203
		
First measurement, pellet number 204	Second measurement, pellet number 204	Third measurement, pellet number 204

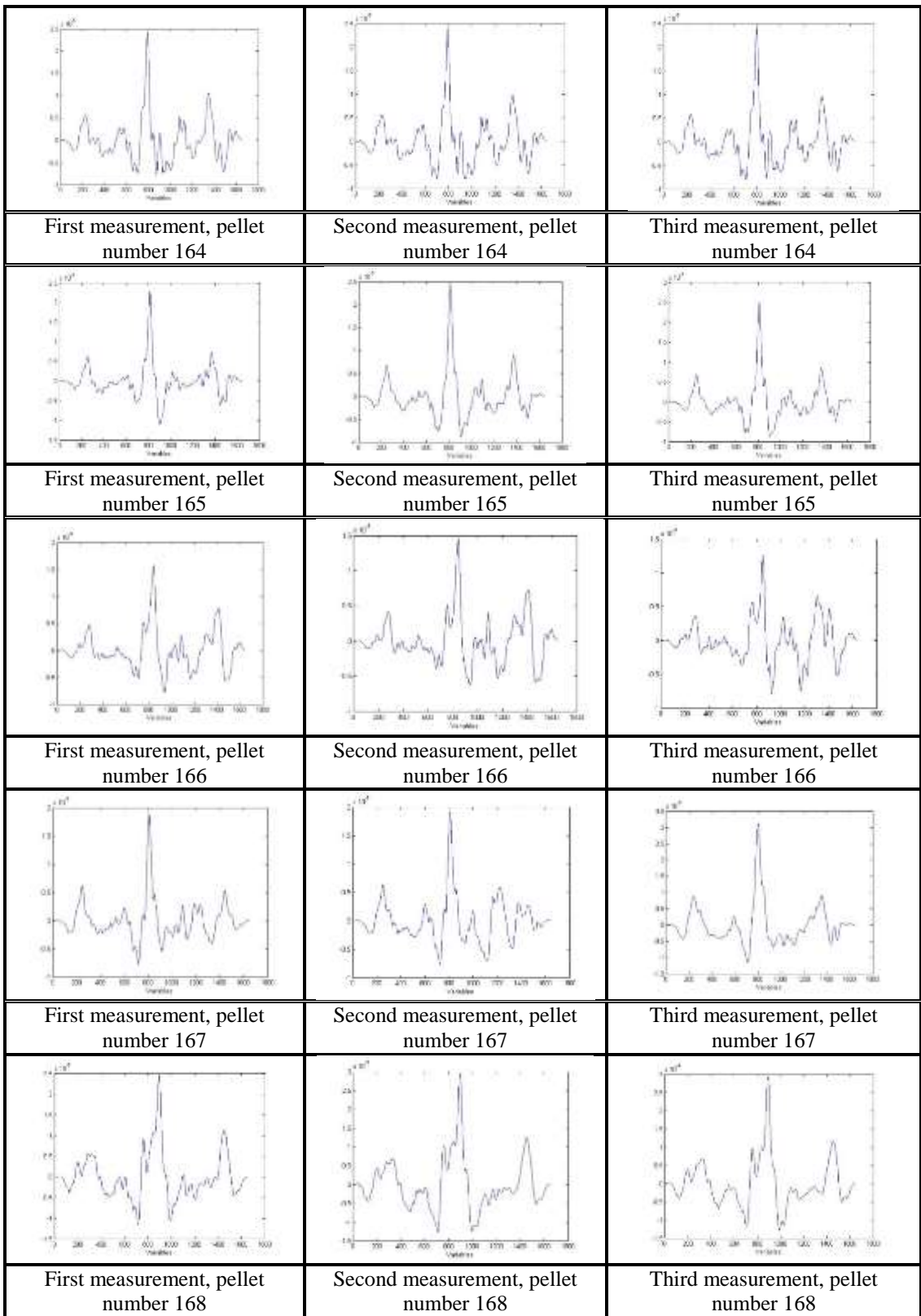
		
First measurement, pellet number 205	Second measurement, pellet number 205	Third measurement, pellet number 205
		
First measurement, pellet number 206	Second measurement, pellet number 206	Third measurement, pellet number 206
		
First measurement, pellet number 207	Second measurement, pellet number 207	Third measurement, pellet number 207
		
First measurement, pellet number 208	Second measurement, pellet number 208	Third measurement, pellet number 208

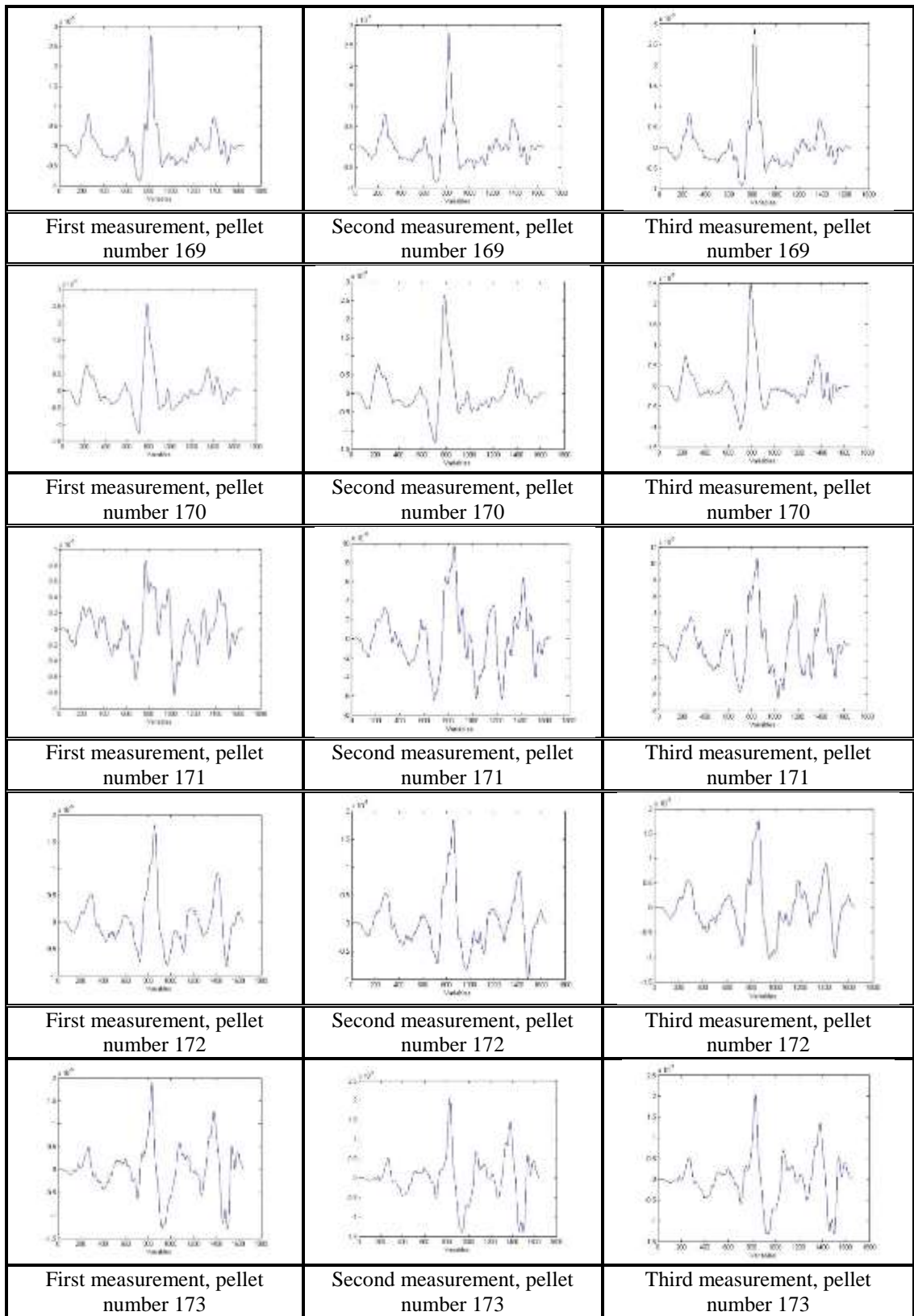


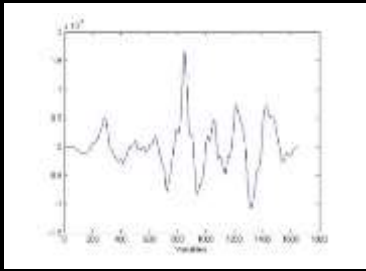
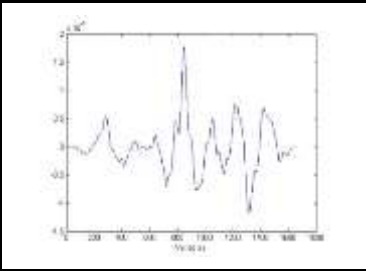
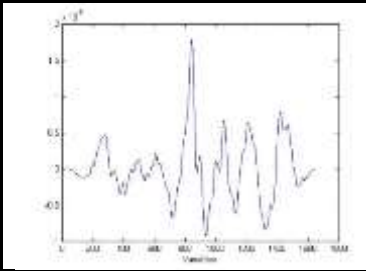
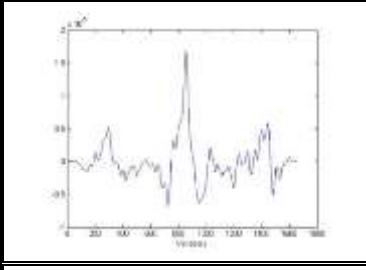
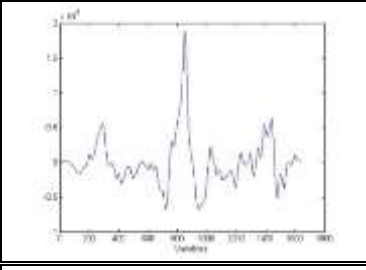
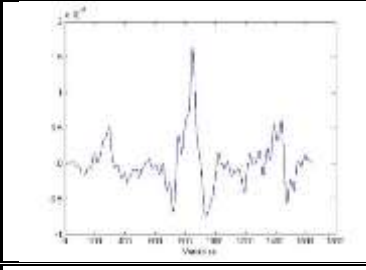
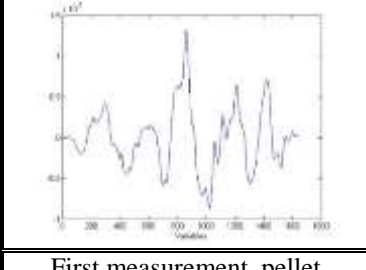
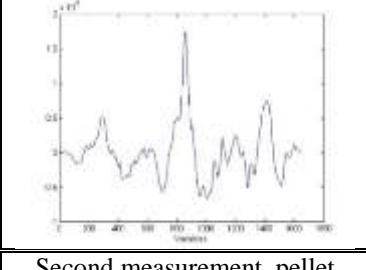
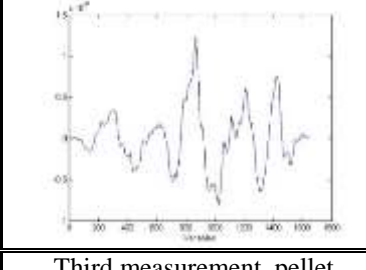
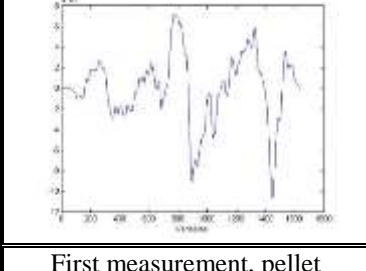
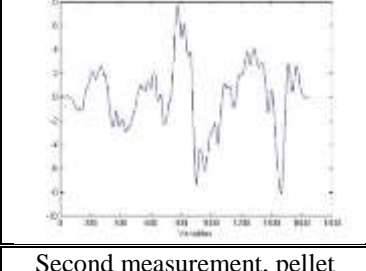
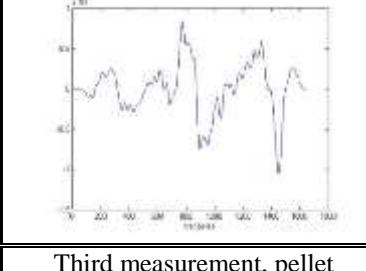
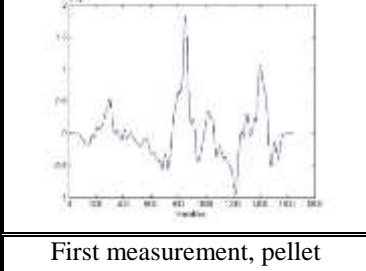
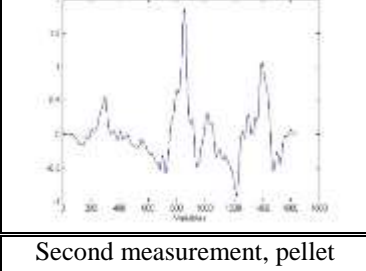
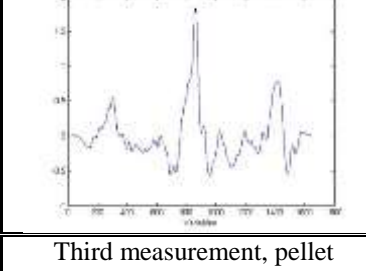
## Appendix 5

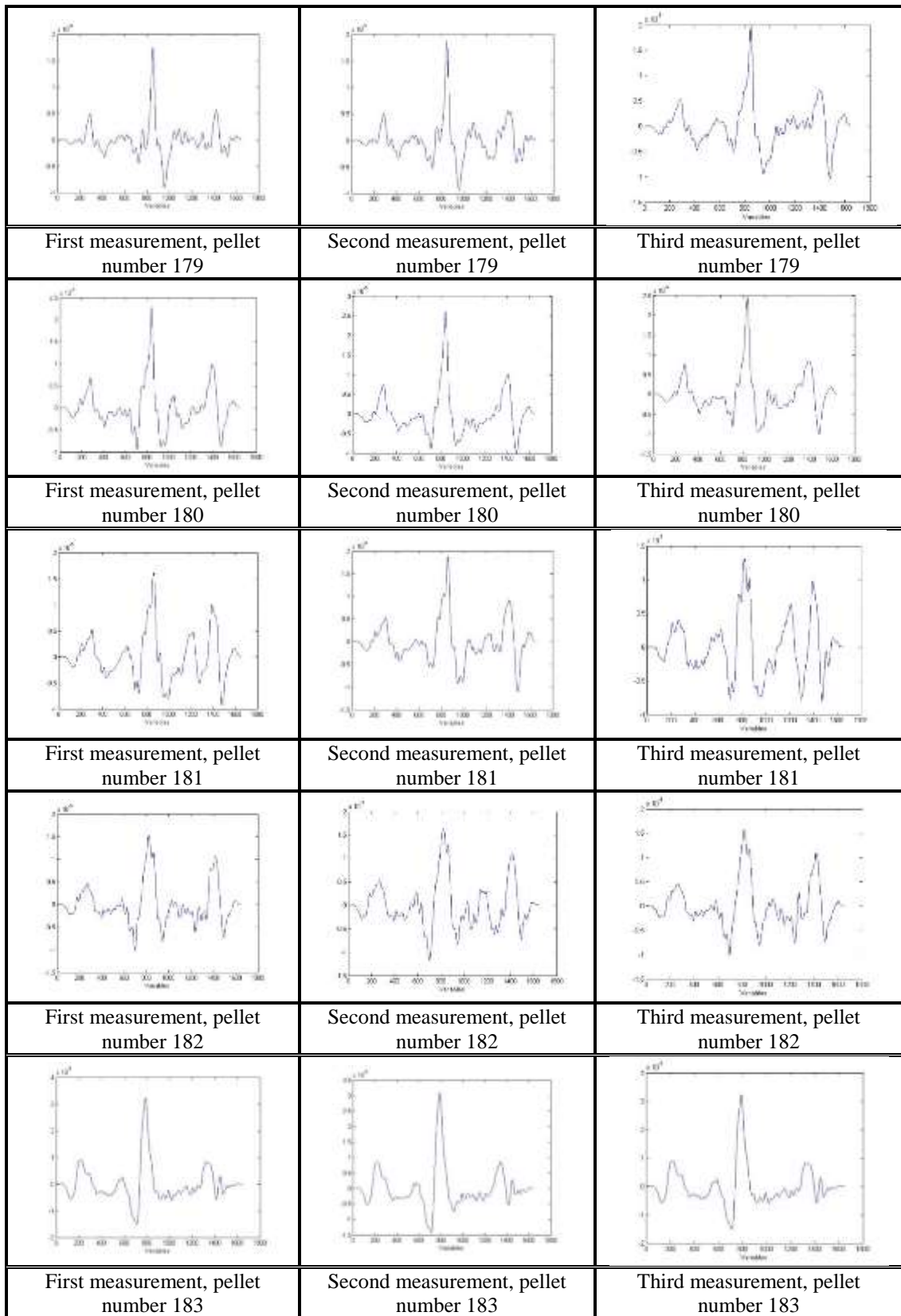
Alignment result for LEA B, pellet number 159 – 208

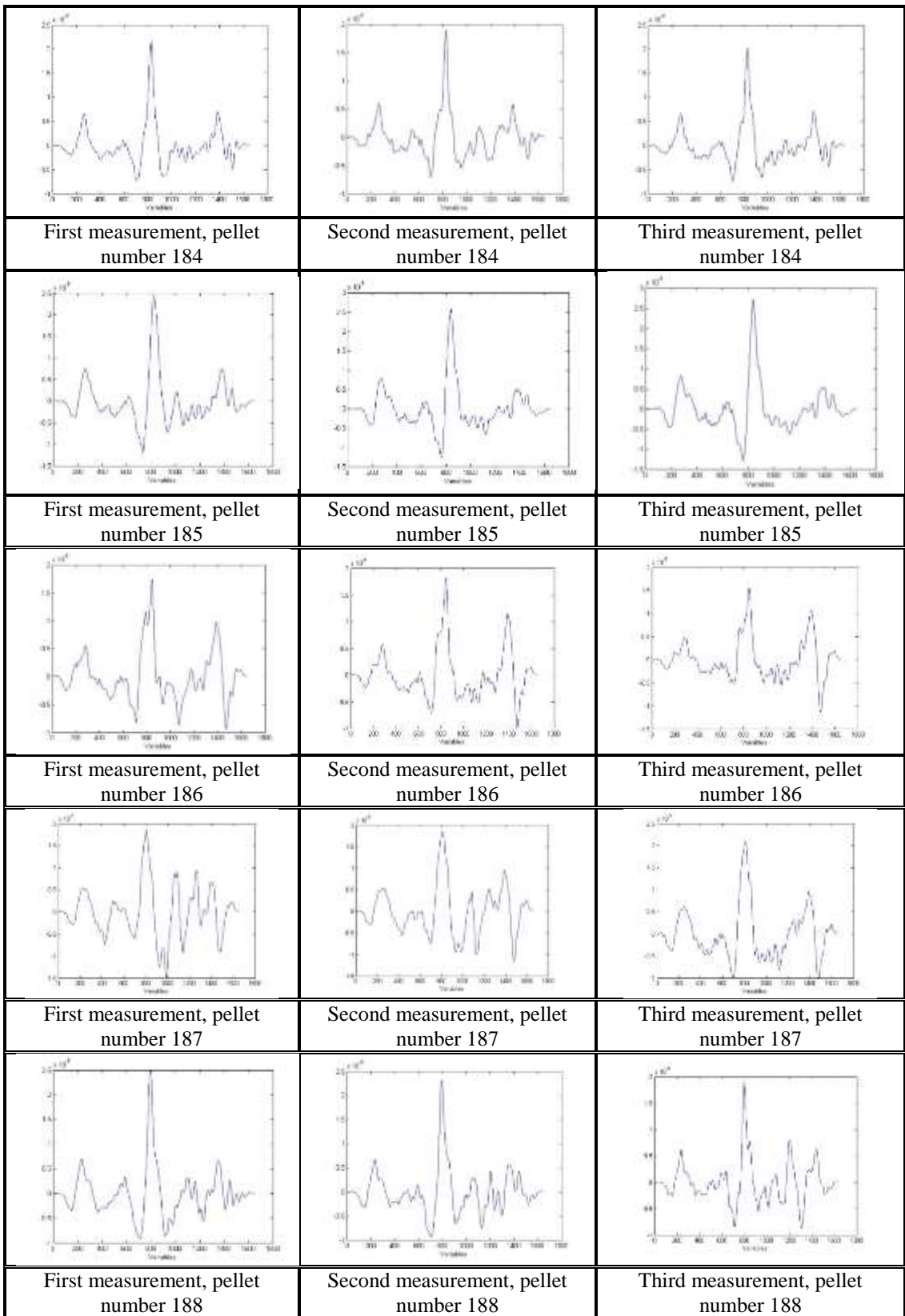
		
	Second measurement, pellet number 159	Third measurement, pellet number 159
		
First measurement, pellet number 160	Second measurement, pellet number 160	Third measurement, pellet number 160
		
First measurement, pellet number 161	Second measurement, pellet number 161	Third measurement, pellet number 161
		
First measurement, pellet number 162	Second measurement, pellet number 162	Third measurement, pellet number 162
		
First measurement, pellet number 163	Second measurement, pellet number 163	Third measurement, pellet number 163

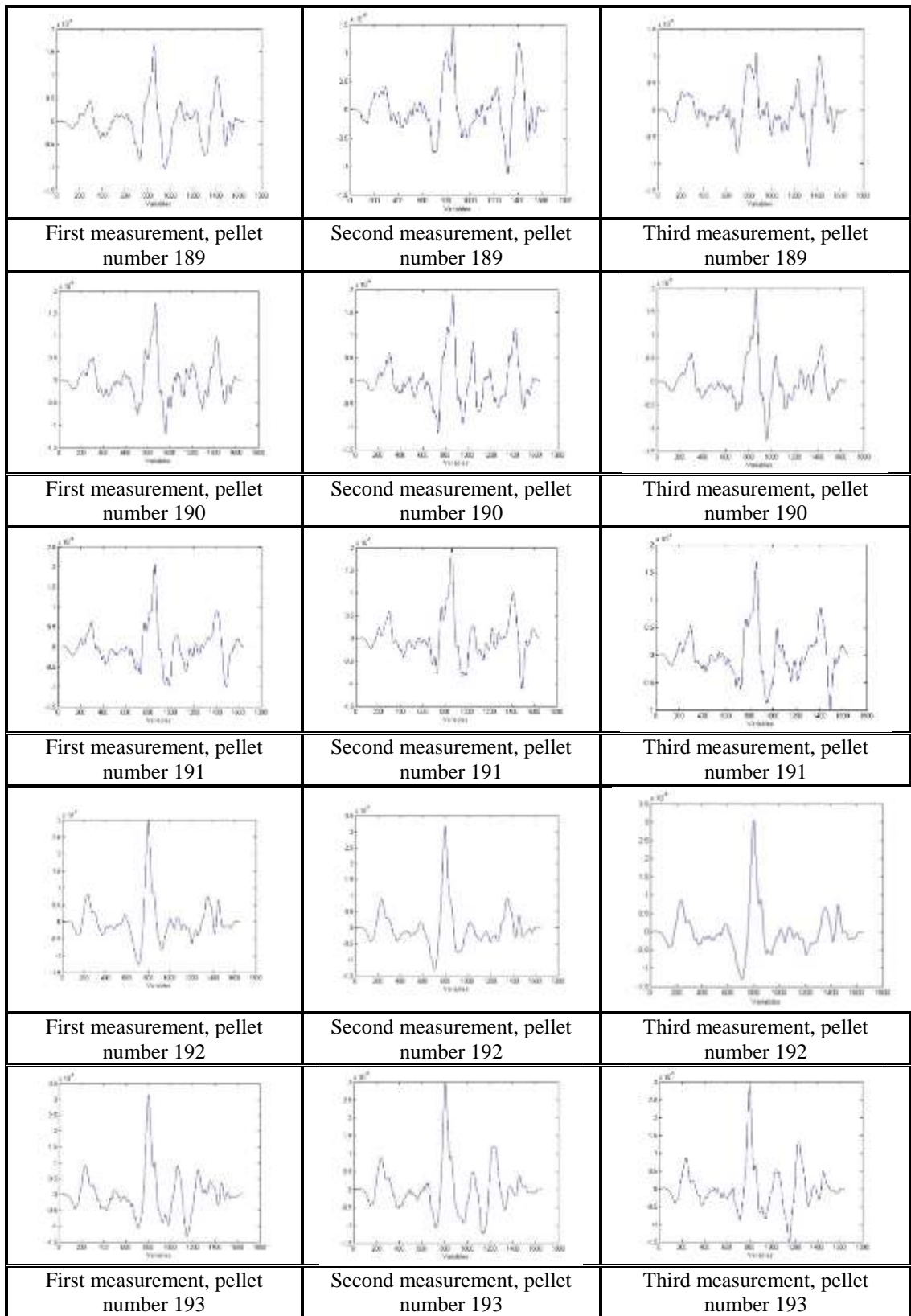


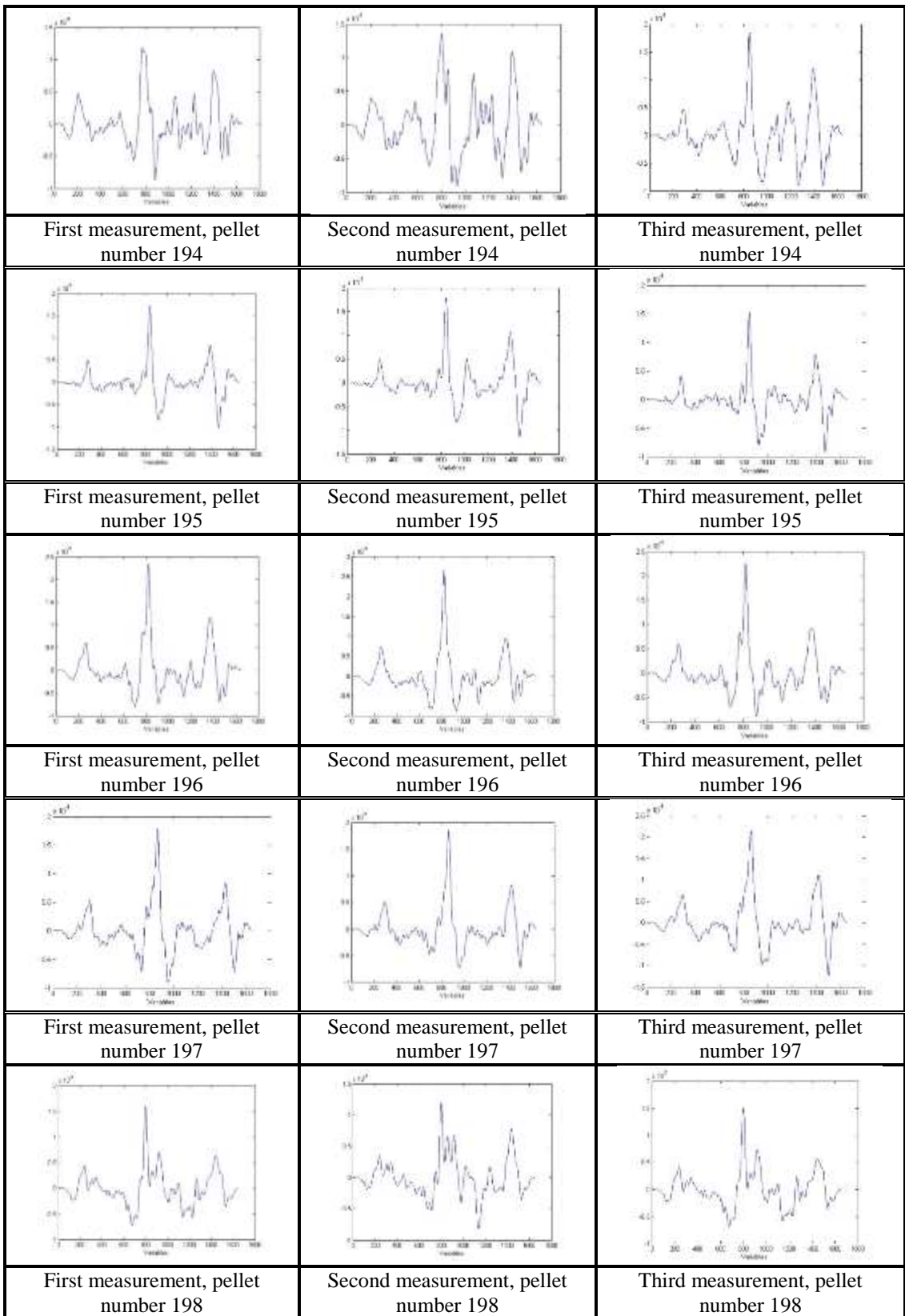


		
First measurement, pellet number 174	Second measurement, pellet number 174	Third measurement, pellet number 174
		
First measurement, pellet number 175	Second measurement, pellet number 175	Third measurement, pellet number 175
		
First measurement, pellet number 176	Second measurement, pellet number 176	Third measurement, pellet number 176
		
First measurement, pellet number 177	Second measurement, pellet number 177	Third measurement, pellet number 177
		
First measurement, pellet number 178	Second measurement, pellet number 178	Third measurement, pellet number 178

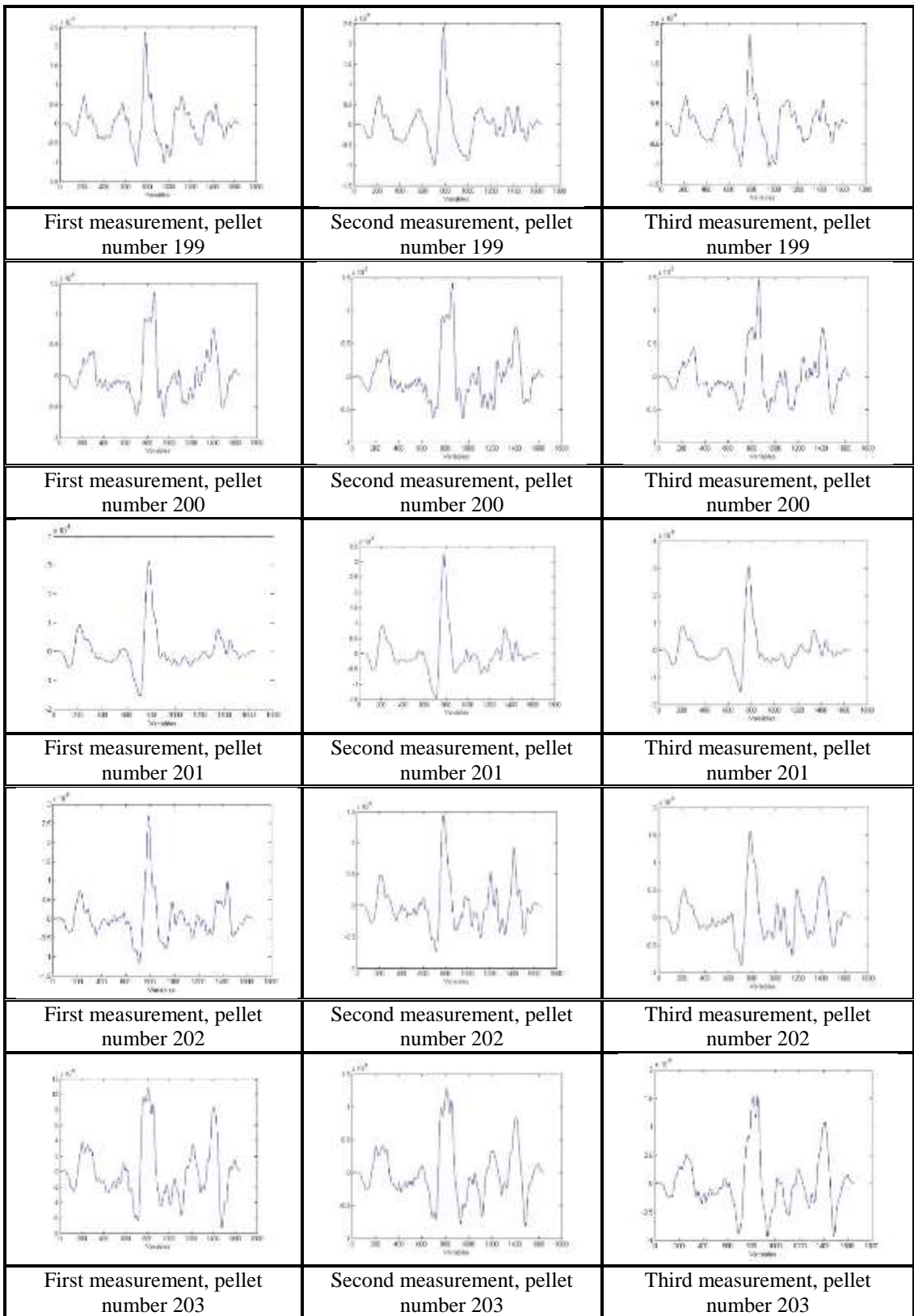


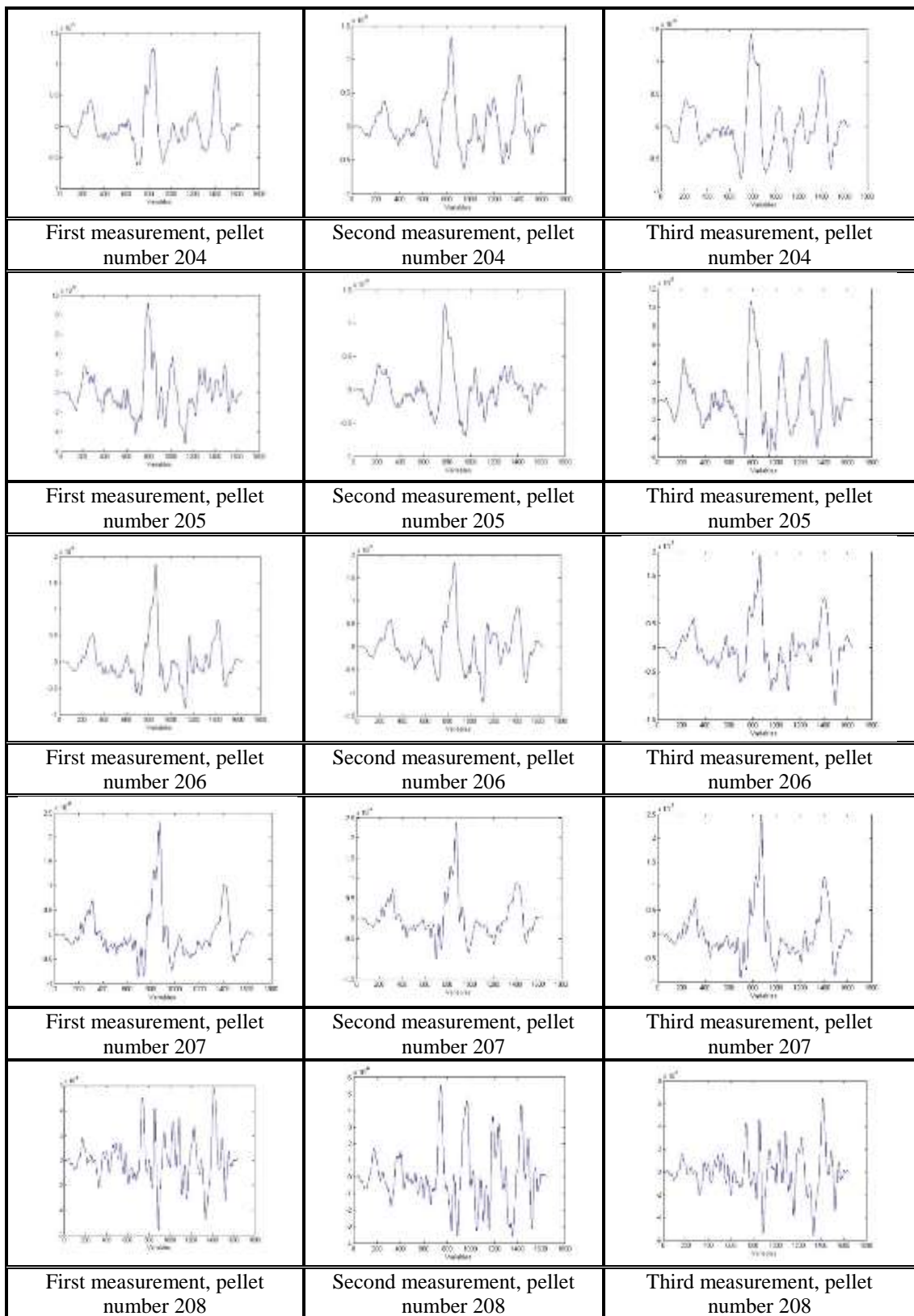






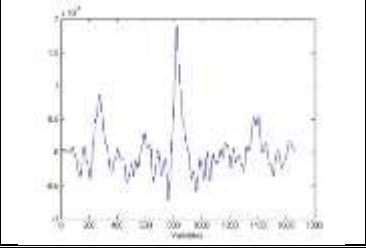
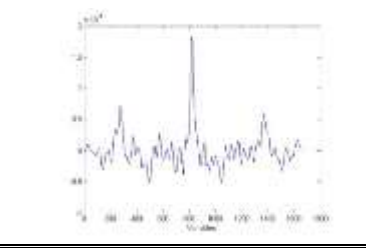
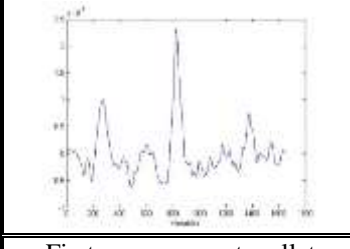
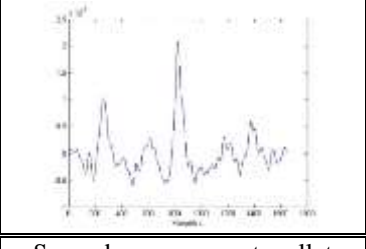
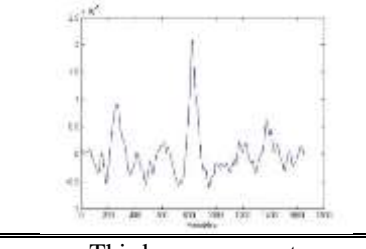
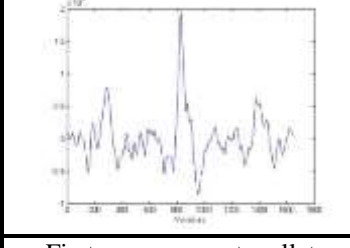
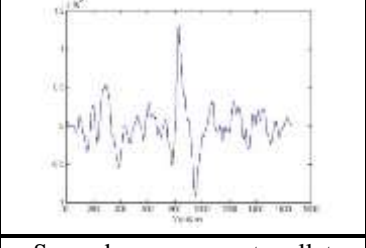
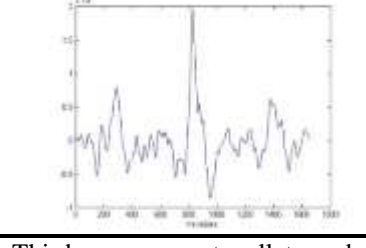
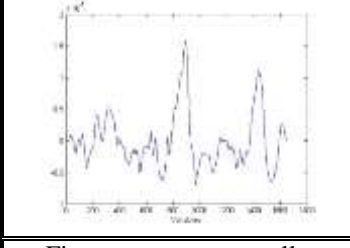
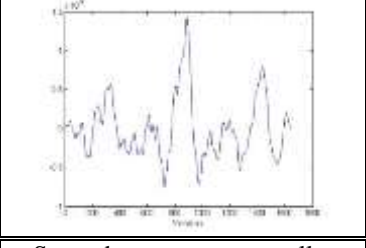
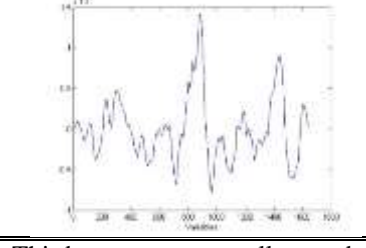
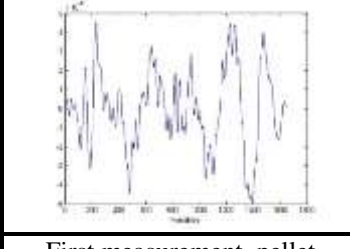
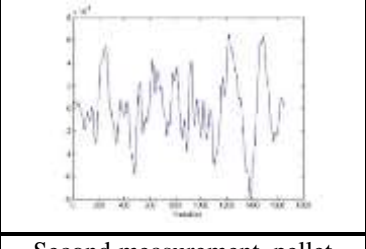
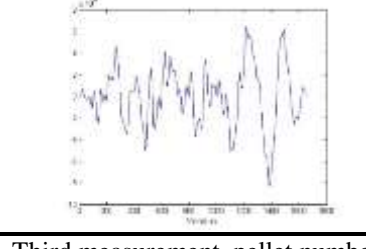


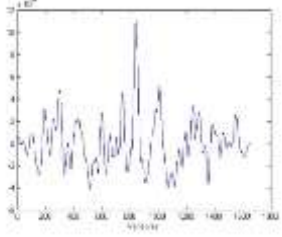
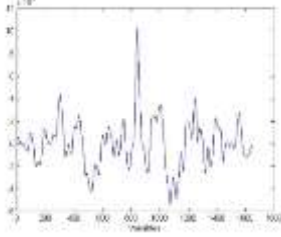
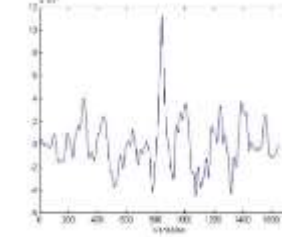
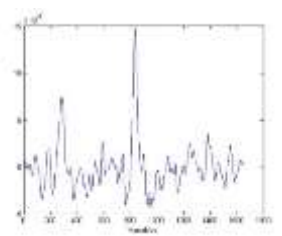
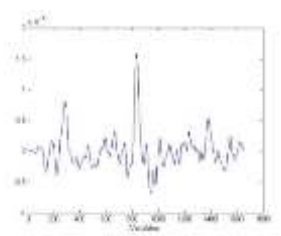
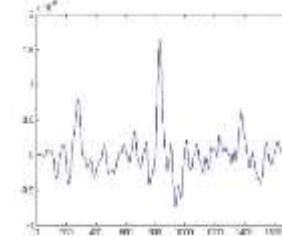
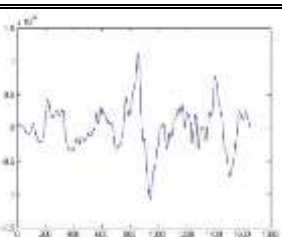
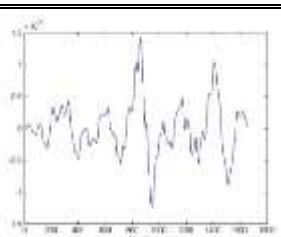
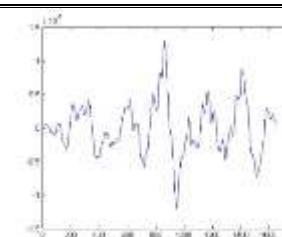
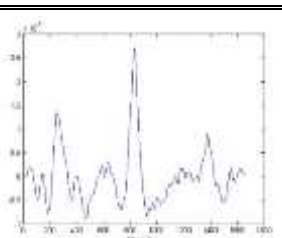
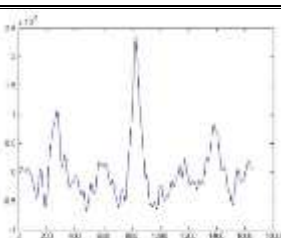
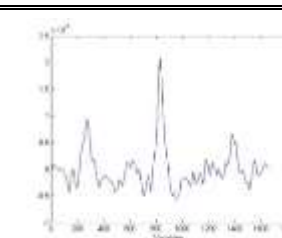
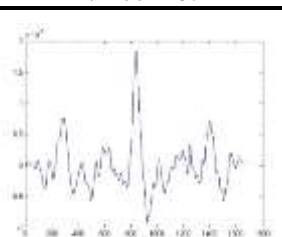
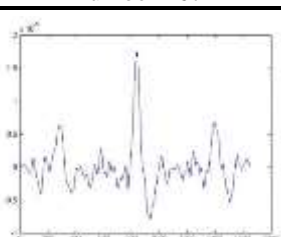
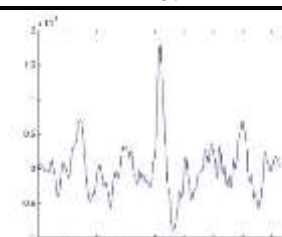


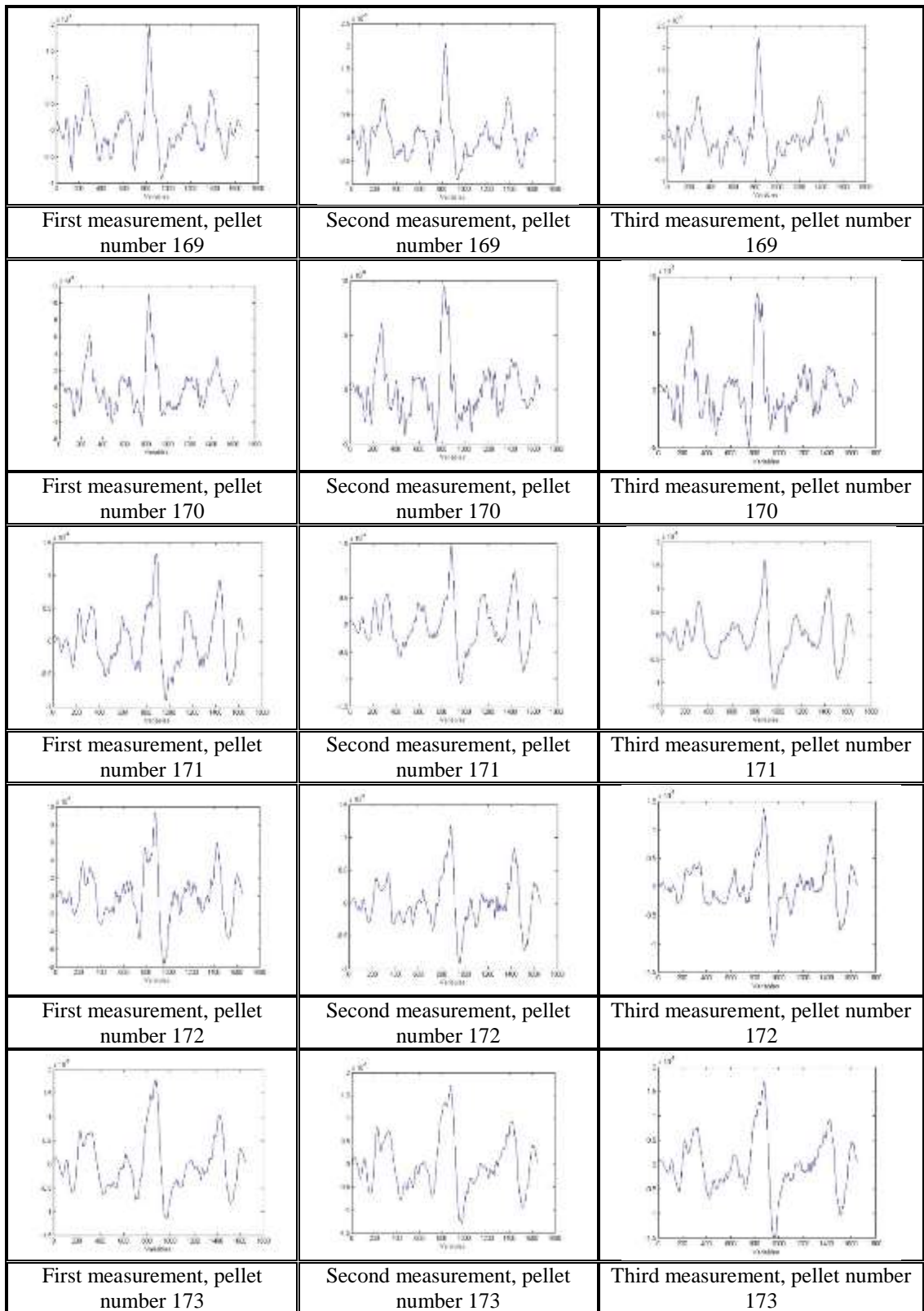


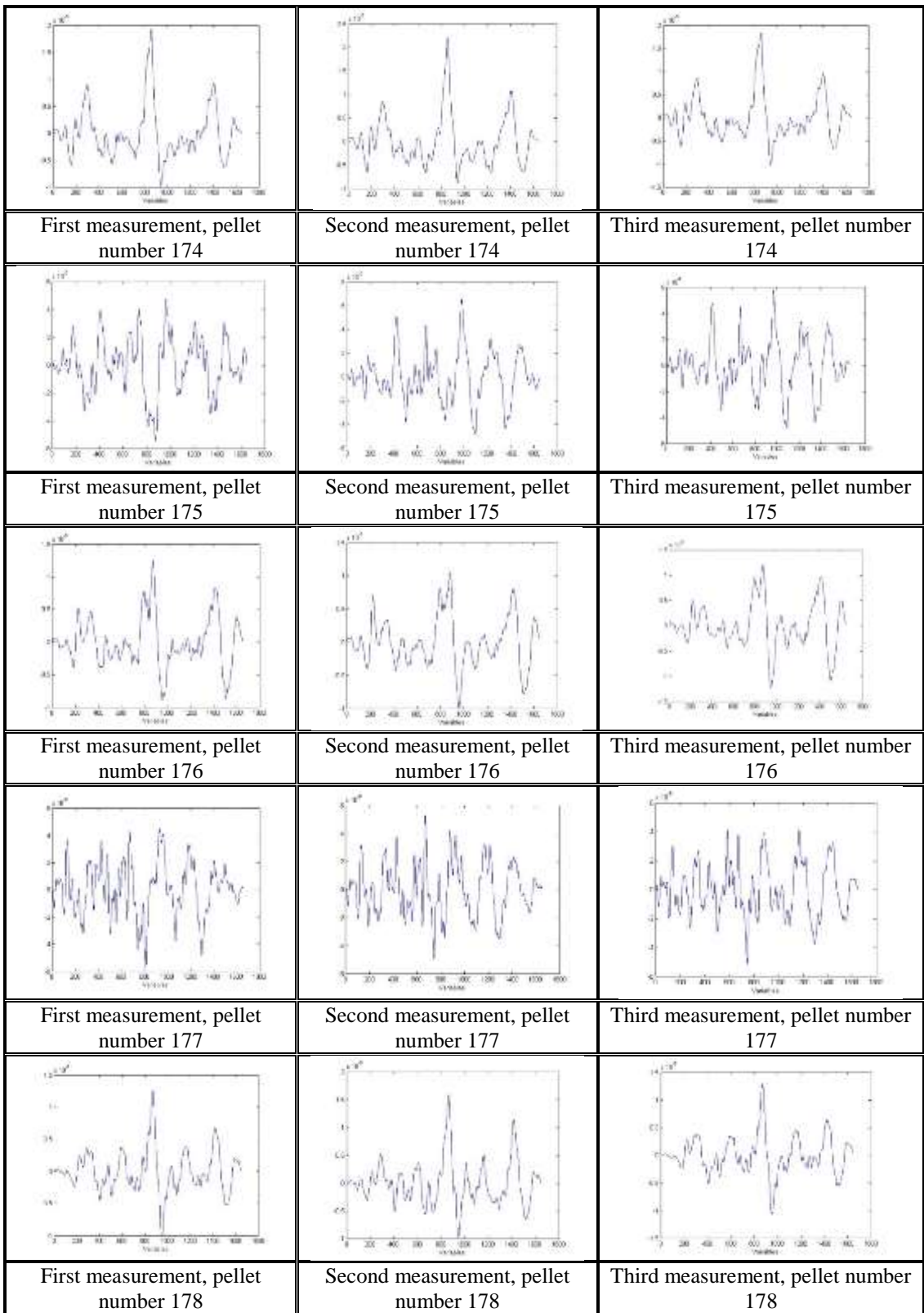
## Appendix 6

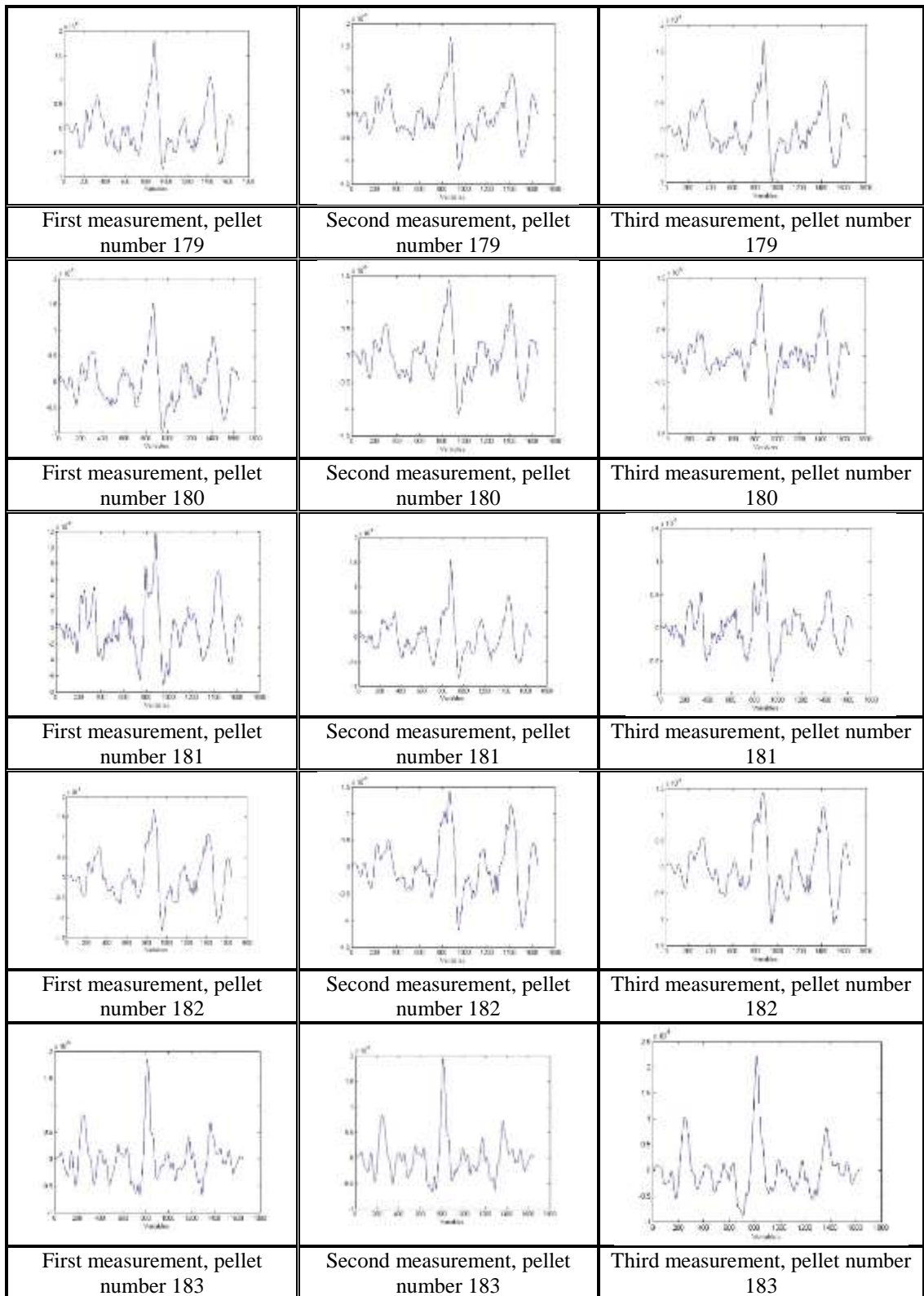
Alignment result for LEA C, pellet number 159 – 208

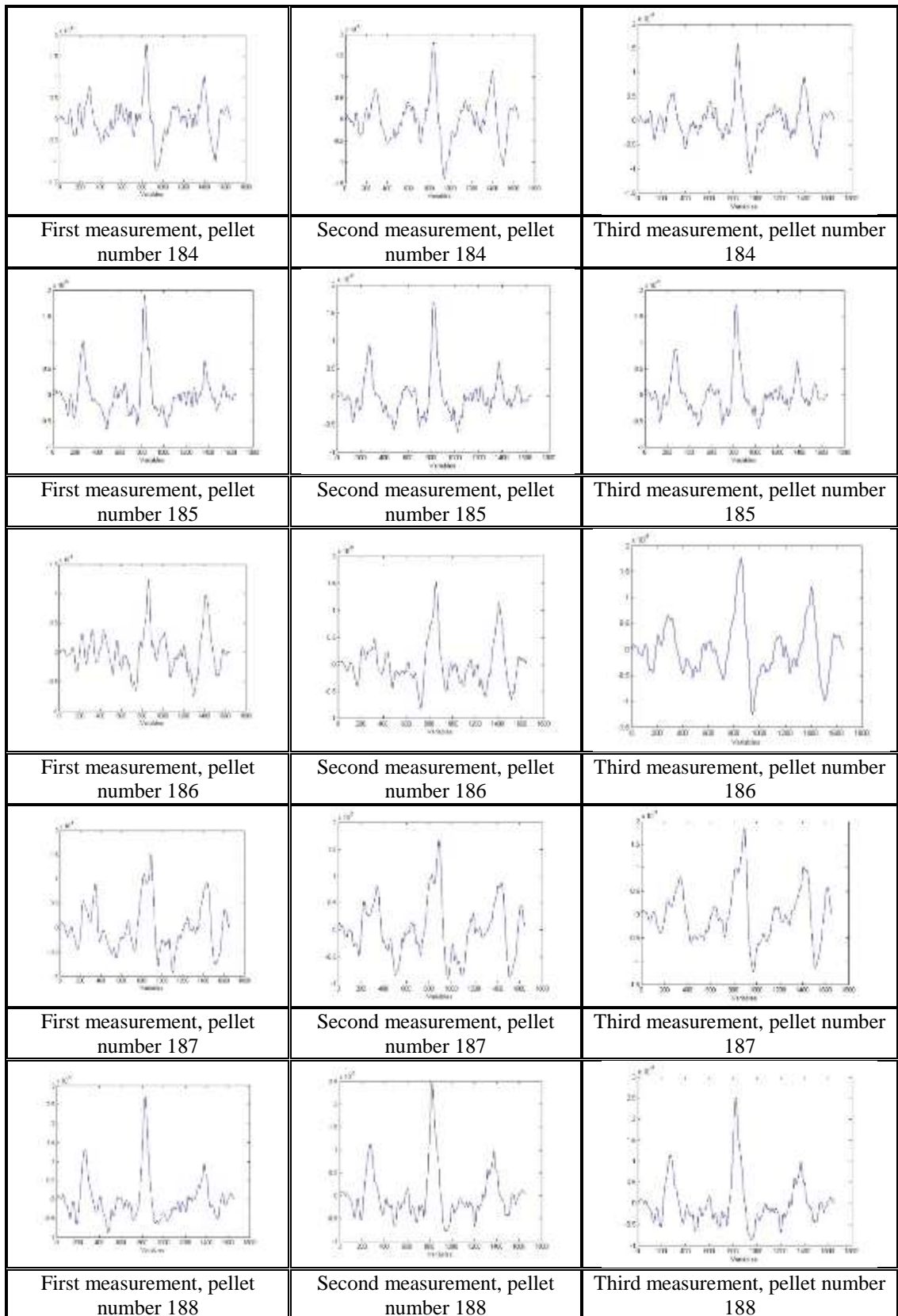
		
	Second measurement, pellet number 159	Third measurement, pellet number 159
		
First measurement, pellet number 160	Second measurement, pellet number 160	Third measurement, pellet number 160
		
First measurement, pellet number 161	Second measurement, pellet number 161	Third measurement, pellet number 161
		
First measurement, pellet number 162	Second measurement, pellet number 162	Third measurement, pellet number 162
		
First measurement, pellet number 163	Second measurement, pellet number 163	Third measurement, pellet number 163

		
First measurement, pellet number 164	Second measurement, pellet number 164	Third measurement, pellet number 164
		
First measurement, pellet number 165	Second measurement, pellet number 165	Third measurement, pellet number 165
		
First measurement, pellet number 166	Second measurement, pellet number 166	Third measurement, pellet number 166
		
First measurement, pellet number 167	Second measurement, pellet number 167	Third measurement, pellet number 167
		
First measurement, pellet number 168	Second measurement, pellet number 168	Third measurement, pellet number 168

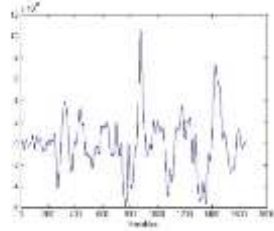
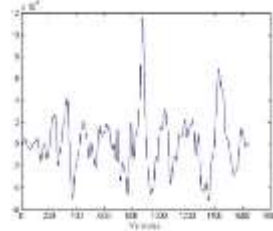
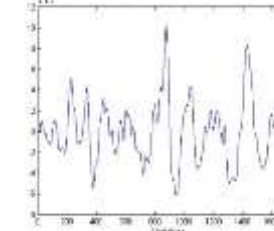
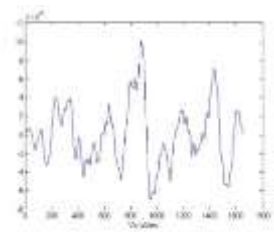
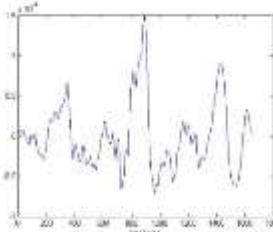
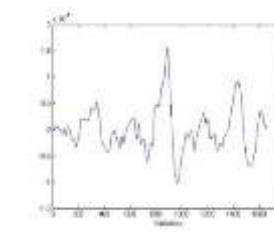
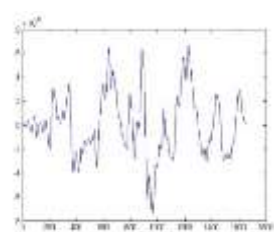
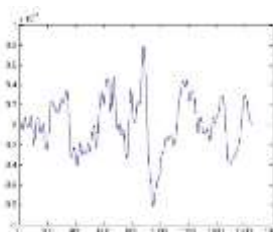
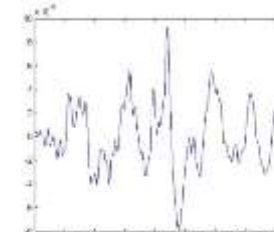
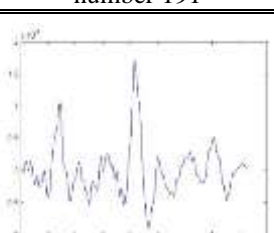
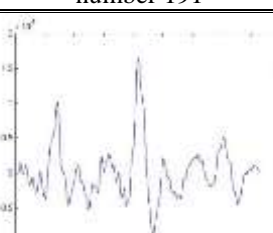
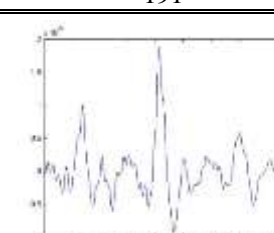
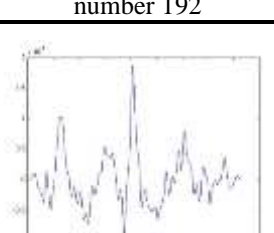
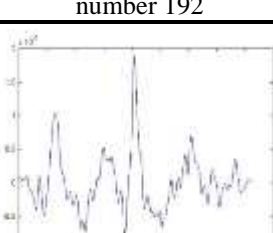
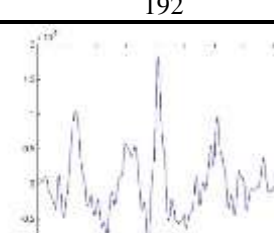


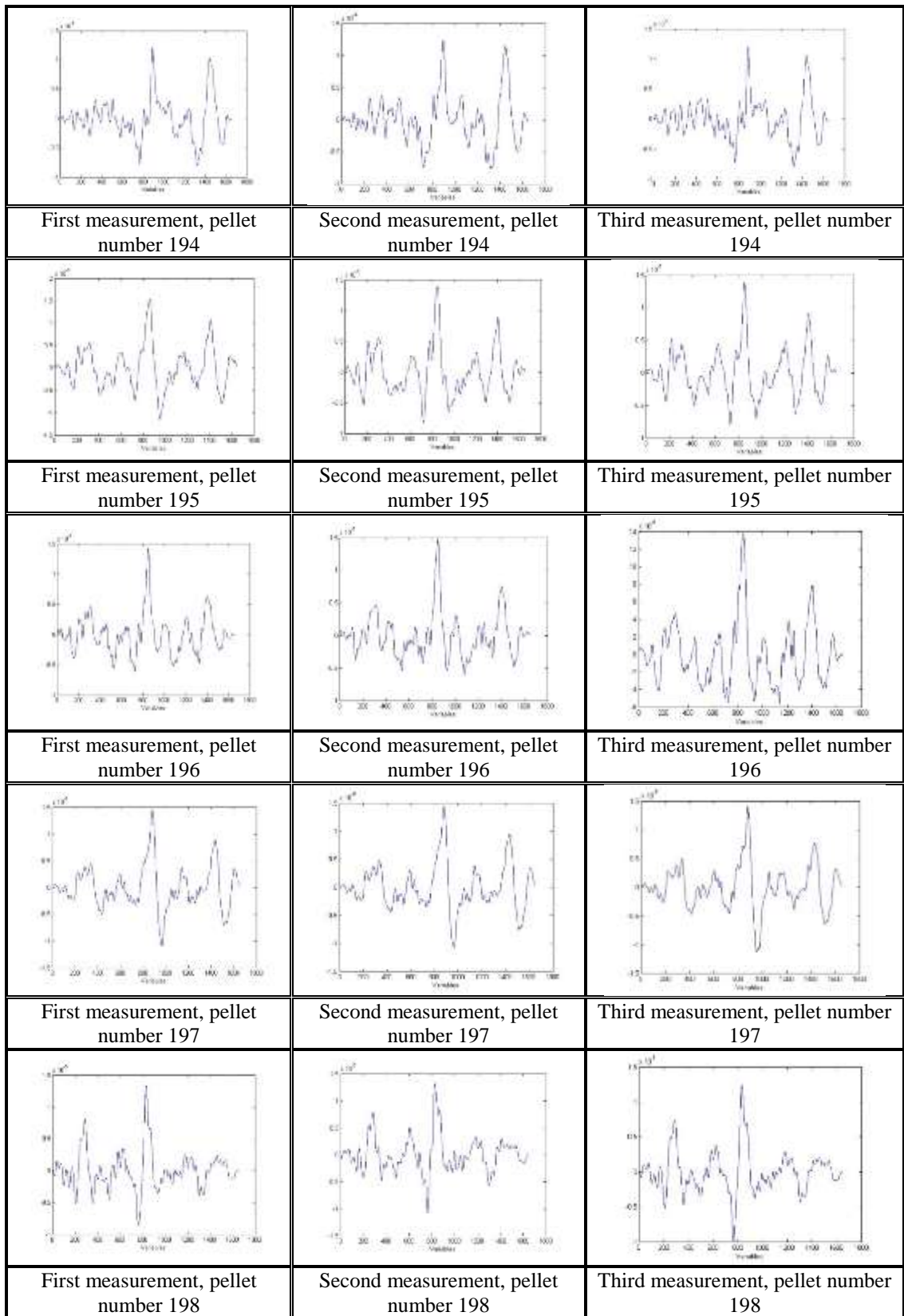


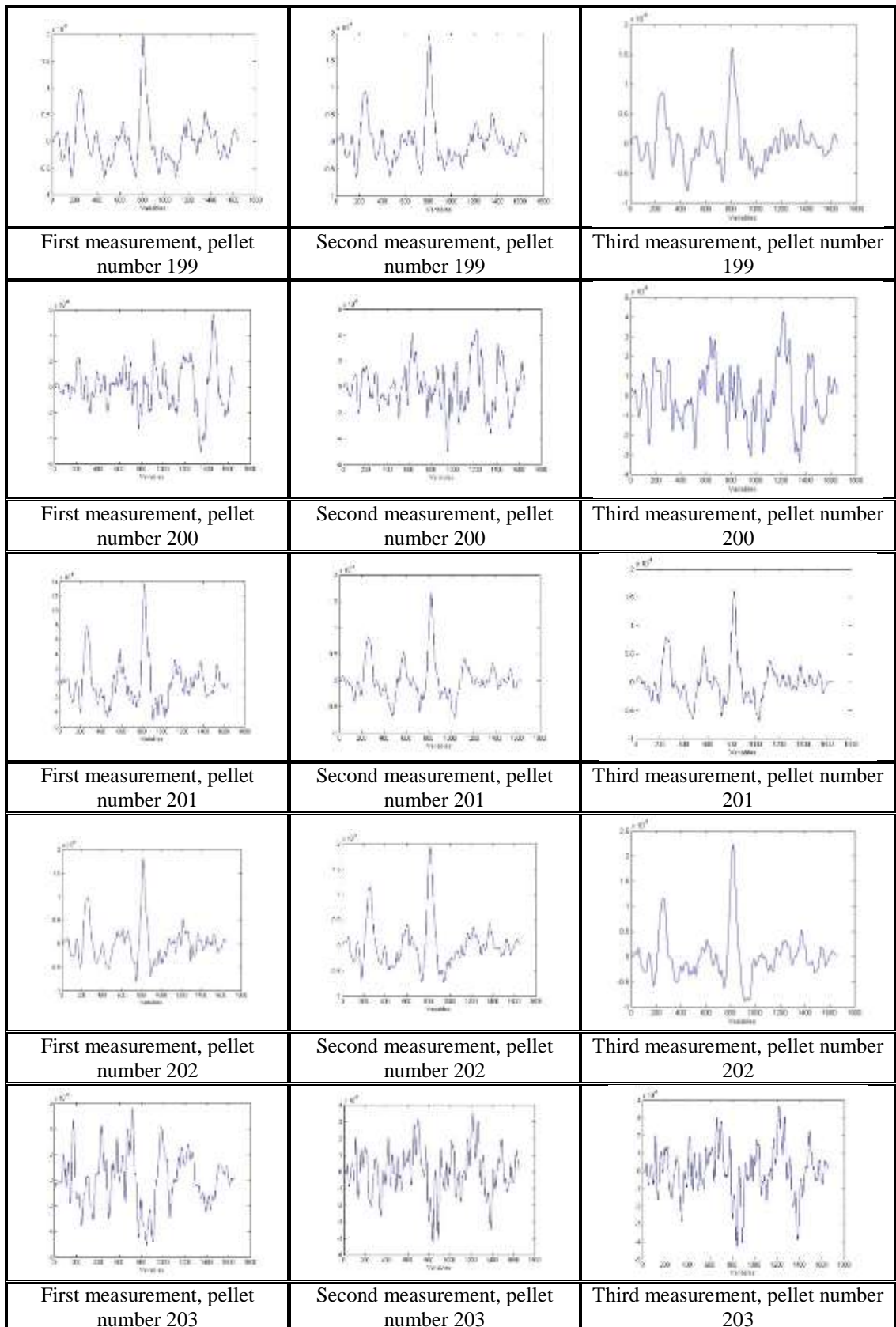


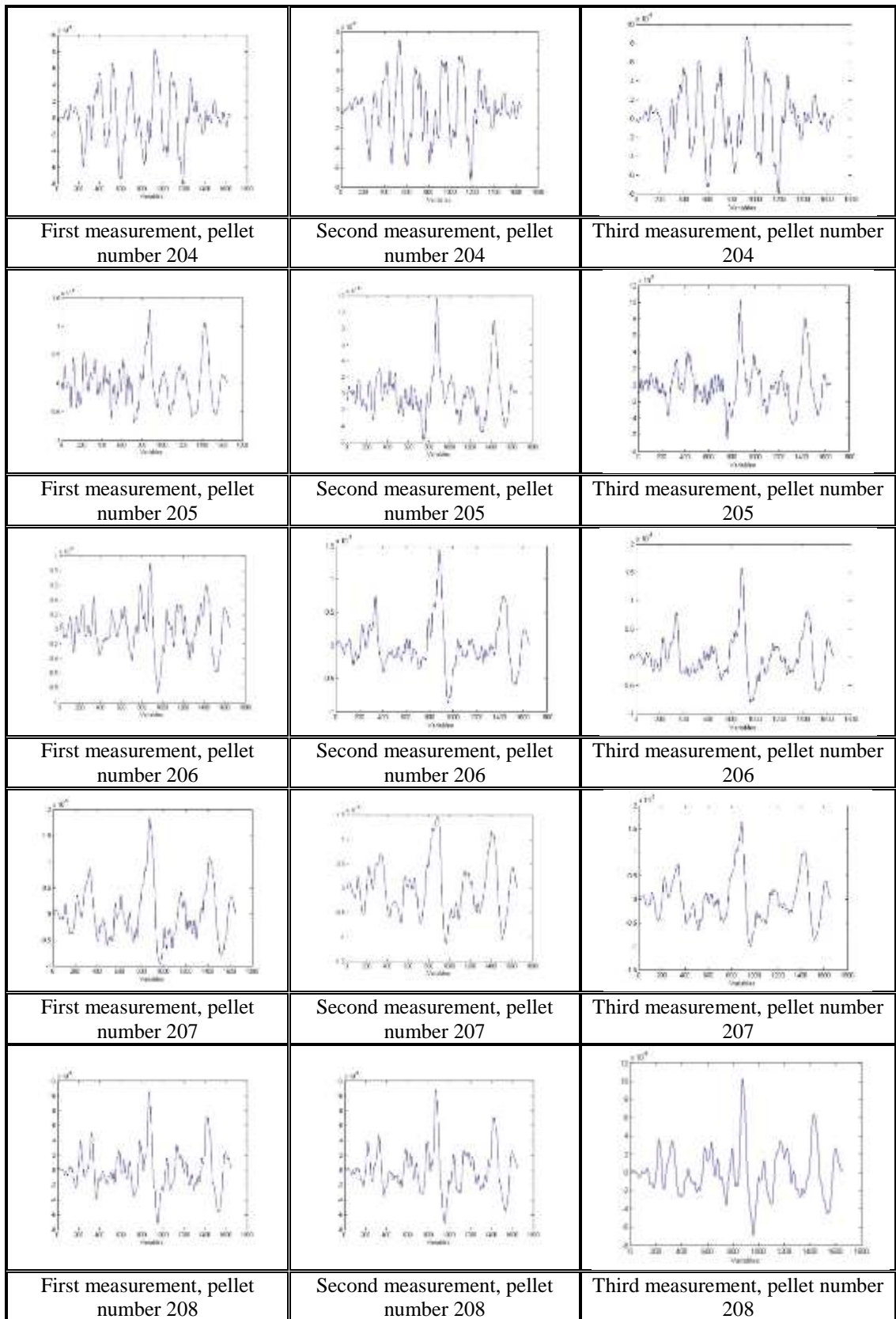




		
First measurement, pellet number 189	Second measurement, pellet number 189	Third measurement, pellet number 189
		
First measurement, pellet number 190	Second measurement, pellet number 190	Third measurement, pellet number 190
		
First measurement, pellet number 191	Second measurement, pellet number 191	Third measurement, pellet number 191
		
First measurement, pellet number 192	Second measurement, pellet number 192	Third measurement, pellet number 192
		
First measurement, pellet number 193	Second measurement, pellet number 193	Third measurement, pellet number 193

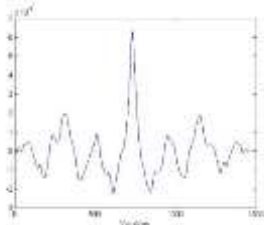
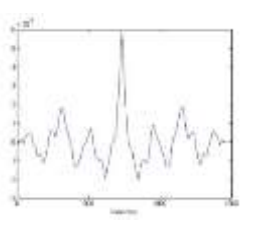
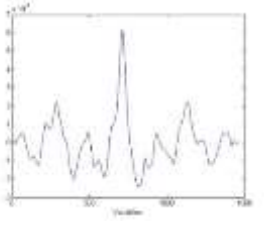
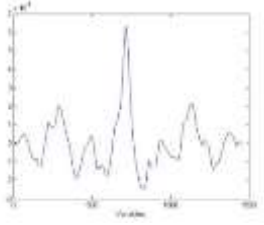
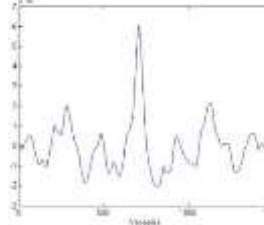
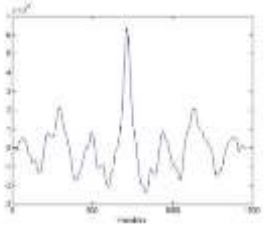
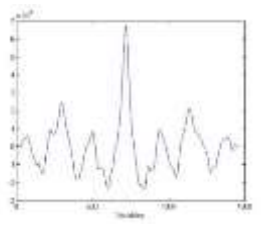
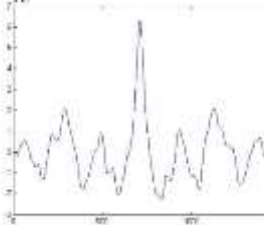
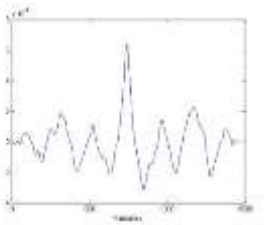
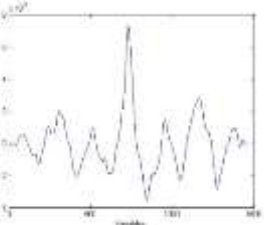
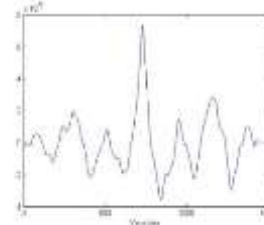
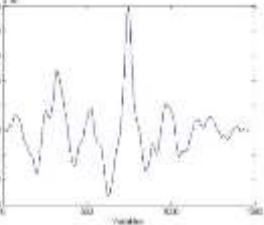
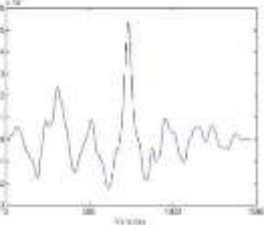
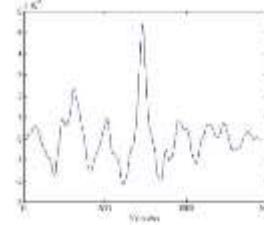


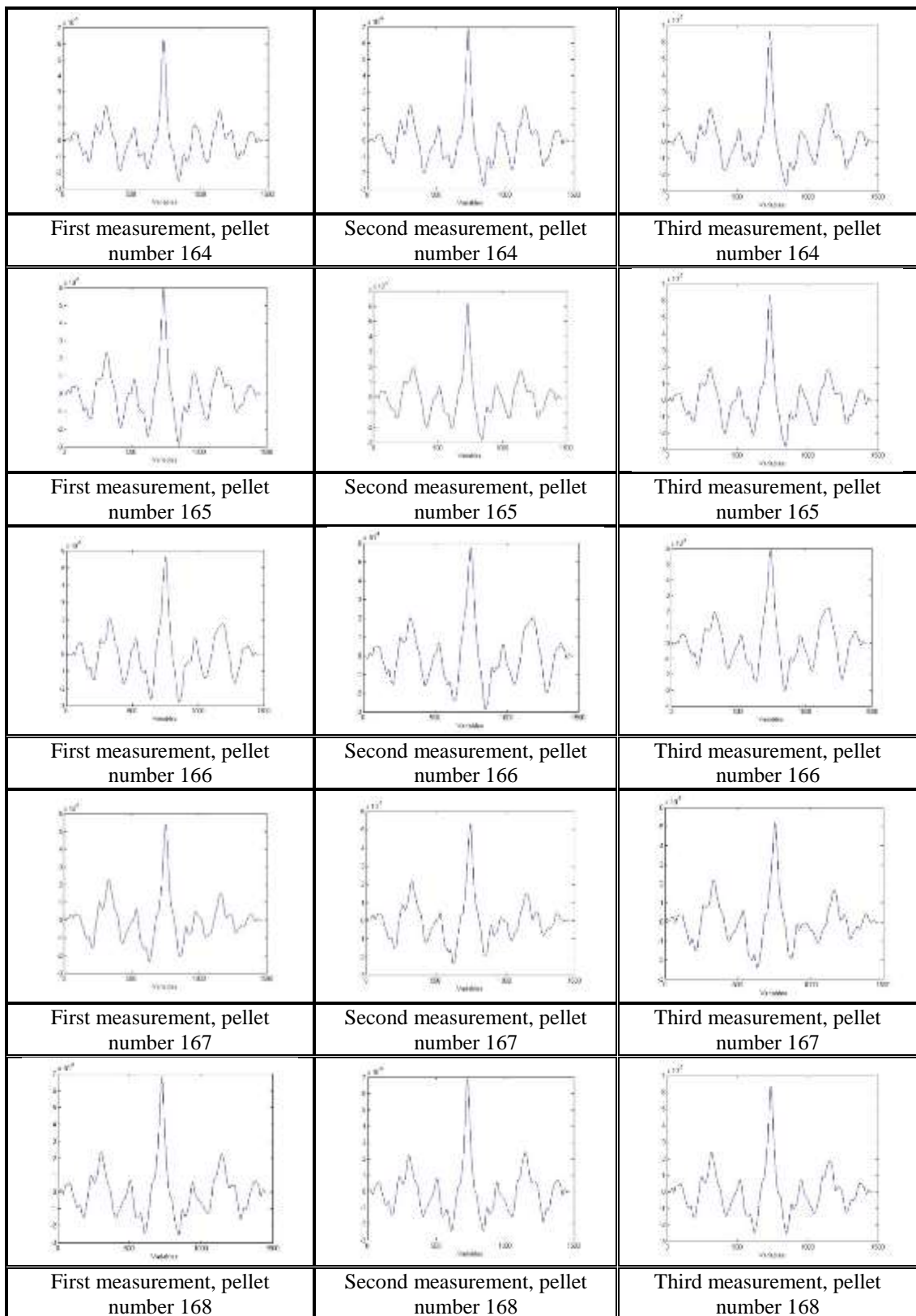


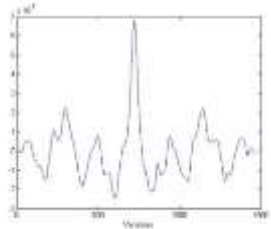
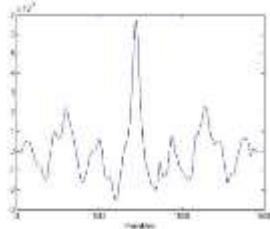
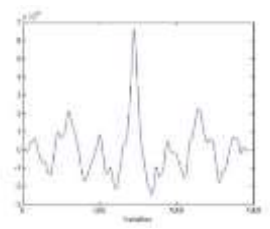
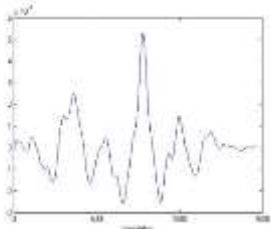
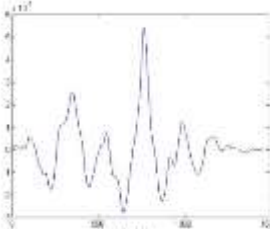
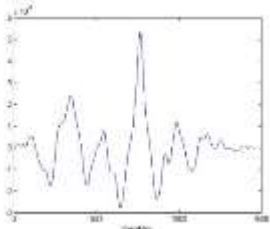
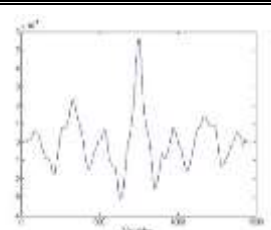
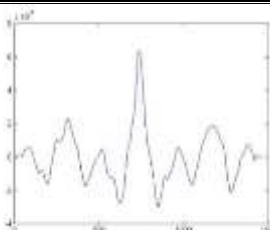
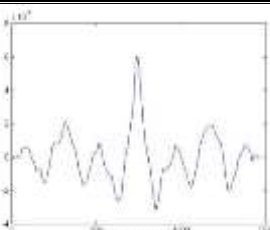
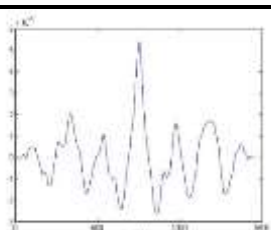
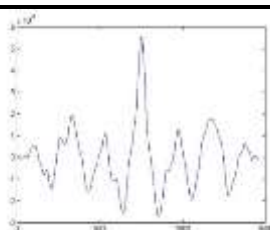
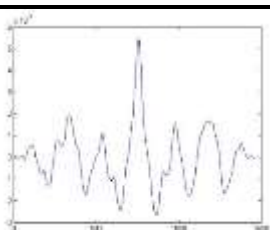
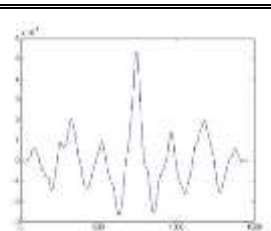
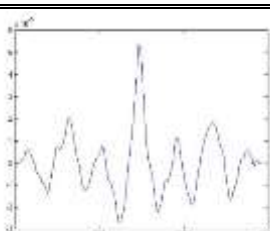
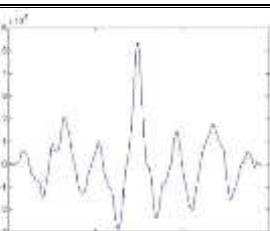


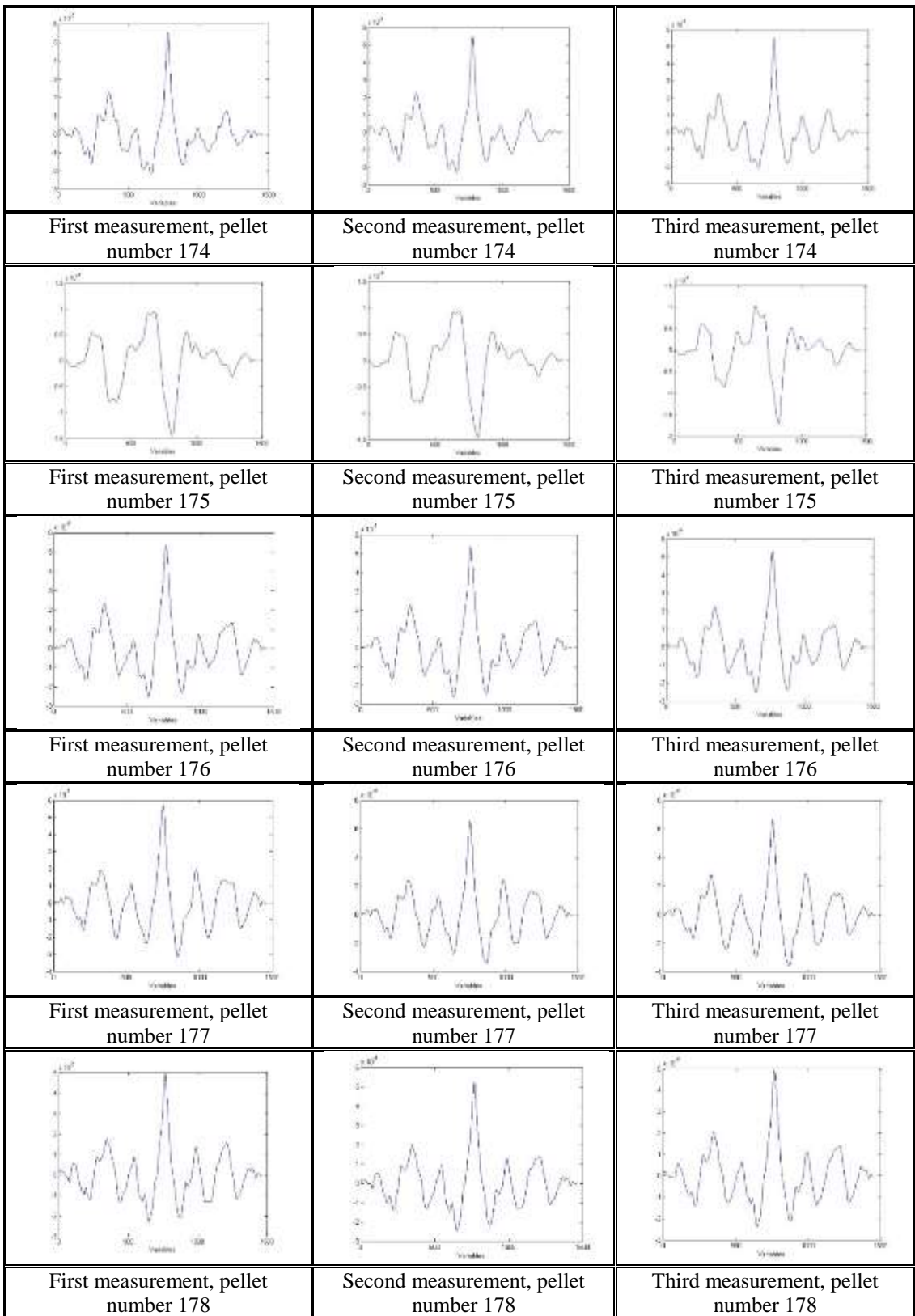
## Appendix 7

Alignment result for LEA D, pellet number 159 – 208

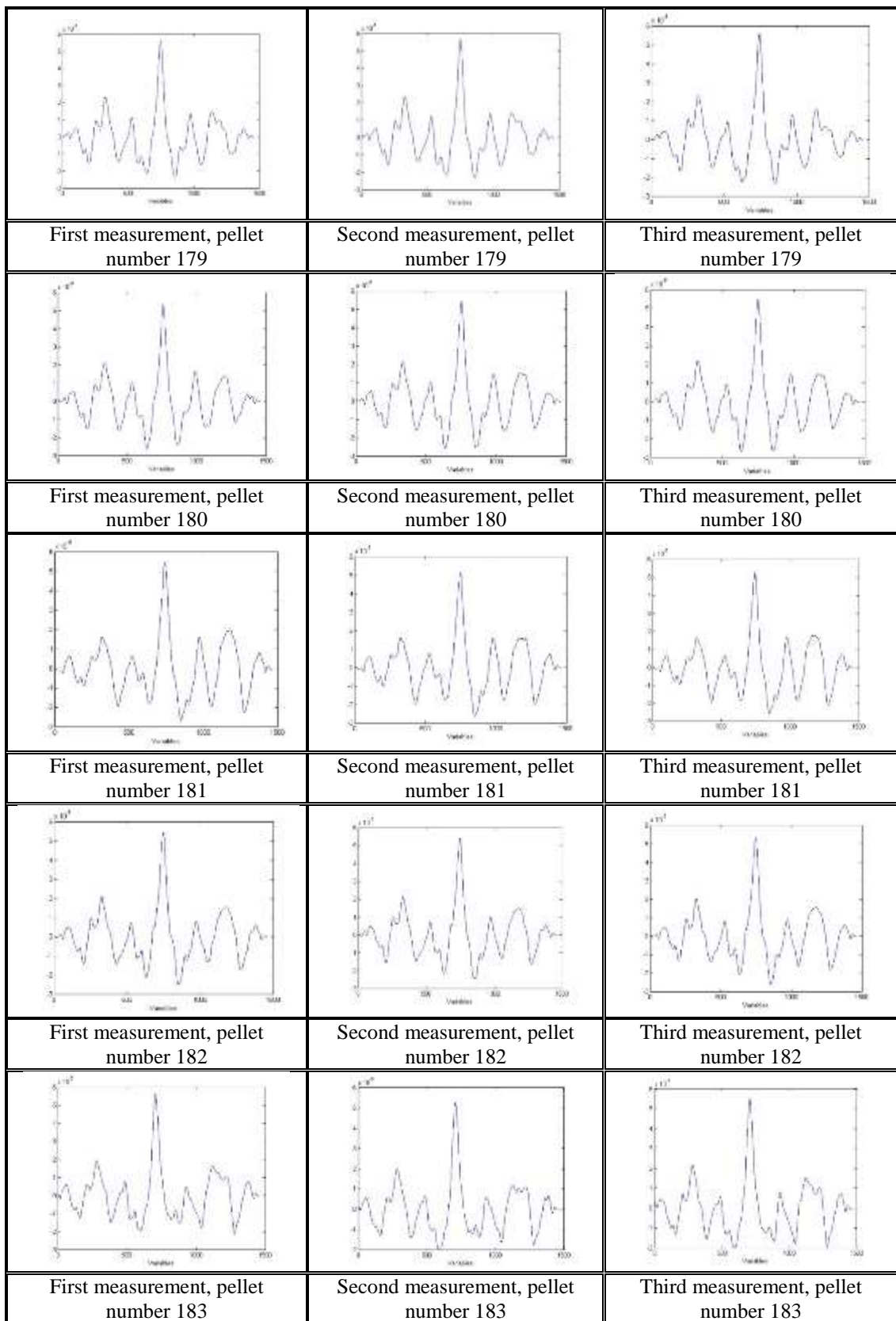
		
	Second measurement, pellet number 159	Third measurement, pellet number 159
		
First measurement, pellet number 160	Second measurement, pellet number 160	Third measurement, pellet number 160
		
First measurement, pellet number 161	Second measurement, pellet number 161	Third measurement, pellet number 161
		
First measurement, pellet number 162	Second measurement, pellet number 162	Third measurement, pellet number 162
		
First measurement, pellet number 163	Second measurement, pellet number 163	Third measurement, pellet number 163

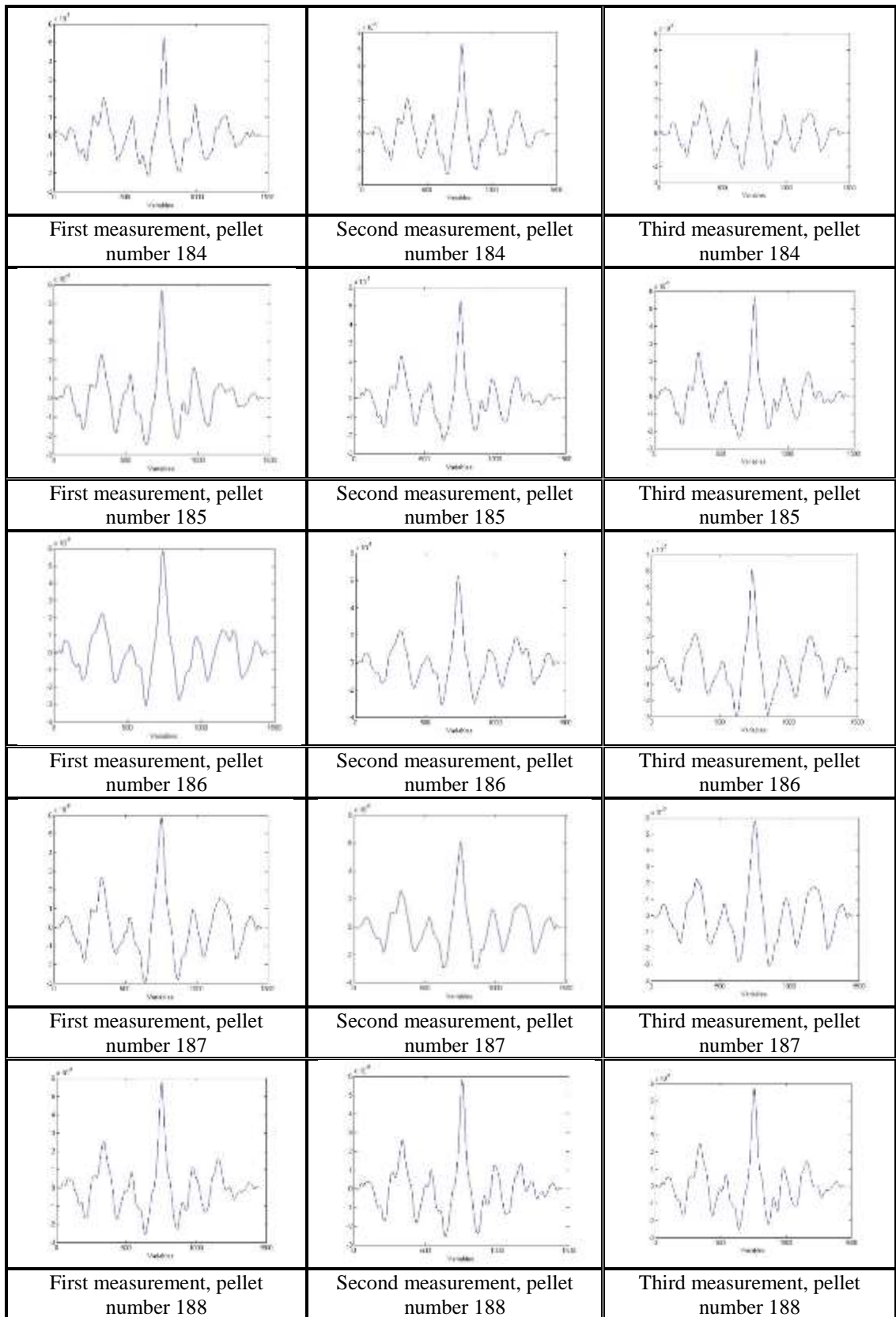


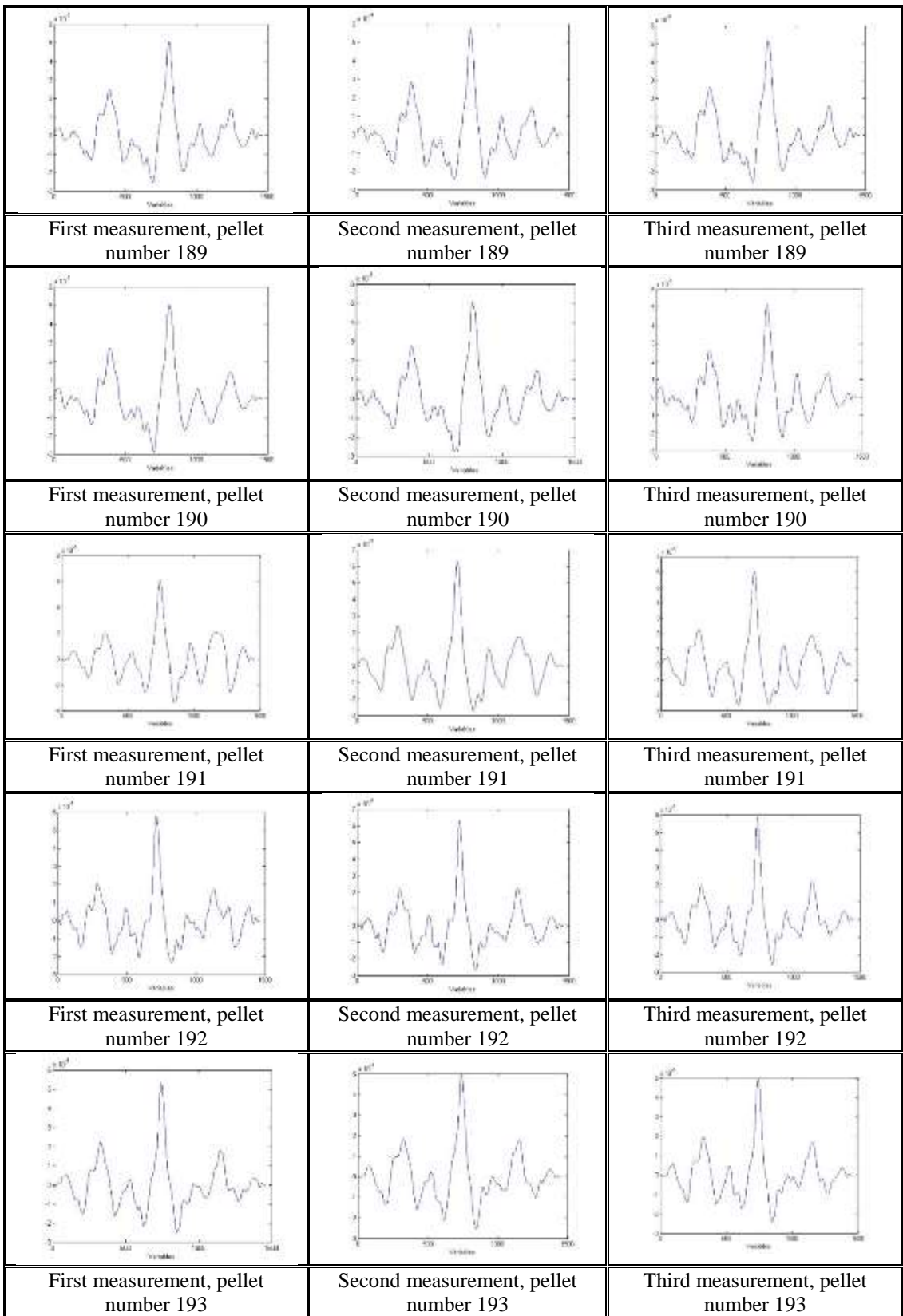
		
First measurement, pellet number 169	Second measurement, pellet number 169	Third measurement, pellet number 169
		
First measurement, pellet number 170	Second measurement, pellet number 170	Third measurement, pellet number 170
		
First measurement, pellet number 171	Second measurement, pellet number 171	Third measurement, pellet number 171
		
First measurement, pellet number 172	Second measurement, pellet number 172	Third measurement, pellet number 172
		
First measurement, pellet number 173	Second measurement, pellet number 173	Third measurement, pellet number 173

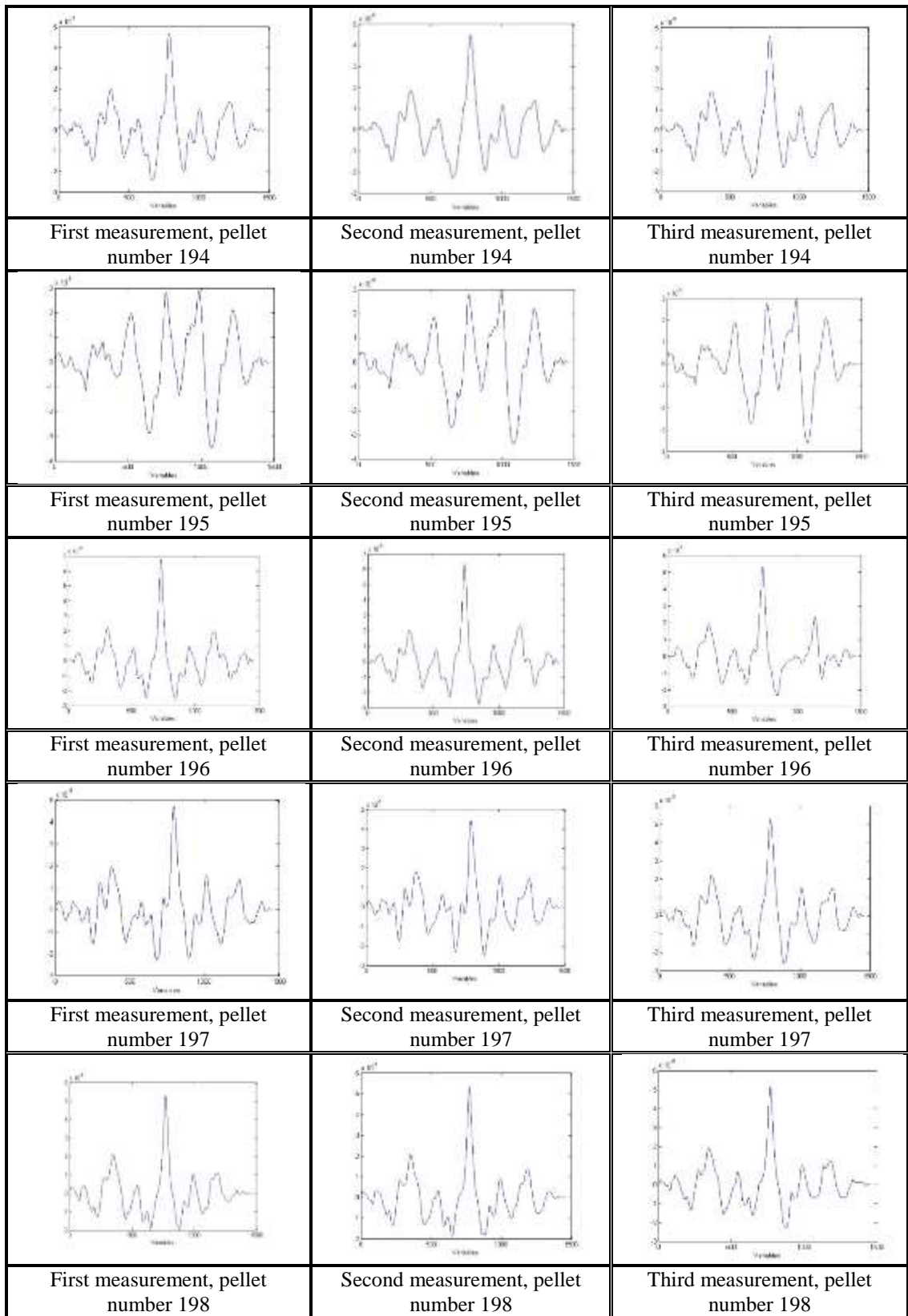


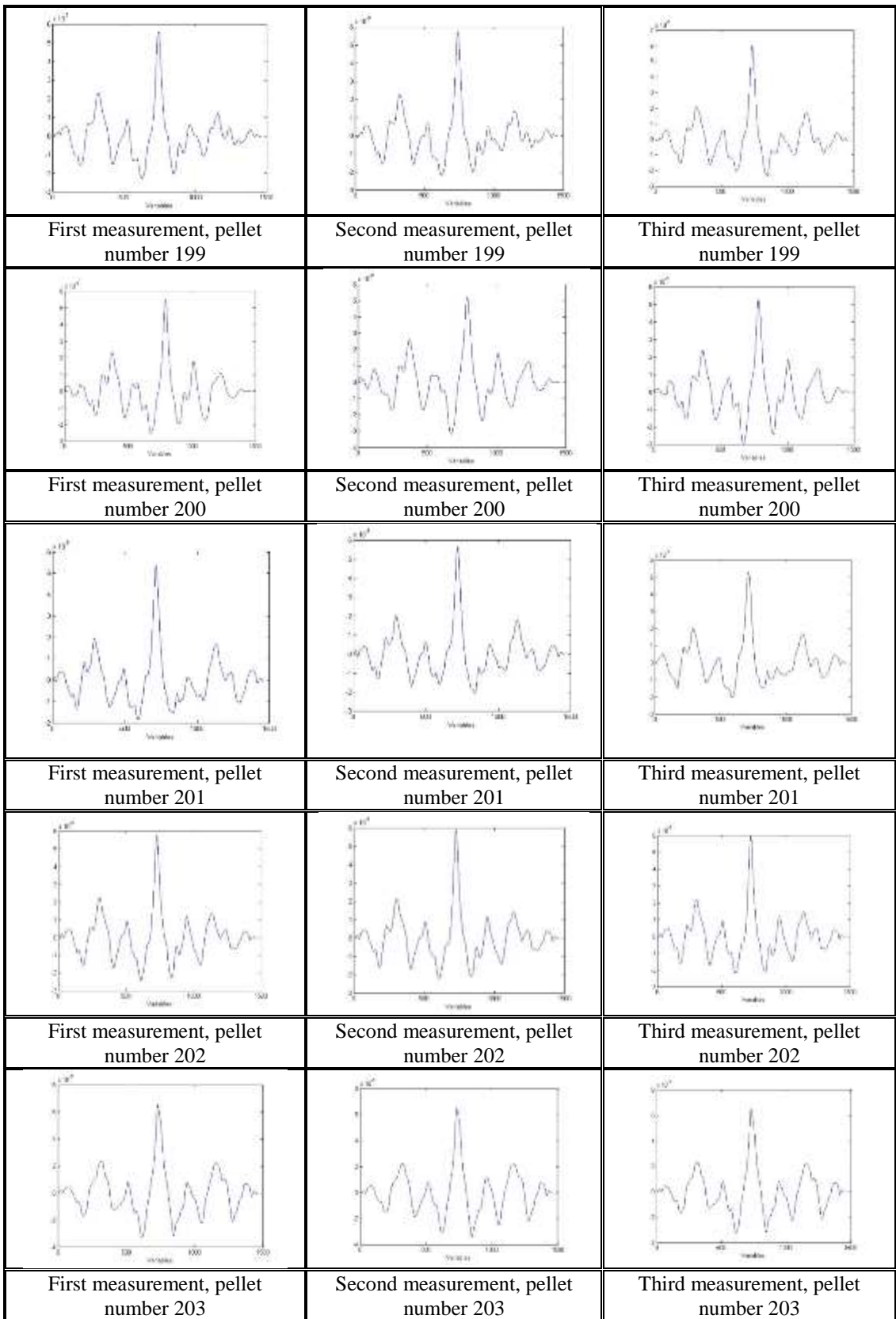


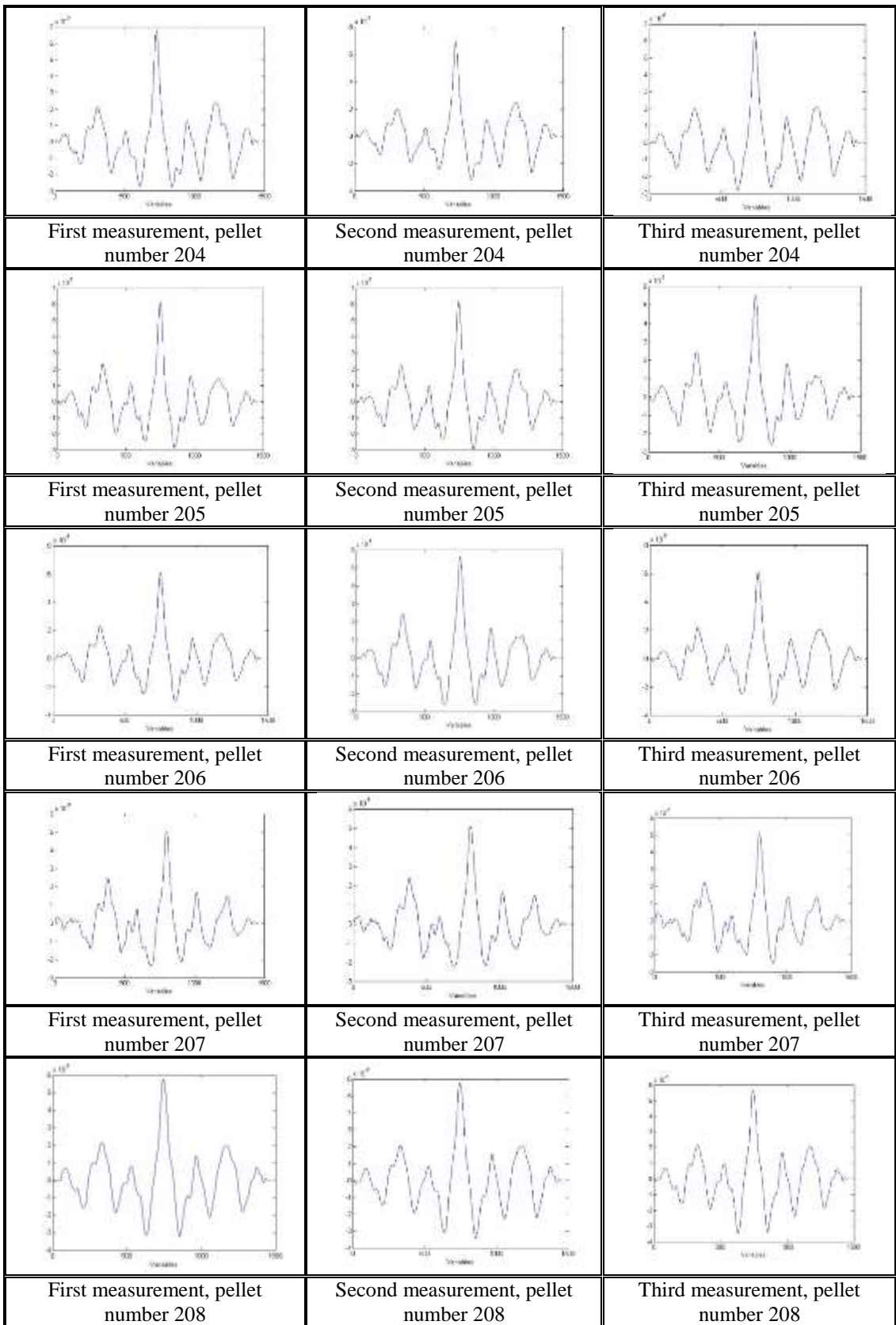






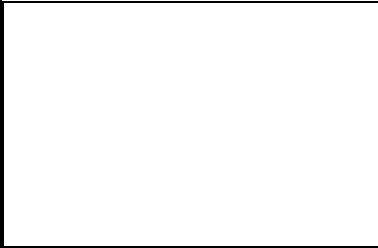
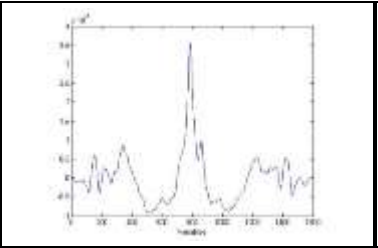
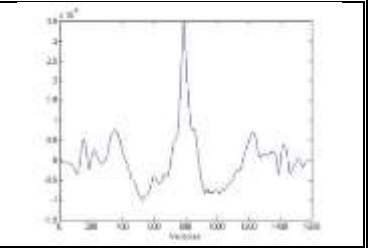
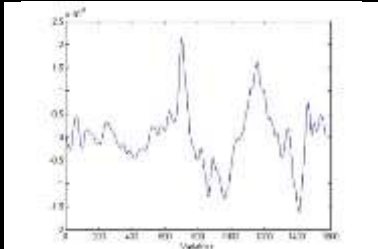
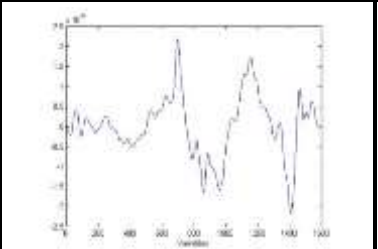
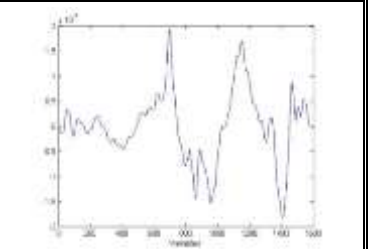
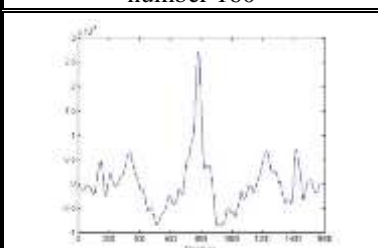
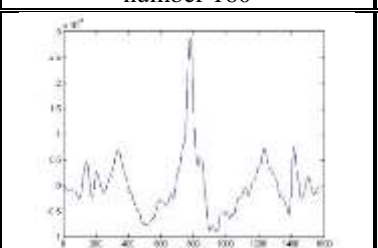
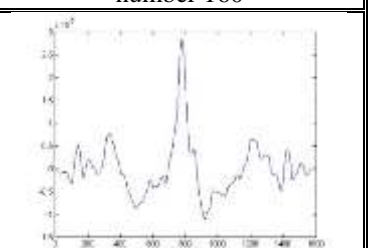
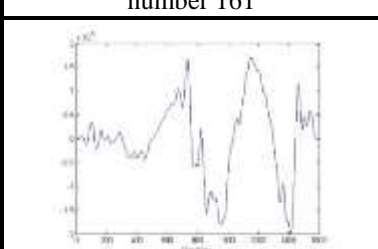
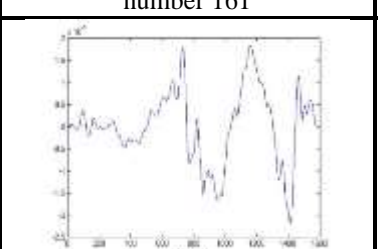
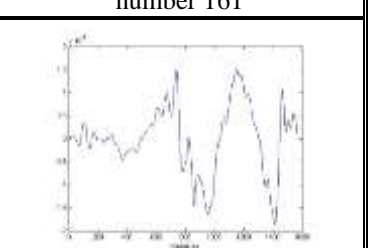
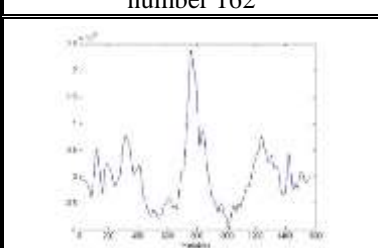
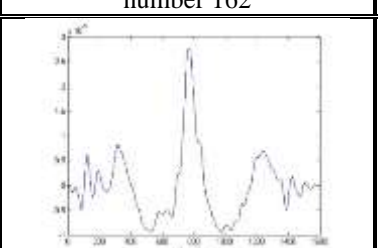
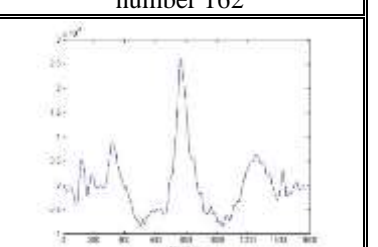


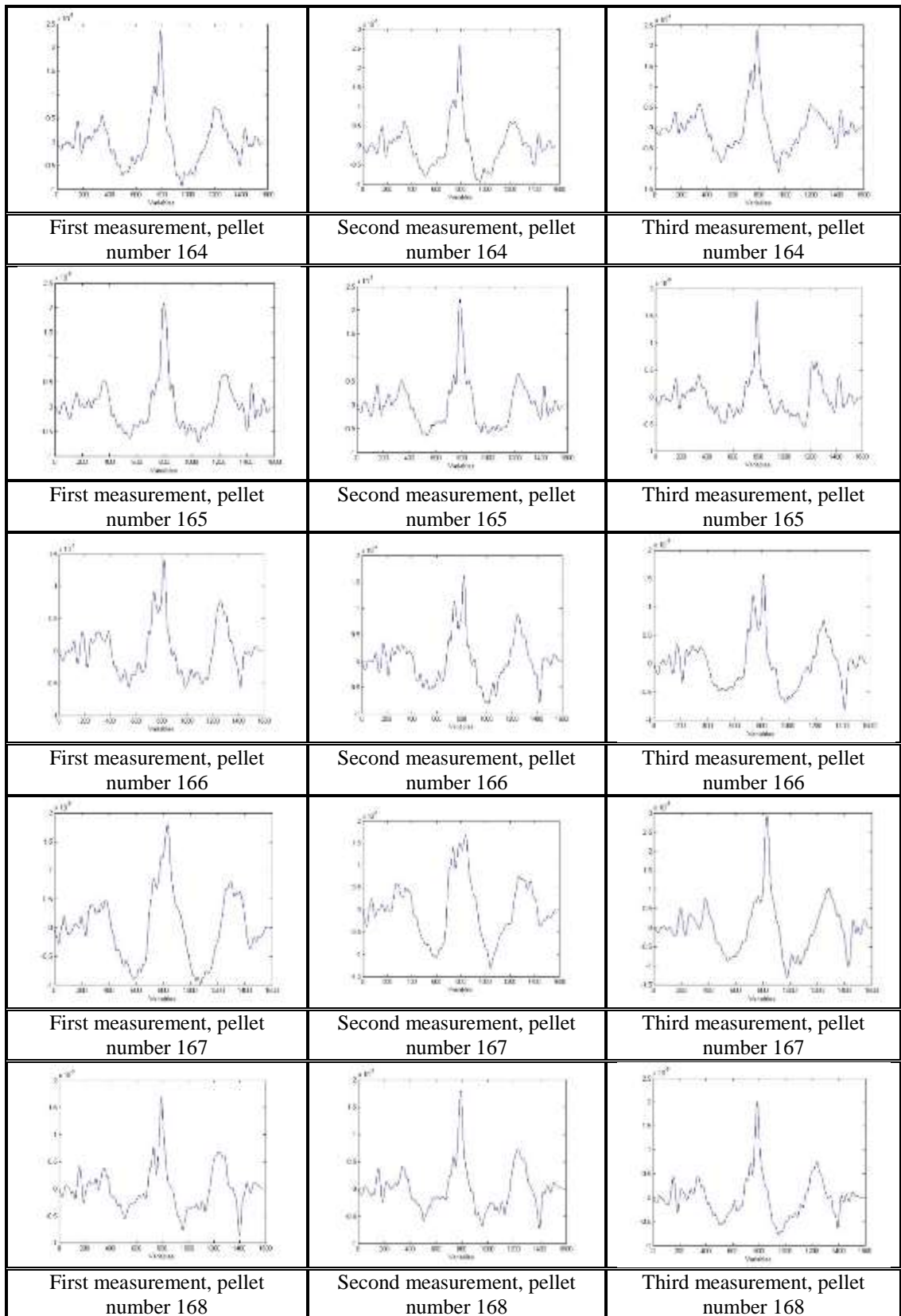




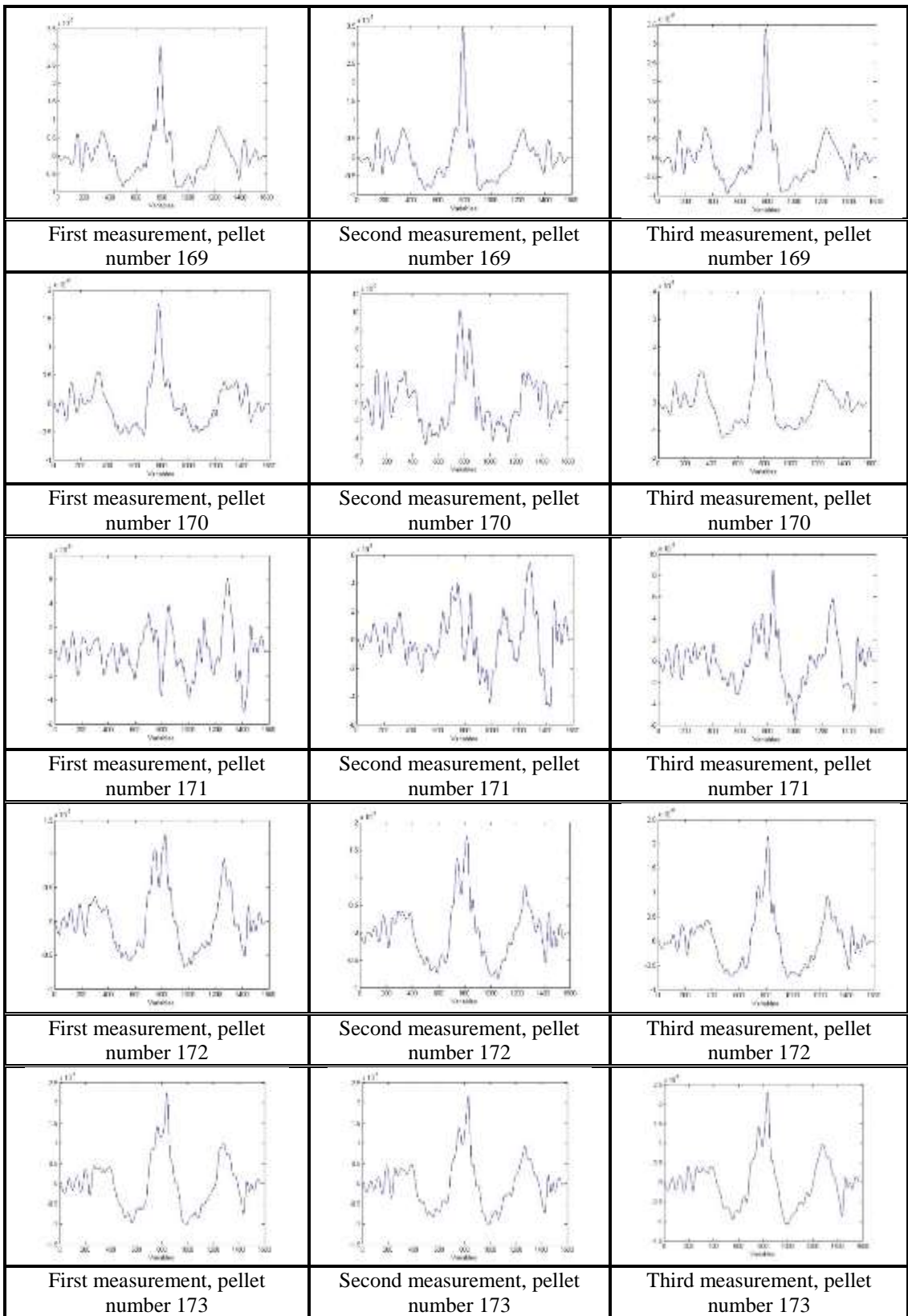
## Appendix 8

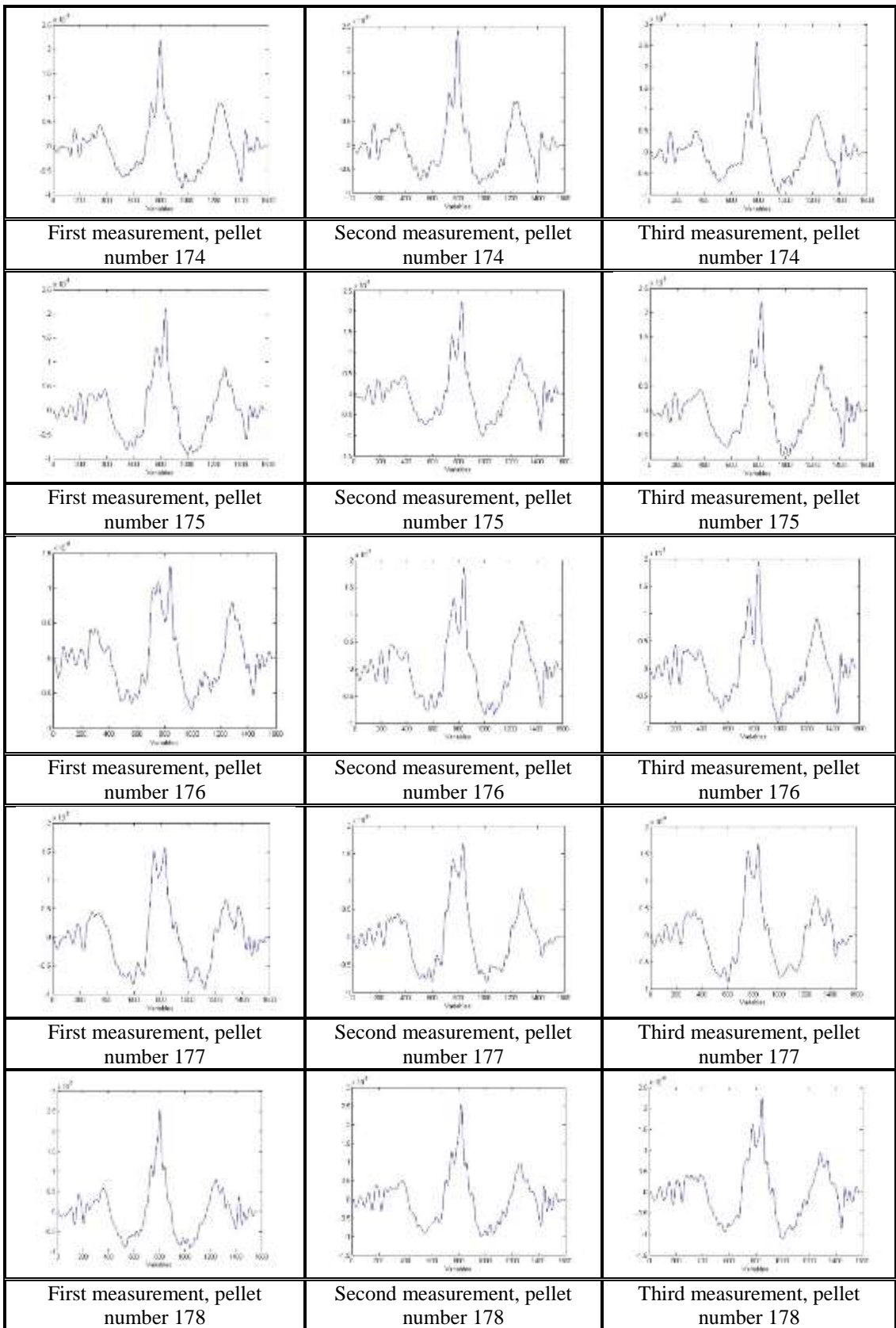
Alignment result for LEA E, pellet number 159 – 208

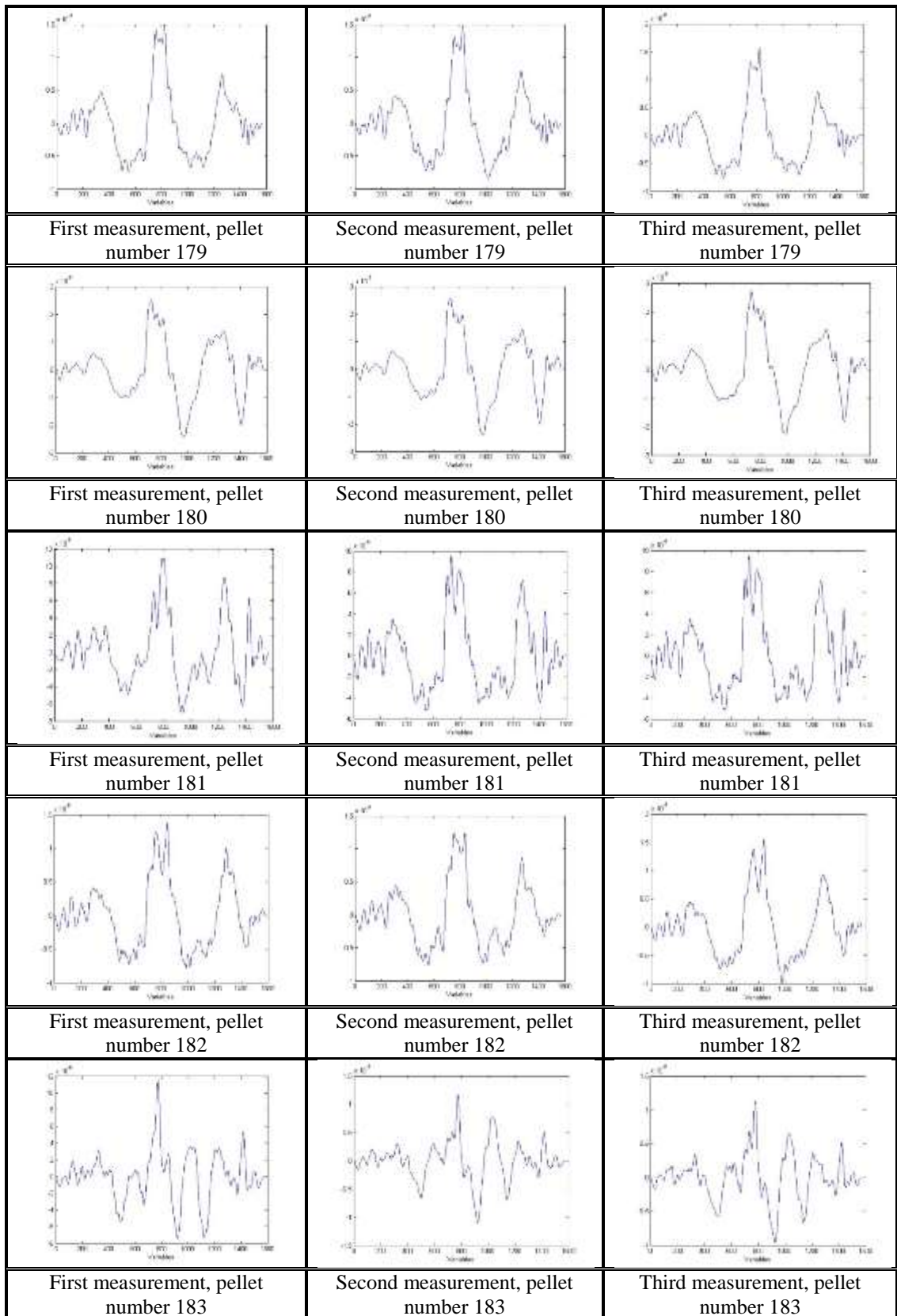
		
	Second measurement, pellet number 159	Third measurement, pellet number 159
		
First measurement, pellet number 160	Second measurement, pellet number 160	Third measurement, pellet number 160
		
First measurement, pellet number 161	Second measurement, pellet number 161	Third measurement, pellet number 161
		
First measurement, pellet number 162	Second measurement, pellet number 162	Third measurement, pellet number 162
		
First measurement, pellet number 163	Second measurement, pellet number 163	Third measurement, pellet number 163

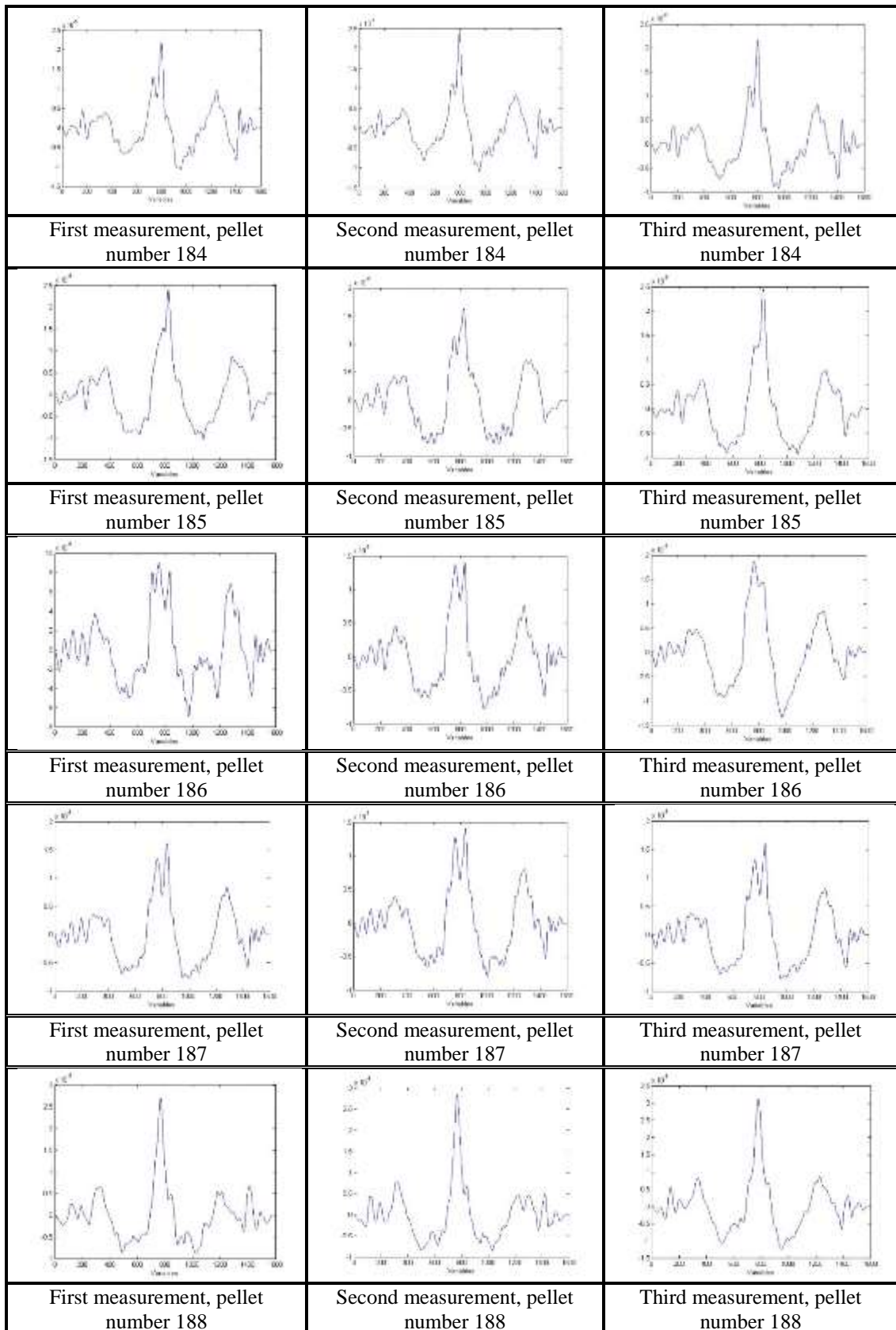


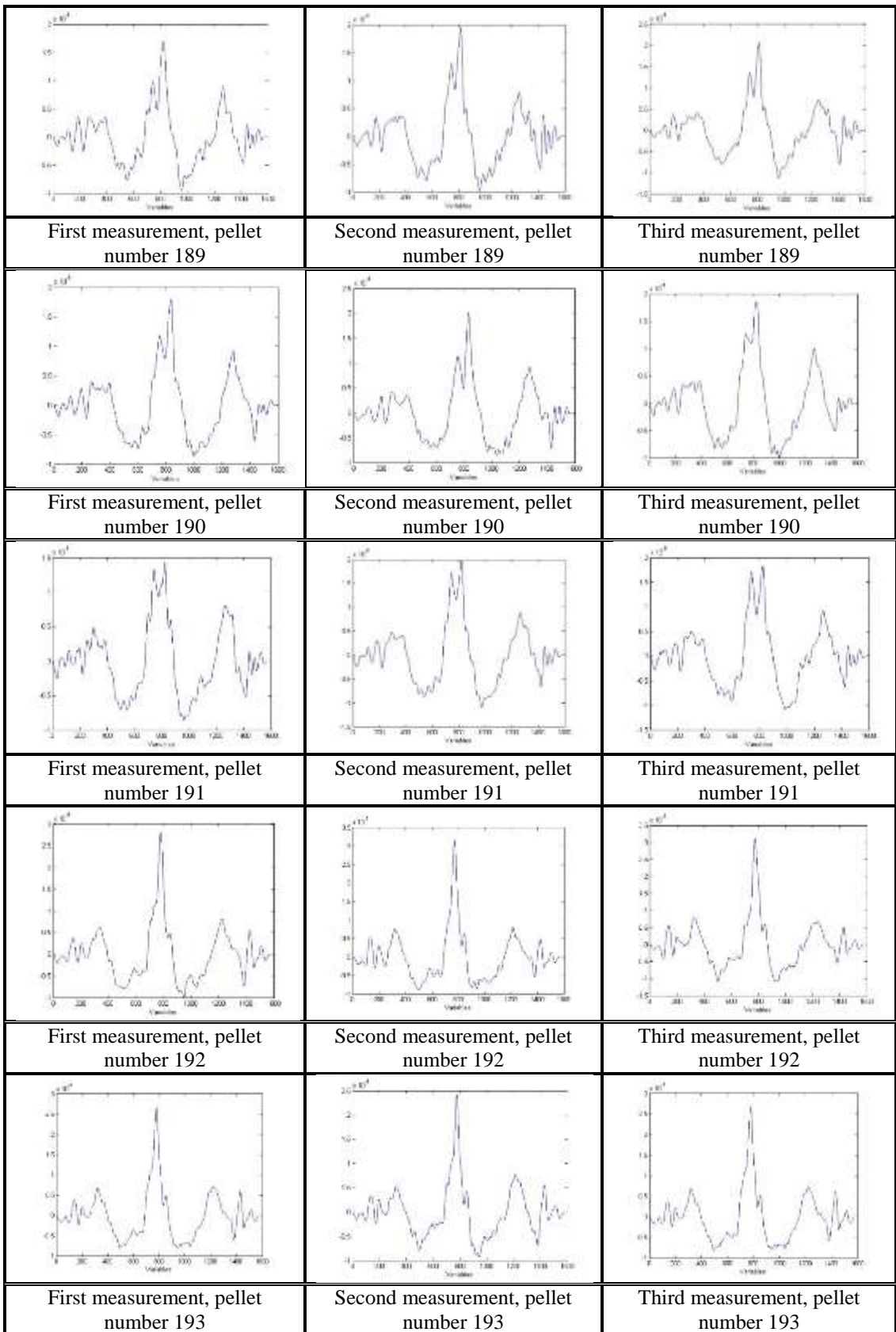


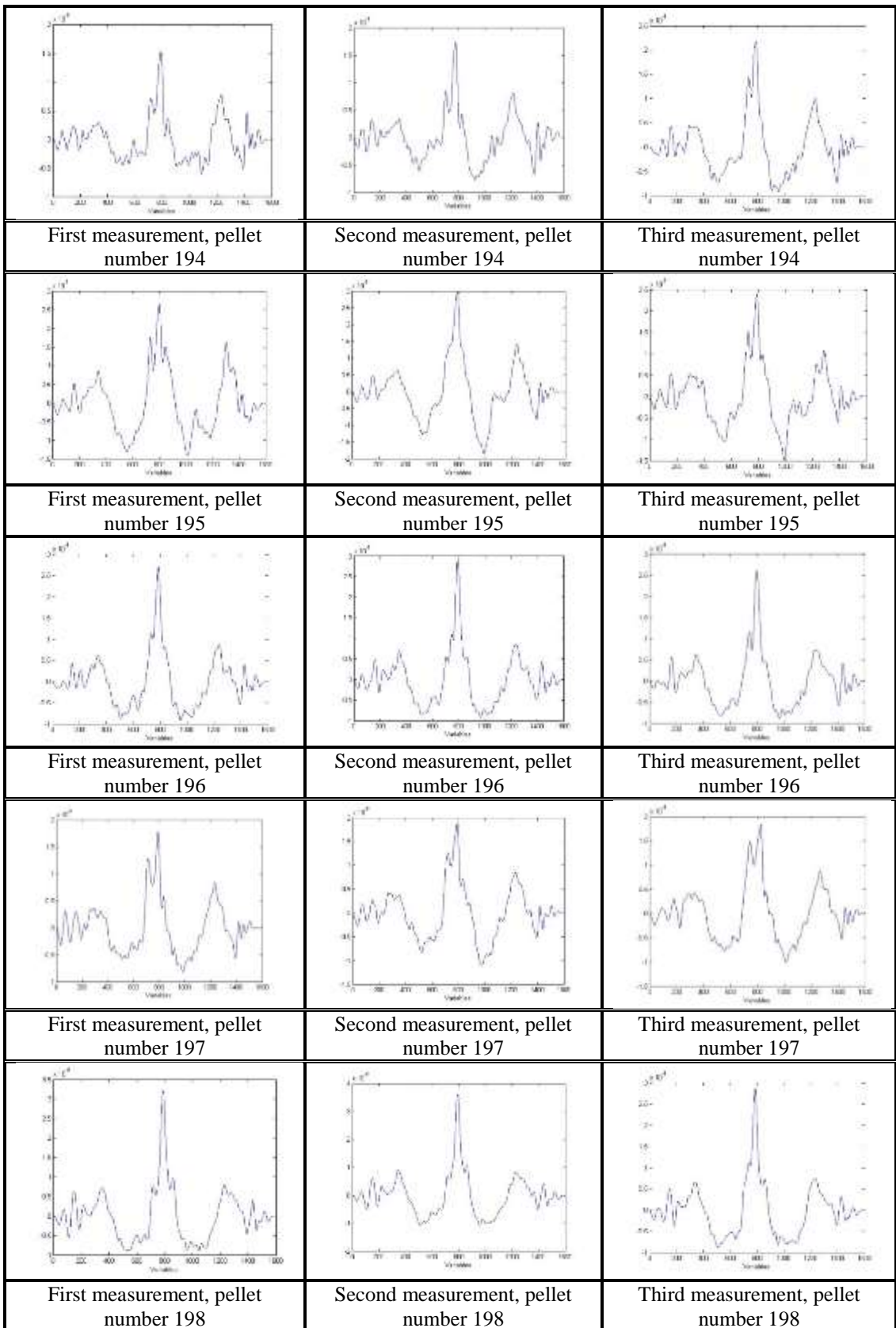


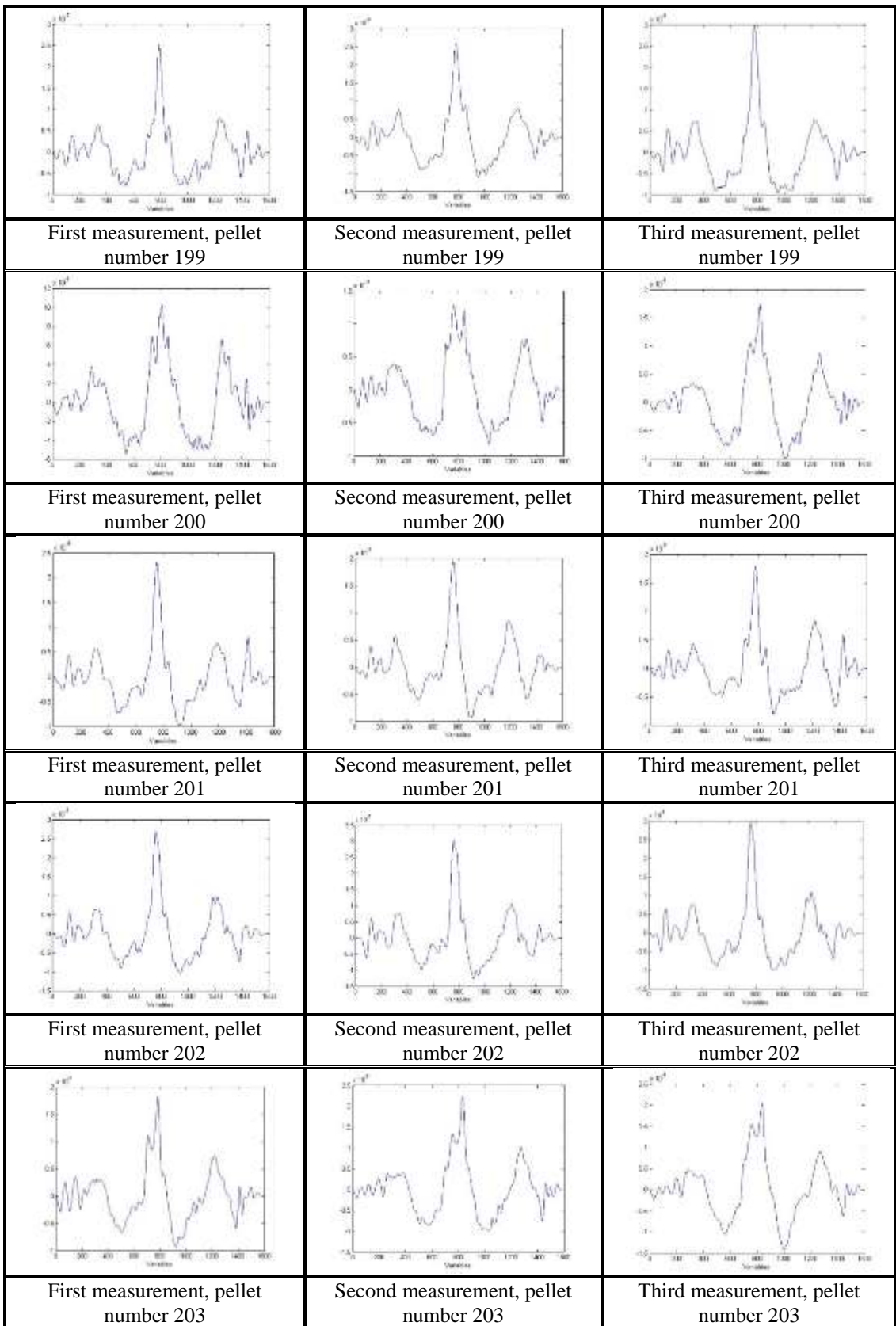


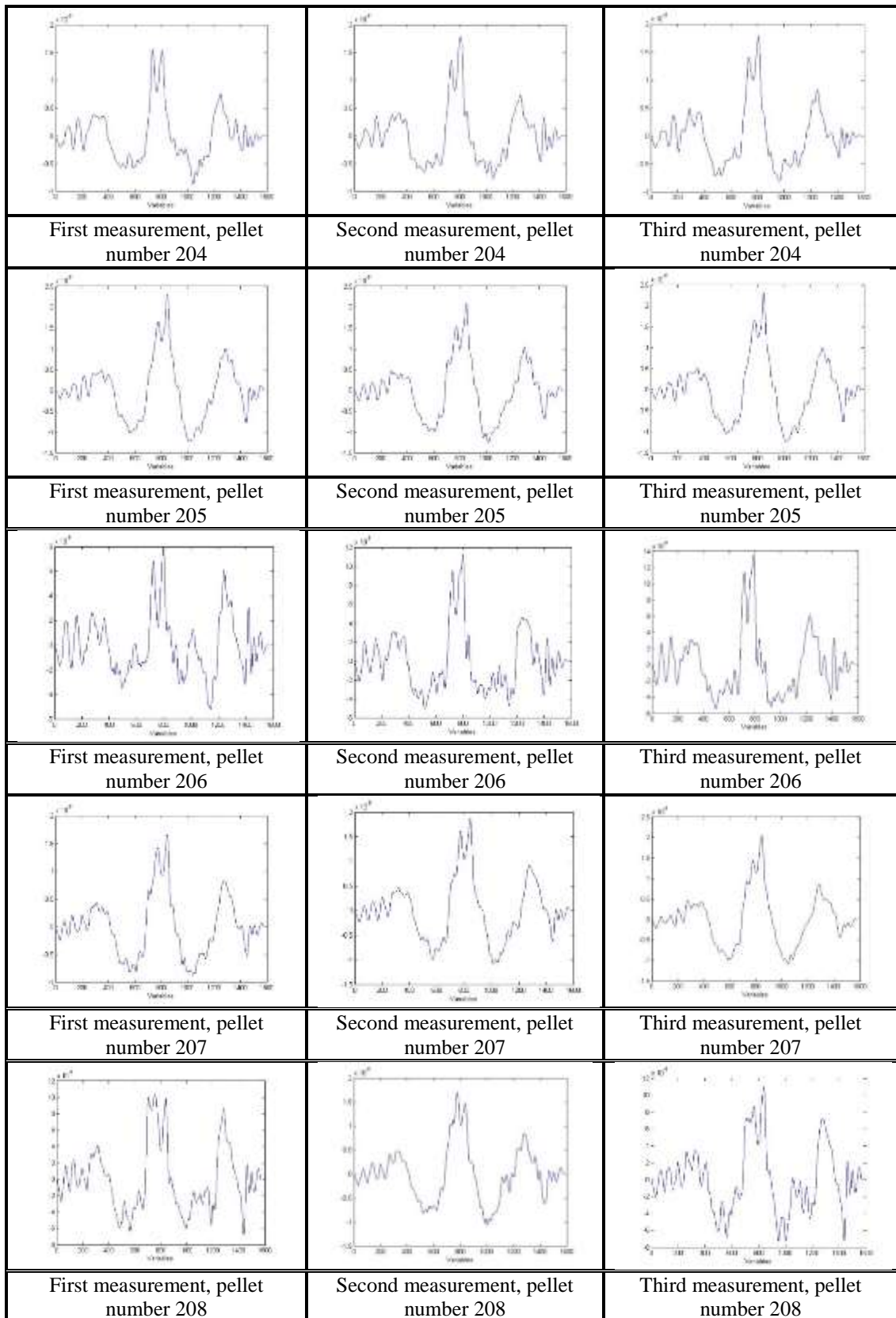








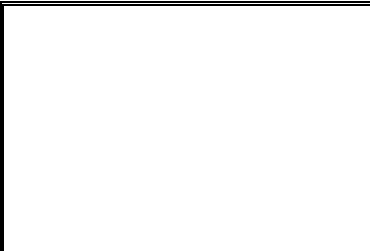
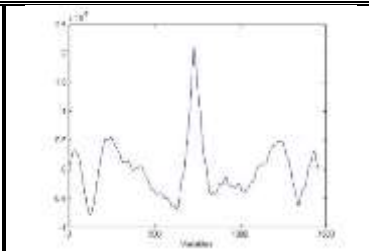
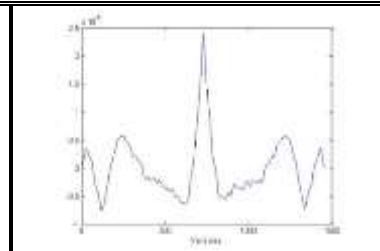
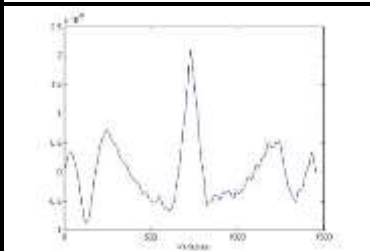
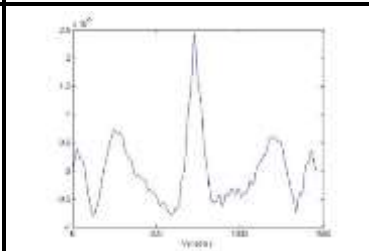
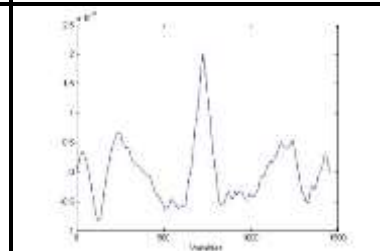
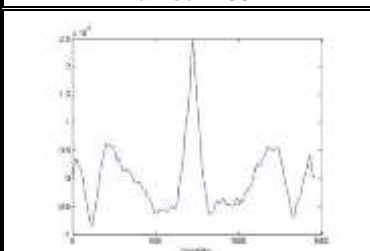
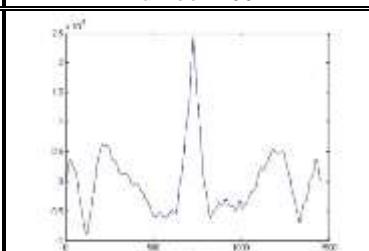
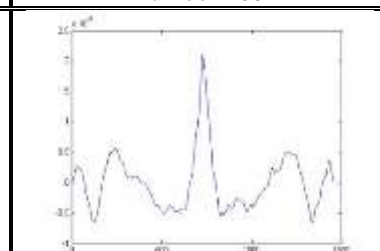
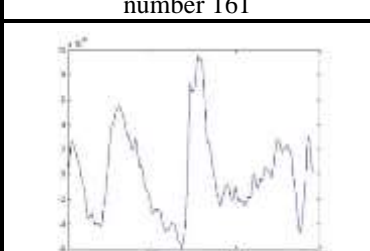
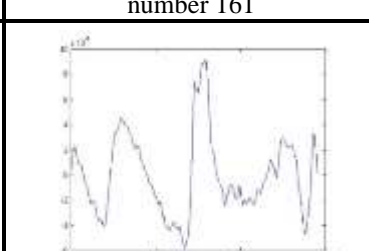
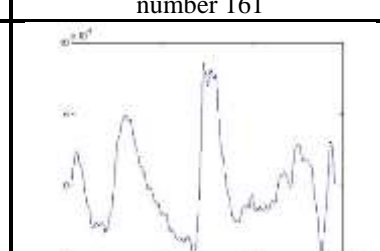
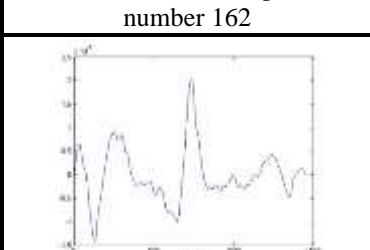
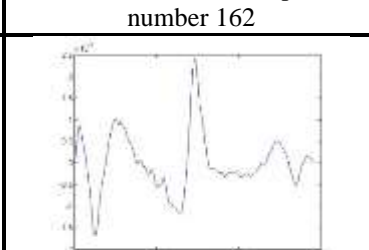
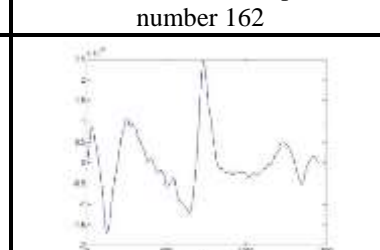


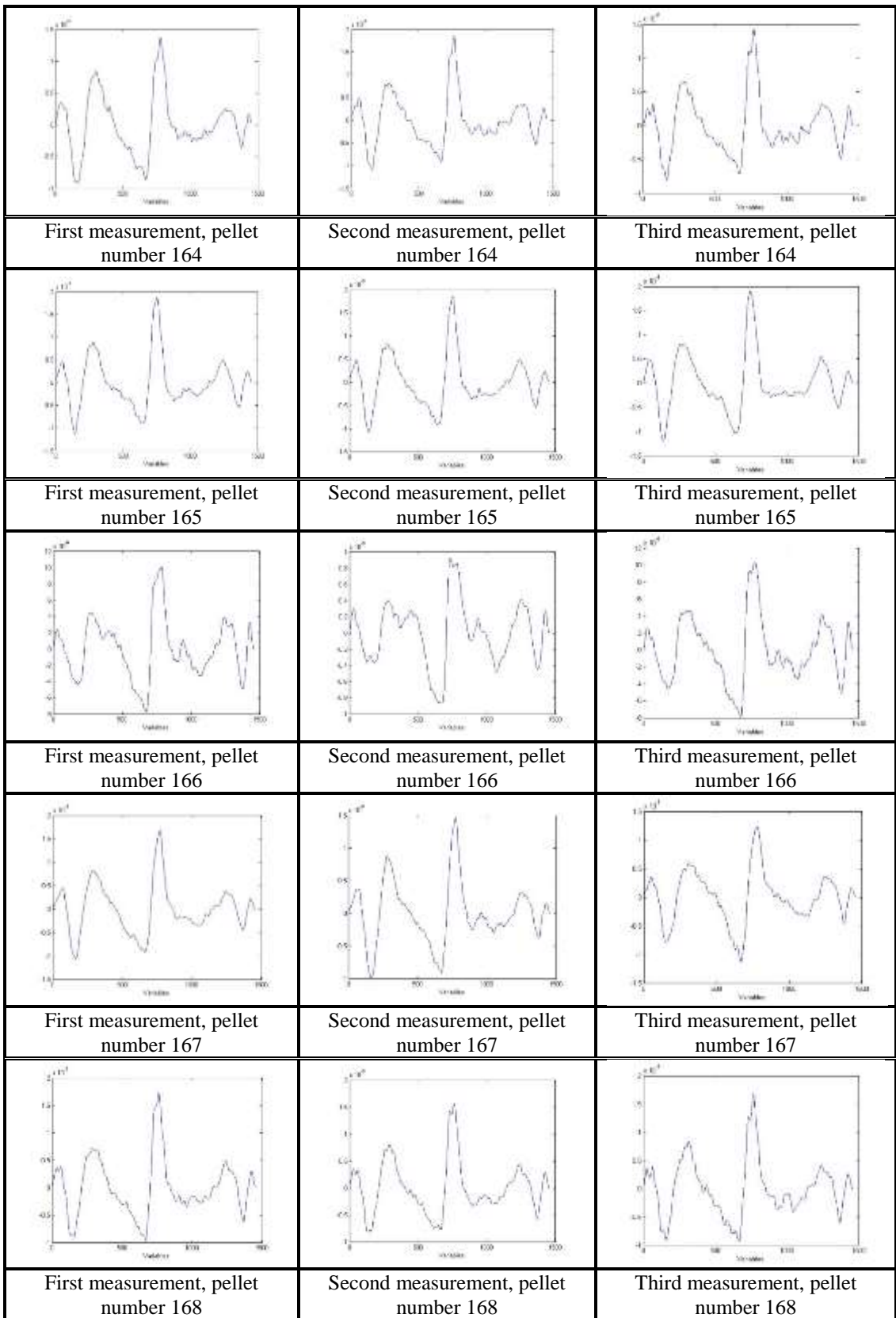


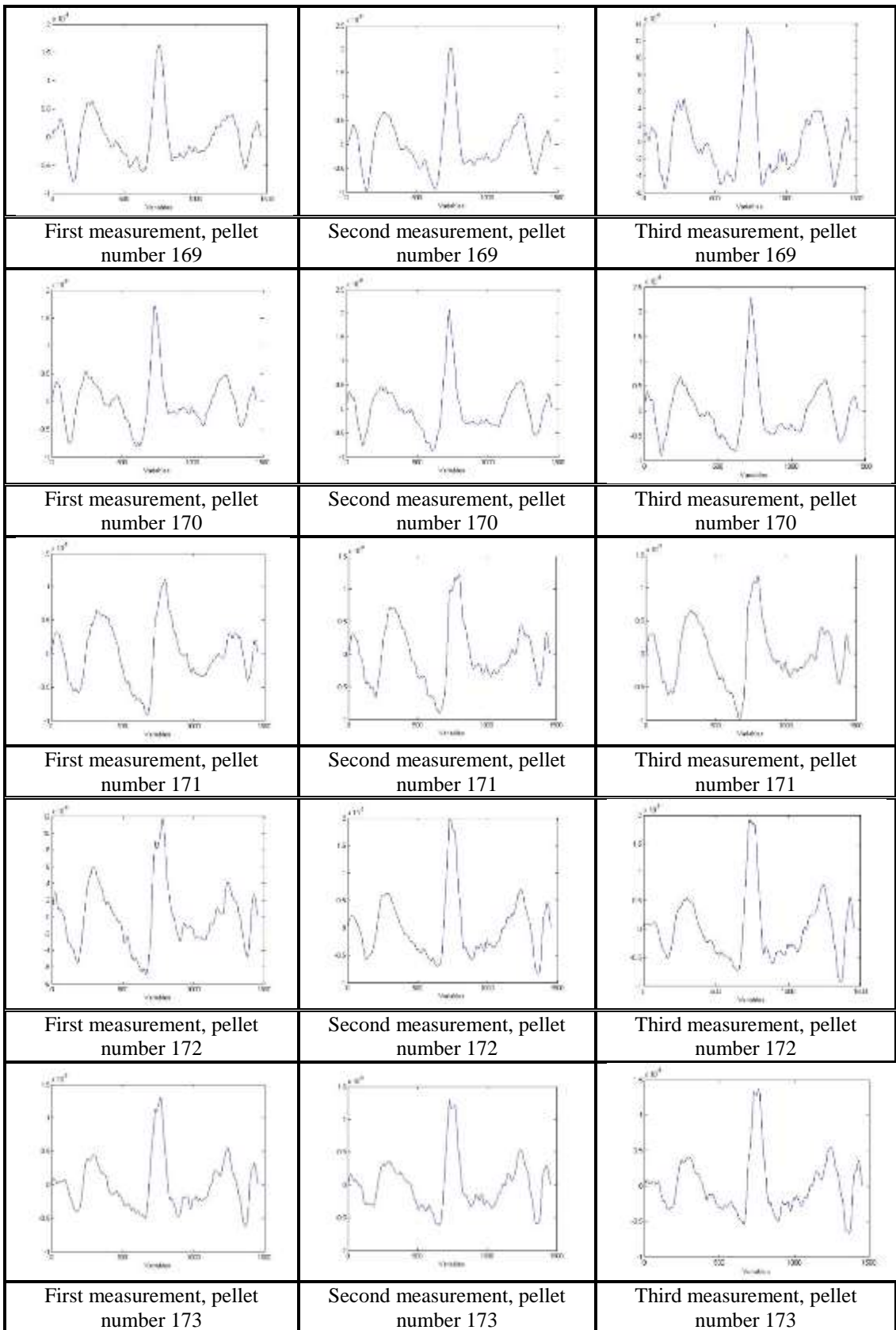


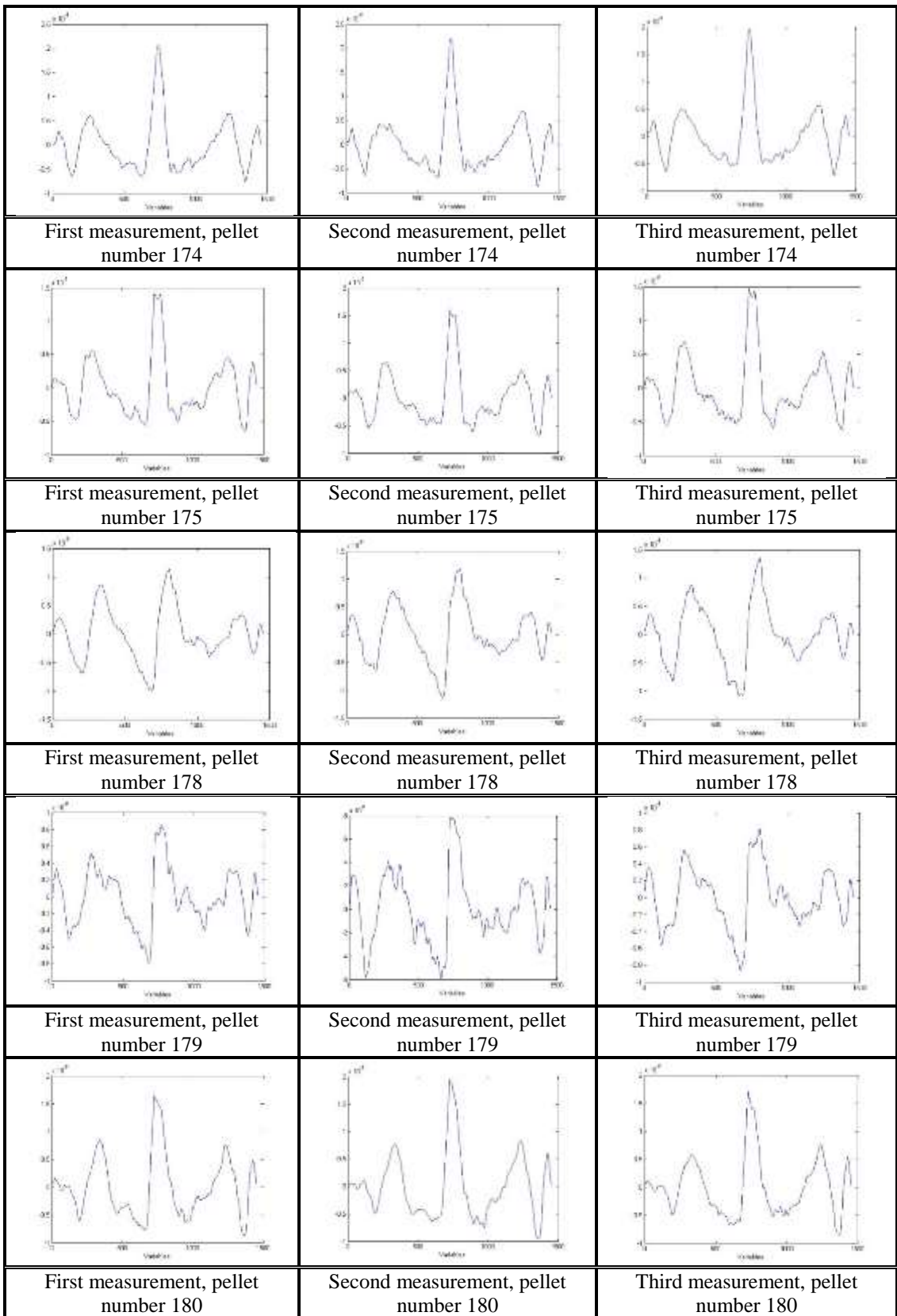
## Appendix 9

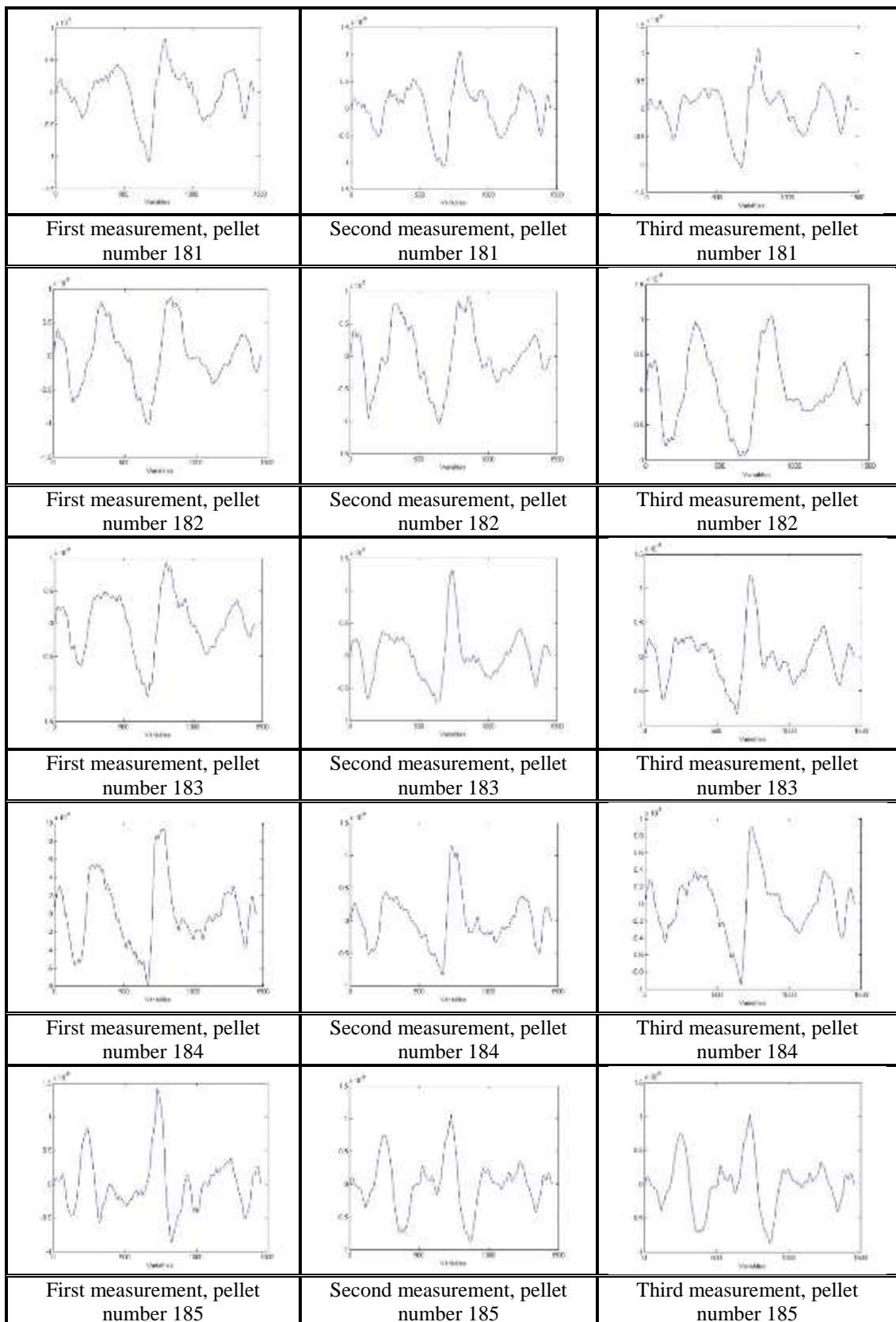
Alignment result for LEA F, pellet number 159 – 208

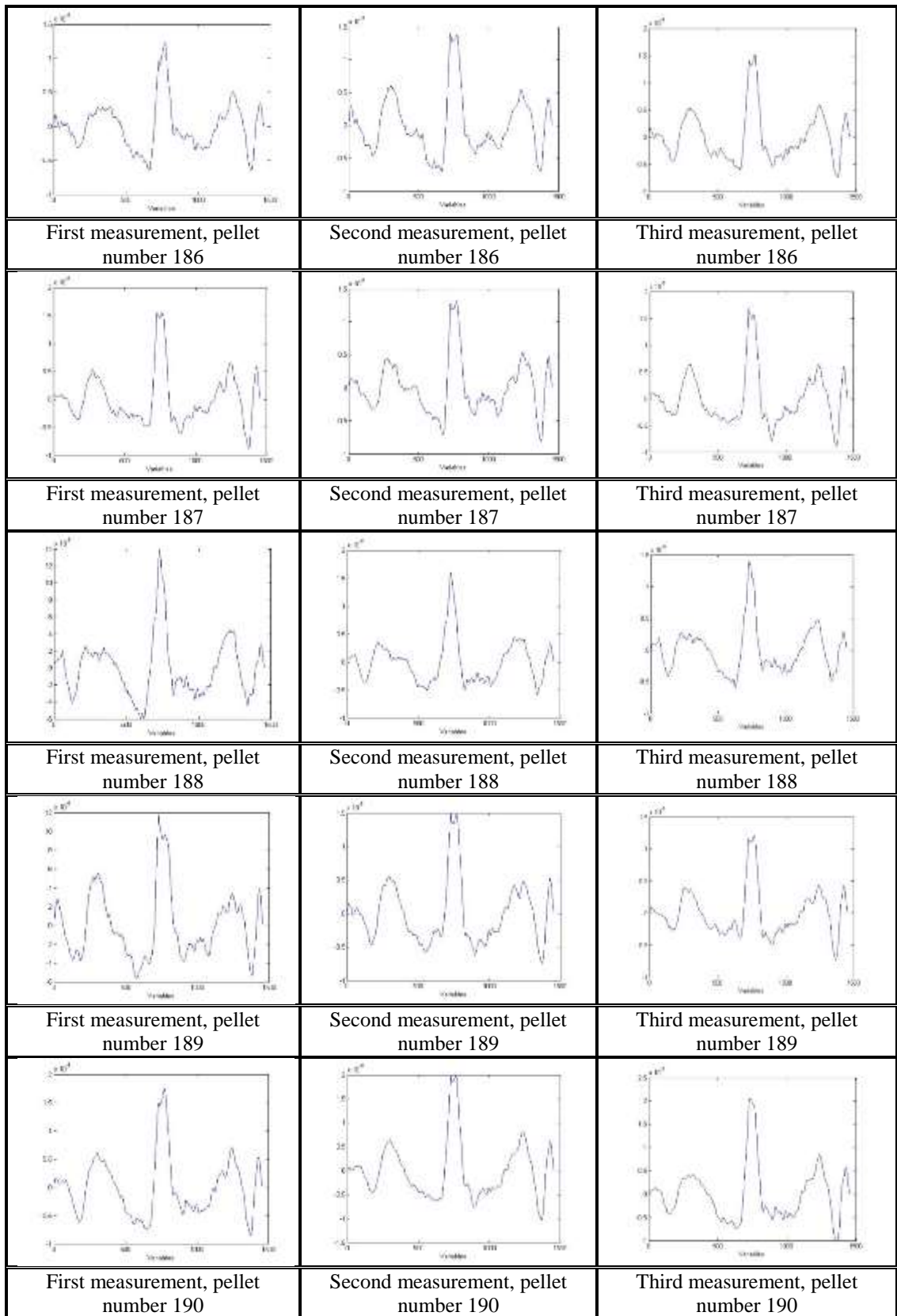
		
	Second measurement, pellet number 159	Third measurement, pellet number 159
		
First measurement, pellet number 160	Second measurement, pellet number 160	Third measurement, pellet number 160
		
First measurement, pellet number 161	Second measurement, pellet number 161	Third measurement, pellet number 161
		
First measurement, pellet number 162	Second measurement, pellet number 162	Third measurement, pellet number 162
		
First measurement, pellet number 163	Second measurement, pellet number 163	Third measurement, pellet number 163

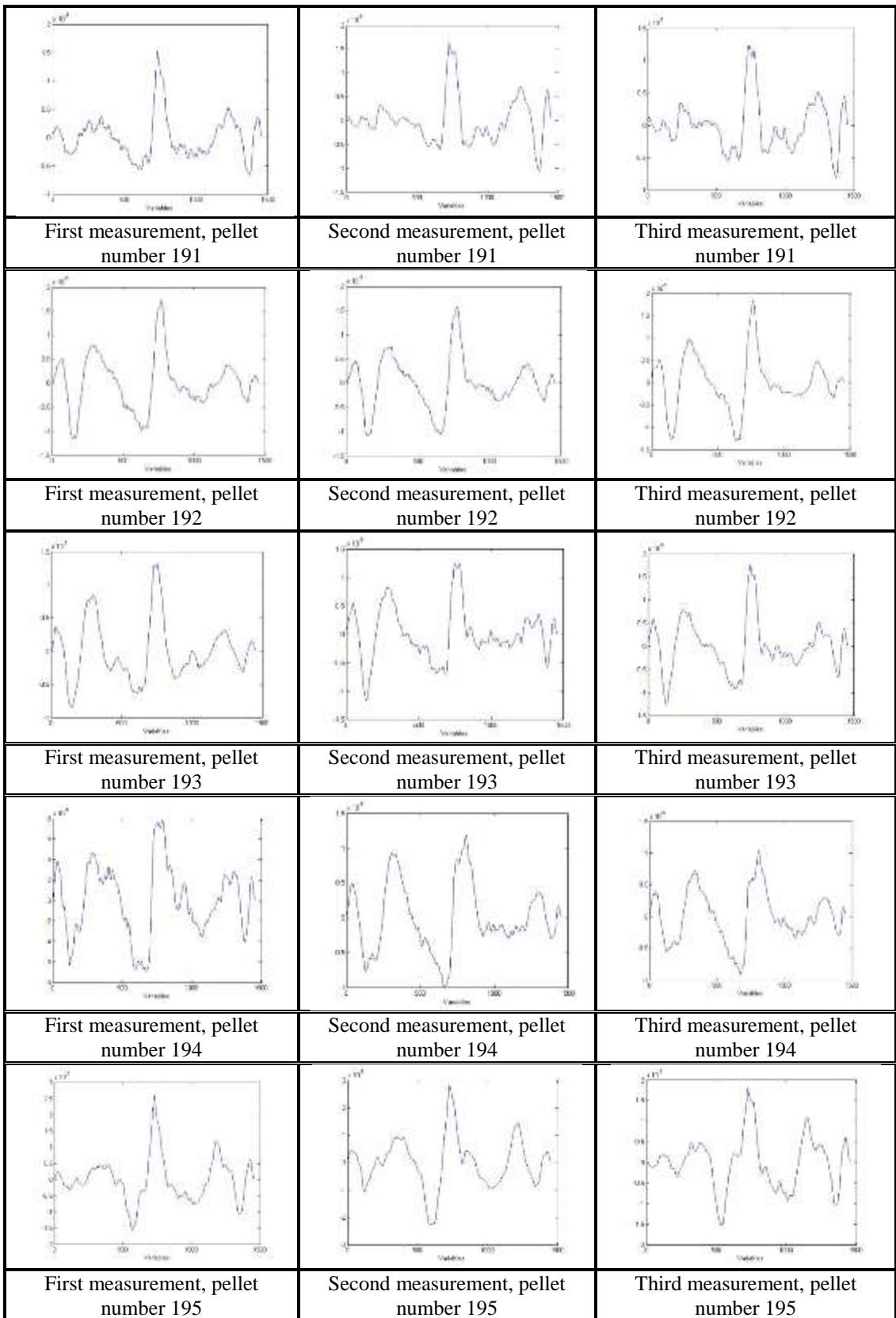


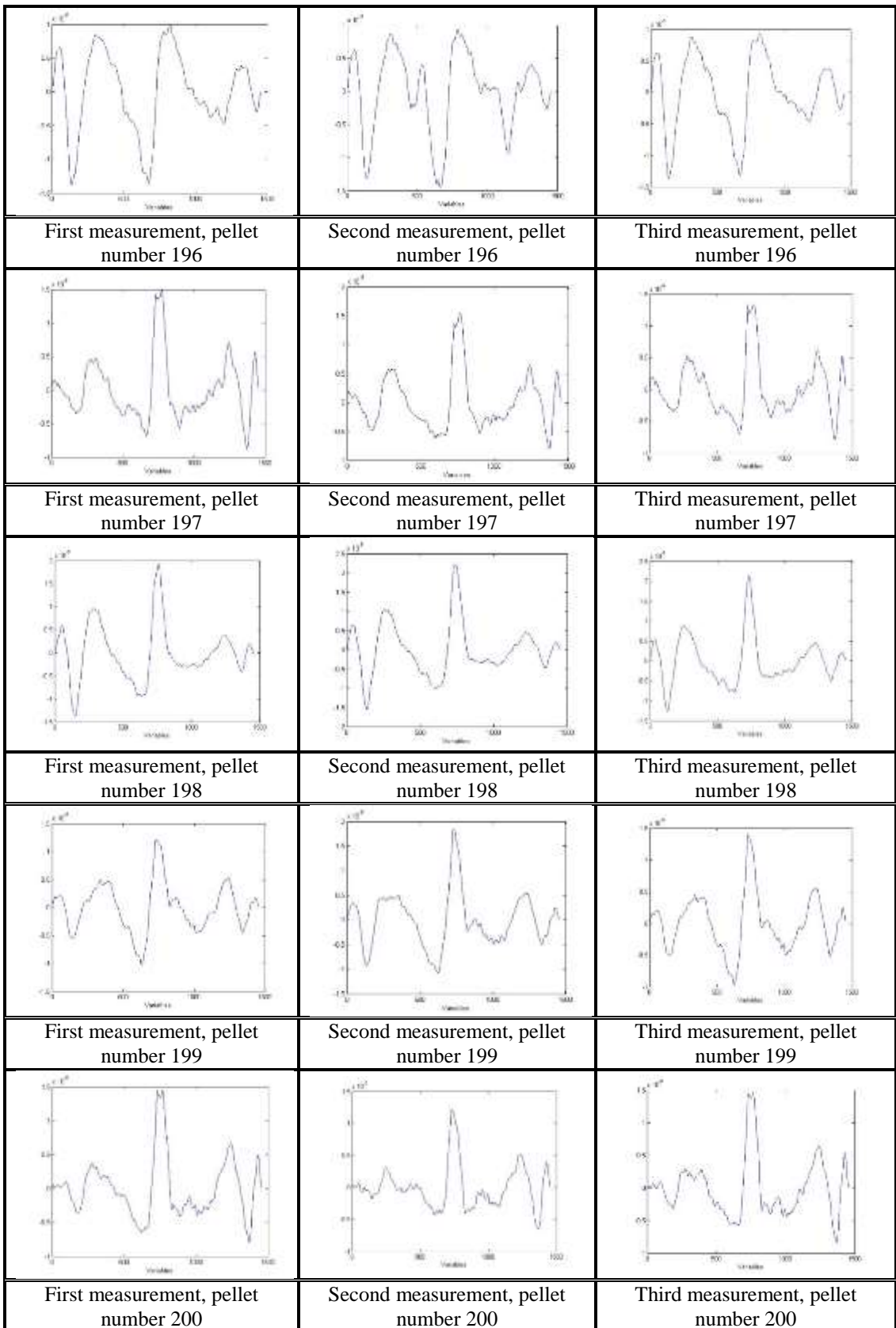




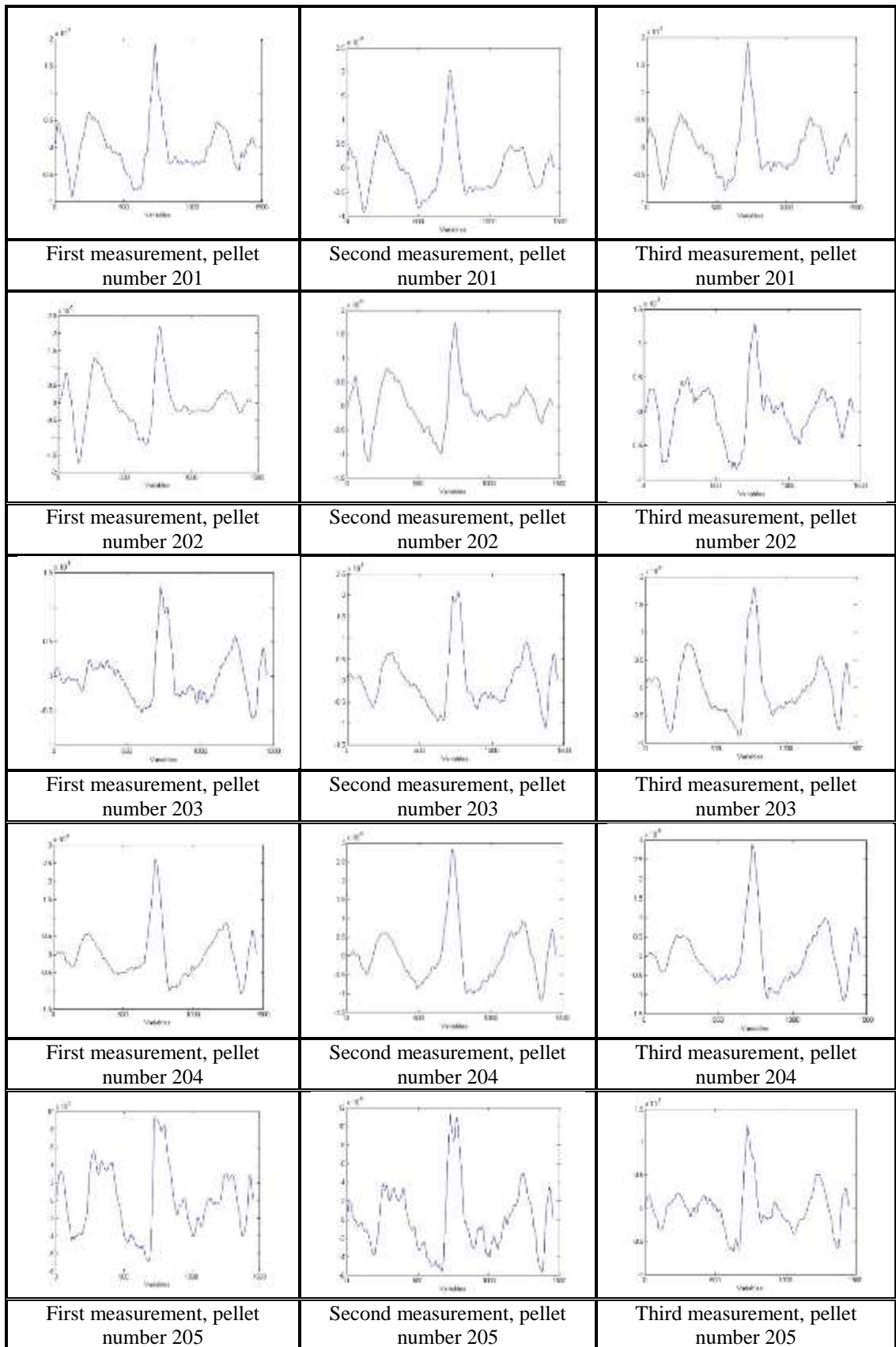


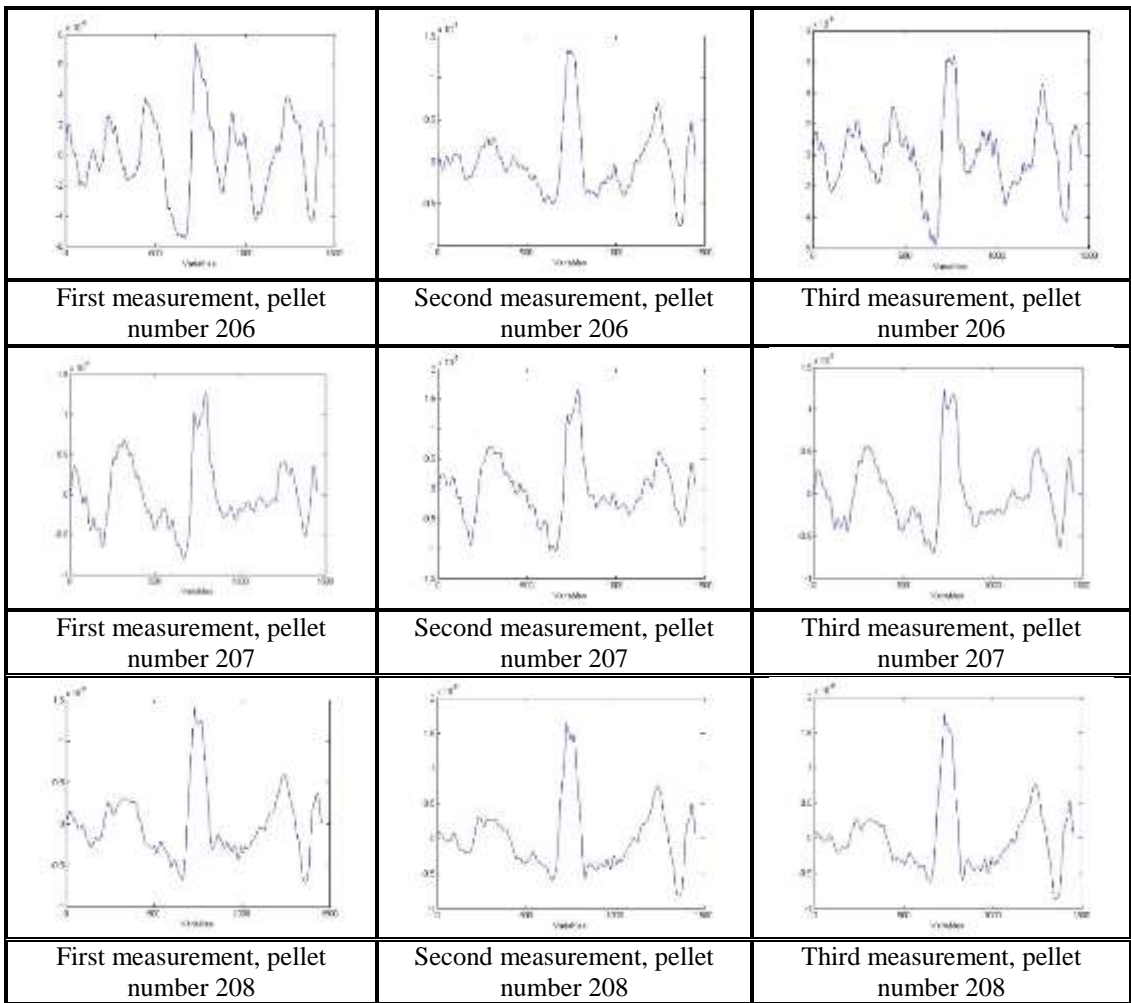






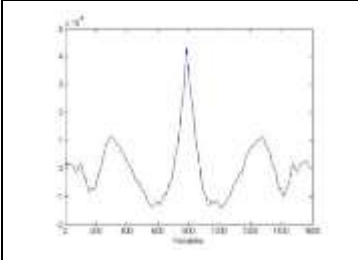
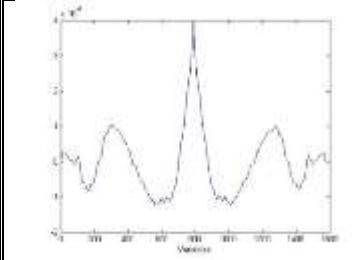
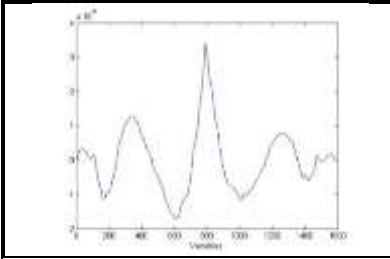
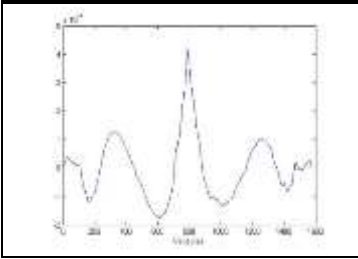
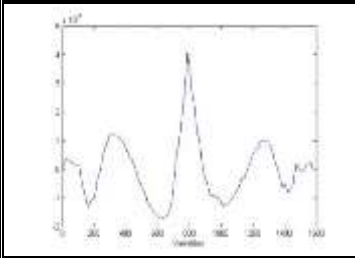
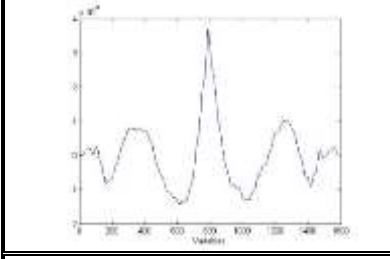
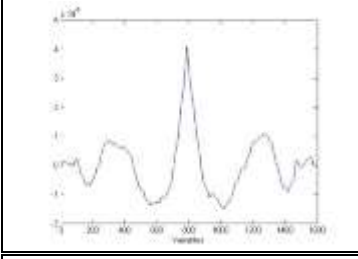
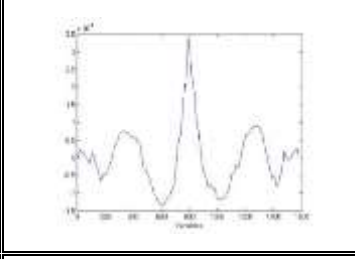
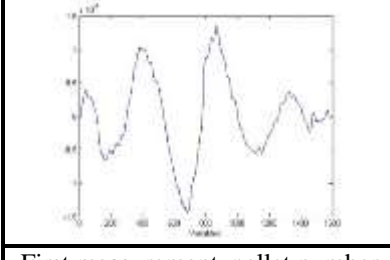
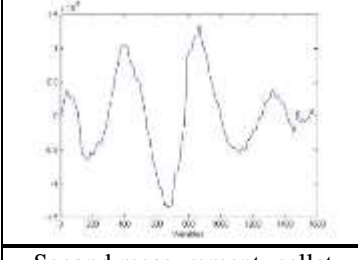
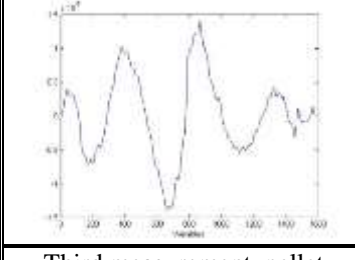
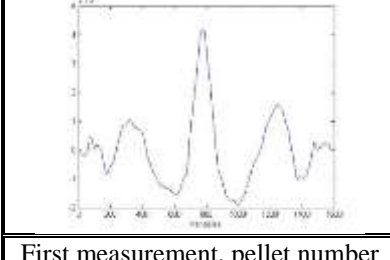
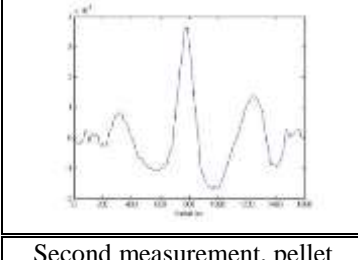
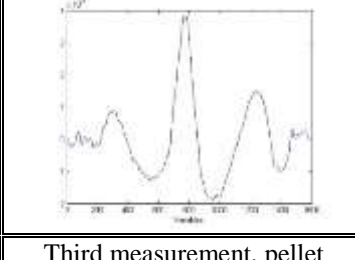


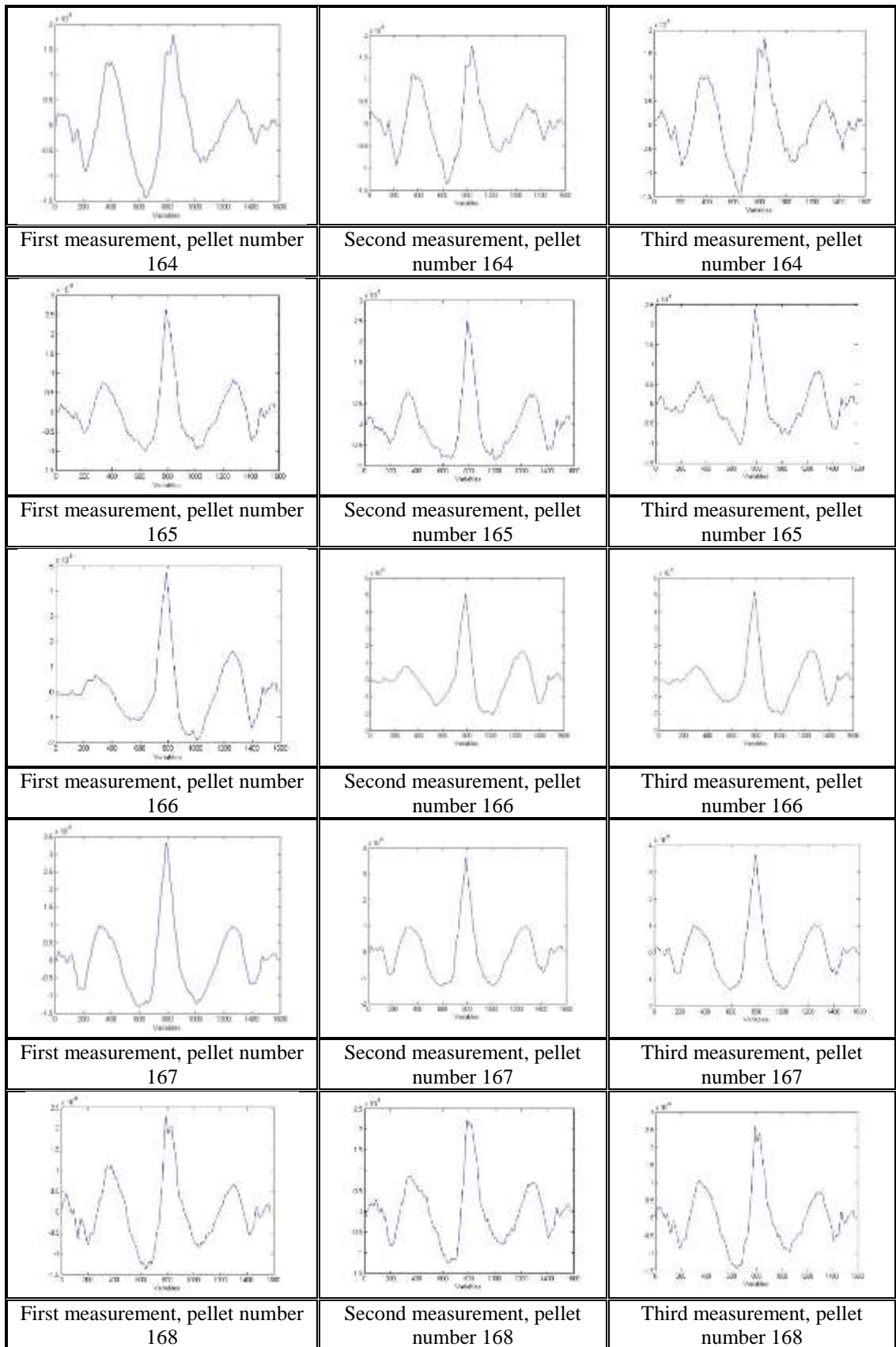


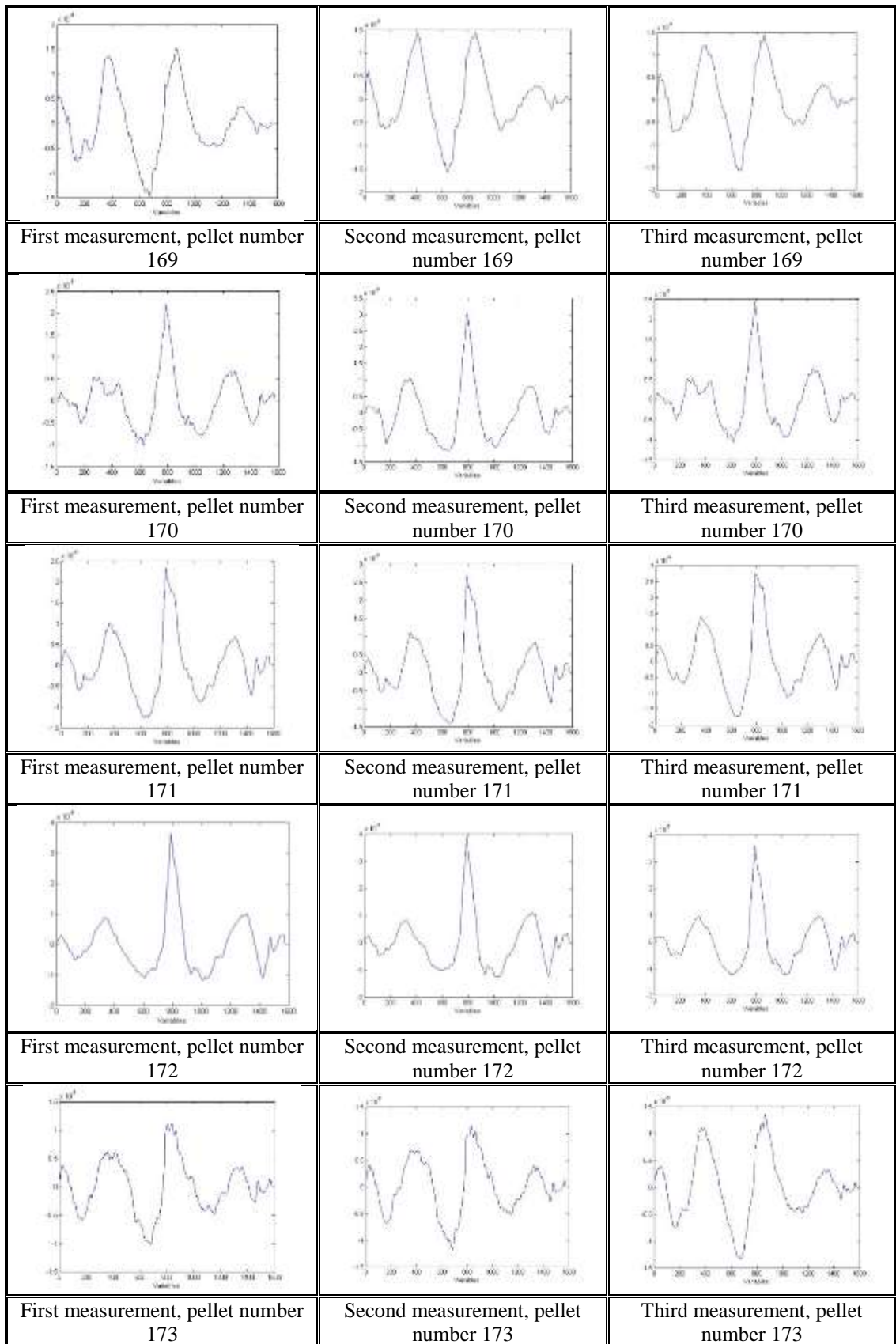


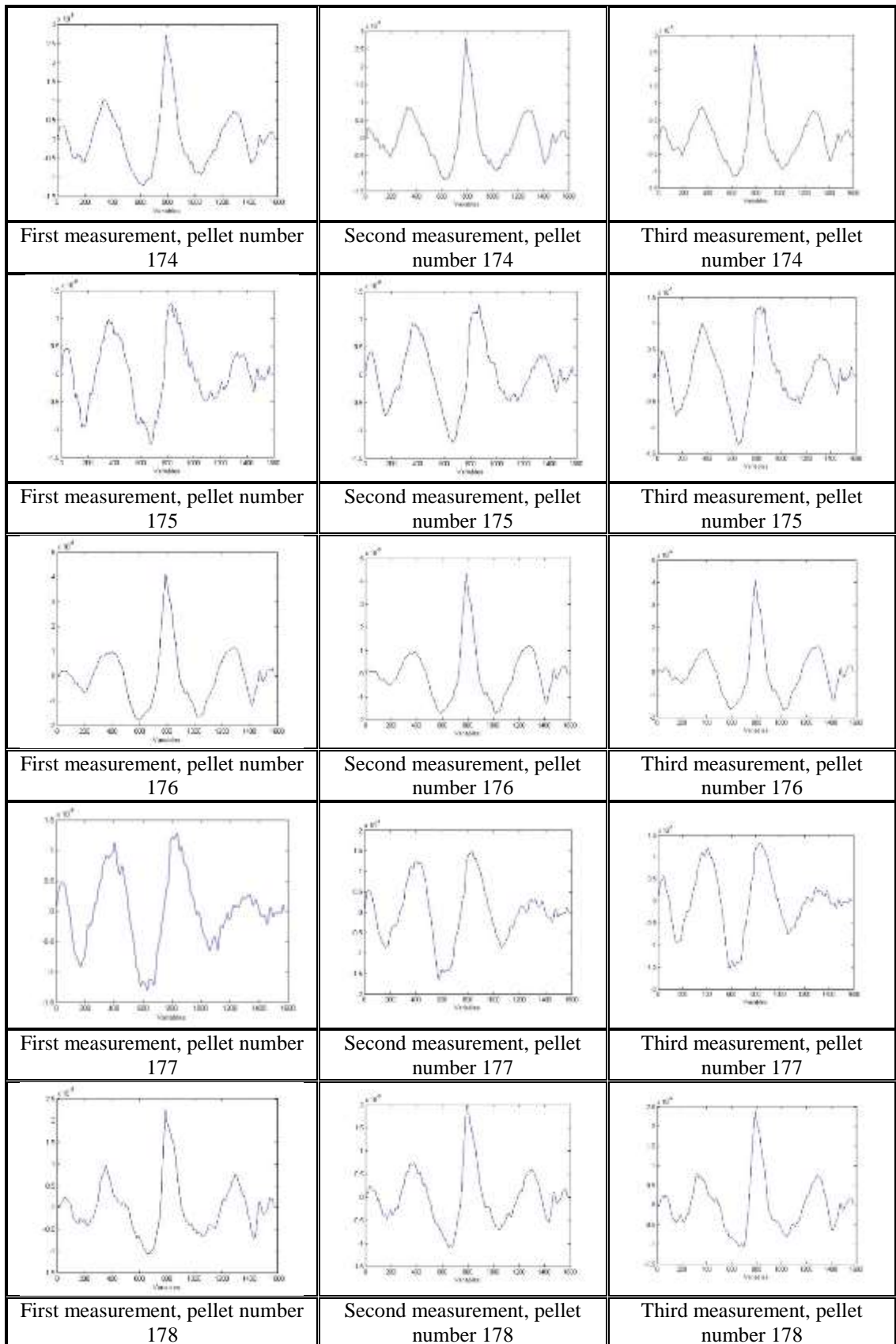
## Appendix 10

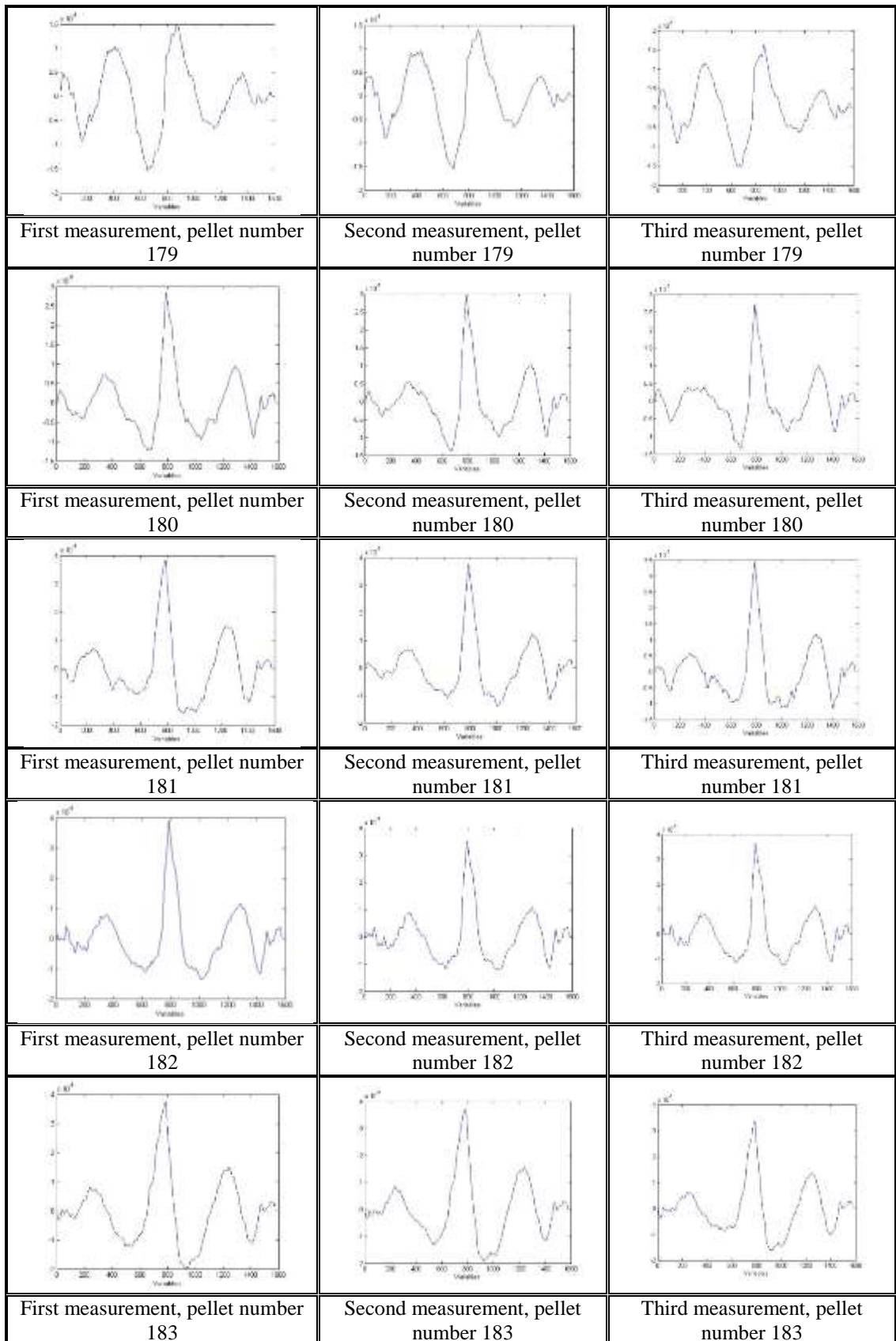
Alignment result for LEA G, pellet number 159 – 208

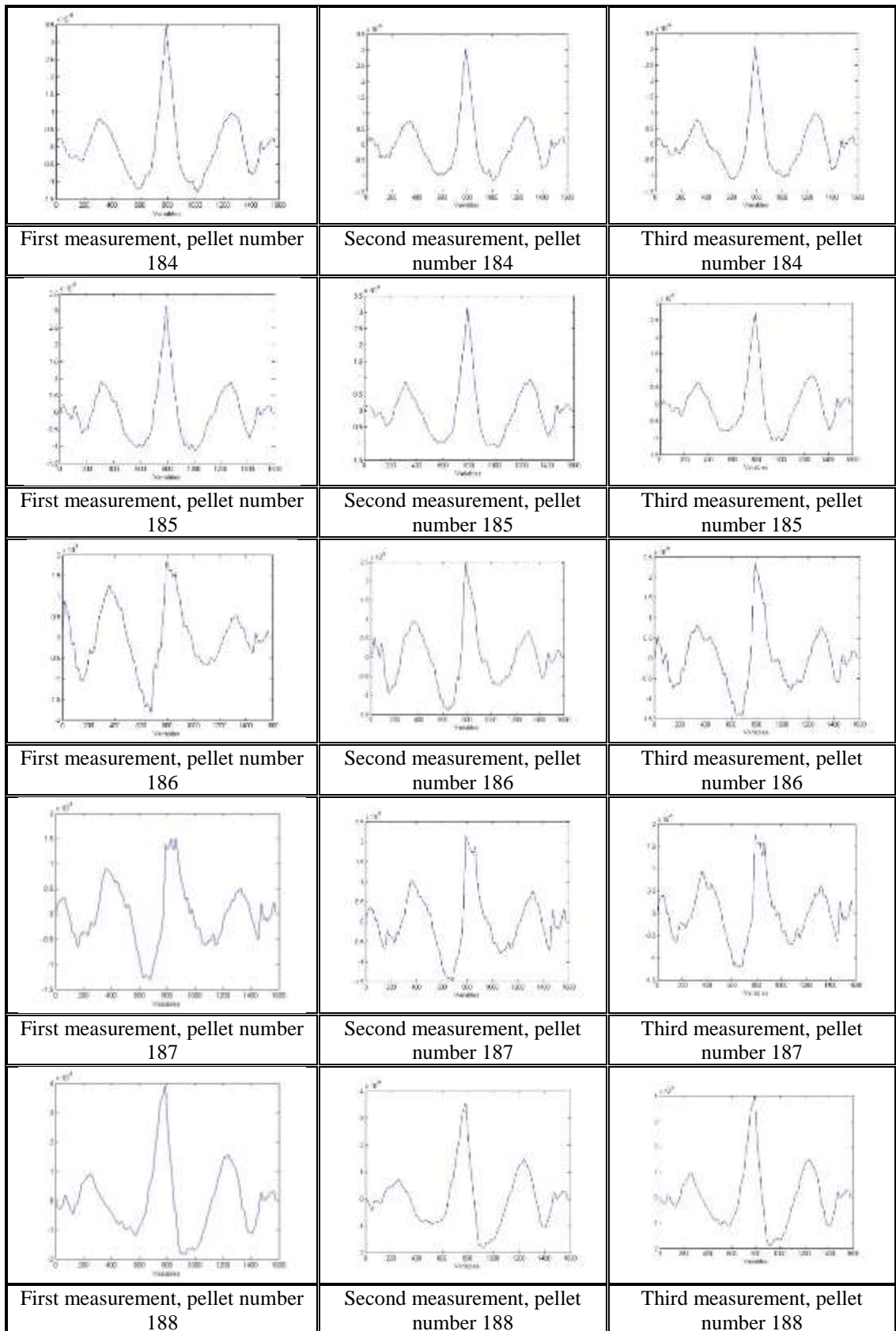
		
	Second measurement, pellet number 159	Third measurement, pellet number 159
		
First measurement, pellet number 160	Second measurement, pellet number 160	Third measurement, pellet number 160
		
First measurement, pellet number 161	Second measurement, pellet number 161	Third measurement, pellet number 161
		
First measurement, pellet number 162	Second measurement, pellet number 162	Third measurement, pellet number 162
		
First measurement, pellet number 163	Second measurement, pellet number 163	Third measurement, pellet number 163



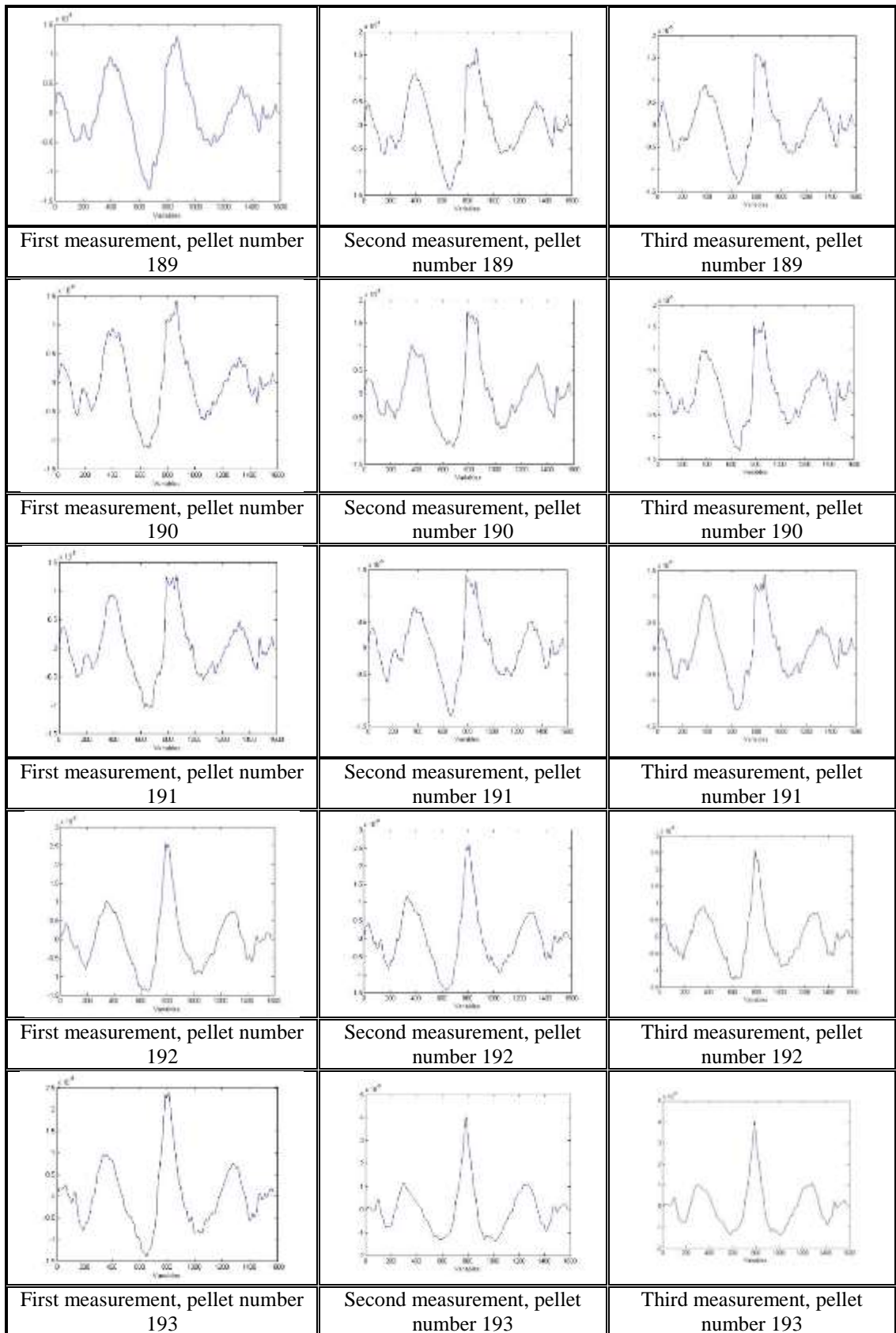


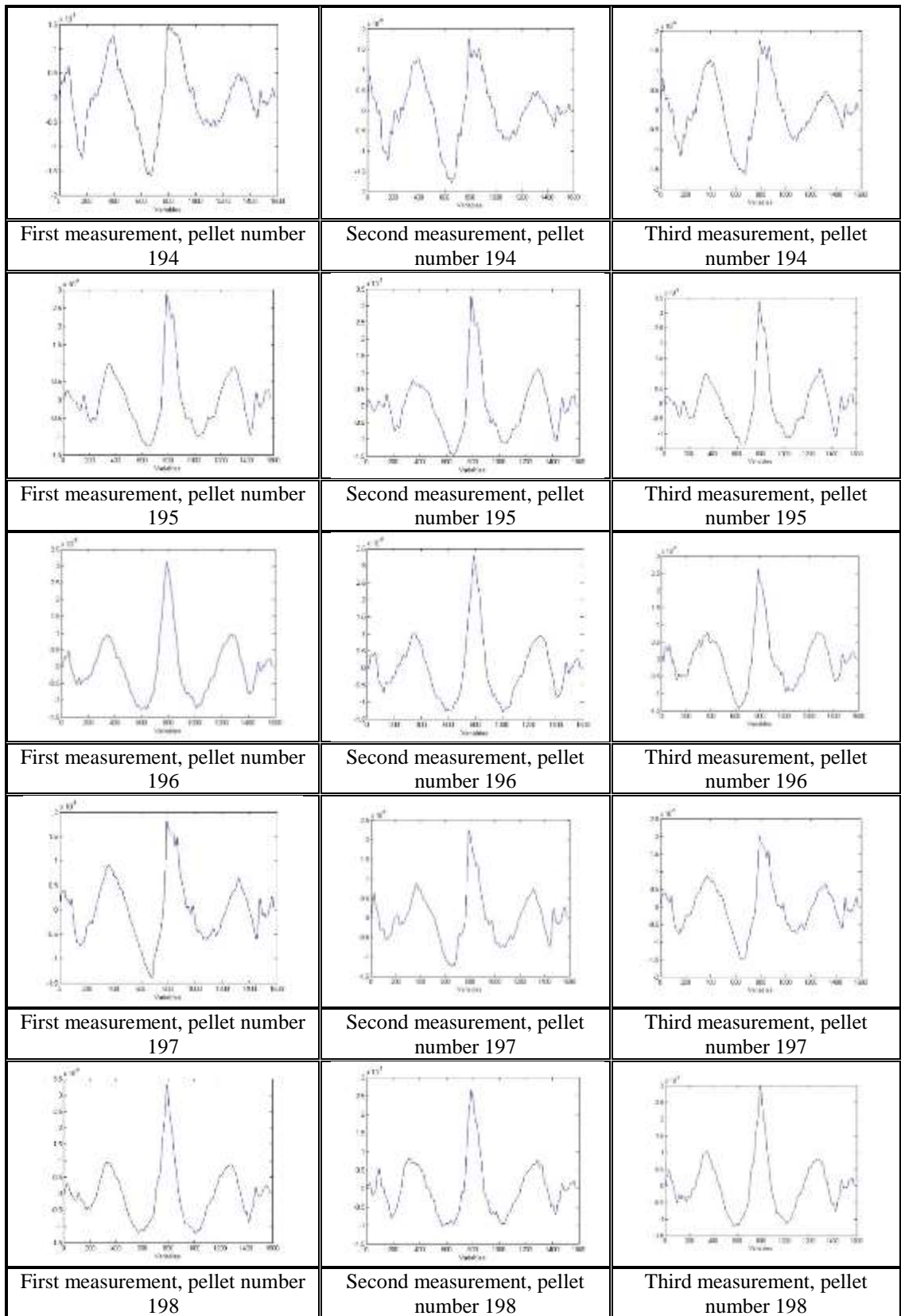


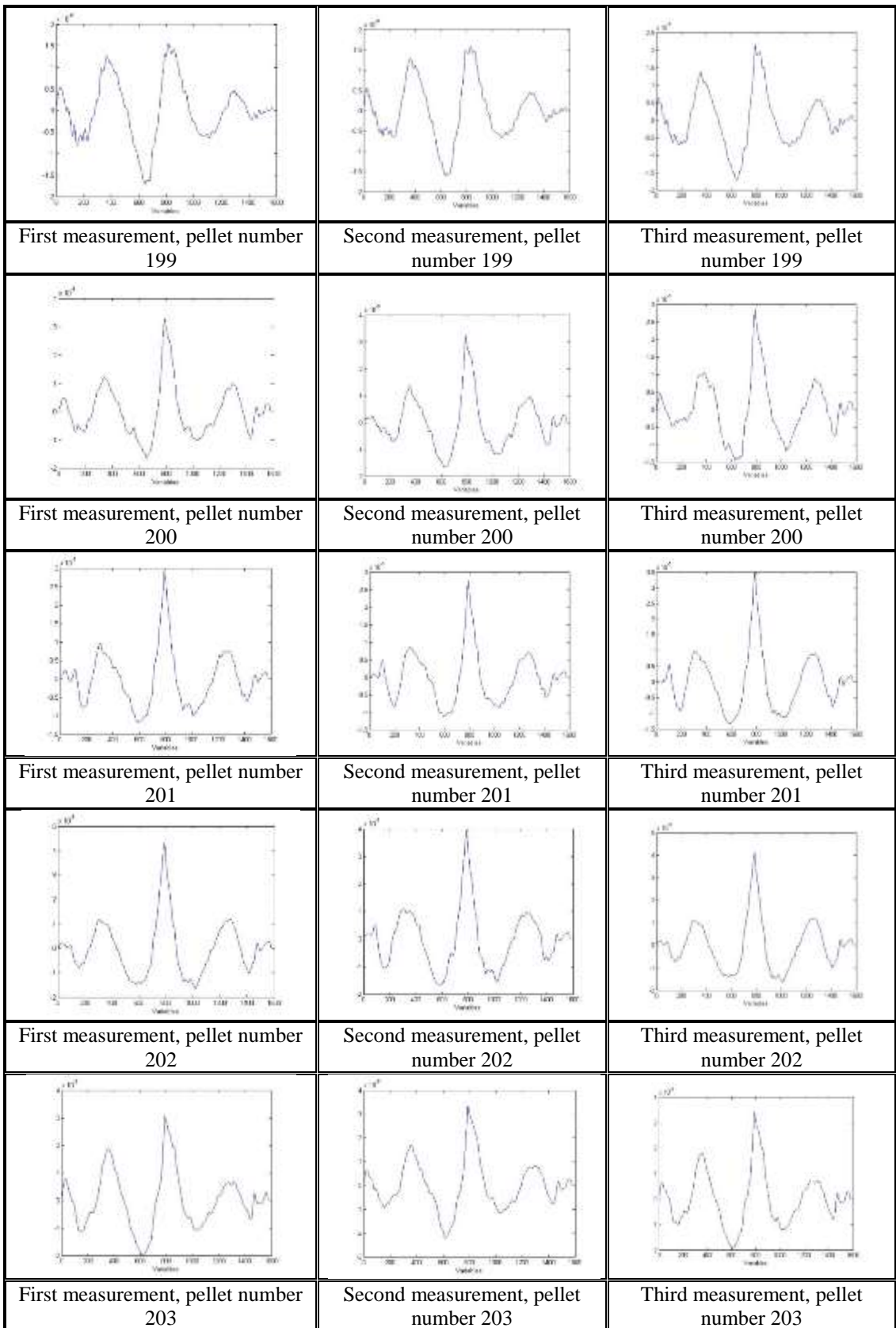


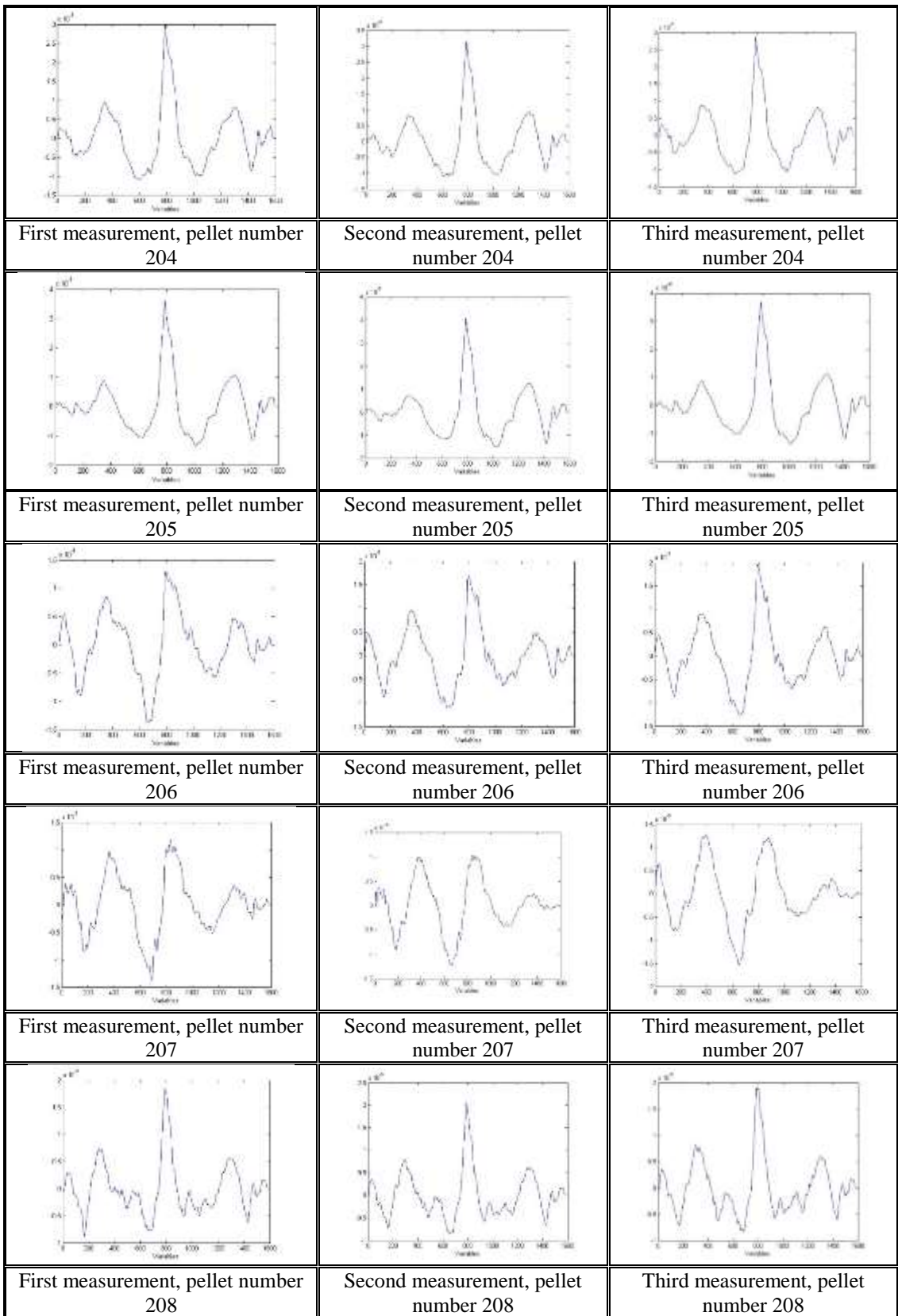






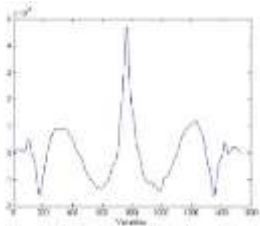
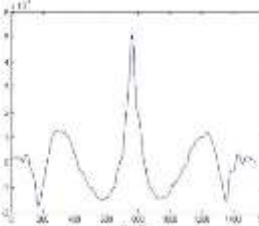
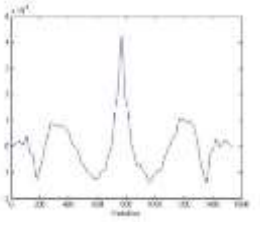
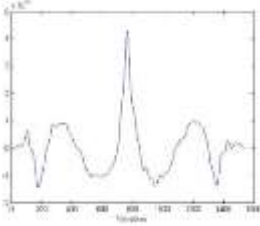
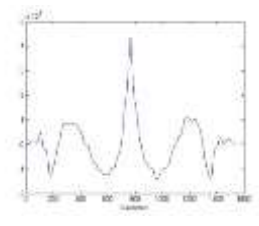
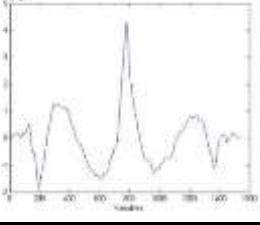
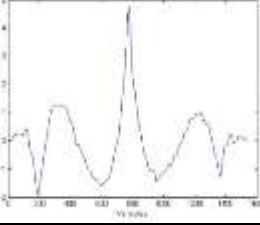
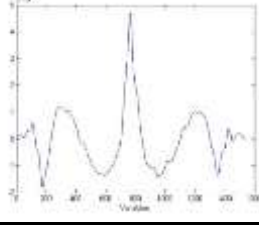
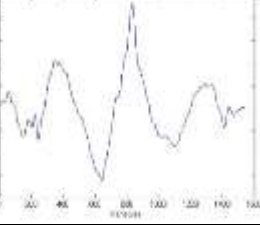
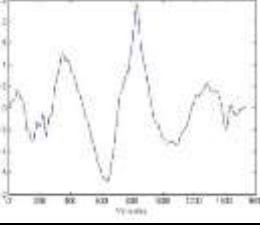
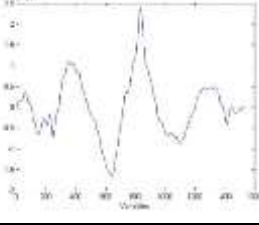
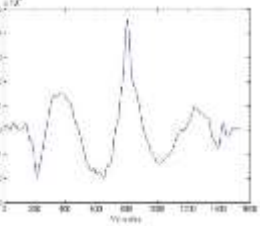
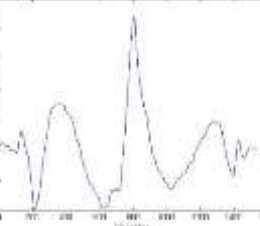
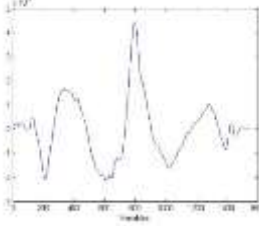


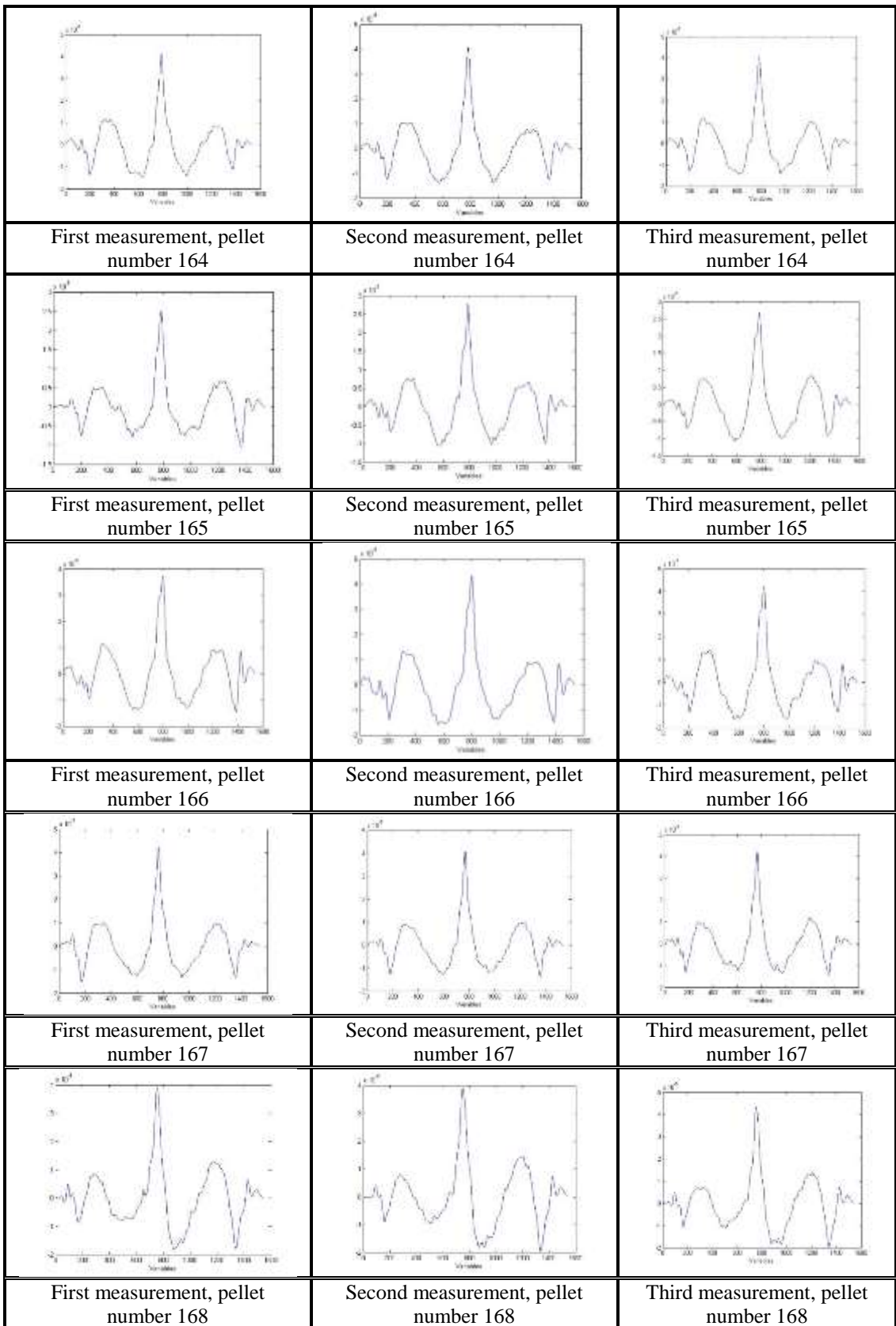


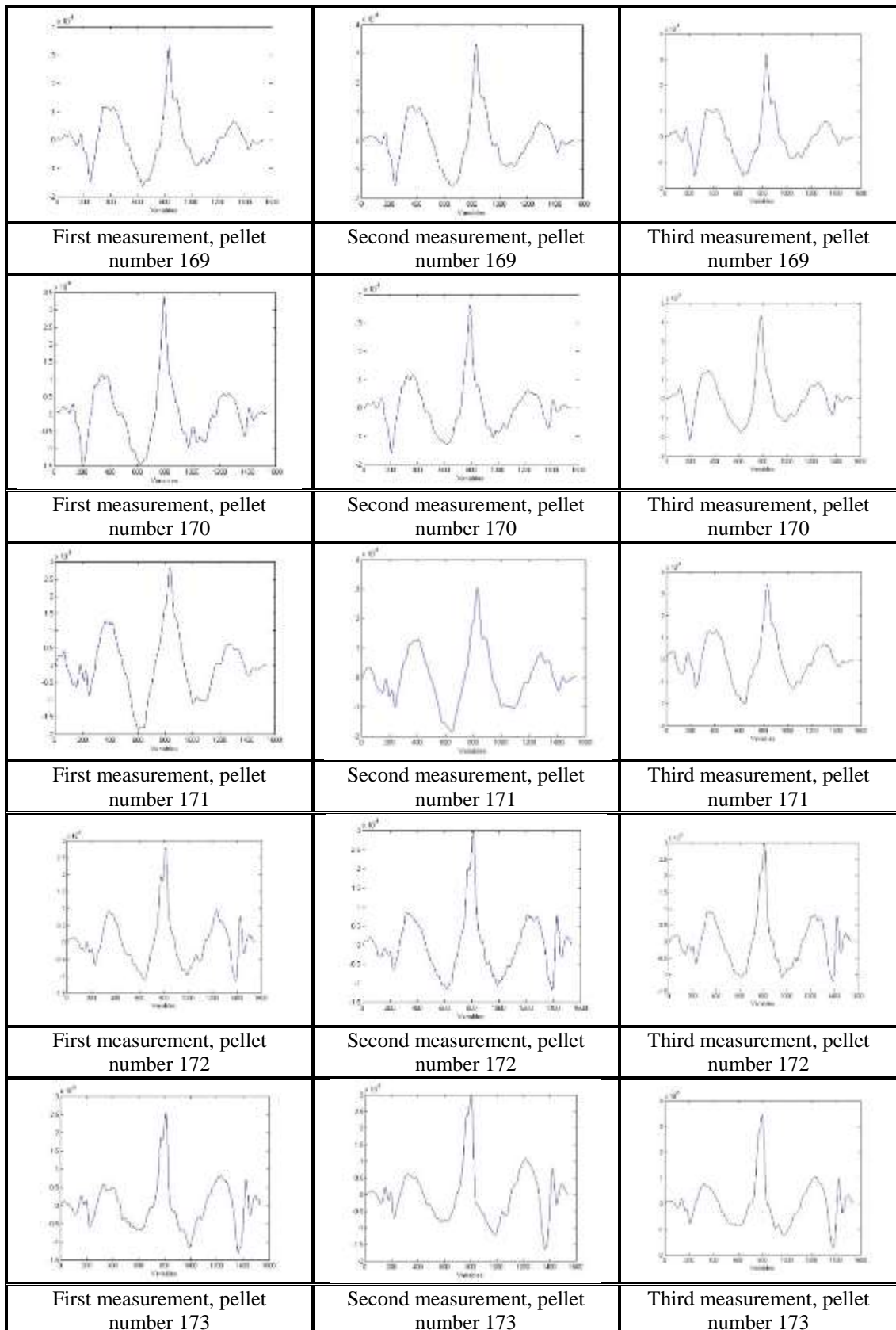


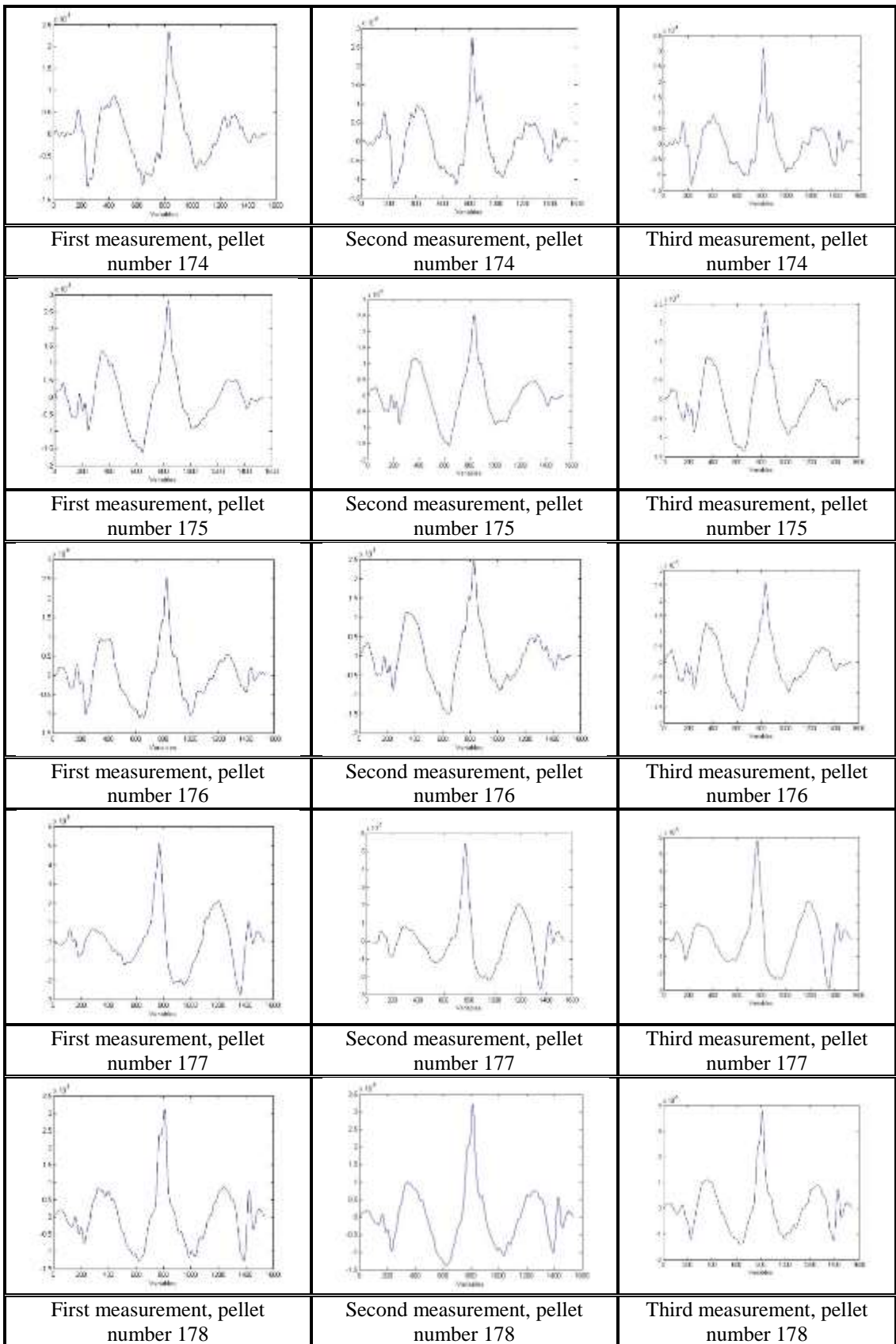
## Appendix 11

Alignment result for LEA H, pellet number 159 – 208

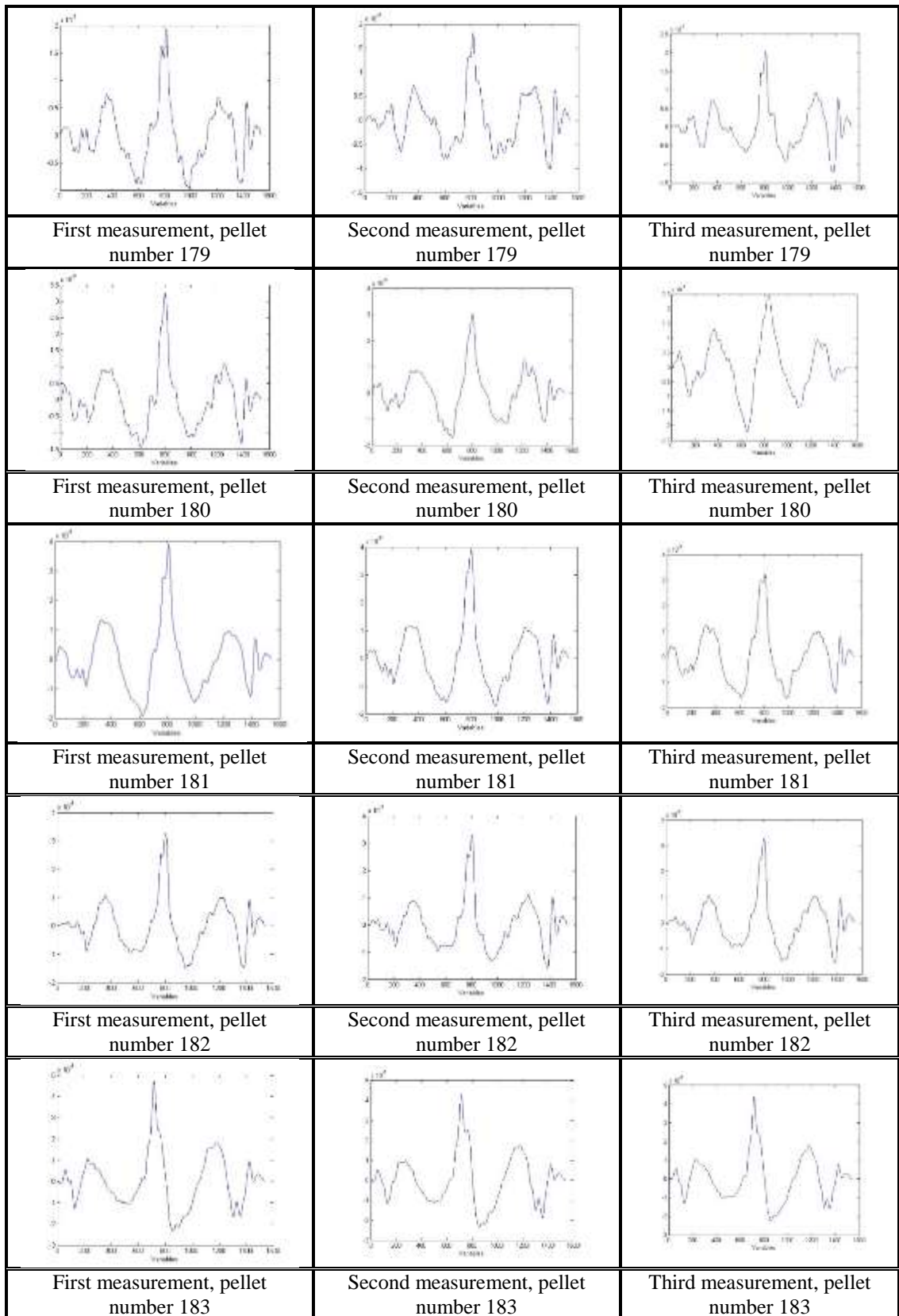
		
	Second measurement, pellet number 159	Third measurement, pellet number 159
		
First measurement, pellet number 160	Second measurement, pellet number 160	Third measurement, pellet number 160
		
First measurement, pellet number 161	Second measurement, pellet number 161	Third measurement, pellet number 161
		
First measurement, pellet number 162	Second measurement, pellet number 162	Third measurement, pellet number 162
		
First measurement, pellet number 163	Second measurement, pellet number 163	Third measurement, pellet number 163

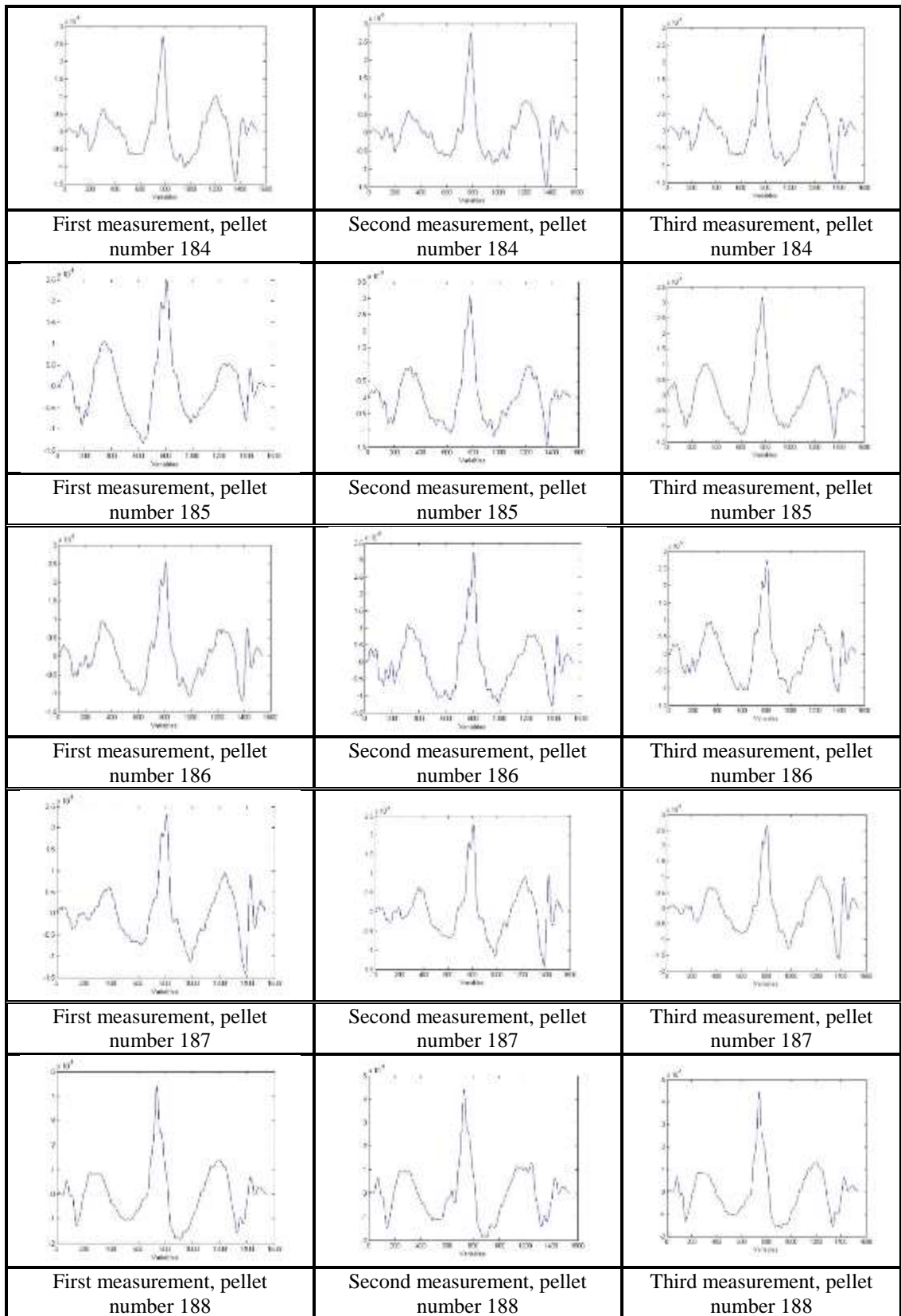


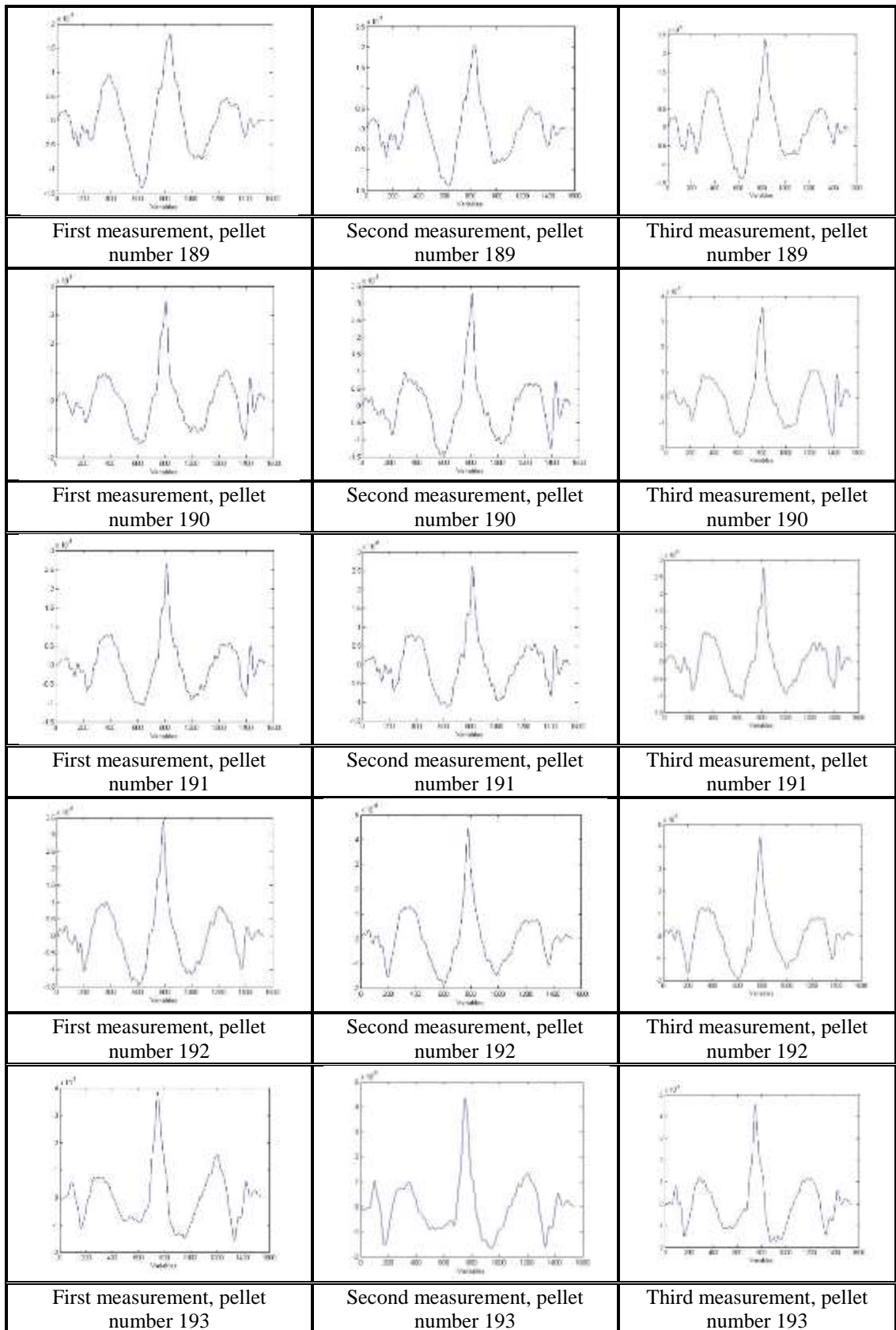


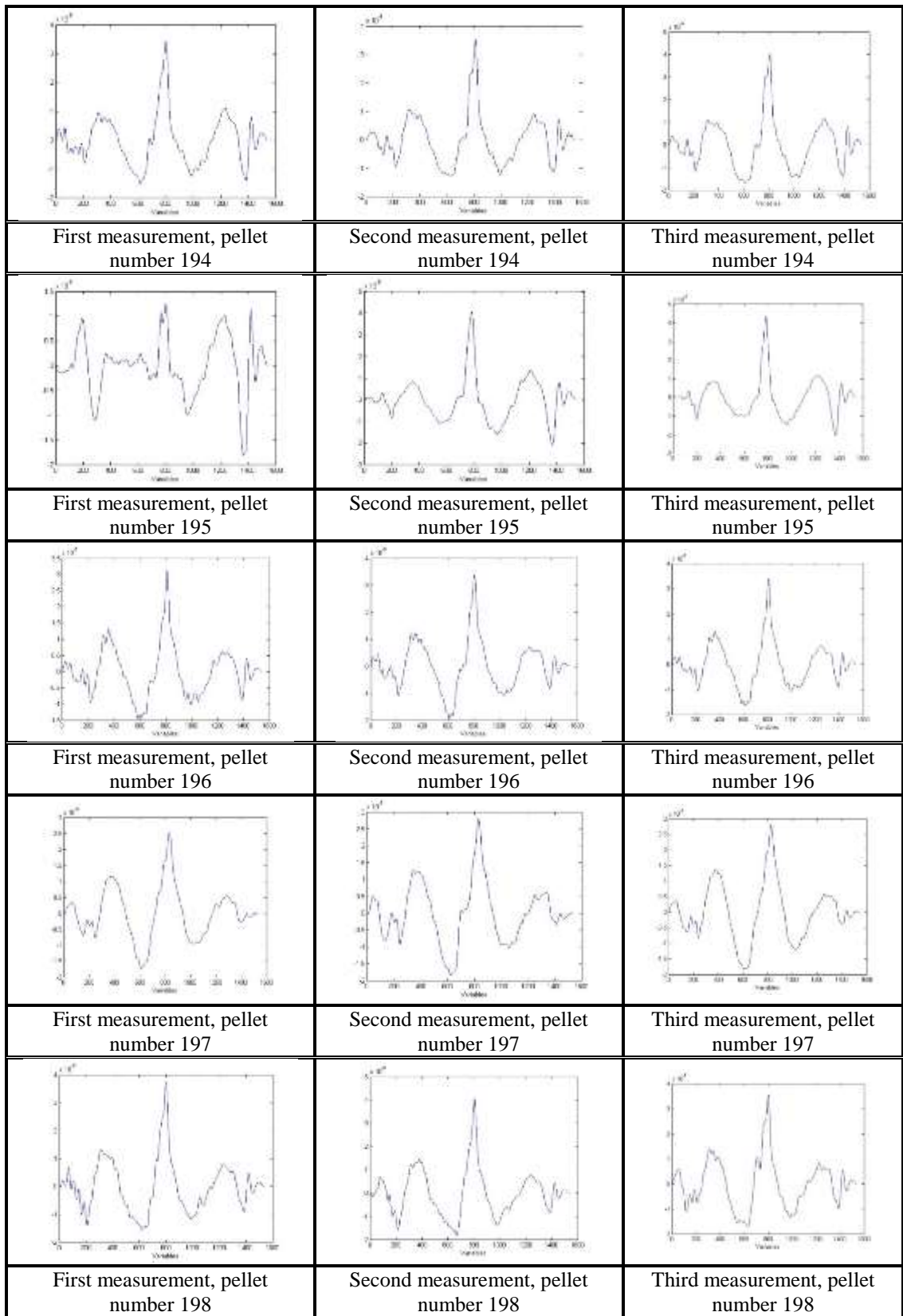


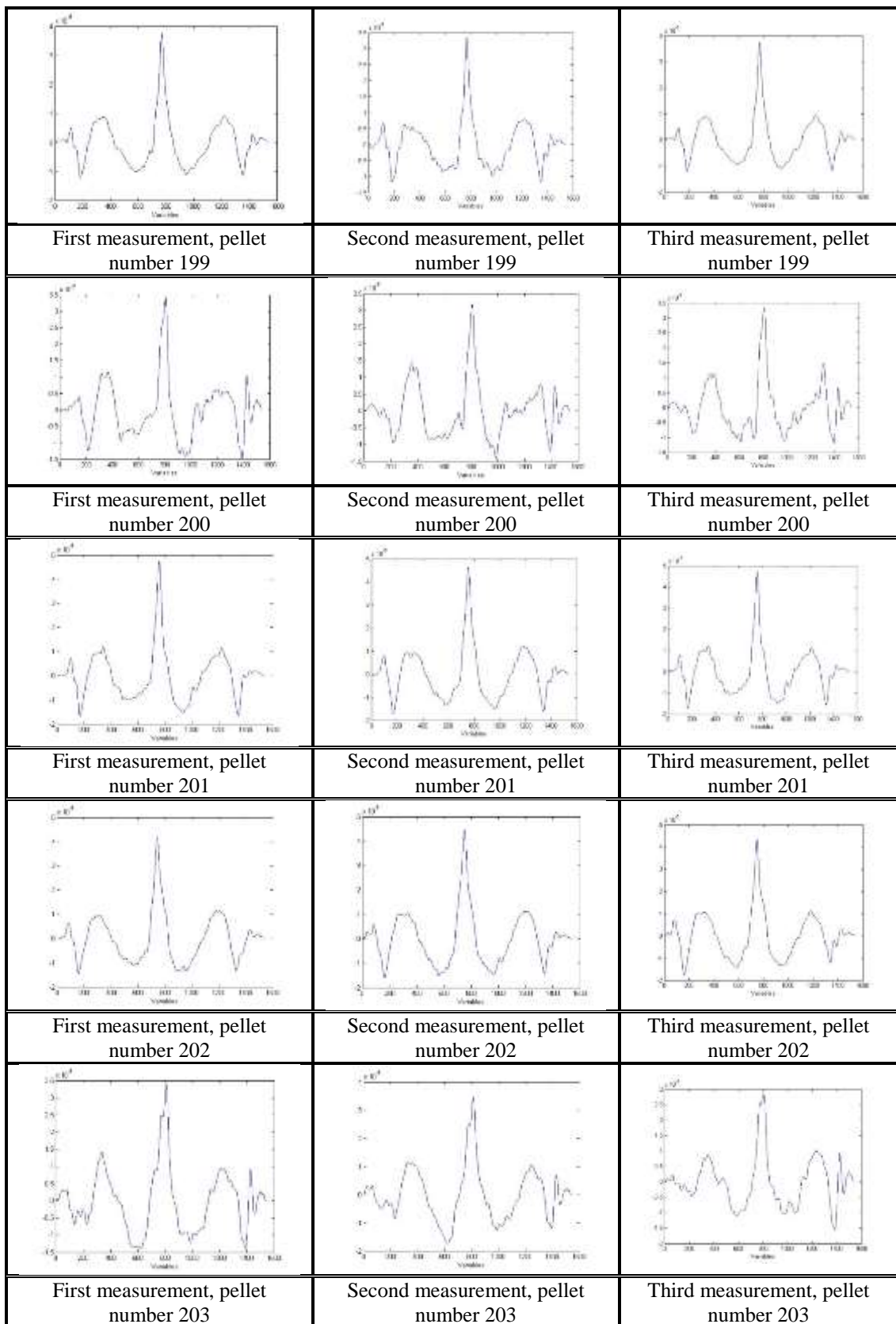


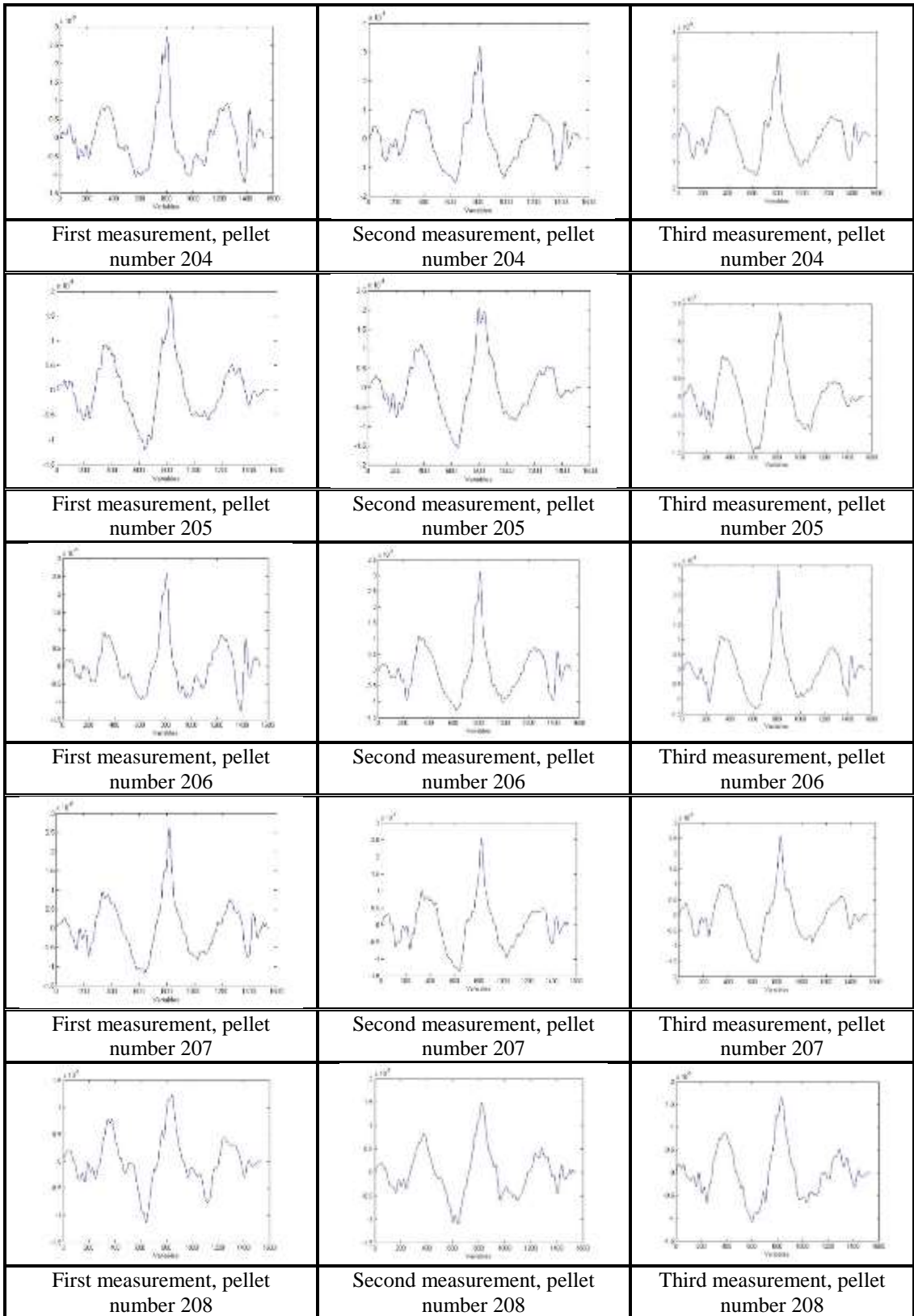







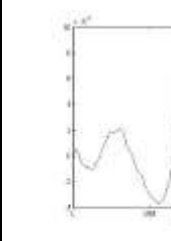
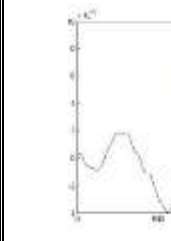
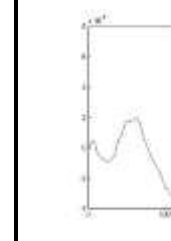
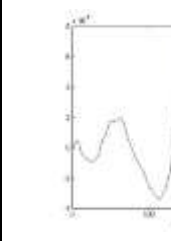
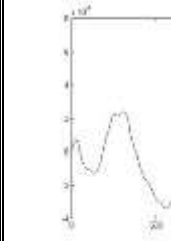

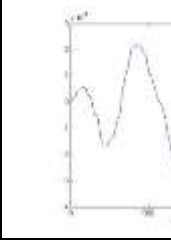
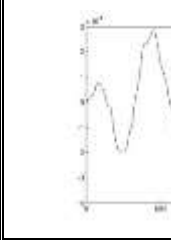
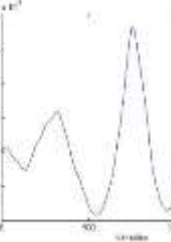




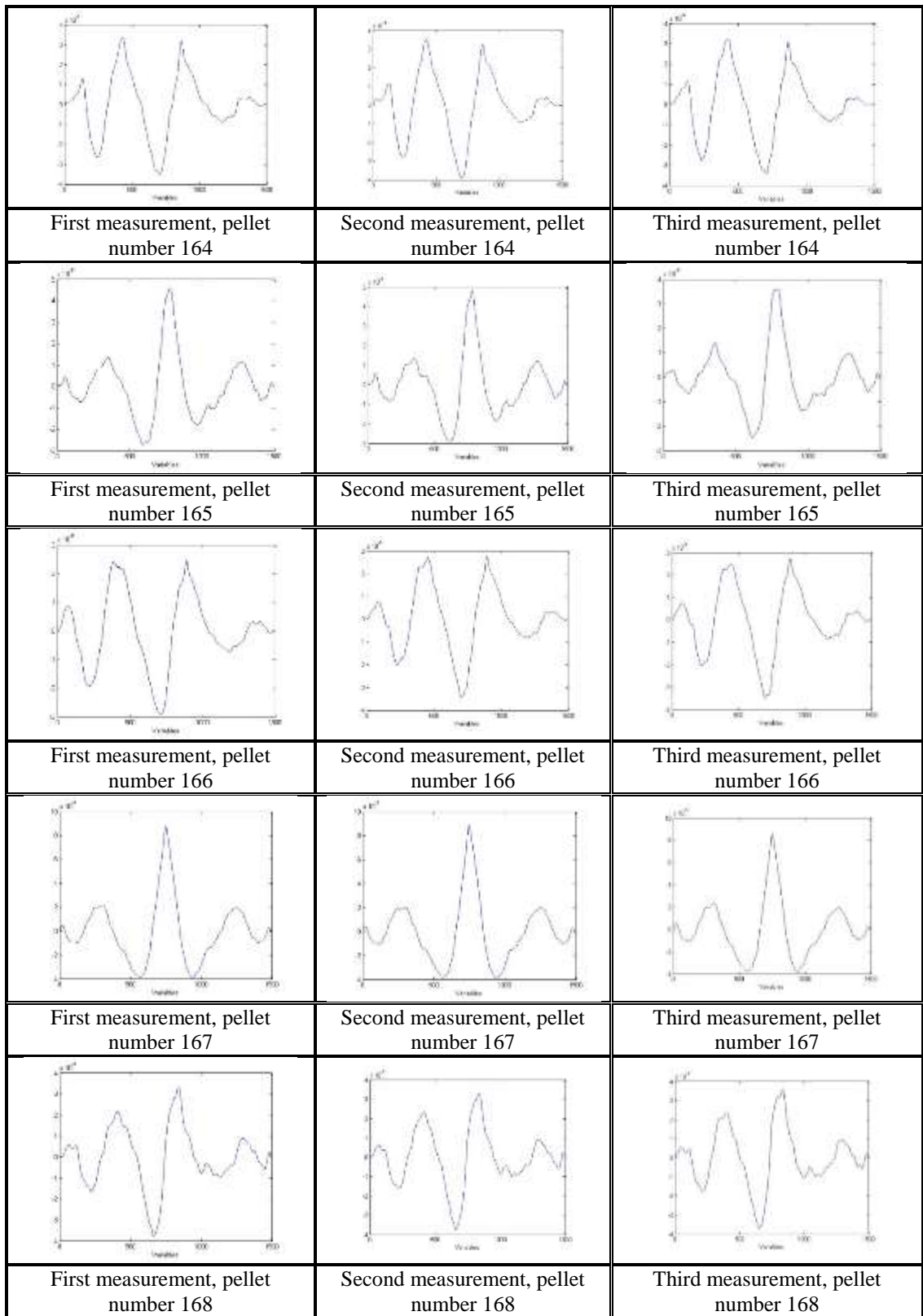




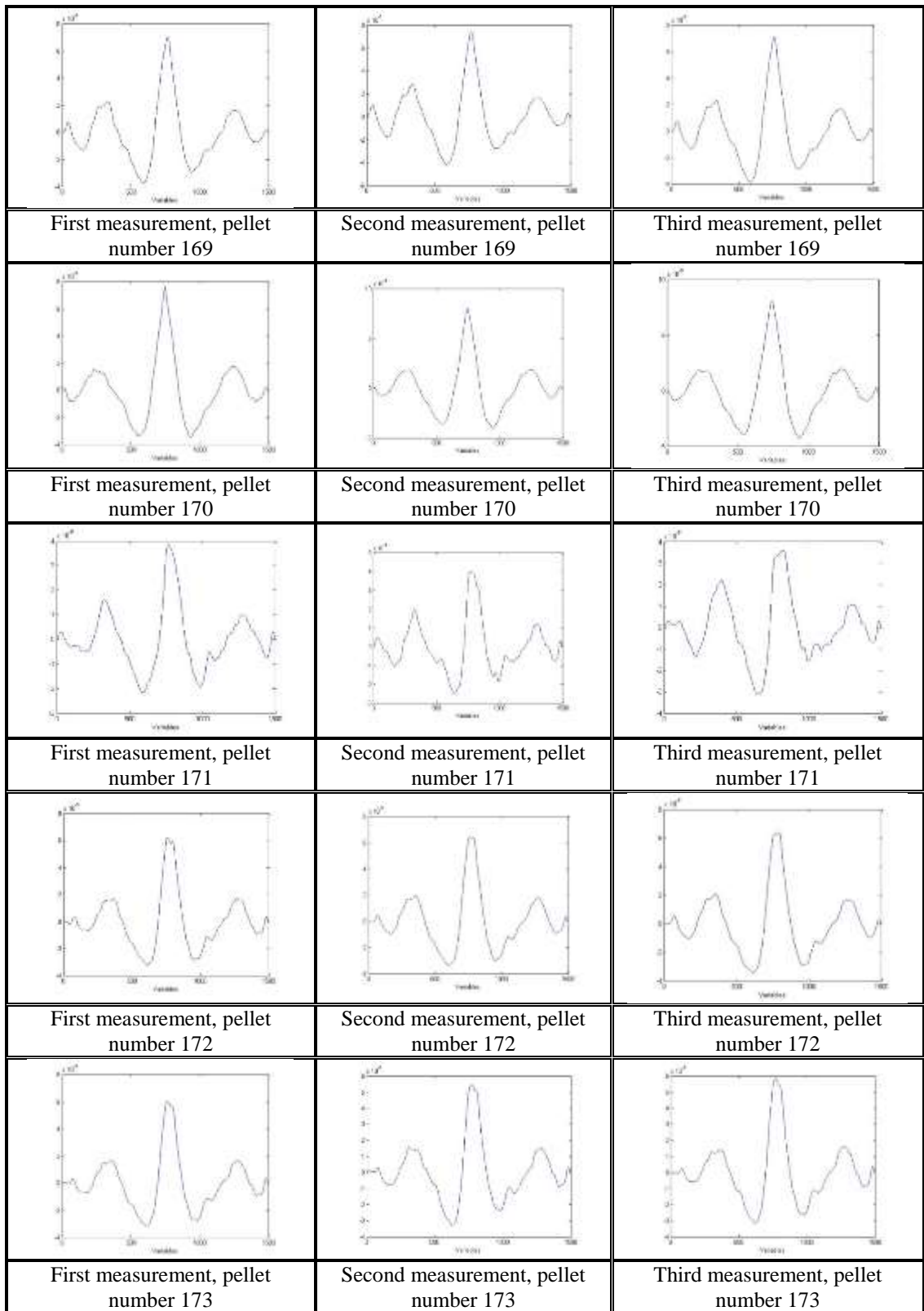
## Appendix 12

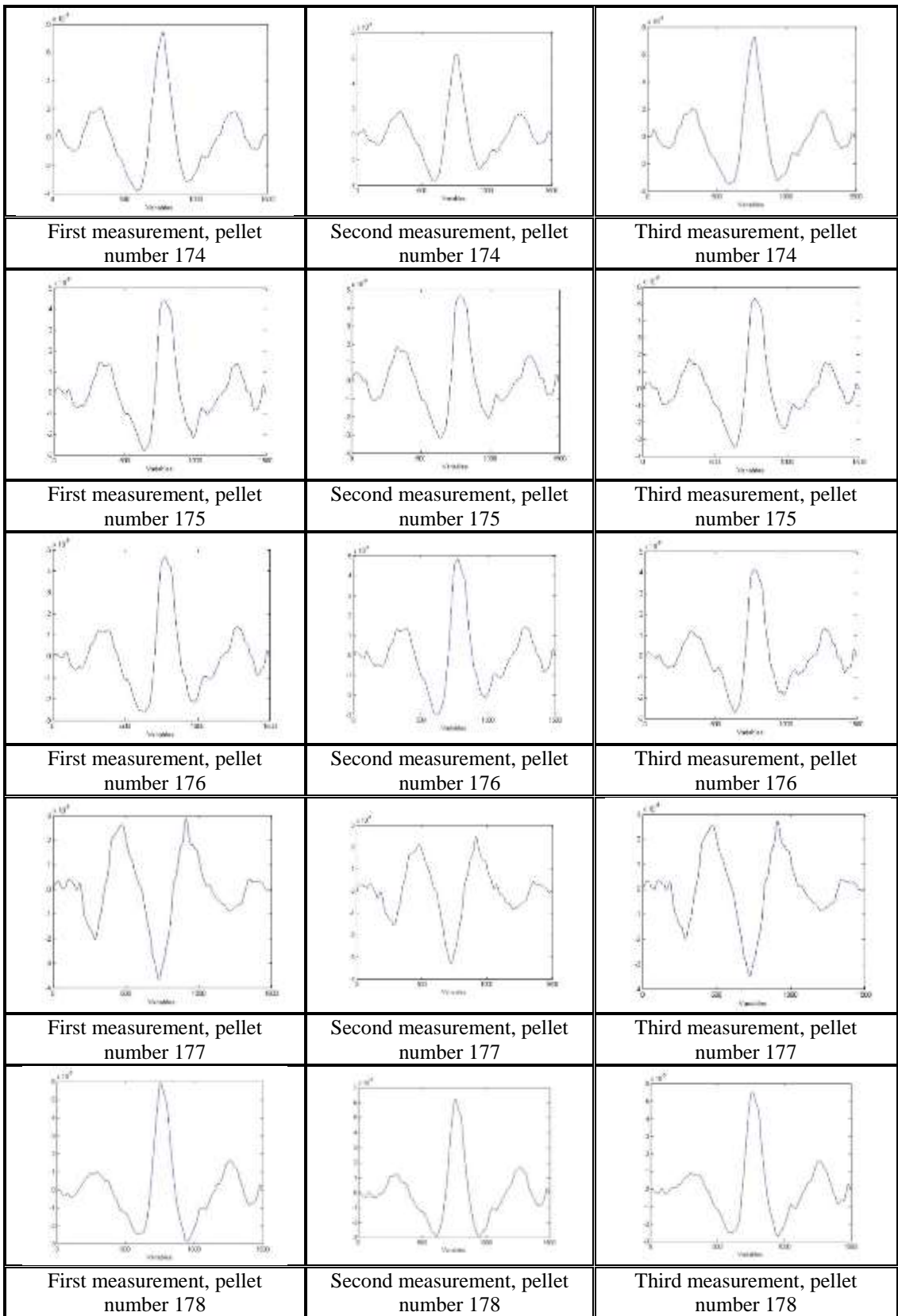
Alignment result for LEA I, pellet number 159 – 208

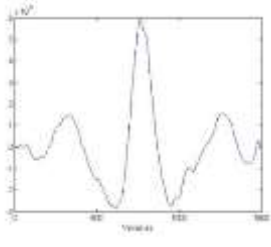
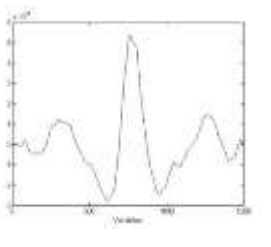
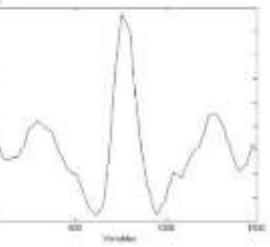
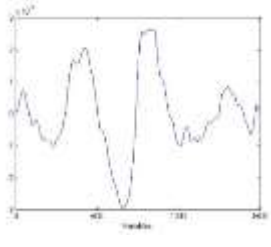
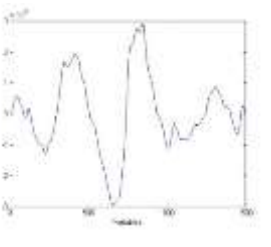
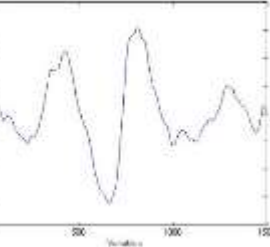
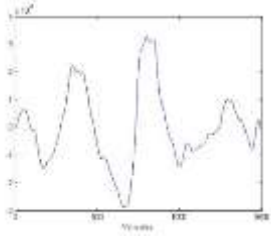
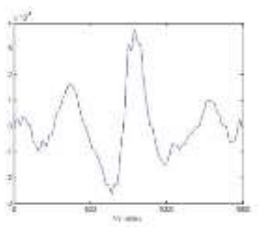
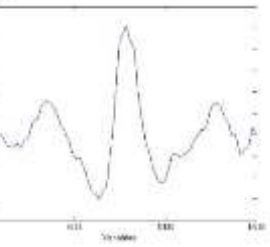
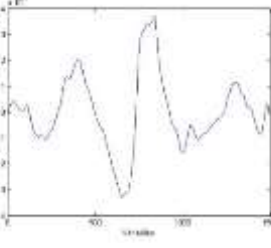
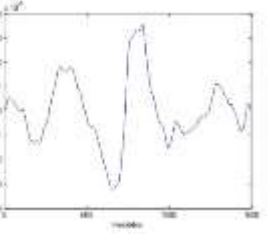
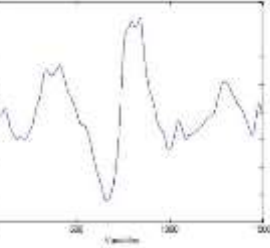
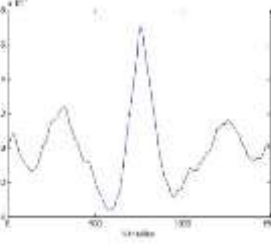
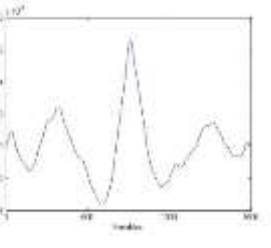
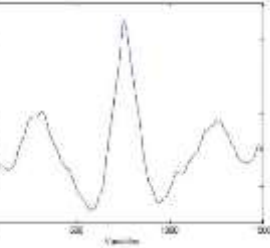
	Second measurement, pellet number 159	Third measurement, pellet number 159
		
First measurement, pellet number 160	Second measurement, pellet number 160	Third measurement, pellet number 160
		
First measurement, pellet number 161	Second measurement, pellet number 161	Third measurement, pellet number 161
		
First measurement, pellet number 162	Second measurement, pellet number 162	Third measurement, pellet number 162
		
First measurement, pellet number 163	Second measurement, pellet number 163	Third measurement, pellet number 163

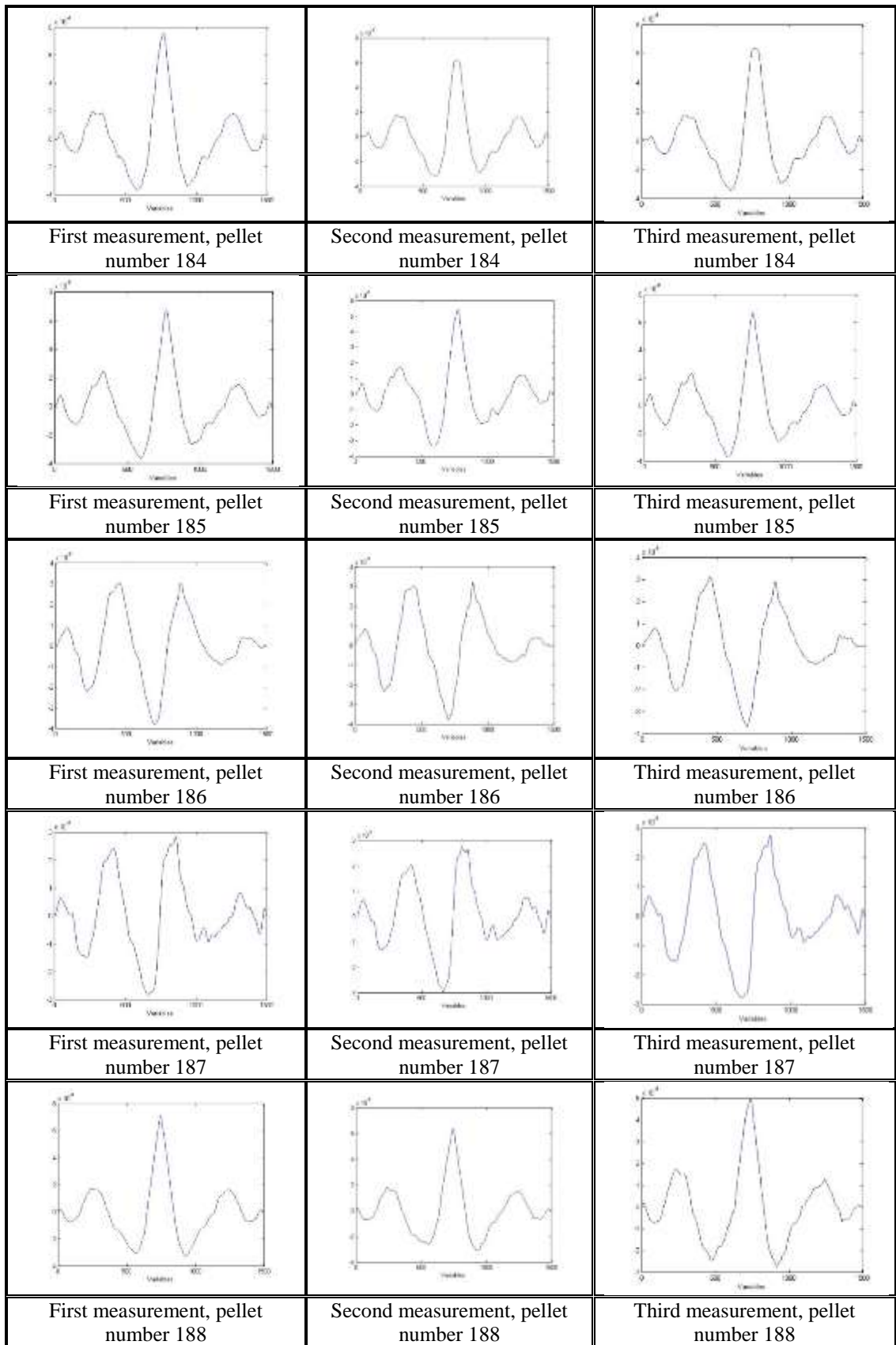


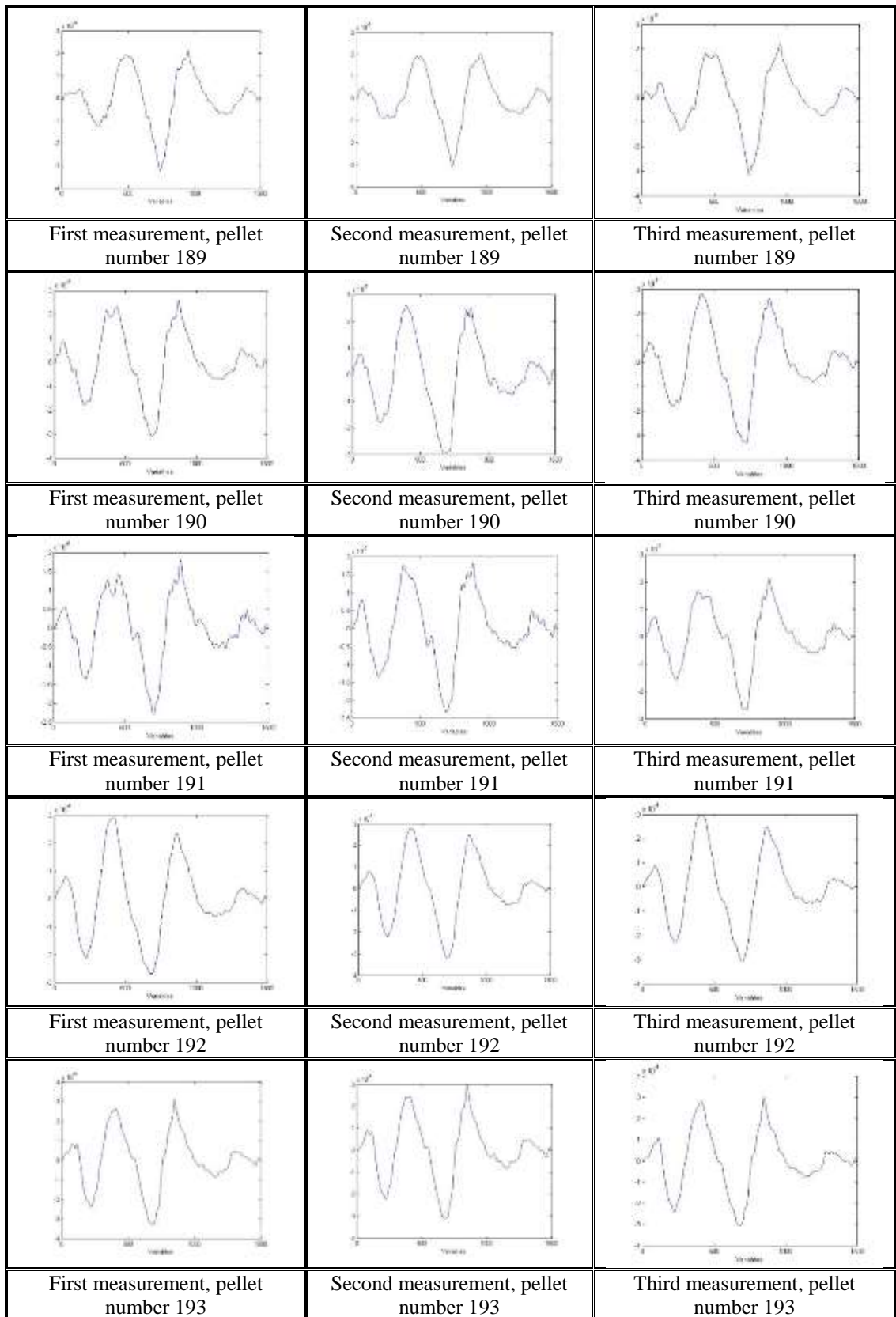


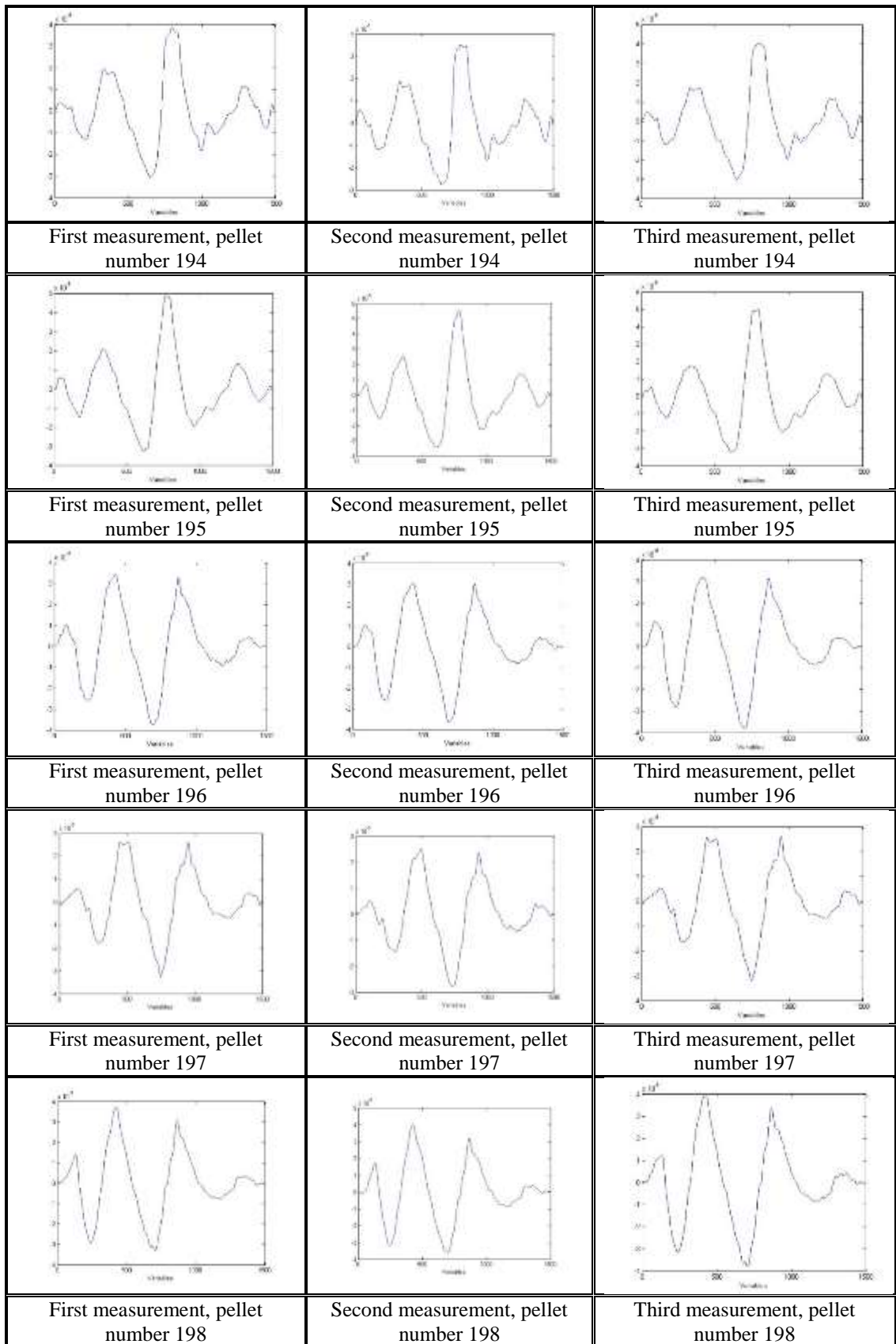


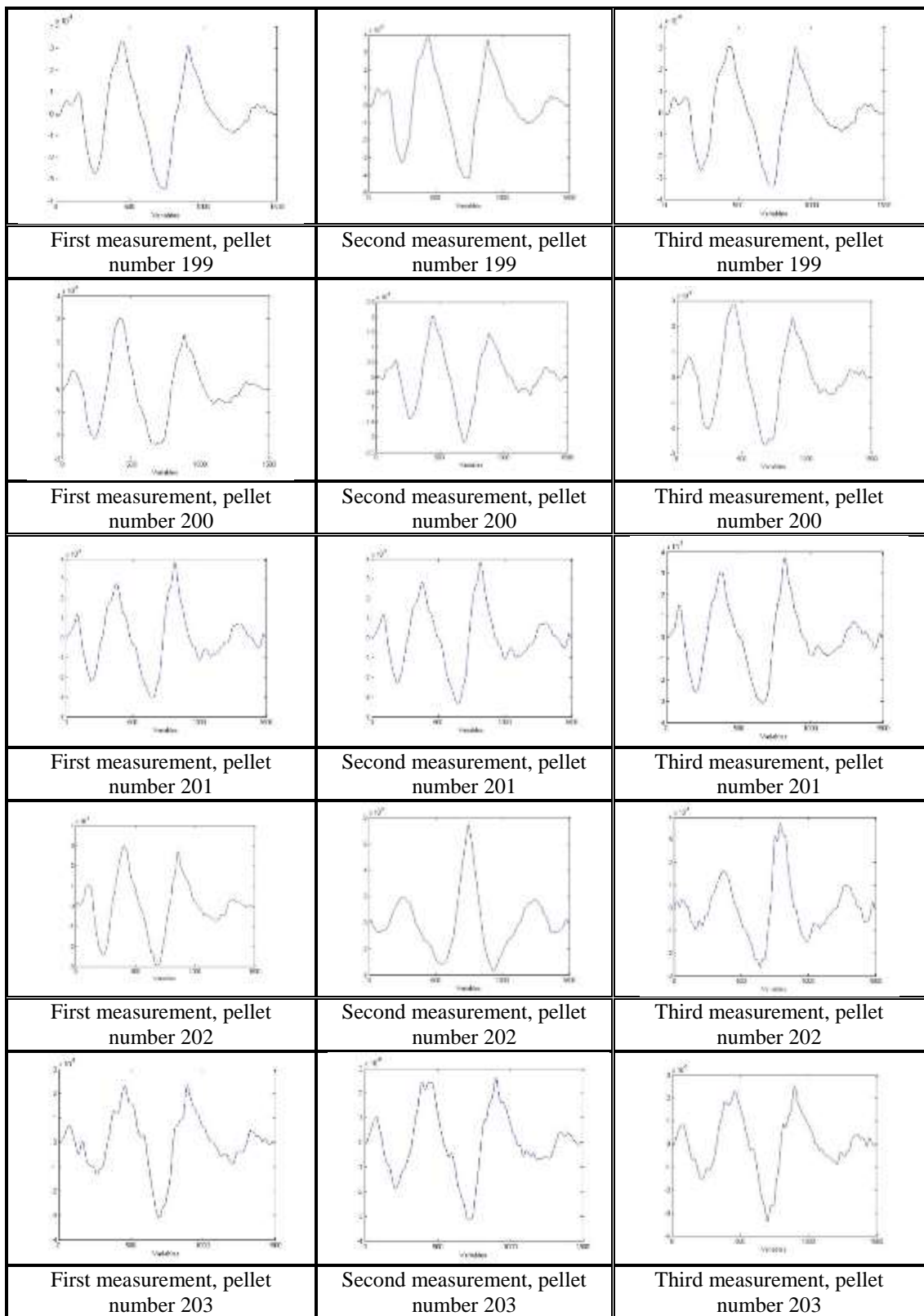


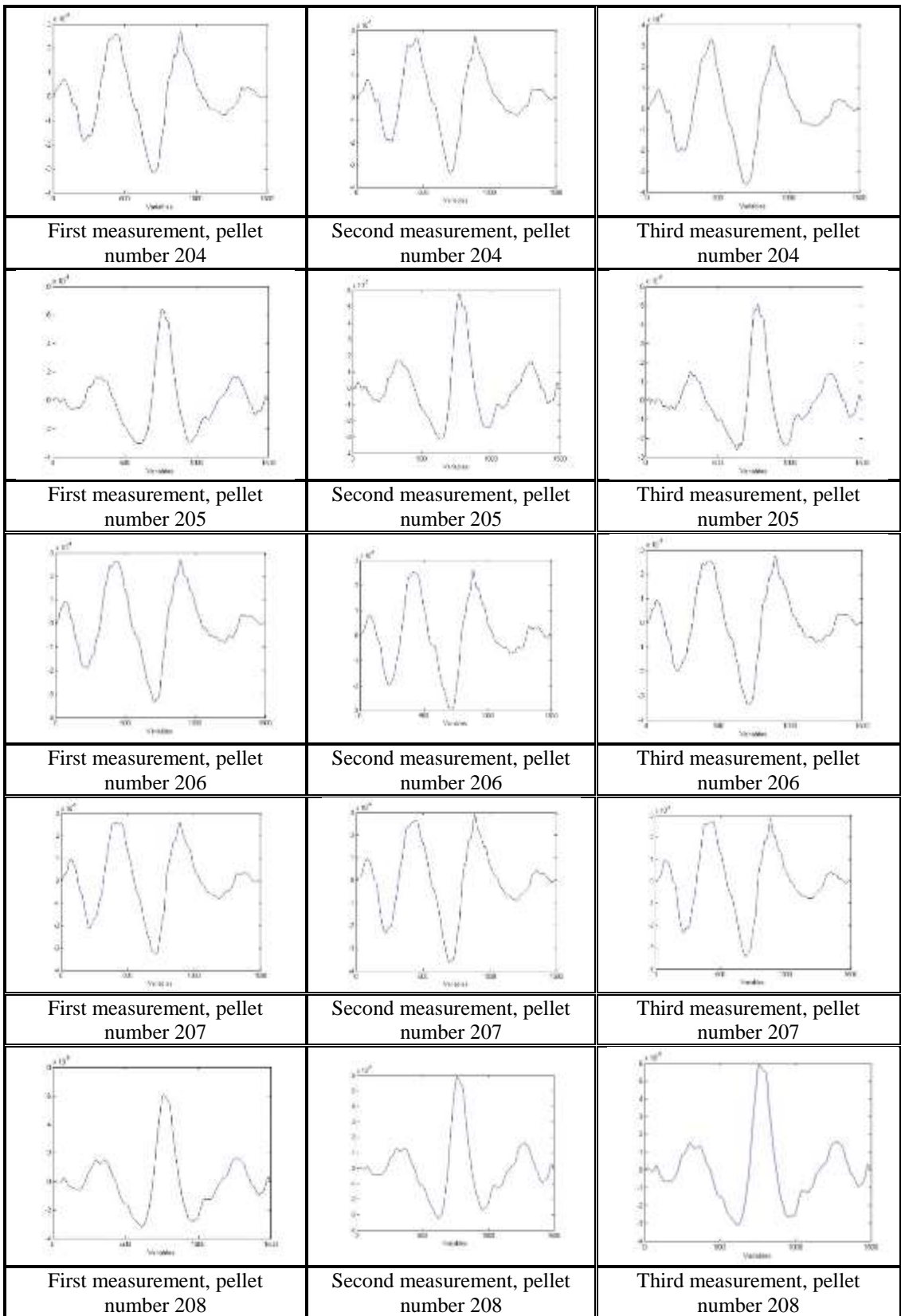
		
First measurement, pellet number 179	Second measurement, pellet number 179	Third measurement, pellet number 179
		
First measurement, pellet number 180	Second measurement, pellet number 180	Third measurement, pellet number 180
		
First measurement, pellet number 181	Second measurement, pellet number 181	Third measurement, pellet number 181
		
First measurement, pellet number 182	Second measurement, pellet number 182	Third measurement, pellet number 182
		
First measurement, pellet number 183	Second measurement, pellet number 183	Third measurement, pellet number 183







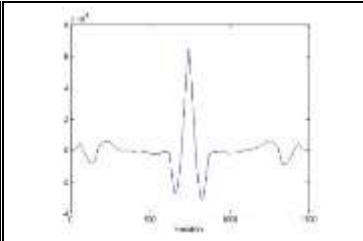
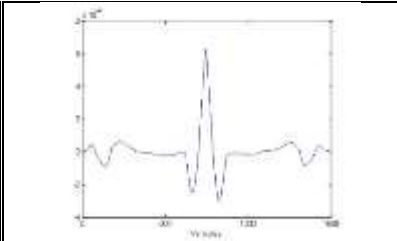
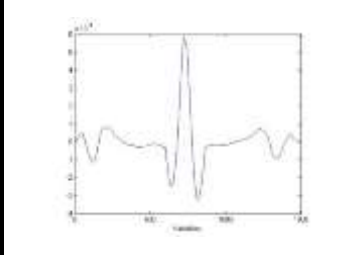
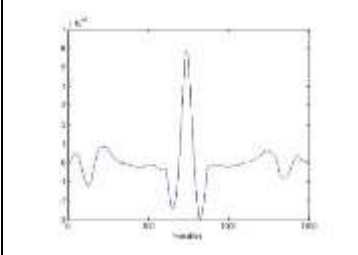
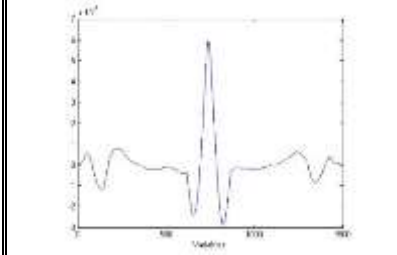
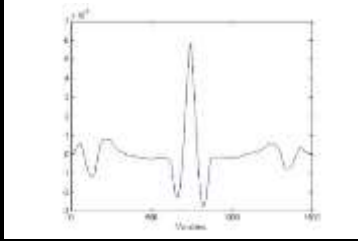
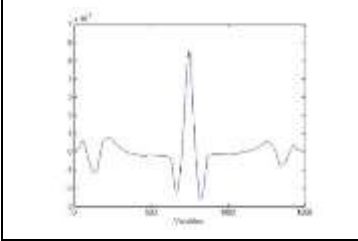
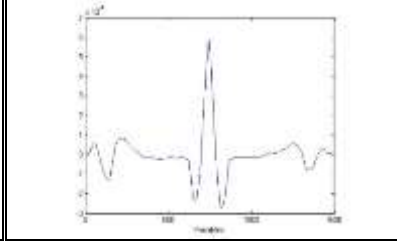
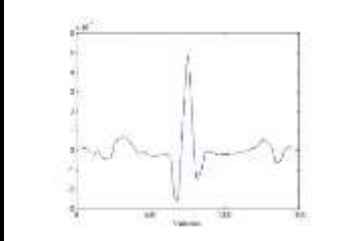
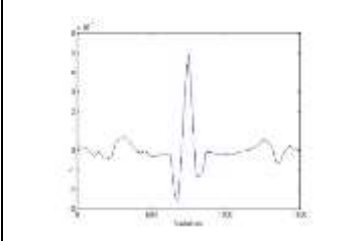
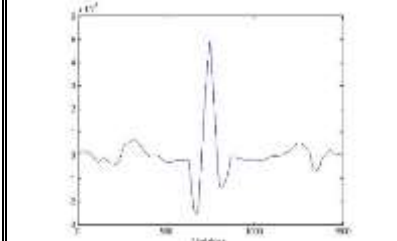
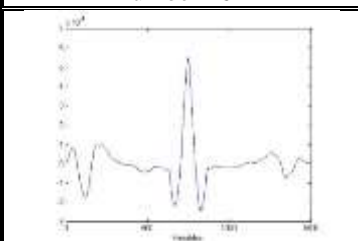
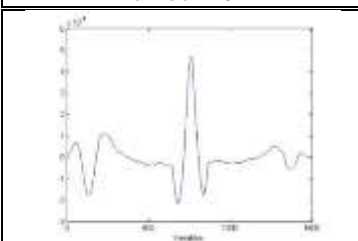
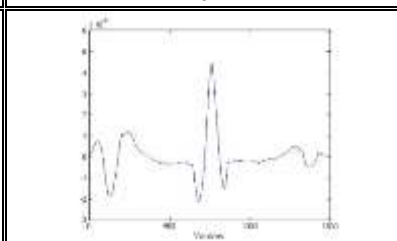


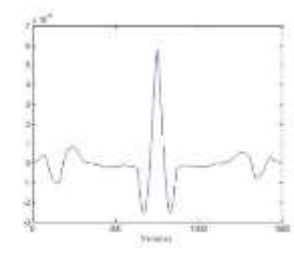
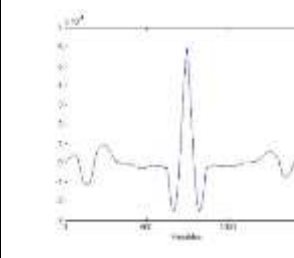
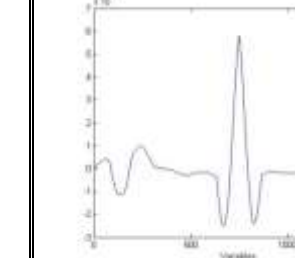
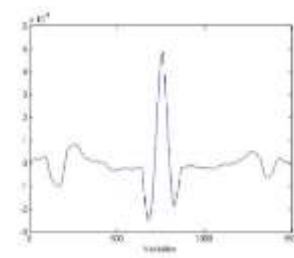
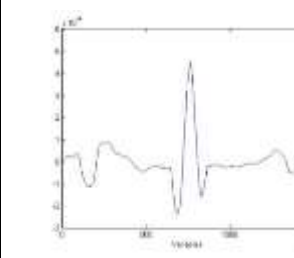
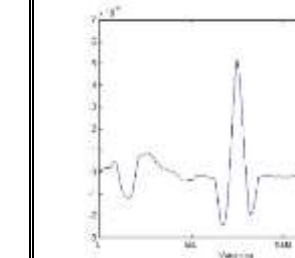
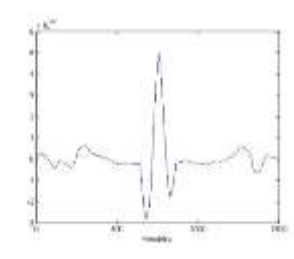
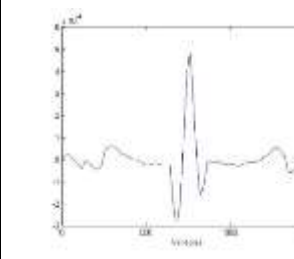
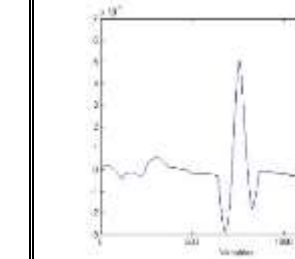
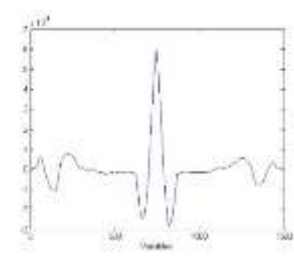
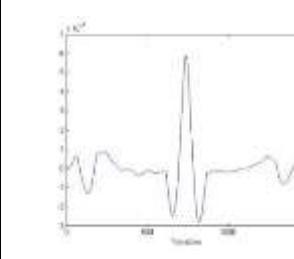
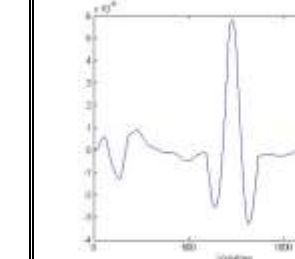
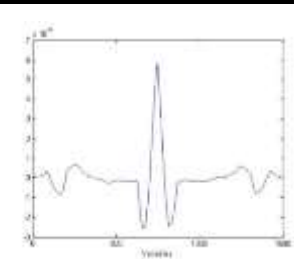
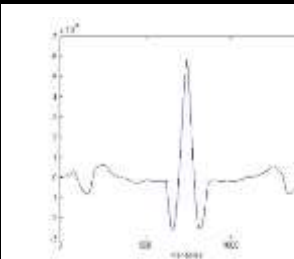
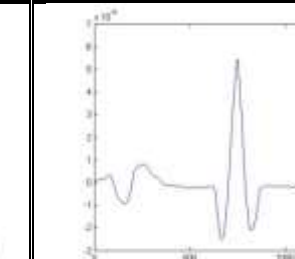




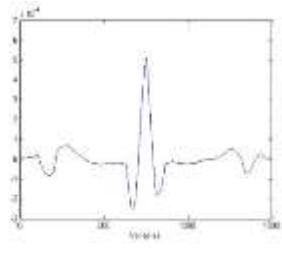
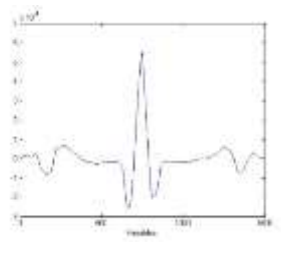
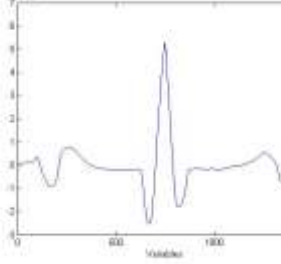
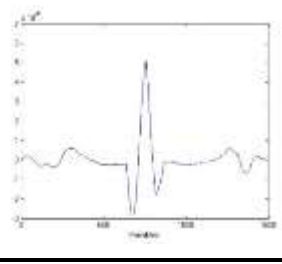
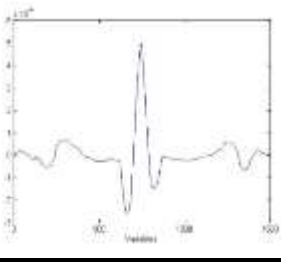
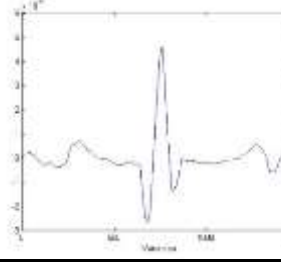
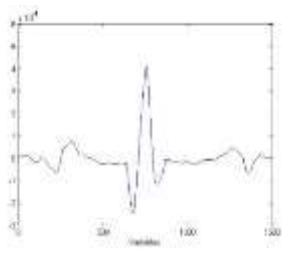
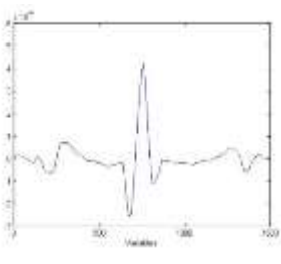
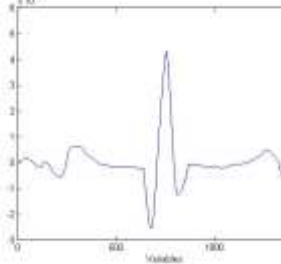
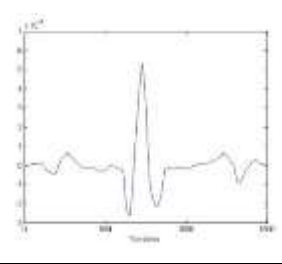
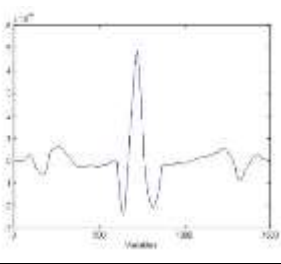
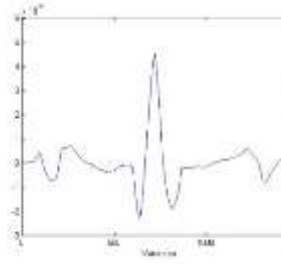
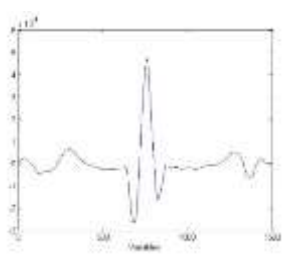
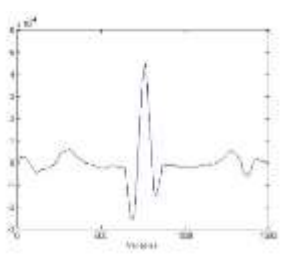
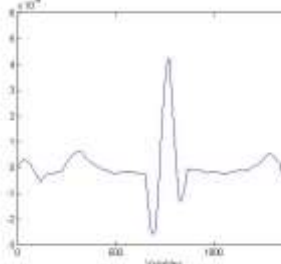
## Appendix 13

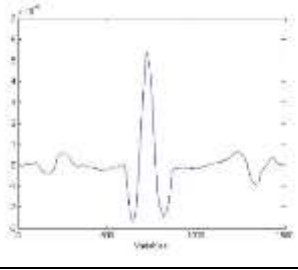
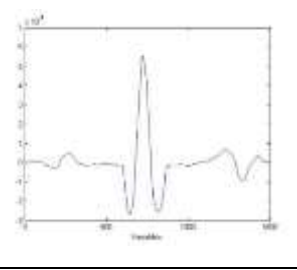
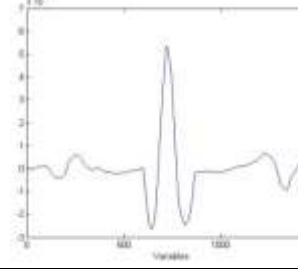
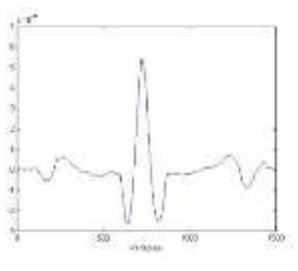
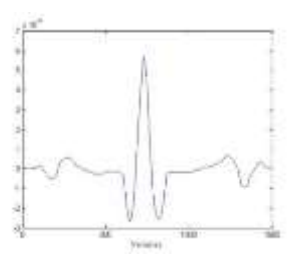
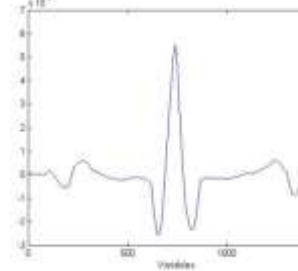
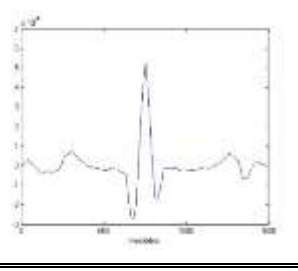
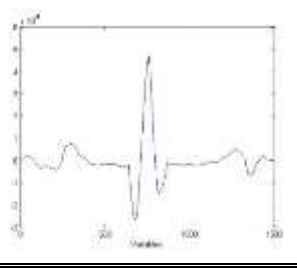
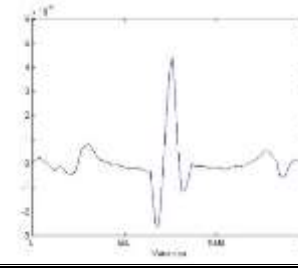
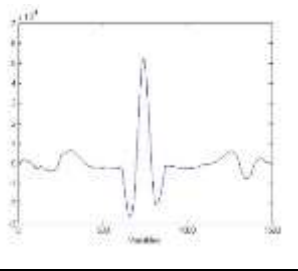
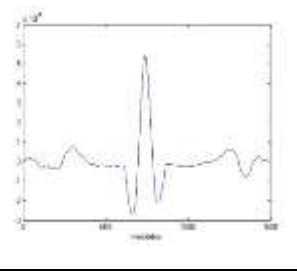
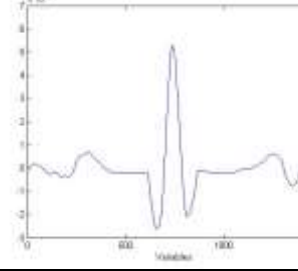
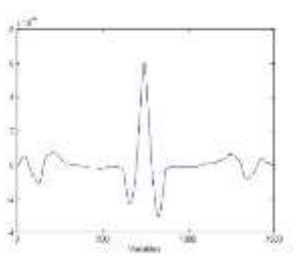
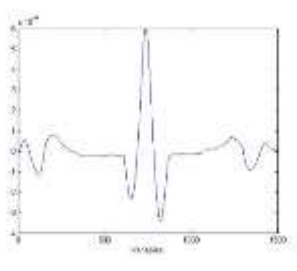
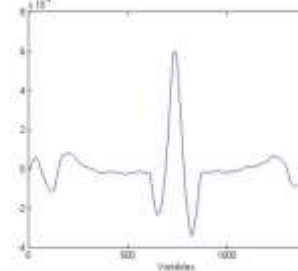
Alignment result for LEA J, pellet number 159 – 208

		
	Second measurement, pellet number 159	Third measurement, pellet number 159
		
First measurement, pellet number 160	Second measurement, pellet number 160	Third measurement, pellet number 160
		
First measurement, pellet number 161	Second measurement, pellet number 161	Third measurement, pellet number 161
		
First measurement, pellet number 162	Second measurement, pellet number 162	Third measurement, pellet number 162
		
First measurement, pellet number 163	Second measurement, pellet number 163	Third measurement, pellet number 163

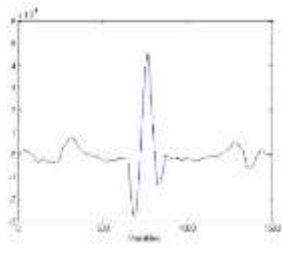
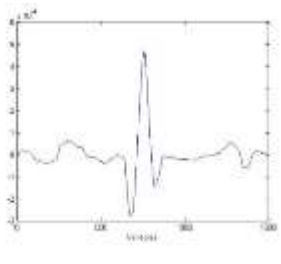
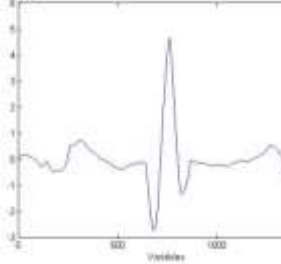
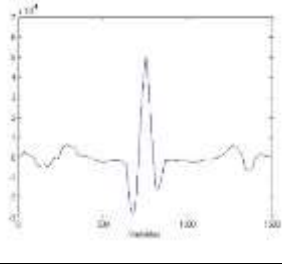
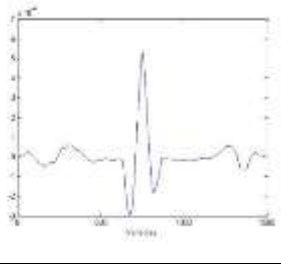
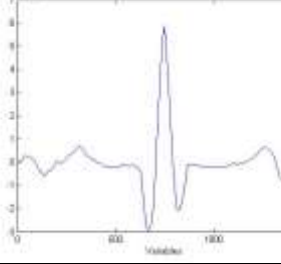
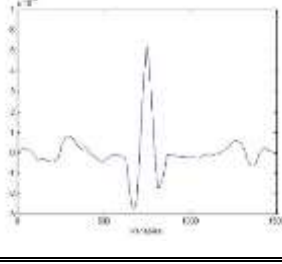
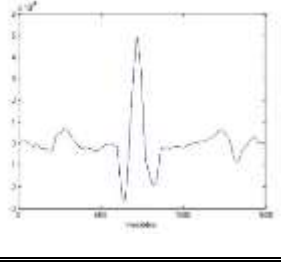
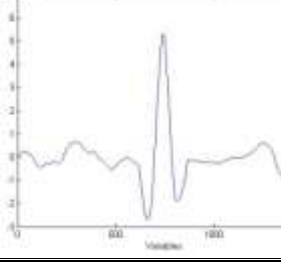
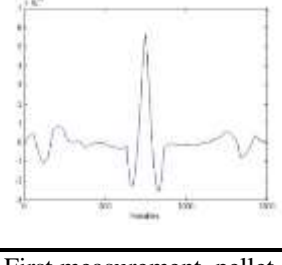
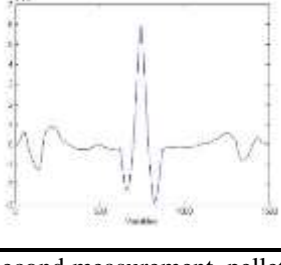
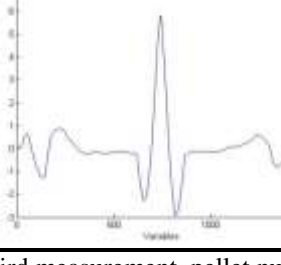
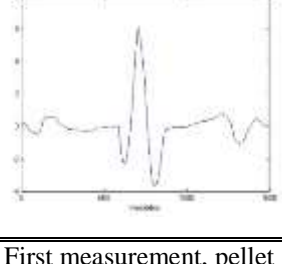
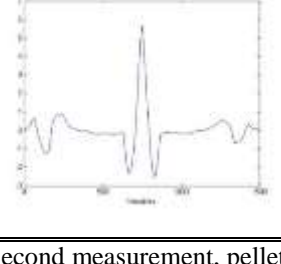
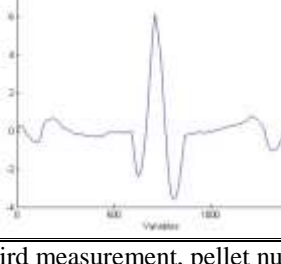
		
First measurement, pellet number 164	Second measurement, pellet number 164	Third measurement, pellet number 164
		
First measurement, pellet number 165	Second measurement, pellet number 165	Third measurement, pellet number 165
		
First measurement, pellet number 166	Second measurement, pellet number 166	Third measurement, pellet number 166
		
First measurement, pellet number 167	Second measurement, pellet number 167	Third measurement, pellet number 167
		
First measurement, pellet number 168	Second measurement, pellet number 168	Third measurement, pellet number 168

First measurement, pellet number 169	Second measurement, pellet number 169	Third measurement, pellet number 169
First measurement, pellet number 170	Second measurement, pellet number 170	Third measurement, pellet number 170
First measurement, pellet number 171	Second measurement, pellet number 171	Third measurement, pellet number 171
First measurement, pellet number 172	Second measurement, pellet number 172	Third measurement, pellet number 172
First measurement, pellet number 173	Second measurement, pellet number 173	Third measurement, pellet number 173

		
First measurement, pellet number 174	Second measurement, pellet number 174	Third measurement, pellet number 174
		
First measurement, pellet number 175	Second measurement, pellet number 175	Third measurement, pellet number 175
		
First measurement, pellet number 176	Second measurement, pellet number 176	Third measurement, pellet number 176
		
First measurement, pellet number 177	Second measurement, pellet number 177	Third measurement, pellet number 177
		
First measurement, pellet number 178	Second measurement, pellet number 178	Third measurement, pellet number 178

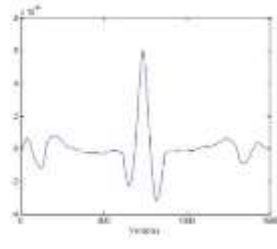
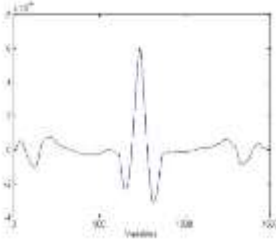
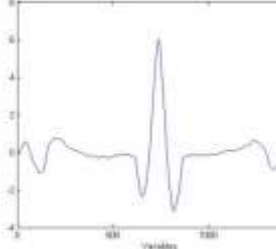
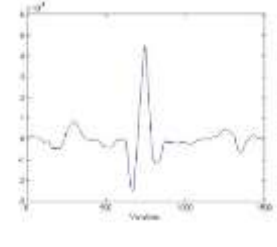
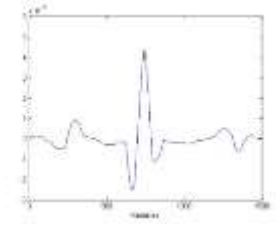
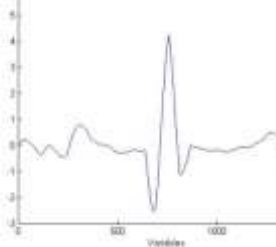
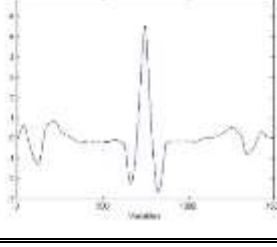
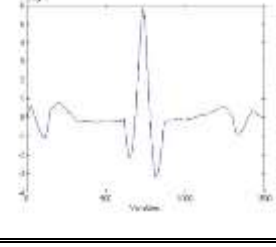
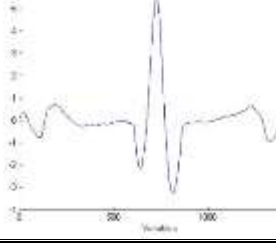
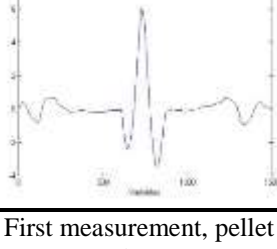
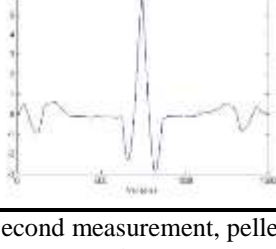
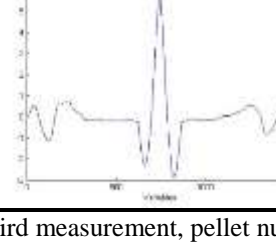
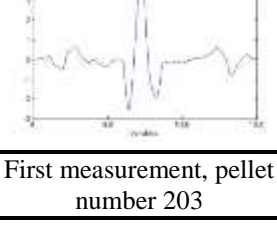
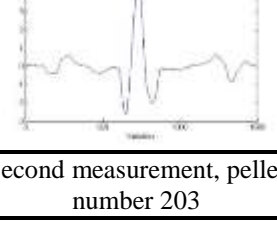
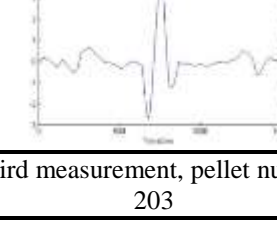
		
First measurement, pellet number 179	Second measurement, pellet number 179	Third measurement, pellet number 179
		
First measurement, pellet number 180	Second measurement, pellet number 180	Third measurement, pellet number 180
		
First measurement, pellet number 181	Second measurement, pellet number 181	Third measurement, pellet number 181
		
First measurement, pellet number 182	Second measurement, pellet number 182	Third measurement, pellet number 182
		
First measurement, pellet number 183	Second measurement, pellet number 183	Third measurement, pellet number 183

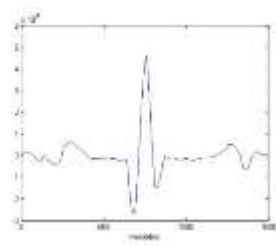
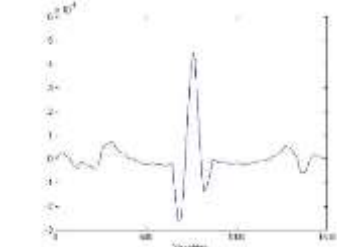
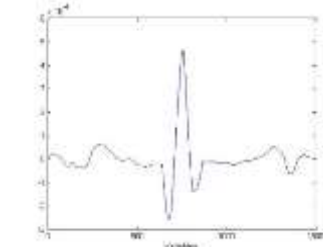
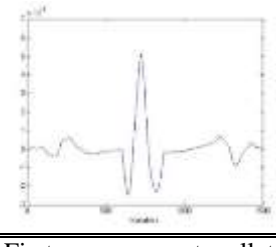
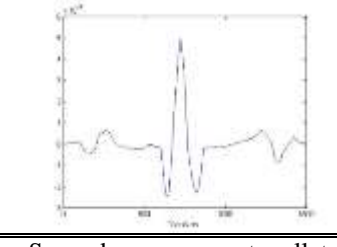
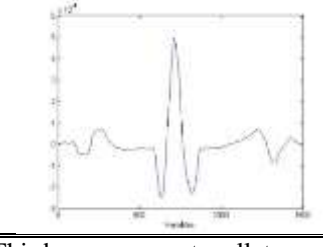
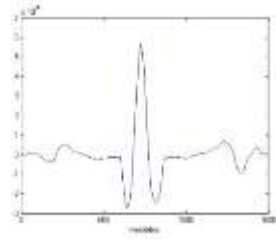
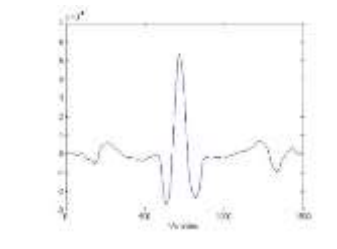
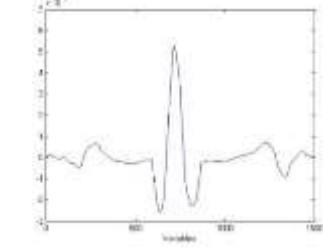
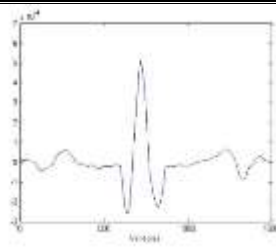
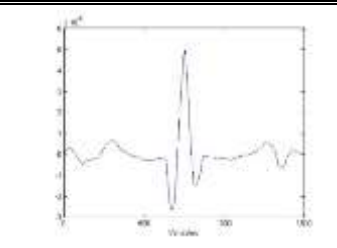
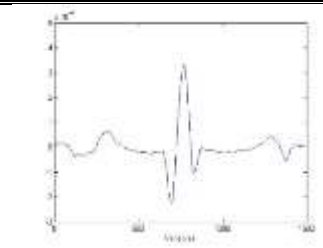
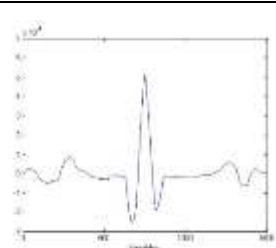
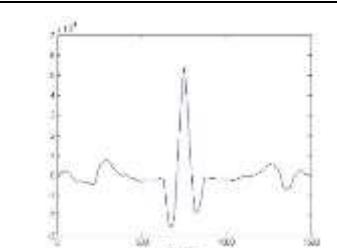
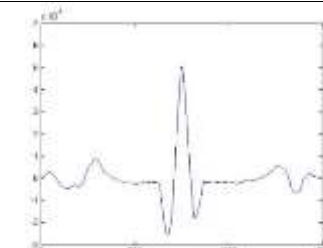
First measurement, pellet number 184	Second measurement, pellet number 184	Third measurement, pellet number 184
First measurement, pellet number 185	Second measurement, pellet number 185	Third measurement, pellet number 185
First measurement, pellet number 186	Second measurement, pellet number 186	Third measurement, pellet number 186
First measurement, pellet number 187	Second measurement, pellet number 187	Third measurement, pellet number 187
First measurement, pellet number 188	Second measurement, pellet number 188	Third measurement, pellet number 188

		
First measurement, pellet number 189	Second measurement, pellet number 189	Third measurement, pellet number 189
		
First measurement, pellet number 190	Second measurement, pellet number 190	Third measurement, pellet number 190
		
First measurement, pellet number 191	Second measurement, pellet number 191	Third measurement, pellet number 191
		
First measurement, pellet number 192	Second measurement, pellet number 192	Third measurement, pellet number 192
		
First measurement, pellet number 193	Second measurement, pellet number 193	Third measurement, pellet number 193

First measurement, pellet number 194	Second measurement, pellet number 194	Third measurement, pellet number 194
First measurement, pellet number 195	Second measurement, pellet number 195	Third measurement, pellet number 195
First measurement, pellet number 196	Second measurement, pellet number 196	Third measurement, pellet number 196
First measurement, pellet number 197	Second measurement, pellet number 197	Third measurement, pellet number 197
First measurement, pellet number 198	Second measurement, pellet number 198	Third measurement, pellet number 198

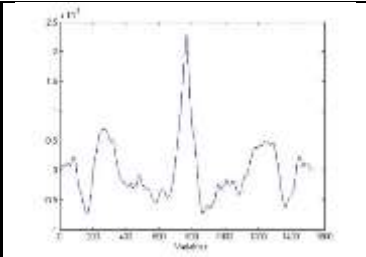
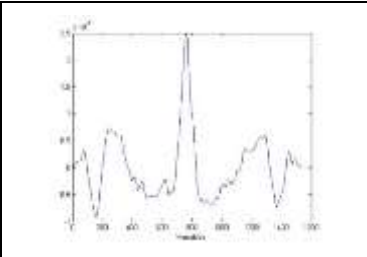
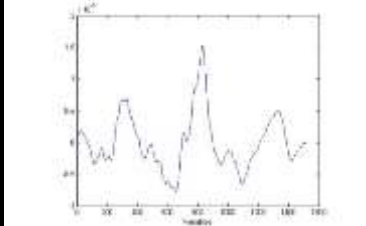
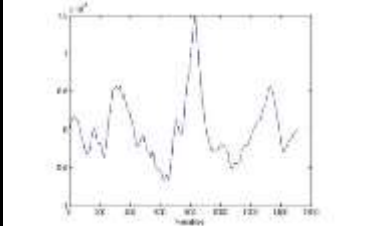
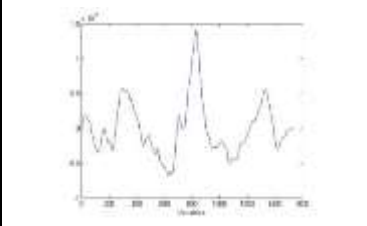
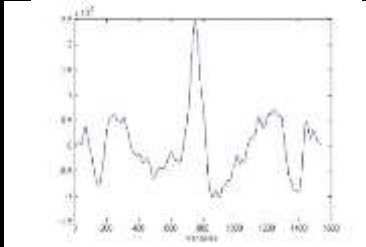
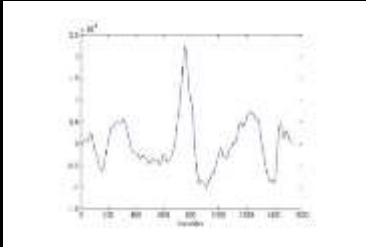
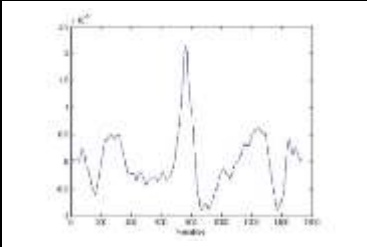
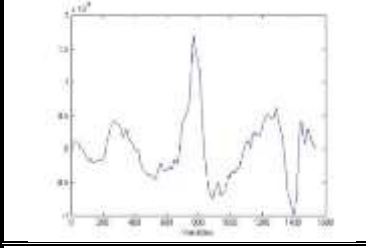
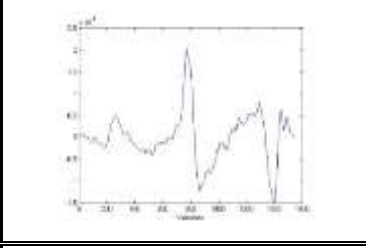
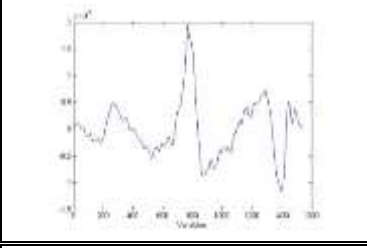
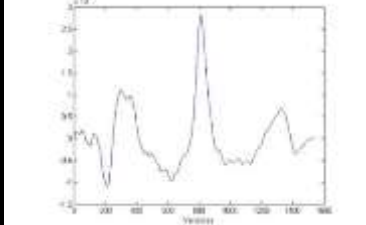
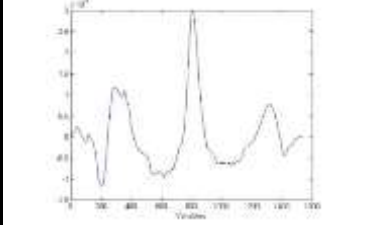
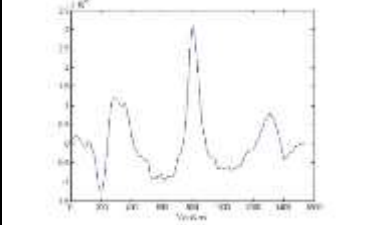


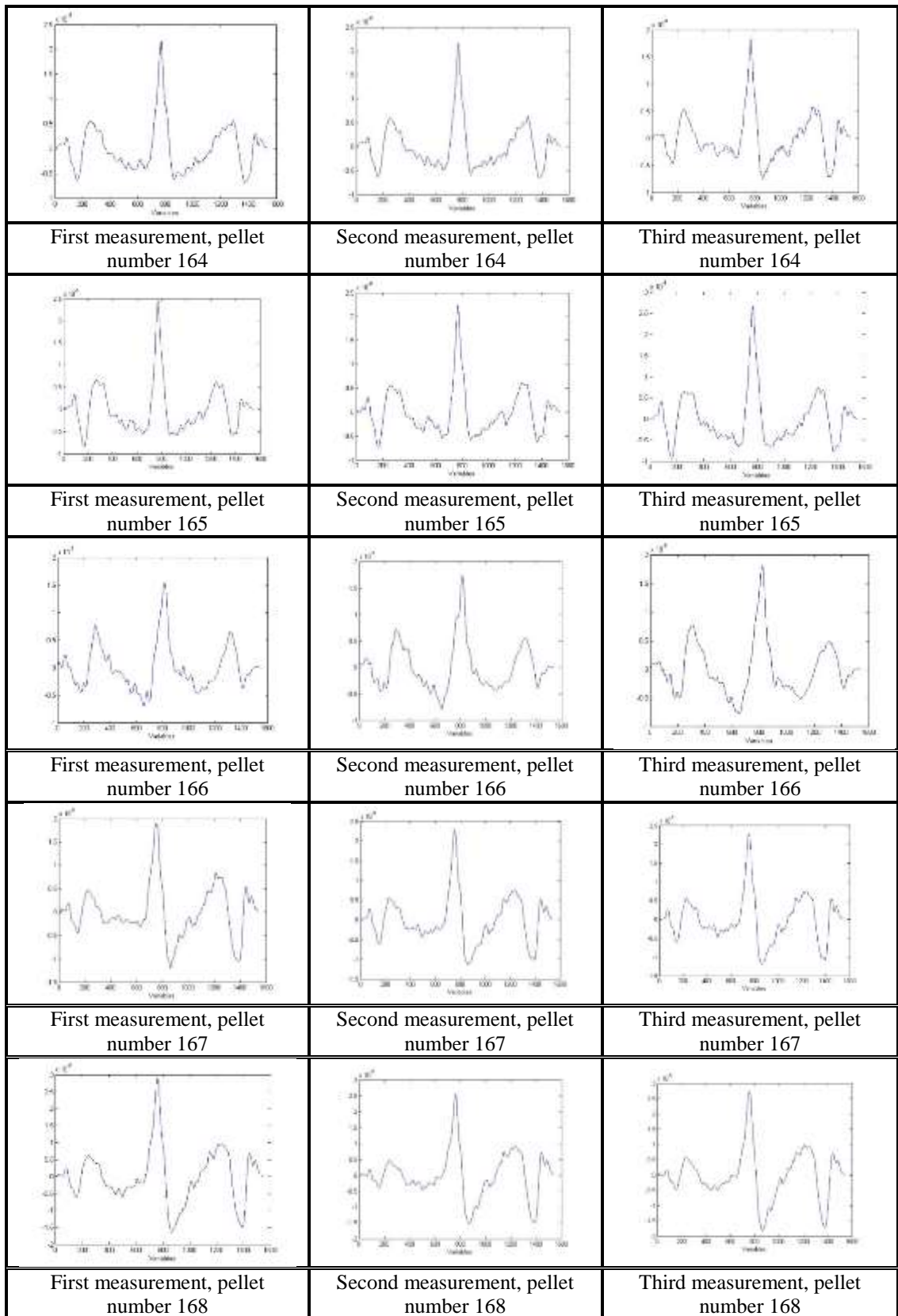
		
First measurement, pellet number 199	Second measurement, pellet number 199	Third measurement, pellet number 199
		
First measurement, pellet number 200	Second measurement, pellet number 200	Third measurement, pellet number 200
		
First measurement, pellet number 201	Second measurement, pellet number 201	Third measurement, pellet number 201
		
First measurement, pellet number 202	Second measurement, pellet number 202	Third measurement, pellet number 202
		
First measurement, pellet number 203	Second measurement, pellet number 203	Third measurement, pellet number 203

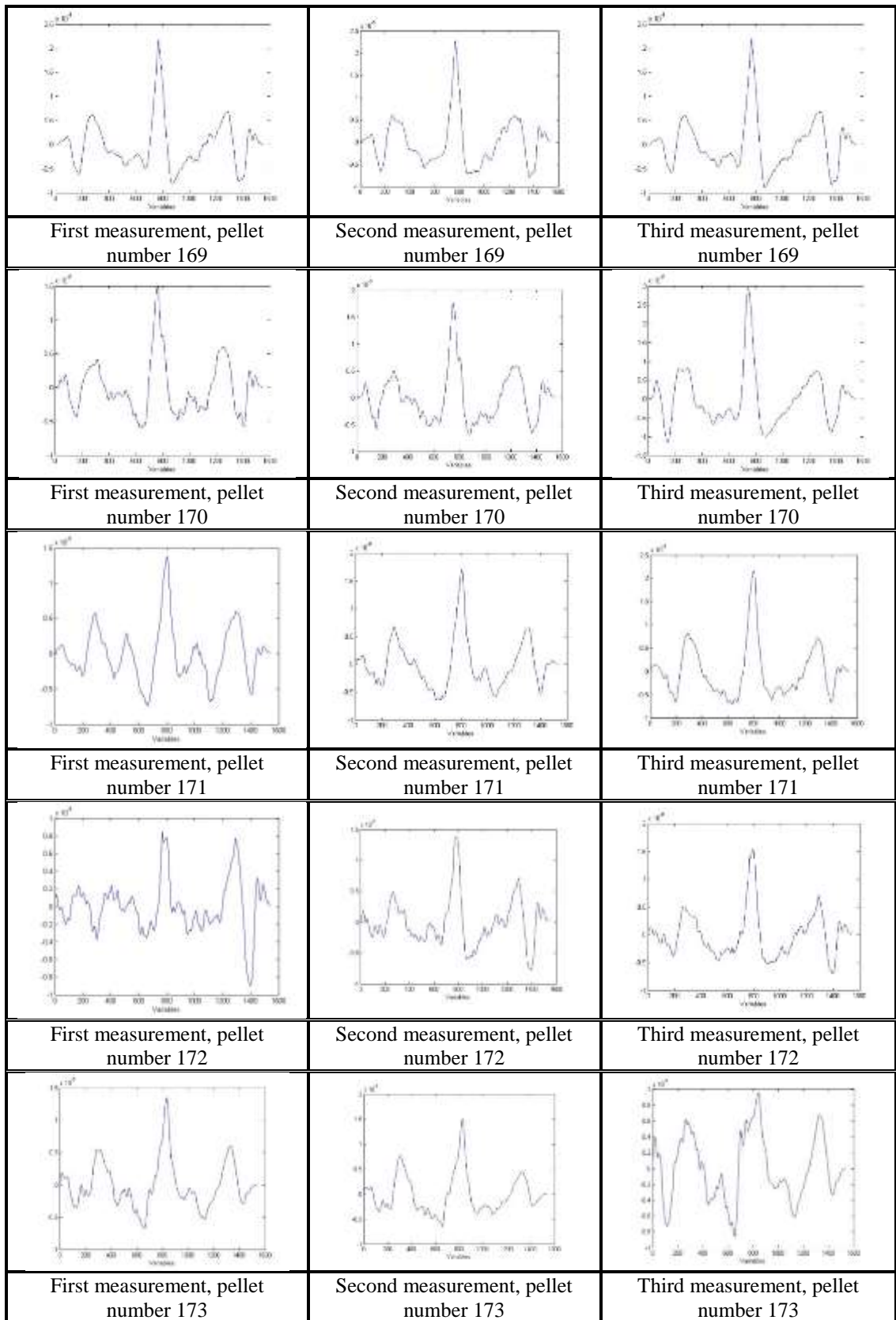
		
First measurement, pellet number 204	Second measurement, pellet number 204	Third measurement, pellet number 204
		
First measurement, pellet number 205	Second measurement, pellet number 205	Third measurement, pellet number 205
		
First measurement, pellet number 206	Second measurement, pellet number 206	Third measurement, pellet number 206
		
First measurement, pellet number 207	Second measurement, pellet number 207	Third measurement, pellet number 207
		
First measurement, pellet number 208	Second measurement, pellet number 208	Third measurement, pellet number 208

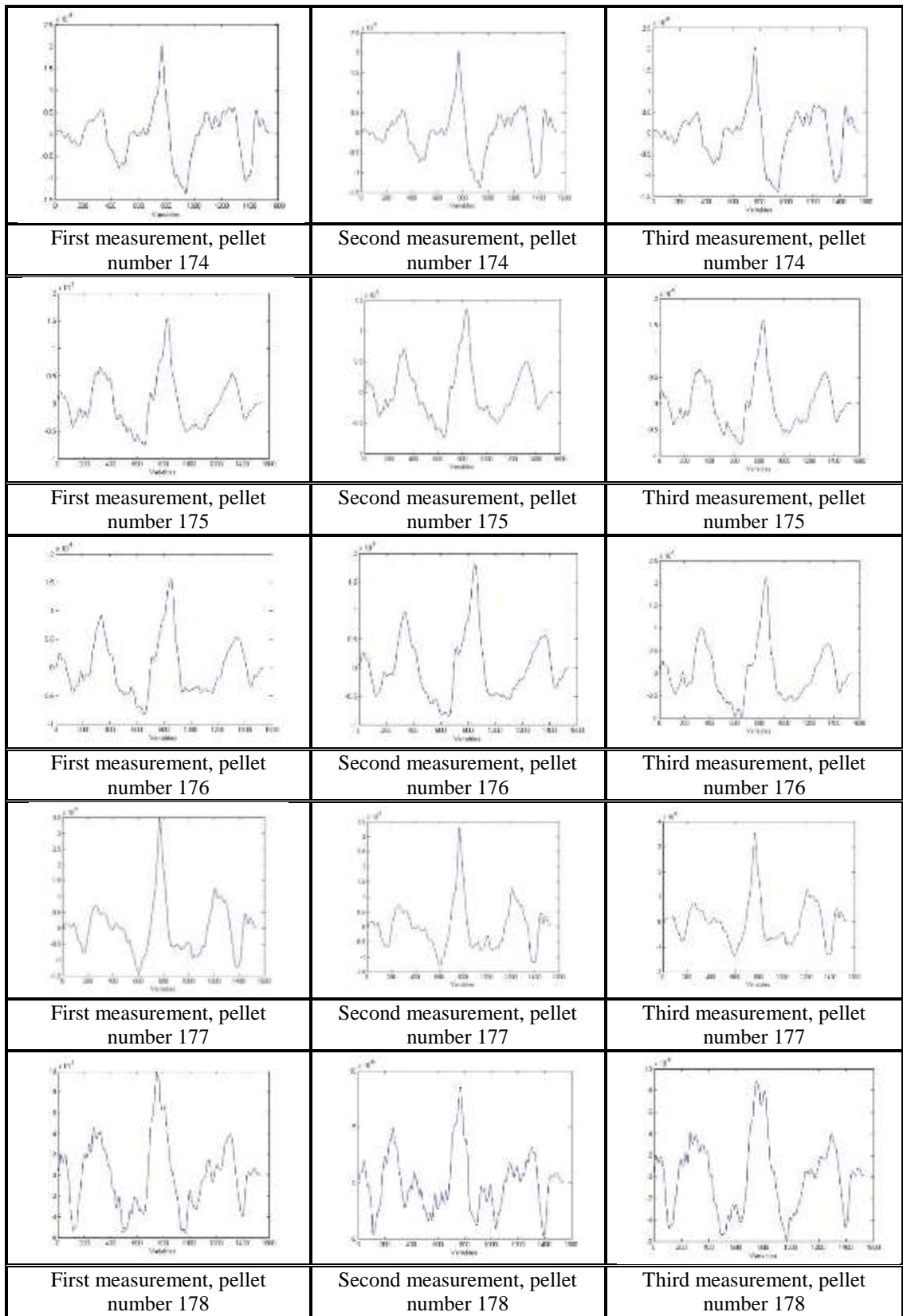
## Appendix 14

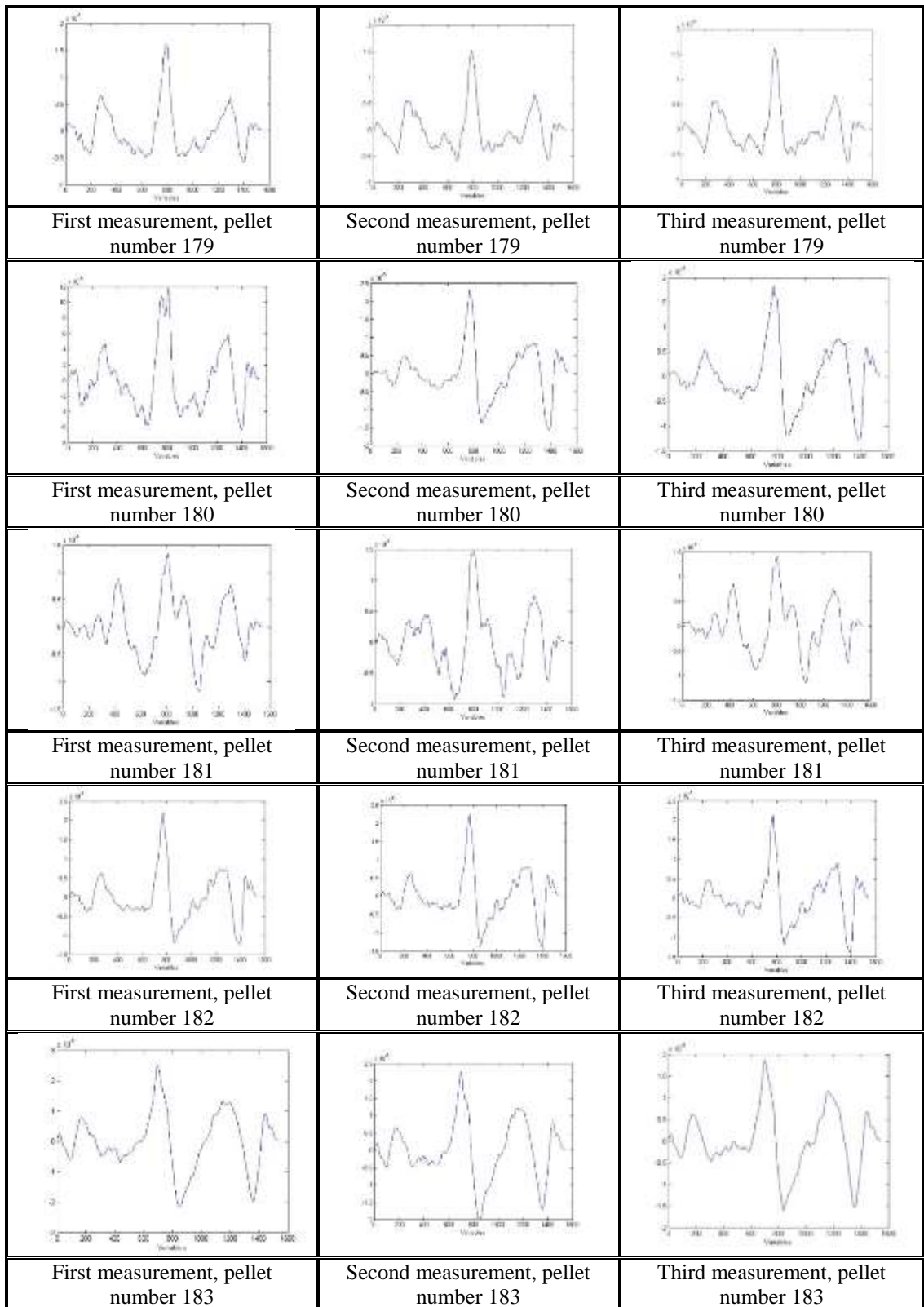
Alignment result for LEA K, pellet number 159 – 208

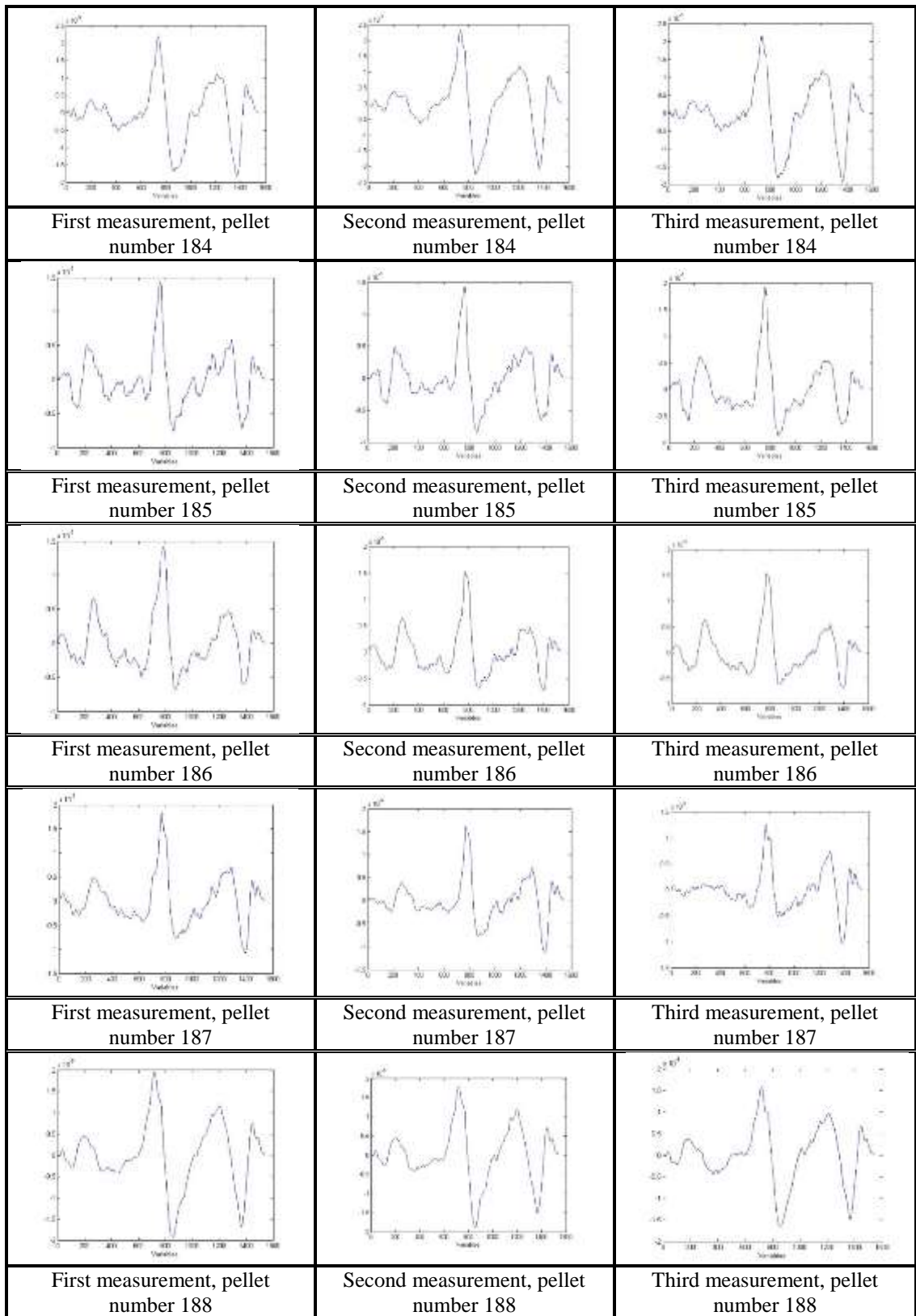
		
	Second measurement, pellet number 159	Third measurement, pellet number 159
		
First measurement, pellet number 160	Second measurement, pellet number 160	Third measurement, pellet number 160
		
First measurement, pellet number 161	Second measurement, pellet number 161	Third measurement, pellet number 161
		
First measurement, pellet number 162	Second measurement, pellet number 162	Third measurement, pellet number 162
		
First measurement, pellet number 163	Second measurement, pellet number 163	Third measurement, pellet number 163



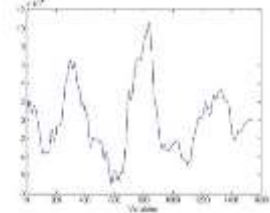
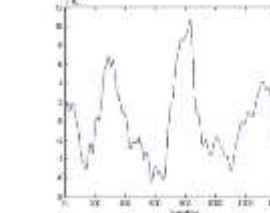
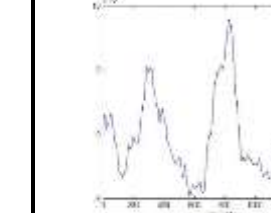
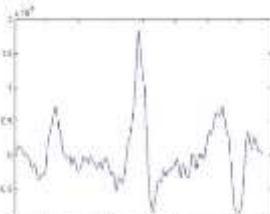
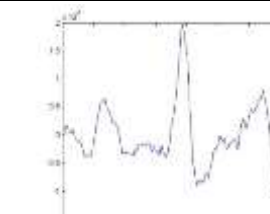
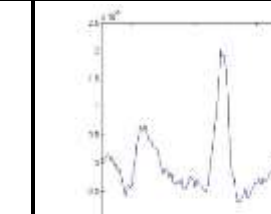
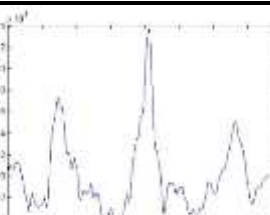
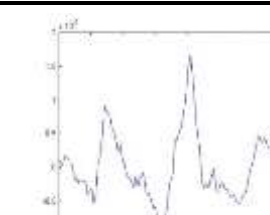
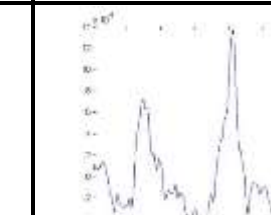

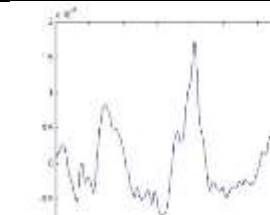
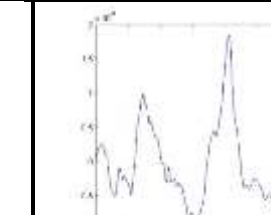
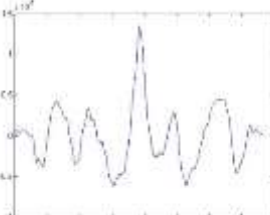
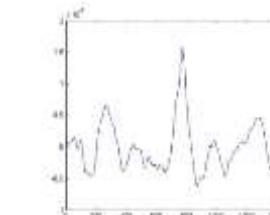
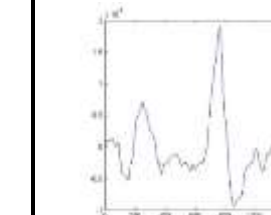


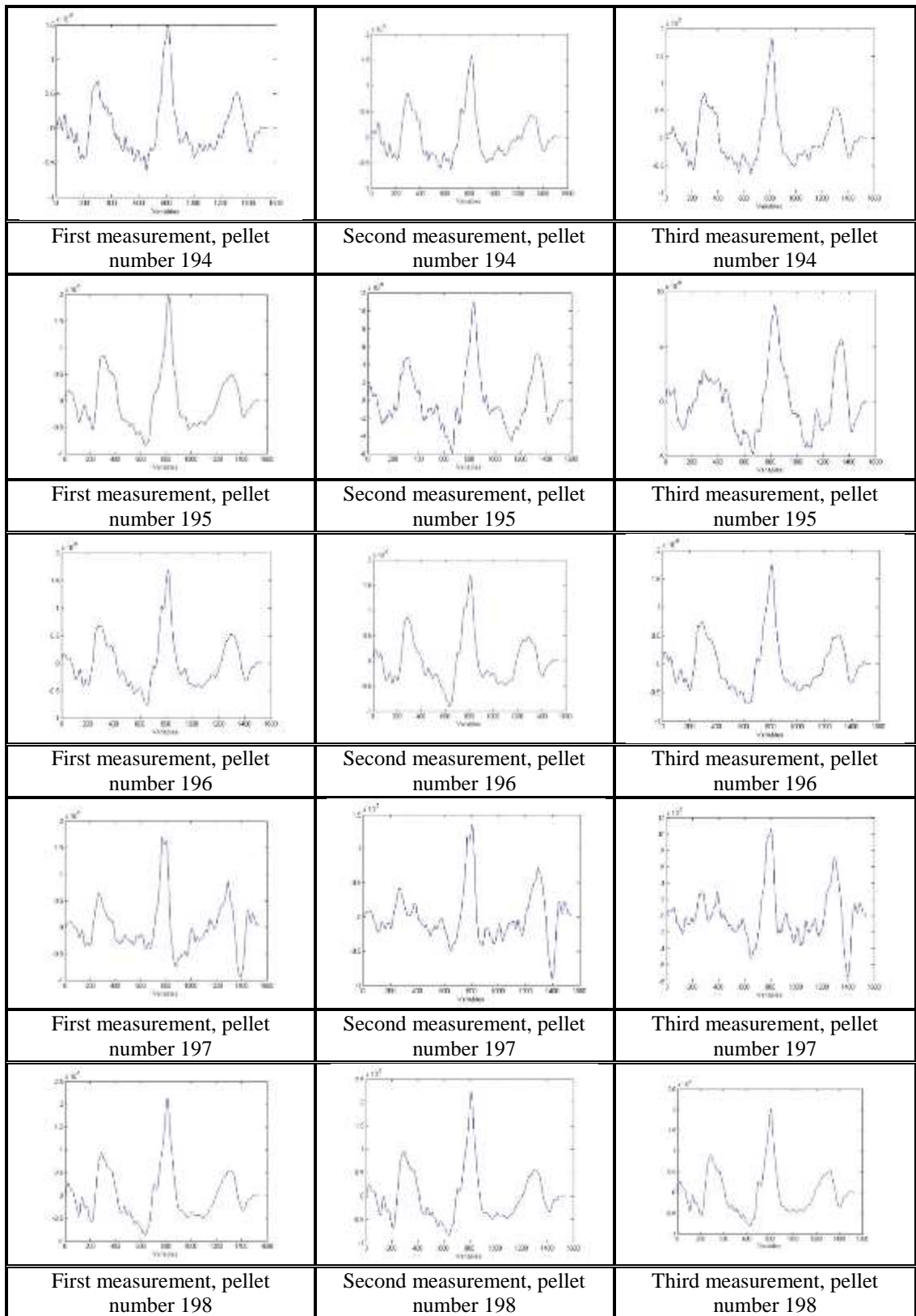


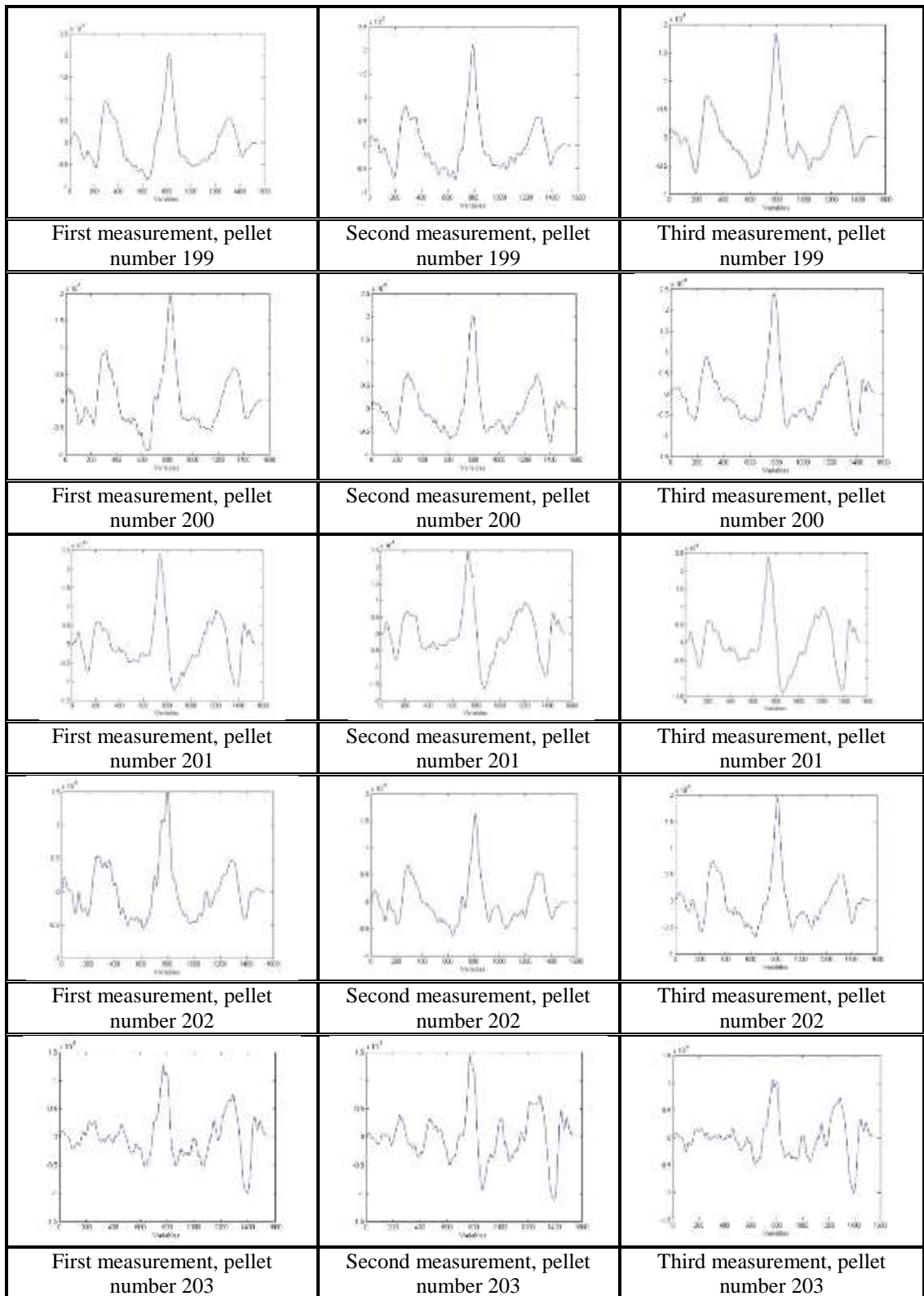


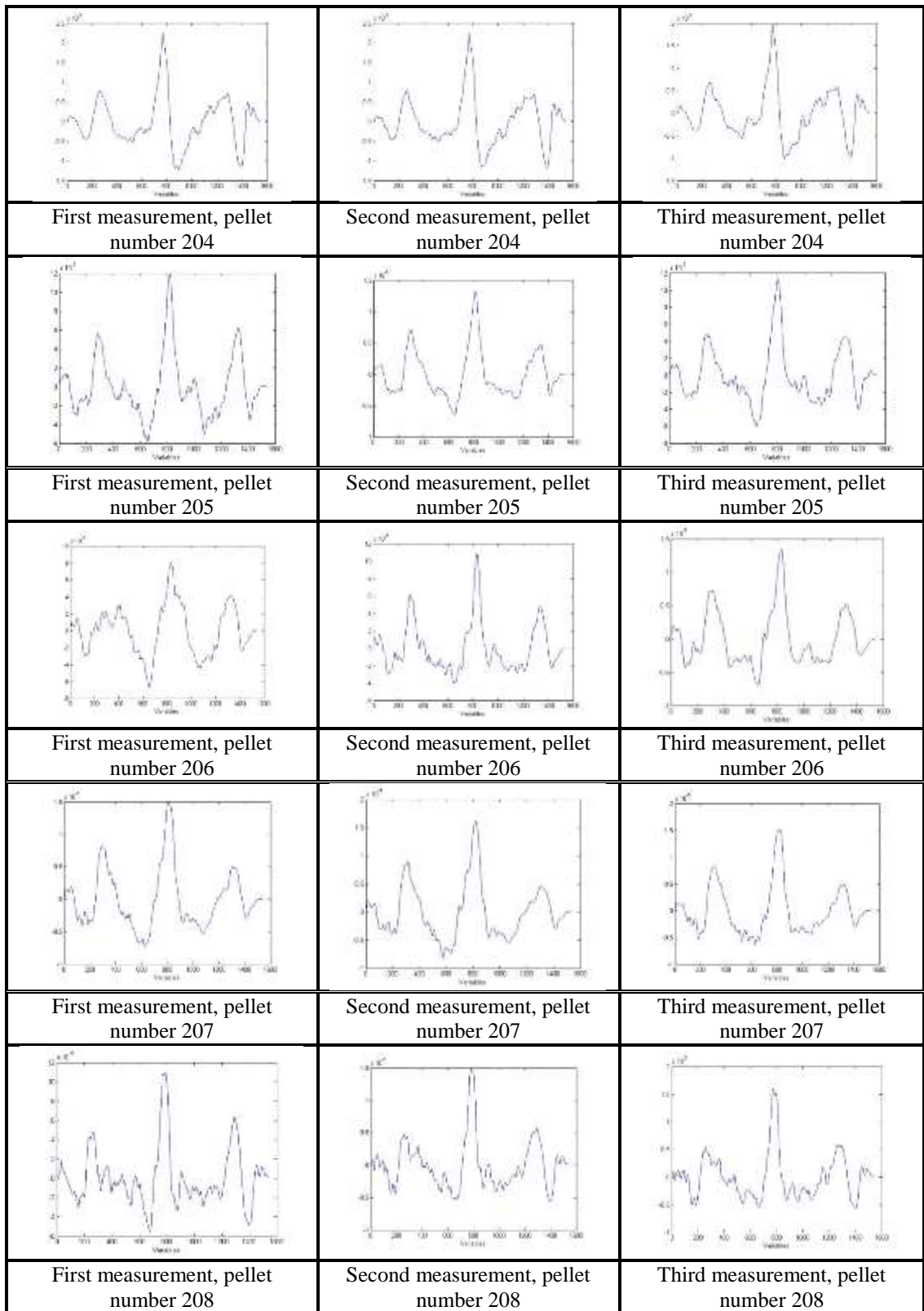




		
First measurement, pellet number 189	Second measurement, pellet number 189	Third measurement, pellet number 189
		
First measurement, pellet number 190	Second measurement, pellet number 190	Third measurement, pellet number 190
		
First measurement, pellet number 191	Second measurement, pellet number 191	Third measurement, pellet number 191
		
First measurement, pellet number 192	Second measurement, pellet number 192	Third measurement, pellet number 192
		
First measurement, pellet number 193	Second measurement, pellet number 193	Third measurement, pellet number 193

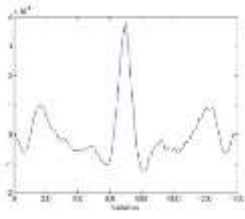
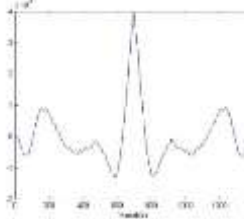
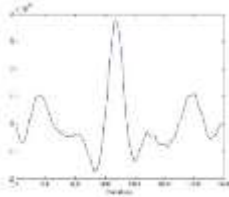
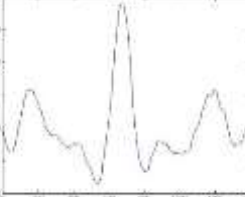
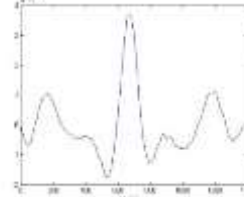
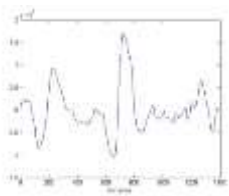
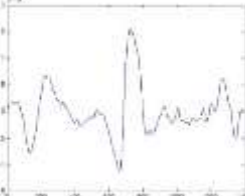
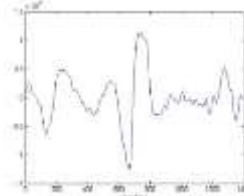
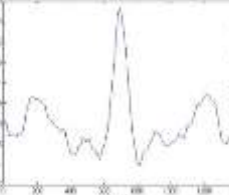
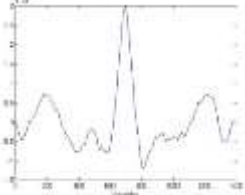
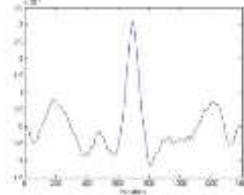
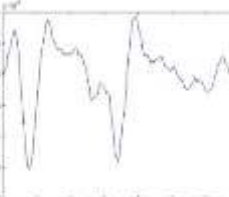
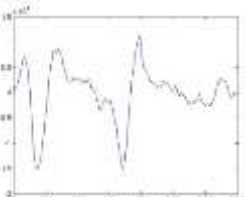
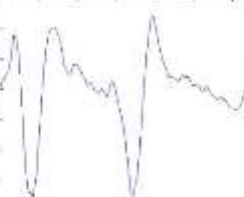


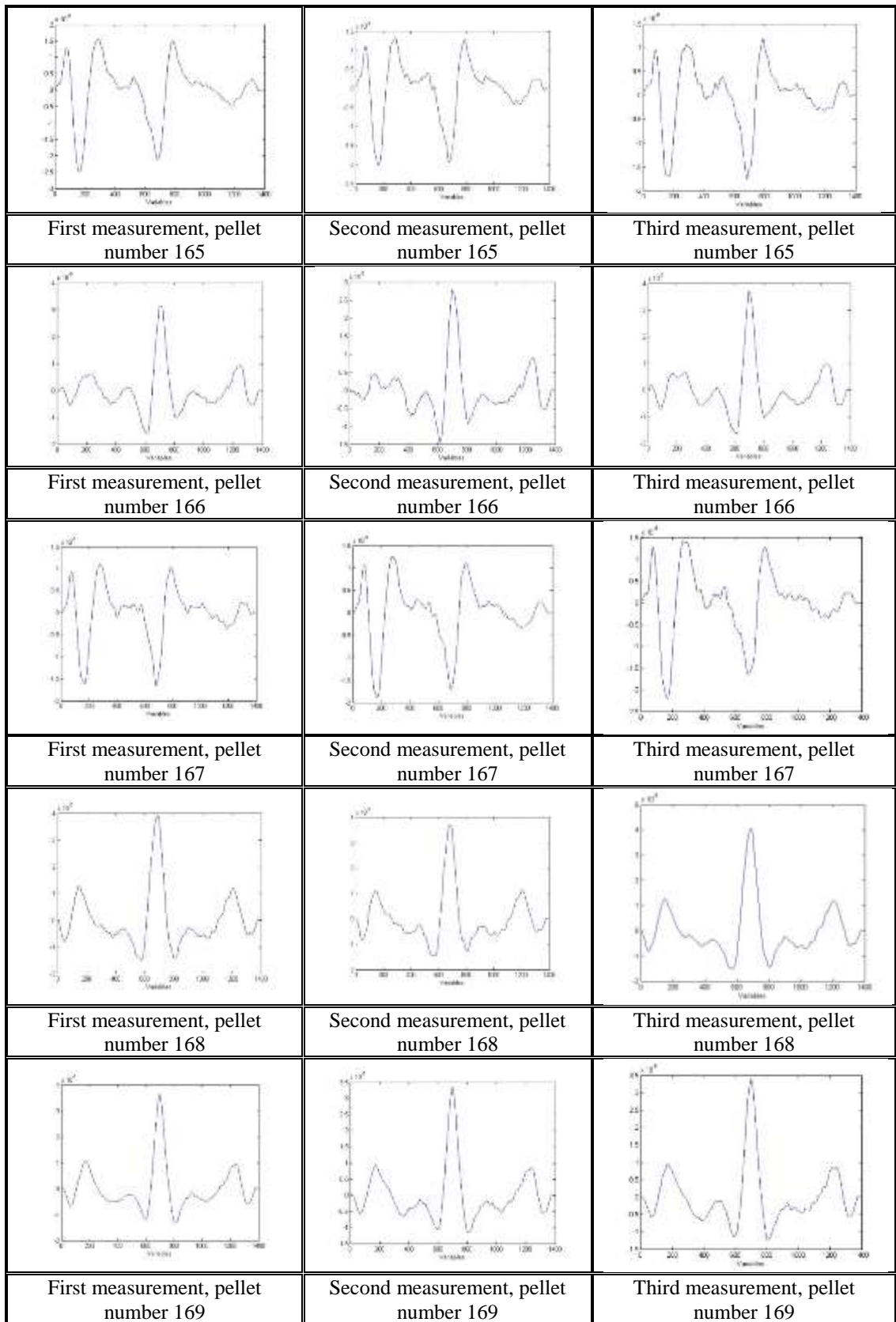


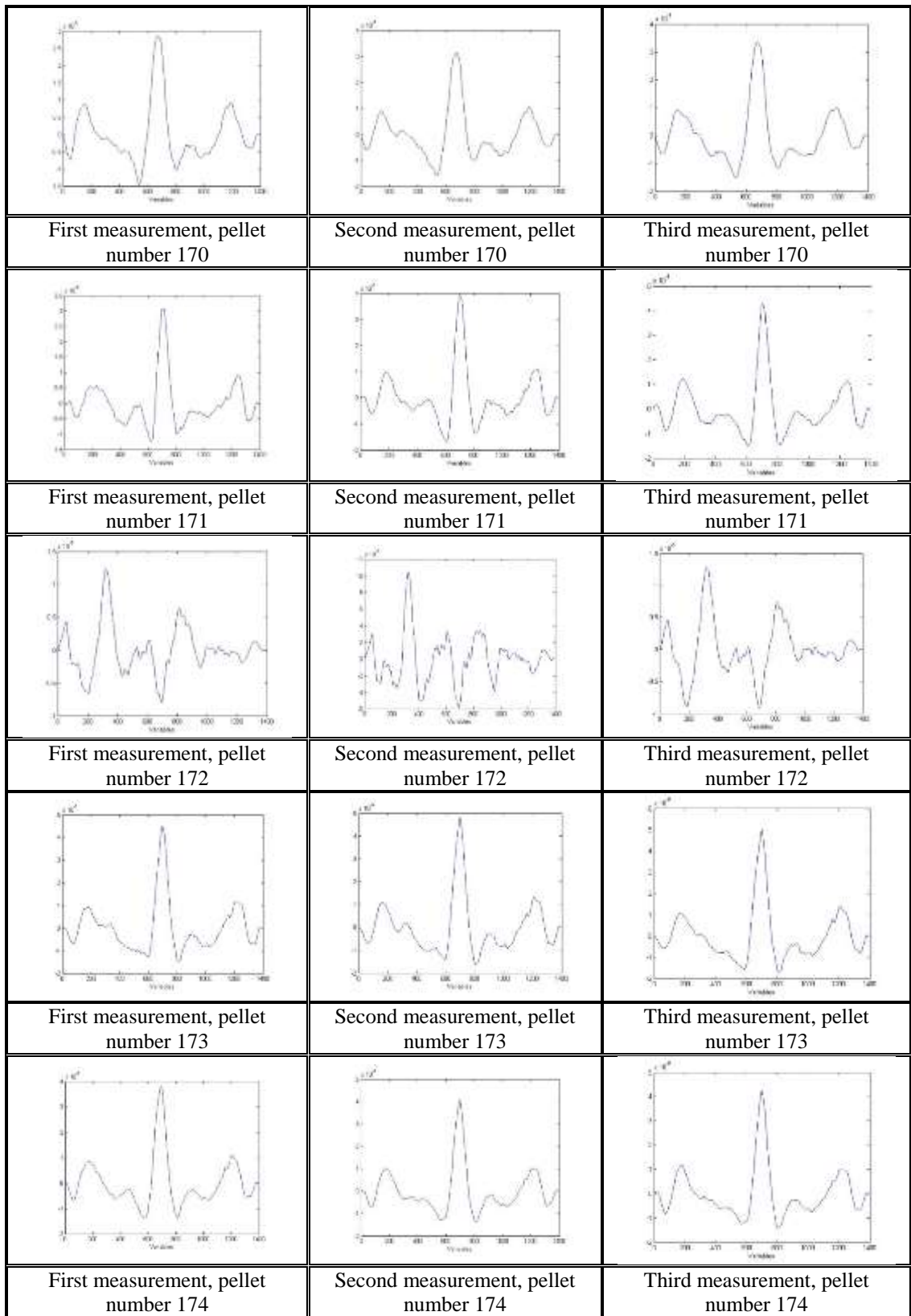


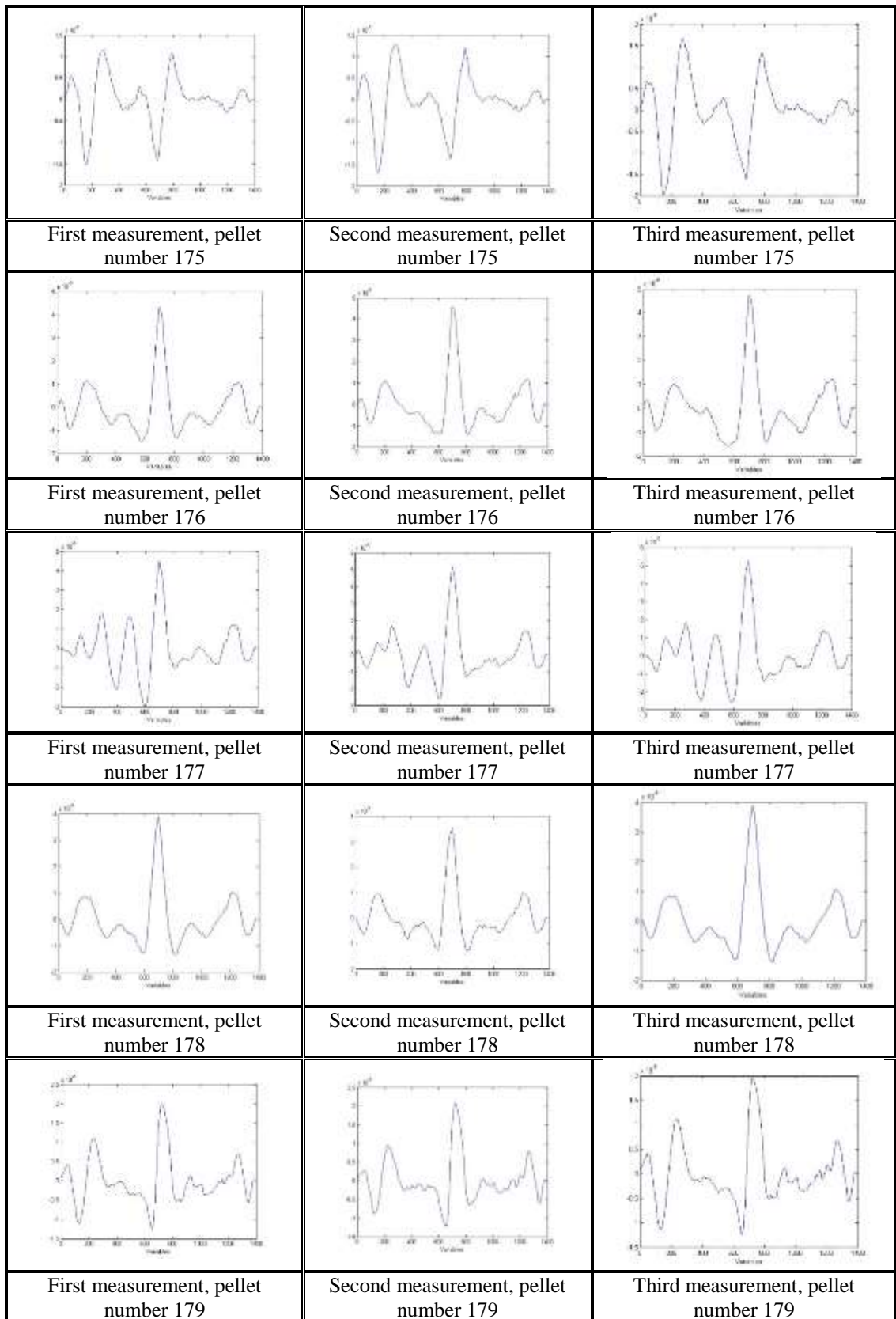
## Appendix 15

Alignment result for LEA L, pellet number 159 – 208

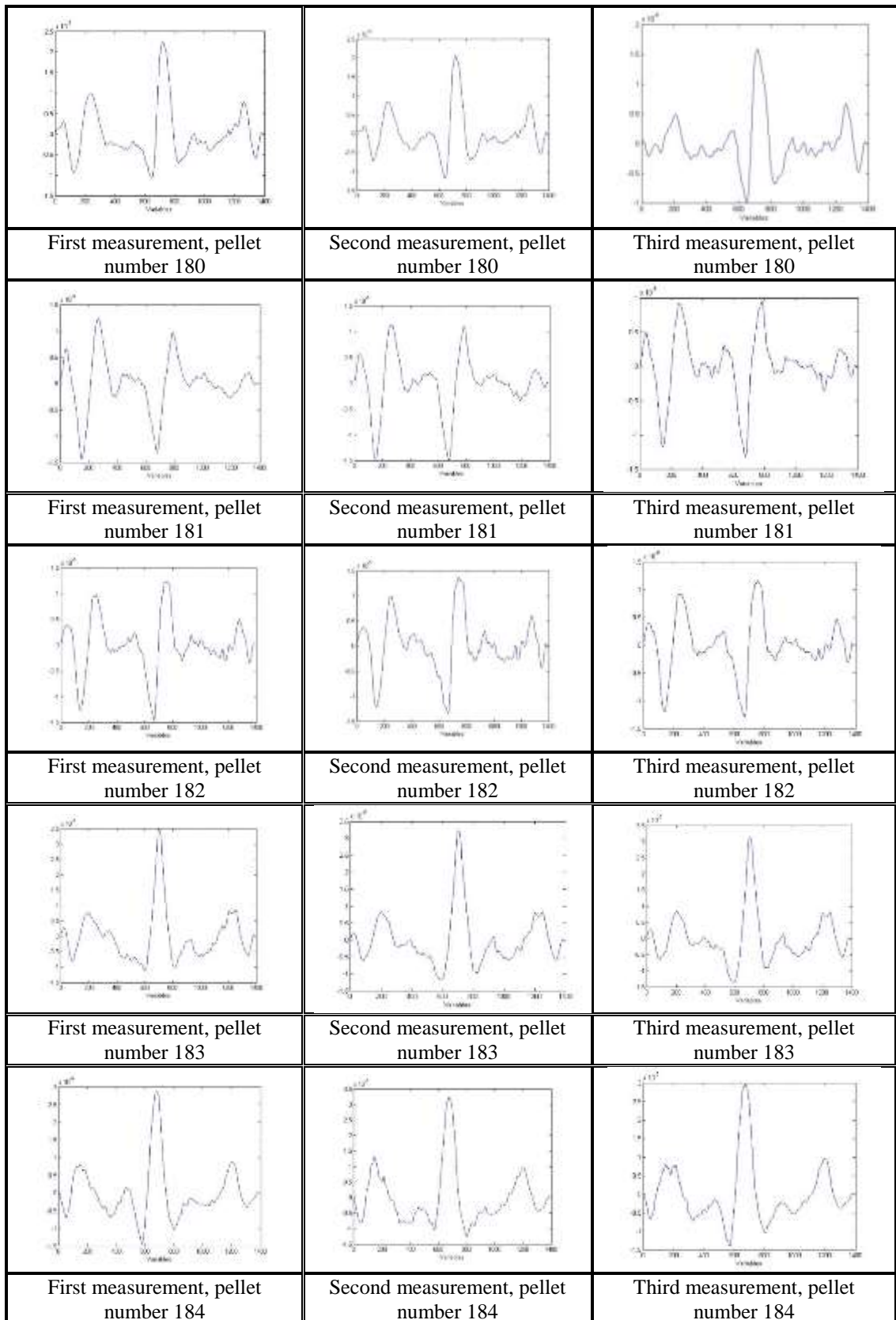
		
	Second measurement, pellet number 159	Third measurement, pellet number 159
		
First measurement, pellet number 160	Second measurement, pellet number 160	Third measurement, pellet number 160
		
First measurement, pellet number 162	Second measurement, pellet number 162	Third measurement, pellet number 162
		
First measurement, pellet number 163	Second measurement, pellet number 163	Third measurement, pellet number 163
		
First measurement, pellet number 164	Second measurement, pellet number 164	Third measurement, pellet number 164

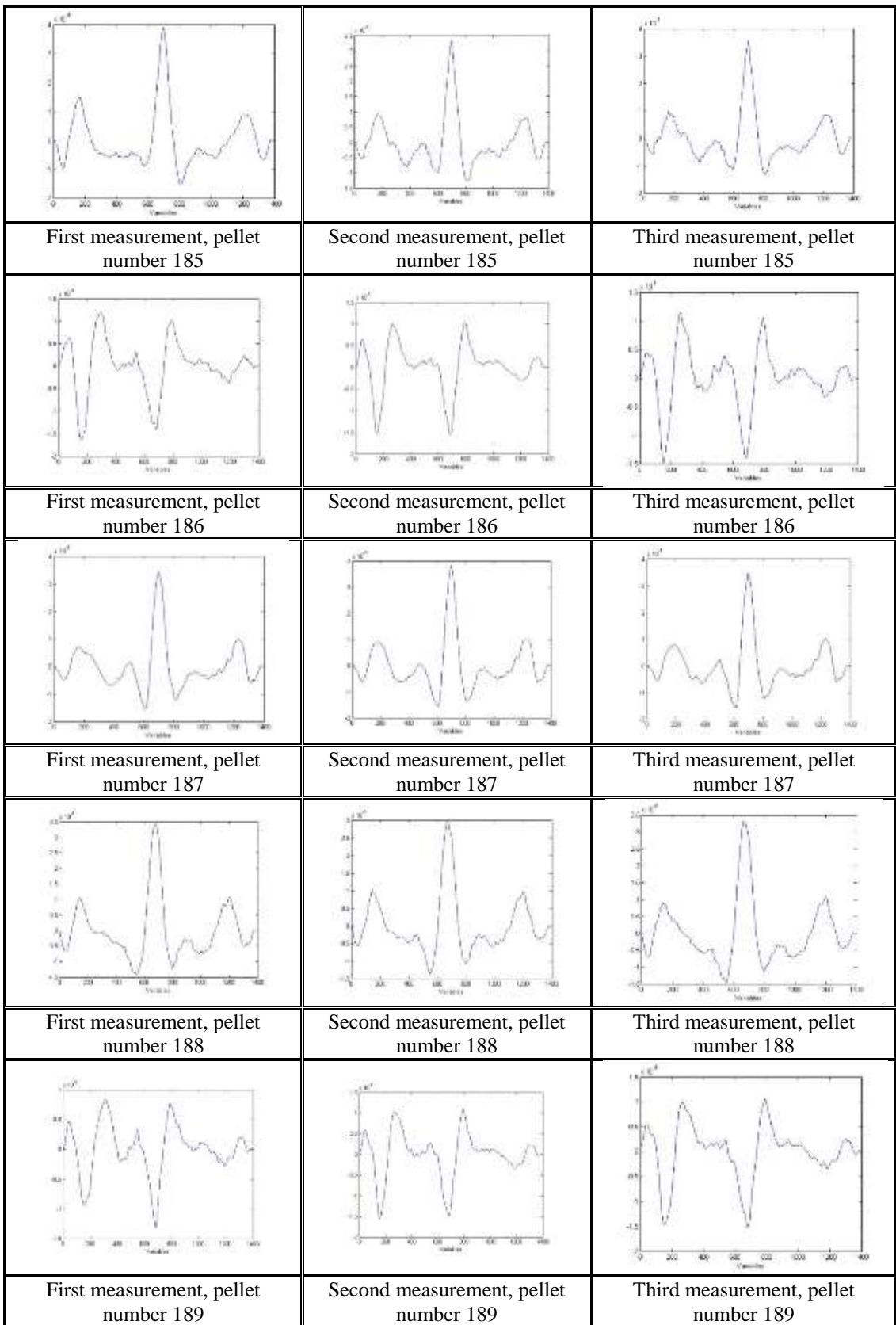


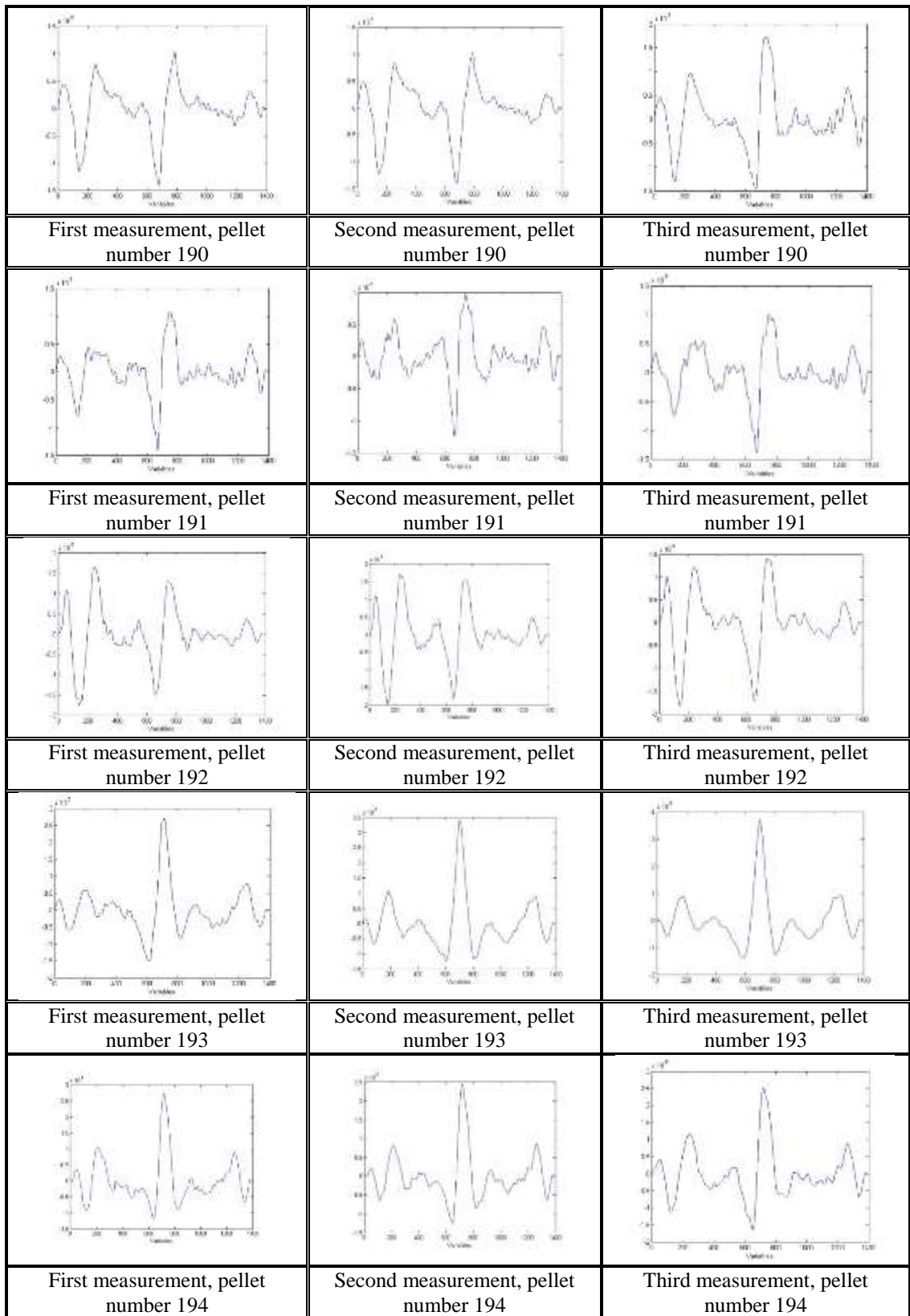


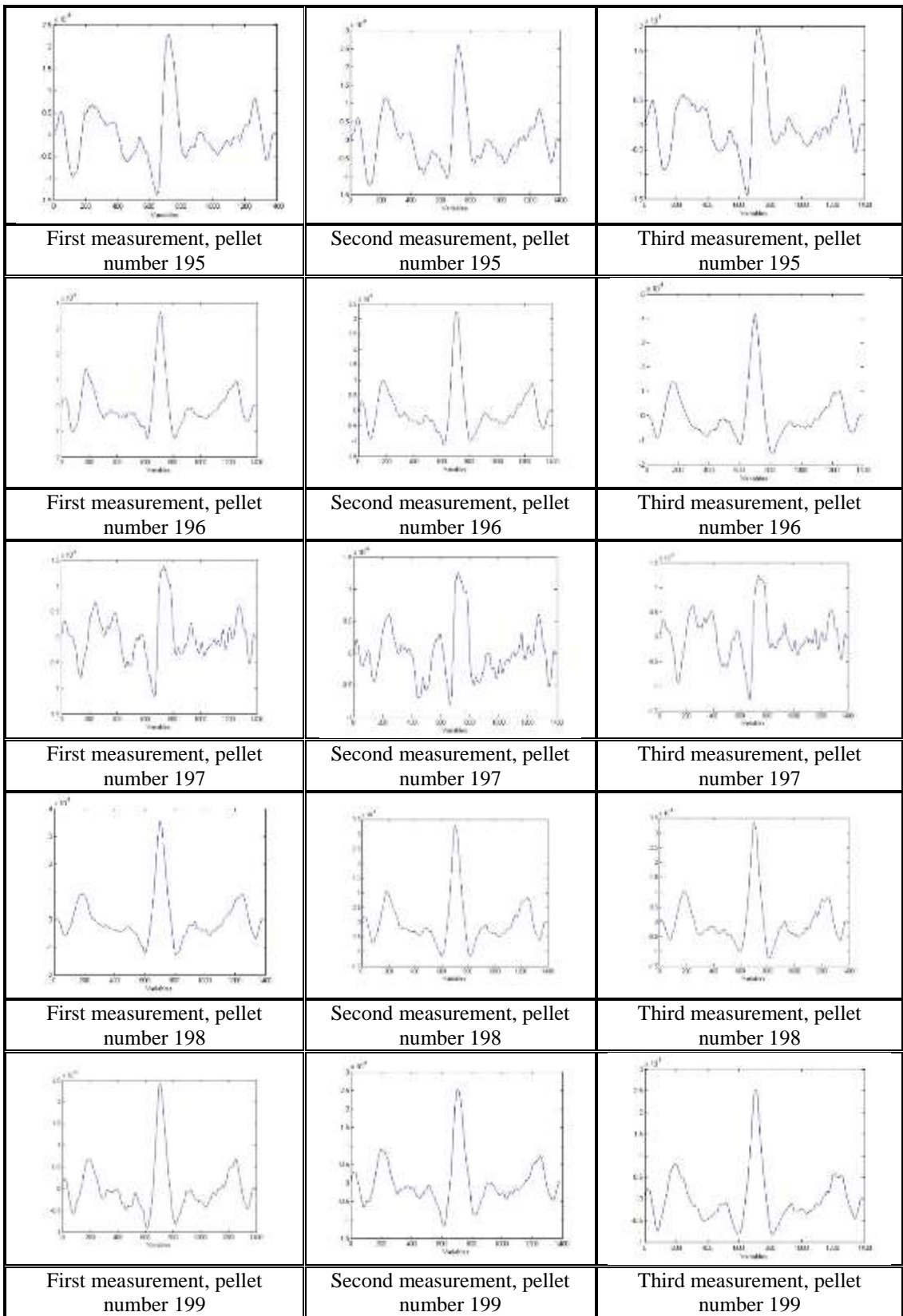


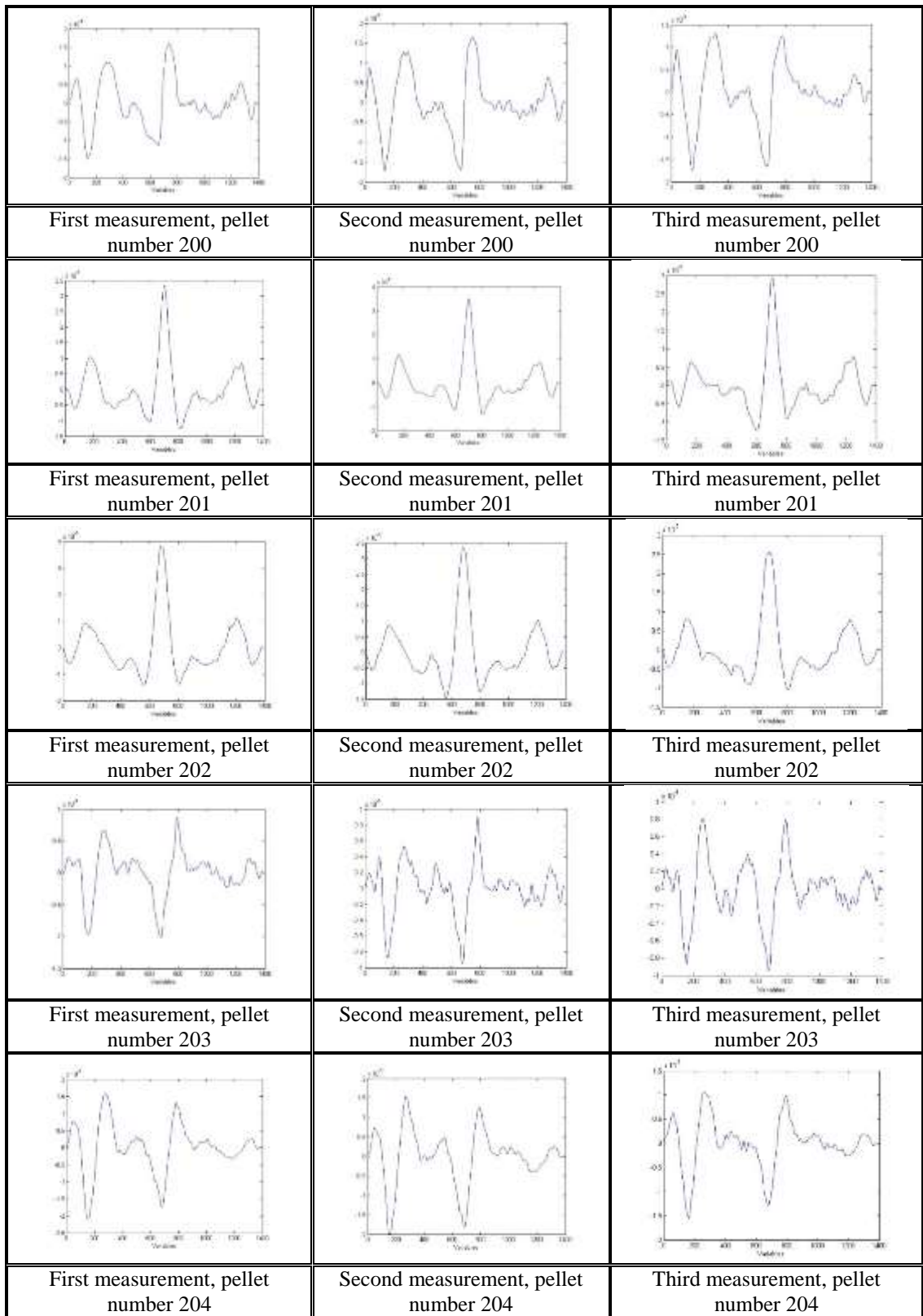


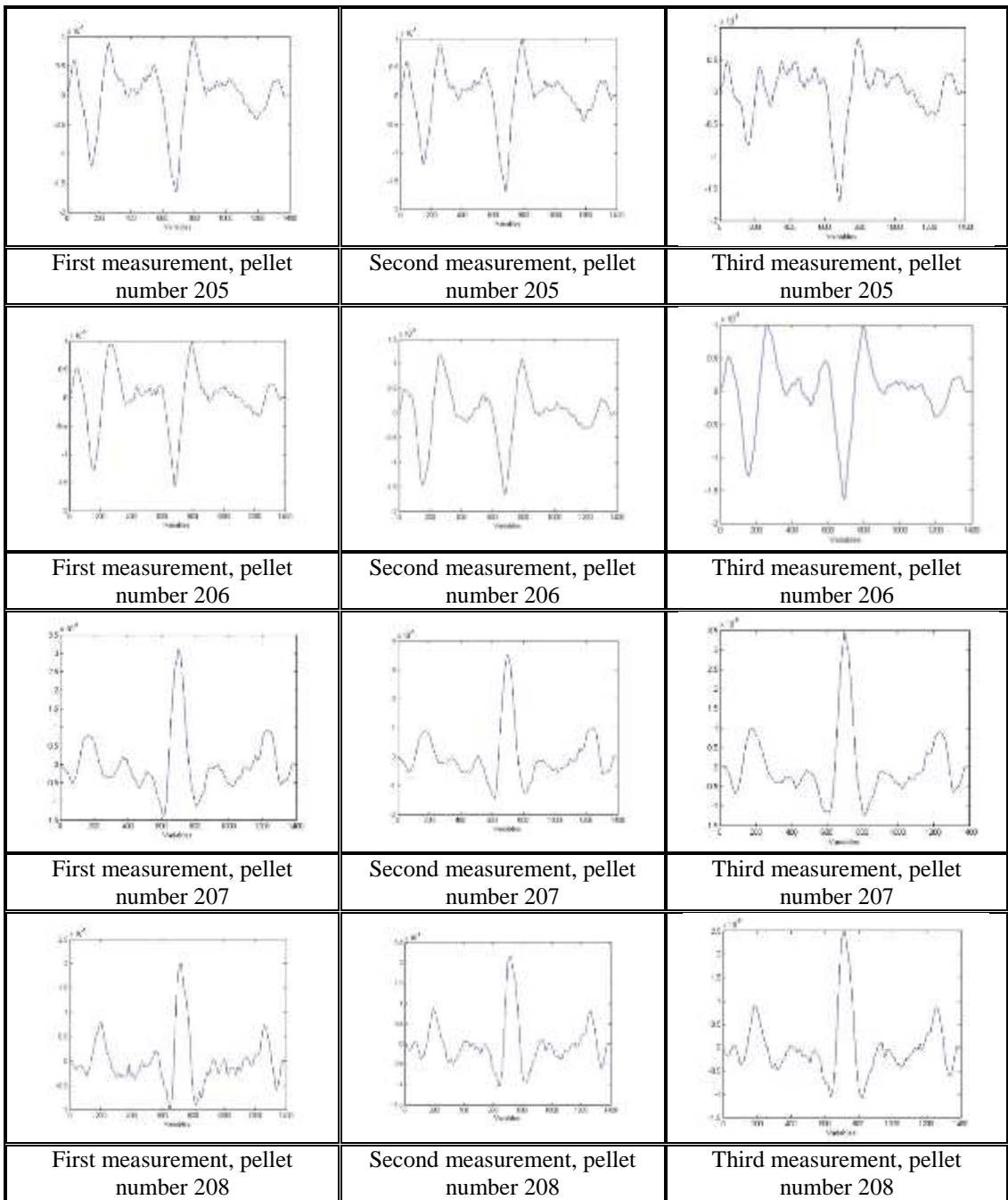






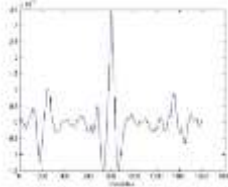
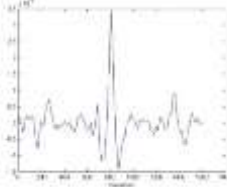
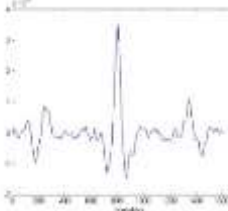
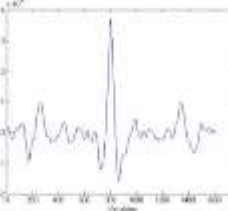
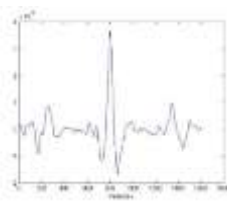
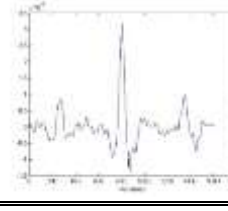
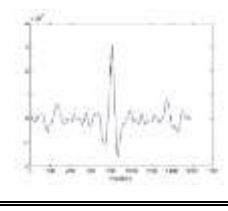
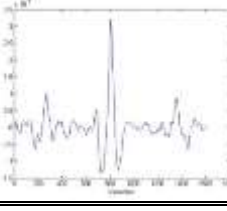
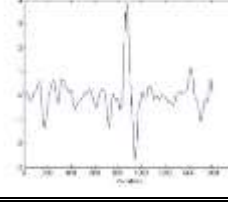
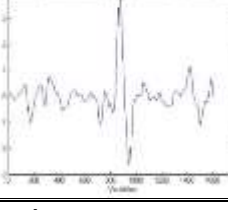
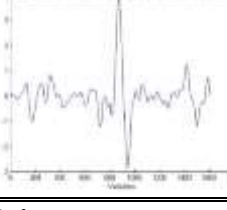
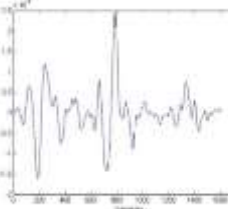

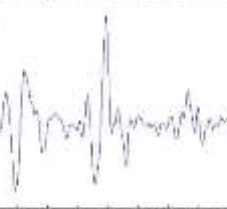


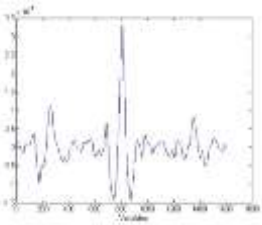
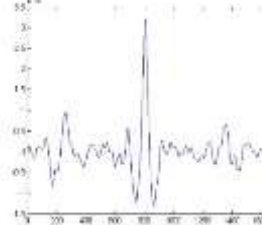
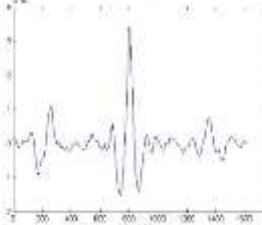
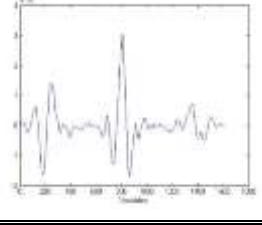
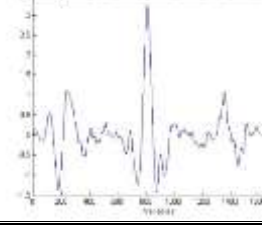
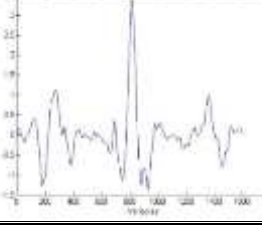
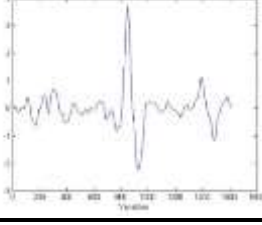
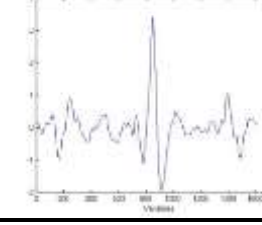
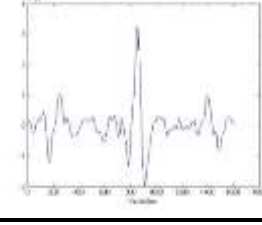
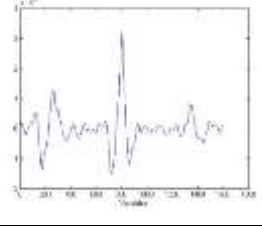
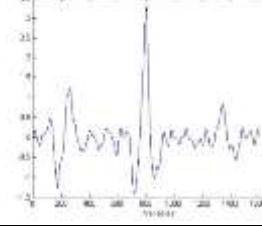
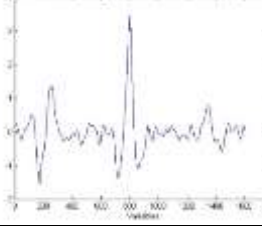
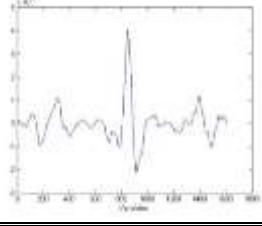
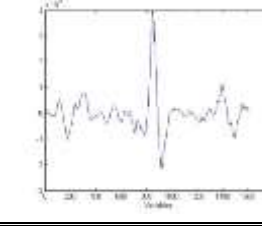
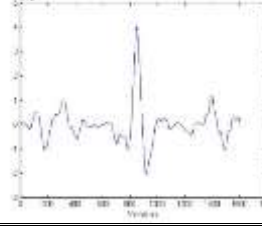




## Appendix 16

Topographical profiles obtained from the microscopic measurements for samples 159-168, LEA A

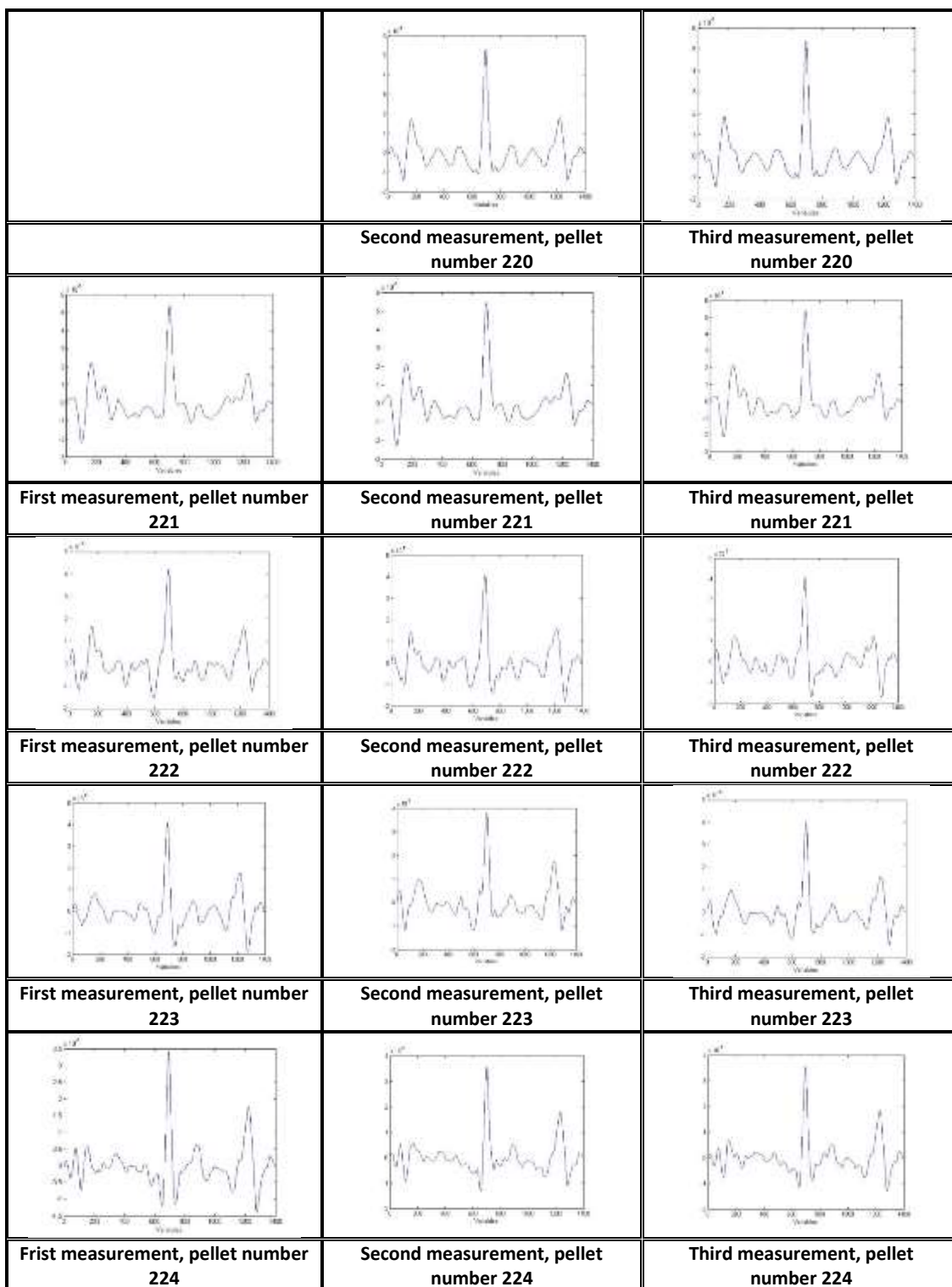
		
	<b>Second measurement, pellet number 159</b>	<b>Third measurement, pellet number 159</b>
		
<b>First measurement, pellet number 160</b>	<b>Second measurement, pellet number 160</b>	<b>Third measurement, pellet number 160</b>
		
<b>First measurement, pellet number 161</b>	<b>Second measurement, pellet number 161</b>	<b>Third measurement, pellet number 161</b>
		
<b>First measurement, pellet number 162</b>	<b>Second measurement, pellet number 162</b>	<b>Third measurement, pellet number 162</b>
		
<b>First measurement, pellet number 163</b>	<b>Second measurement, pellet number 163</b>	<b>Third measurement, pellet number 163</b>

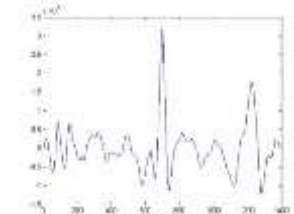
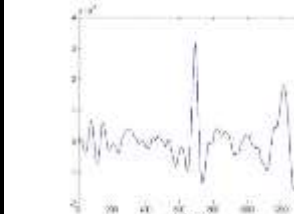
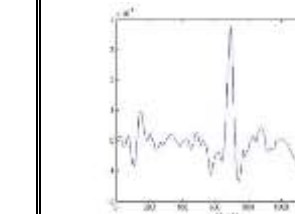
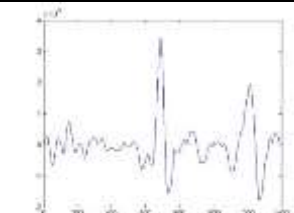
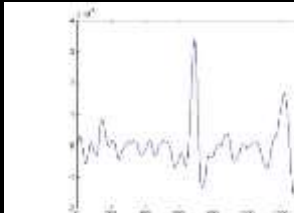
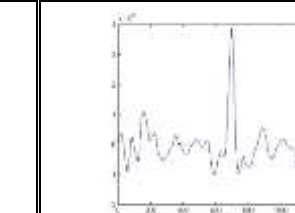
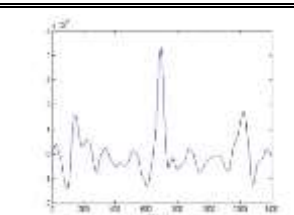
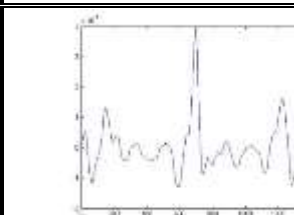
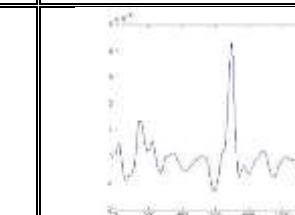


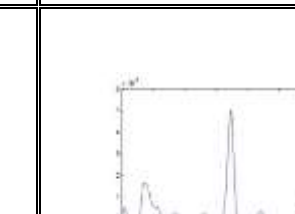
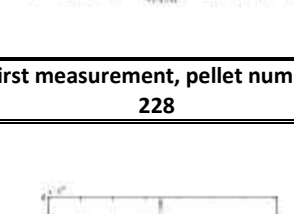
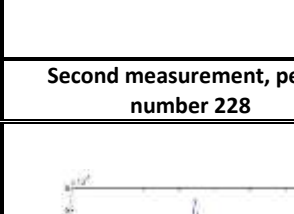
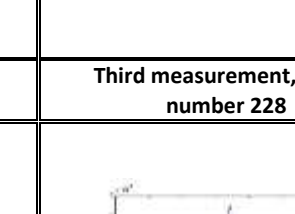
		
<b>First measurement, pellet number 164</b>	<b>Second measurement, pellet number 164</b>	<b>Third measurement, pellet number 164</b>
		
<b>First measurement, pellet number 165</b>	<b>Second measurement, pellet number 165</b>	<b>Third measurement, pellet number 165</b>
		
<b>First measurement, pellet number 166</b>	<b>Second measurement, pellet number 166</b>	<b>Third measurement, pellet number 166</b>
		
<b>First measurement, pellet number 167</b>	<b>Second measurement, pellet number 167</b>	<b>Third measurement, pellet number 167</b>
		
<b>First measurement, pellet number 168</b>	<b>Second measurement, pellet number 168</b>	<b>Third measurement, pellet number 168</b>



## Appendix 17

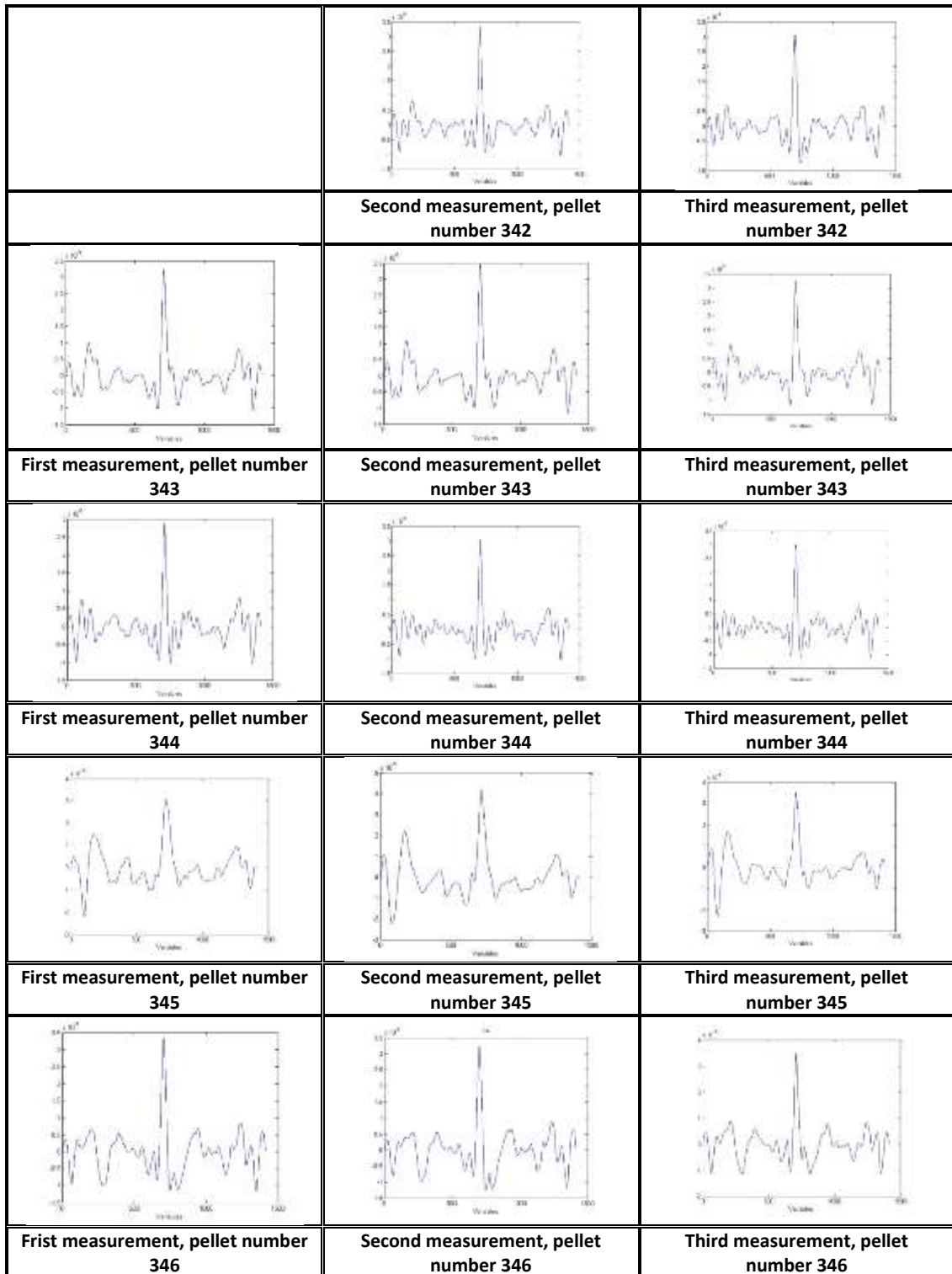
Topographical profiles obtained from the microscopic measurements for samples 220-229, LEA A

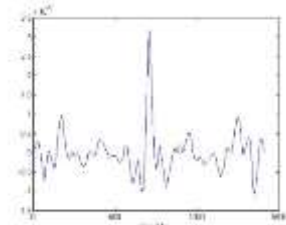
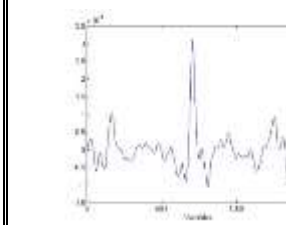
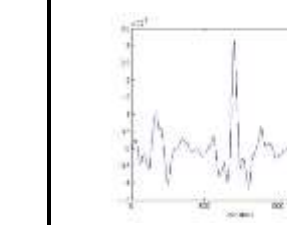
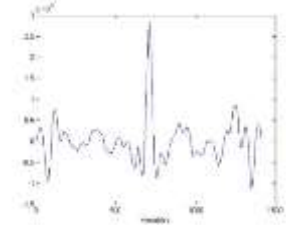
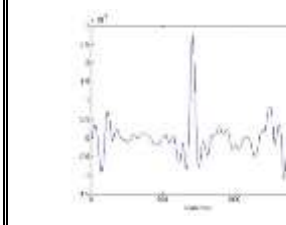
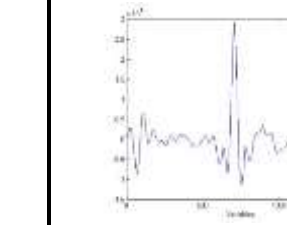
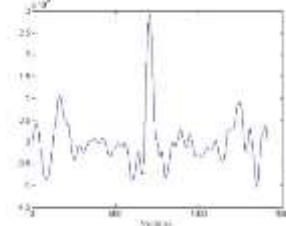
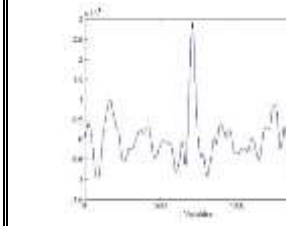
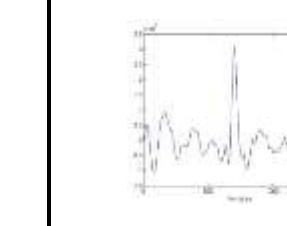
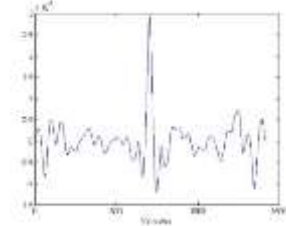
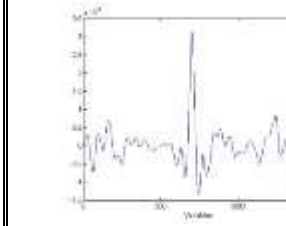
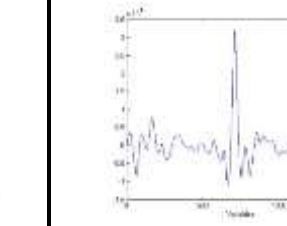
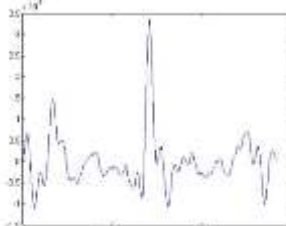
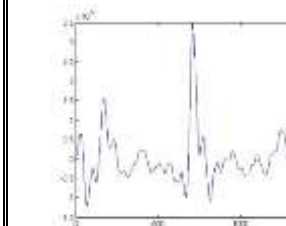
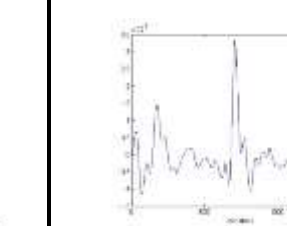


		
<b>First measurement, pellet number 225</b>	<b>Second measurement, pellet number 225</b>	<b>Third measurement, pellet number 225</b>
		
<b>First measurement, pellet number 226</b>	<b>Second measurement, pellet number 226</b>	<b>Third measurement, pellet number 226</b>
		
<b>First measurement, pellet number 227</b>	<b>Second measurement, pellet number 227</b>	<b>Third measurement, pellet number 227</b>
		
<b>First measurement, pellet number 228</b>	<b>Second measurement, pellet number 228</b>	<b>Third measurement, pellet number 228</b>
		
<b>First measurement, pellet number 229</b>	<b>Second measurement, pellet number 229</b>	<b>Third measurement, pellet number 229</b>

## Appendix 18

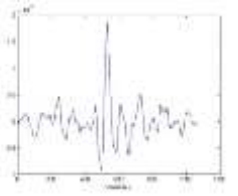
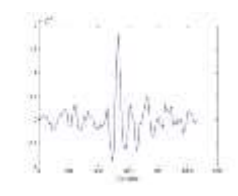
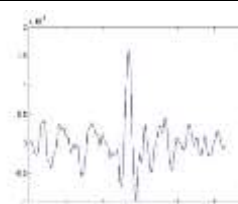
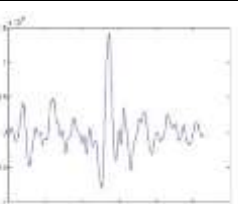
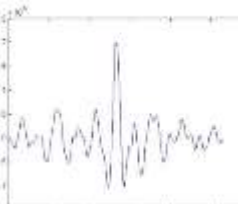


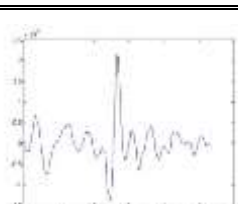
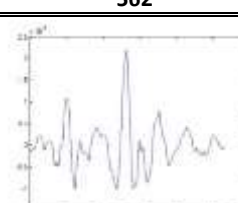

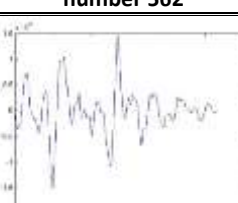
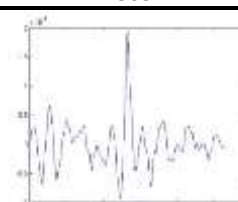
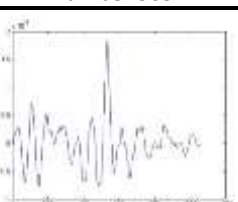
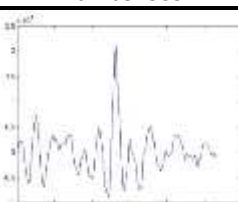
Topographical profiles obtained from the microscopic measurements for samples 342-351, LEA A

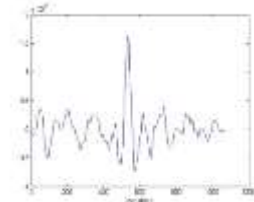
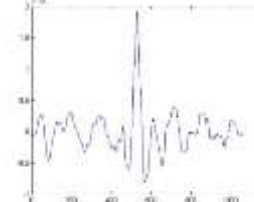
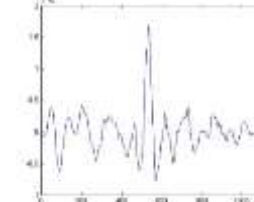
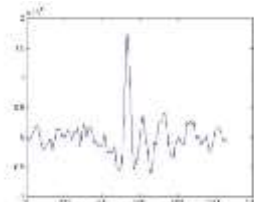
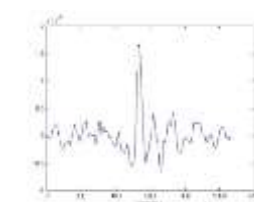
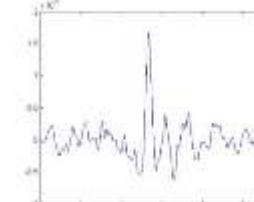
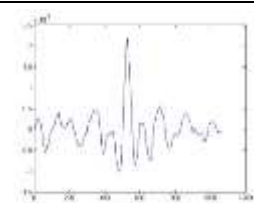
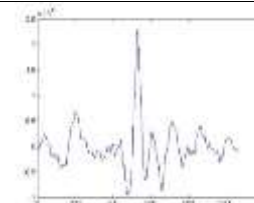
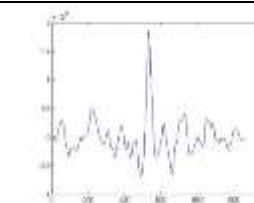
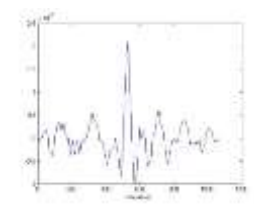
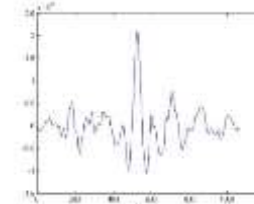
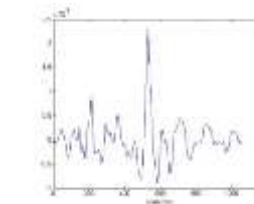
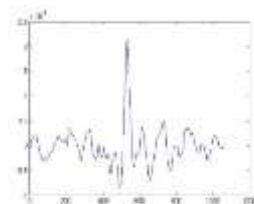
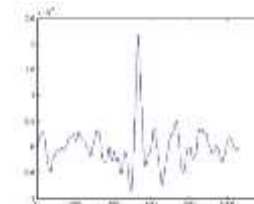
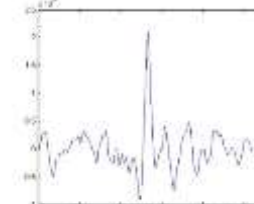


		
<b>First measurement, pellet number 347</b>	<b>Second measurement, pellet number 347</b>	<b>Third measurement, pellet number 347</b>
		
<b>First measurement, pellet number 348</b>	<b>Second measurement, pellet number 348</b>	<b>Third measurement, pellet number 348</b>
		
<b>First measurement, pellet number 349</b>	<b>Second measurement, pellet number 349</b>	<b>Third measurement, pellet number 349</b>
		
<b>First measurement, pellet number 350</b>	<b>Second measurement, pellet number 350</b>	<b>Third measurement, pellet number 350</b>
		
<b>First measurement, pellet number 351</b>	<b>Second measurement, pellet number 351</b>	<b>Third measurement, pellet number 351</b>

## Appendix 19

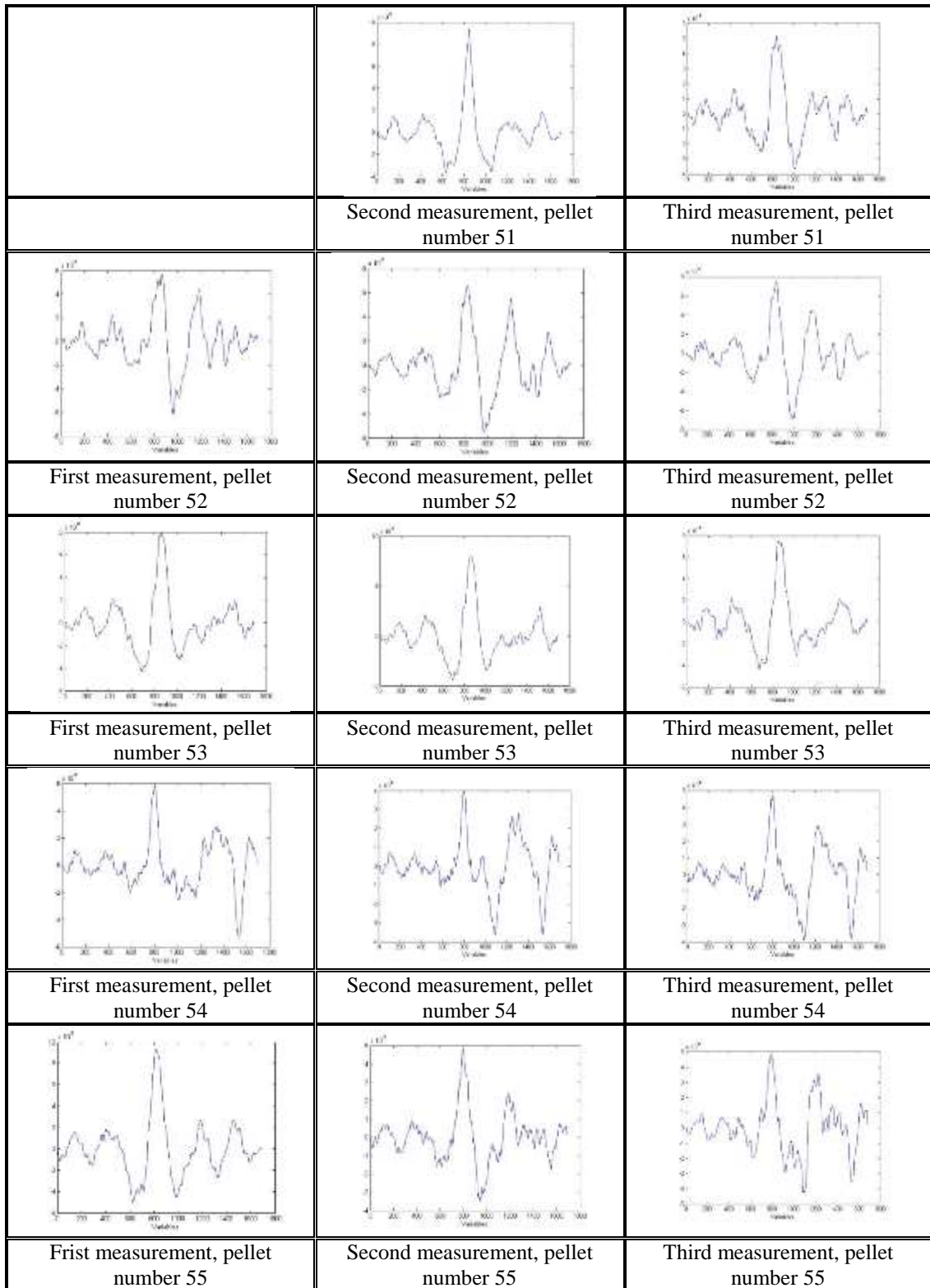
Topographical profiles obtained from the microscopic measurements for samples 560-569, LEA A

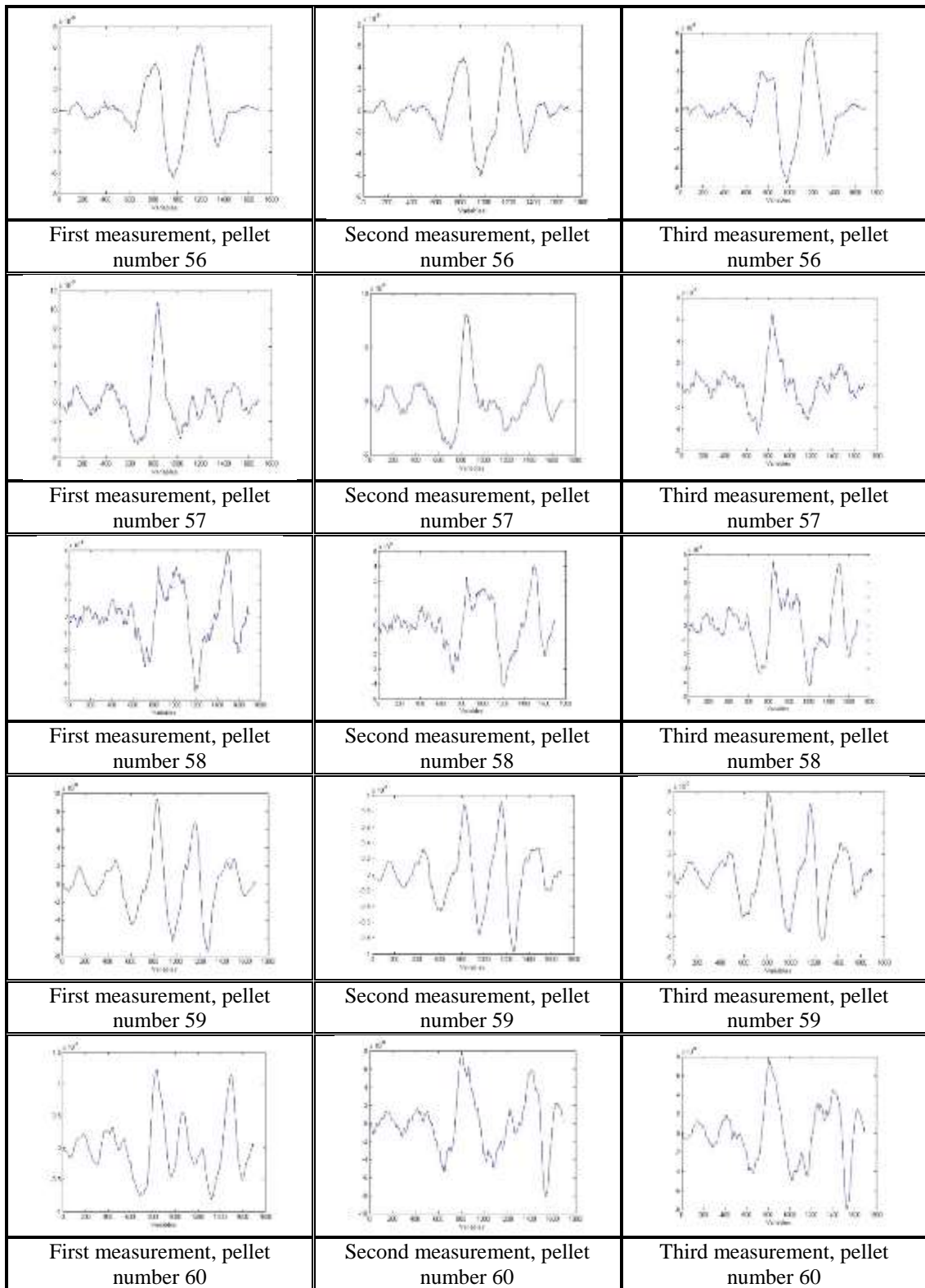
		
	Second measurement, pellet number 560	Third measurement, pellet number 560
		
First measurement, pellet number 561	Second measurement, pellet number 561	Third measurement, pellet number 561
		
First measurement, pellet number 562	Second measurement, pellet number 562	Third measurement, pellet number 562
		
First measurement, pellet number 563	Second measurement, pellet number 563	Third measurement, pellet number 563
		
First measurement, pellet number 564	Second measurement, pellet number 564	Third measurement, pellet number 564

		
<b>First measurement, pellet number 565</b>	<b>Second measurement, pellet number 565</b>	<b>Third measurement, pellet number 565</b>
		
<b>First measurement, pellet number 566</b>	<b>Second measurement, pellet number 566</b>	<b>Third measurement, pellet number 566</b>
		
<b>First measurement, pellet number 567</b>	<b>Second measurement, pellet number 567</b>	<b>Third measurement, pellet number 567</b>
		
<b>First measurement, pellet number 568</b>	<b>Second measurement, pellet number 568</b>	<b>Third measurement, pellet number 568</b>
		
<b>First measurement, pellet number 569</b>	<b>Second measurement, pellet number 569</b>	<b>Third measurement, pellet number 569</b>

## Appendix 20

Topographical profiles obtained from the microscopic measurements for samples 51-60, LEA B

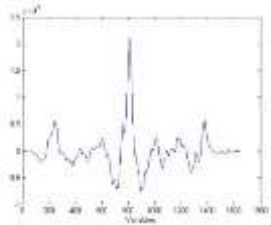
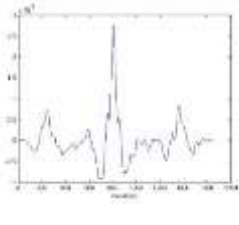
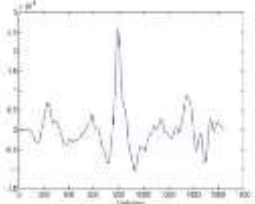
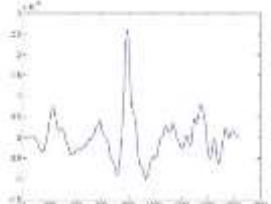
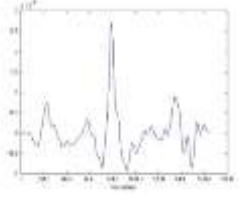

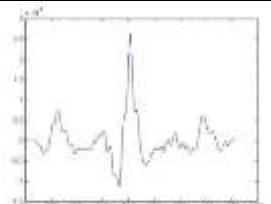
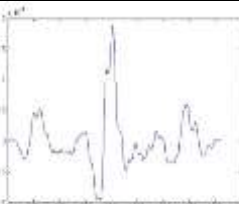

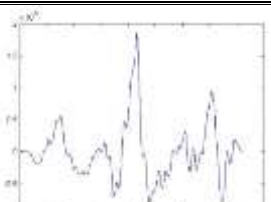
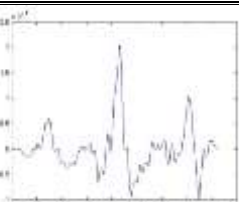





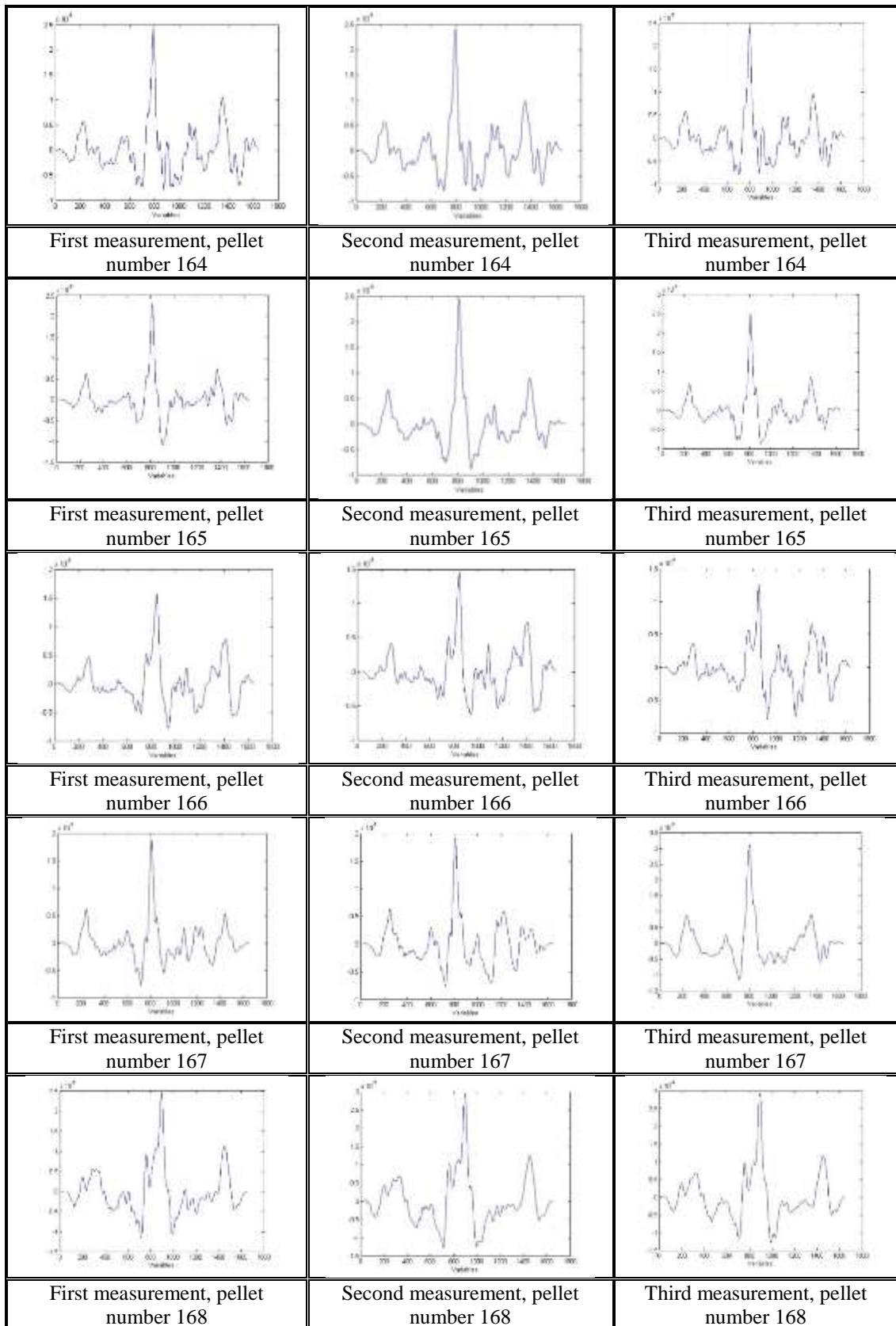




## Appendix 21

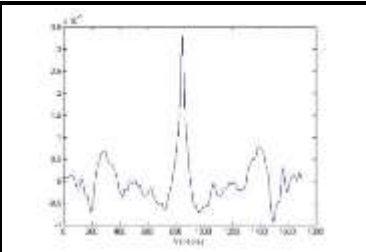
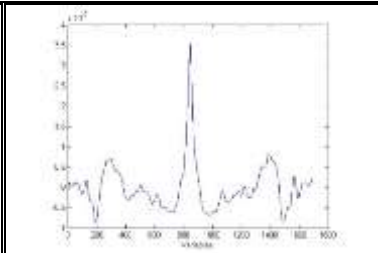
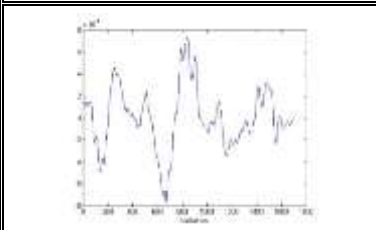
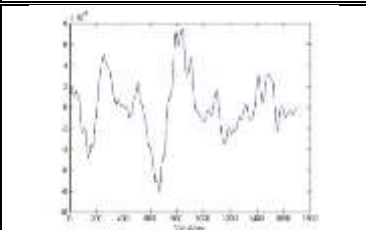
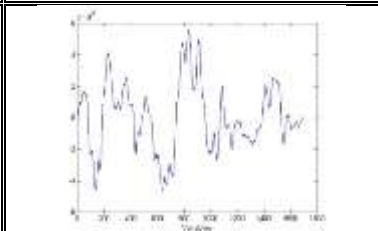
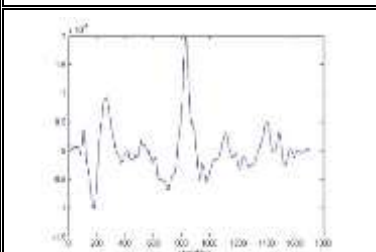
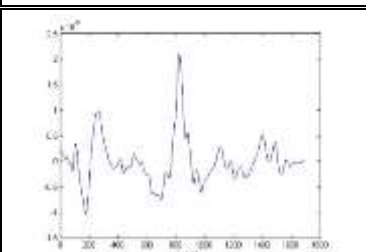
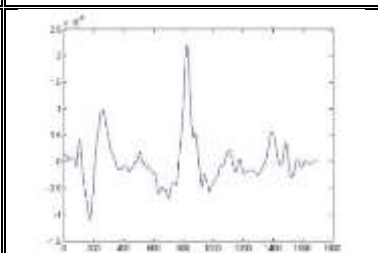
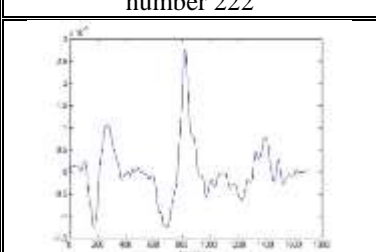
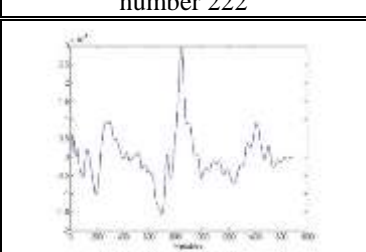
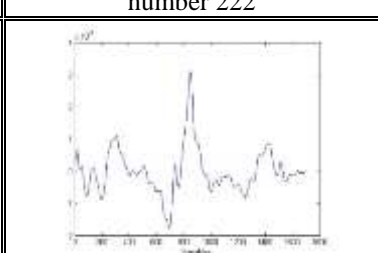
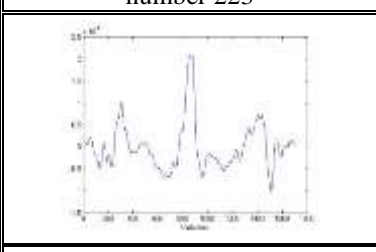
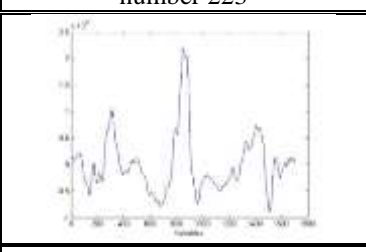
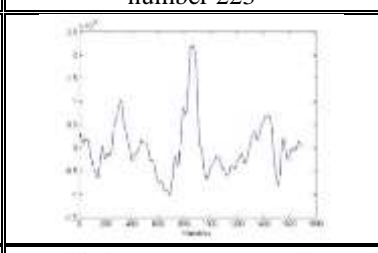
Topographical profiles obtained from the microscopic measurements for samples 159-168, LEA B

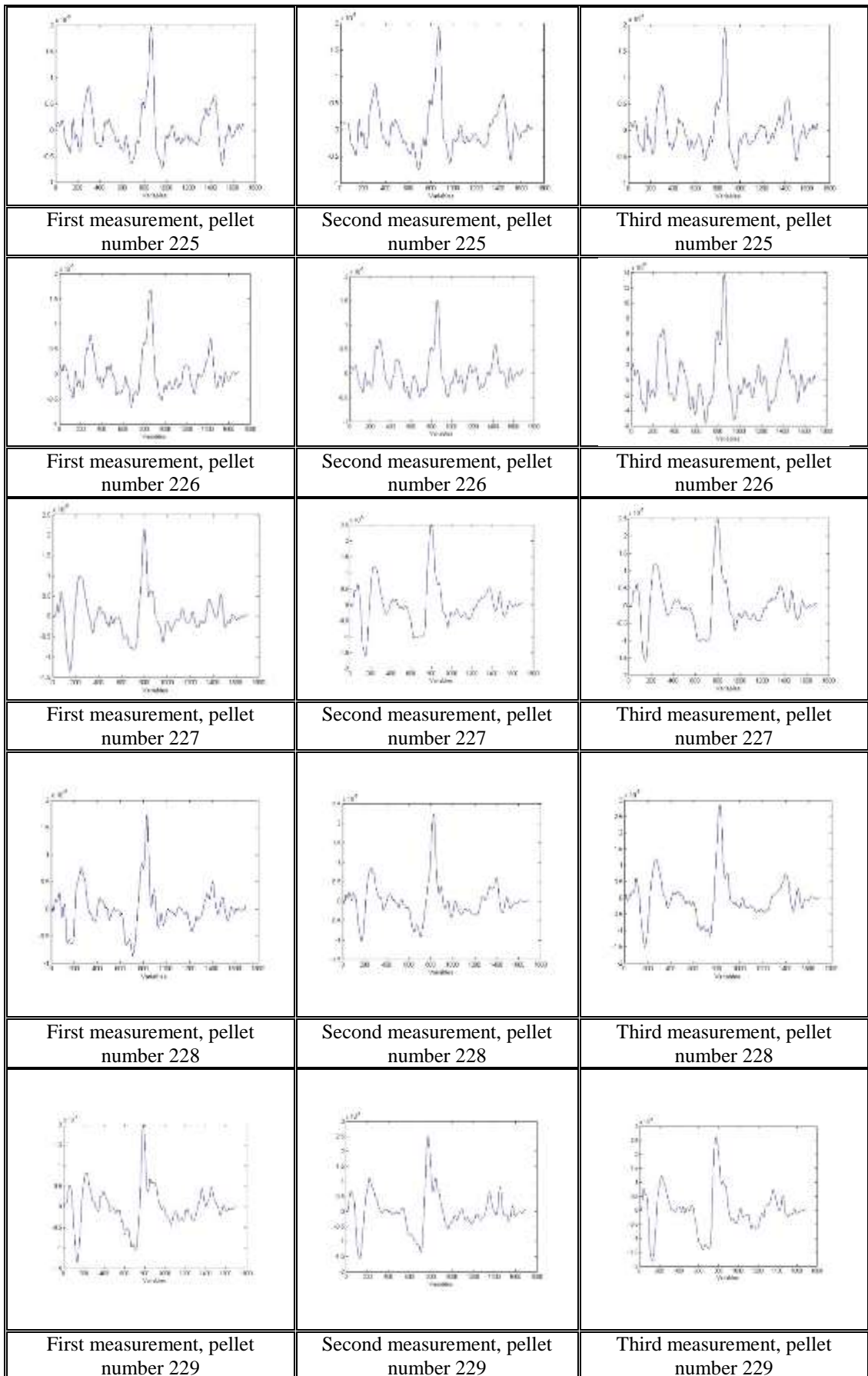
		
	Second measurement, pellet number 159	Third measurement, pellet number 159
		
First measurement, pellet number 160	Second measurement, pellet number 160	Third measurement, pellet number 160
		
First measurement, pellet number 161	Second measurement, pellet number 161	Third measurement, pellet number 161
		
First measurement, pellet number 162	Second measurement, pellet number 162	Third measurement, pellet number 162
		
First measurement, pellet number 163	Second measurement, pellet number 163	Third measurement, pellet number 163



## Appendix 22

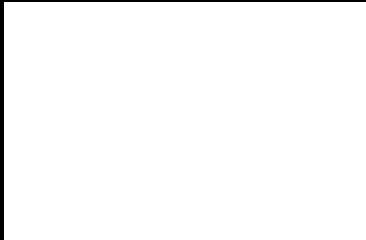
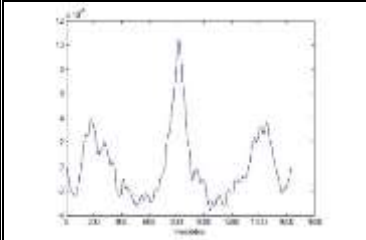
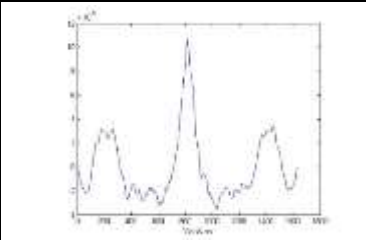
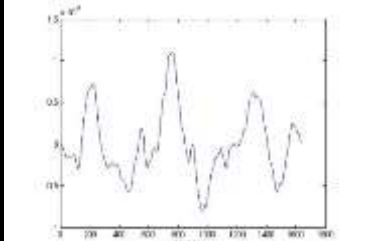
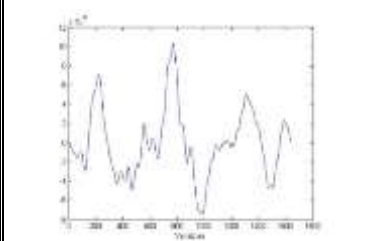
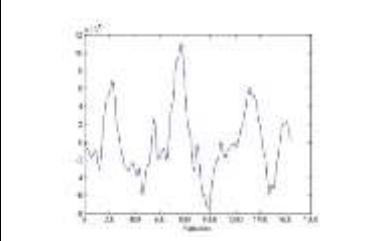
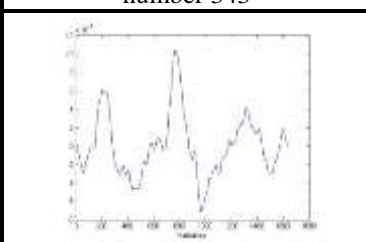
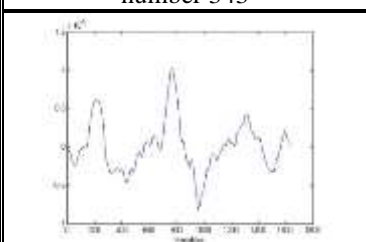
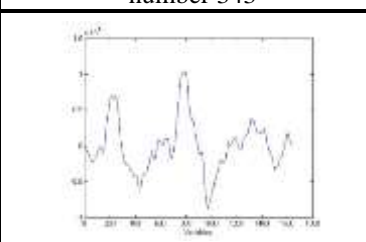
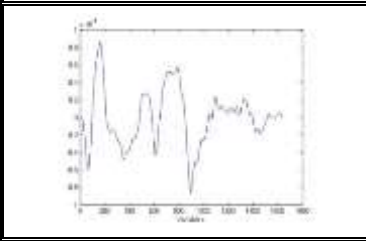
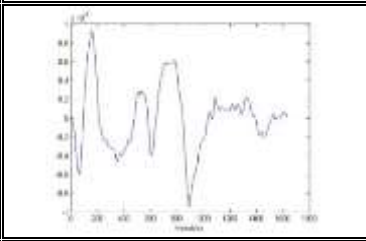
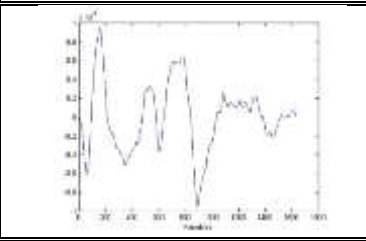
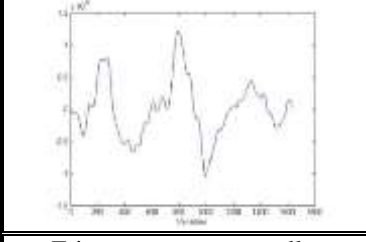
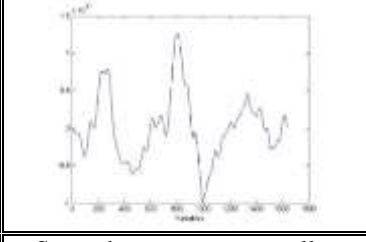
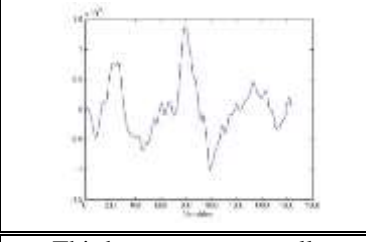
Topographical profiles obtained from the microscopic measurements for samples 220-229, LEA B

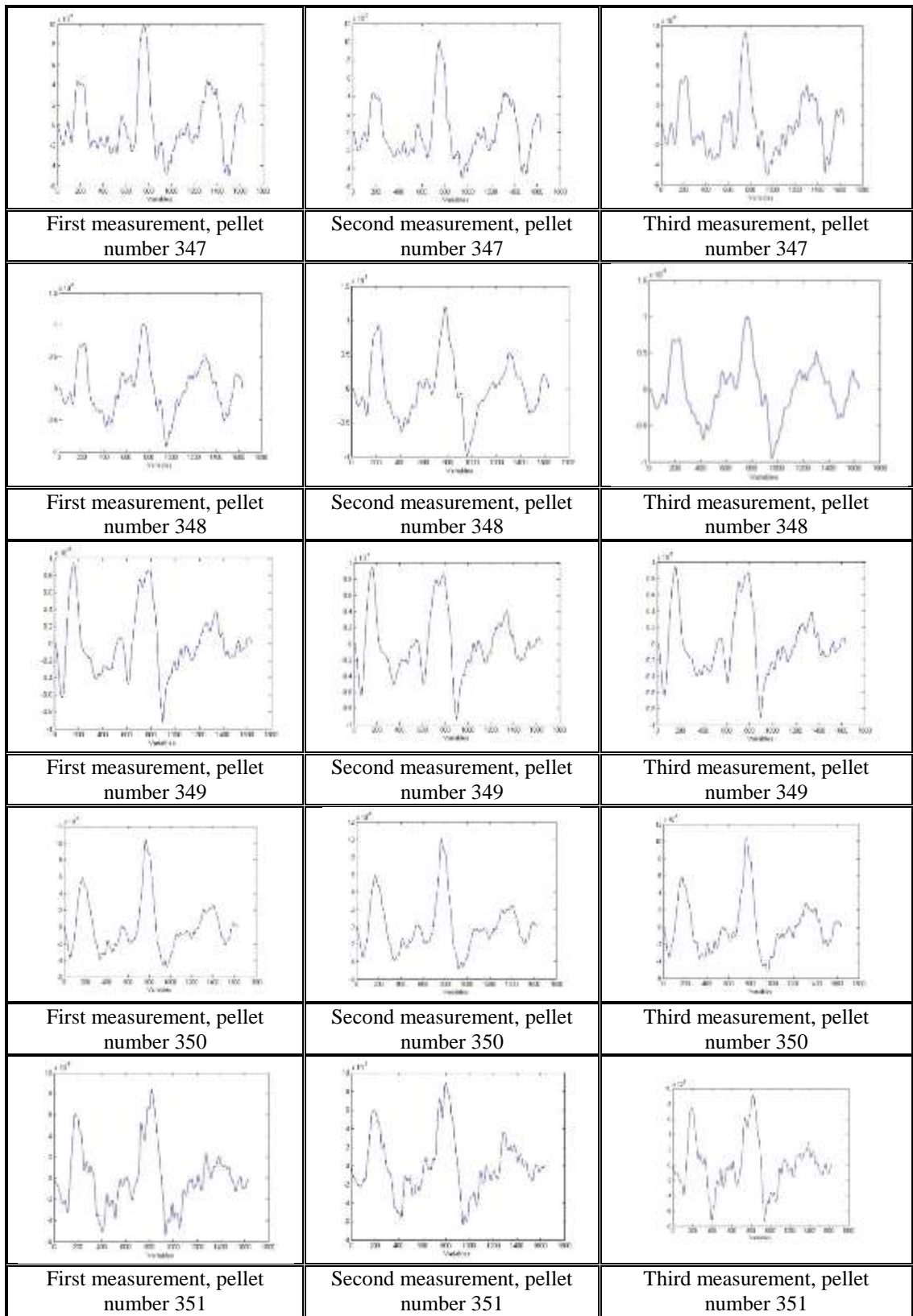
		
	Second measurement, pellet number 220	Third measurement, pellet number 220
		
First measurement, pellet number 221	Second measurement, pellet number 221	Third measurement, pellet number 221
		
First measurement, pellet number 222	Second measurement, pellet number 222	Third measurement, pellet number 222
		
First measurement, pellet number 223	Second measurement, pellet number 223	Third measurement, pellet number 223
		
First measurement, pellet number 224	Second measurement, pellet number 224	Third measurement, pellet number 224



## Appendix 23

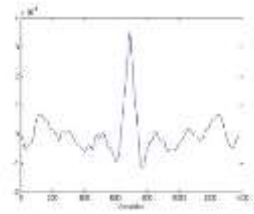
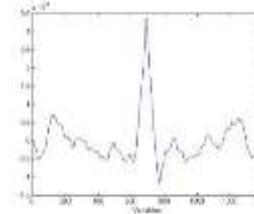
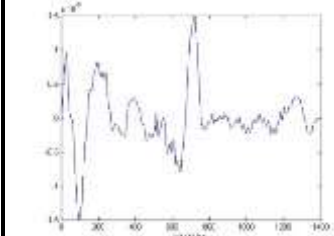
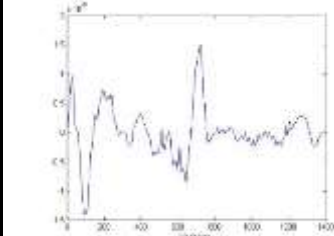
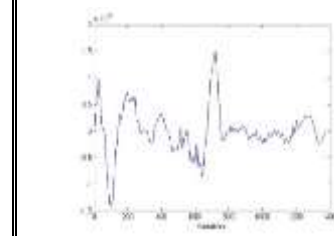
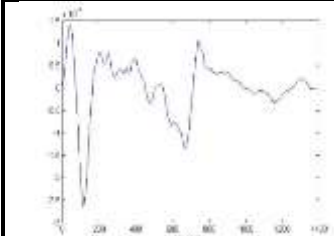
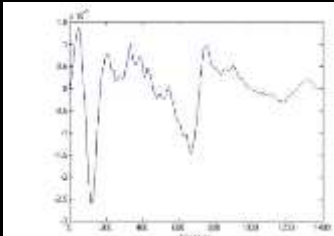
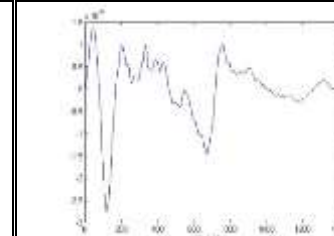
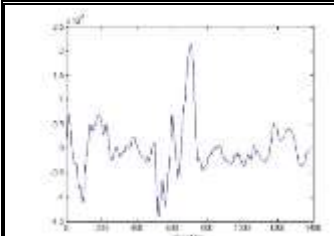
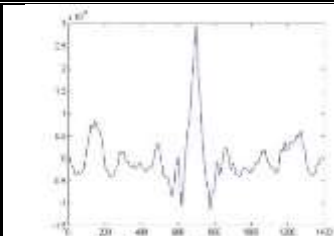
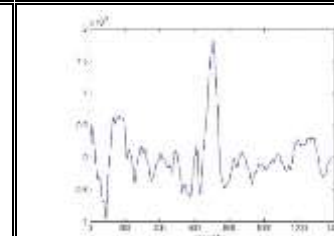
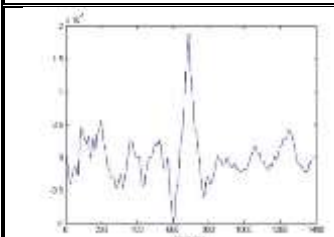
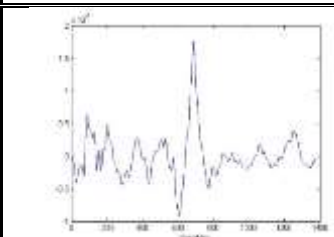
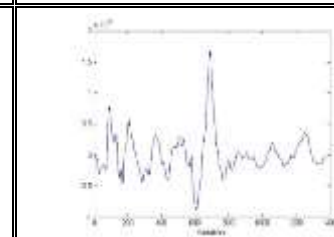
Topographical profiles obtained from the microscopic measurements for samples 342-351, LEA B

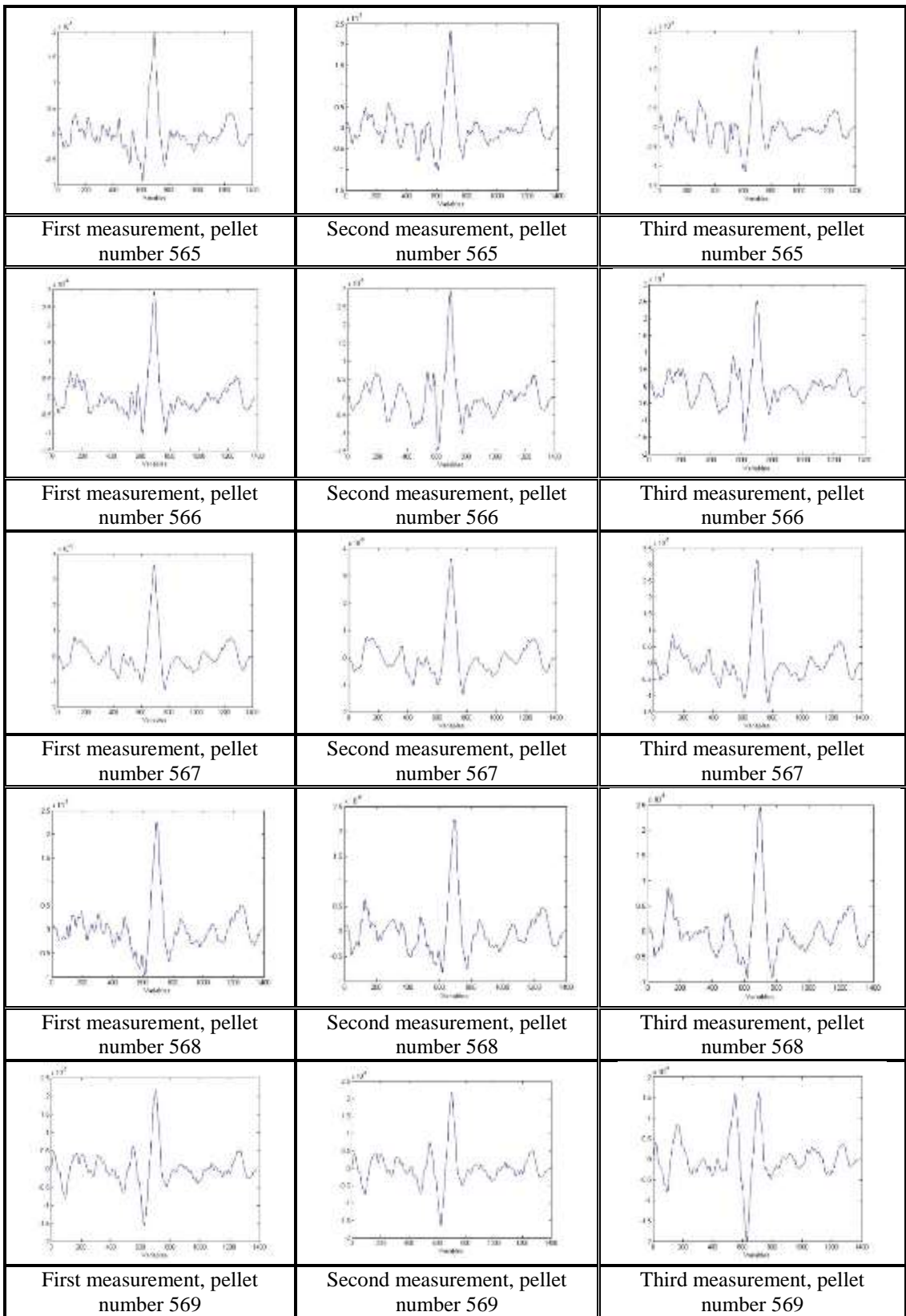
		
	Second measurement, pellet number 342	Third measurement, pellet number 342
		
First measurement, pellet number 343	Second measurement, pellet number 343	Third measurement, pellet number 343
		
First measurement, pellet number 344	Second measurement, pellet number 344	Third measurement, pellet number 344
		
First measurement, pellet number 345	Second measurement, pellet number 345	Third measurement, pellet number 345
		
First measurement, pellet number 346	Second measurement, pellet number 346	Third measurement, pellet number 346



## Appendix 24

Topographical profiles obtained from the microscopic measurements for samples 560-569, LEA B

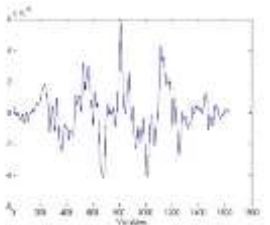
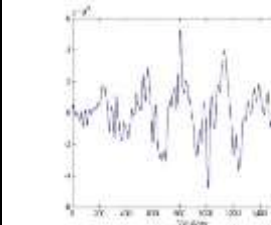
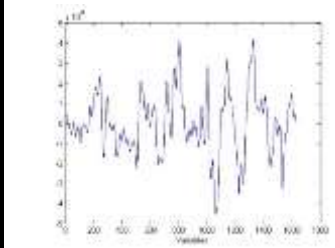
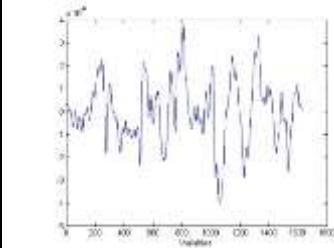
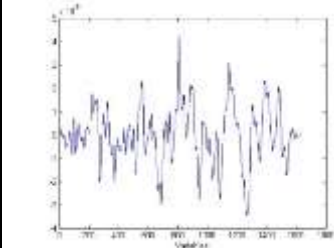
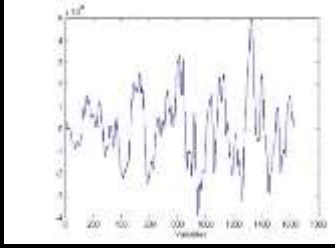
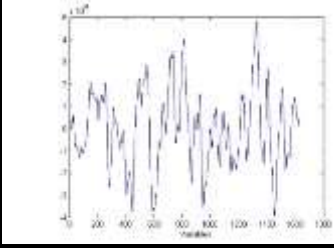
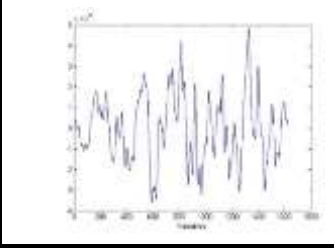
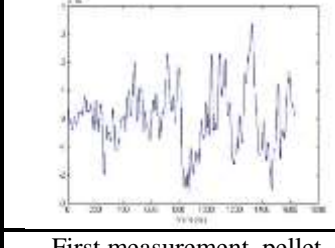
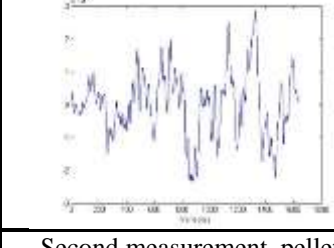
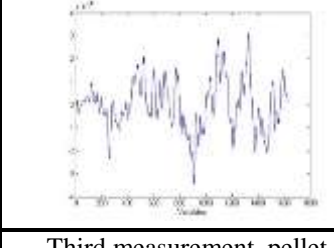
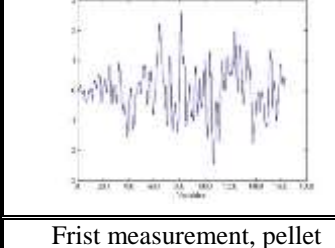
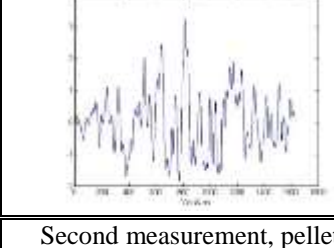
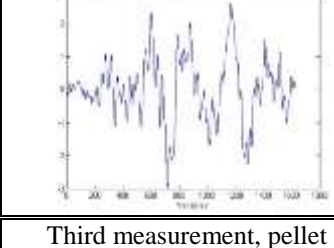
		
	Second measurement, pellet number 560	Third measurement, pellet number 560
		
First measurement, pellet number 561	Second measurement, pellet number 561	Third measurement, pellet number 561
		
First measurement, pellet number 562	Second measurement, pellet number 562	Third measurement, pellet number 562
		
First measurement, pellet number 563	Second measurement, pellet number 563	Third measurement, pellet number 563
		
First measurement, pellet number 564	Second measurement, pellet number 564	Third measurement, pellet number 564

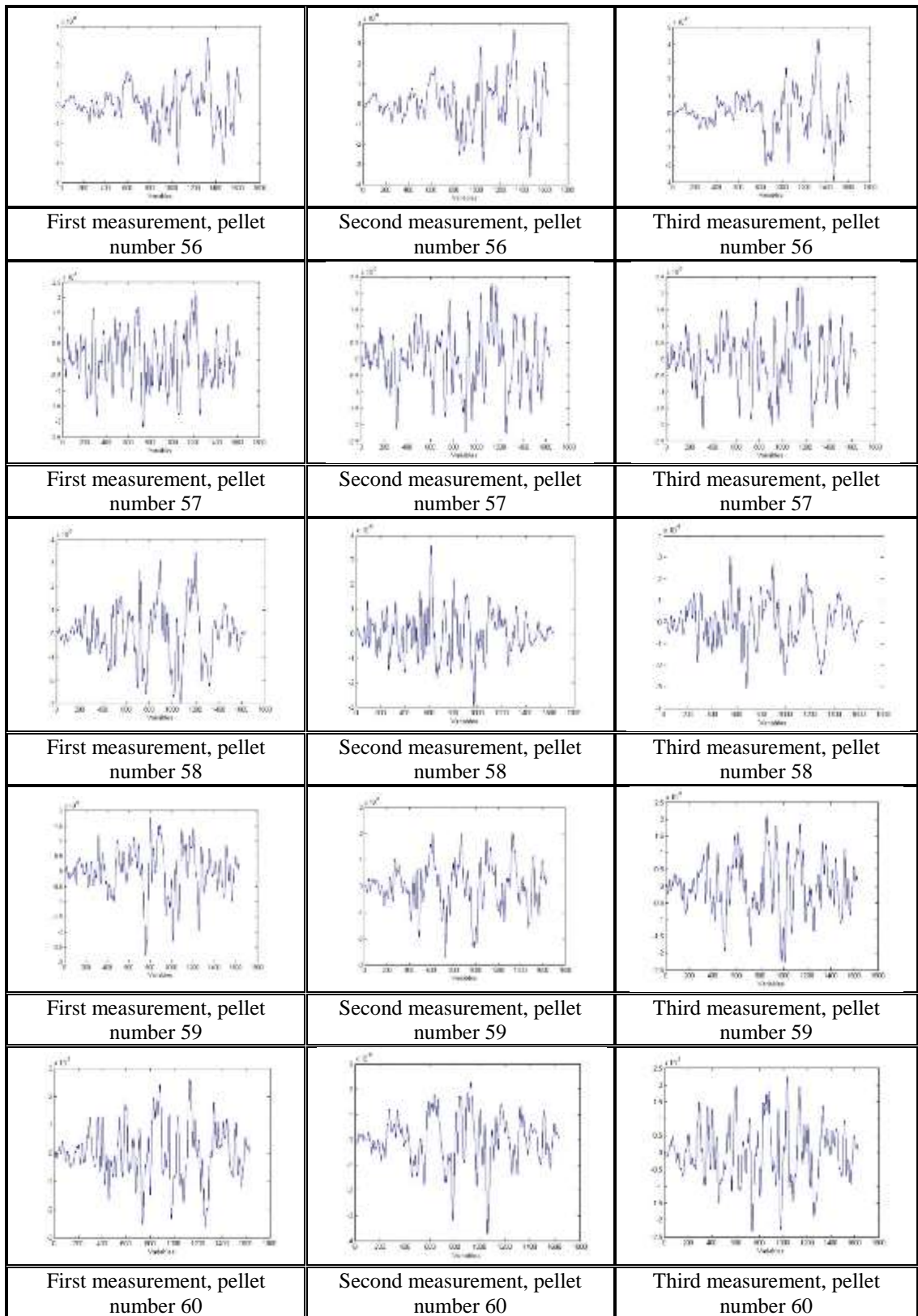




## Appendix 25

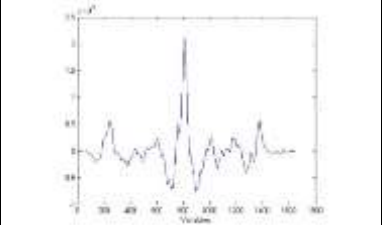
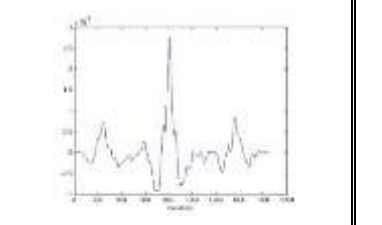
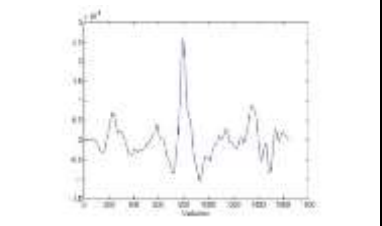
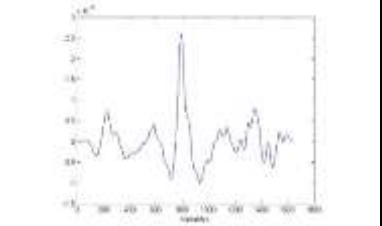
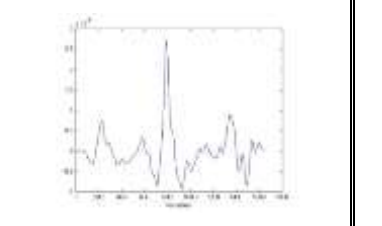
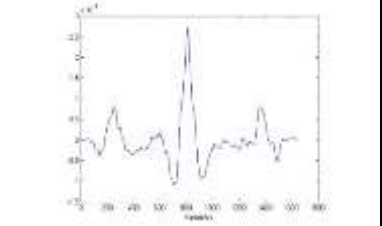
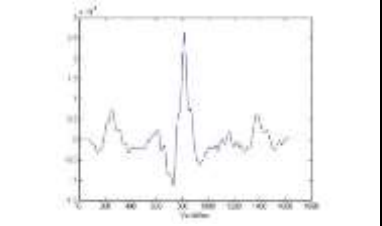
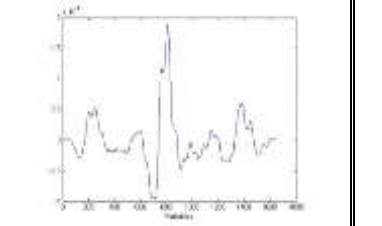
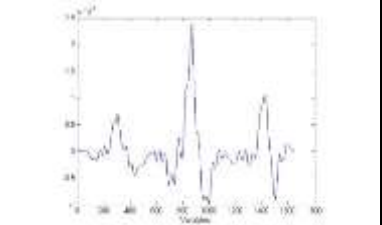
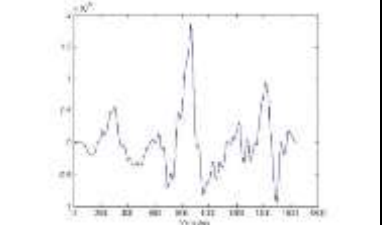
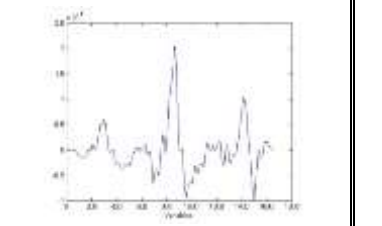
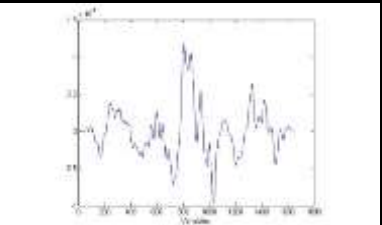
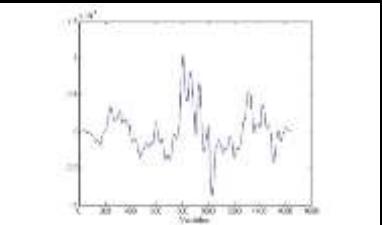
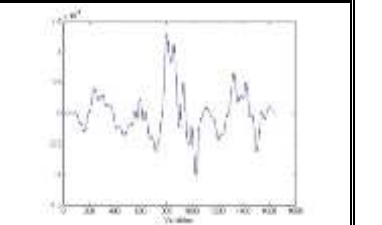
Topographical profiles obtained from the microscopic measurements for samples 51-60, LEA C

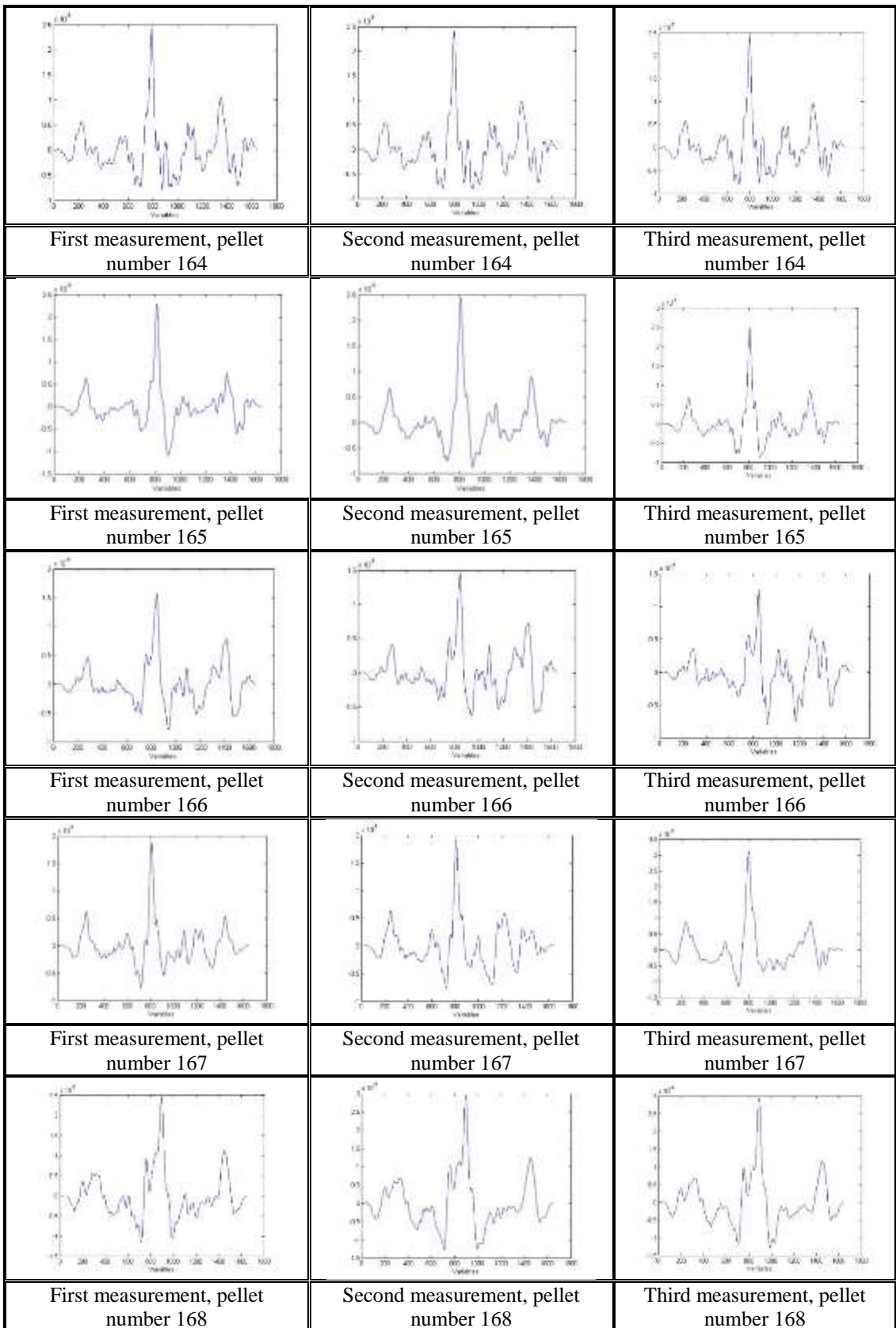
		
	Second measurement, pellet number 51	Third measurement, pellet number 51
		
First measurement, pellet number 52	Second measurement, pellet number 52	Third measurement, pellet number 52
		
First measurement, pellet number 53	Second measurement, pellet number 53	Third measurement, pellet number 53
		
First measurement, pellet number 54	Second measurement, pellet number 54	Third measurement, pellet number 54
		
First measurement, pellet number 55	Second measurement, pellet number 55	Third measurement, pellet number 55



## Appendix 26

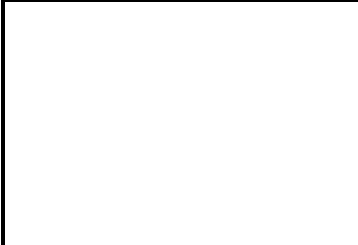
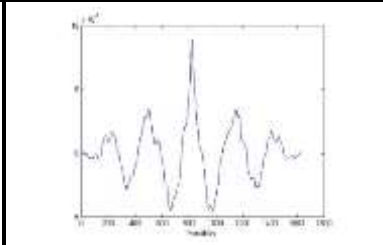
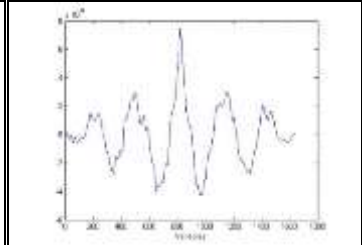
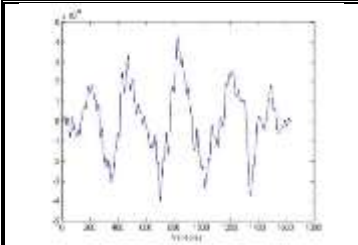
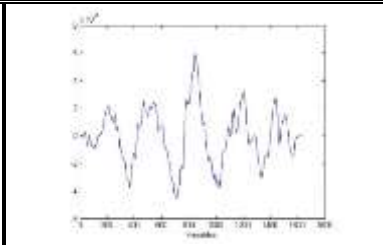
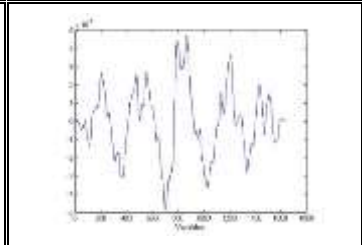
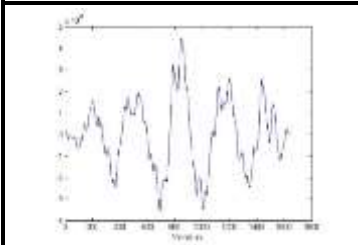
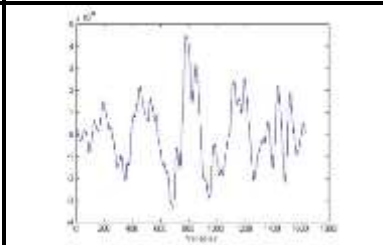
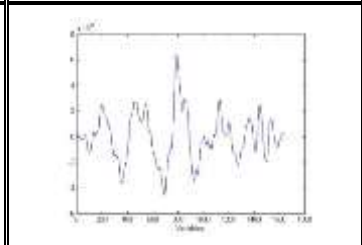
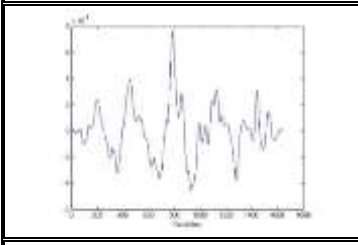
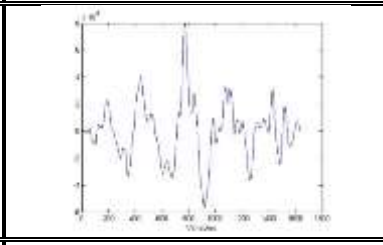
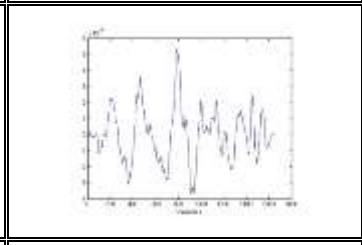
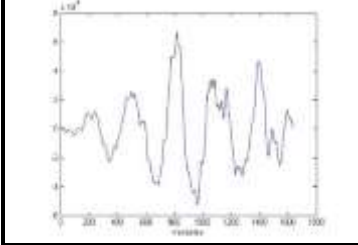
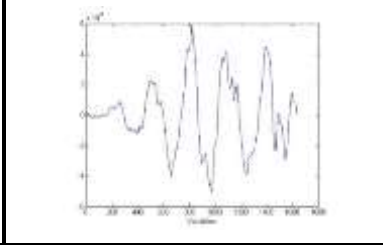
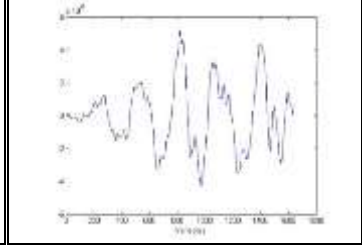
Topographical profiles obtained from the microscopic measurements for samples 159-168, LEA C

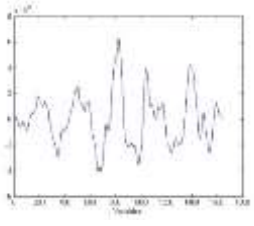
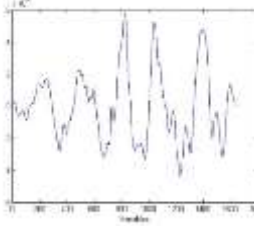
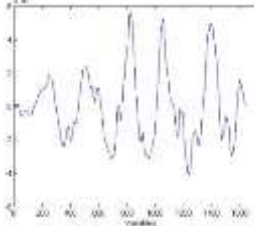
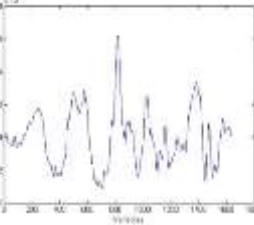
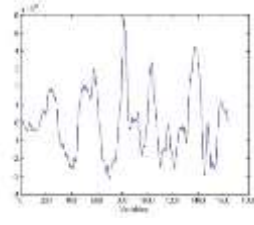
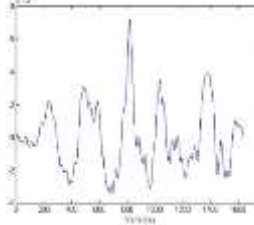
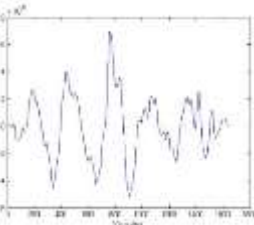
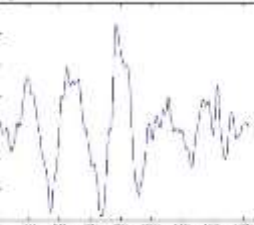
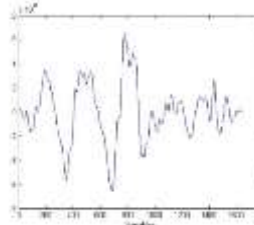
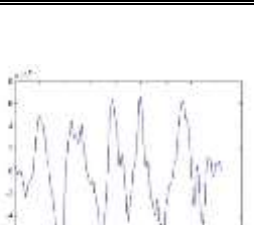
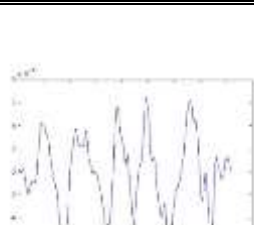
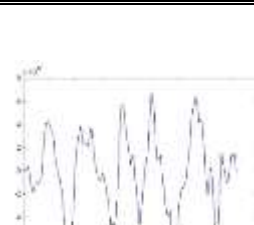
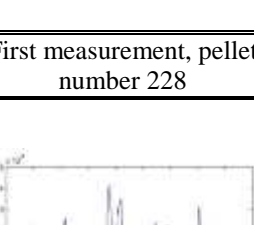
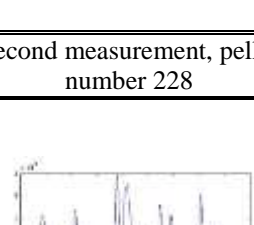
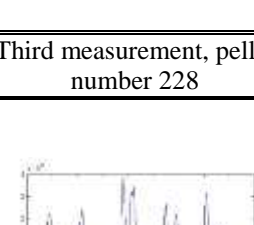
		
	Second measurement, pellet number 159	Third measurement, pellet number 159
		
First measurement, pellet number 160	Second measurement, pellet number 160	Third measurement, pellet number 160
		
First measurement, pellet number 161	Second measurement, pellet number 161	Third measurement, pellet number 161
		
First measurement, pellet number 162	Second measurement, pellet number 162	Third measurement, pellet number 162
		
First measurement, pellet number 163	Second measurement, pellet number 163	Third measurement, pellet number 163



## Appendix 27

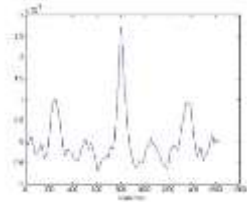
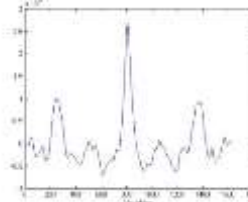
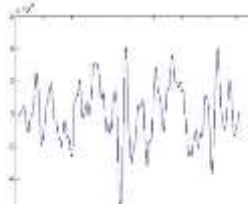
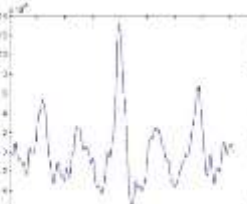
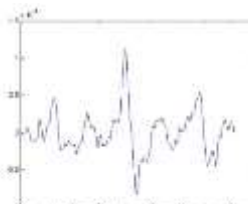
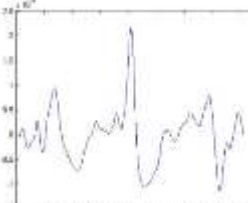
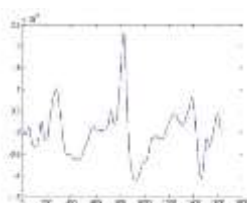
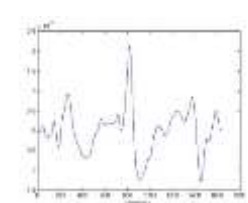
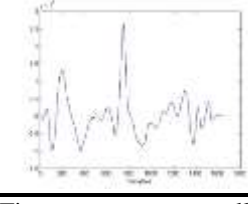
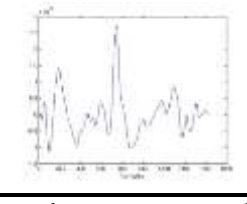
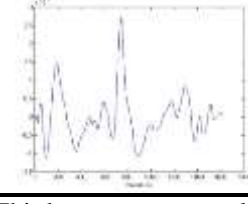
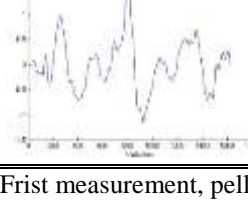
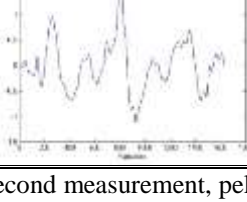
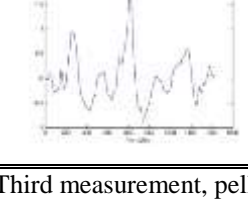
Topographical profiles obtained from the microscopic measurements for samples 220-229, LEA C

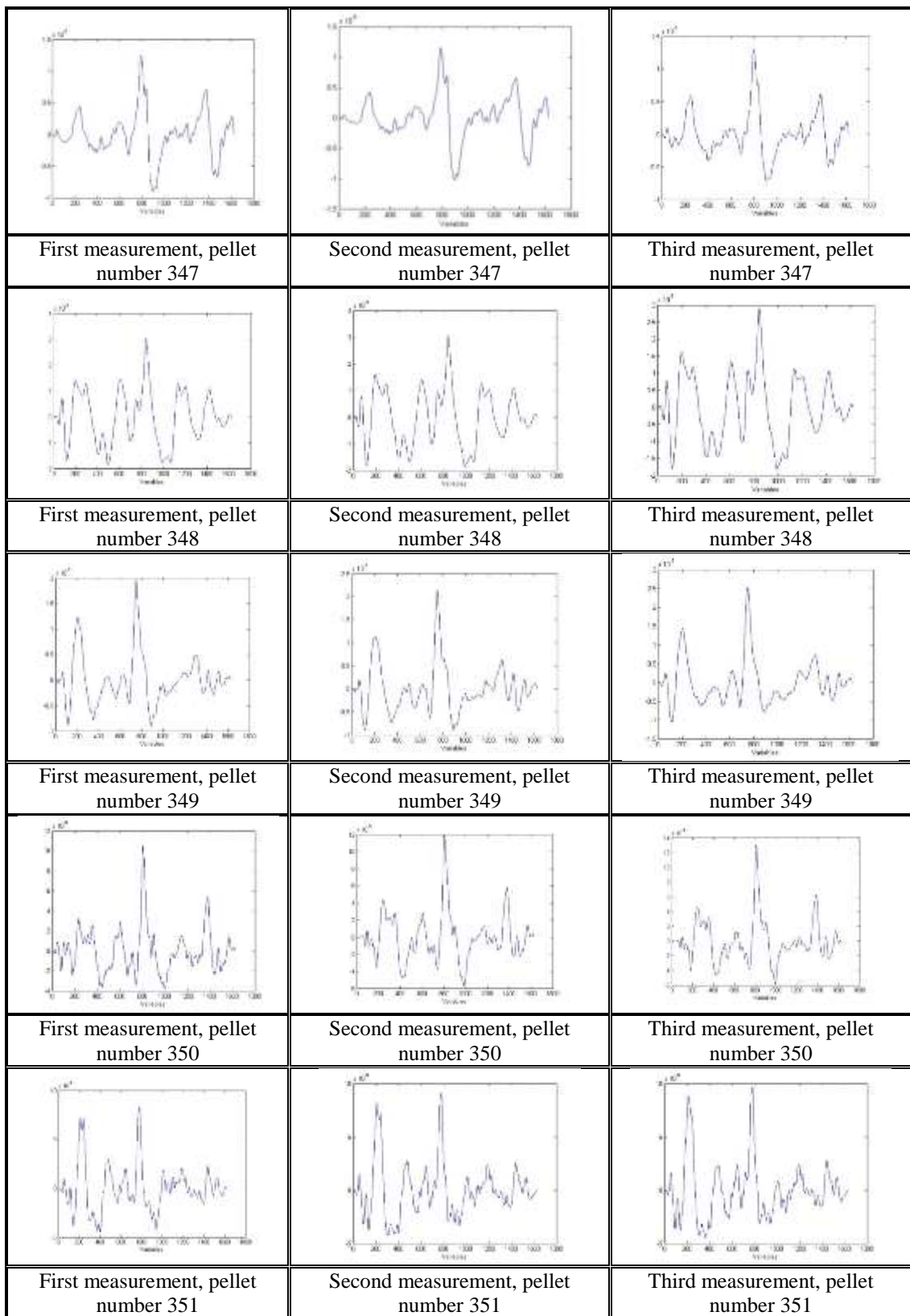
		
	Second measurement, pellet number 220	Third measurement, pellet number 220
		
First measurement, pellet number 221	Second measurement, pellet number 221	Third measurement, pellet number 221
		
First measurement, pellet number 222	Second measurement, pellet number 222	Third measurement, pellet number 222
		
First measurement, pellet number 223	Second measurement, pellet number 223	Third measurement, pellet number 223
		
First measurement, pellet number 224	Second measurement, pellet number 224	Third measurement, pellet number 224

		
First measurement, pellet number 225	Second measurement, pellet number 225	Third measurement, pellet number 225
		
First measurement, pellet number 226	Second measurement, pellet number 226	Third measurement, pellet number 226
		
First measurement, pellet number 227	Second measurement, pellet number 227	Third measurement, pellet number 227
		
First measurement, pellet number 228	Second measurement, pellet number 228	Third measurement, pellet number 228
		
First measurement, pellet number 229	Second measurement, pellet number 229	Third measurement, pellet number 229

## Appendix 28

Topographical profiles obtained from the microscopic measurements for samples 342-351, LEA C

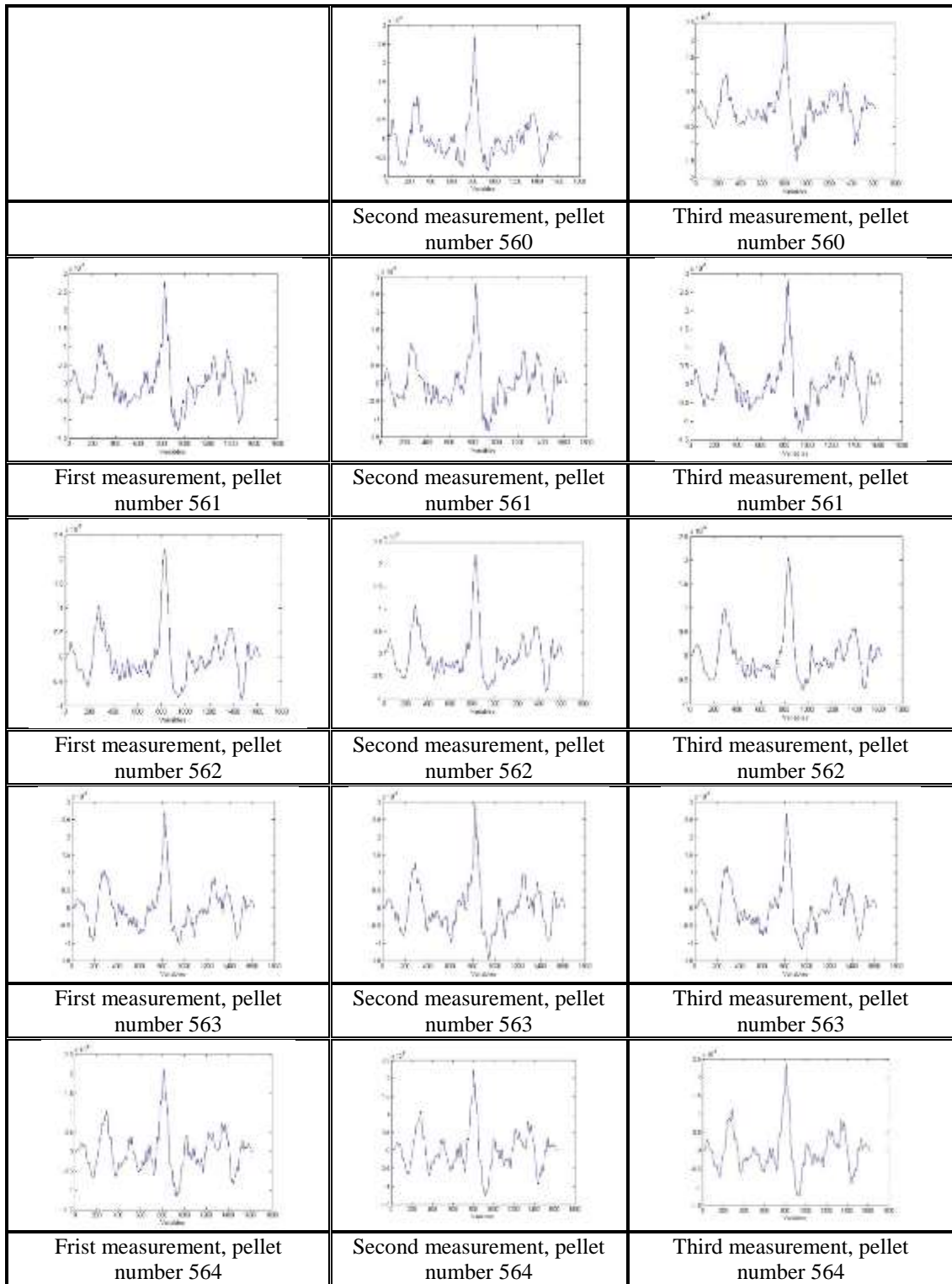
		
	Second measurement, pellet number 342	Third measurement, pellet number 342
		
First measurement, pellet number 343	Second measurement, pellet number 343	Third measurement, pellet number 343
		
First measurement, pellet number 344	Second measurement, pellet number 344	Third measurement, pellet number 344
		
First measurement, pellet number 345	Second measurement, pellet number 345	Third measurement, pellet number 345
		
First measurement, pellet number 346	Second measurement, pellet number 346	Third measurement, pellet number 346

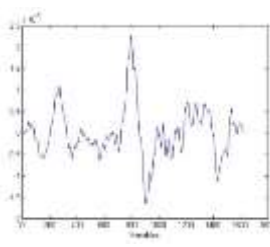
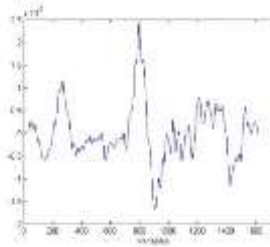
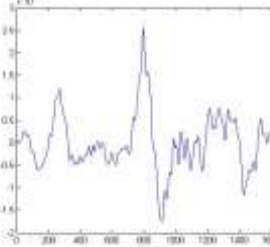
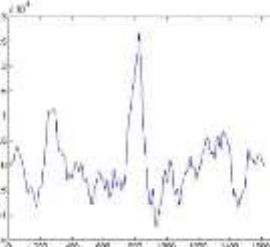
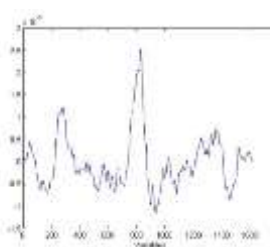
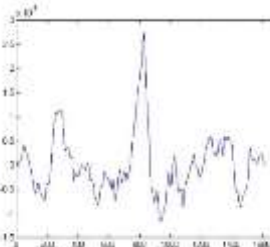
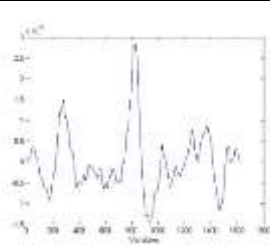
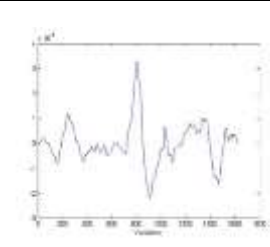
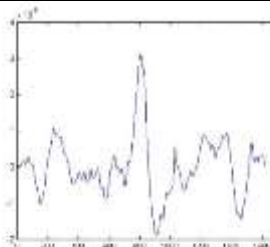
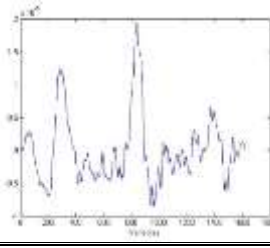
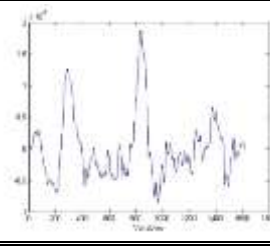
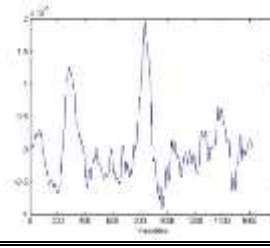
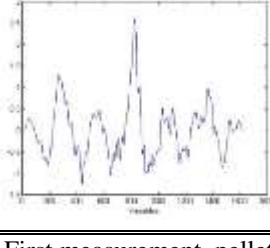
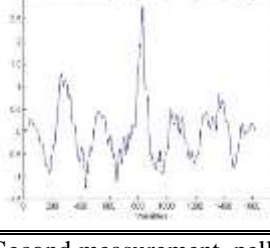
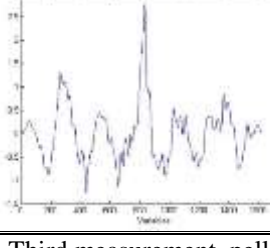




## Appendix 29

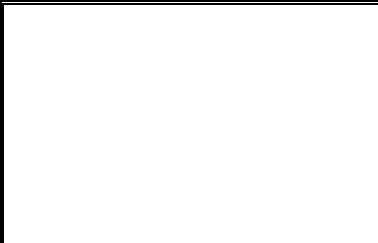
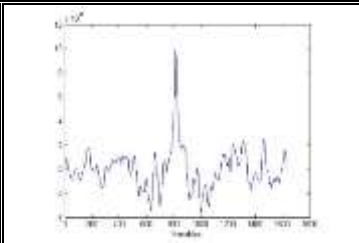
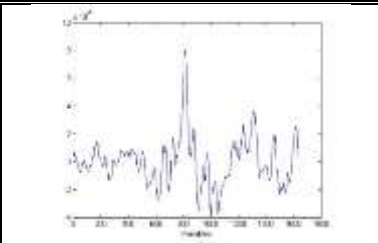
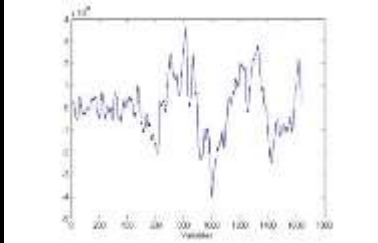
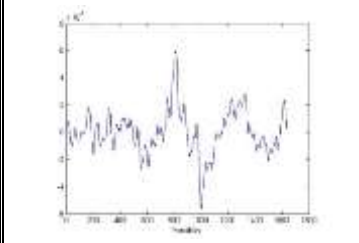
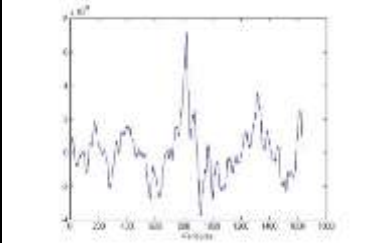
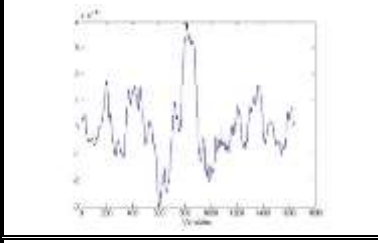
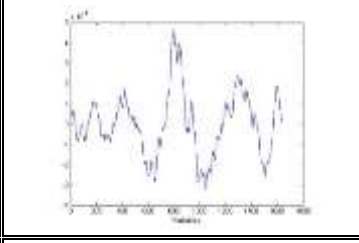
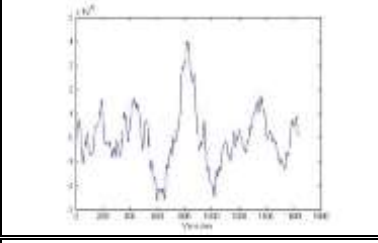
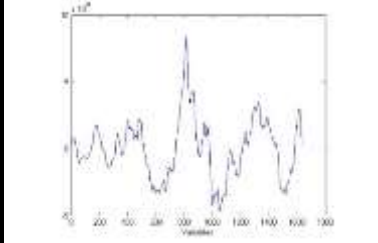
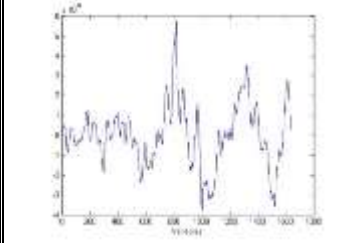
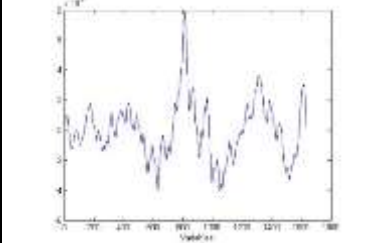
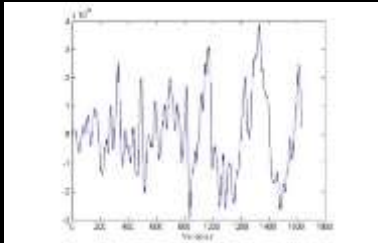
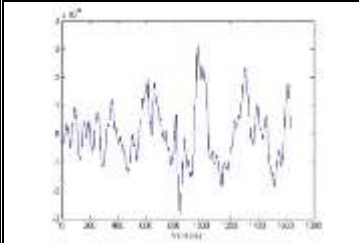
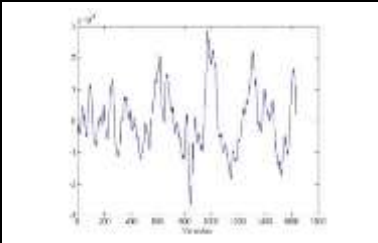
Topographical profiles obtained from the microscopic measurements for samples 560-569, LEA C

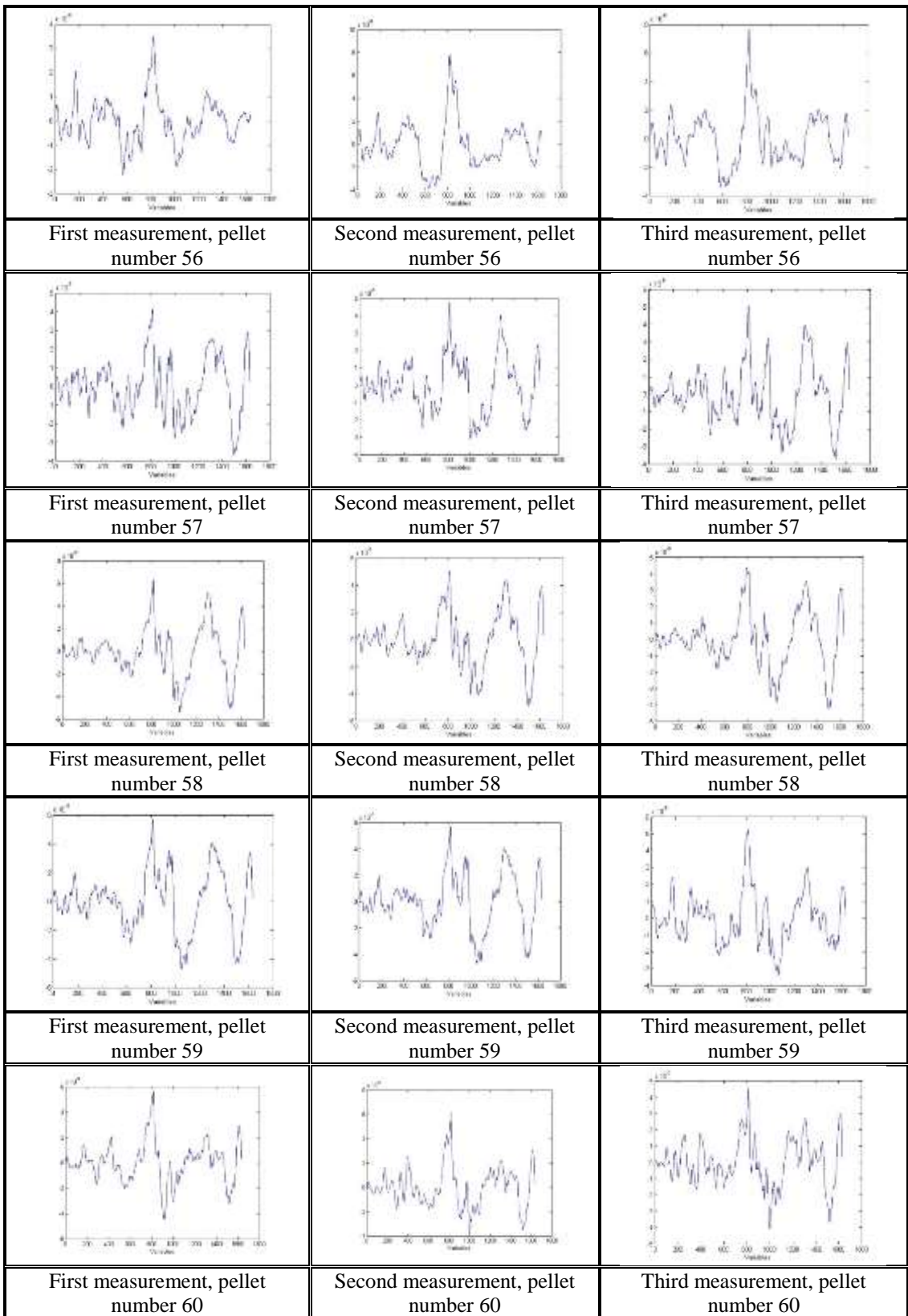


		
First measurement, pellet number 565	Second measurement, pellet number 565	Third measurement, pellet number 565
		
First measurement, pellet number 566	Second measurement, pellet number 566	Third measurement, pellet number 566
		
First measurement, pellet number 567	Second measurement, pellet number 567	Third measurement, pellet number 567
		
First measurement, pellet number 568	Second measurement, pellet number 568	Third measurement, pellet number 568
		
First measurement, pellet number 569	Second measurement, pellet number 569	Third measurement, pellet number 569

## Appendix 30

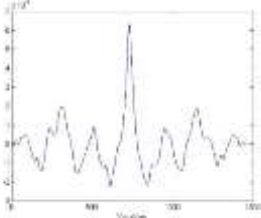
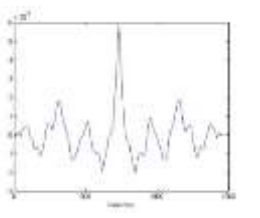
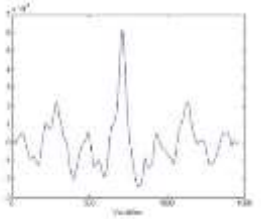
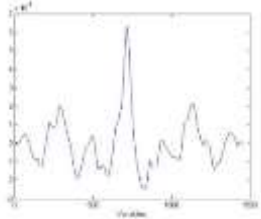
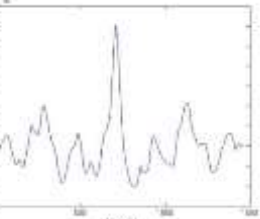
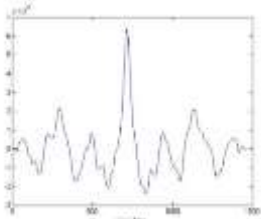
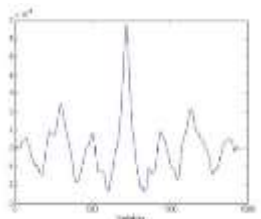
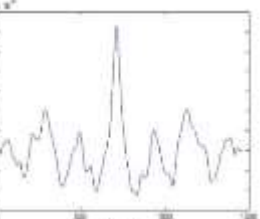
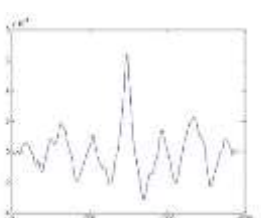
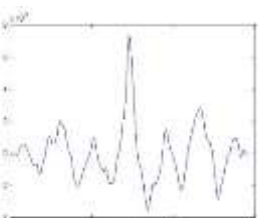

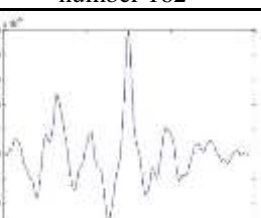

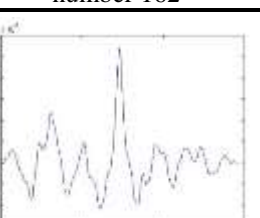
Topographical profiles obtained from the microscopic measurements for samples 51-60,  
LEA D

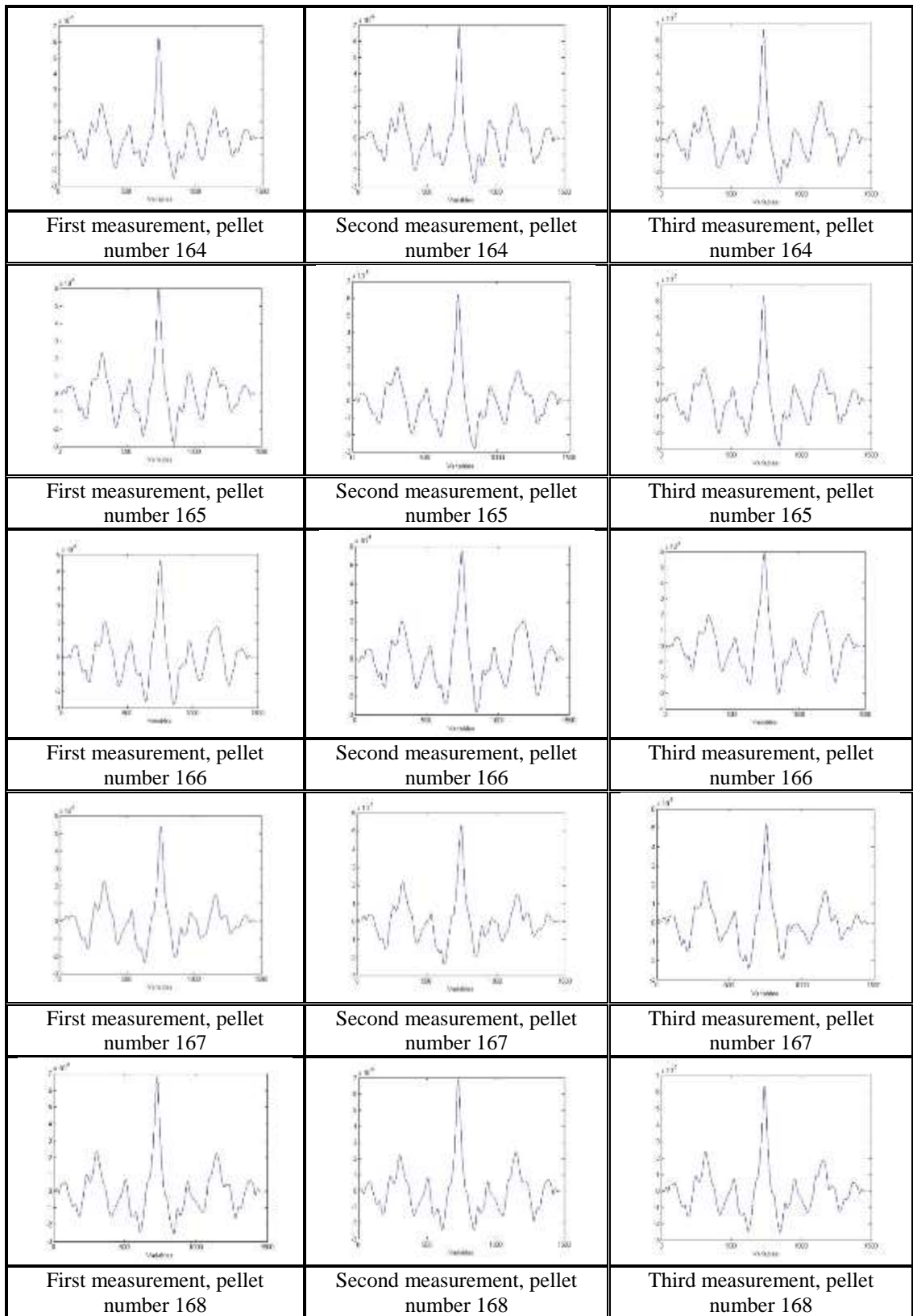
		
	Second measurement, pellet number 51	Third measurement, pellet number 51
		
First measurement, pellet number 52	Second measurement, pellet number 52	Third measurement, pellet number 52
		
First measurement, pellet number 53	Second measurement, pellet number 53	Third measurement, pellet number 53
		
First measurement, pellet number 54	Second measurement, pellet number 54	Third measurement, pellet number 54
		
First measurement, pellet number 55	Second measurement, pellet number 55	Third measurement, pellet number 55



## Appendix 31

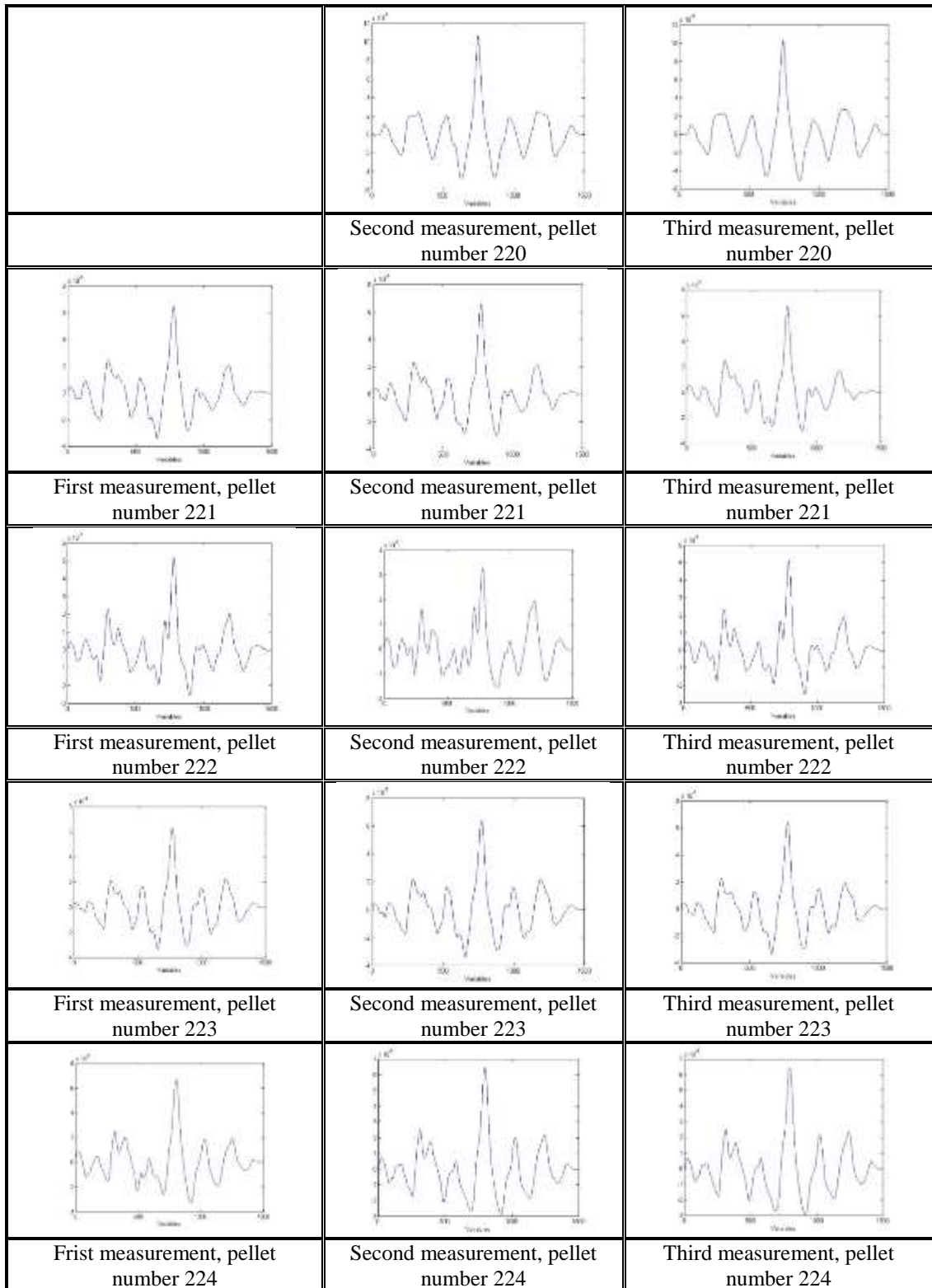
Topographical profiles obtained from the microscopic measurements for samples 159-168, LEA D

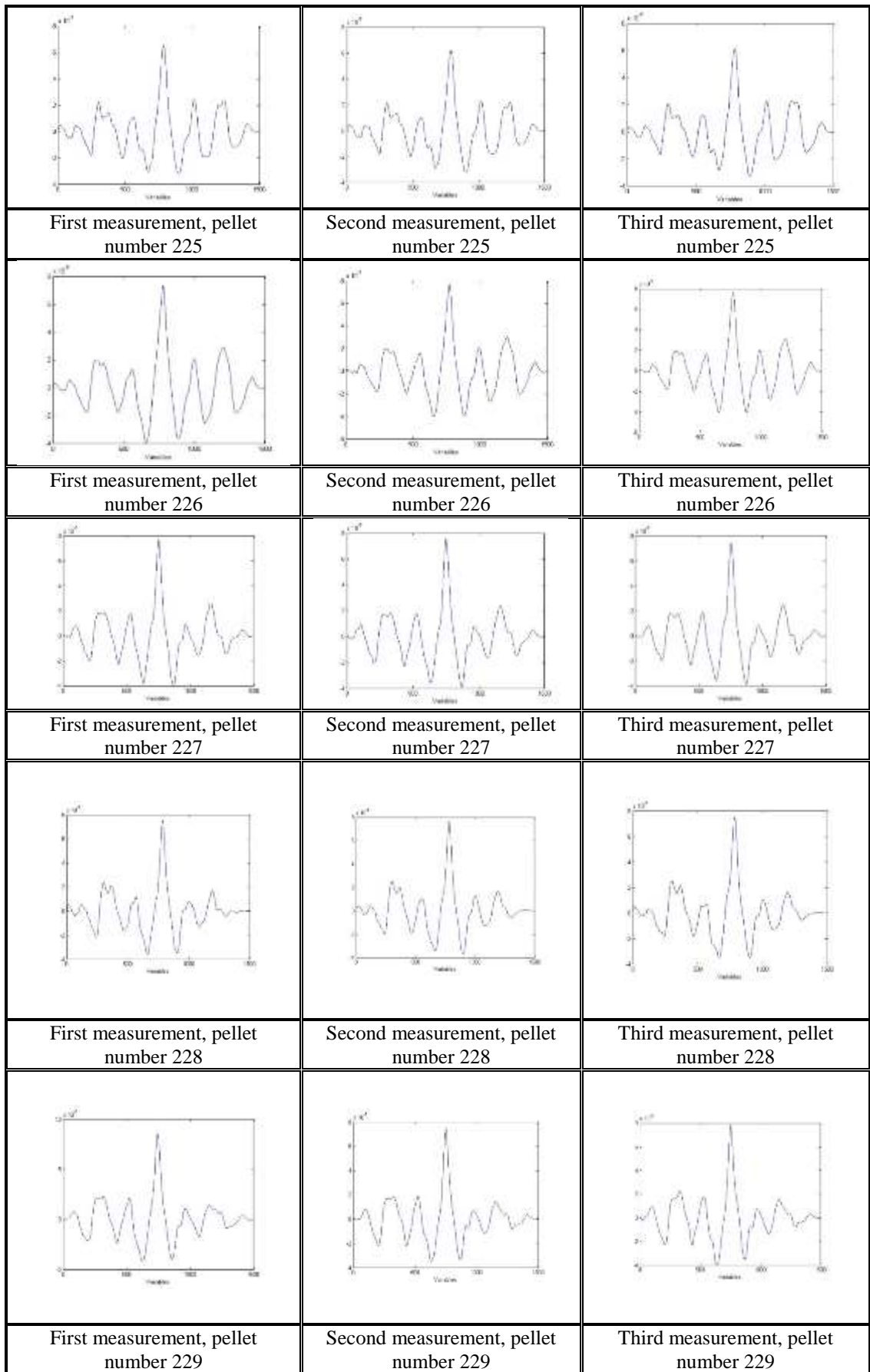
		
	Second measurement, pellet number 159	Third measurement, pellet number 159
		
First measurement, pellet number 160	Second measurement, pellet number 160	Third measurement, pellet number 160
		
First measurement, pellet number 161	Second measurement, pellet number 161	Third measurement, pellet number 161
		
First measurement, pellet number 162	Second measurement, pellet number 162	Third measurement, pellet number 162
		
First measurement, pellet number 163	Second measurement, pellet number 163	Third measurement, pellet number 163



## Appendix 32

Topographical profiles obtained from the microscopic measurements for samples 220-229, LEA D

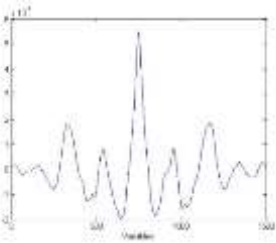
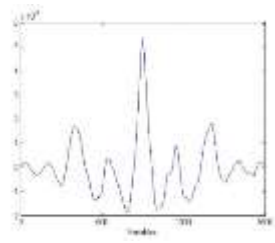
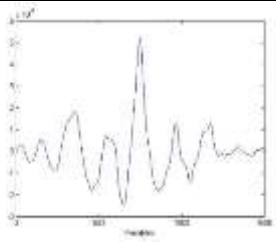
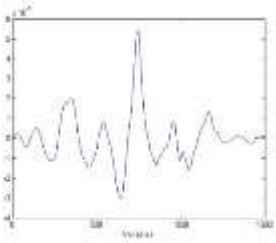
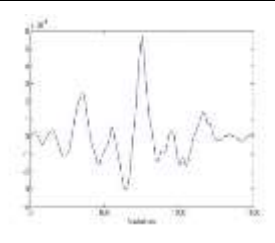
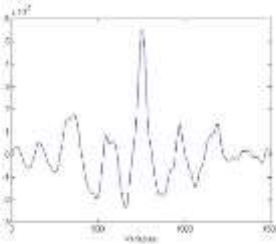
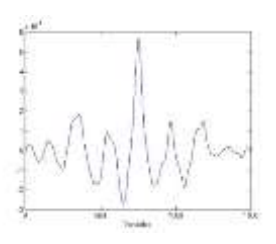
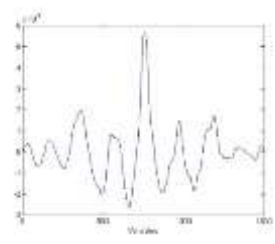
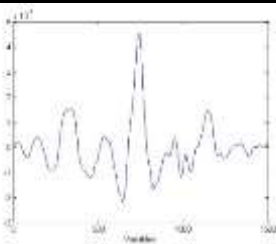
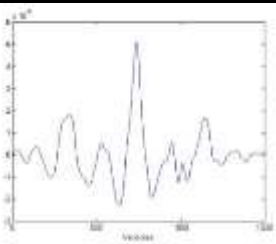
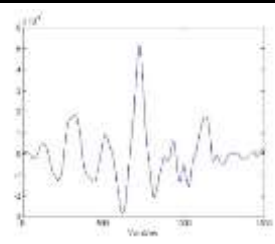
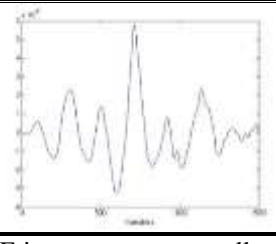
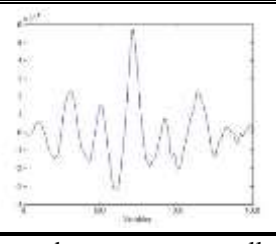
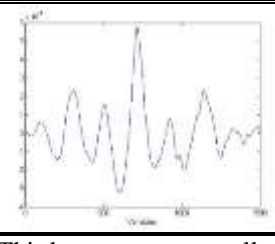


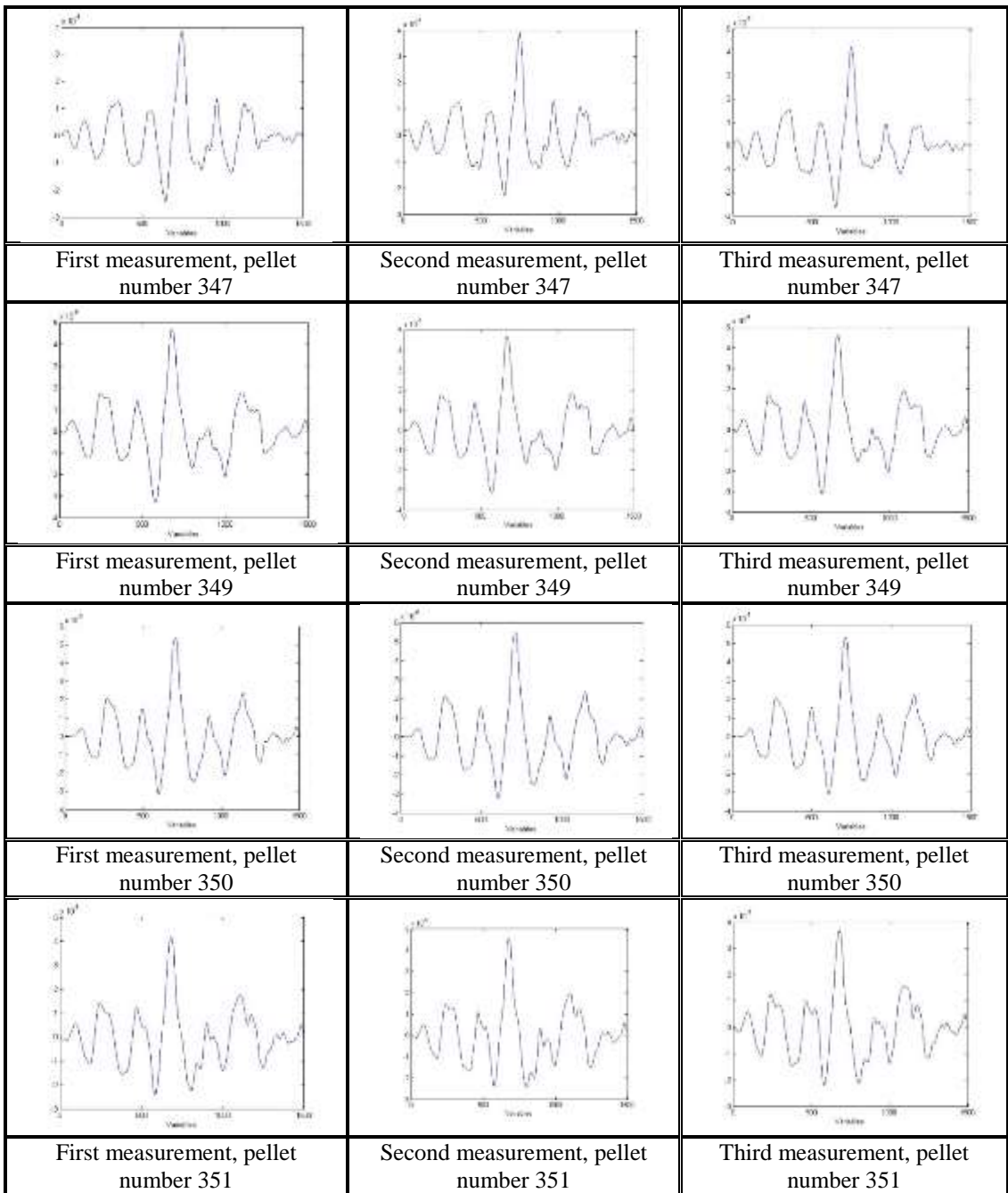




### Appendix 33

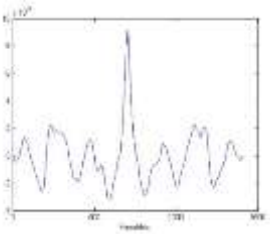
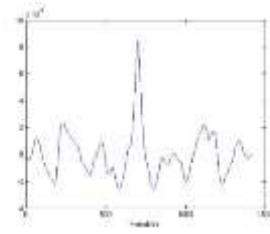
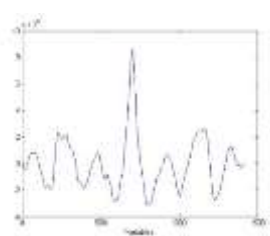
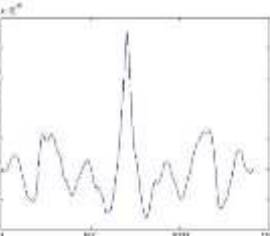
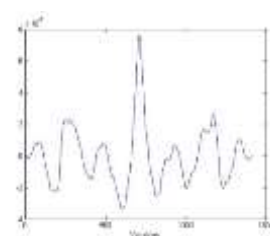
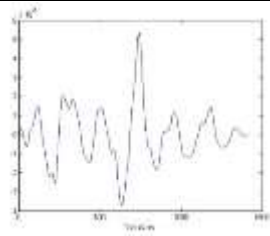
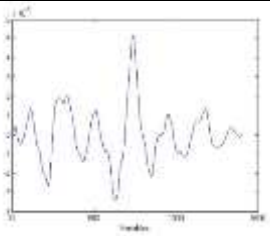
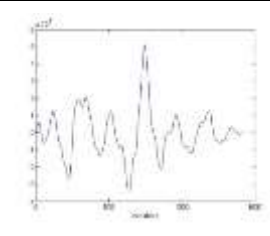
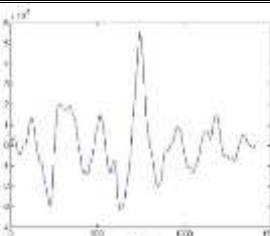
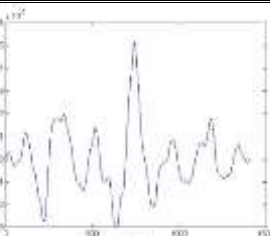
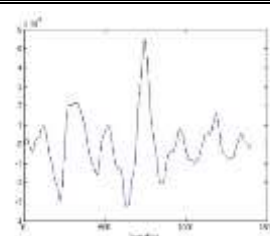
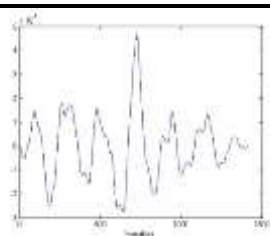
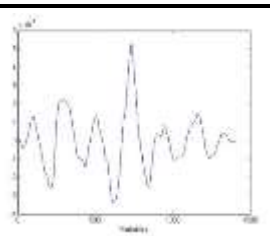
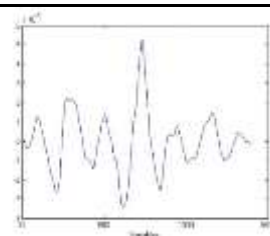
Topographical profiles obtained from the microscopic measurements for samples 342-351, LEA D

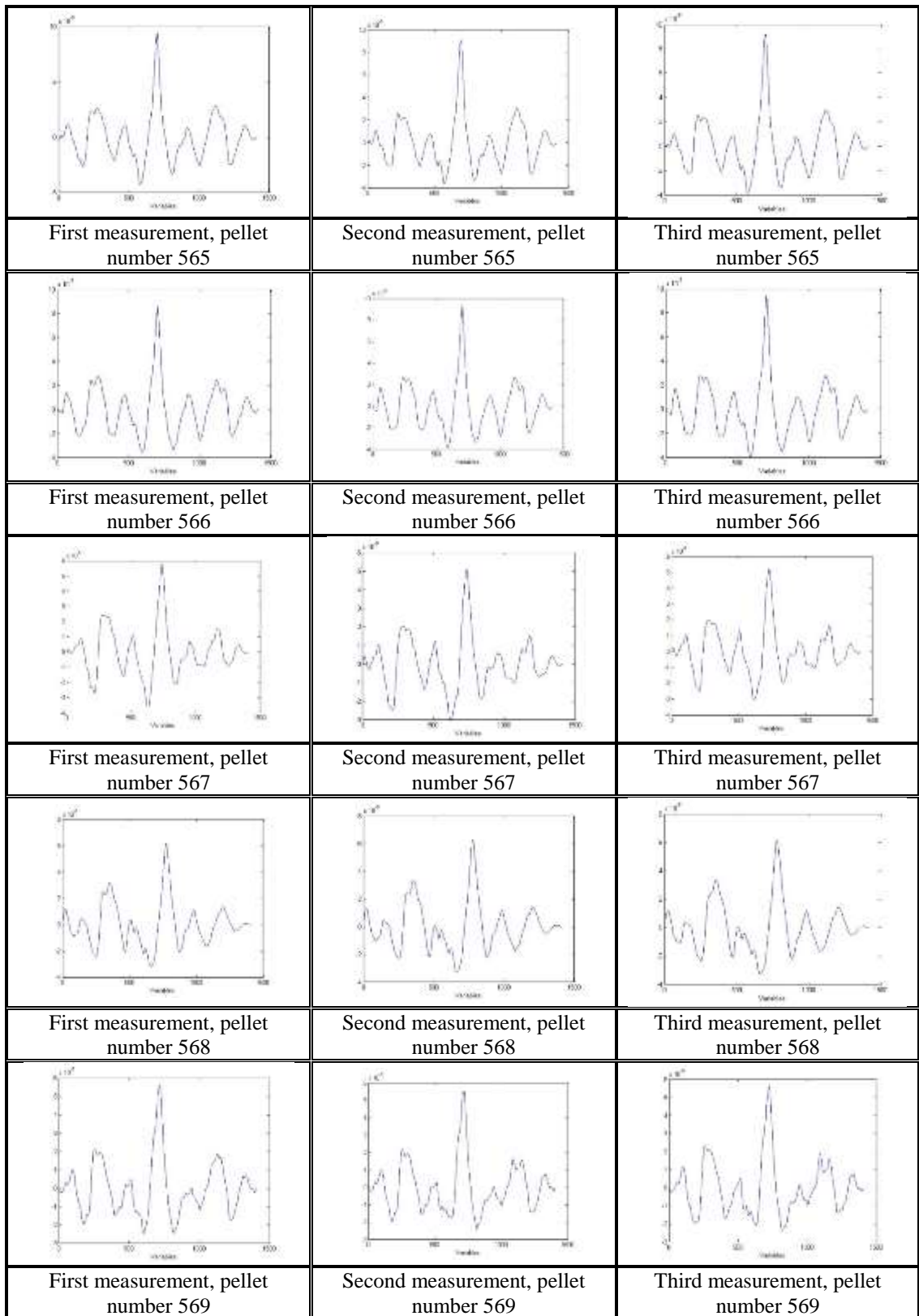
		
	Second measurement, pellet number 342	Third measurement, pellet number 342
		
First measurement, pellet number 343	Second measurement, pellet number 343	Third measurement, pellet number 343
		
First measurement, pellet number 344	Second measurement, pellet number 344	Third measurement, pellet number 344
		
First measurement, pellet number 345	Second measurement, pellet number 345	Third measurement, pellet number 345
		
First measurement, pellet number 346	Second measurement, pellet number 346	Third measurement, pellet number 346



## Appendix 34

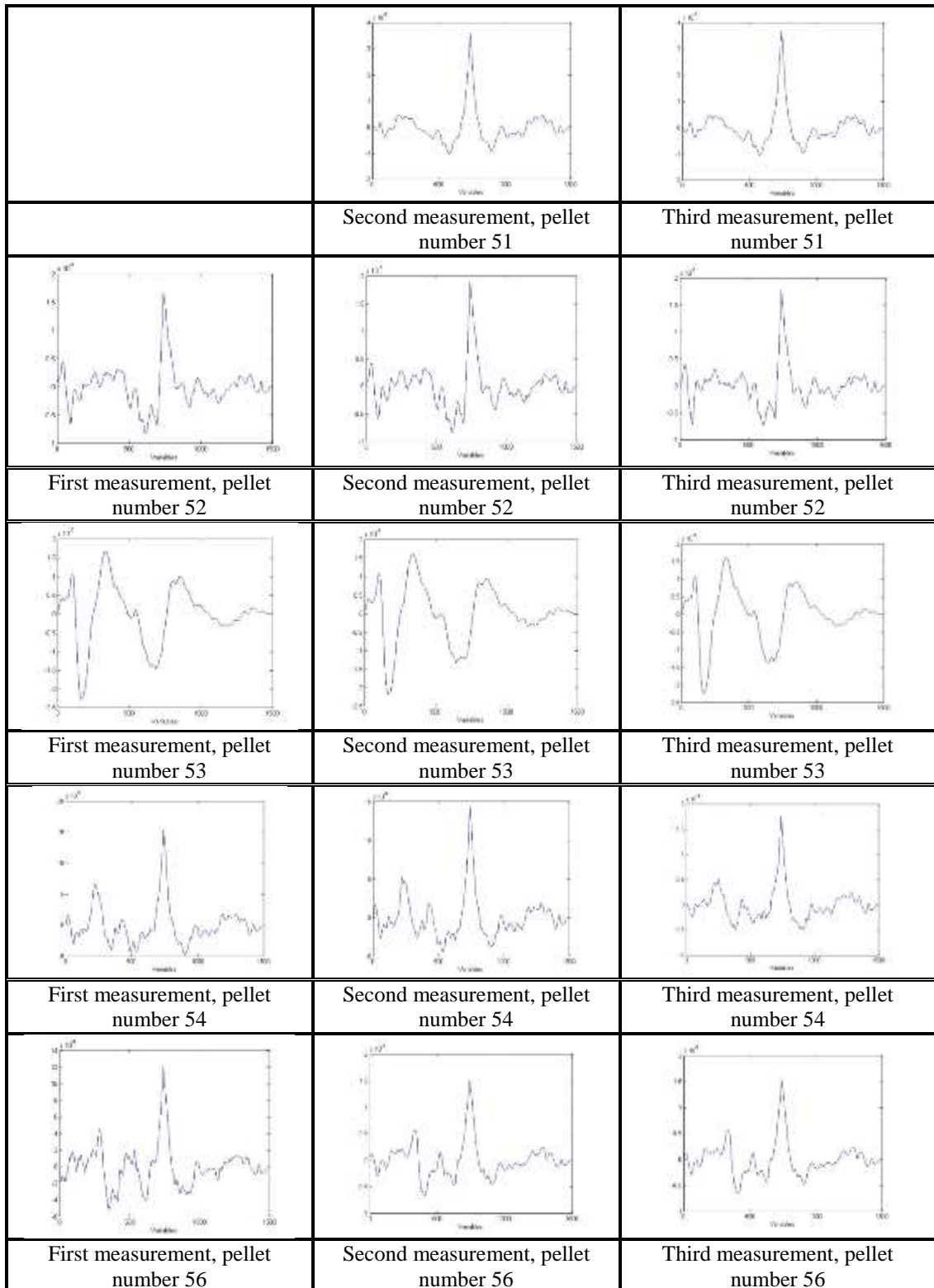
Topographical profiles obtained from the microscopic measurements for samples 560-569, LEA D

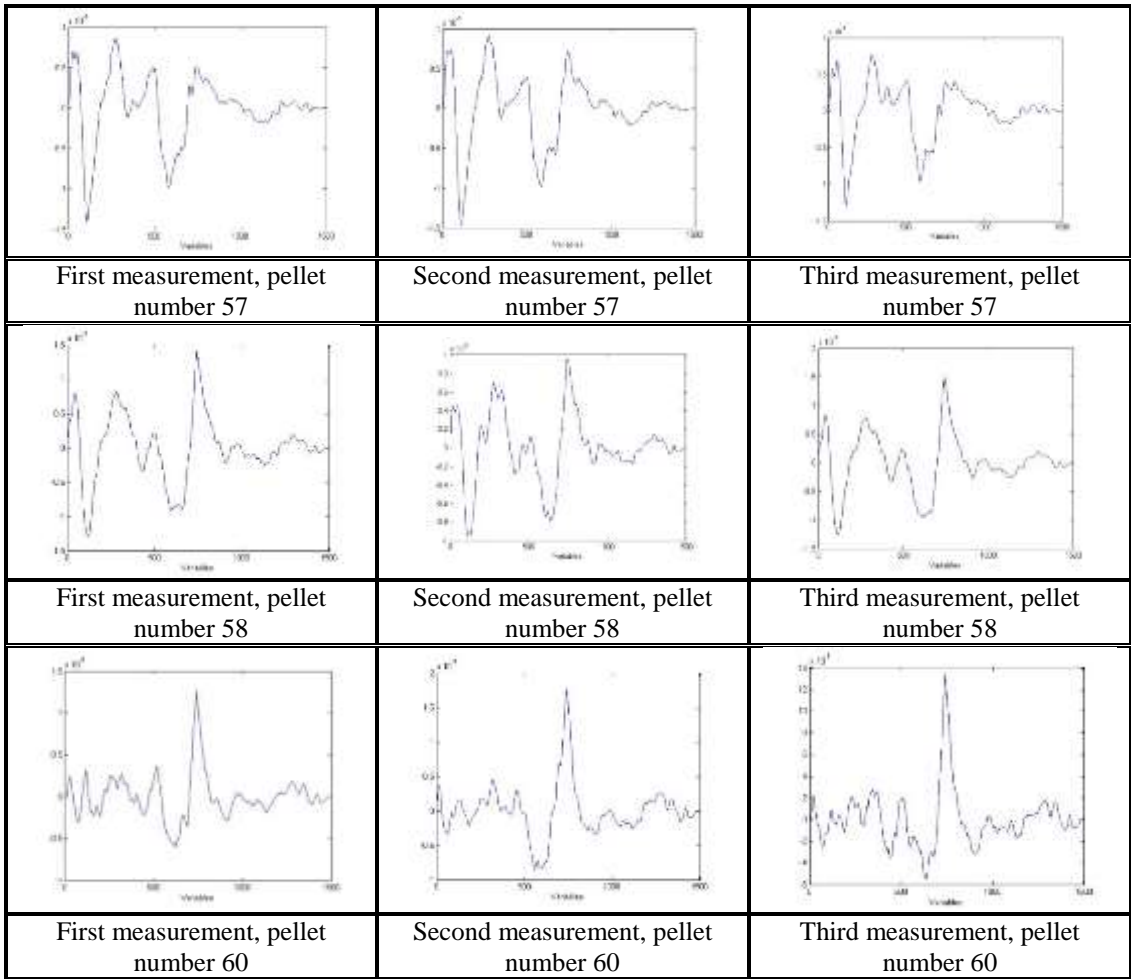
		
	Second measurement, pellet number 560	Third measurement, pellet number 560
		
First measurement, pellet number 561	Second measurement, pellet number 561	Third measurement, pellet number 561
		
First measurement, pellet number 562	Second measurement, pellet number 562	Third measurement, pellet number 562
		
First measurement, pellet number 563	Second measurement, pellet number 563	Third measurement, pellet number 563
		
First measurement, pellet number 564	Second measurement, pellet number 564	Third measurement, pellet number 564



## Appendix 35

Topographical profiles obtained from the microscopic measurements for samples 51-60, LEA E

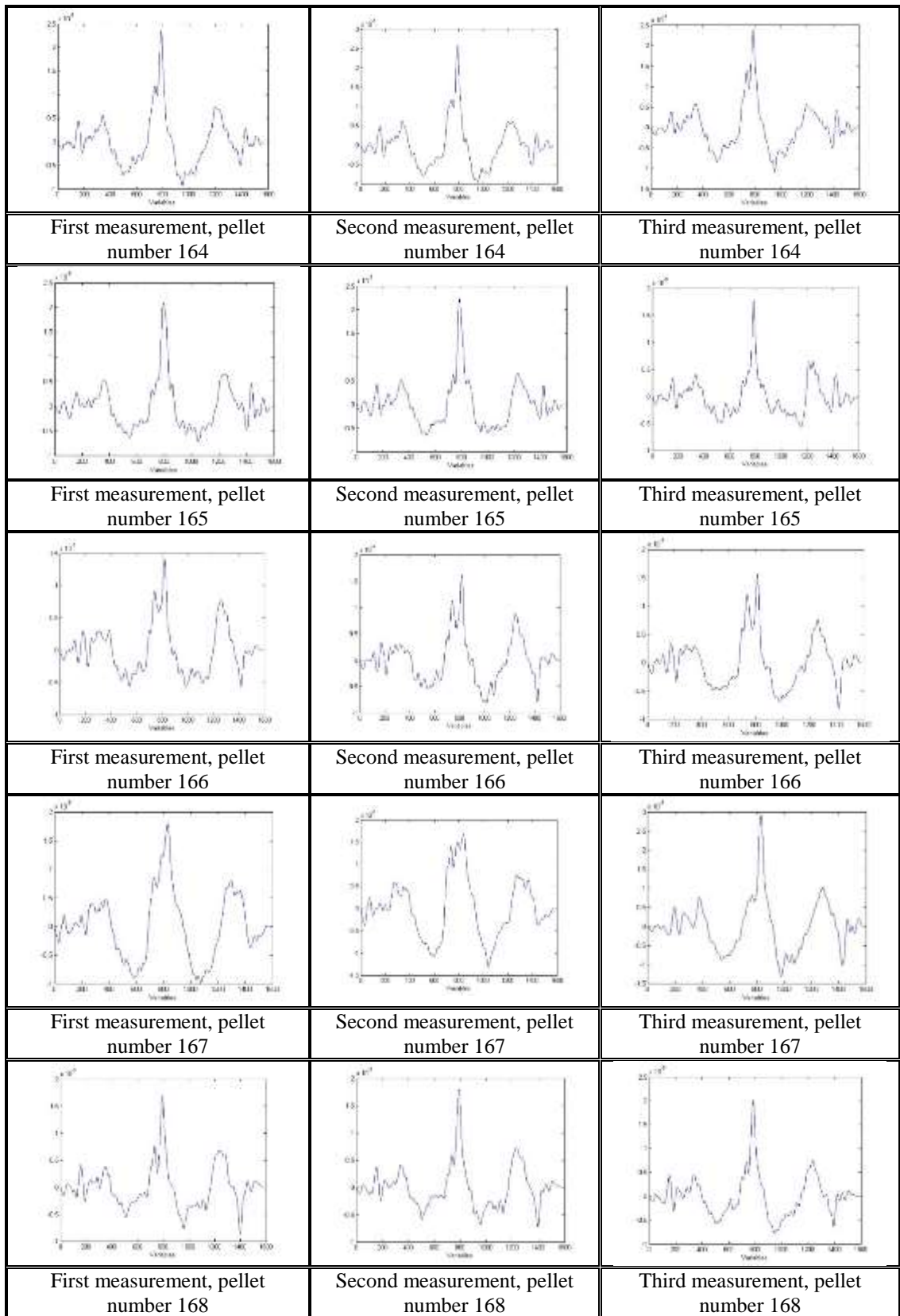




## Appendix 36

Topographical profiles obtained from the microscopic measurements for samples 159-168, LEA E

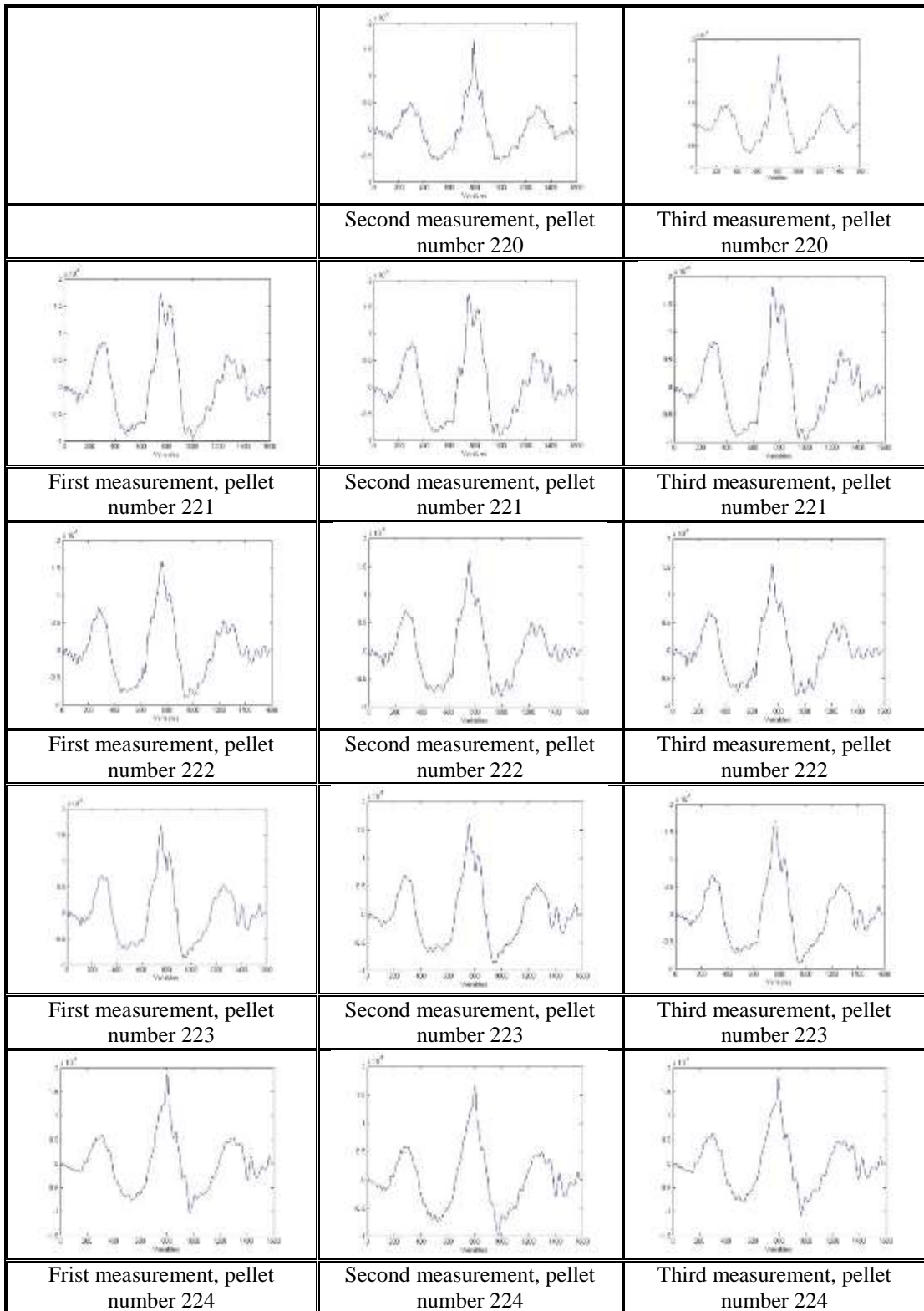
	Second measurement, pellet number 159	Third measurement, pellet number 159
First measurement, pellet number 160	Second measurement, pellet number 160	Third measurement, pellet number 160
First measurement, pellet number 161	Second measurement, pellet number 161	Third measurement, pellet number 161
First measurement, pellet number 162	Second measurement, pellet number 162	Third measurement, pellet number 162
First measurement, pellet number 163	Second measurement, pellet number 163	Third measurement, pellet number 163

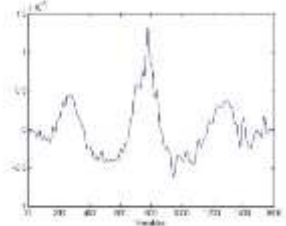
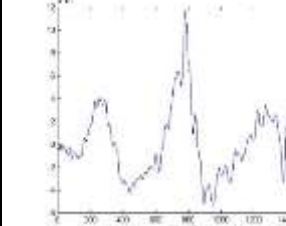
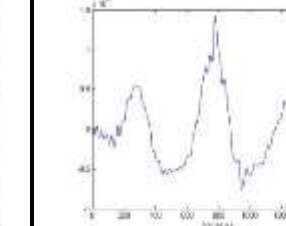
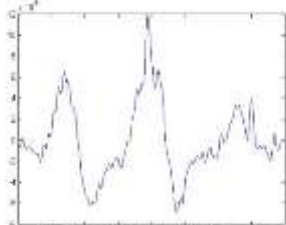
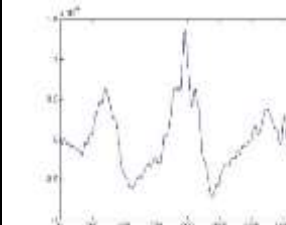
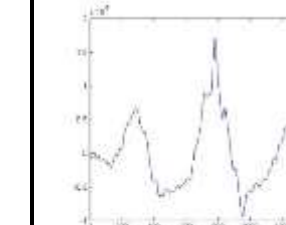
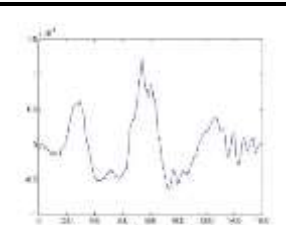
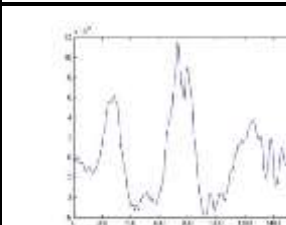
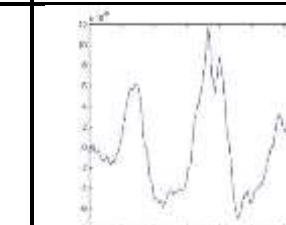
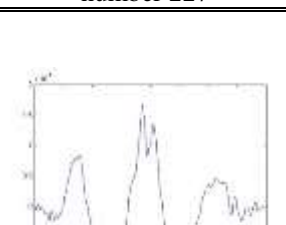
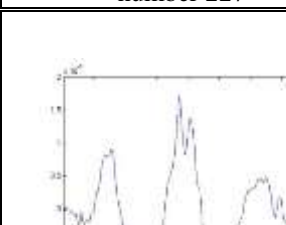
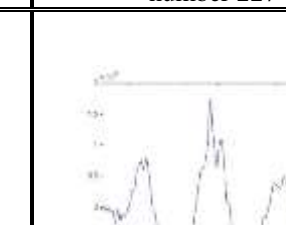
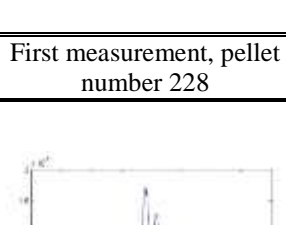
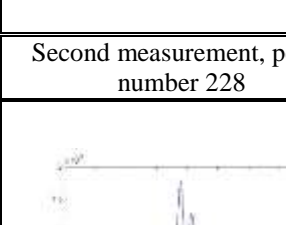
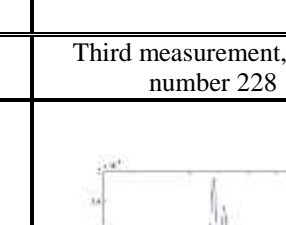




## Appendix 37

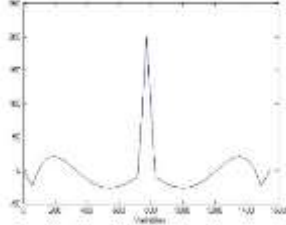
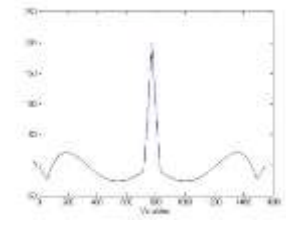
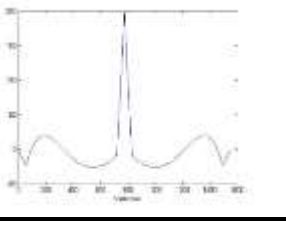
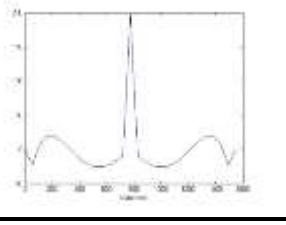
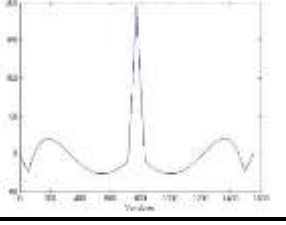
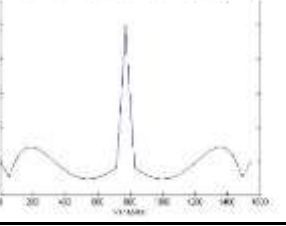
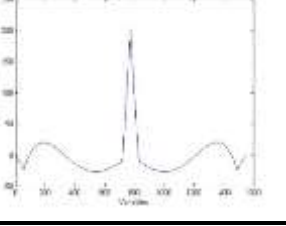
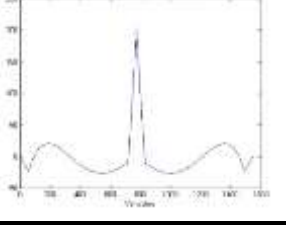
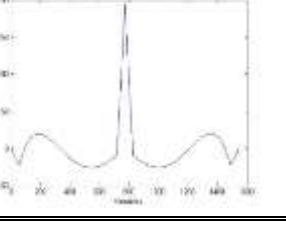
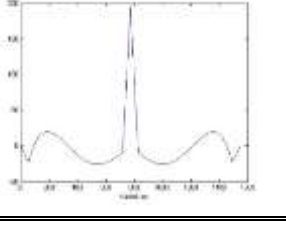
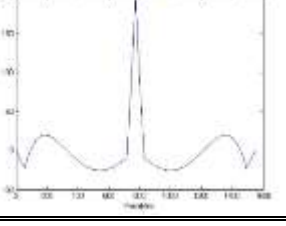
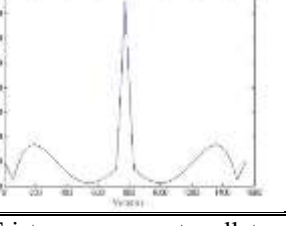
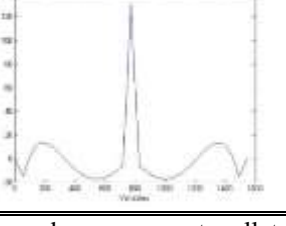
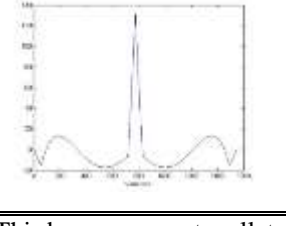
Topographical profiles obtained from the microscopic measurements for samples 220-229, LEA E

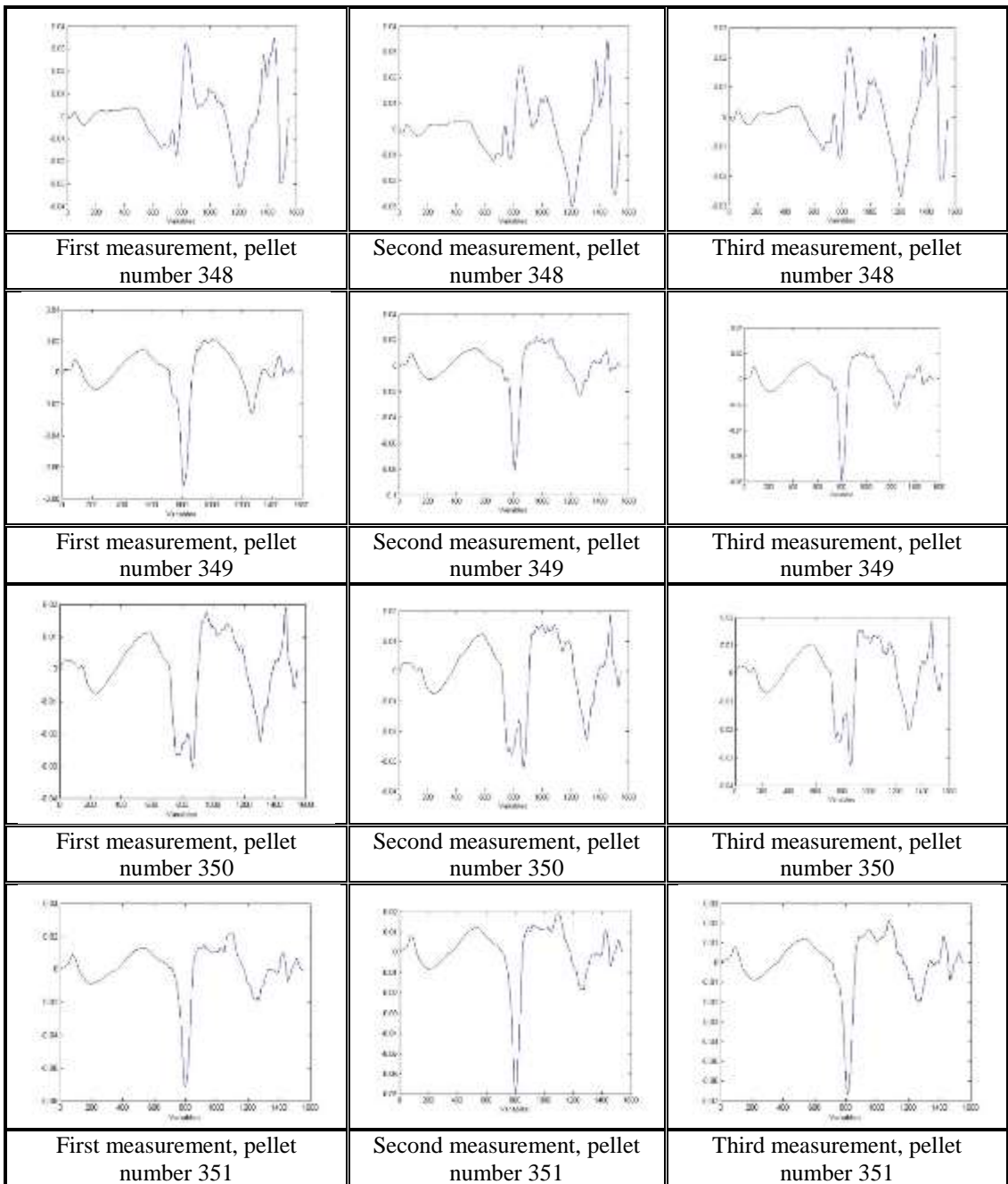


		
First measurement, pellet number 225	Second measurement, pellet number 225	Third measurement, pellet number 225
		
First measurement, pellet number 226	Second measurement, pellet number 226	Third measurement, pellet number 226
		
First measurement, pellet number 227	Second measurement, pellet number 227	Third measurement, pellet number 227
		
First measurement, pellet number 228	Second measurement, pellet number 228	Third measurement, pellet number 228
		
First measurement, pellet number 229	Second measurement, pellet number 229	Third measurement, pellet number 229

## Appendix 38

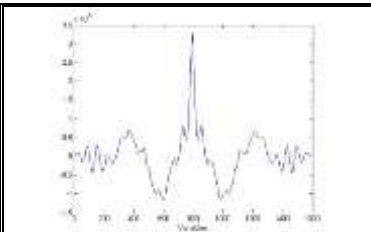
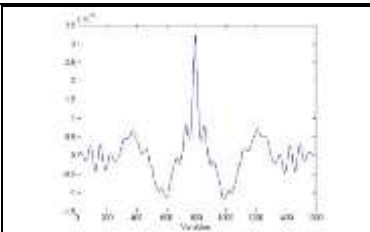
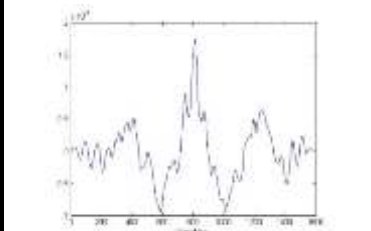
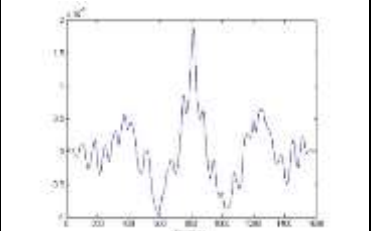
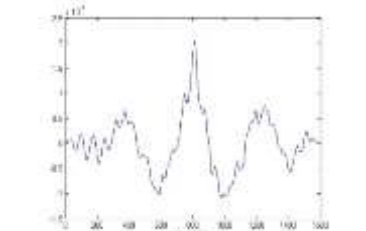
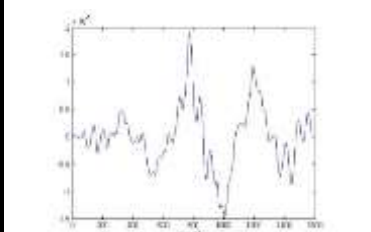
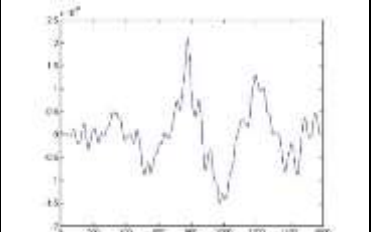
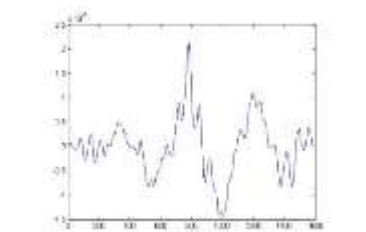
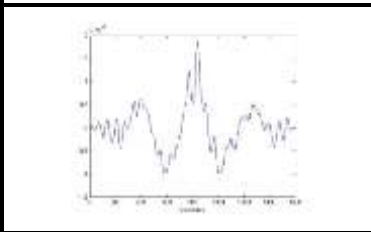
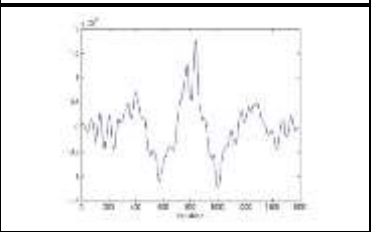
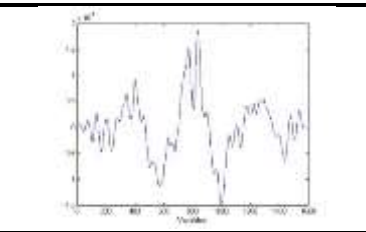
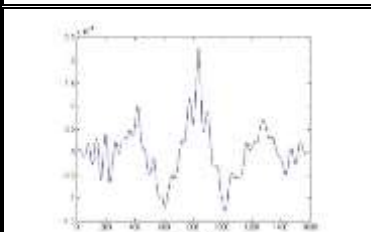
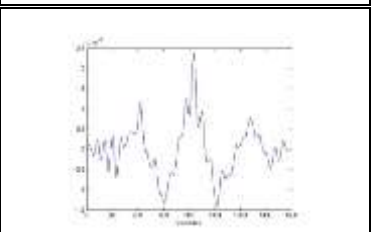
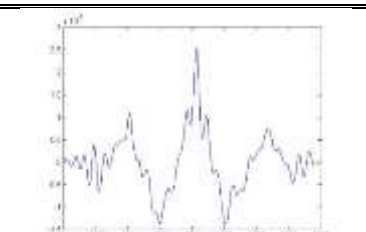
Topographical profiles obtained from the microscopic measurements for samples 342-351, LEA E

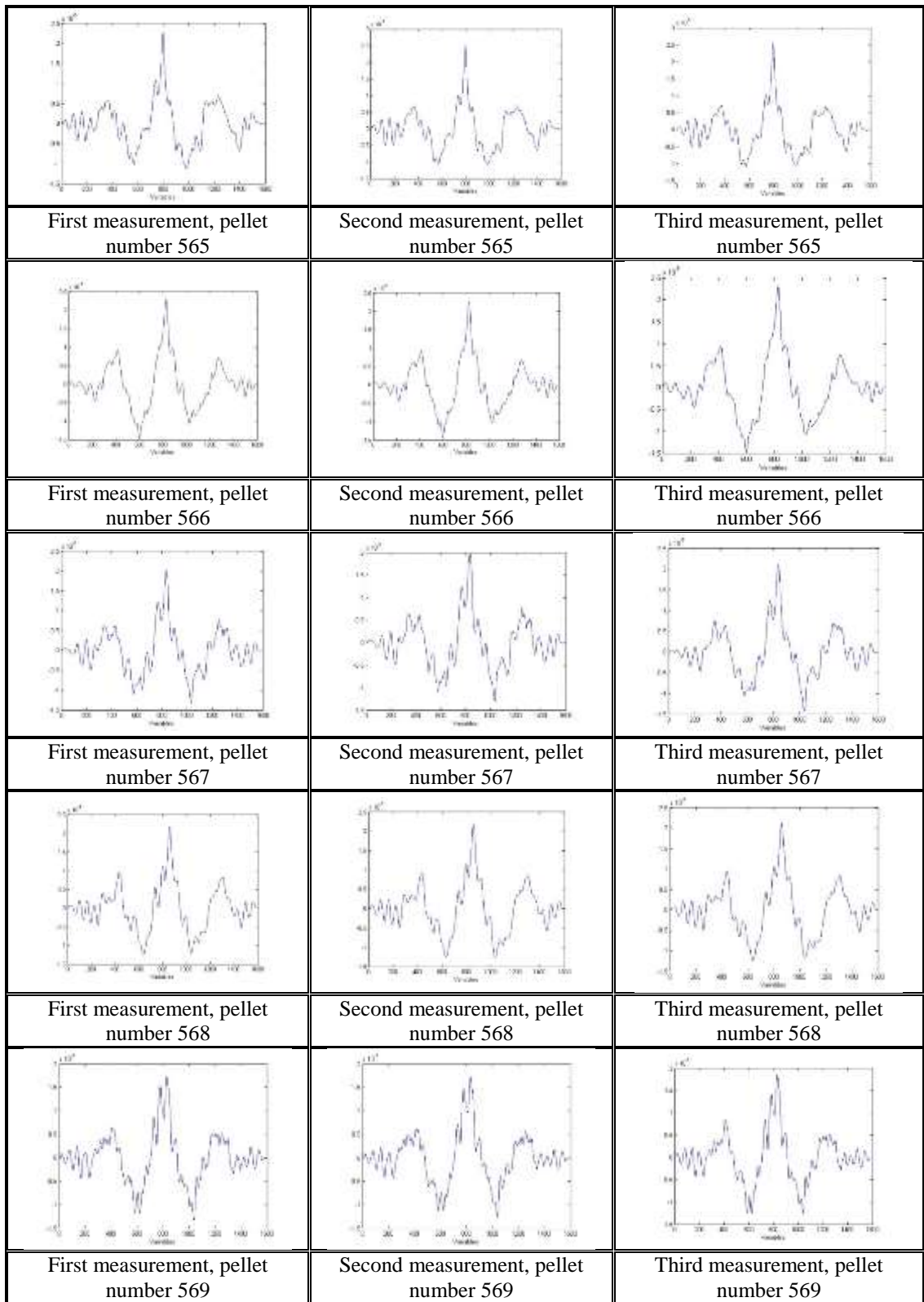
		
	Second measurement, pellet number 342	Third measurement, pellet number 342
		
First measurement, pellet number 343	Second measurement, pellet number 343	Third measurement, pellet number 343
		
First measurement, pellet number 344	Second measurement, pellet number 344	Third measurement, pellet number 344
		
First measurement, pellet number 345	Second measurement, pellet number 345	Third measurement, pellet number 345
		
First measurement, pellet number 346	Second measurement, pellet number 346	Third measurement, pellet number 346



## Appendix 39

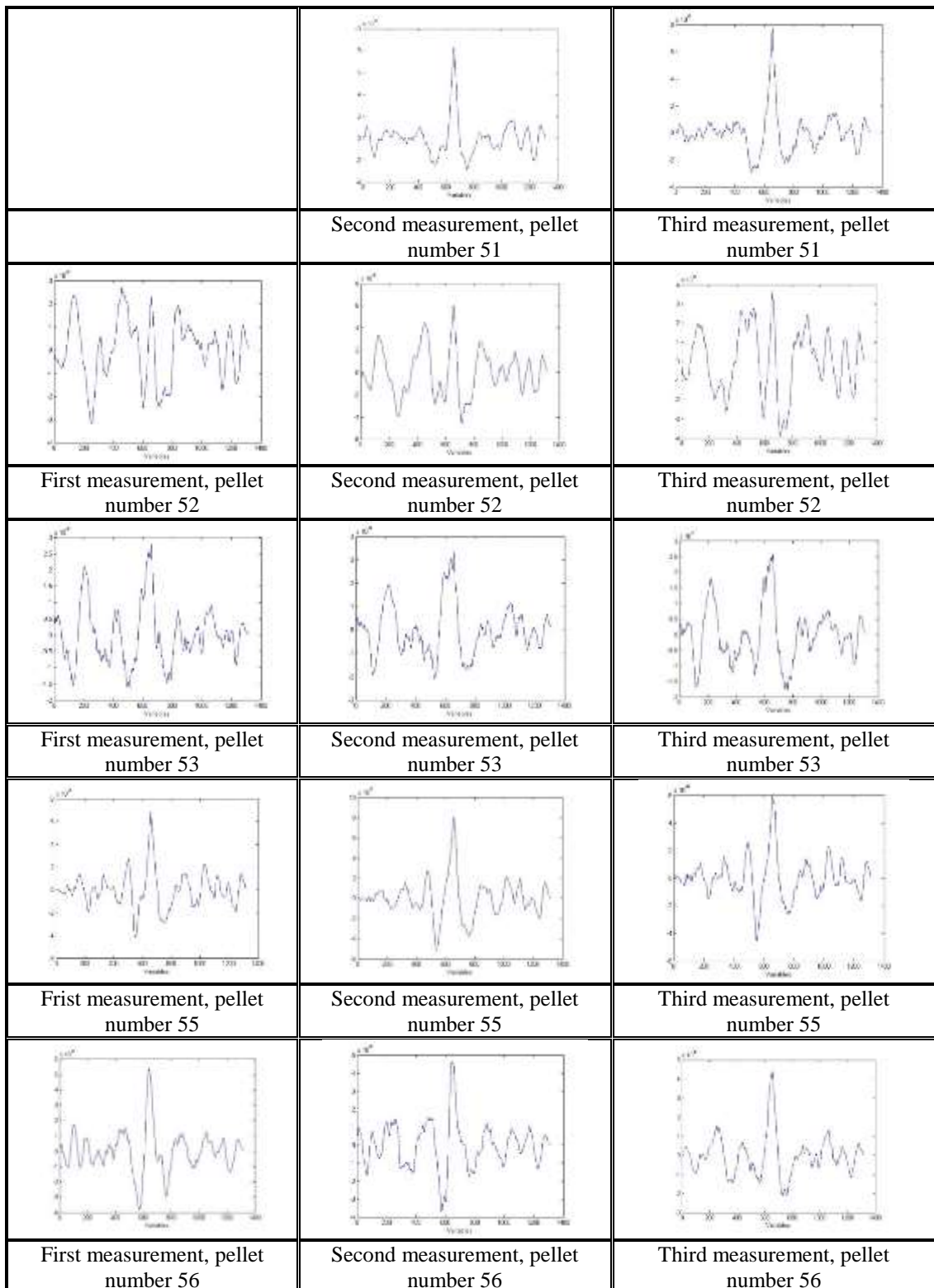
Topographical profiles obtained from the microscopic measurements for samples 560-569, LEA E

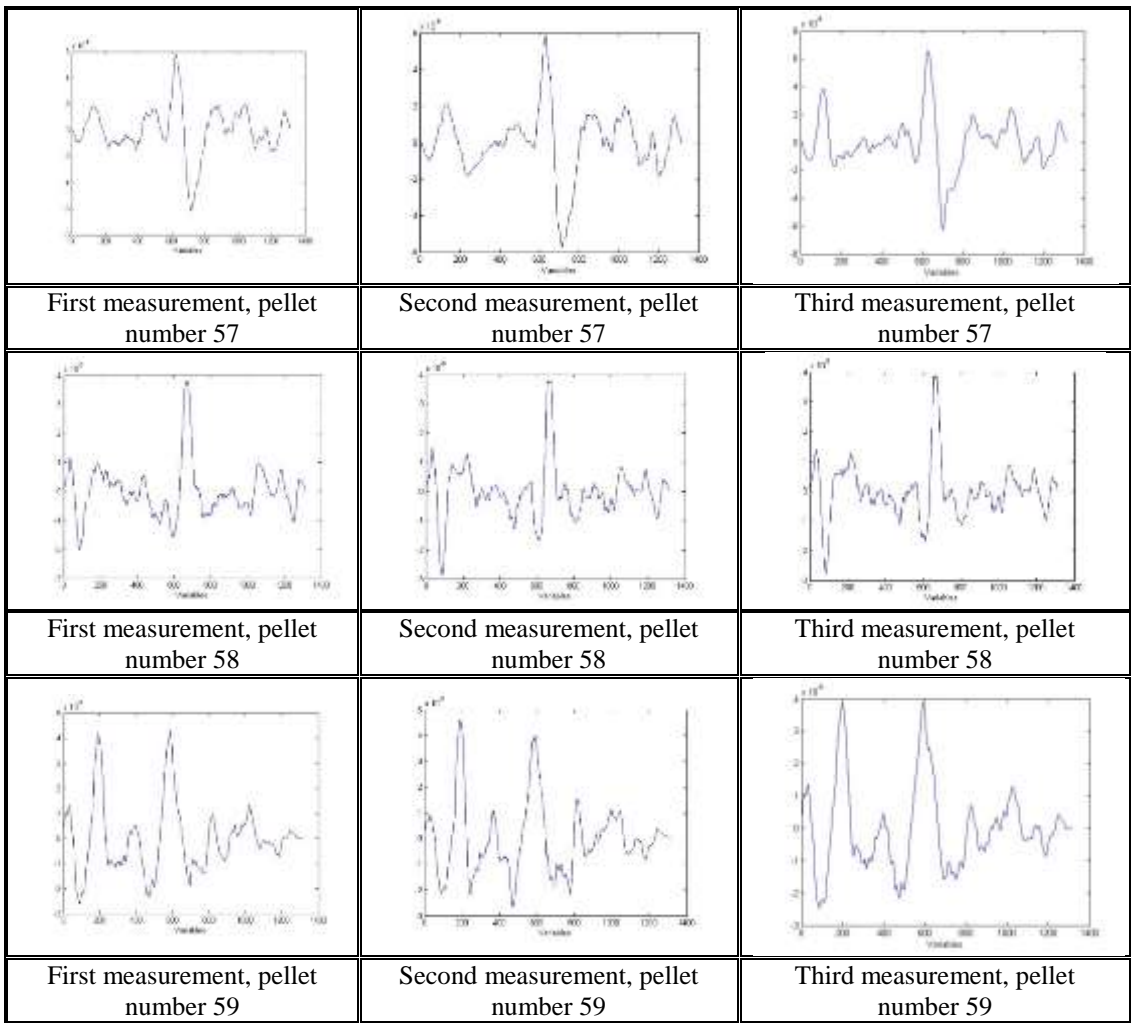
		
	Second measurement, pellet number 560	Third measurement, pellet number 560
		
First measurement, pellet number 561	Second measurement, pellet number 561	Third measurement, pellet number 561
		
First measurement, pellet number 562	Second measurement, pellet number 562	Third measurement, pellet number 562
		
First measurement, pellet number 563	Second measurement, pellet number 563	Third measurement, pellet number 563
		
First measurement, pellet number 564	Second measurement, pellet number 564	Third measurement, pellet number 564



## Appendix 40

Topographical profiles obtained from the microscopic measurements for samples 51-60, LEA F


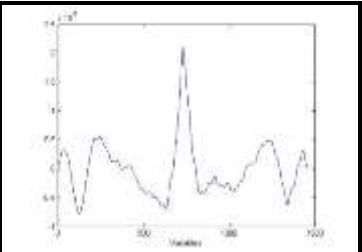
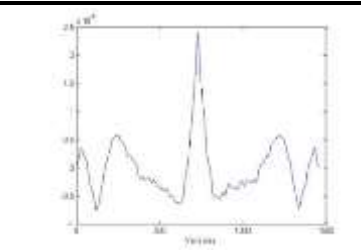
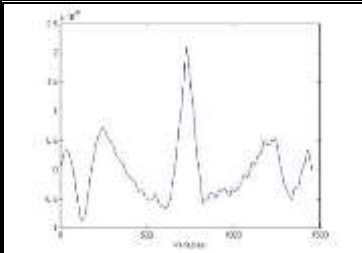
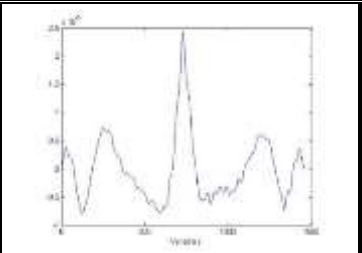
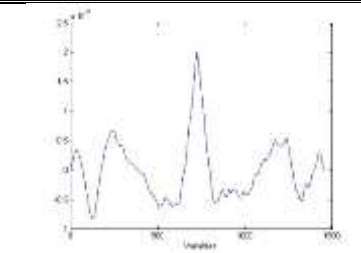
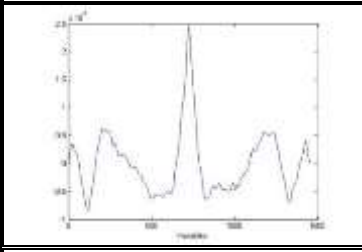
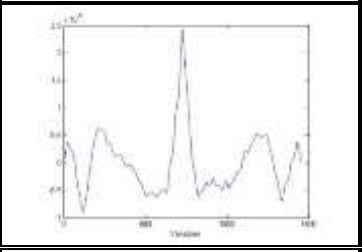
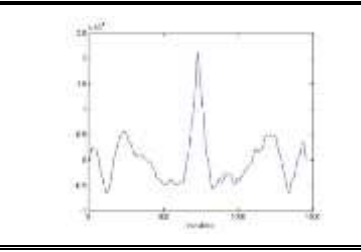
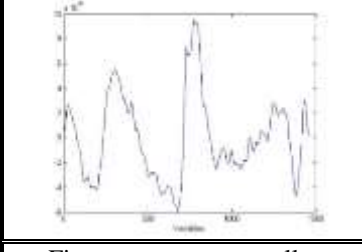
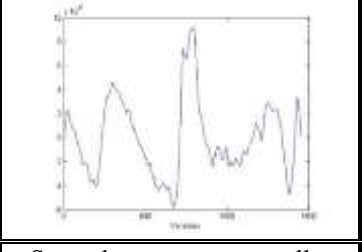
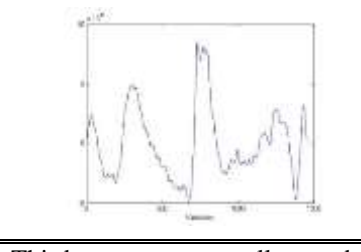
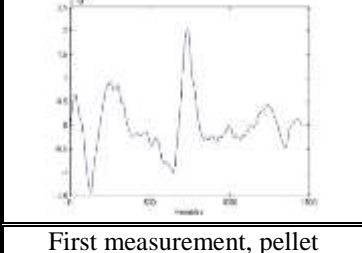
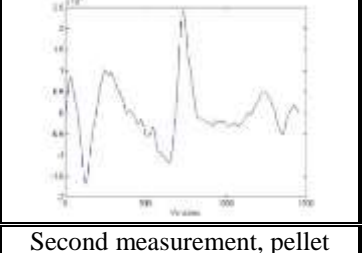
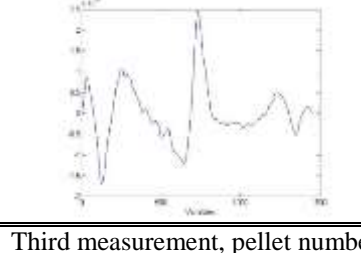


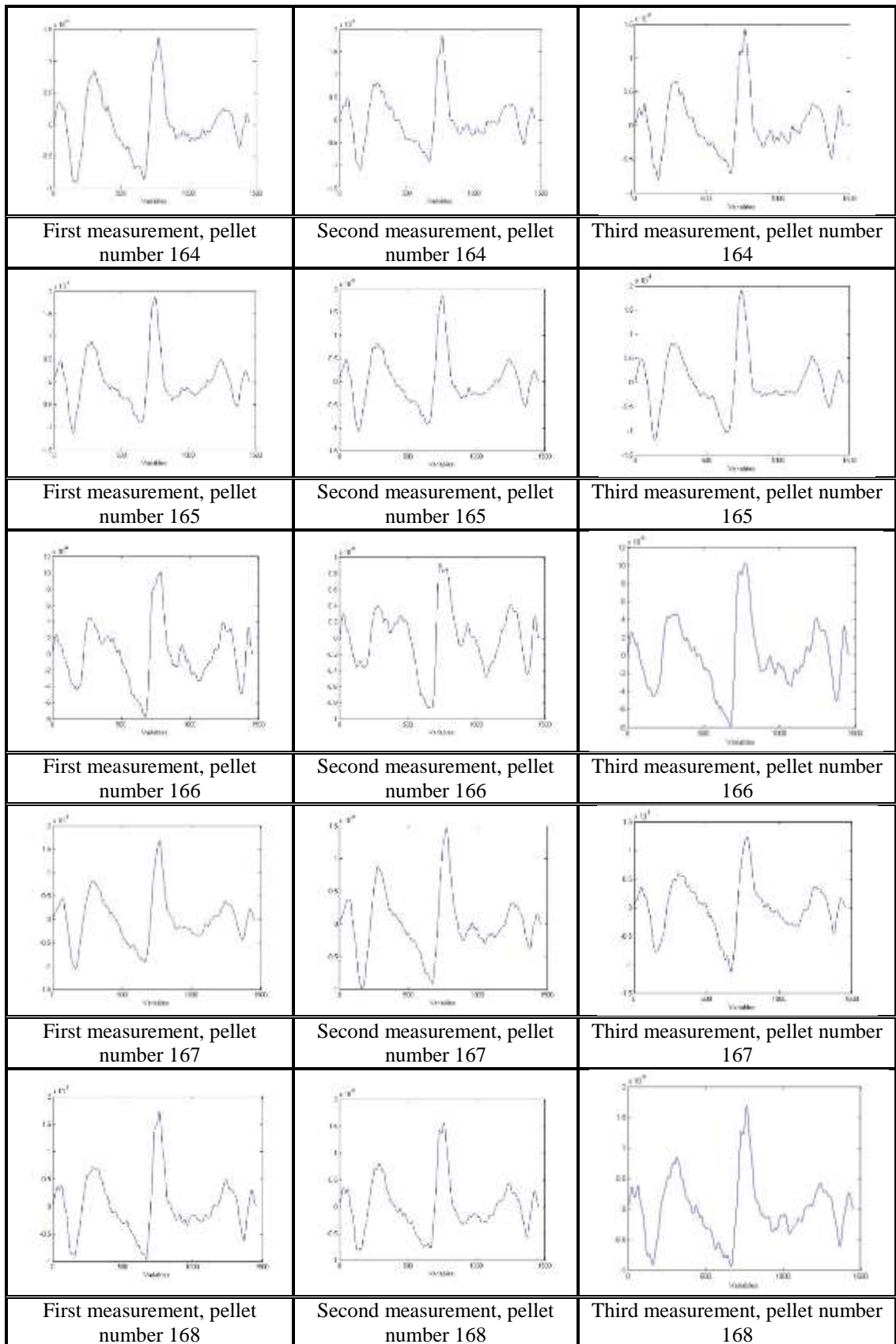




## Appendix 41

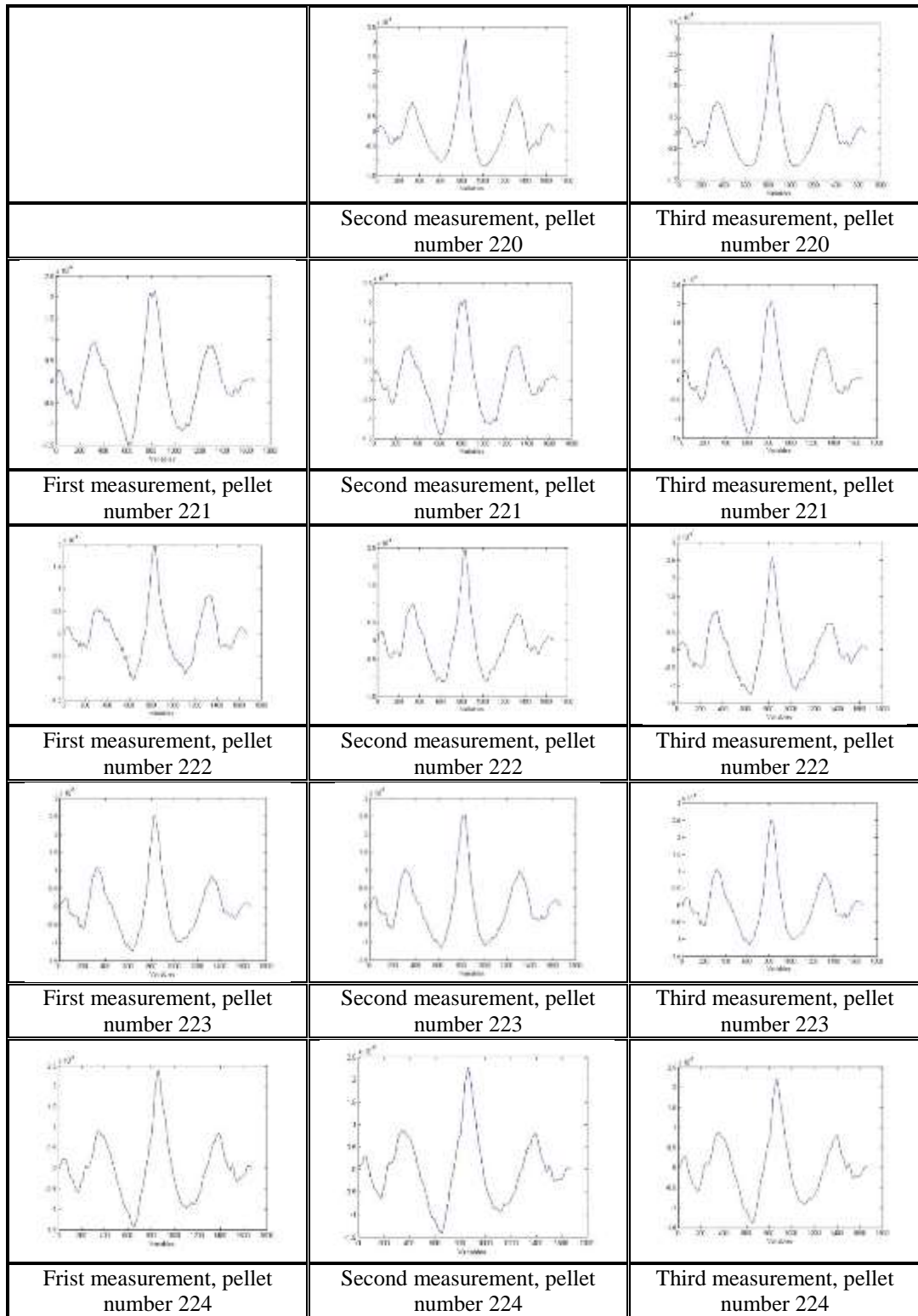
Topographical profiles obtained from the microscopic measurements for samples 159-168, LEA F

		
	Second measurement, pellet number 159	Third measurement, pellet number 159
		
First measurement, pellet number 160	Second measurement, pellet number 160	Third measurement, pellet number 160
		
First measurement, pellet number 161	Second measurement, pellet number 161	Third measurement, pellet number 161
		
First measurement, pellet number 162	Second measurement, pellet number 162	Third measurement, pellet number 162
		
First measurement, pellet number 163	Second measurement, pellet number 163	Third measurement, pellet number 163



## Appendix 42

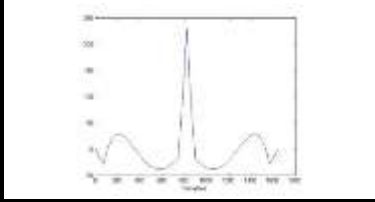
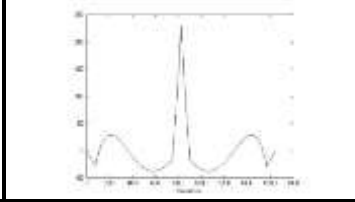
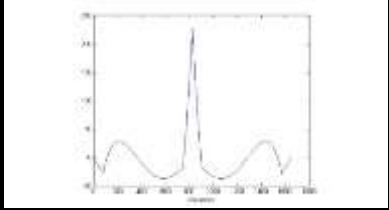
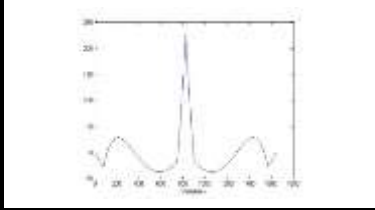
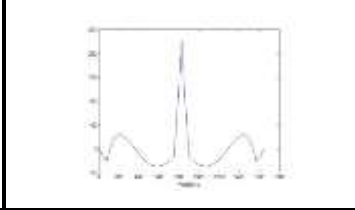
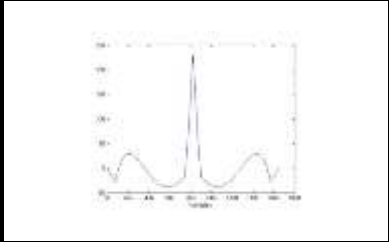
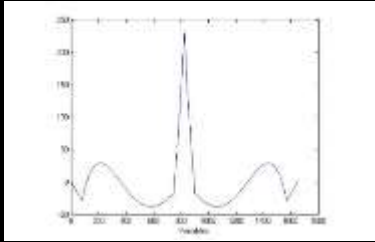
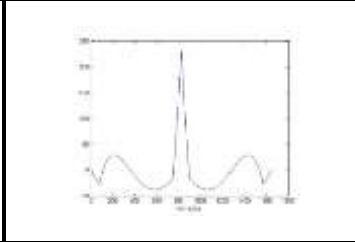
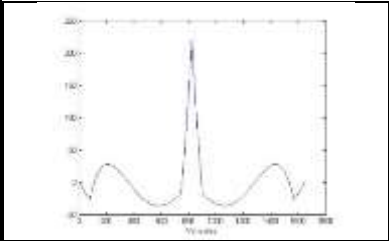
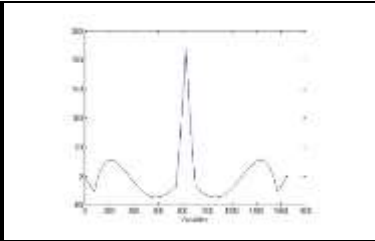
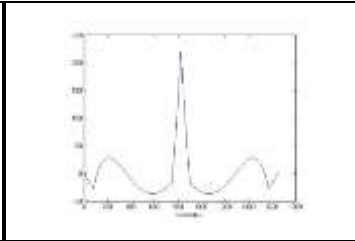
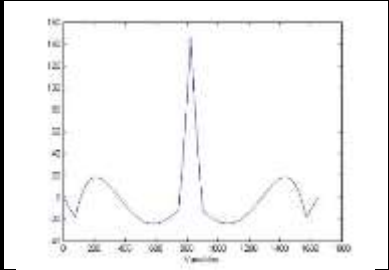
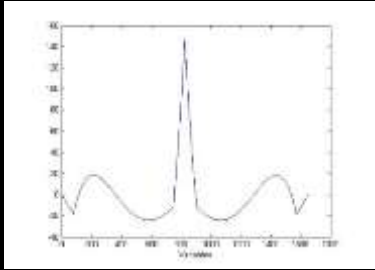
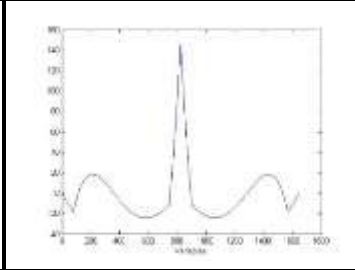
Topographical profiles obtained from the microscopic measurements for samples 220-229, LEA F

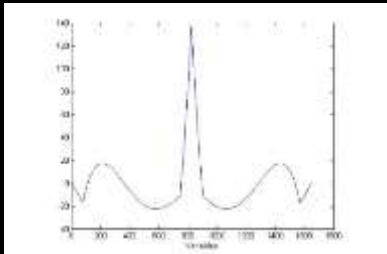
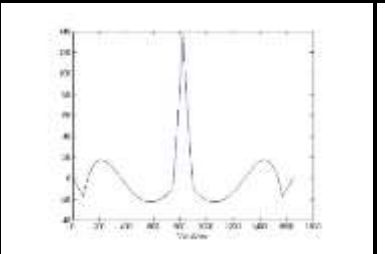
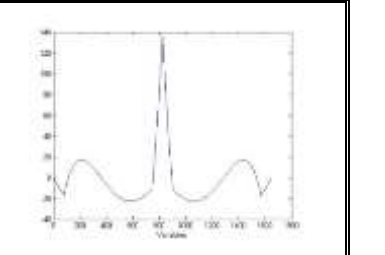
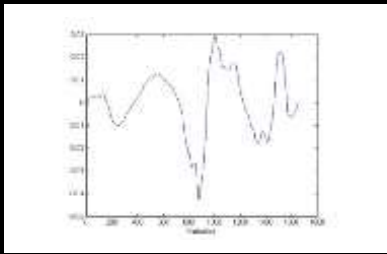
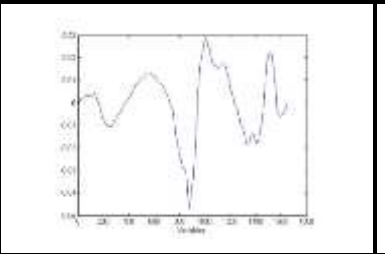
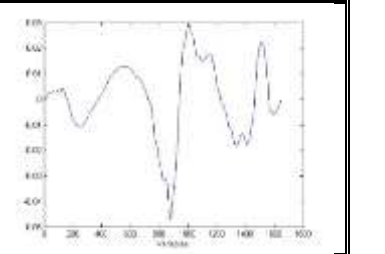
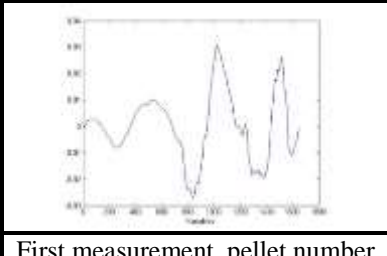
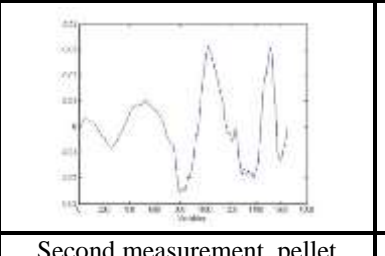
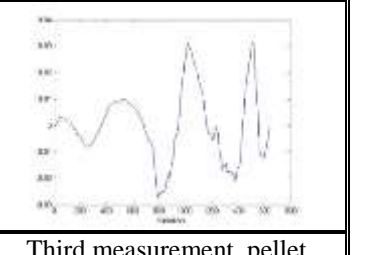
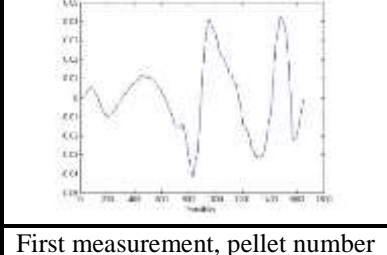
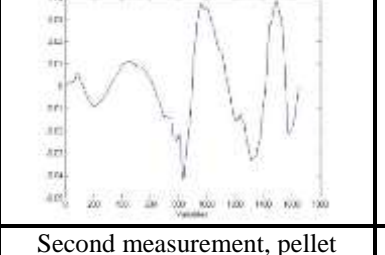
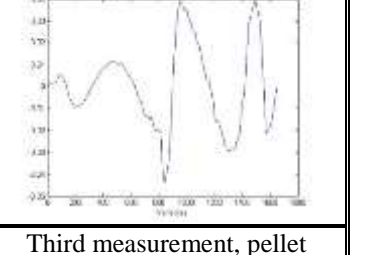


First measurement, pellet number 225	Second measurement, pellet number 225	Third measurement, pellet number 225
First measurement, pellet number 226	Second measurement, pellet number 226	Third measurement, pellet number 226
First measurement, pellet number 227	Second measurement, pellet number 227	Third measurement, pellet number 227
First measurement, pellet number 228	Second measurement, pellet number 228	Third measurement, pellet number 228
First measurement, pellet number 229	Second measurement, pellet number 229	Third measurement, pellet number 229

### Appendix 43

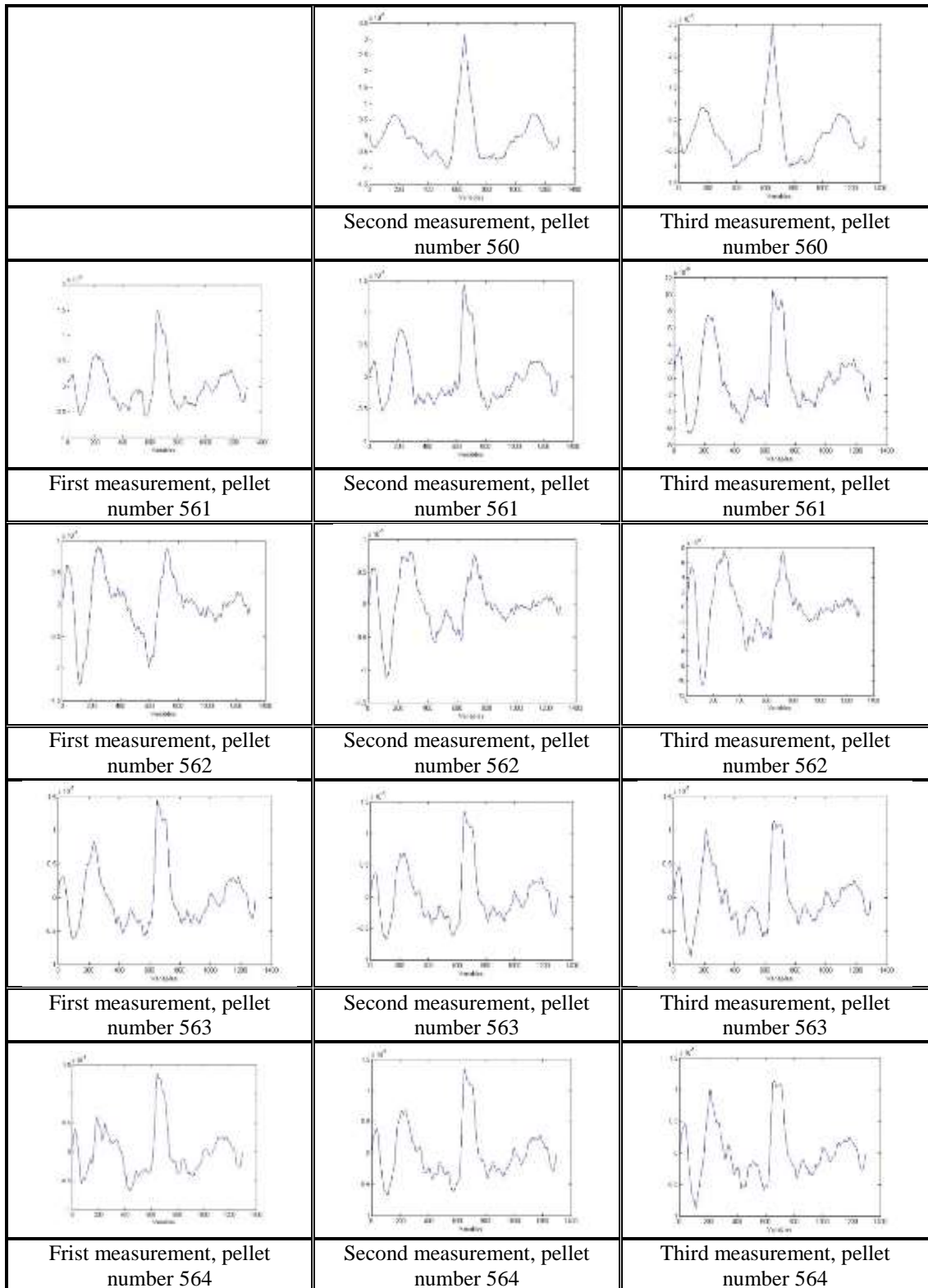
Topographical profiles obtained from the microscopic measurements for samples 342-351, LEA F

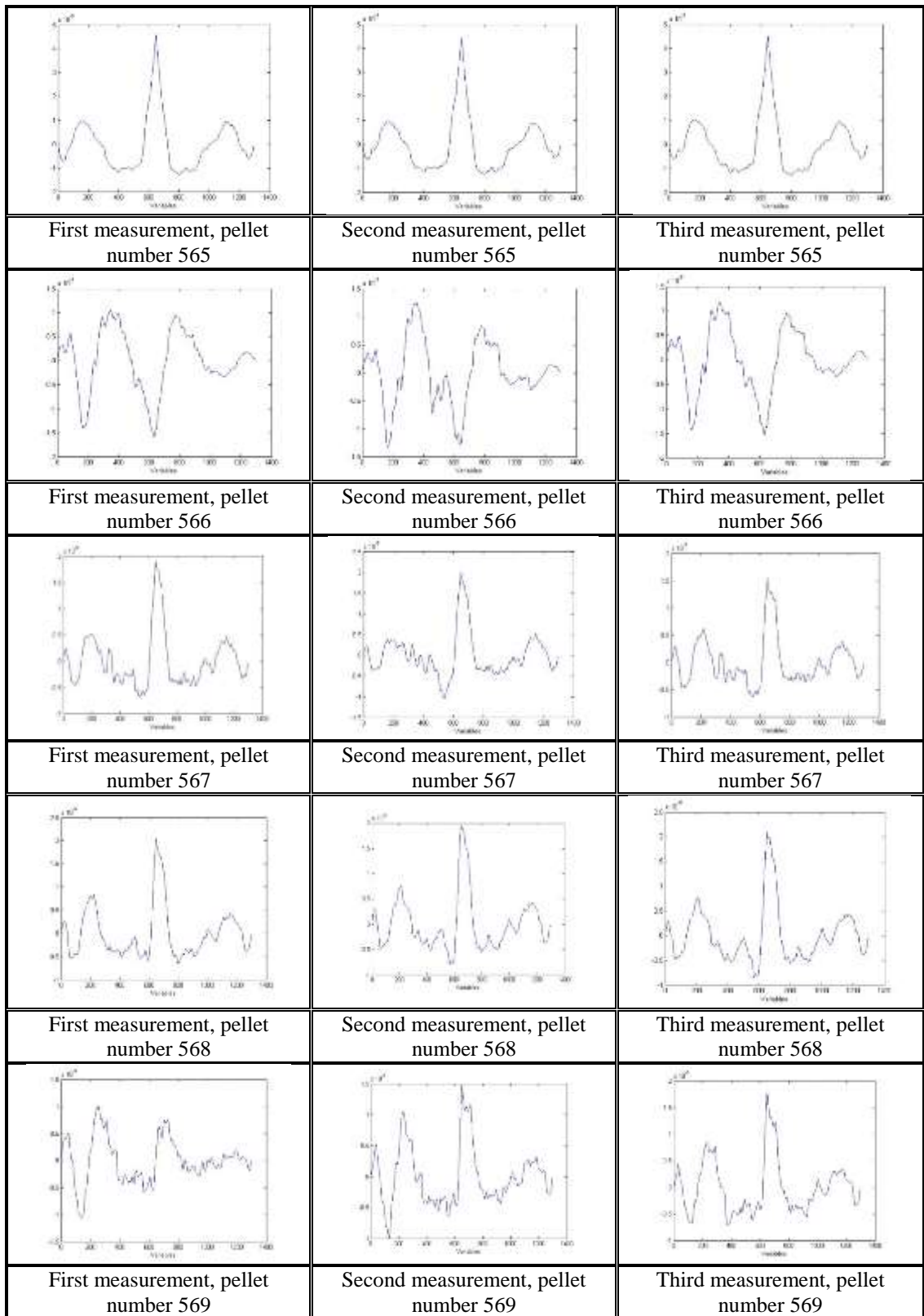
		
	Second measurement, pellet number 342	Third measurement, pellet number 342
		
First measurement, pellet number 343	Second measurement, pellet number 343	Third measurement, pellet number 343
		
First measurement, pellet number 344	Second measurement, pellet number 344	Third measurement, pellet number 344
		
First measurement, pellet number 345	Second measurement, pellet number 345	Third measurement, pellet number 345
		
First measurement, pellet number 346	Second measurement, pellet number 346	Third measurement, pellet number 346

		
First measurement, pellet number 347	Second measurement, pellet number 347	Third measurement, pellet number 347
		
First measurement, pellet number 349	Second measurement, pellet number 349	Third measurement, pellet number 349
		
First measurement, pellet number 350	Second measurement, pellet number 350	Third measurement, pellet number 350
		
First measurement, pellet number 351	Second measurement, pellet number 351	Third measurement, pellet number 351

## Appendix 44

Topographical profiles obtained from the microscopic measurements for samples 560-569, LEA F

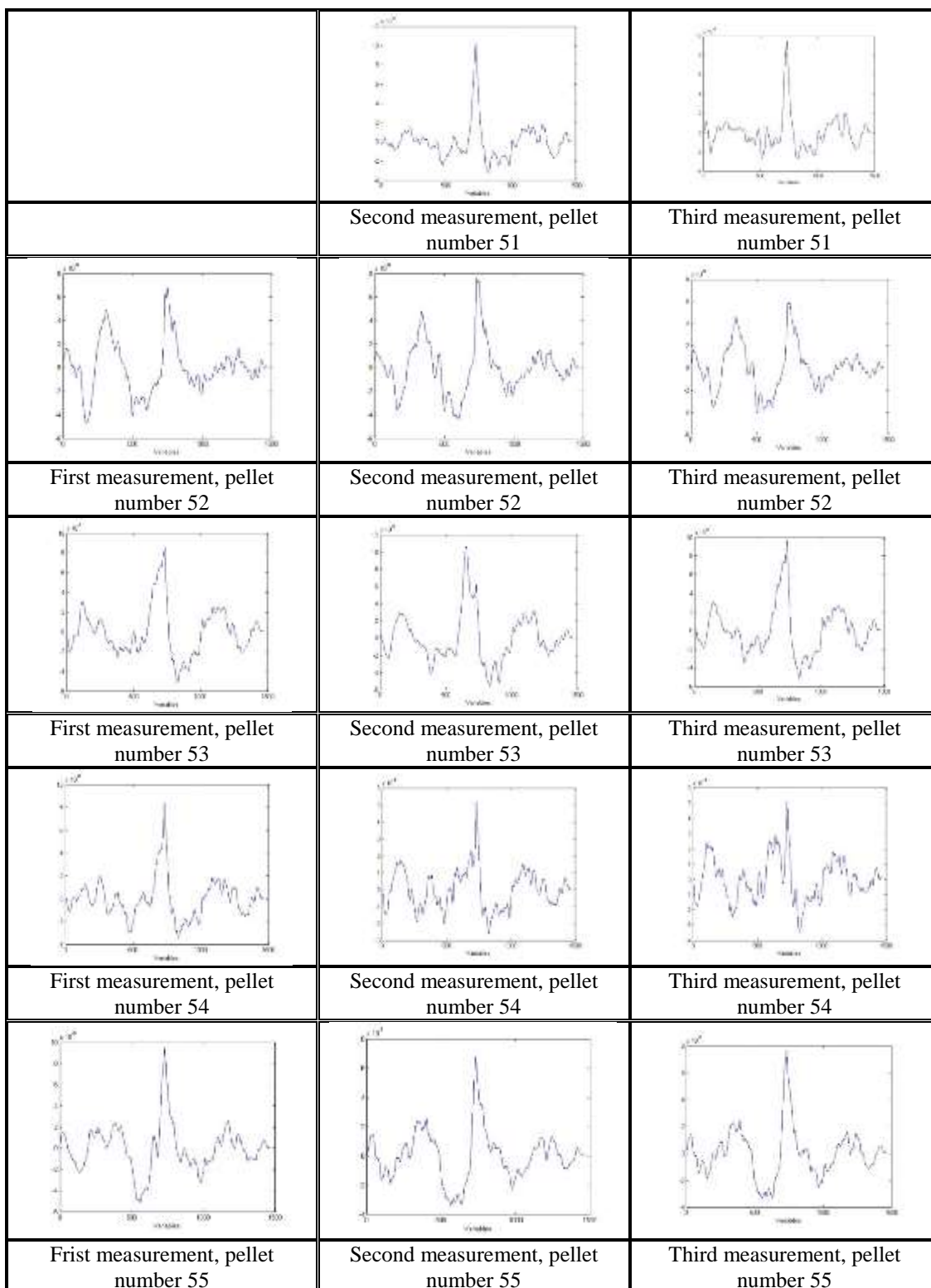


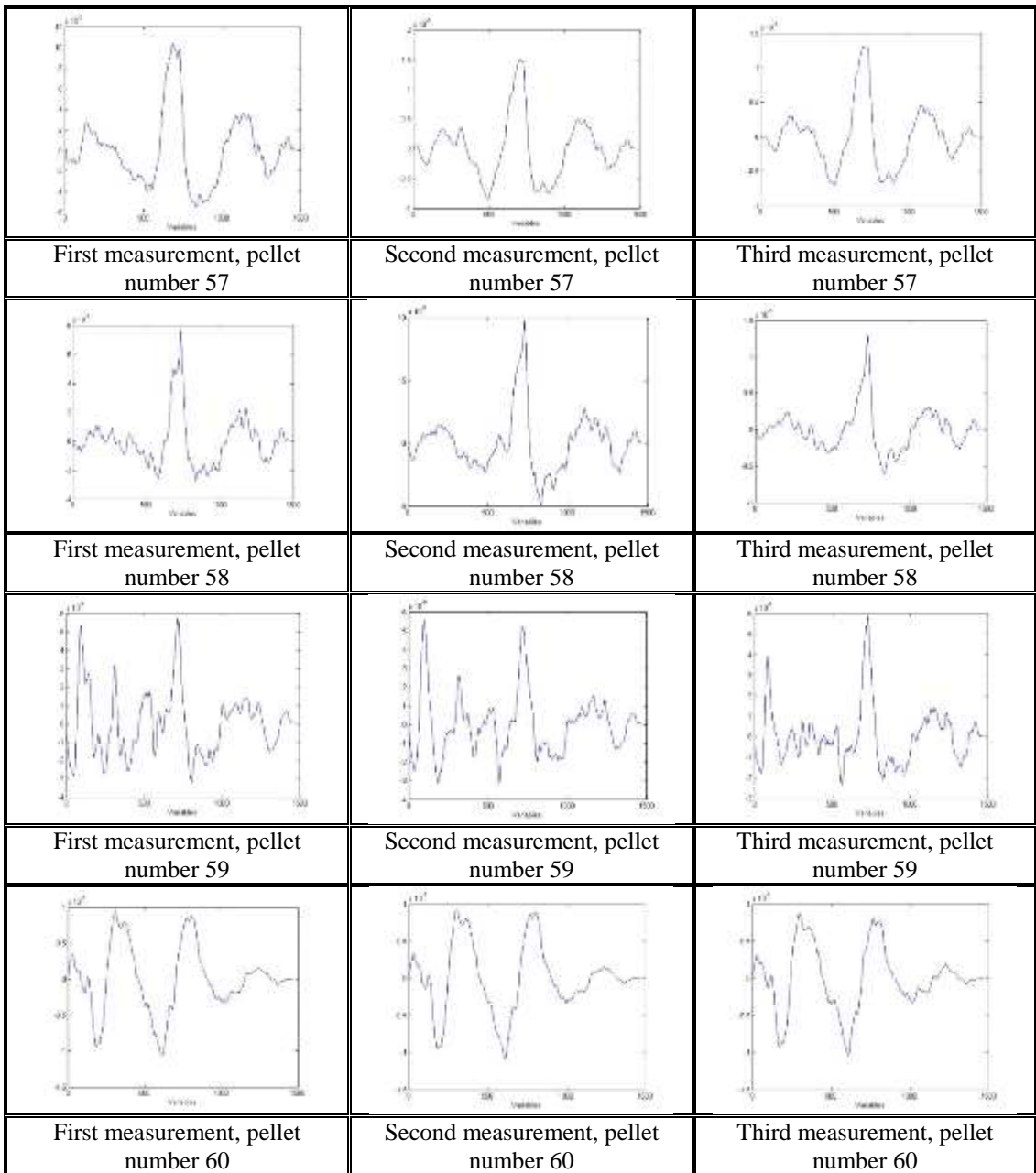




## Appendix 45

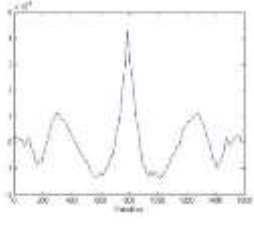
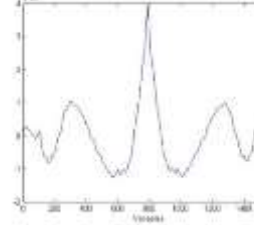
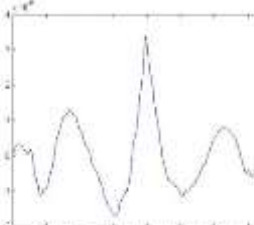
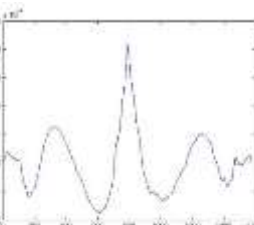
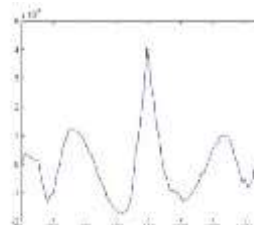
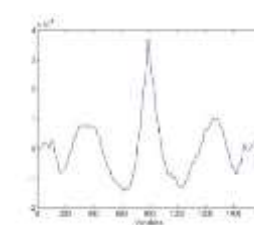
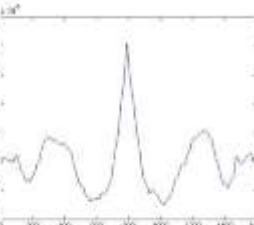
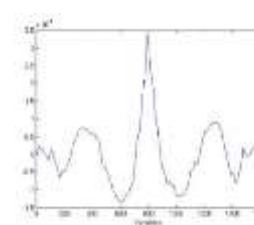
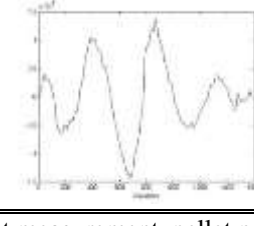
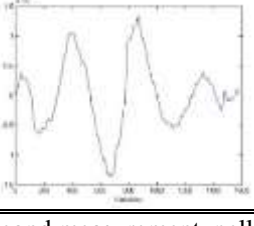
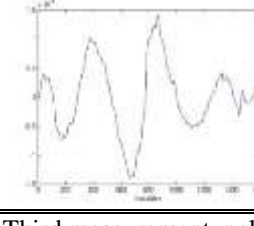
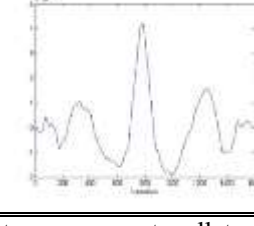
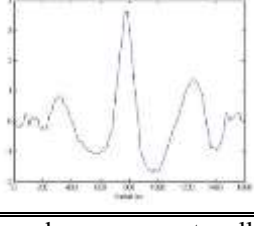
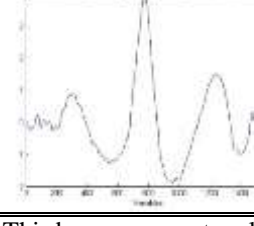
Topographical profiles obtained from the microscopic measurements for samples 51-60, LEA G

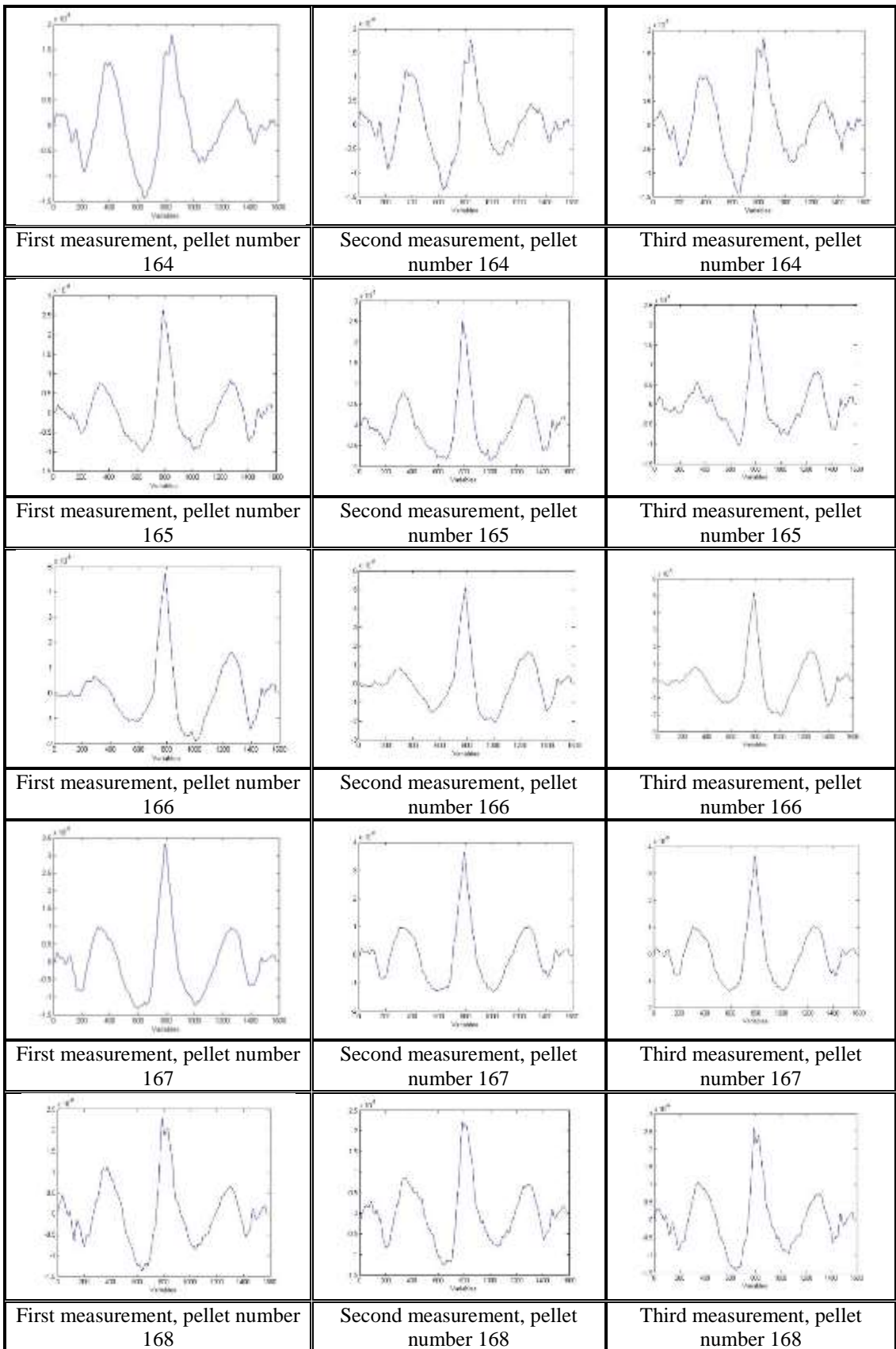




## Appendix 46

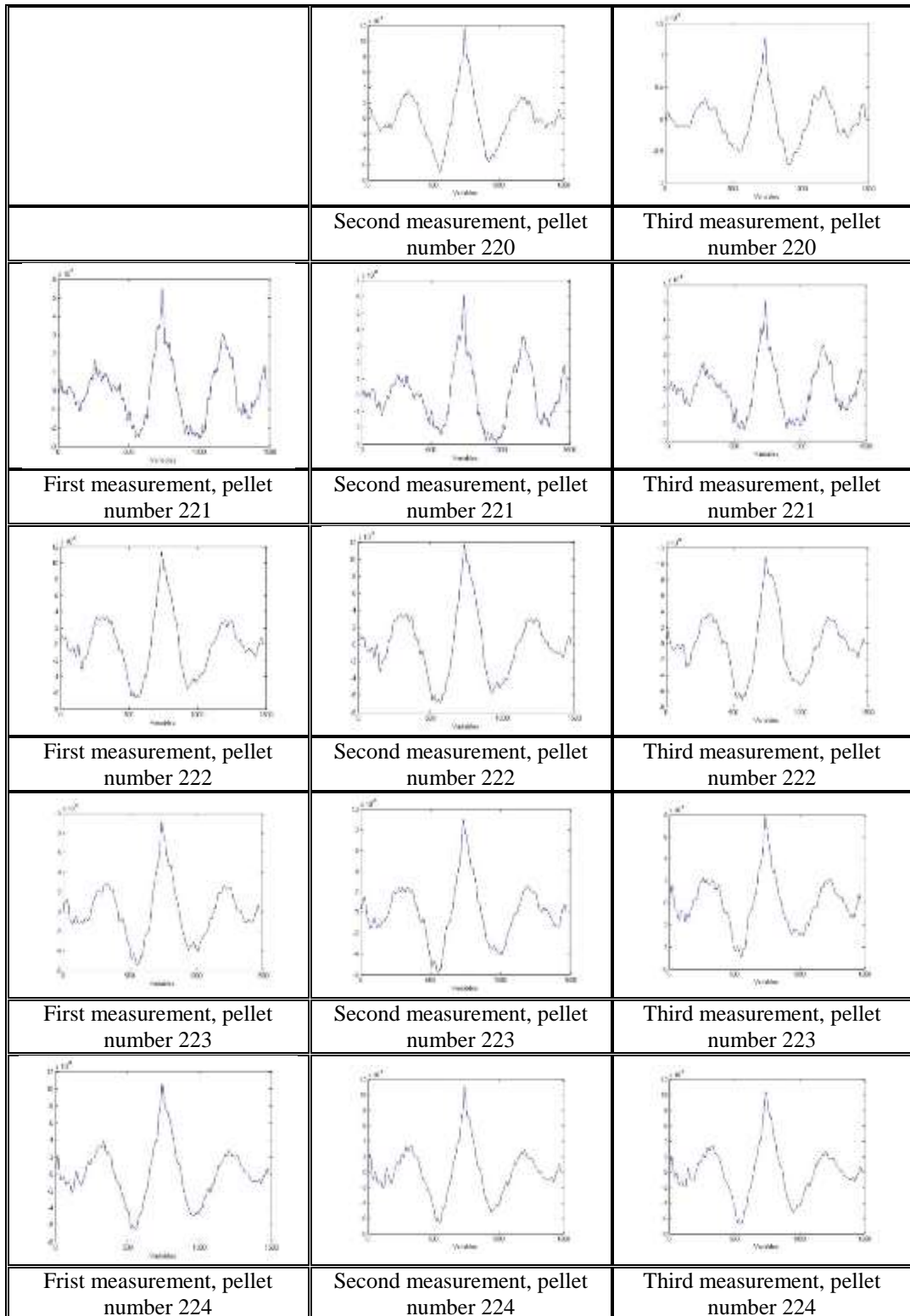
Topographical profiles obtained from the microscopic measurements for samples 159-168, LEA G

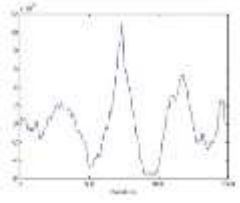
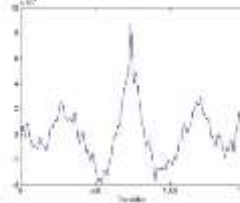
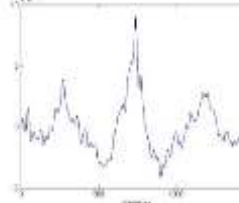
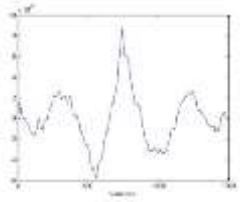
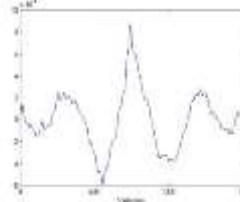
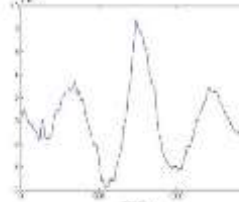
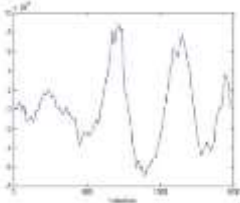
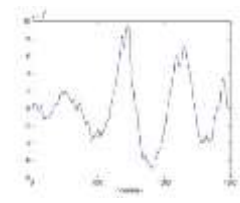
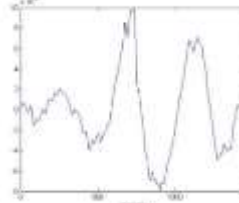
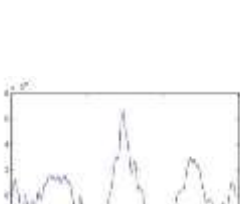
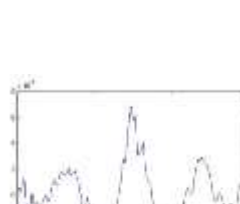
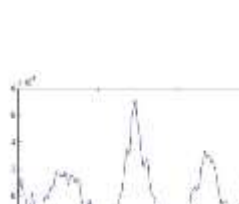
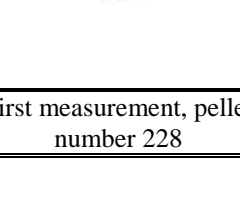
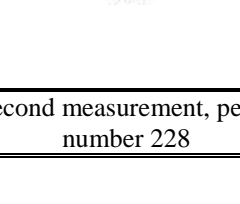
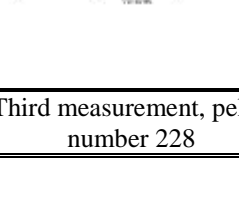
		
	Second measurement, pellet number 159	Third measurement, pellet number 159
		
First measurement, pellet number 160	Second measurement, pellet number 160	Third measurement, pellet number 160
		
First measurement, pellet number 161	Second measurement, pellet number 161	Third measurement, pellet number 161
		
First measurement, pellet number 162	Second measurement, pellet number 162	Third measurement, pellet number 162
		
First measurement, pellet number 163	Second measurement, pellet number 163	Third measurement, pellet number 163



## Appendix 47

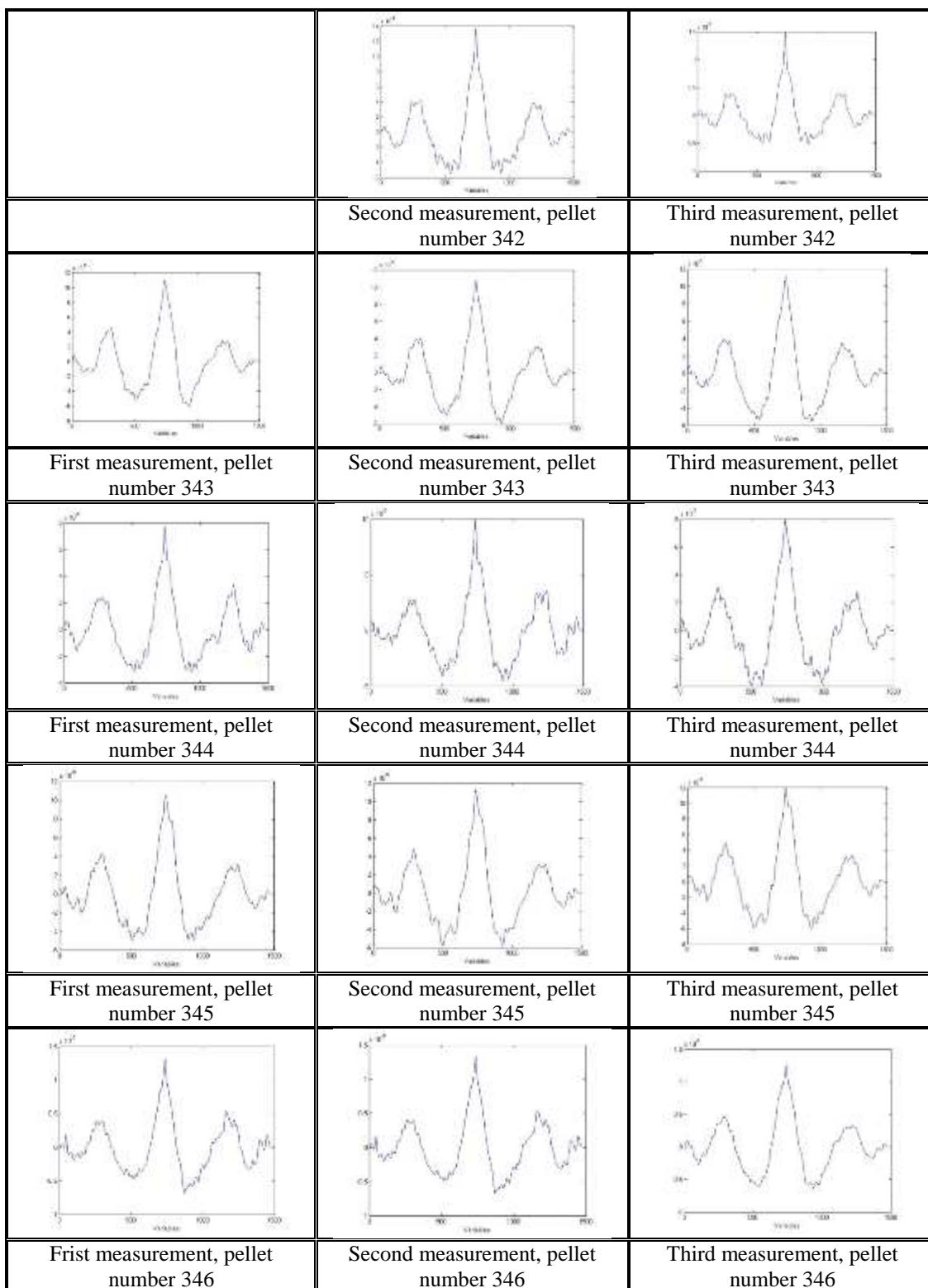
Topographical profiles obtained from the microscopic measurements for samples 220-229, LEA G

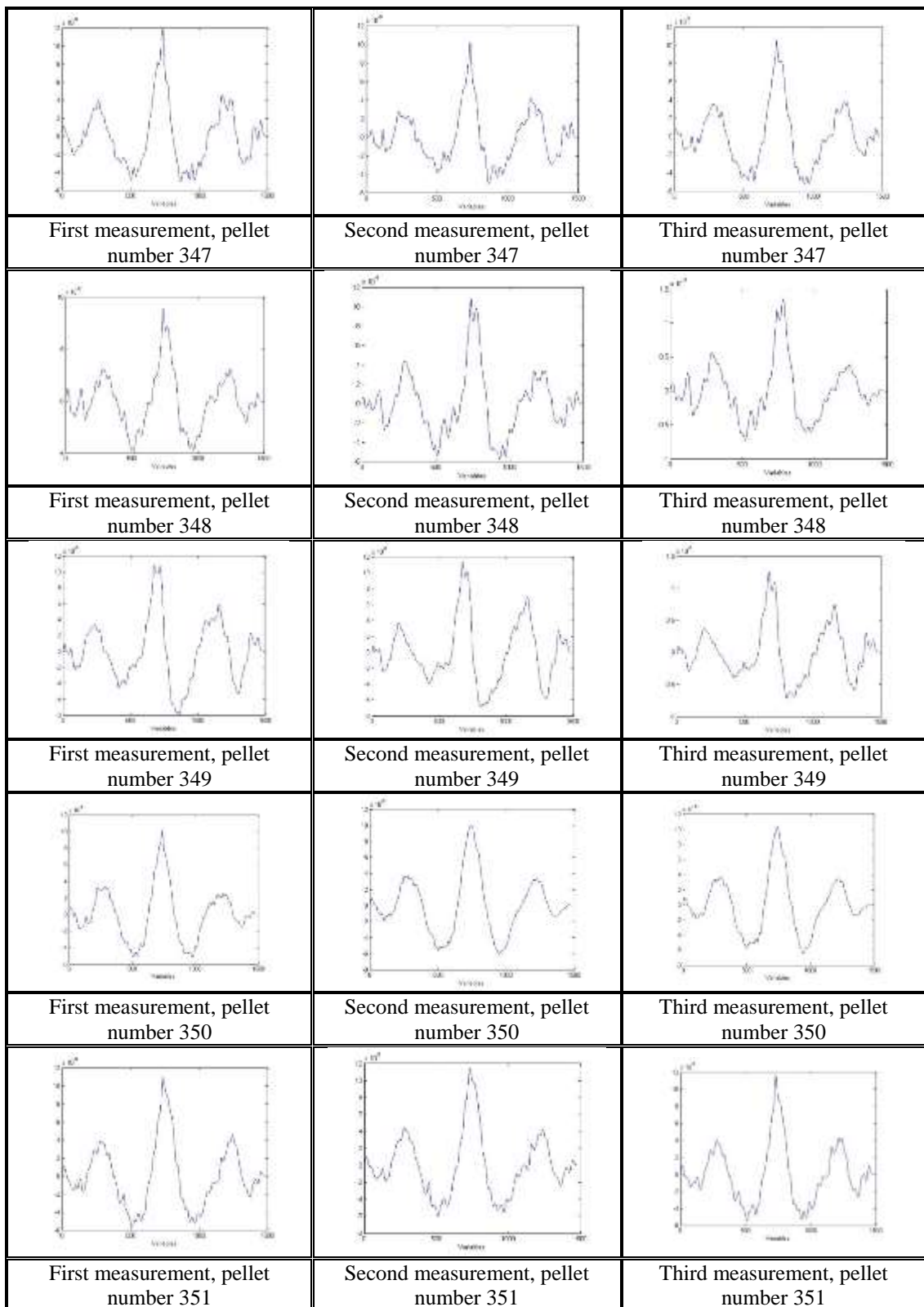


		
First measurement, pellet number 225	Second measurement, pellet number 225	Third measurement, pellet number 225
		
First measurement, pellet number 226	Second measurement, pellet number 226	Third measurement, pellet number 226
		
First measurement, pellet number 227	Second measurement, pellet number 227	Third measurement, pellet number 227
		
First measurement, pellet number 228	Second measurement, pellet number 228	Third measurement, pellet number 228
		
First measurement, pellet number 229	Second measurement, pellet number 229	Third measurement, pellet number 229

## Appendix 48

Topographical profiles obtained from the microscopic measurements for samples 342-351, LEA G

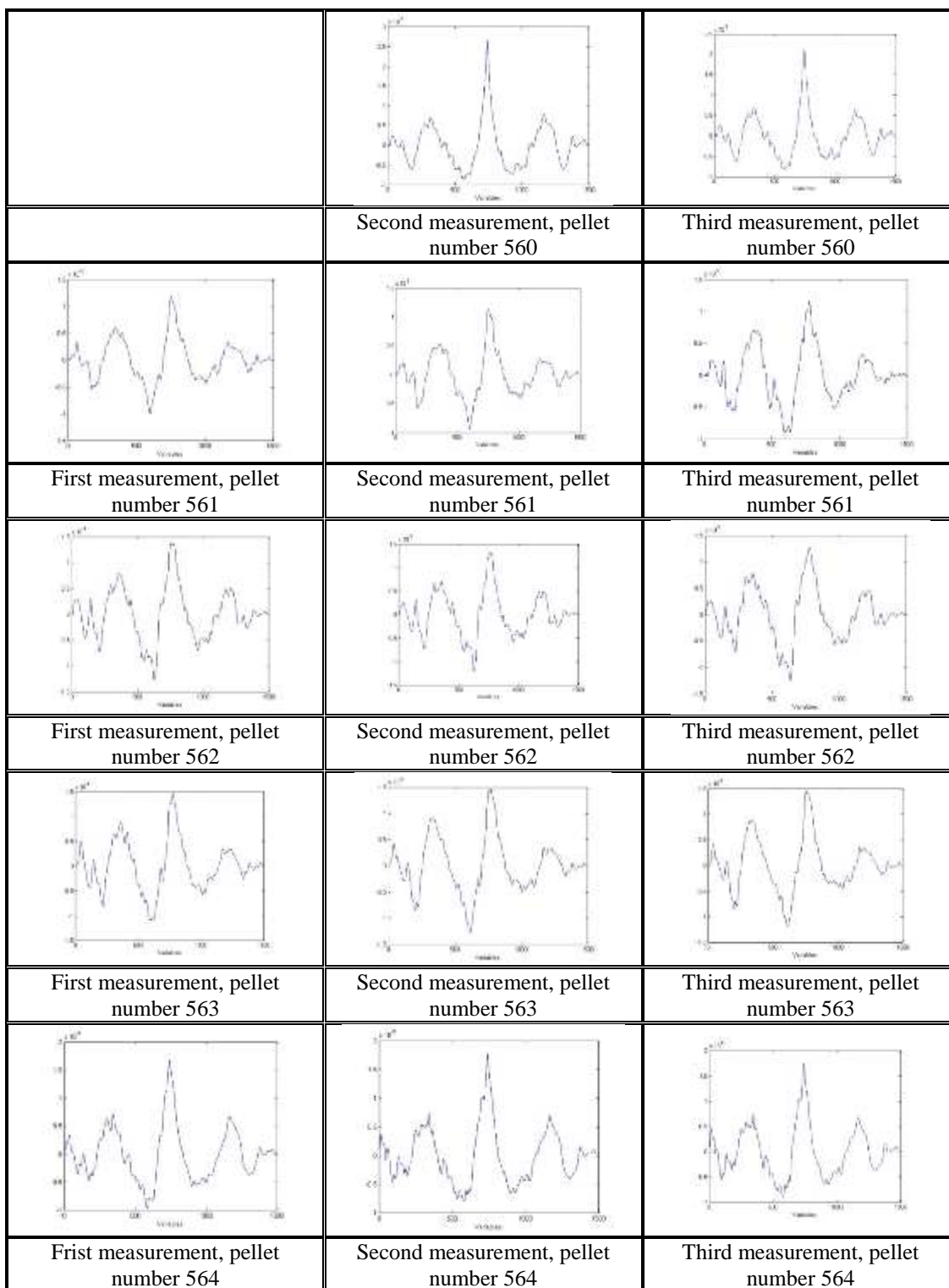


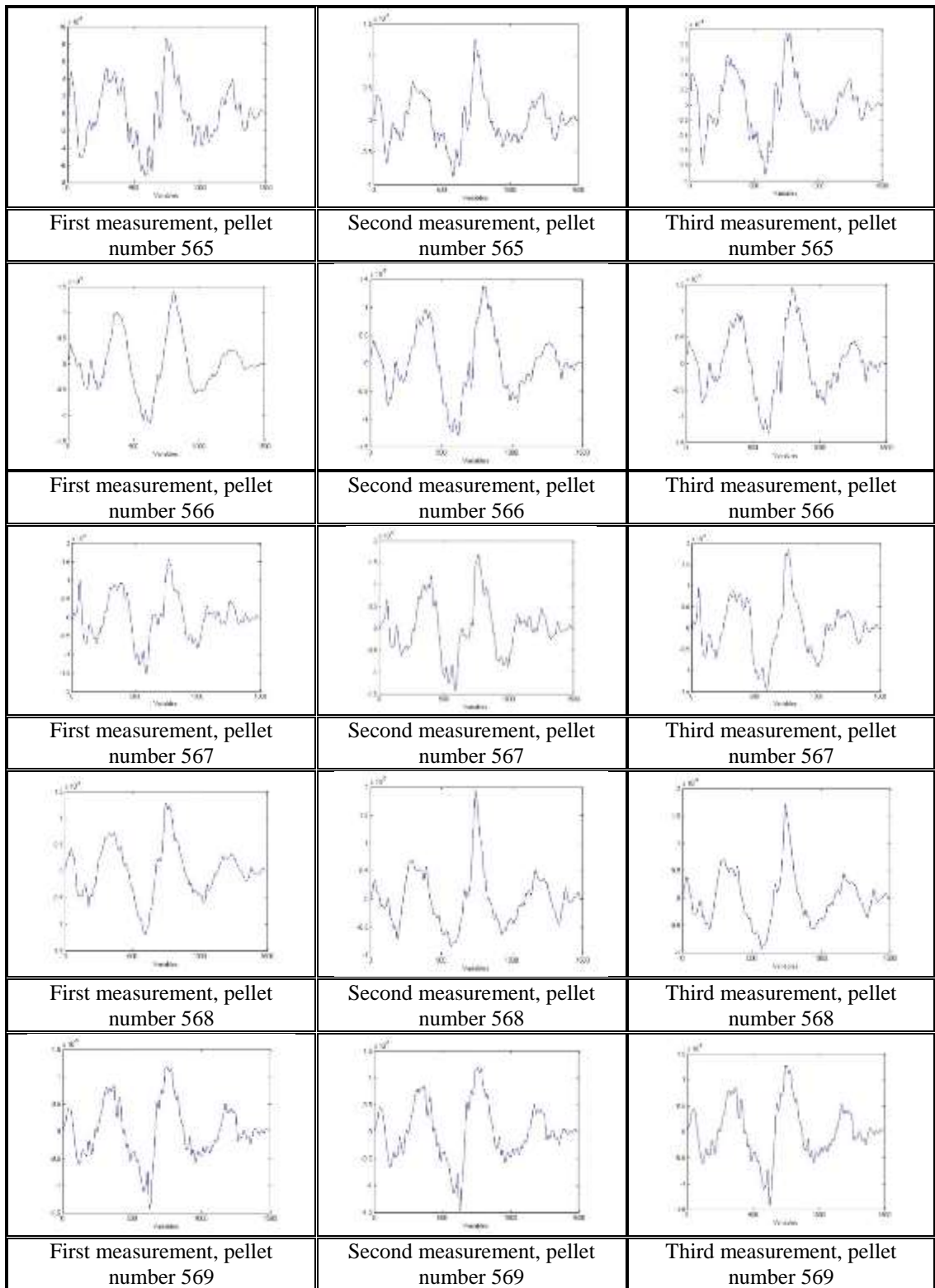




## Appendix 49

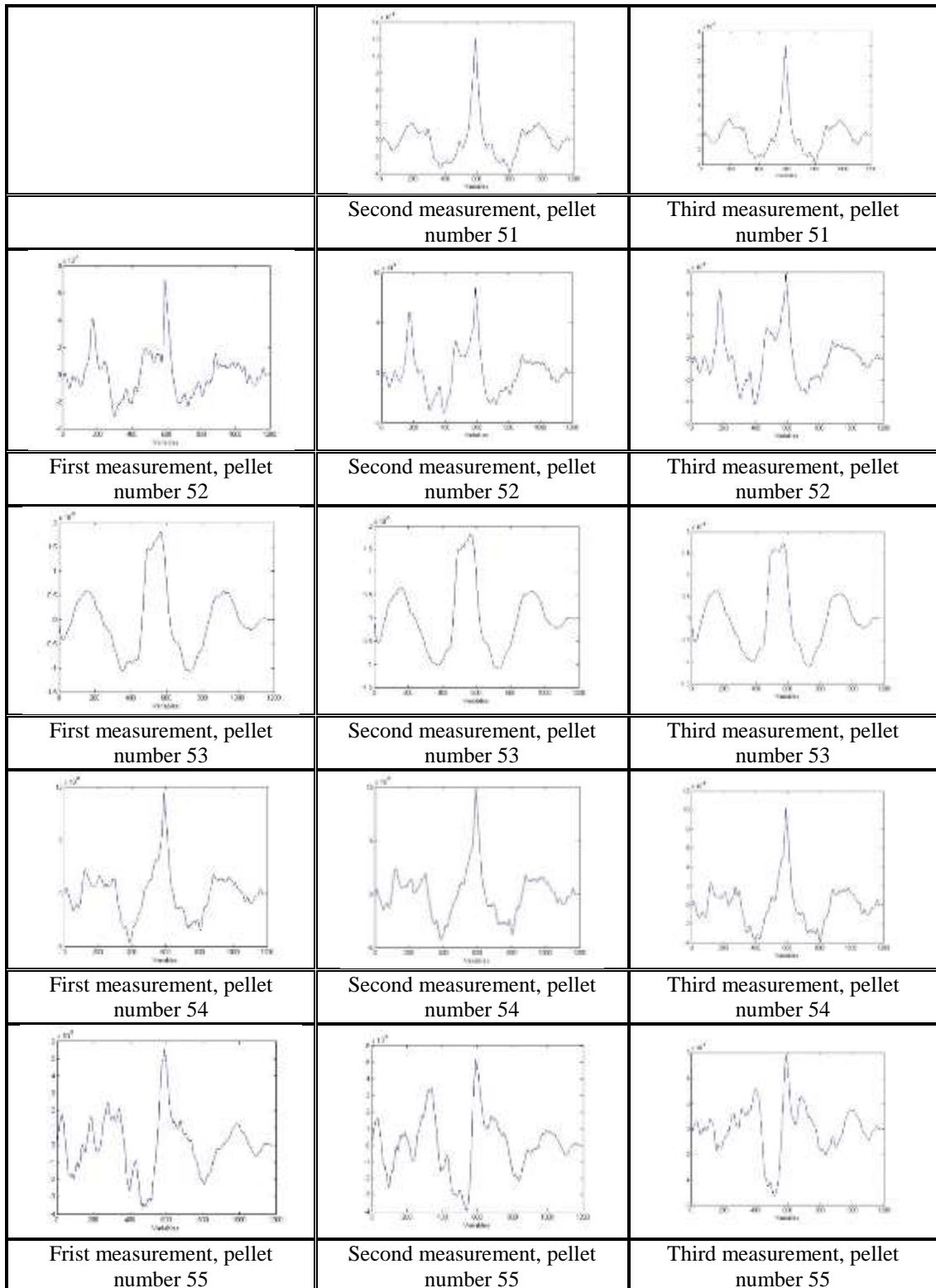
Topographical profiles obtained from the microscopic measurements for samples 560-569, LEA G

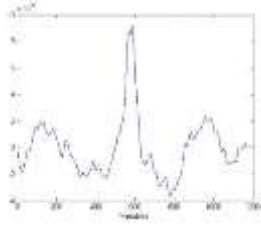
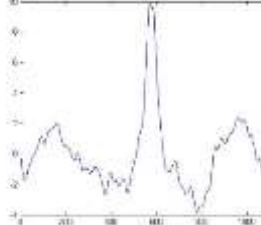
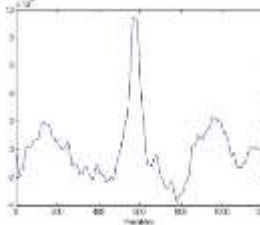
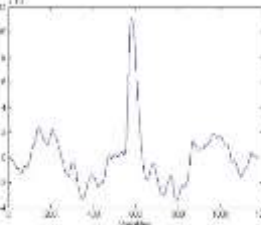
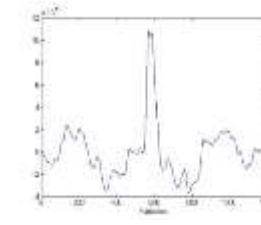
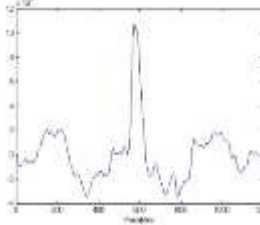
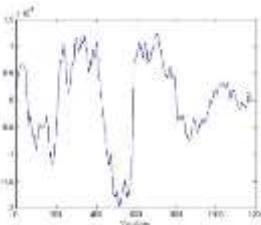
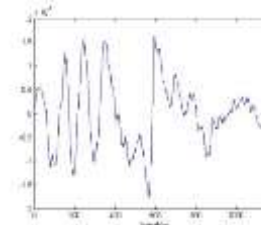
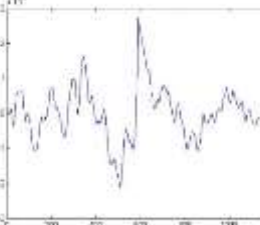
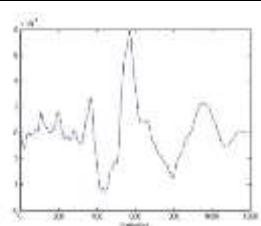
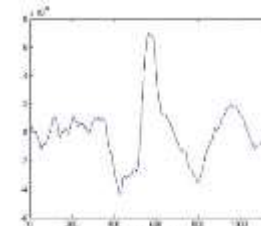
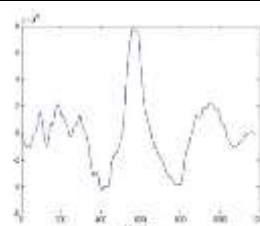
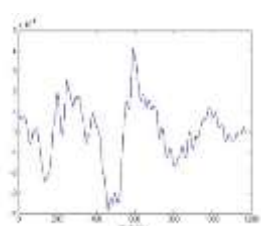
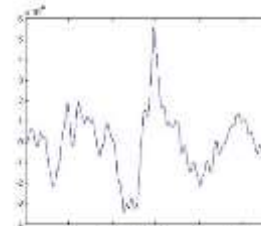
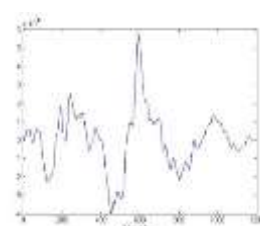




## Appendix 50

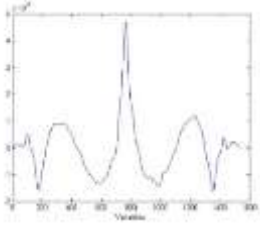
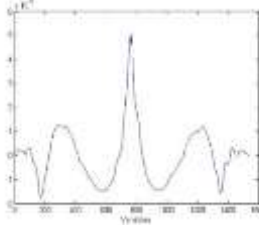
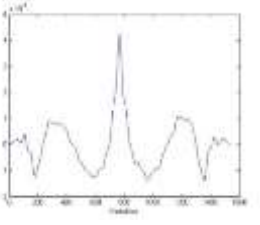
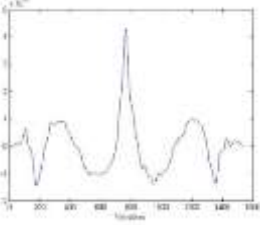
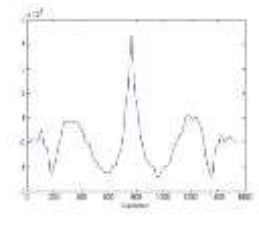
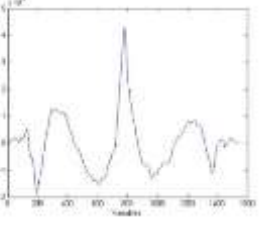
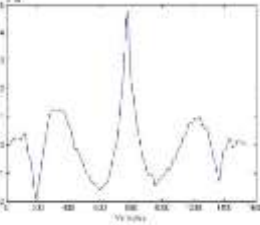
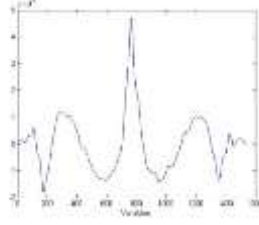
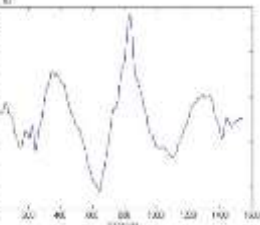
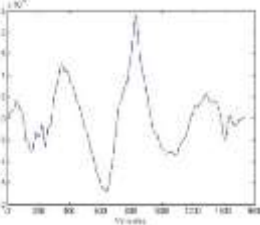
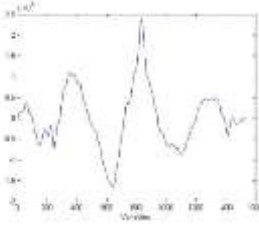
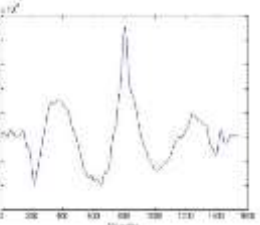
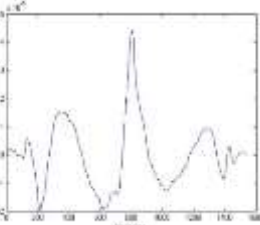
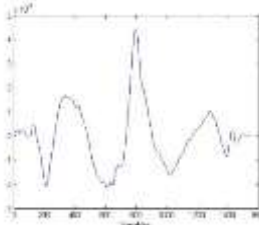
Topographical profiles obtained from the microscopic measurements for samples 51-60, LEA H

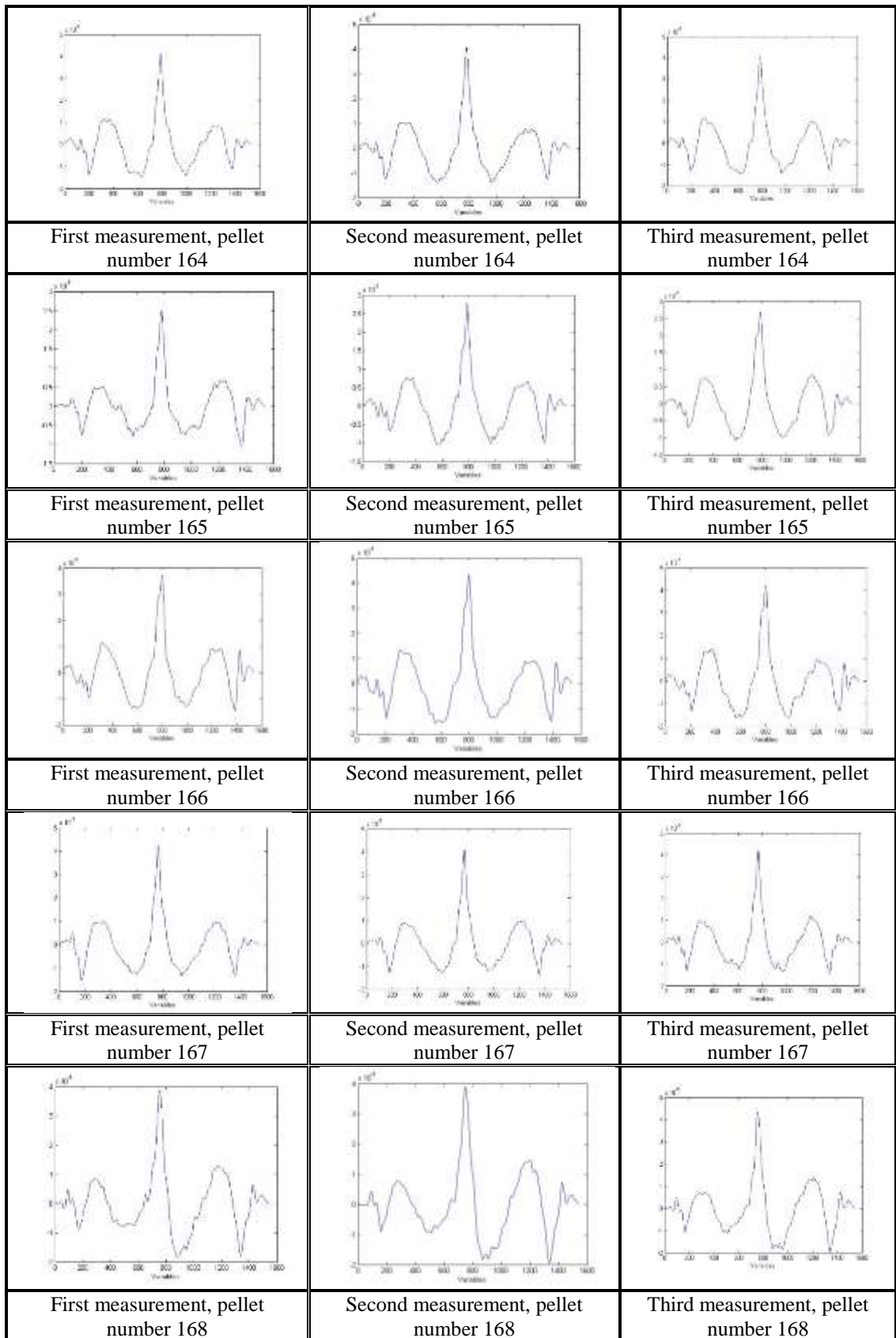


		
First measurement, pellet number 56	Second measurement, pellet number 56	Third measurement, pellet number 56
		
First measurement, pellet number 57	Second measurement, pellet number 57	Third measurement, pellet number 57
		
First measurement, pellet number 58	Second measurement, pellet number 58	Third measurement, pellet number 58
		
First measurement, pellet number 59	Second measurement, pellet number 59	Third measurement, pellet number 59
		
First measurement, pellet number 60	Second measurement, pellet number 60	Third measurement, pellet number 60

## Appendix 51

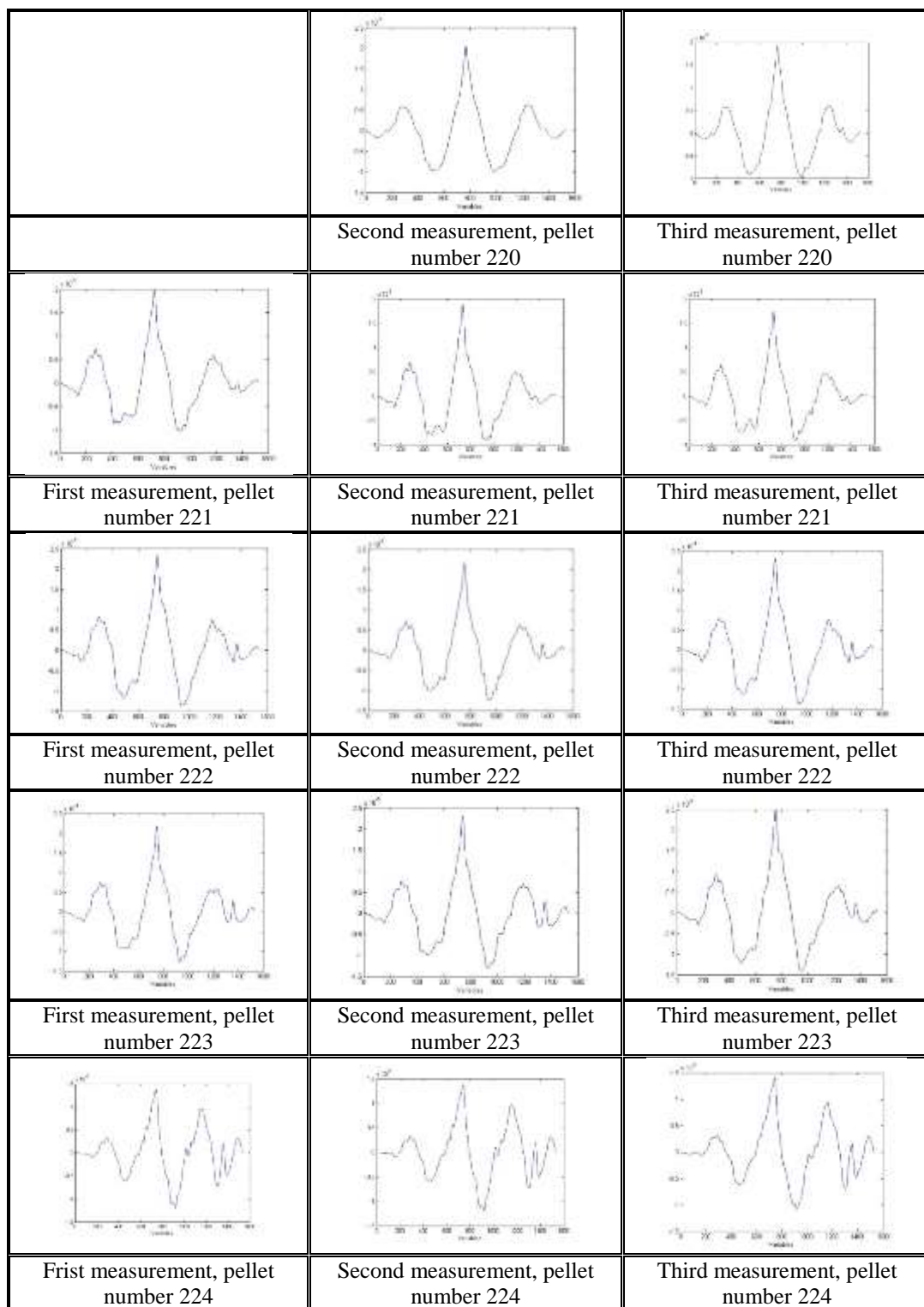
Topographical profiles obtained from the microscopic measurements for samples 159-168, LEA H

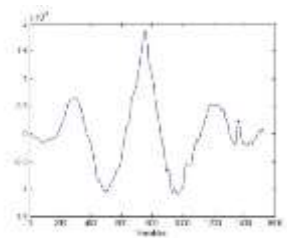
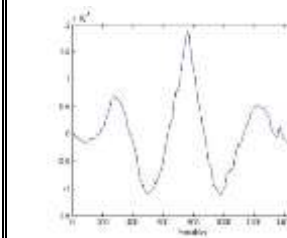
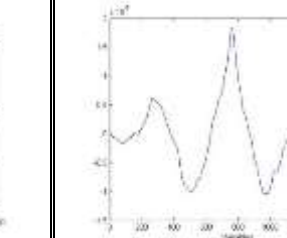
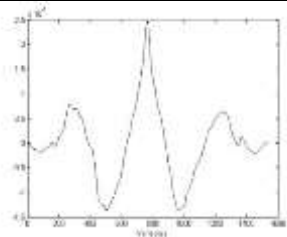
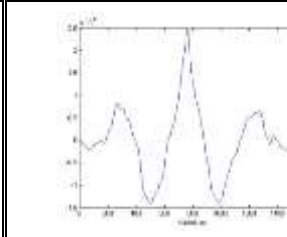
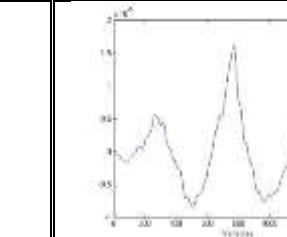
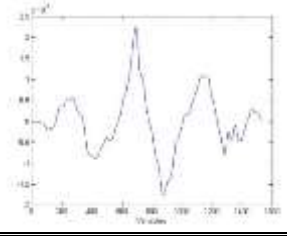
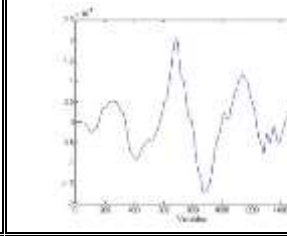
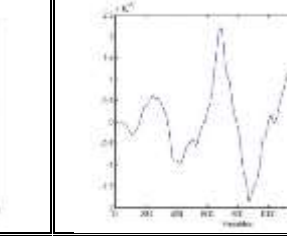
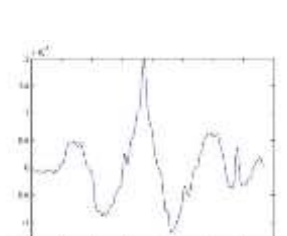
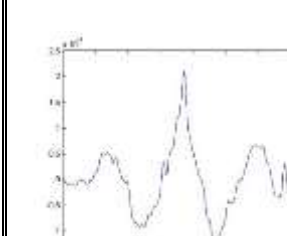
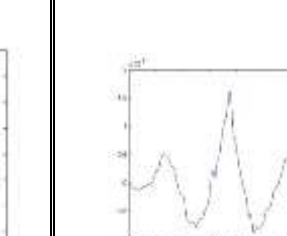
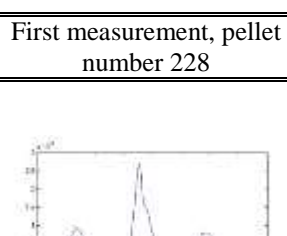
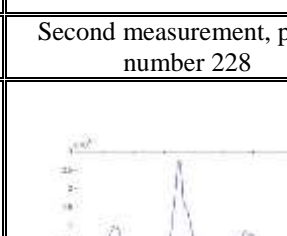
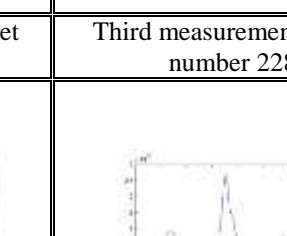
		
	Second measurement, pellet number 159	Third measurement, pellet number 159
		
First measurement, pellet number 160	Second measurement, pellet number 160	Third measurement, pellet number 160
		
First measurement, pellet number 161	Second measurement, pellet number 161	Third measurement, pellet number 161
		
First measurement, pellet number 162	Second measurement, pellet number 162	Third measurement, pellet number 162
		
First measurement, pellet number 163	Second measurement, pellet number 163	Third measurement, pellet number 163



## Appendix 52

Topographical profiles obtained from the microscopic measurements for samples 220-229, LEA H

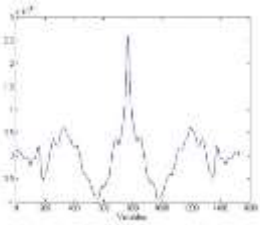
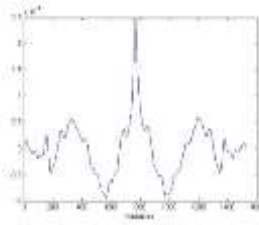
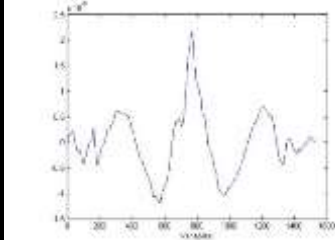
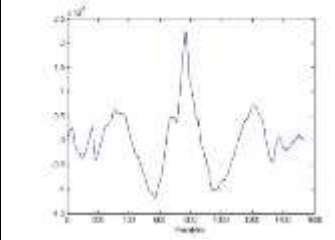
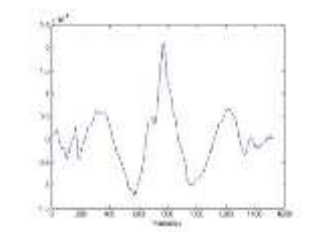
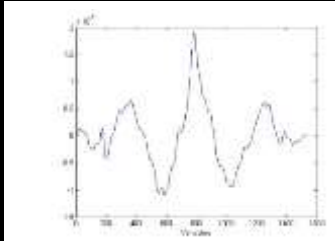
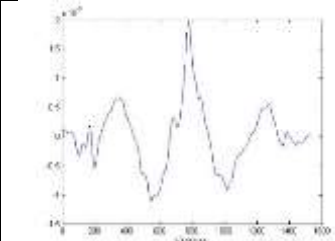
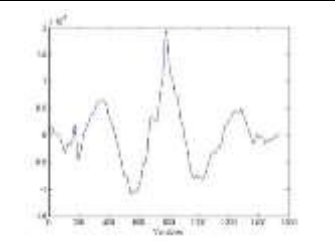
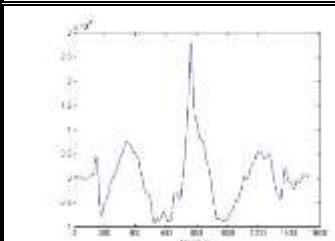
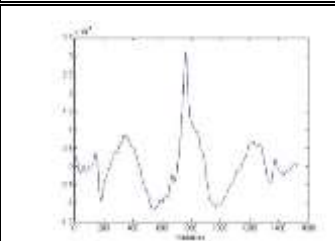
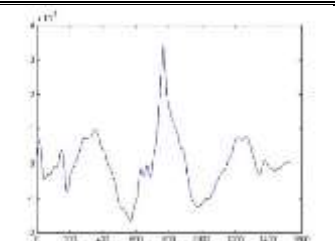
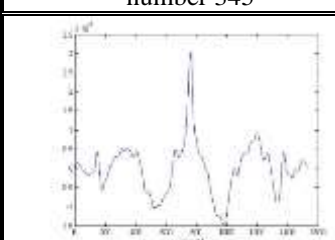
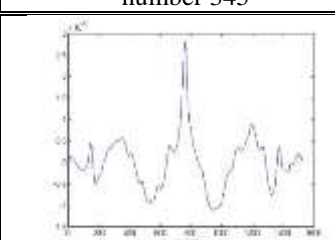
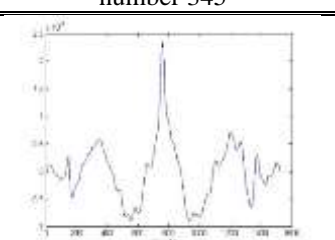


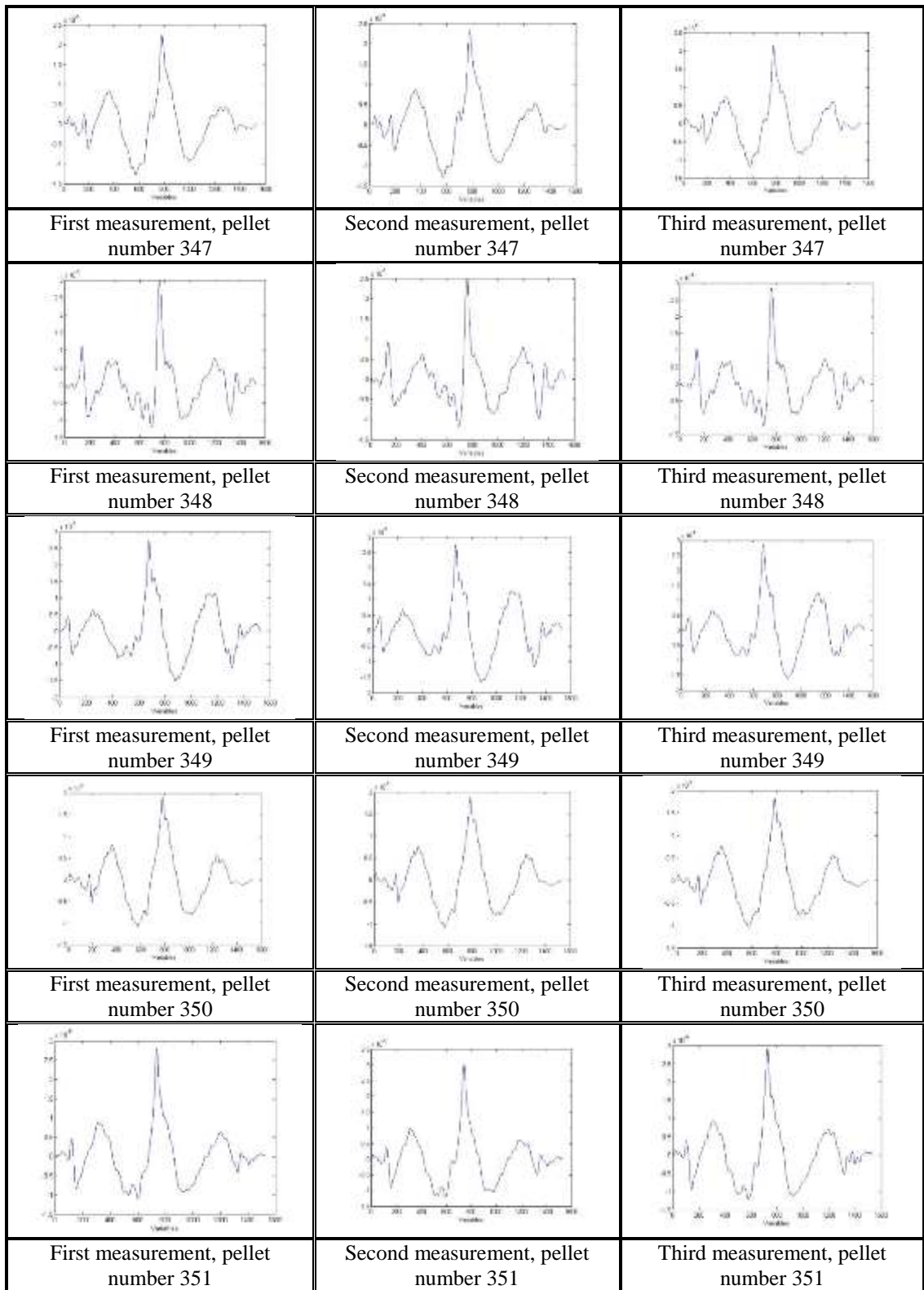
		
First measurement, pellet number 225	Second measurement, pellet number 225	Third measurement, pellet number 225
		
First measurement, pellet number 226	Second measurement, pellet number 226	Third measurement, pellet number 226
		
First measurement, pellet number 227	Second measurement, pellet number 227	Third measurement, pellet number 227
		
First measurement, pellet number 228	Second measurement, pellet number 228	Third measurement, pellet number 228
		
First measurement, pellet number 229	Second measurement, pellet number 229	Third measurement, pellet number 229



## Appendix 53

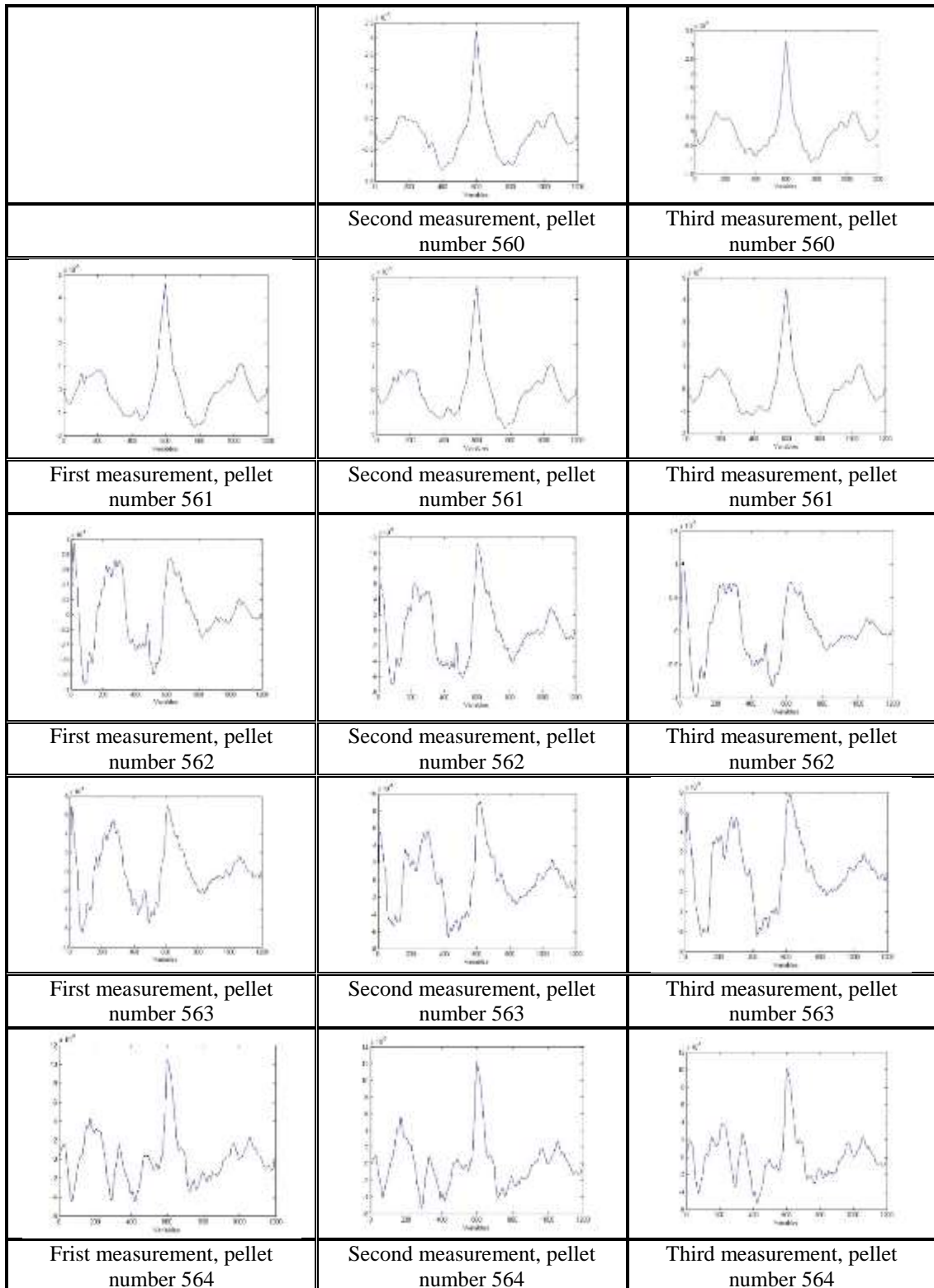
Topographical profiles obtained from the microscopic measurements for samples 342-351, LEA H

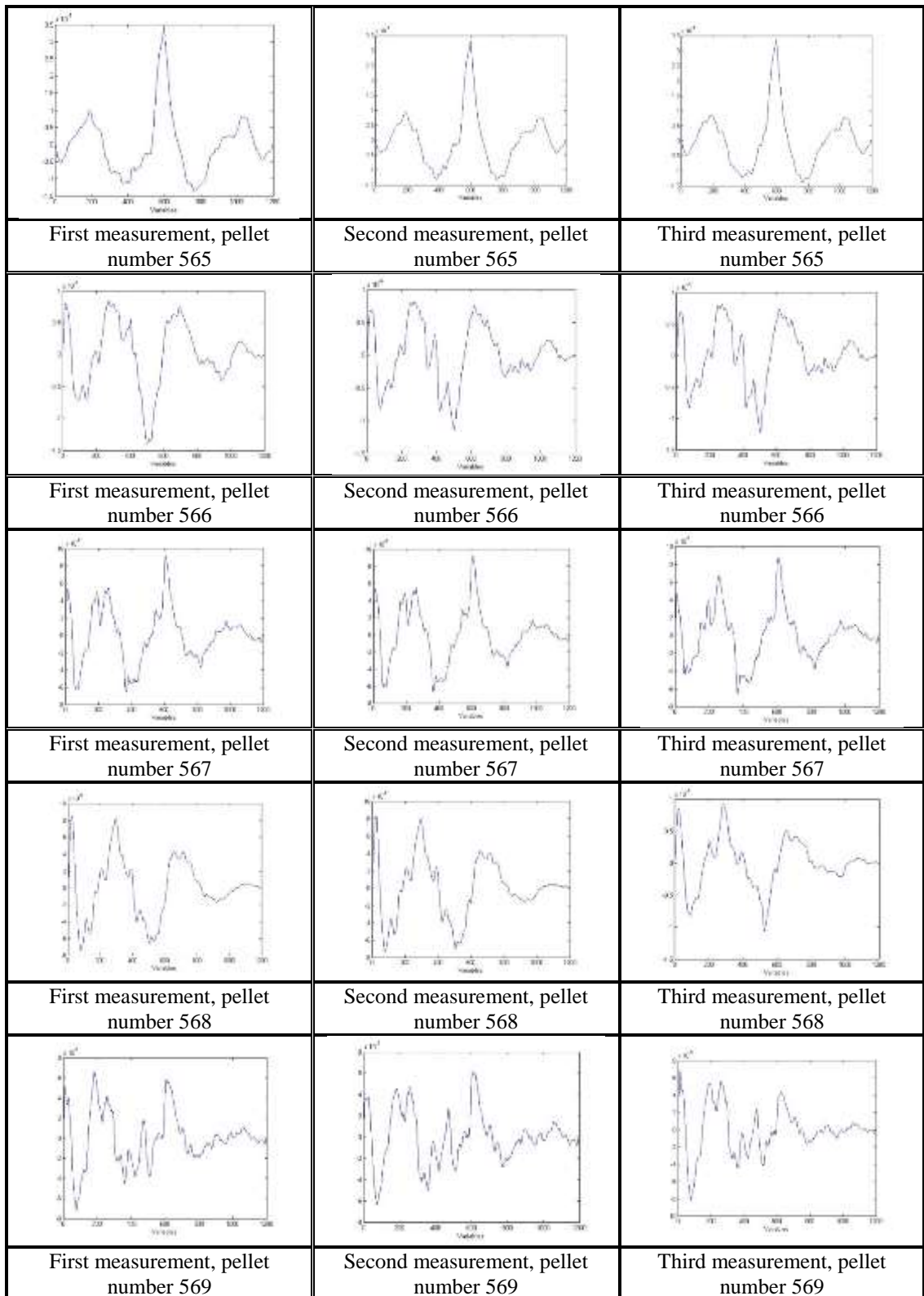
		
	Second measurement, pellet number 342	Third measurement, pellet number 342
		
First measurement, pellet number 343	Second measurement, pellet number 343	Third measurement, pellet number 343
		
First measurement, pellet number 344	Second measurement, pellet number 344	Third measurement, pellet number 344
		
First measurement, pellet number 345	Second measurement, pellet number 345	Third measurement, pellet number 345
		
First measurement, pellet number 346	Second measurement, pellet number 346	Third measurement, pellet number 346



## Appendix 54

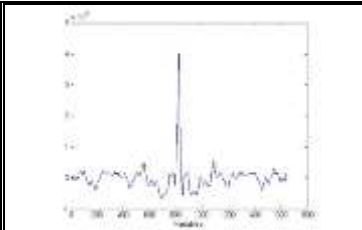
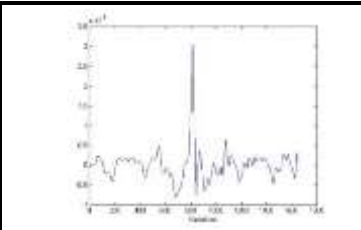
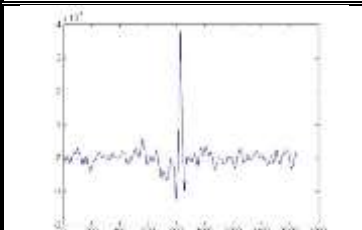
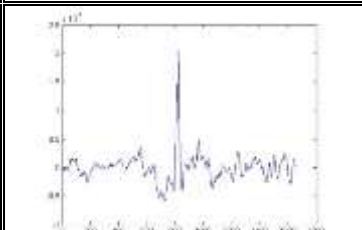
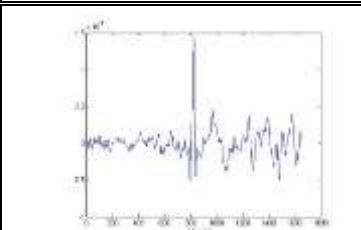

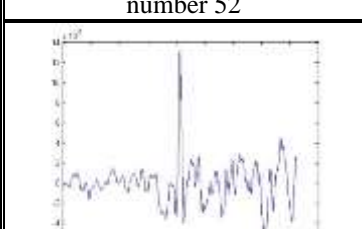
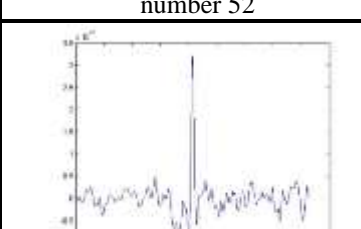



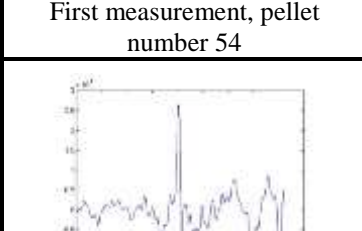
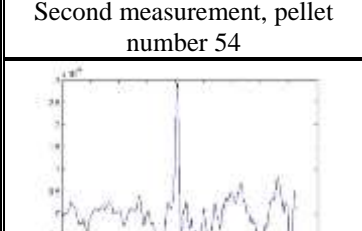
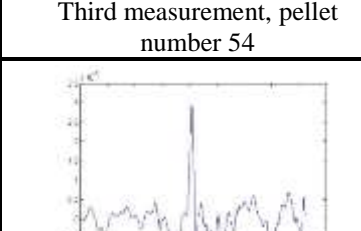
Topographical profiles obtained from the microscopic measurements for samples 560-569, LEA H

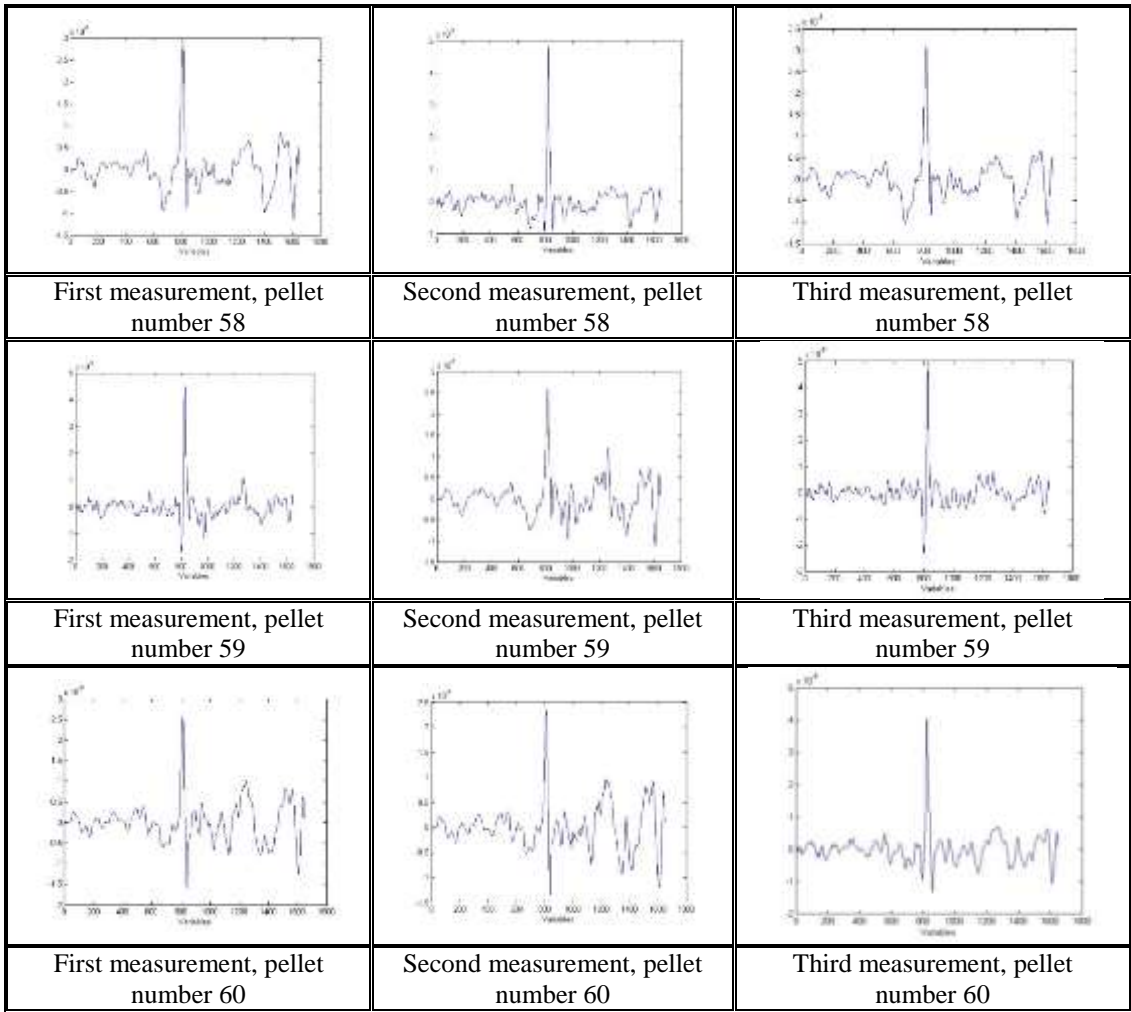




## Appendix 55

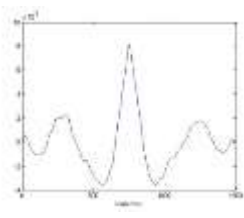
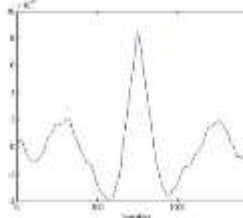
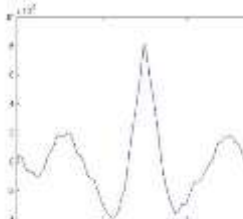
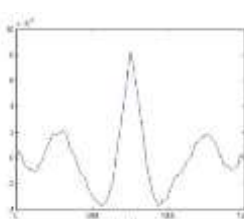
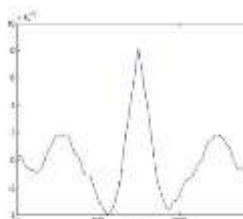
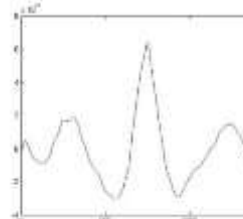
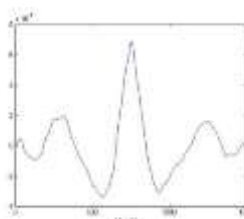
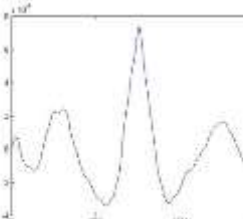
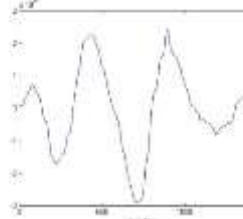
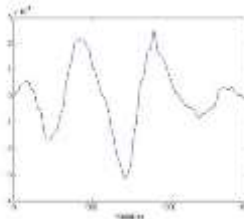
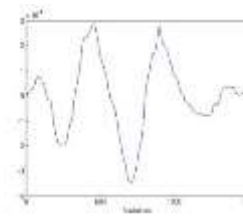
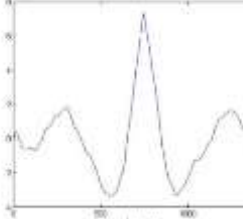
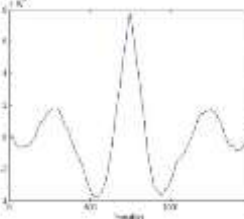
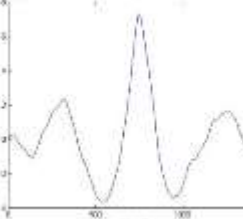
Topographical profiles obtained from the microscopic measurements for samples 51-60, LEA I

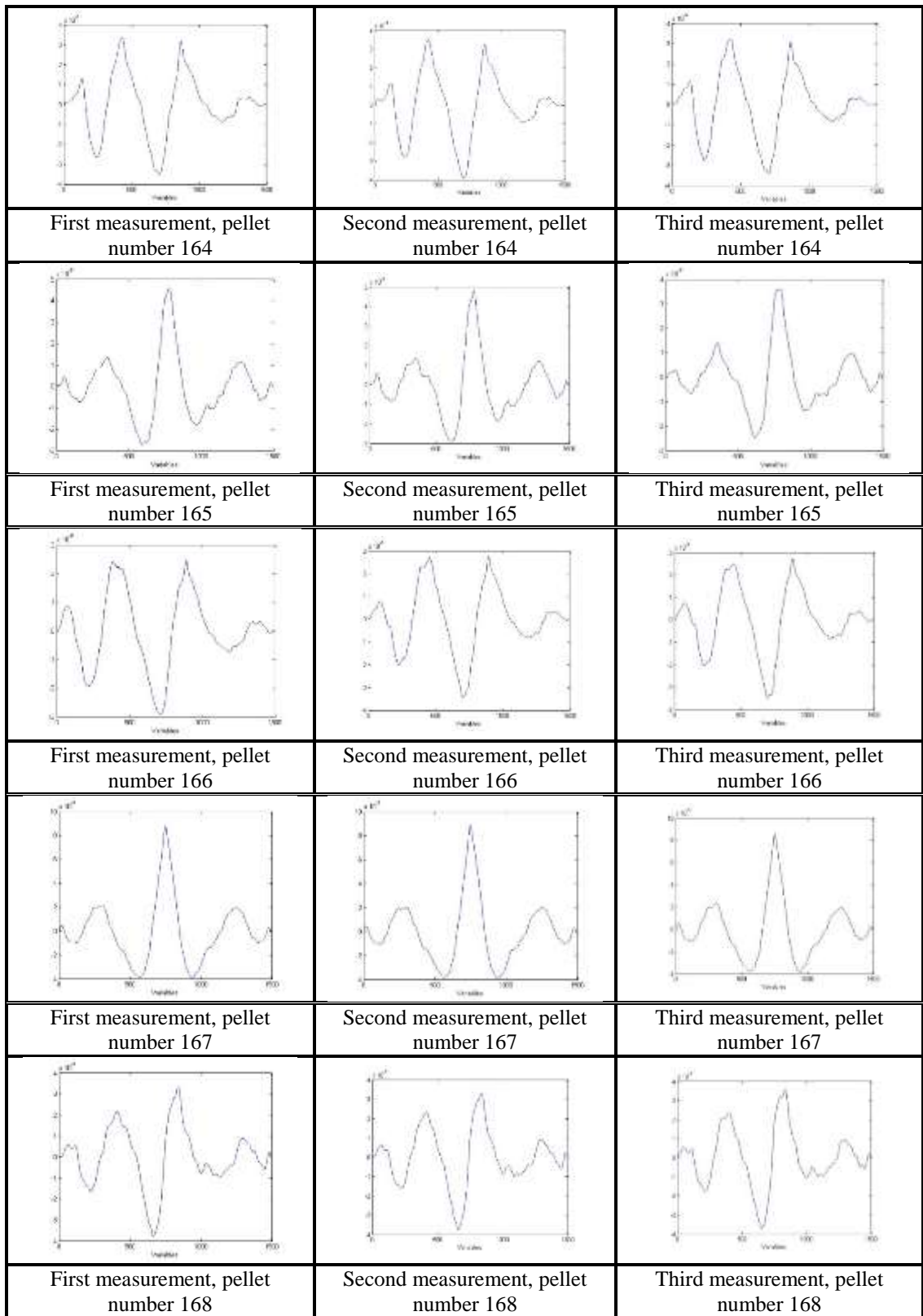
		
	Second measurement, pellet number 51	Third measurement, pellet number 51
		
First measurement, pellet number 52	Second measurement, pellet number 52	Third measurement, pellet number 52
		
First measurement, pellet number 53	Second measurement, pellet number 53	Third measurement, pellet number 53
		
First measurement, pellet number 54	Second measurement, pellet number 54	Third measurement, pellet number 54
		
First measurement, pellet number 57	Second measurement, pellet number 57	Third measurement, pellet number 57



## Appendix 56

Topographical profiles obtained from the microscopic measurements for samples 159-168, LEA I

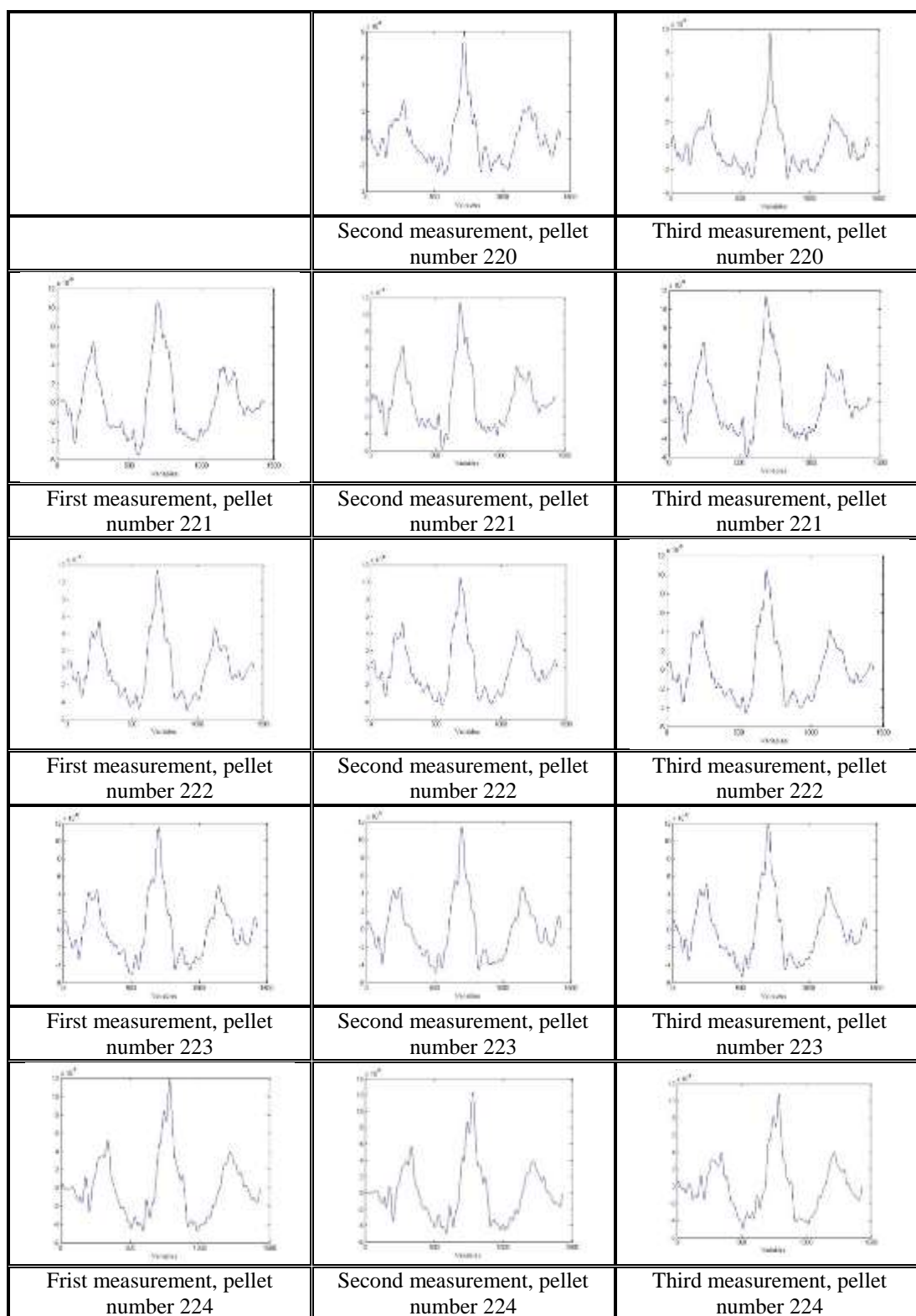
		
	Second measurement, pellet number 159	Third measurement, pellet number 159
		
First measurement, pellet number 160	Second measurement, pellet number 160	Third measurement, pellet number 160
		
First measurement, pellet number 161	Second measurement, pellet number 161	Third measurement, pellet number 161
		
First measurement, pellet number 162	Second measurement, pellet number 162	Third measurement, pellet number 162
		
First measurement, pellet number 163	Second measurement, pellet number 163	Third measurement, pellet number 163

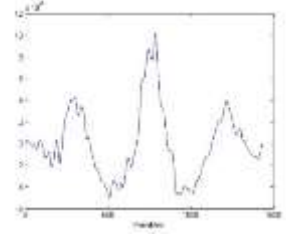
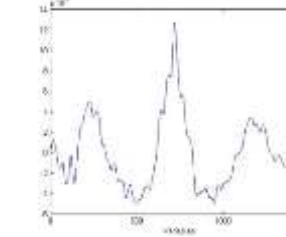
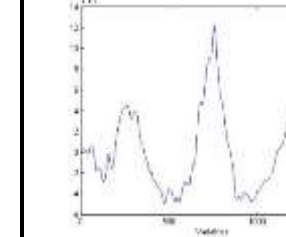
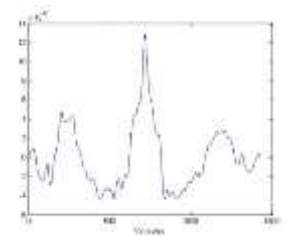
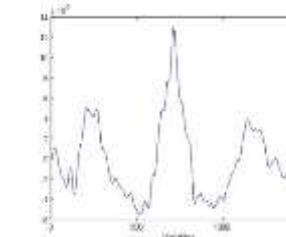
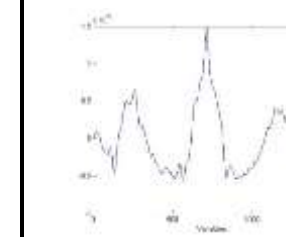
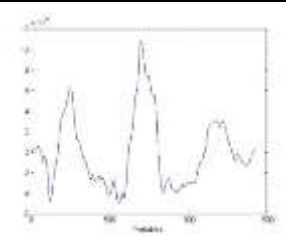
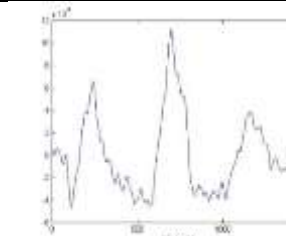
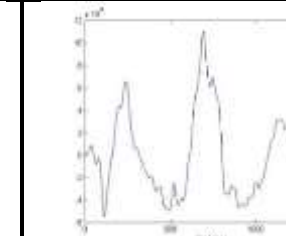
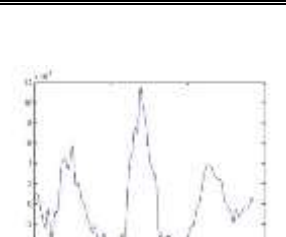
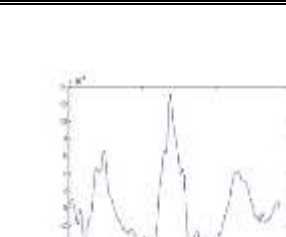
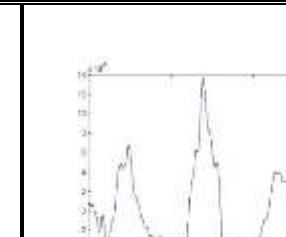
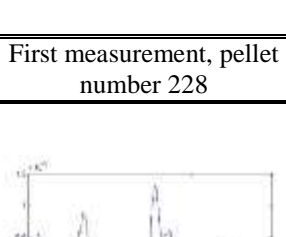
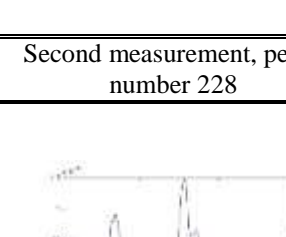
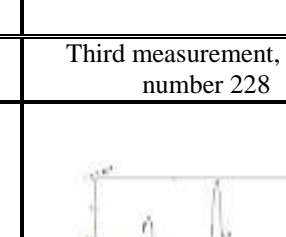




## Appendix 57

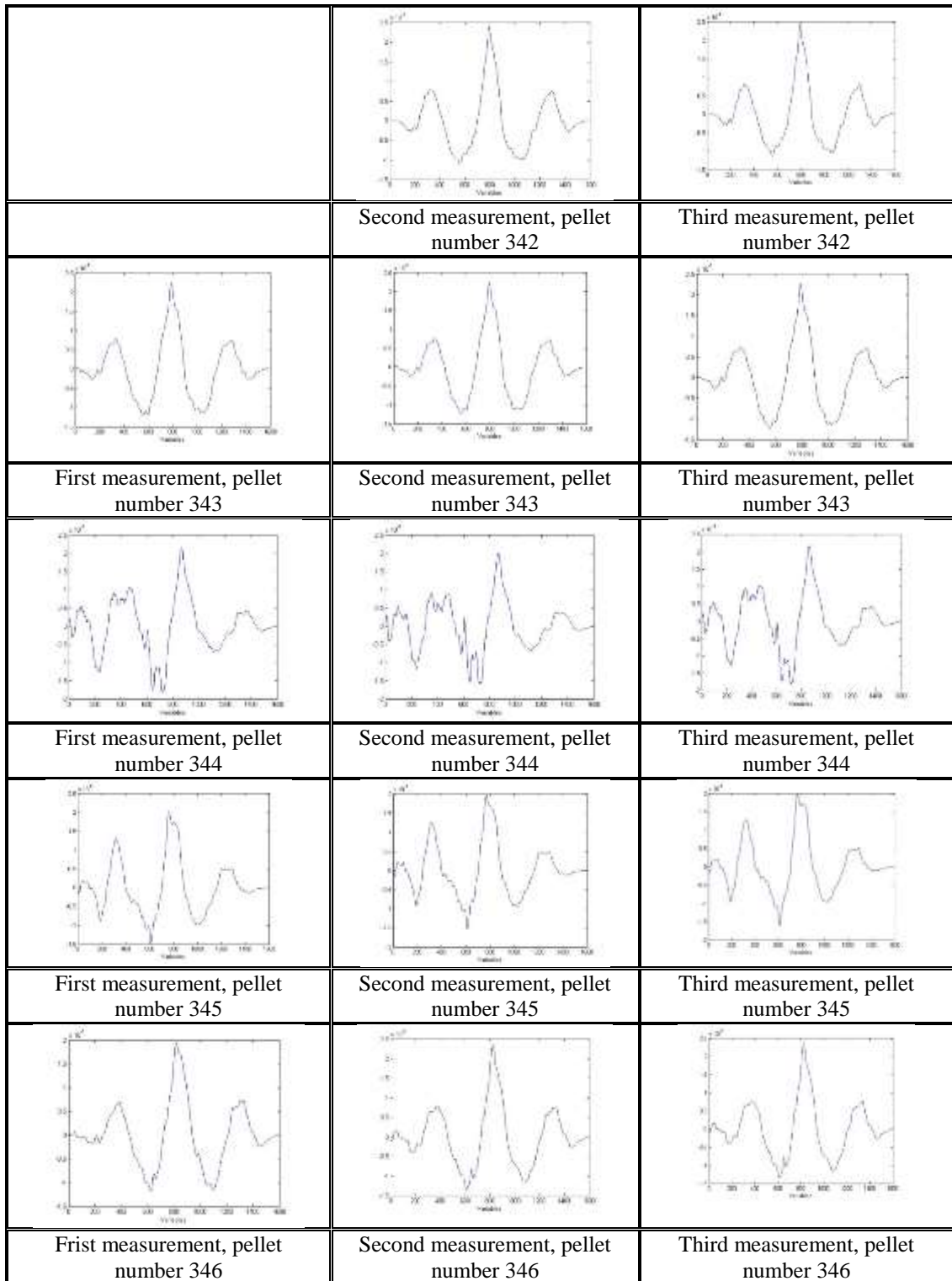
Topographical profiles obtained from the microscopic measurements for samples 220-229, LEA I

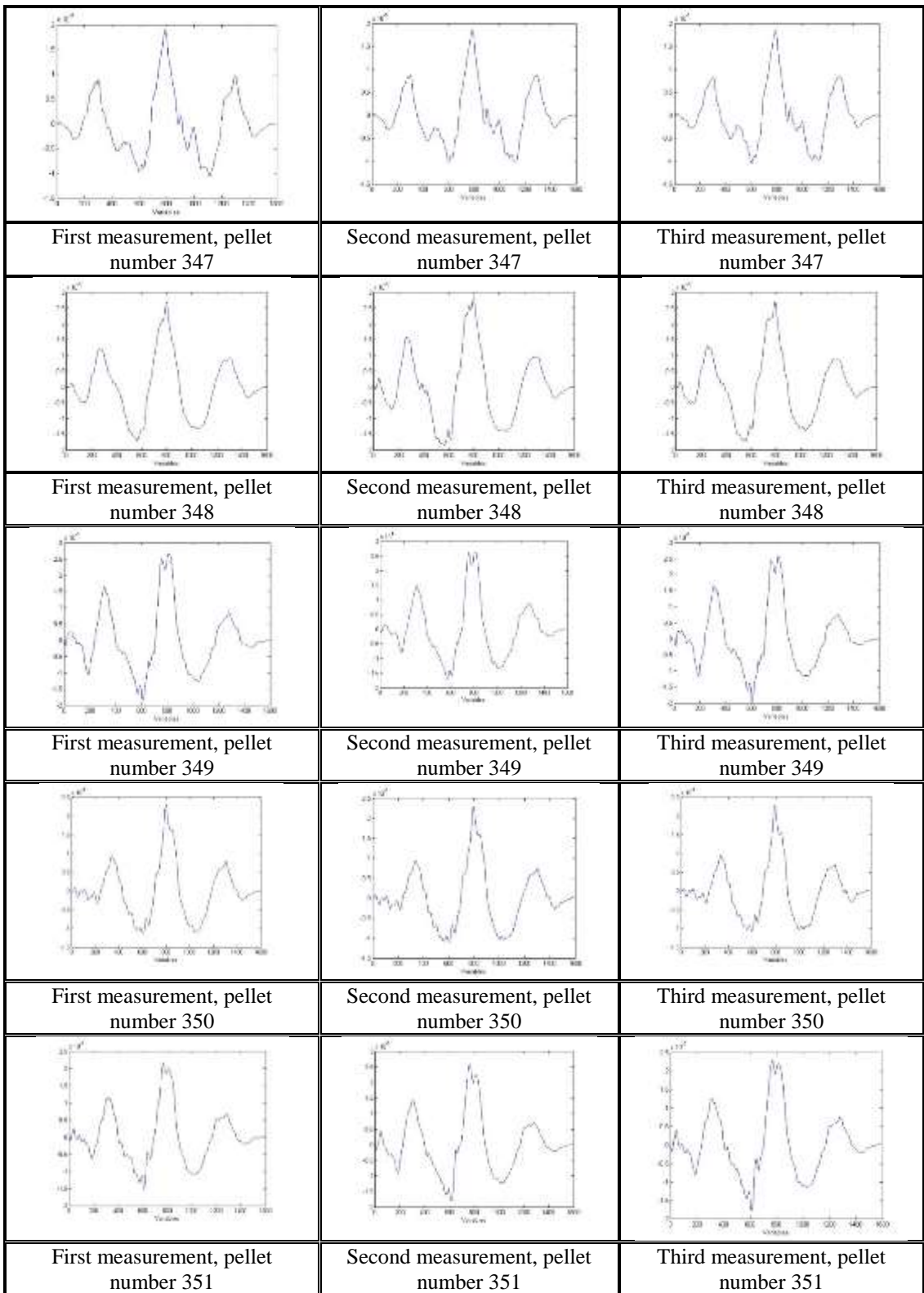


		
First measurement, pellet number 225	Second measurement, pellet number 225	Third measurement, pellet number 225
		
First measurement, pellet number 226	Second measurement, pellet number 226	Third measurement, pellet number 226
		
First measurement, pellet number 227	Second measurement, pellet number 227	Third measurement, pellet number 227
		
First measurement, pellet number 228	Second measurement, pellet number 228	Third measurement, pellet number 228
		
First measurement, pellet number 229	Second measurement, pellet number 229	Third measurement, pellet number 229

## Appendix 58

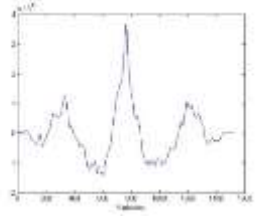
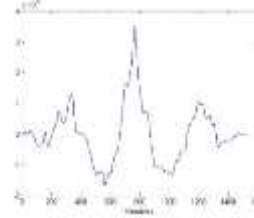
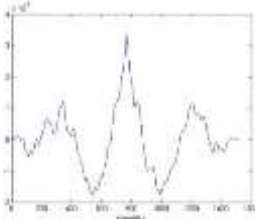
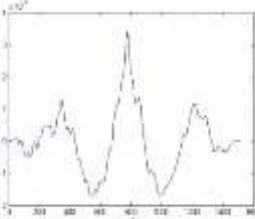
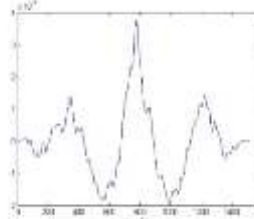
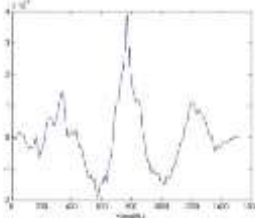
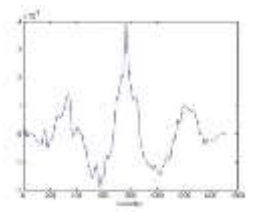
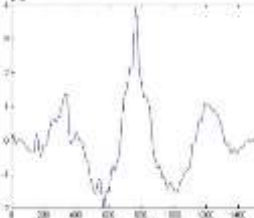
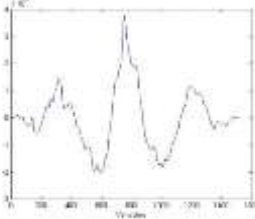
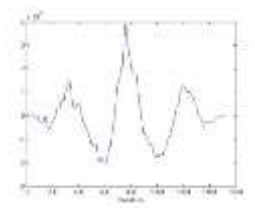
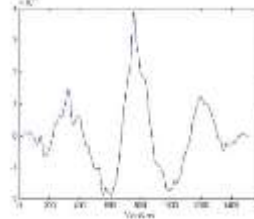
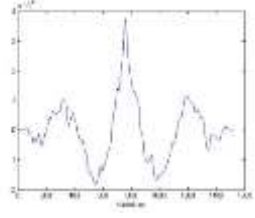
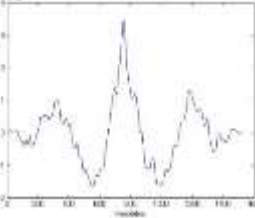
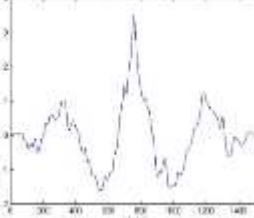
Topographical profiles obtained from the microscopic measurements for samples 342-351, LEA I

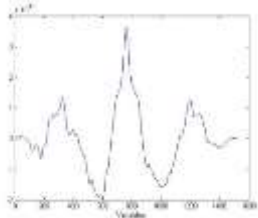
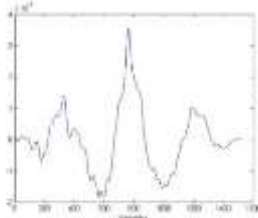
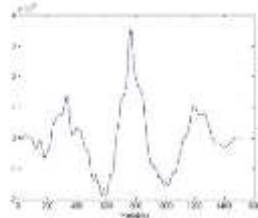
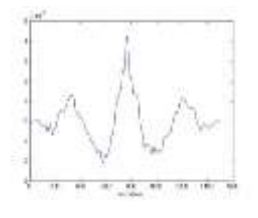
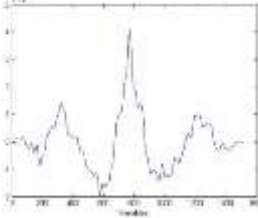
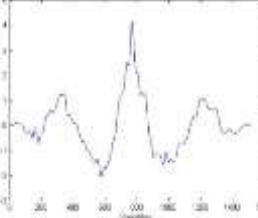
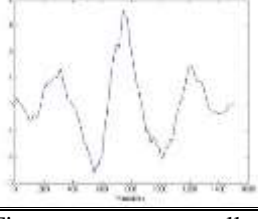
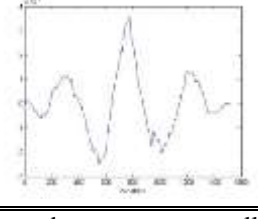
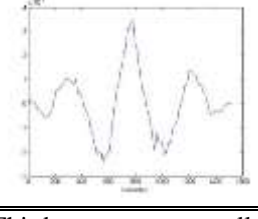
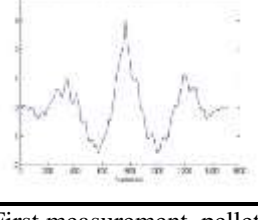

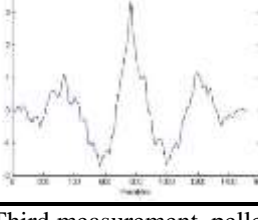




## Appendix 59

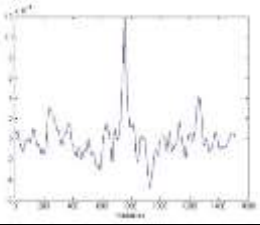
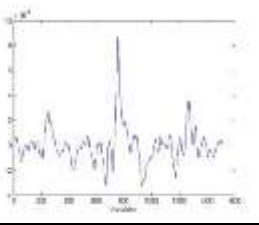
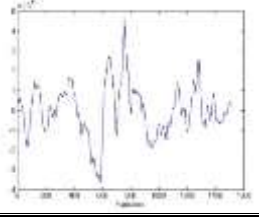
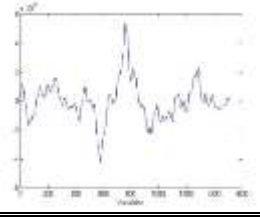
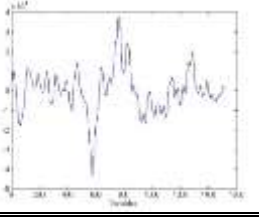
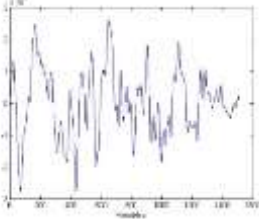
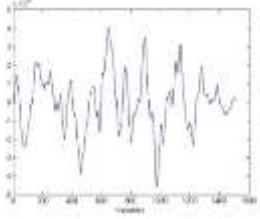
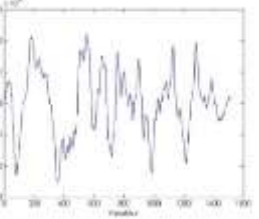
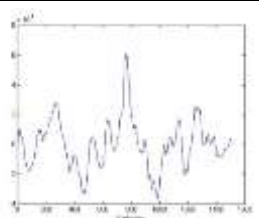
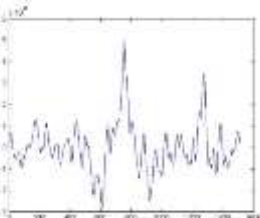
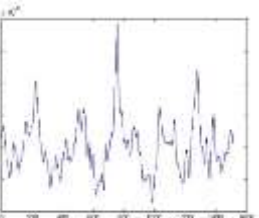
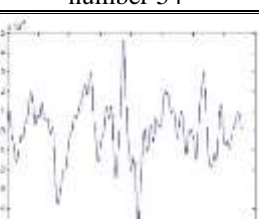
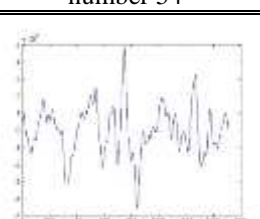
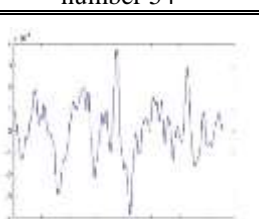
Topographical profiles obtained from the microscopic measurements for samples 560-569, LEA I

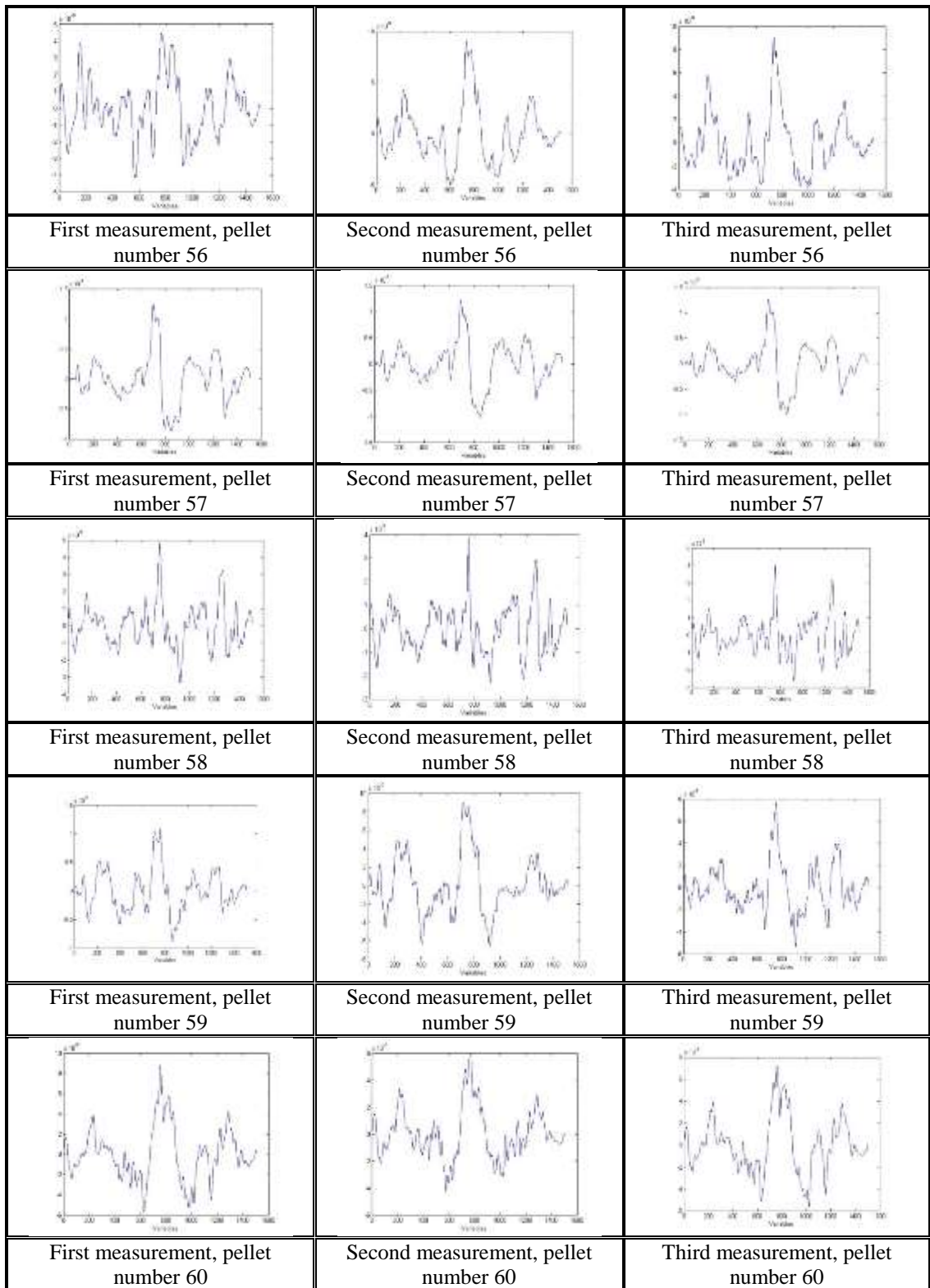
		
	Second measurement, pellet number 561	Third measurement, pellet number 561
		
First measurement, pellet number 562	Second measurement, pellet number 562	Third measurement, pellet number 562
		
First measurement, pellet number 563	Second measurement, pellet number 563	Third measurement, pellet number 563
		
First measurement, pellet number 564	Second measurement, pellet number 564	Third measurement, pellet number 564
		
First measurement, pellet number 565	Second measurement, pellet number 565	Third measurement, pellet number 565

		
First measurement, pellet number 566	Second measurement, pellet number 566	Third measurement, pellet number 566
		
First measurement, pellet number 567	Second measurement, pellet number 567	Third measurement, pellet number 567
		
First measurement, pellet number 568	Second measurement, pellet number 568	Third measurement, pellet number 568
		
First measurement, pellet number 569	Second measurement, pellet number 569	Third measurement, pellet number 569

## Appendix 60

Topographical profiles obtained from the microscopic measurements for samples 51-60, LEA J

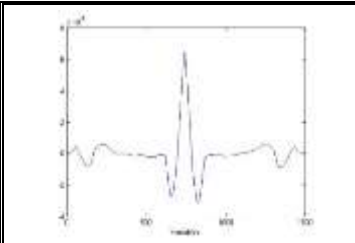
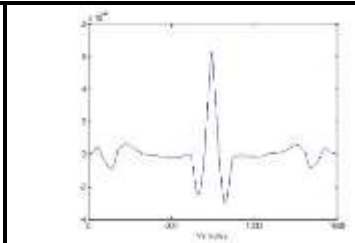
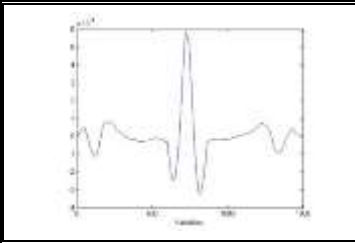
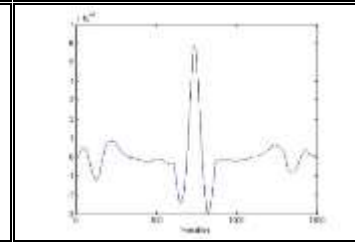
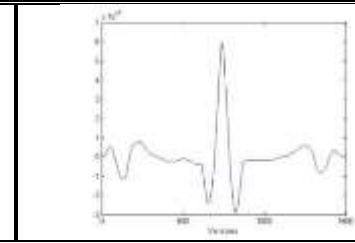
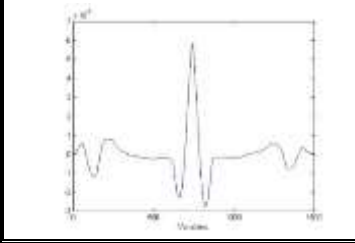
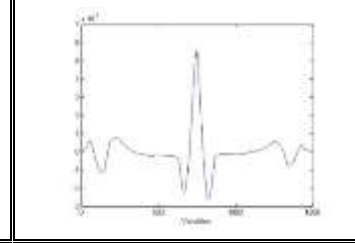
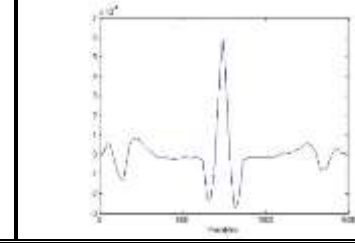
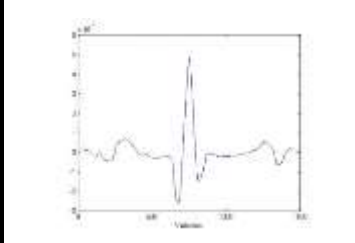
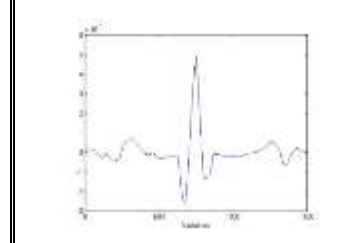
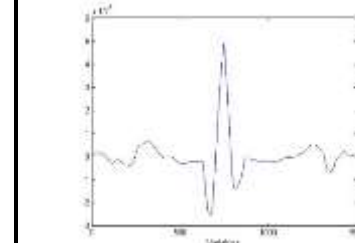
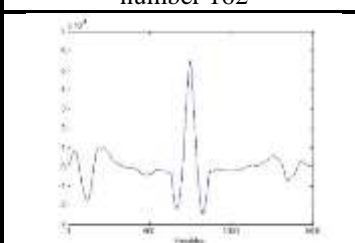
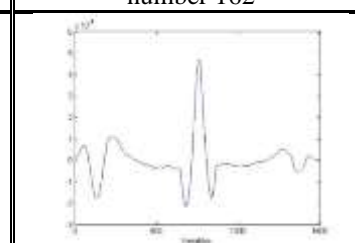
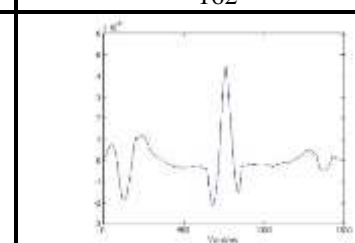
		
	Second measurement, pellet number 51	Third measurement, pellet number 51
		
First measurement, pellet number 52	Second measurement, pellet number 52	Third measurement, pellet number 52
		
First measurement, pellet number 53	Second measurement, pellet number 53	Third measurement, pellet number 53
		
First measurement, pellet number 54	Second measurement, pellet number 54	Third measurement, pellet number 54
		
First measurement, pellet number 55	Second measurement, pellet number 55	Third measurement, pellet number 55

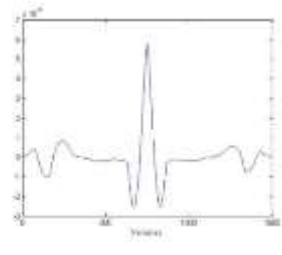
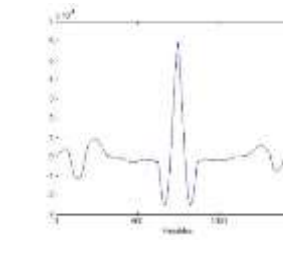
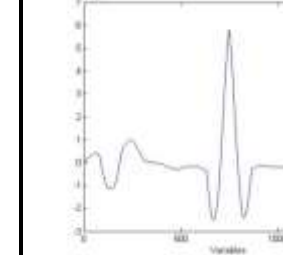
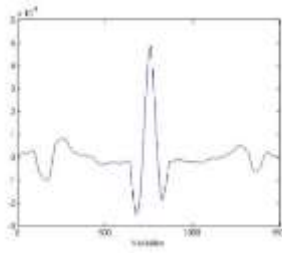
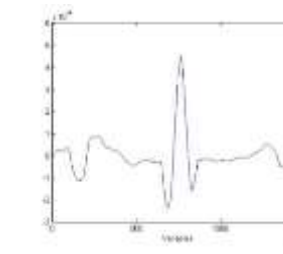
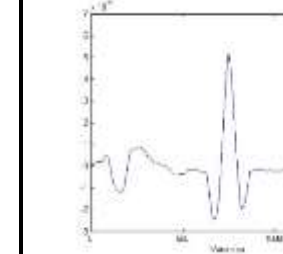
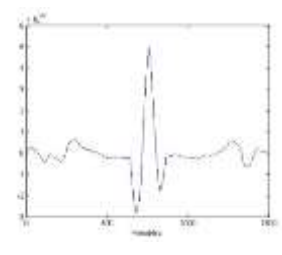
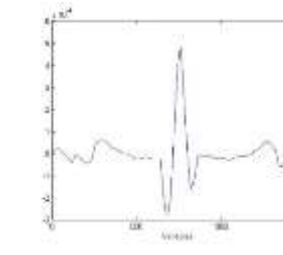
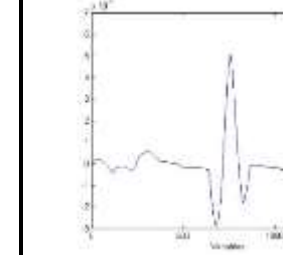
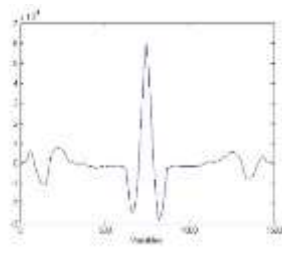
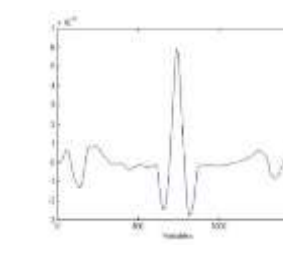
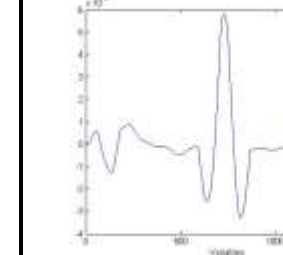
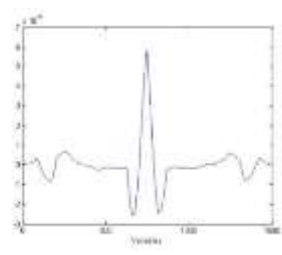
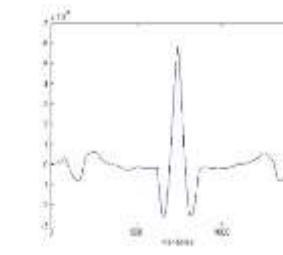
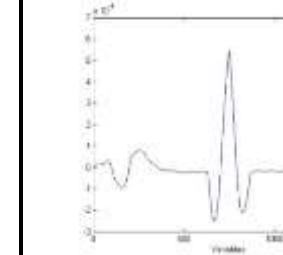




## Appendix 61

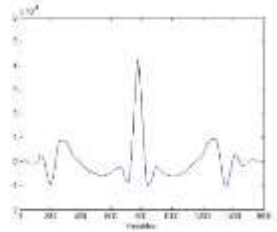
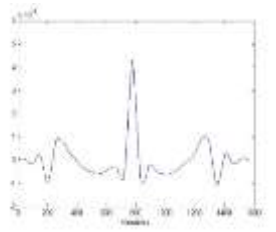
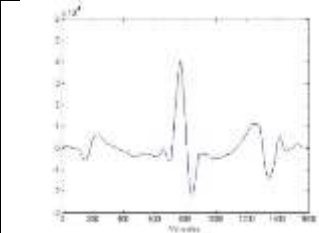
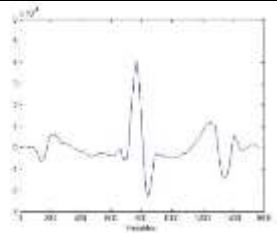
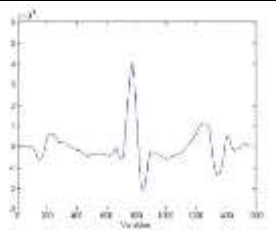
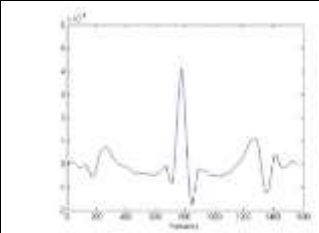
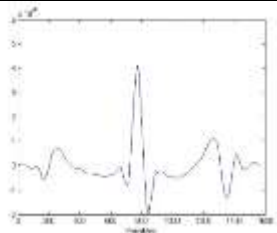
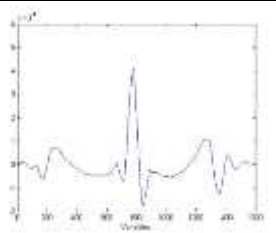
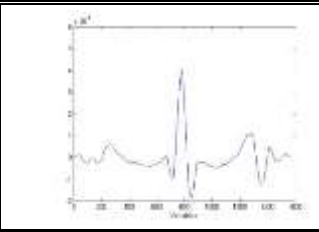
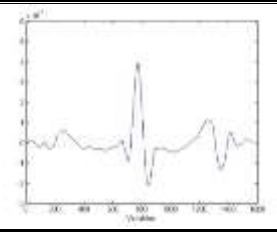
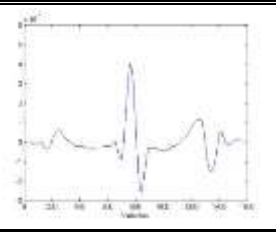
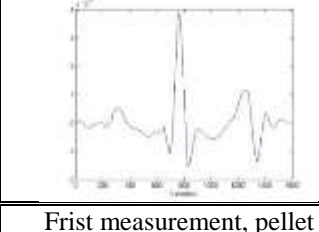
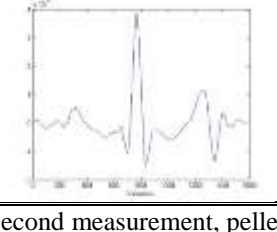
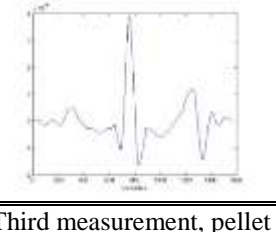
Topographical profiles obtained from the microscopic measurements for samples 159-168, LEA J

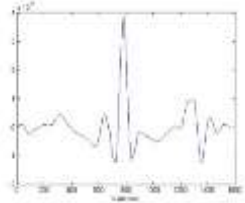
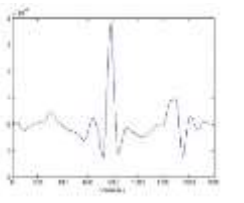
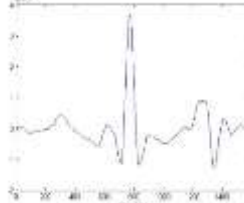
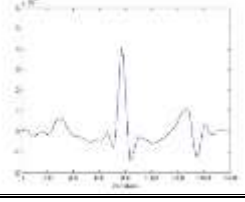
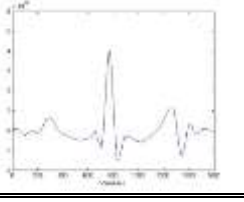
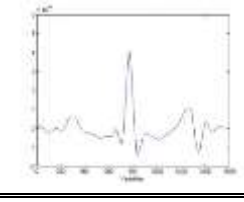
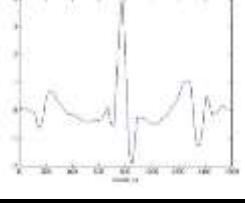
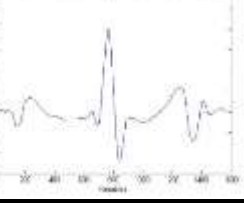
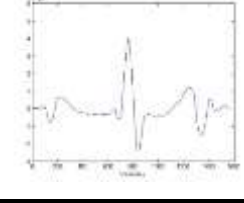
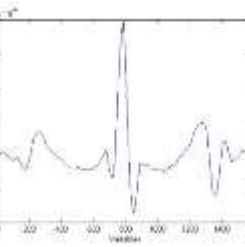
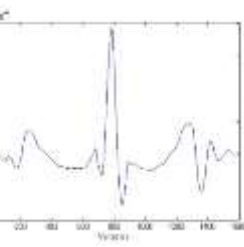
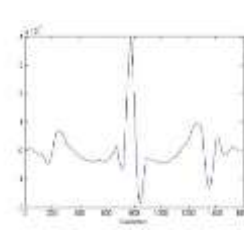
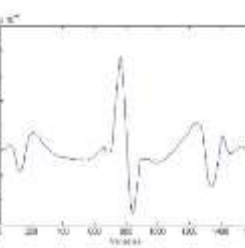
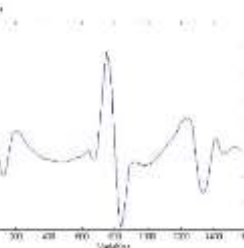
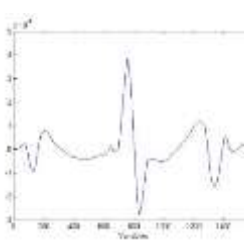
		
	Second measurement, pellet number 159	Third measurement, pellet number 159
		
First measurement, pellet number 160	Second measurement, pellet number 160	Third measurement, pellet number 160
		
First measurement, pellet number 161	Second measurement, pellet number 161	Third measurement, pellet number 161
		
First measurement, pellet number 162	Second measurement, pellet number 162	Third measurement, pellet number 162
		
First measurement, pellet number 163	Second measurement, pellet number 163	Third measurement, pellet number 163

		
First measurement, pellet number 164	Second measurement, pellet number 164	Third measurement, pellet number 164
		
First measurement, pellet number 165	Second measurement, pellet number 165	Third measurement, pellet number 165
		
First measurement, pellet number 166	Second measurement, pellet number 166	Third measurement, pellet number 166
		
First measurement, pellet number 167	Second measurement, pellet number 167	Third measurement, pellet number 167
		
First measurement, pellet number 168	Second measurement, pellet number 168	Third measurement, pellet number 168

## Appendix 62

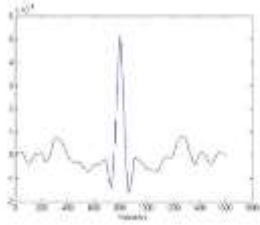
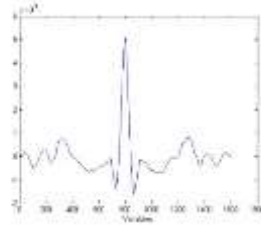
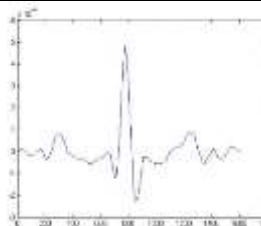
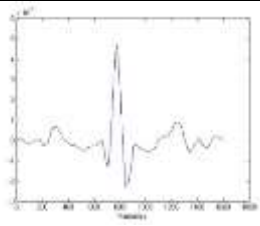
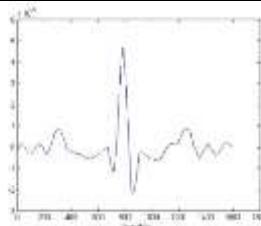
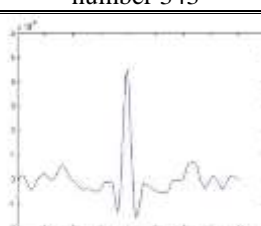
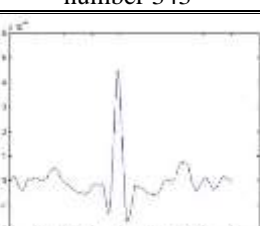
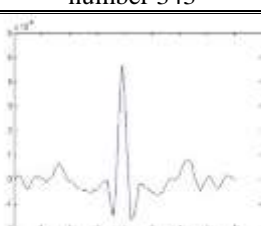


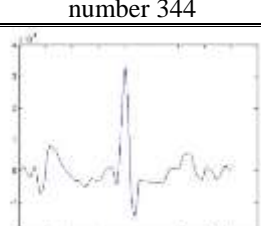

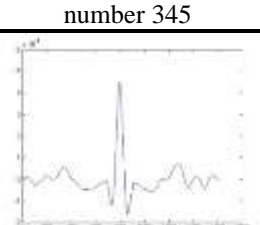
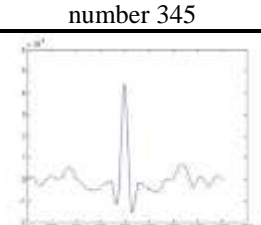
Topographical profiles obtained from the microscopic measurements for samples 220-229, LEA J

		
	Second measurement, pellet number 220	Third measurement, pellet number 220
		
First measurement, pellet number 221	Second measurement, pellet number 221	Third measurement, pellet number 221
		
First measurement, pellet number 222	Second measurement, pellet number 222	Third measurement, pellet number 222
		
First measurement, pellet number 223	Second measurement, pellet number 223	Third measurement, pellet number 223
		
First measurement, pellet number 224	Second measurement, pellet number 224	Third measurement, pellet number 224

		
First measurement, pellet number 225	Second measurement, pellet number 225	Third measurement, pellet number 225
		
First measurement, pellet number 226	Second measurement, pellet number 226	Third measurement, pellet number 226
		
First measurement, pellet number 227	Second measurement, pellet number 227	Third measurement, pellet number 227
		
First measurement, pellet number 228	Second measurement, pellet number 228	Third measurement, pellet number 228
		
First measurement, pellet number 229	Second measurement, pellet number 229	Third measurement, pellet number 229

## Appendix 63

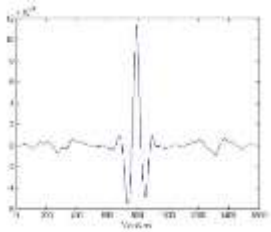
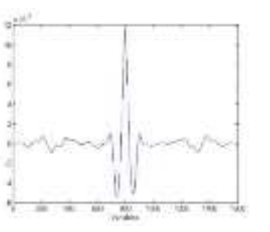
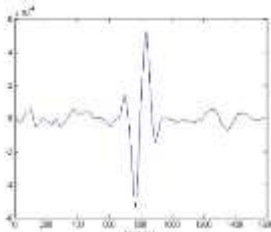
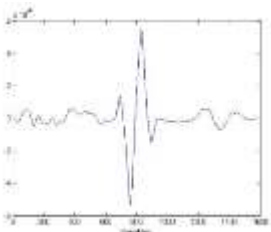
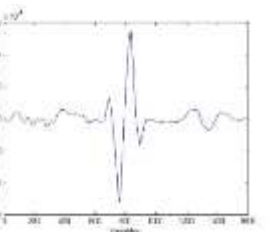
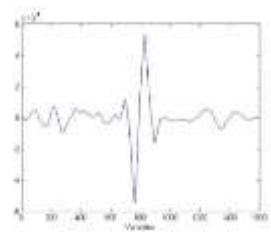
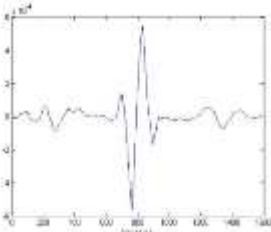
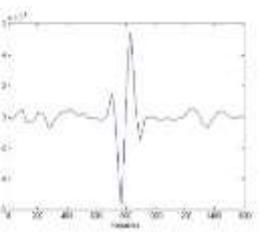
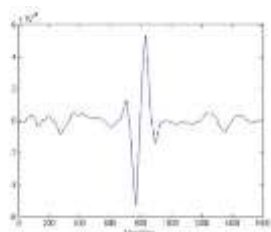
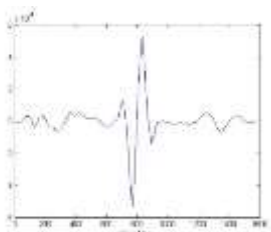
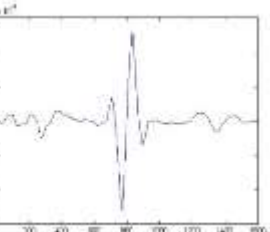
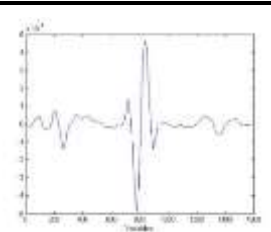

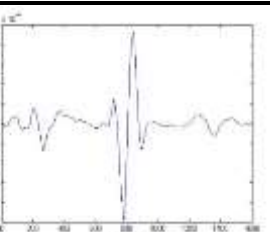
Topographical profiles obtained from the microscopic measurements for samples 342-351, LEA J

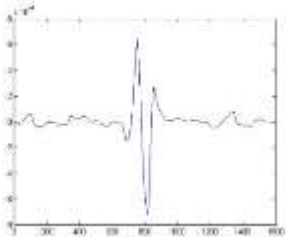
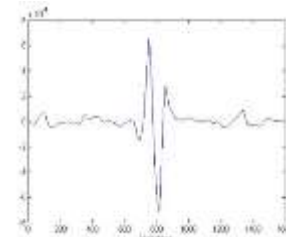
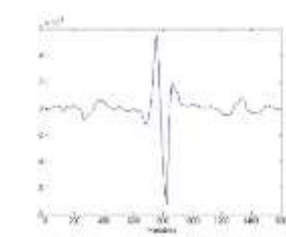
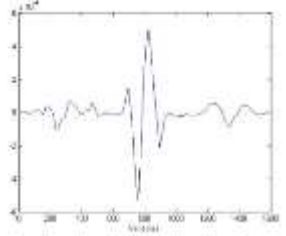
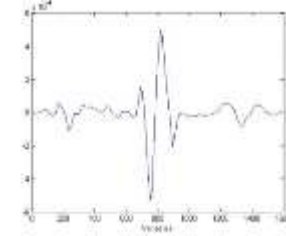
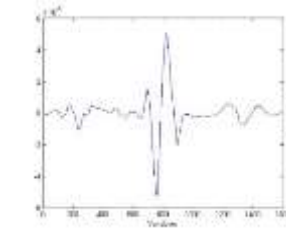
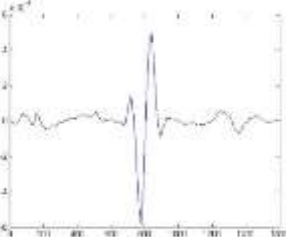
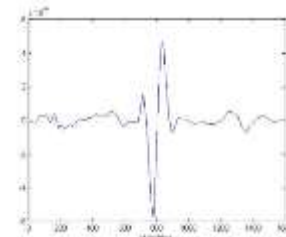
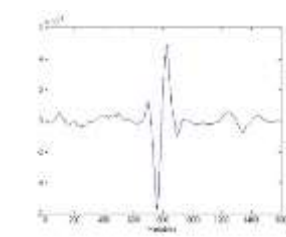
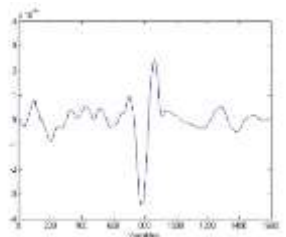
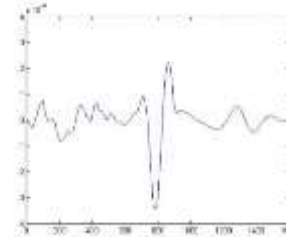
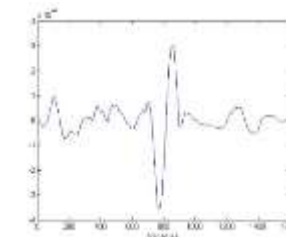
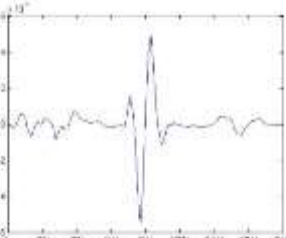
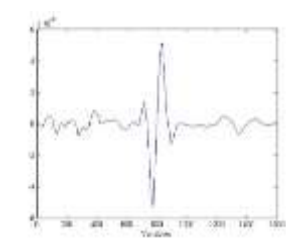
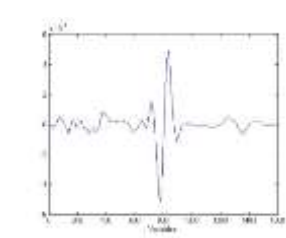
		
	Second measurement, pellet number 342	Third measurement, pellet number 342
		
First measurement, pellet number 343	Second measurement, pellet number 343	Third measurement, pellet number 343
		
First measurement, pellet number 344	Second measurement, pellet number 344	Third measurement, pellet number 344
		
First measurement, pellet number 345	Second measurement, pellet number 345	Third measurement, pellet number 345
		
First measurement, pellet number 346	Second measurement, pellet number 346	Third measurement, pellet number 346

First measurement, pellet number 347	Second measurement, pellet number 347	Third measurement, pellet number 347
First measurement, pellet number 348	Second measurement, pellet number 348	Third measurement, pellet number 348
First measurement, pellet number 349	Second measurement, pellet number 349	Third measurement, pellet number 349
First measurement, pellet number 350	Second measurement, pellet number 350	Third measurement, pellet number 350
First measurement, pellet number 351	Second measurement, pellet number 351	Third measurement, pellet number 351

## Appendix 64

Topographical profiles obtained from the microscopic measurements for samples 560-569, LEA J

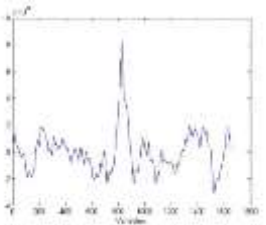
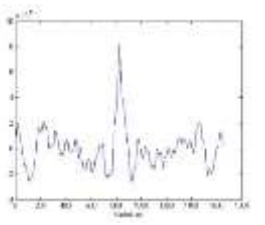
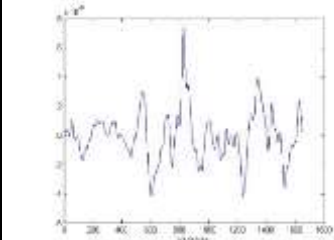
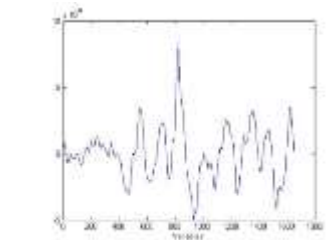
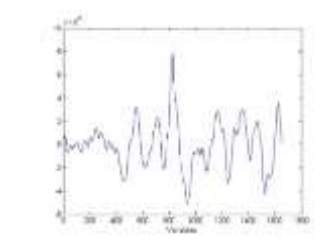
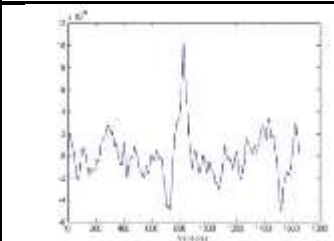
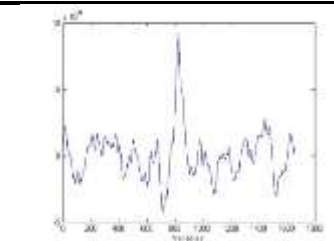
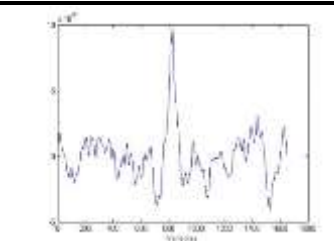
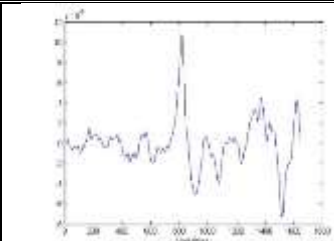
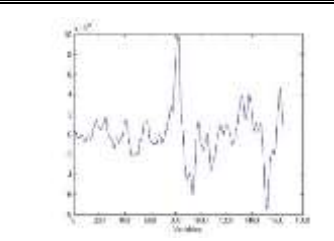
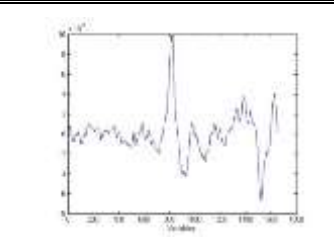
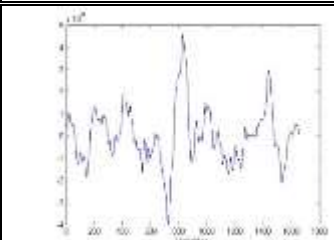
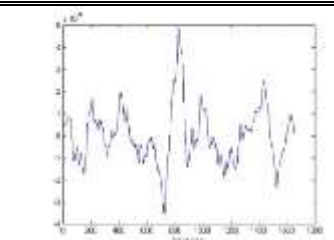
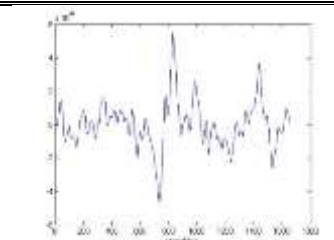
		
	Second measurement, pellet number 560	Third measurement, pellet number 560
		
First measurement, pellet number 561	Second measurement, pellet number 561	Third measurement, pellet number 561
		
First measurement, pellet number 562	Second measurement, pellet number 562	Third measurement, pellet number 562
		
First measurement, pellet number 563	Second measurement, pellet number 563	Third measurement, pellet number 563
		
First measurement, pellet number 564	Second measurement, pellet number 564	Third measurement, pellet number 564

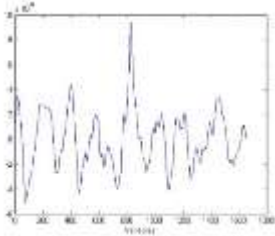
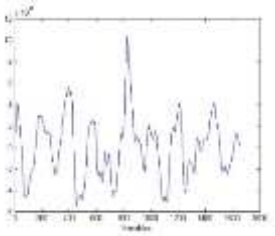
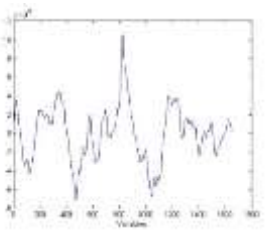
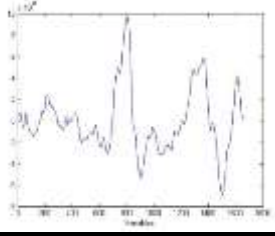
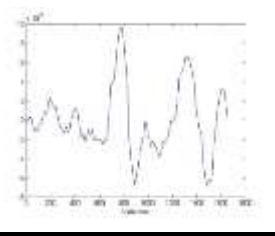
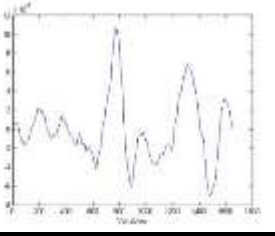
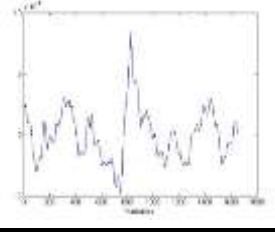
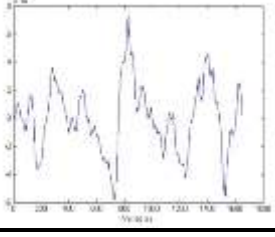
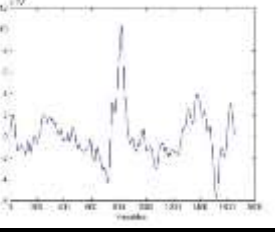
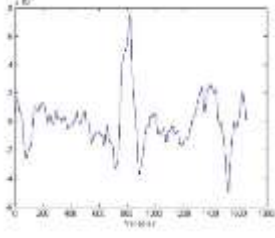
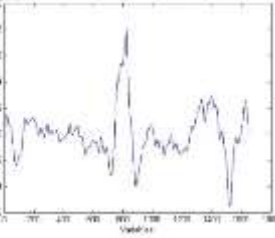
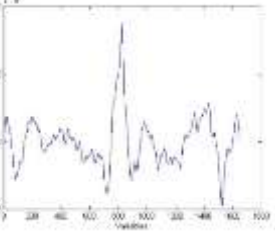
		
First measurement, pellet number 565	Second measurement, pellet number 565	Third measurement, pellet number 565
		
First measurement, pellet number 566	Second measurement, pellet number 566	Third measurement, pellet number 566
		
First measurement, pellet number 567	Second measurement, pellet number 567	Third measurement, pellet number 567
		
First measurement, pellet number 568	Second measurement, pellet number 568	Third measurement, pellet number 568
		
First measurement, pellet number 569	Second measurement, pellet number 569	Third measurement, pellet number 569



## Appendix 65

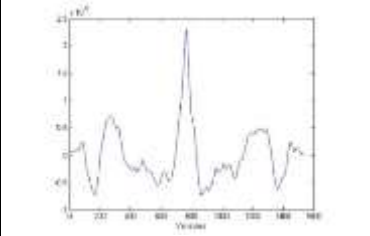
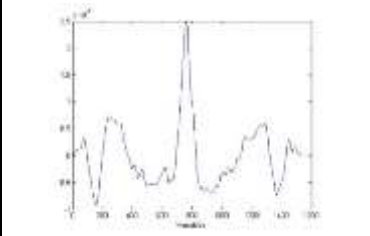
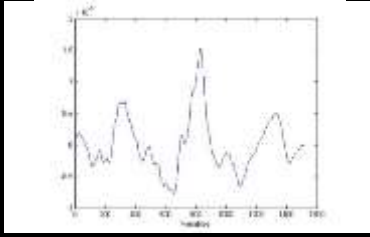
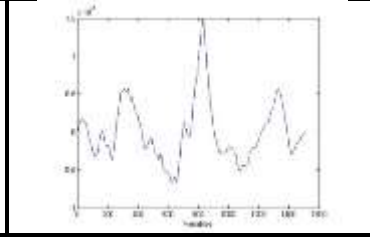
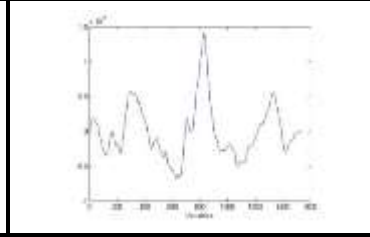
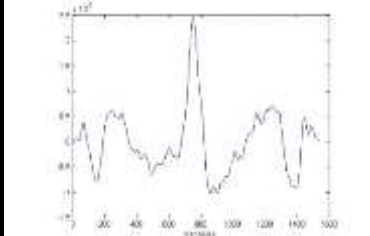
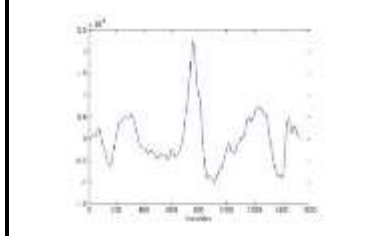
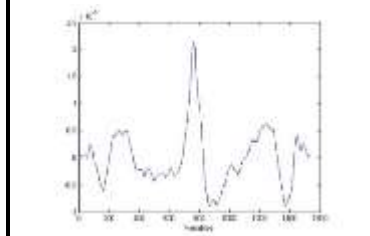
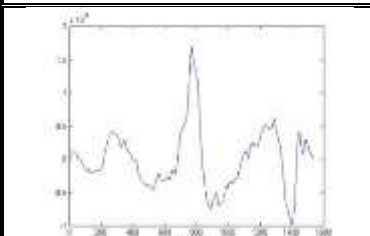
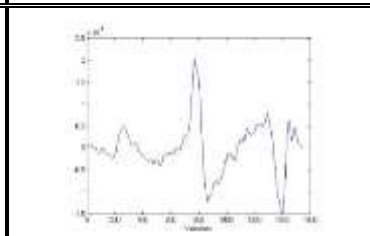
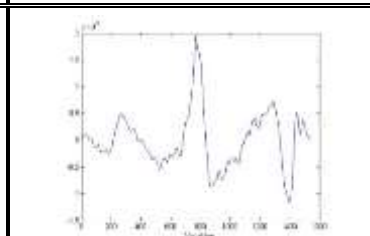
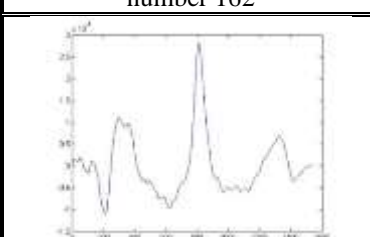
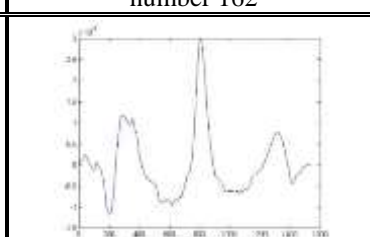
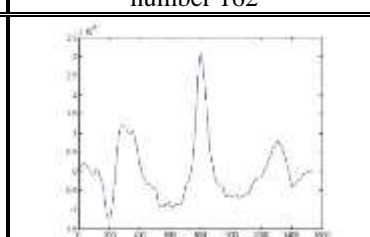
Topographical profiles obtained from the microscopic measurements for samples 51-60, LEA K

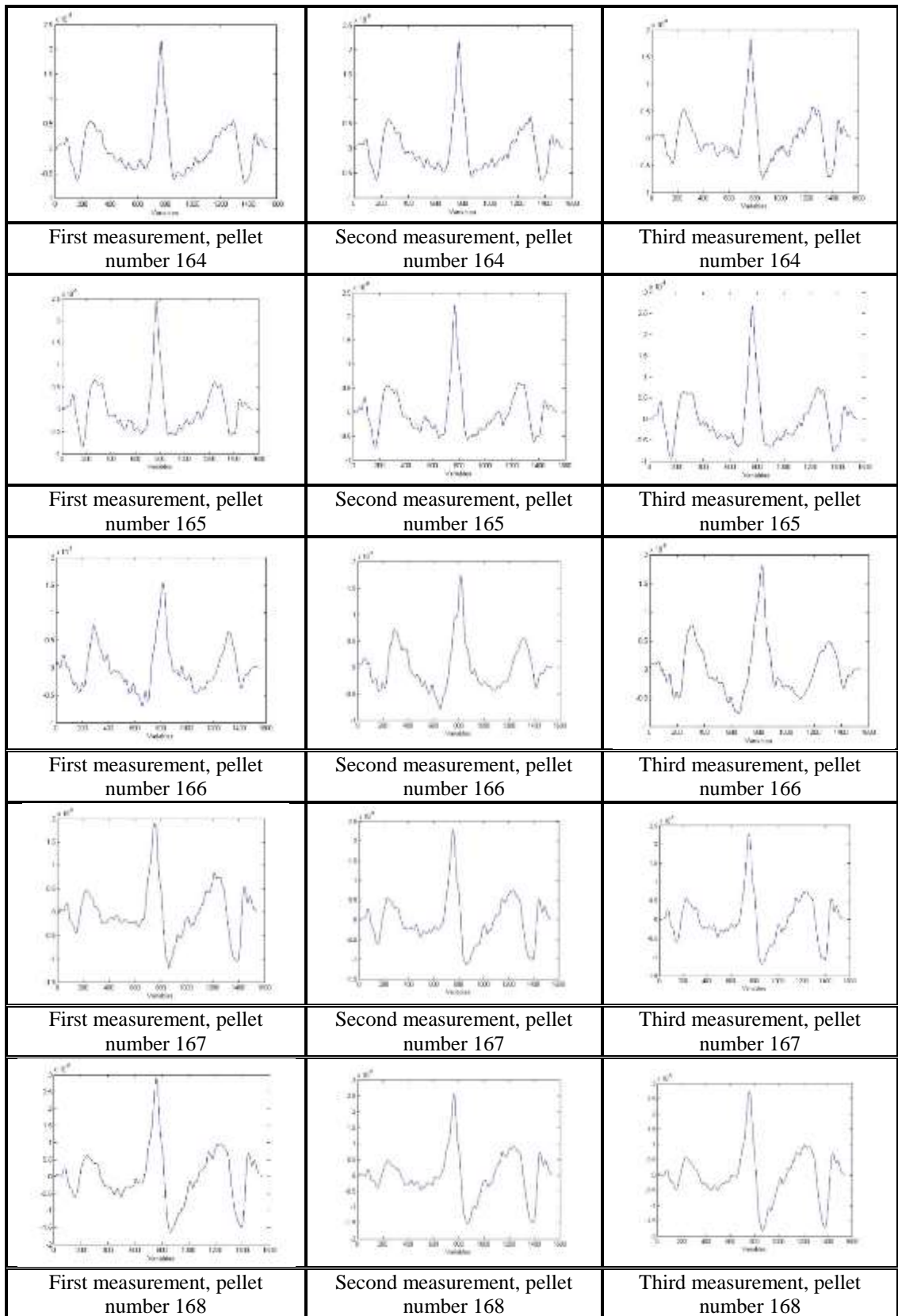
		
	Second measurement, pellet number 51	Third measurement, pellet number 51
		
First measurement, pellet number 52	Second measurement, pellet number 52	Third measurement, pellet number 52
		
First measurement, pellet number 53	Second measurement, pellet number 53	Third measurement, pellet number 53
		
First measurement, pellet number 54	Second measurement, pellet number 54	Third measurement, pellet number 54
		
First measurement, pellet number 55	Second measurement, pellet number 55	Third measurement, pellet number 55

		
First measurement, pellet number 56	Second measurement, pellet number 56	Third measurement, pellet number 56
		
First measurement, pellet number 57	Second measurement, pellet number 57	Third measurement, pellet number 57
		
First measurement, pellet number 58	Second measurement, pellet number 58	Third measurement, pellet number 58
		
First measurement, pellet number 60	Second measurement, pellet number 60	Third measurement, pellet number 60

## Appendix 66

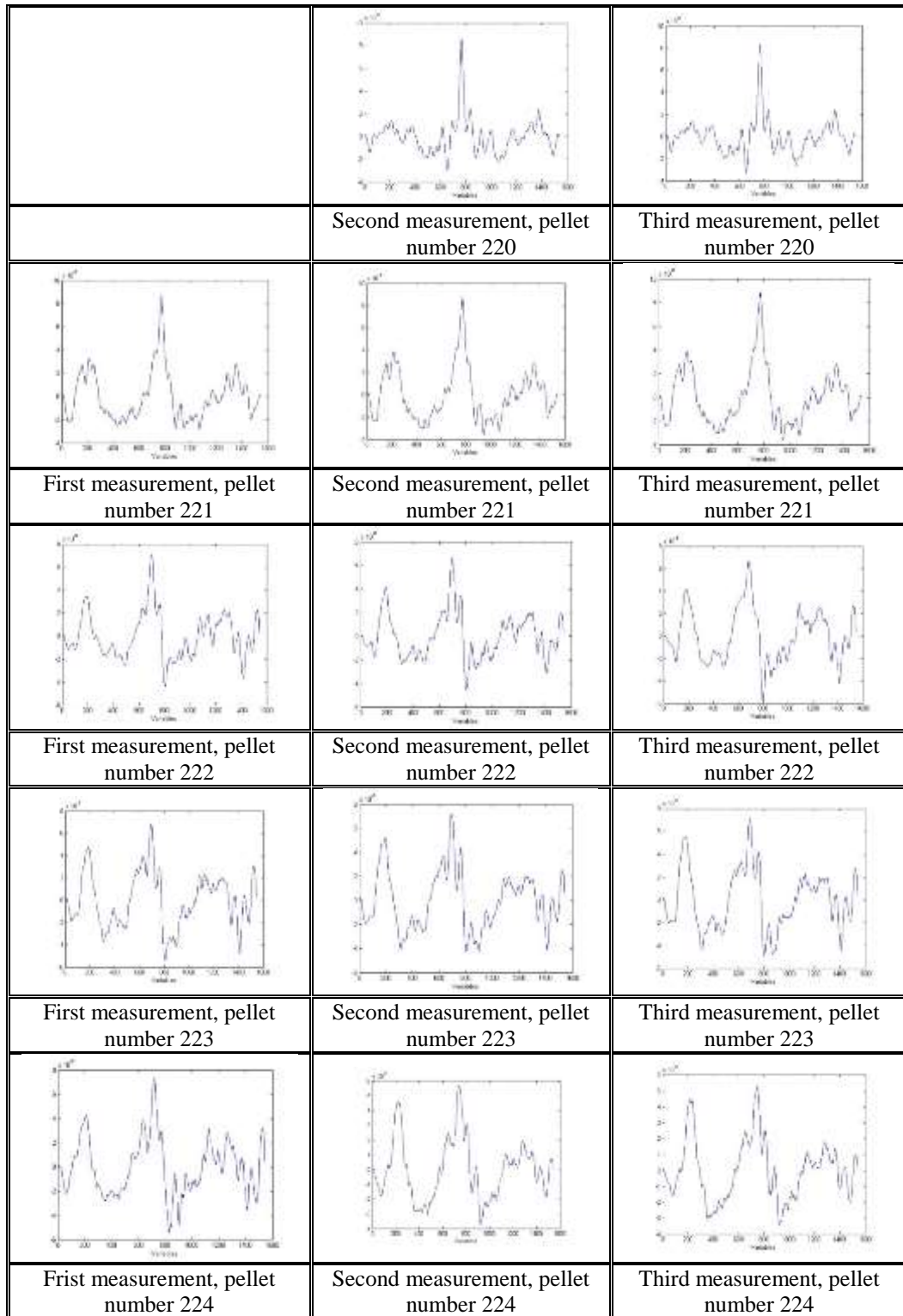
Topographical profiles obtained from the microscopic measurements for samples 159-168, LEA K

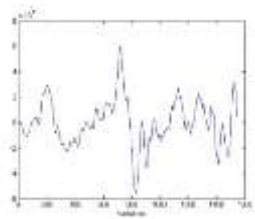
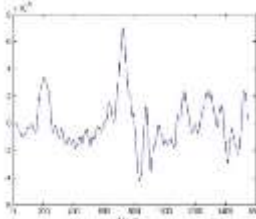
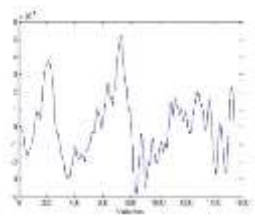
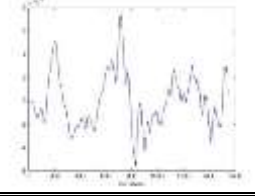
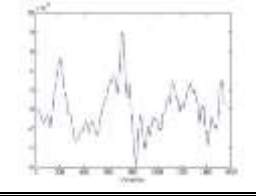
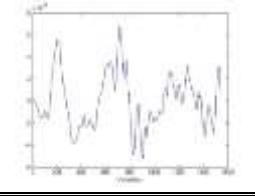
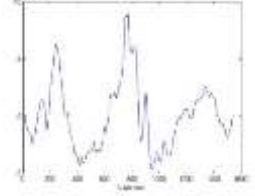
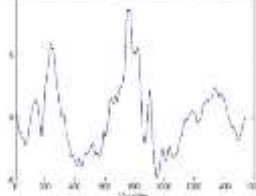
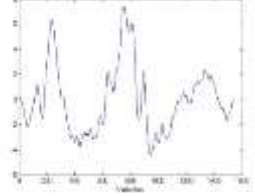
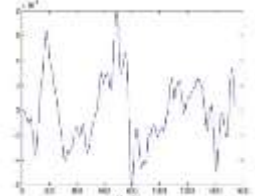
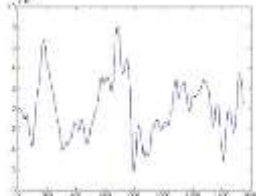
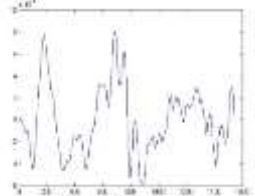
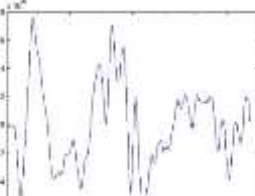
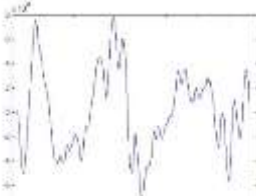
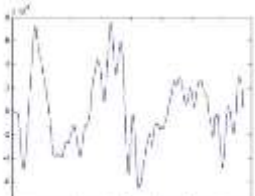
		
	Second measurement, pellet number 159	Third measurement, pellet number 159
		
First measurement, pellet number 160	Second measurement, pellet number 160	Third measurement, pellet number 160
		
First measurement, pellet number 161	Second measurement, pellet number 161	Third measurement, pellet number 161
		
First measurement, pellet number 162	Second measurement, pellet number 162	Third measurement, pellet number 162
		
First measurement, pellet number 163	Second measurement, pellet number 163	Third measurement, pellet number 163



## Appendix 67

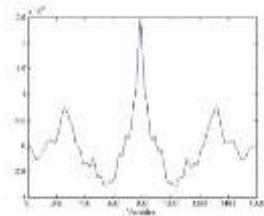
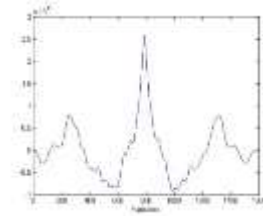
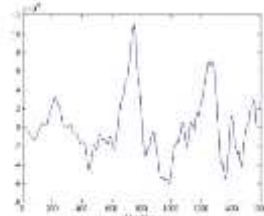
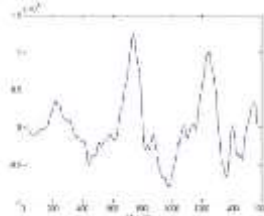
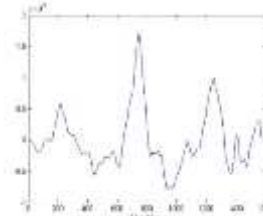
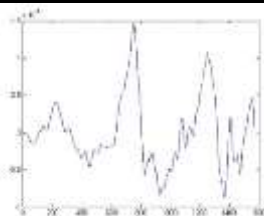
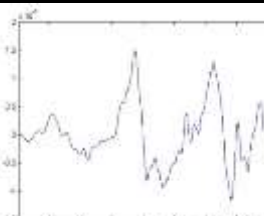
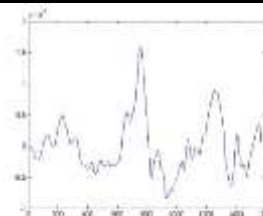



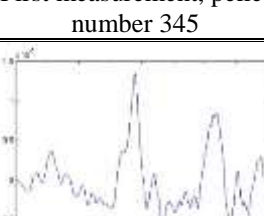
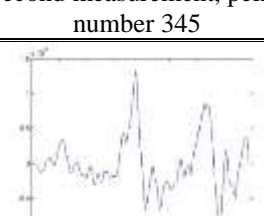
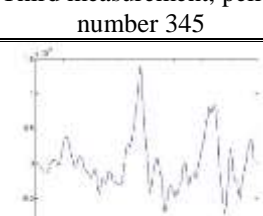
Topographical profiles obtained from the microscopic measurements for samples 220-229, LEA K

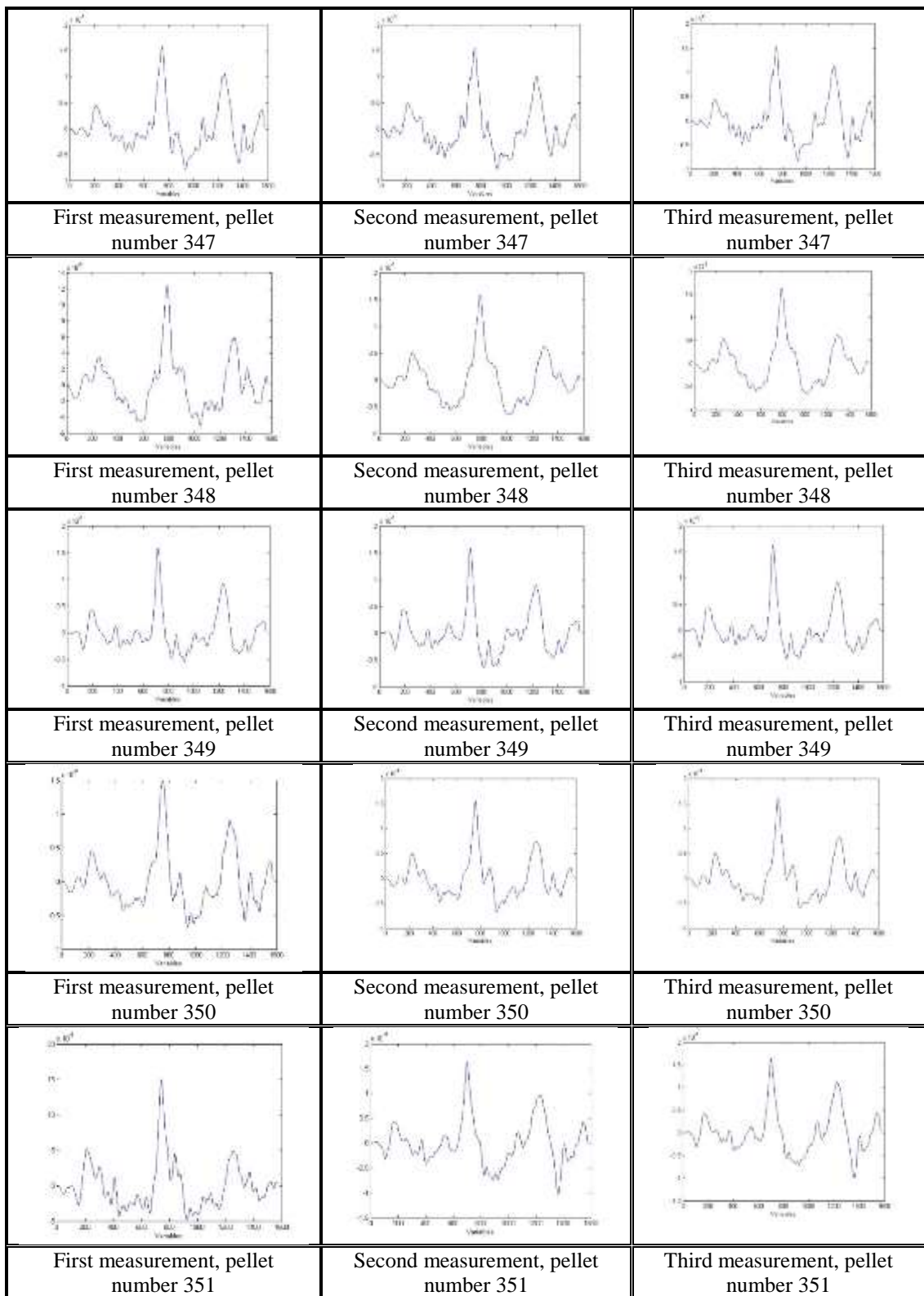


		
First measurement, pellet number 225	Second measurement, pellet number 225	Third measurement, pellet number 225
		
First measurement, pellet number 226	Second measurement, pellet number 226	Third measurement, pellet number 226
		
First measurement, pellet number 227	Second measurement, pellet number 227	Third measurement, pellet number 227
		
First measurement, pellet number 228	Second measurement, pellet number 228	Third measurement, pellet number 228
		
First measurement, pellet number 229	Second measurement, pellet number 229	Third measurement, pellet number 229

## Appendix 68

Topographical profiles obtained from the microscopic measurements for samples 342-351, LEA K

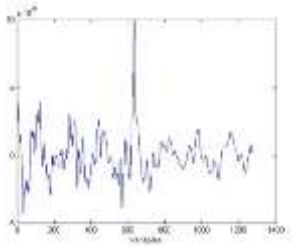
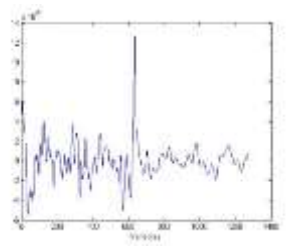
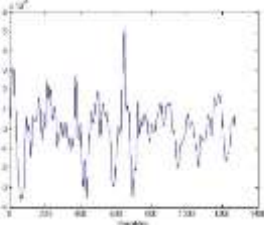
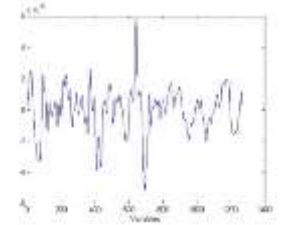
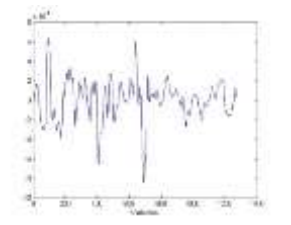
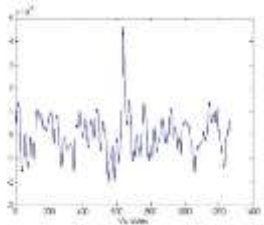
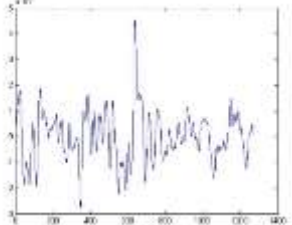
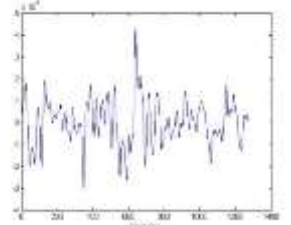
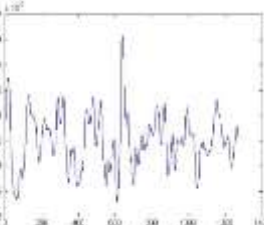
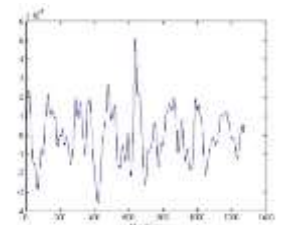
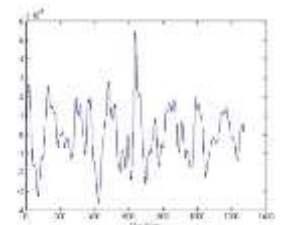
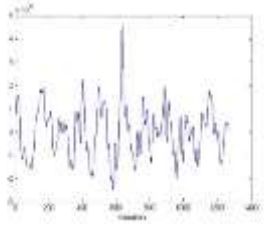
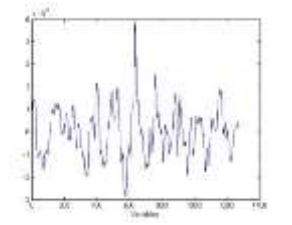
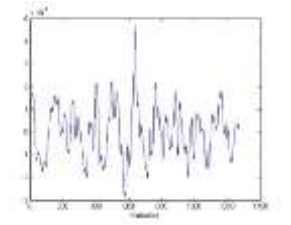
		
	Second measurement, pellet number 342	Third measurement, pellet number 342
		
First measurement, pellet number 343	Second measurement, pellet number 343	Third measurement, pellet number 343
		
First measurement, pellet number 344	Second measurement, pellet number 344	Third measurement, pellet number 344
		
First measurement, pellet number 345	Second measurement, pellet number 345	Third measurement, pellet number 345
		
First measurement, pellet number 346	Second measurement, pellet number 346	Third measurement, pellet number 346

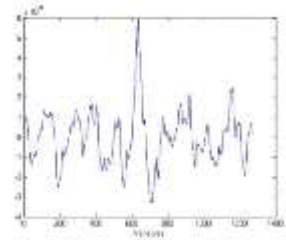
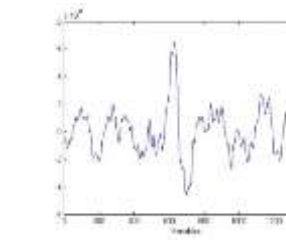
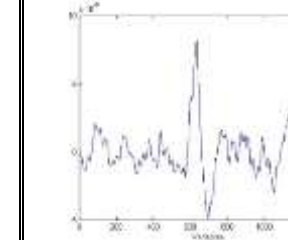
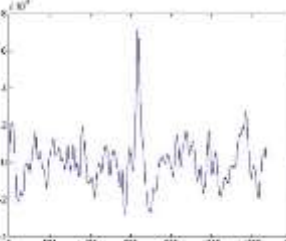
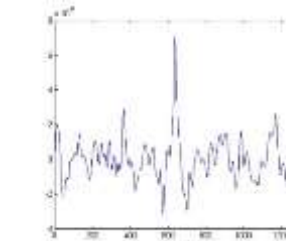
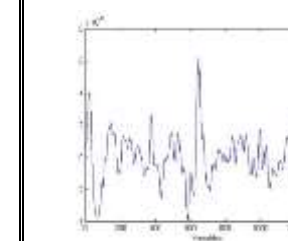
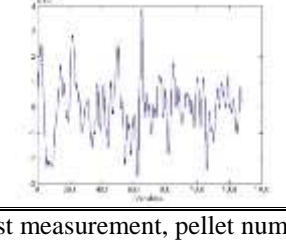
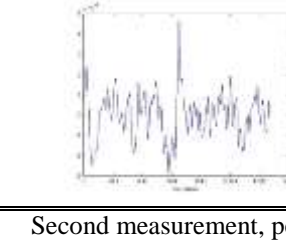
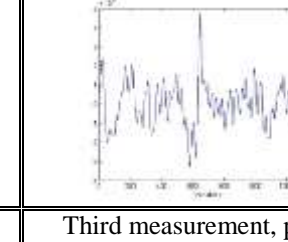
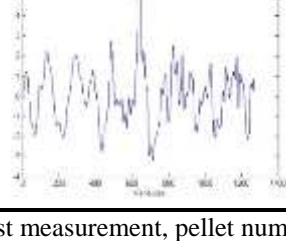
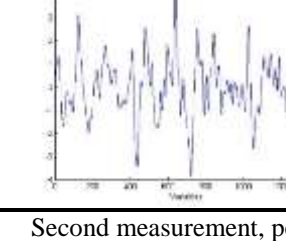
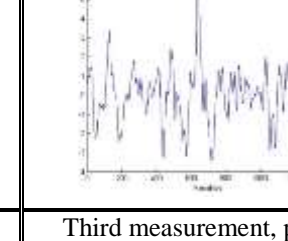




## Appendix 69

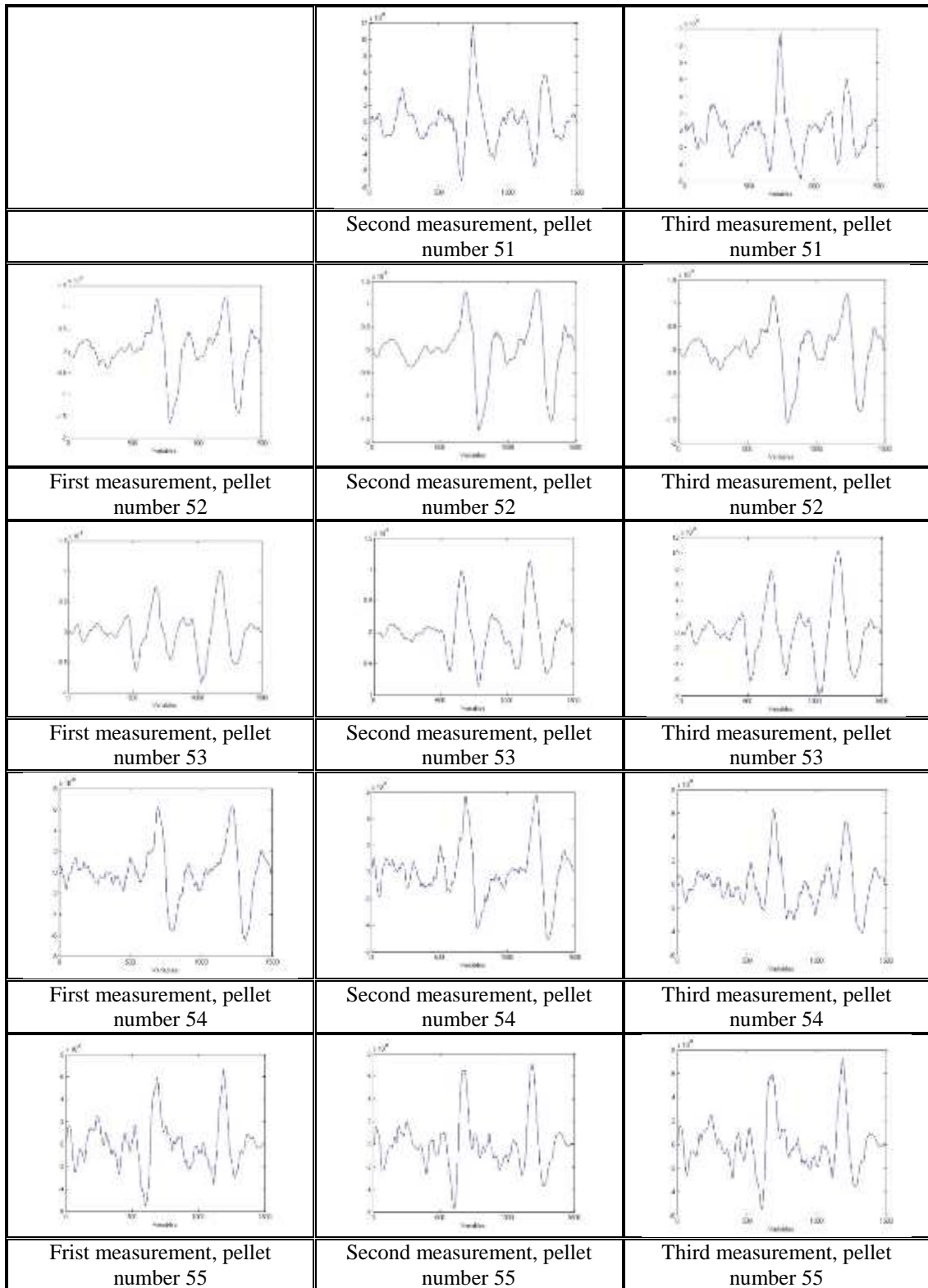
Topographical profiles obtained from the microscopic measurements for samples 560-569, LEA K

		
	Second measurement, pellet number 560	Third measurement, pellet number 560
		
First measurement, pellet number 561	Second measurement, pellet number 561	Third measurement, pellet number 561
		
First measurement, pellet number 562	Second measurement, pellet number 562	Third measurement, pellet number 562
		
First measurement, pellet number 563	Second measurement, pellet number 563	Third measurement, pellet number 563
		
First measurement, pellet number 564	Second measurement, pellet number 564	Third measurement, pellet number 564

		
First measurement, pellet number 565	Second measurement, pellet number 565	Third measurement, pellet number 565
		
First measurement, pellet number 566	Second measurement, pellet number 566	Third measurement, pellet number 566
		
First measurement, pellet number 567	Second measurement, pellet number 567	Third measurement, pellet number 567
		
First measurement, pellet number 569	Second measurement, pellet number 569	Third measurement, pellet number 569

## Appendix 70

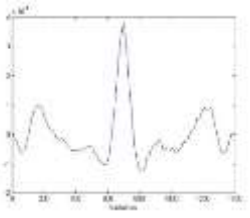
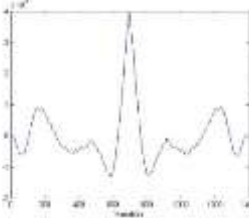
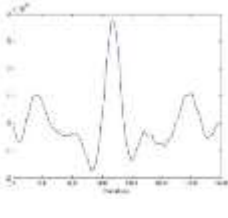
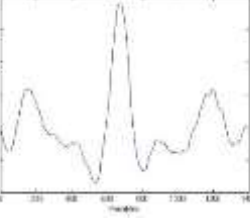
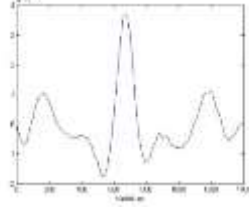
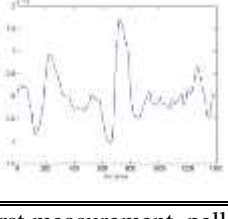
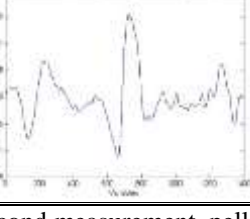
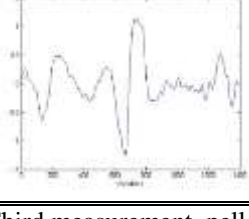
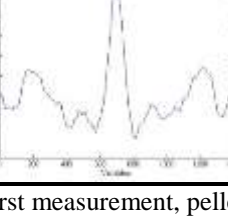
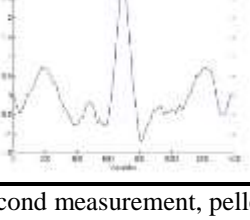
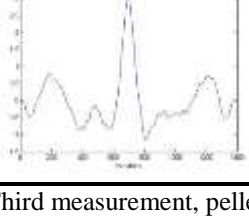
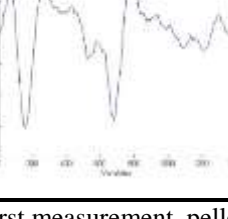
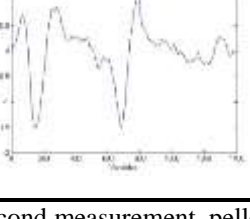

Topographical profiles obtained from the microscopic measurements for samples 51-60, LEA L

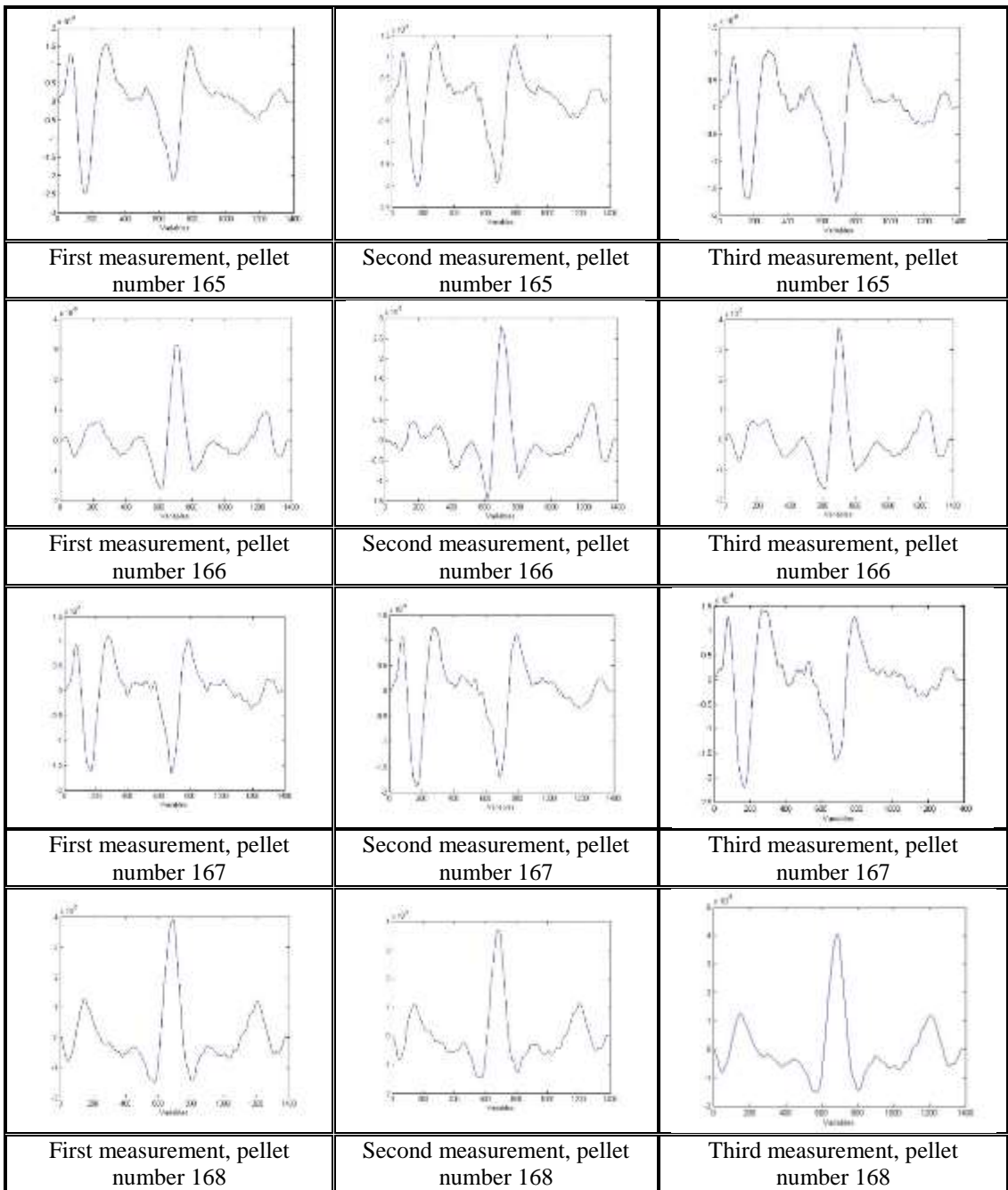


First measurement, pellet number 56	Second measurement, pellet number 56	Third measurement, pellet number 56
First measurement, pellet number 57	Second measurement, pellet number 57	Third measurement, pellet number 57
First measurement, pellet number 58	Second measurement, pellet number 58	Third measurement, pellet number 58
First measurement, pellet number 59	Second measurement, pellet number 59	Third measurement, pellet number 59
First measurement, pellet number 60	Second measurement, pellet number 60	Third measurement, pellet number 60

## Appendix 71

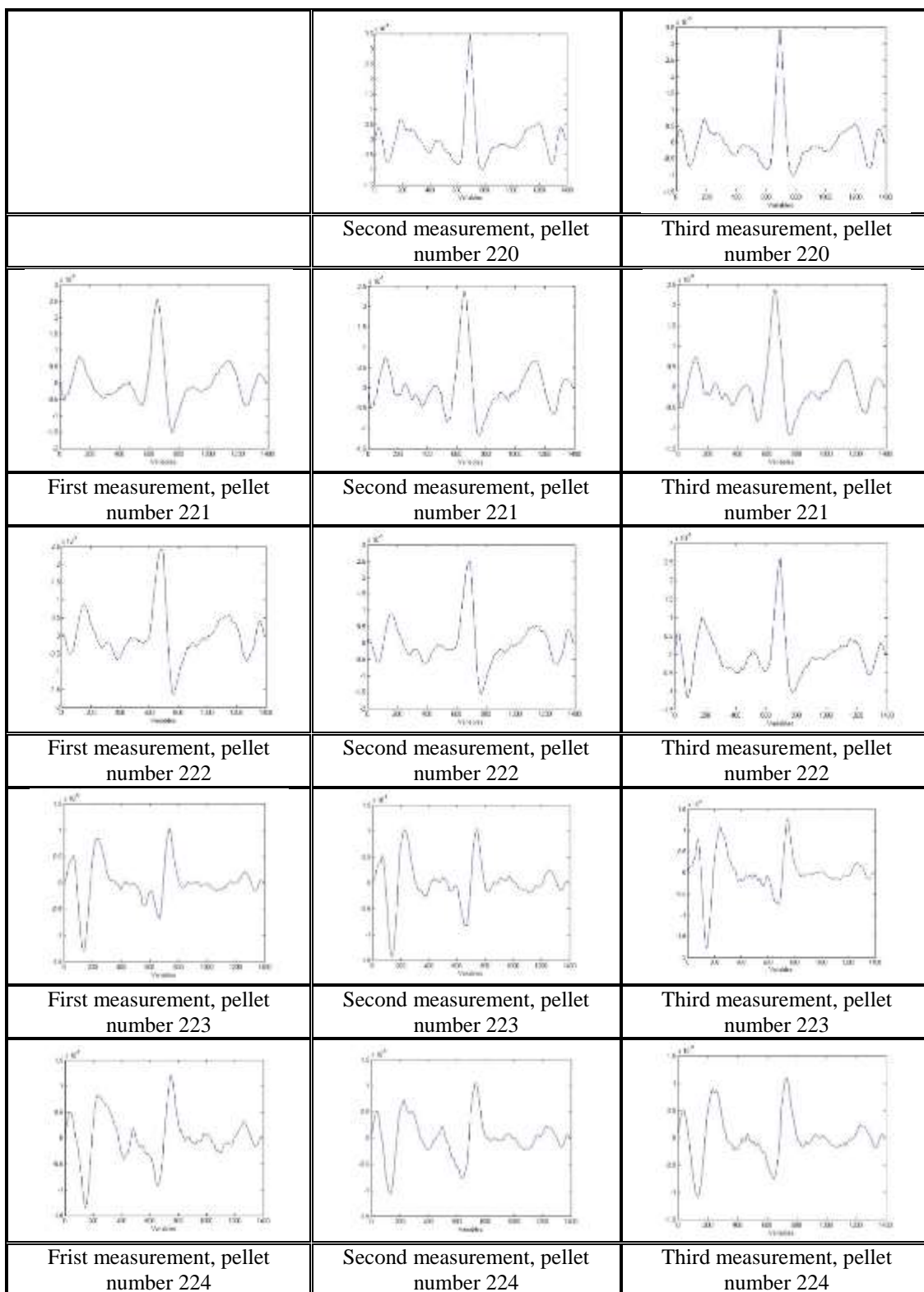
Topographical profiles obtained from the microscopic measurements for samples 159-168, LEA L

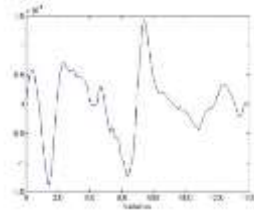
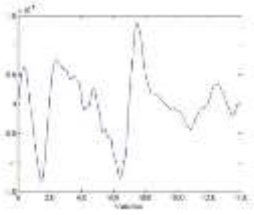
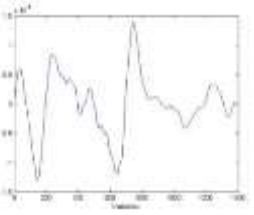
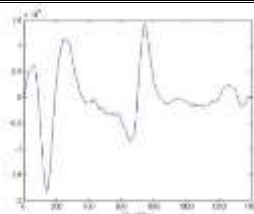
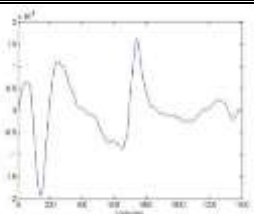
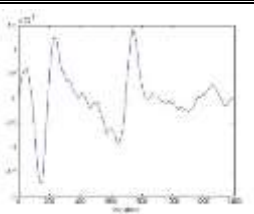
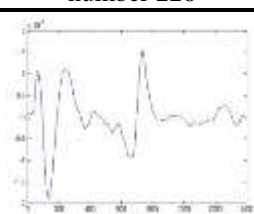
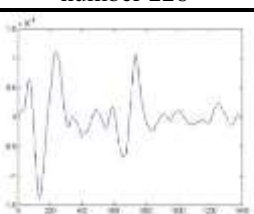
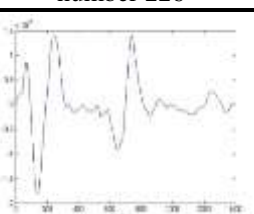
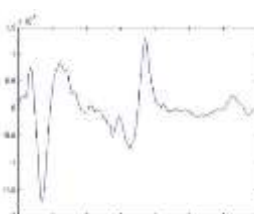
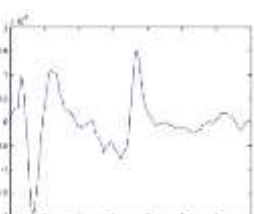
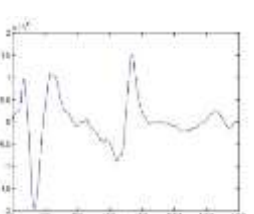
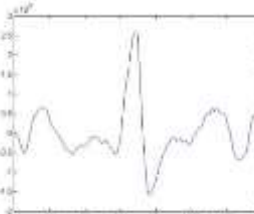
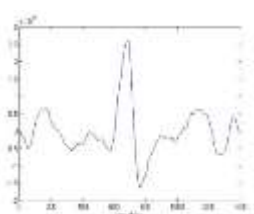
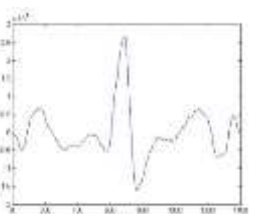
		
	Second measurement, pellet number 159	Third measurement, pellet number 159
		
First measurement, pellet number 160	Second measurement, pellet number 160	Third measurement, pellet number 160
		
First measurement, pellet number 162	Second measurement, pellet number 162	Third measurement, pellet number 162
		
First measurement, pellet number 163	Second measurement, pellet number 163	Third measurement, pellet number 163
		
First measurement, pellet number 164	Second measurement, pellet number 164	Third measurement, pellet number 164



## Appendix 72

Topographical profiles obtained from the microscopic measurements for samples 220-229, LEA L

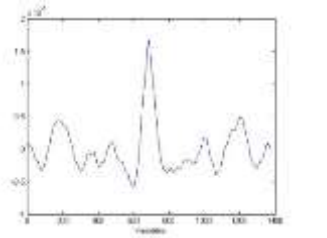
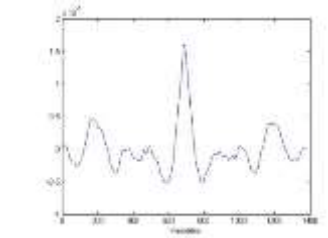
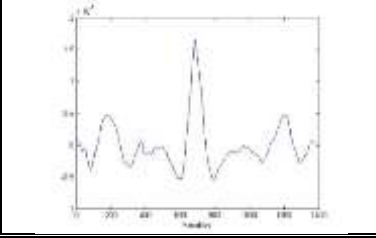
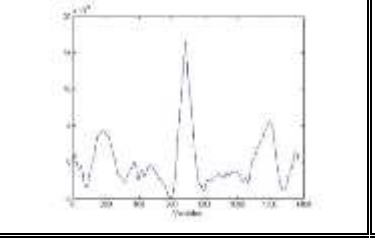
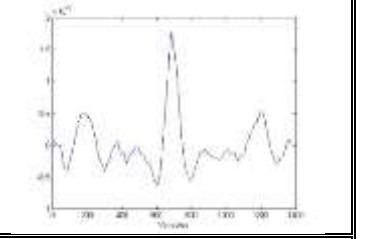
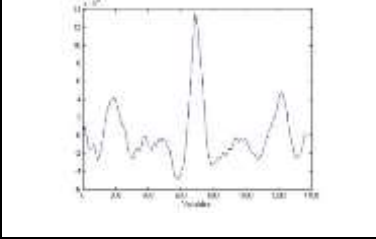
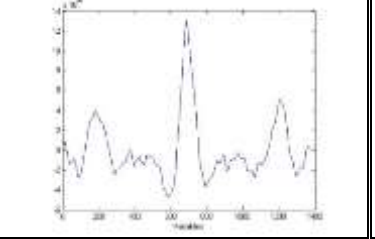
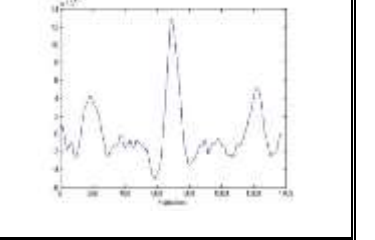
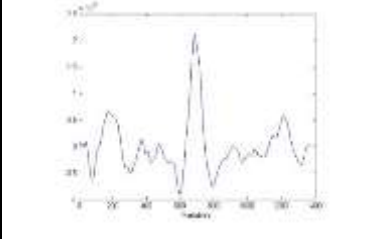
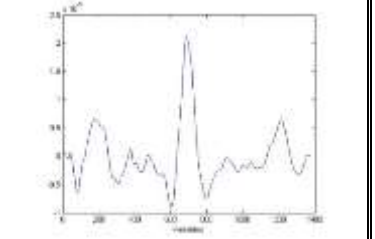
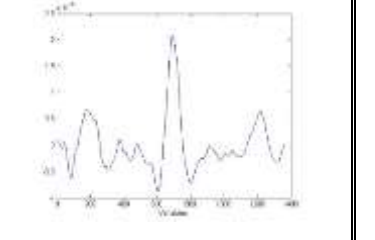
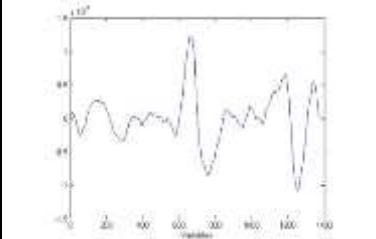
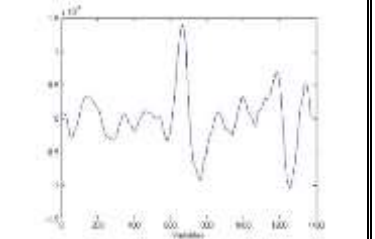
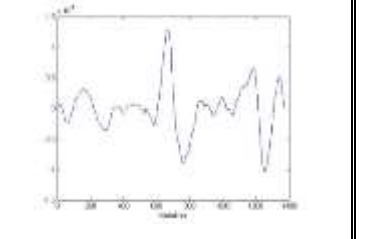


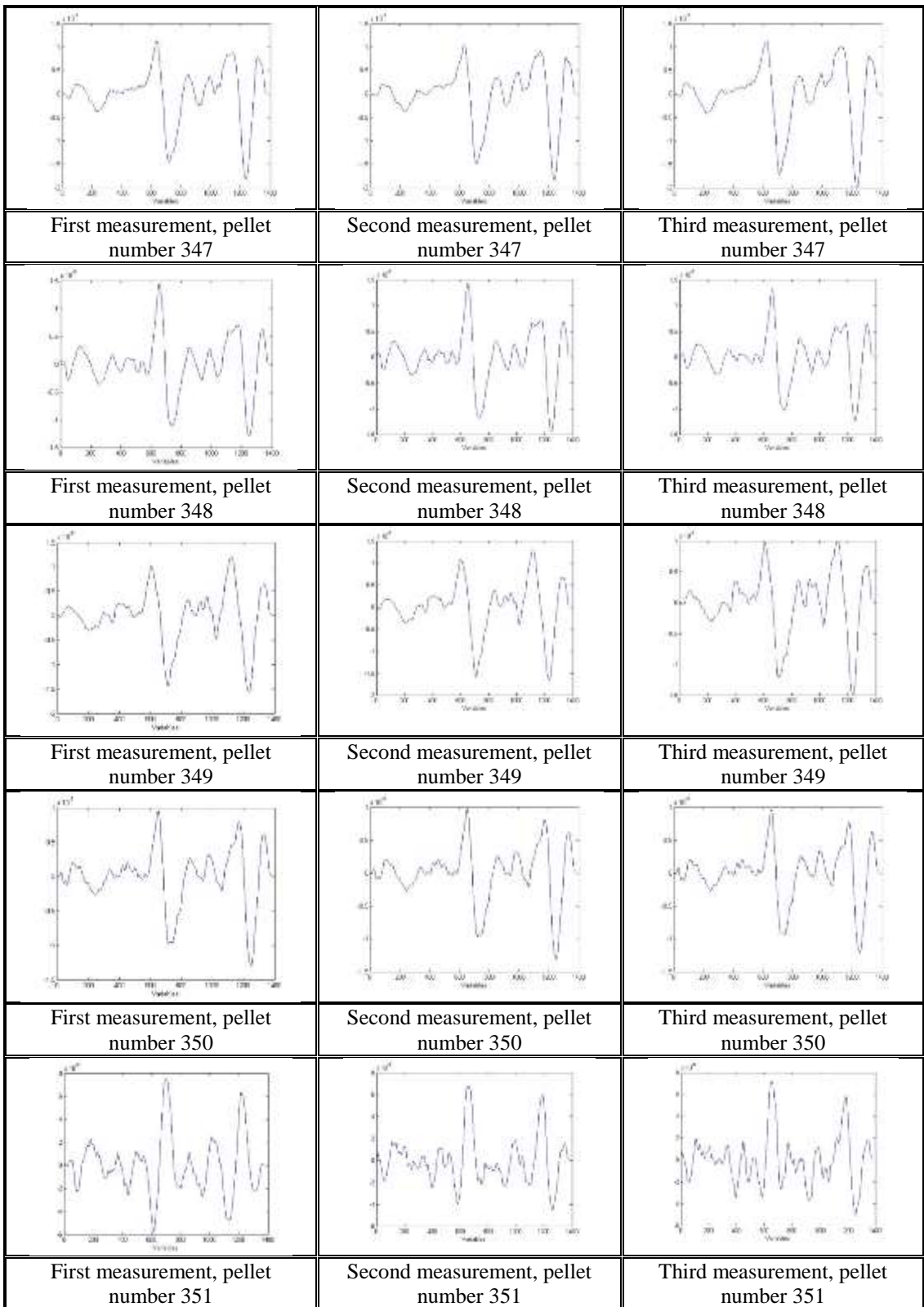
		
First measurement, pellet number 225	Second measurement, pellet number 225	Third measurement, pellet number 225
		
First measurement, pellet number 226	Second measurement, pellet number 226	Third measurement, pellet number 226
		
First measurement, pellet number 227	Second measurement, pellet number 227	Third measurement, pellet number 227
		
First measurement, pellet number 228	Second measurement, pellet number 228	Third measurement, pellet number 228
		
First measurement, pellet number 229	Second measurement, pellet number 229	Third measurement, pellet number 229



### Appendix 73

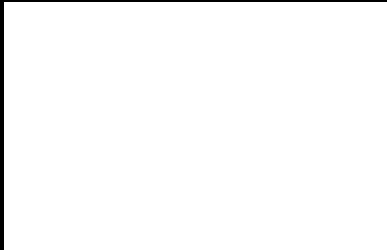
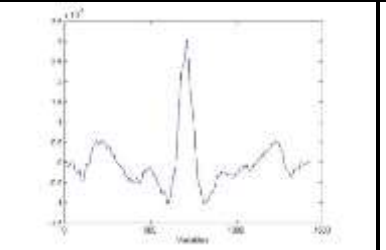
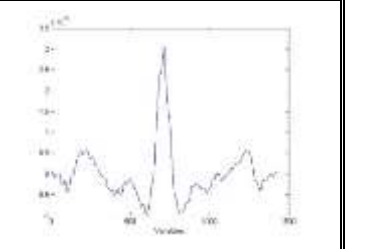
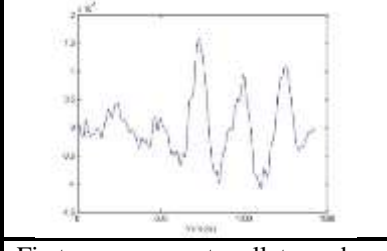
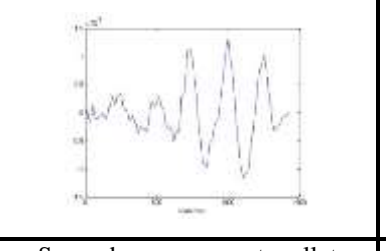
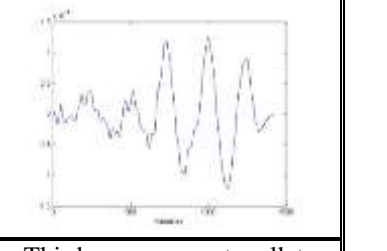
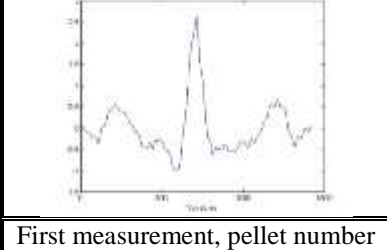
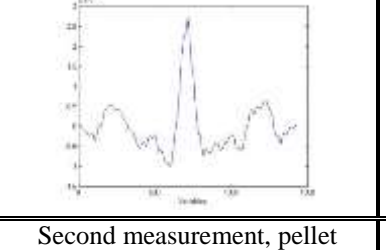
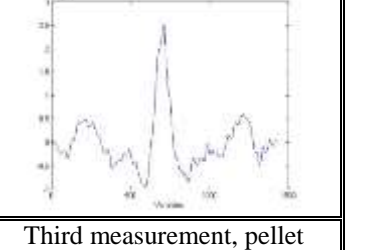
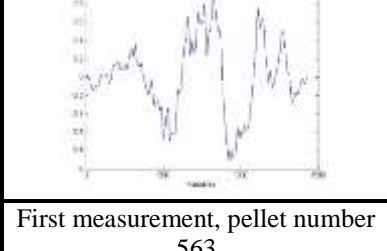
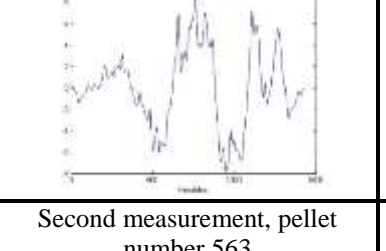
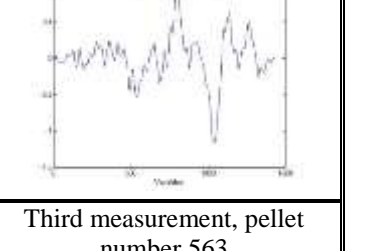
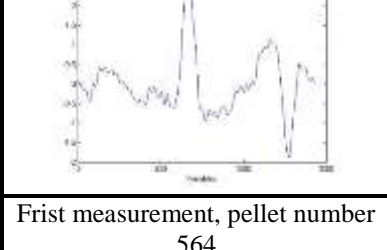
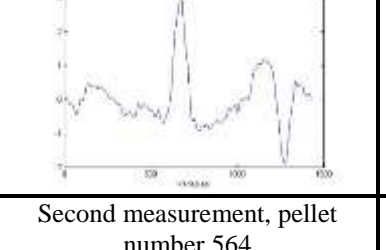
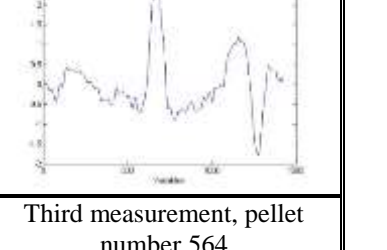
Topographical profiles obtained from the microscopic measurements for samples 342-351, LEA L

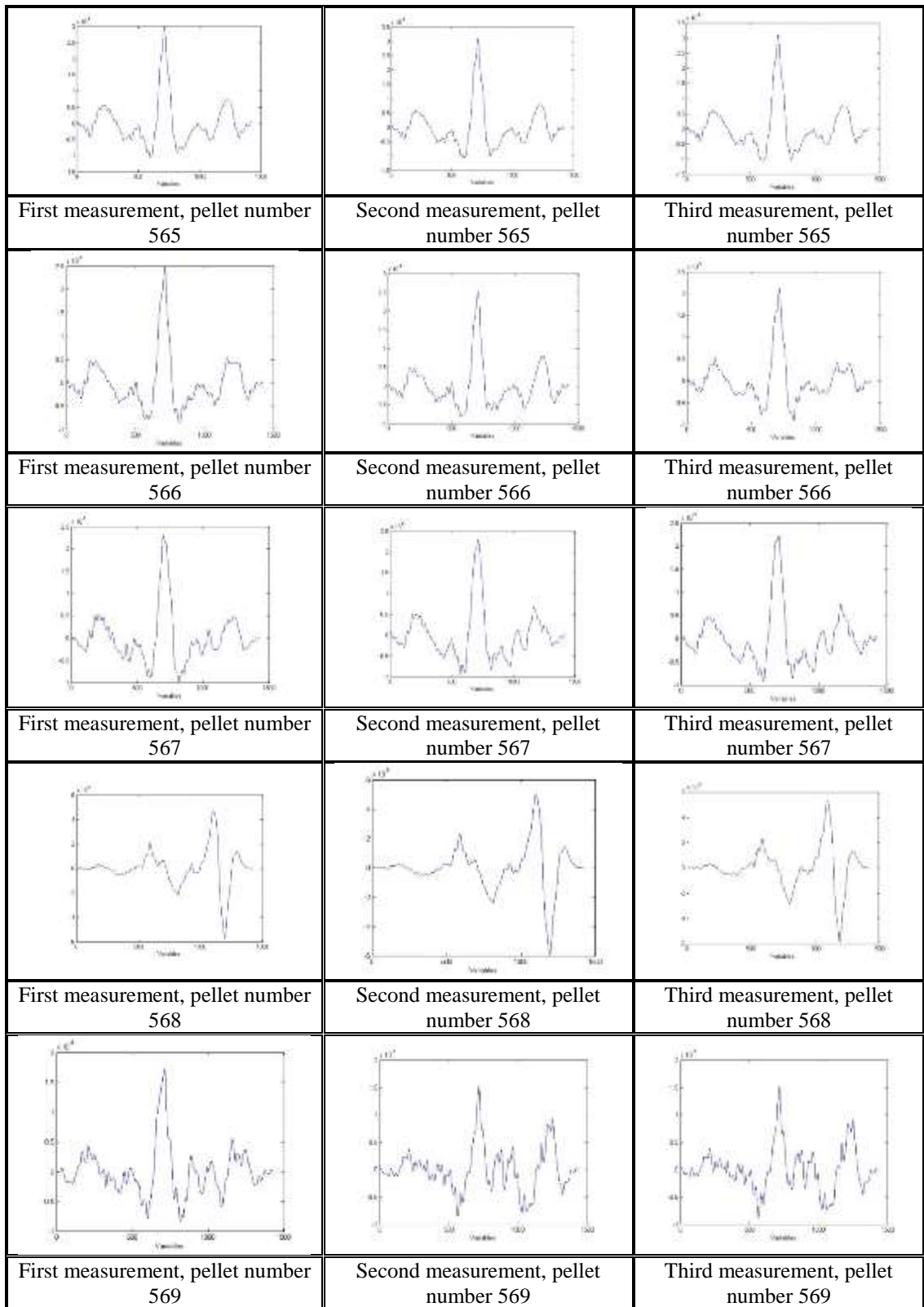
		
	Second measurement, pellet number 342	Third measurement, pellet number 342
		
First measurement, pellet number 343	Second measurement, pellet number 343	Third measurement, pellet number 343
		
First measurement, pellet number 344	Second measurement, pellet number 344	Third measurement, pellet number 344
		
First measurement, pellet number 345	Second measurement, pellet number 345	Third measurement, pellet number 345
		
First measurement, pellet number 346	Second measurement, pellet number 346	Third measurement, pellet number 346



## Appendix 74

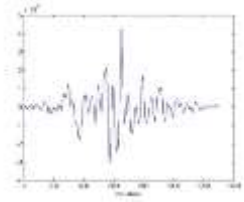
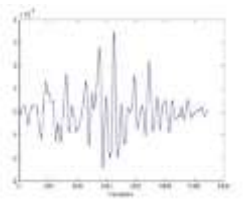
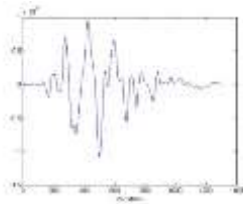
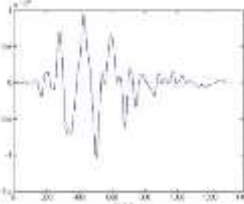
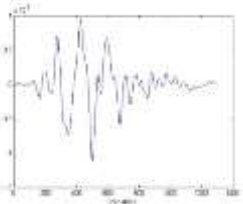
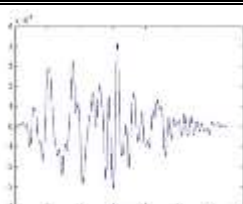
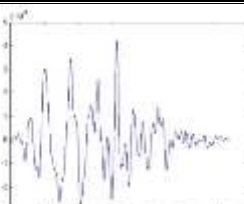


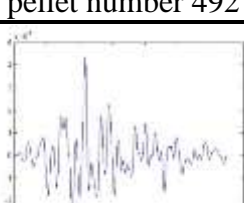
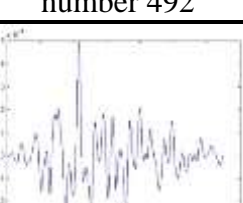
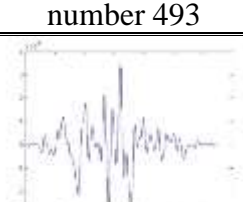
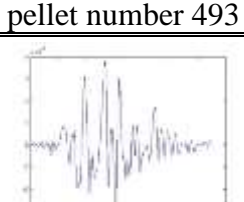

Topographical profiles obtained from the microscopic measurements for samples 560-569, LEA L

		
	Second measurement, pellet number 560	Third measurement, pellet number 560
		
First measurement, pellet number 561	Second measurement, pellet number 561	Third measurement, pellet number 561
		
First measurement, pellet number 562	Second measurement, pellet number 562	Third measurement, pellet number 562
		
First measurement, pellet number 563	Second measurement, pellet number 563	Third measurement, pellet number 563
		
First measurement, pellet number 564	Second measurement, pellet number 564	Third measurement, pellet number 564



## Appendix 75

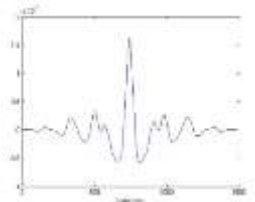
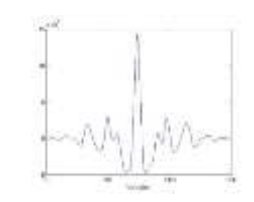
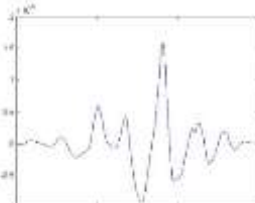
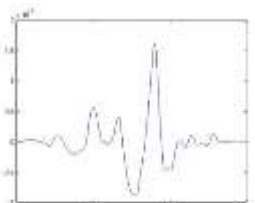
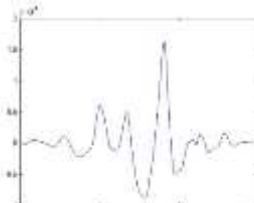
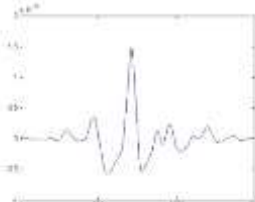
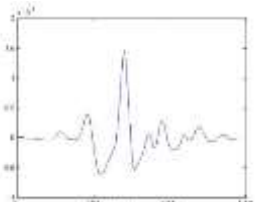
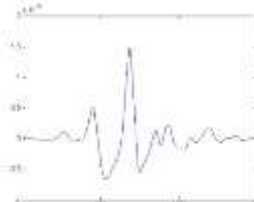
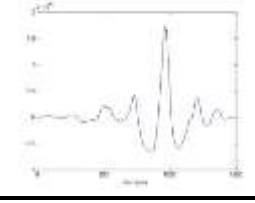
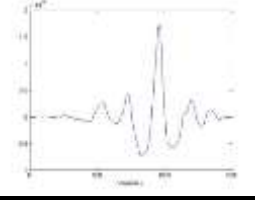
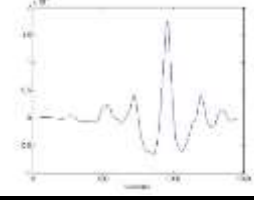
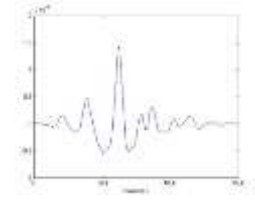
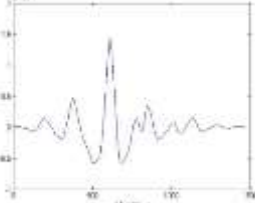
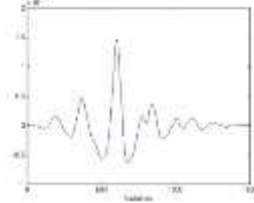
Topographical profiles obtained from the microscopic measurements for samples  
Edgar Brother Model 35, LEA EB

		
	Second measurement, pellet number 490	Third measurement, pellet number 490
		
First measurement, pellet number 491	Second measurement, pellet number 491	Third measurement, pellet number 491
		
First measurement, pellet number 492	Second measurement, pellet number 492	Third measurement, pellet number 492
		
First measurement, pellet number 493	Second measurement, pellet number 493	Third measurement, pellet number 493
		
First measurement, pellet number 494	Second measurement, pellet number 494	Third measurement, pellet number 494

## Appendix 76

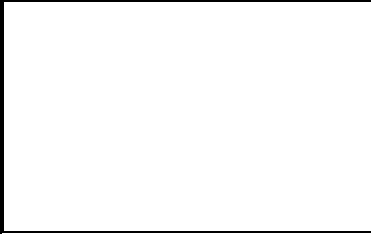
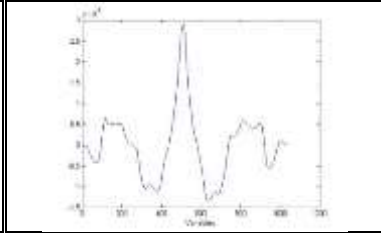
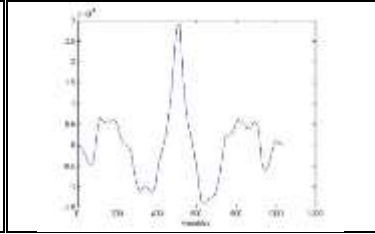
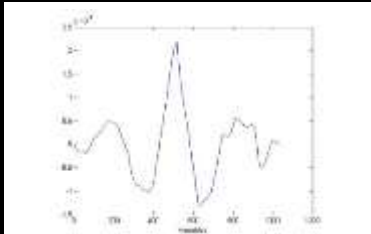
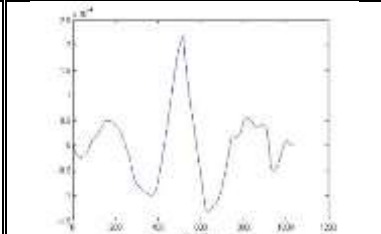
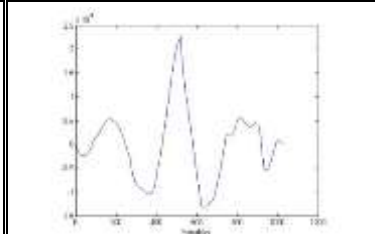
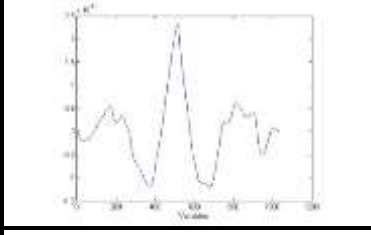
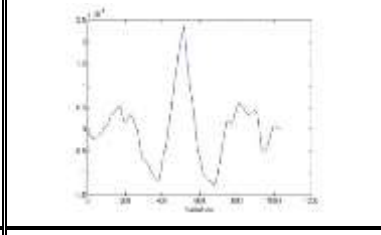
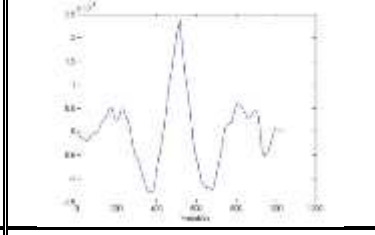
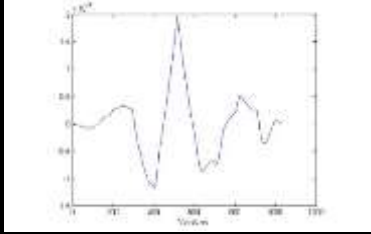
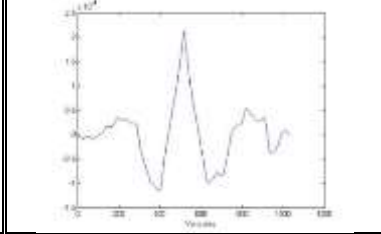
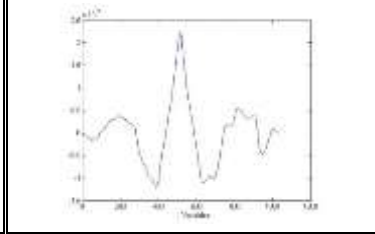
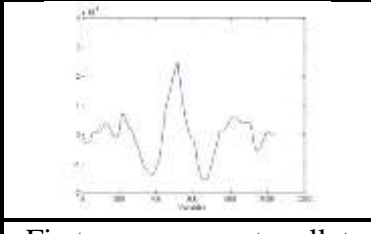
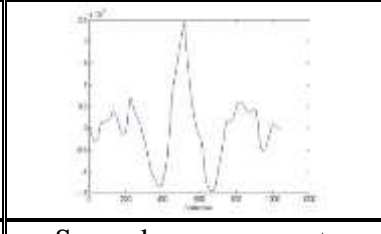
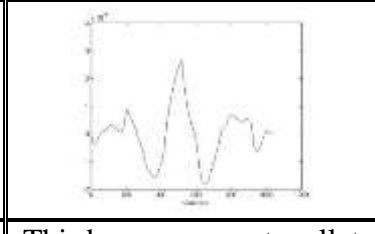
Topographical profiles obtained from the microscopic measurements for samples

Edgar Brother Model 35, LEA EC

		
	Second measurement, pellet number 490	Third measurement, pellet number 490
		
First measurement, pellet number 491	Second measurement, pellet number 491	Third measurement, pellet number 491
		
First measurement, pellet number 492	Second measurement, pellet number 492	Third measurement, pellet number 492
		
First measurement, pellet number 493	Second measurement, pellet number 493	Third measurement, pellet number 493
		
First measurement, pellet number 494	Second measurement, pellet number 494	Third measurement, pellet number 494

## Appendix 77

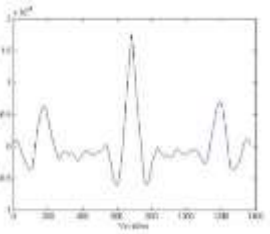
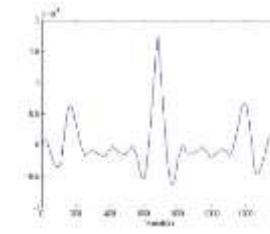
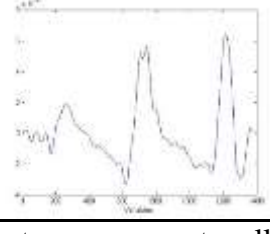
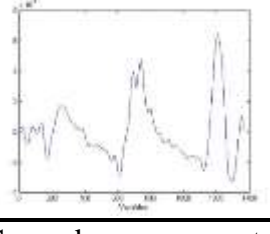
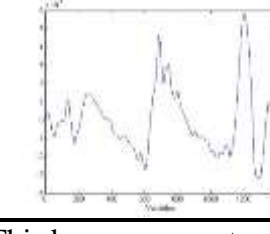
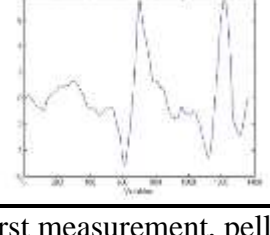
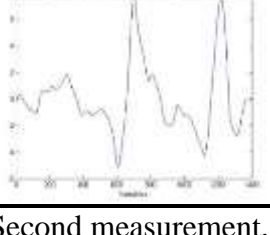

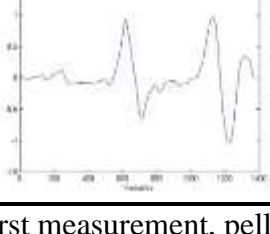
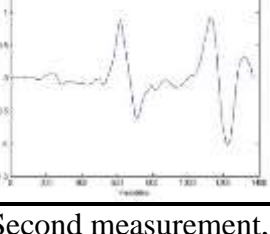

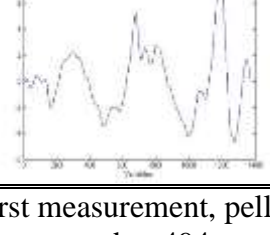
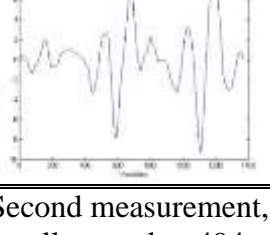
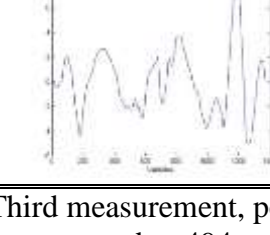
Topographical profiles obtained from the microscopic measurements for samples  
Edgar Brother Model 35, LEA ED

		
	Second measurement, pellet number 490	Third measurement, pellet number 490
		
First measurement, pellet number 491	Second measurement, pellet number 491	Third measurement, pellet number 491
		
First measurement, pellet number 492	Second measurement, pellet number 492	Third measurement, pellet number 492
		
First measurement, pellet number 493	Second measurement, pellet number 493	Third measurement, pellet number 493
		
First measurement, pellet number 494	Second measurement, pellet number 494	Third measurement, pellet number 494

## Appendix 78

Topographical profiles obtained from the microscopic measurements for samples

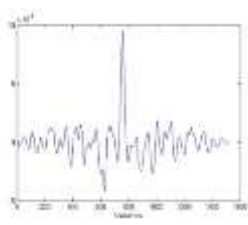
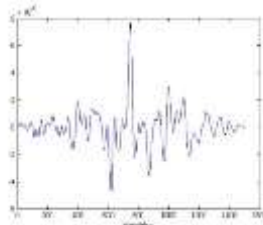
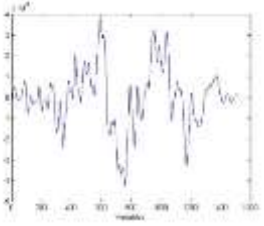
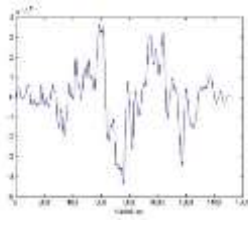
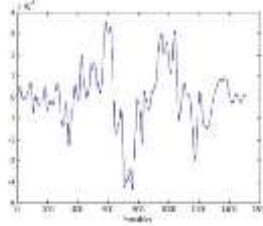
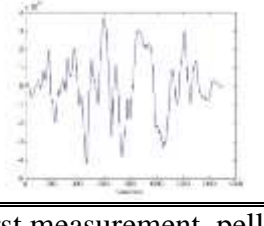
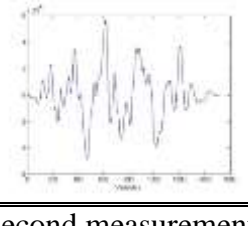
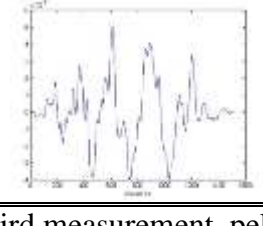
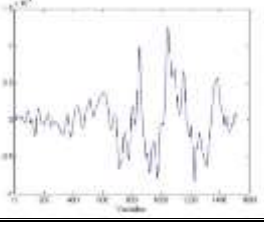
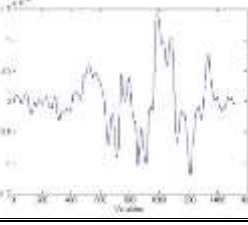
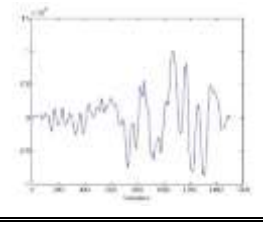
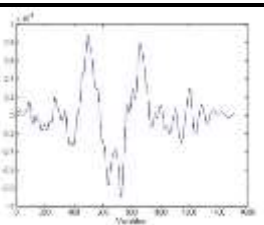
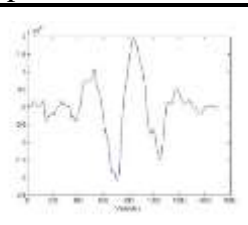
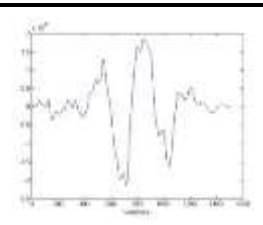
Edgar Brother Model 35, LEA EE

		
	Second measurement, pellet number 490	Third measurement, pellet number 490
		
First measurement, pellet number 491	Second measurement, pellet number 491	Third measurement, pellet number 491
		
First measurement, pellet number 492	Second measurement, pellet number 492	Third measurement, pellet number 492
		
First measurement, pellet number 493	Second measurement, pellet number 493	Third measurement, pellet number 493
		
First measurement, pellet number 494	Second measurement, pellet number 494	Third measurement, pellet number 494



## Appendix 79

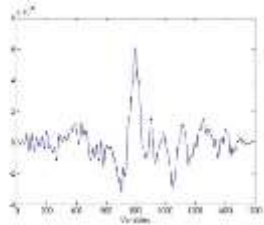
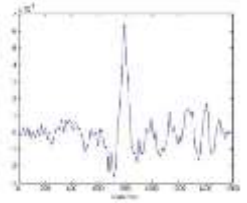
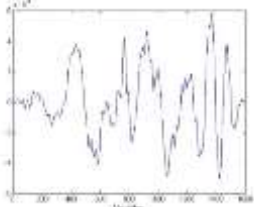
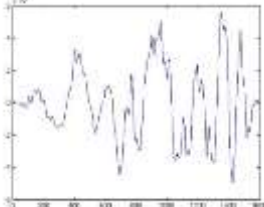
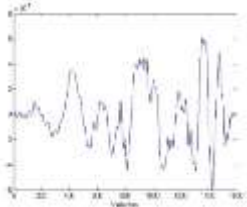
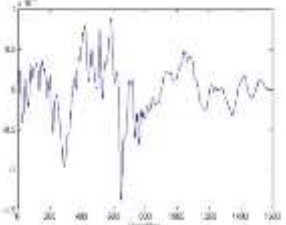
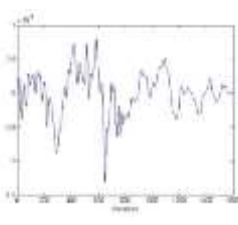
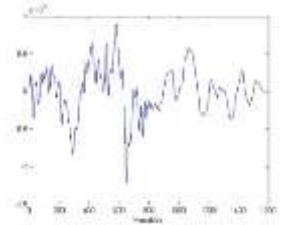
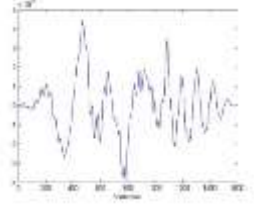
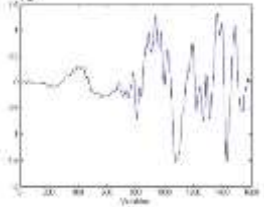
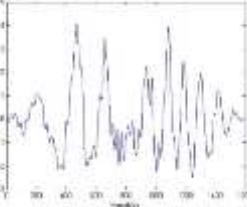
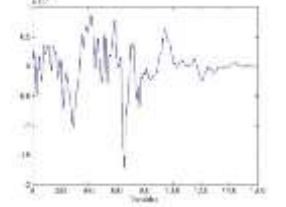
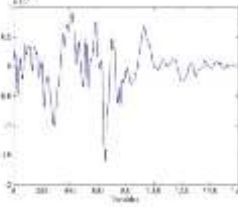
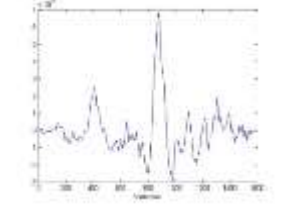
Topographical profiles obtained from the microscopic measurements for samples  
Edgar Brother Model 35, LEA EF

		
	Second measurement, pellet number 490	Third measurement, pellet number 490
		
First measurement, pellet number 491	Second measurement, pellet number 491	Third measurement, pellet number 491
		
First measurement, pellet number 492	Second measurement, pellet number 492	Third measurement, pellet number 492
		
First measurement, pellet number 493	Second measurement, pellet number 493	Third measurement, pellet number 493
		
First measurement, pellet number 494	Second measurement, pellet number 494	Third measurement, pellet number 494

## Appendix 80

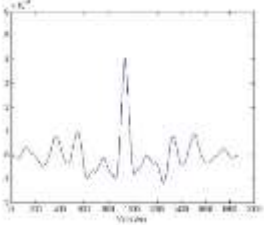
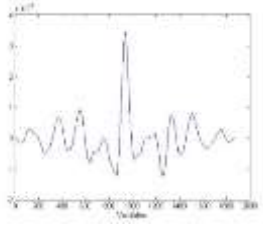
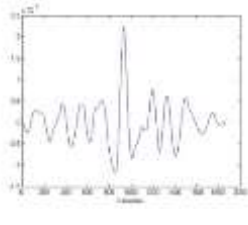
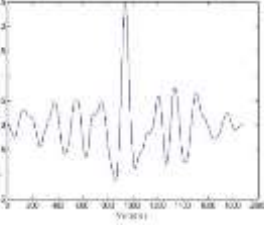
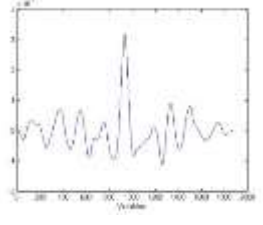
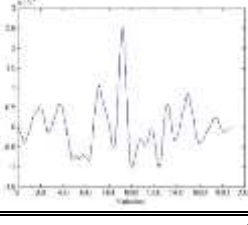
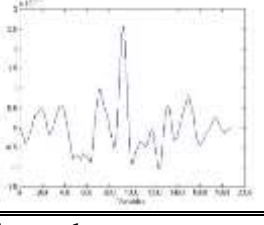
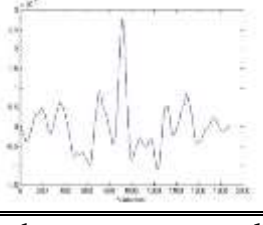
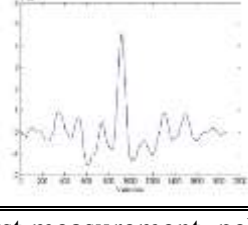
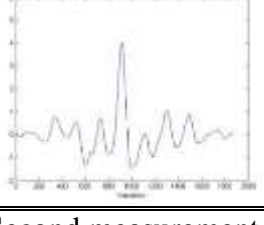
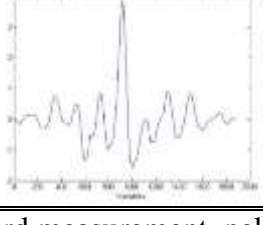
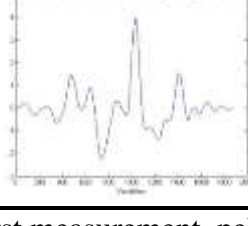
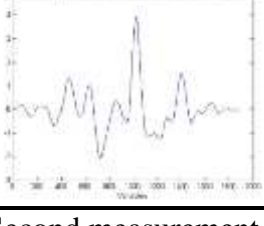
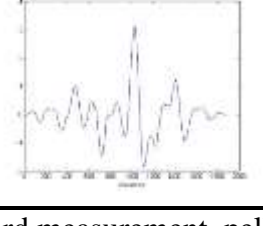
Topographical profiles obtained from the microscopic measurements for samples

Edgar Brother Model 35, LEA EG

		
	Second measurement, pellet number 490	Third measurement, pellet number 490
		
First measurement, pellet number 491	Second measurement, pellet number 491	Third measurement, pellet number 491
		
First measurement, pellet number 492	Second measurement, pellet number 492	Third measurement, pellet number 492
		
First measurement, pellet number 493	Second measurement, pellet number 493	Third measurement, pellet number 493
		
First measurement, pellet number 494	Second measurement, pellet number 494	Third measurement, pellet number 494

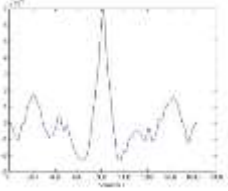
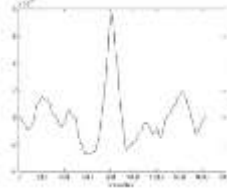
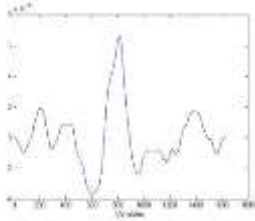
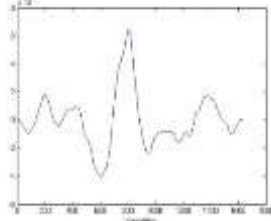
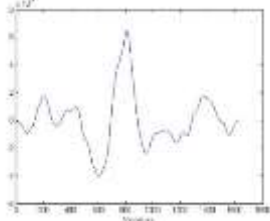
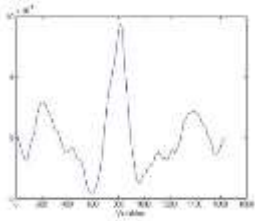
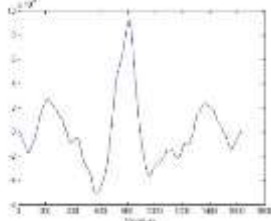
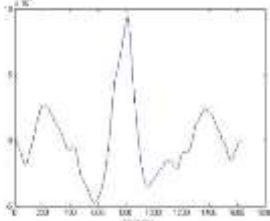
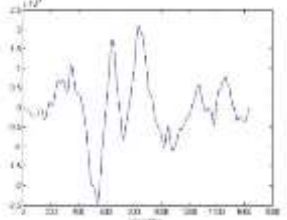
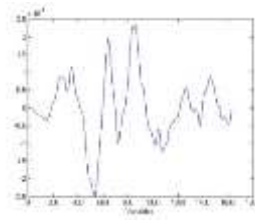
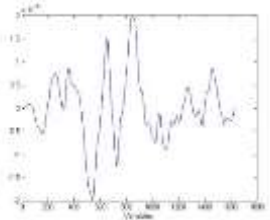
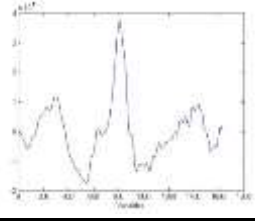
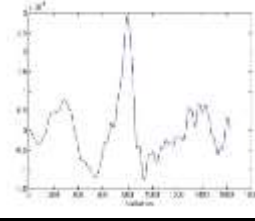
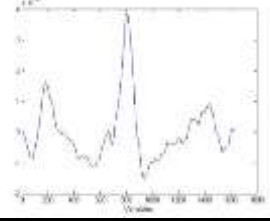
## Appendix 81

Topographical profiles obtained from the microscopic measurements for samples  
Edgar Brother Model 35, LEA EH

		
	Second measurement, pellet number 490	Third measurement, pellet number 490
		
First measurement, pellet number 491	Second measurement, pellet number 491	Third measurement, pellet number 491
		
First measurement, pellet number 492	Second measurement, pellet number 492	Third measurement, pellet number 492
		
First measurement, pellet number 493	Second measurement, pellet number 493	Third measurement, pellet number 493
		
First measurement, pellet number 494	Second measurement, pellet number 494	Third measurement, pellet number 494

## Appendix 82

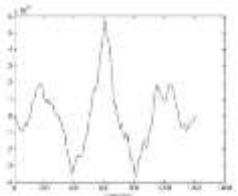
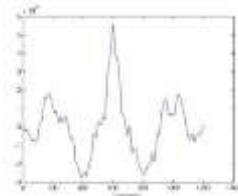
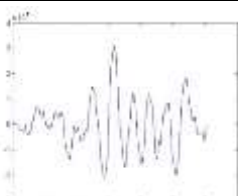
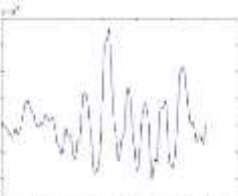
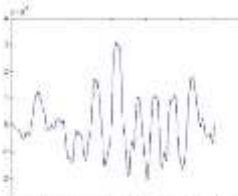
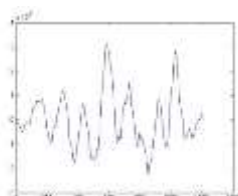
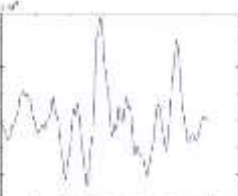
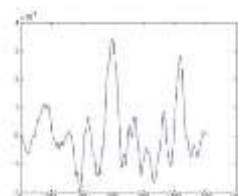
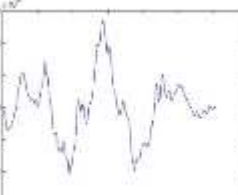
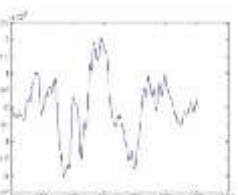
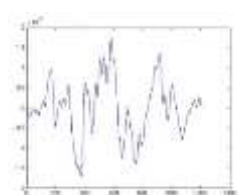
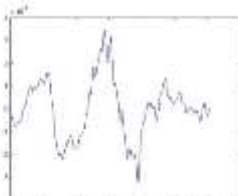
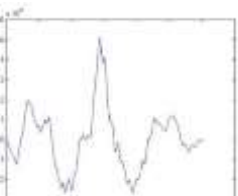
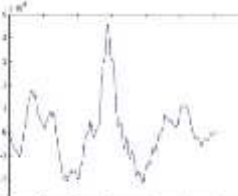
Topographical profiles obtained from the microscopic measurements for samples  
Edgar Brother Model 35, LEA EI

		
	Second measurement, pellet number 490	Third measurement, pellet number 490
		
First measurement, pellet number 491	Second measurement, pellet number 491	Third measurement, pellet number 491
		
First measurement, pellet number 492	Second measurement, pellet number 492	Third measurement, pellet number 492
		
First measurement, pellet number 493	Second measurement, pellet number 493	Third measurement, pellet number 493
		
First measurement, pellet number 494	Second measurement, pellet number 494	Third measurement, pellet number 494

## Appendix 83

Topographical profiles obtained from the microscopic measurements for samples

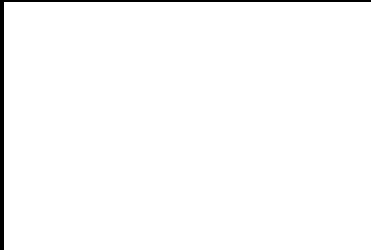
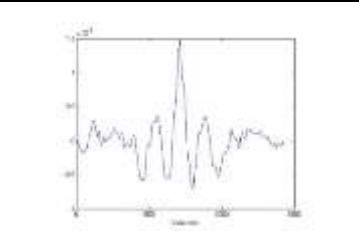
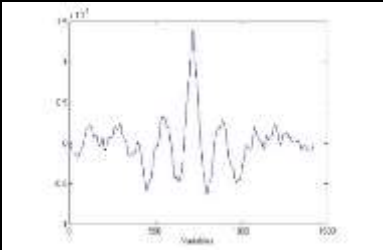
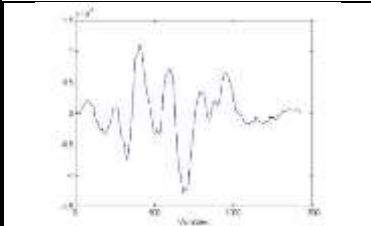
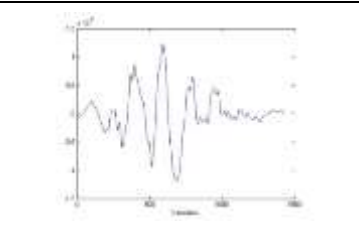
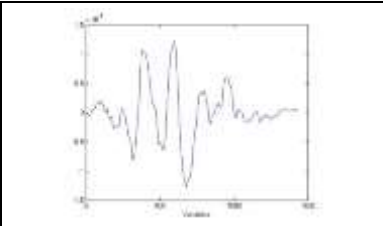
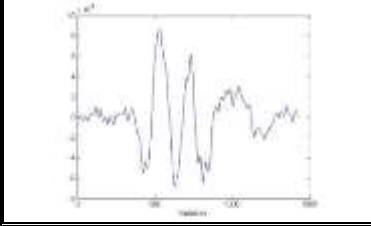
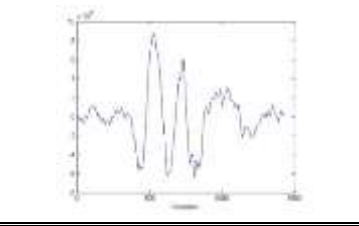
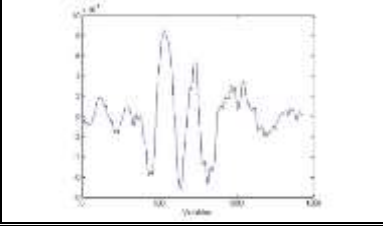
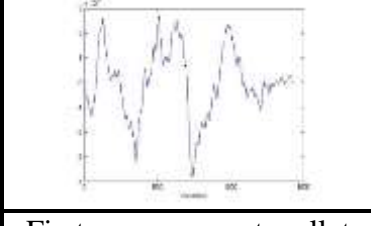
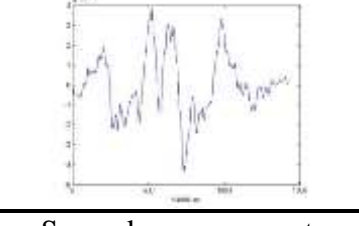
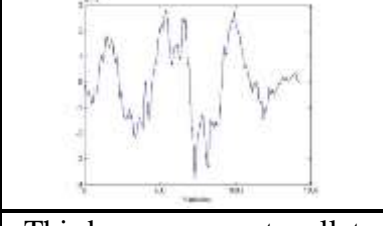
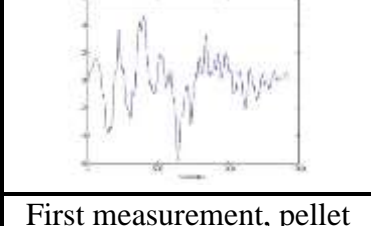
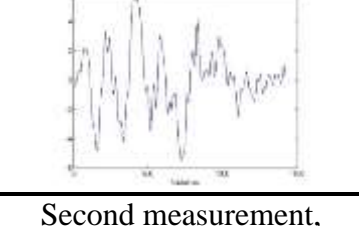
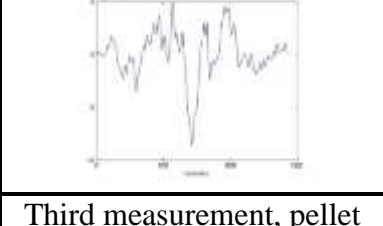
Edgar Brother Model 35, LEA EJ

		
	Second measurement, pellet number 490	Third measurement, pellet number 490
		
First measurement, pellet number 491	Second measurement, pellet number 491	Third measurement, pellet number 491
		
First measurement, pellet number 492	Second measurement, pellet number 492	Third measurement, pellet number 492
		
First measurement, pellet number 493	Second measurement, pellet number 493	Third measurement, pellet number 493
		
First measurement, pellet number 494	Second measurement, pellet number 494	Third measurement, pellet number 494

## Appendix 84

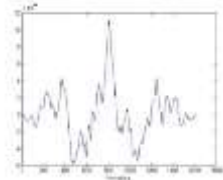
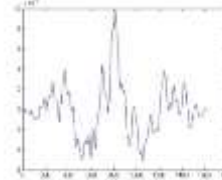
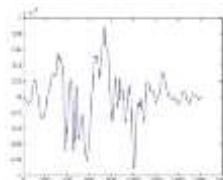
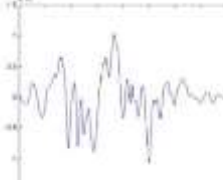
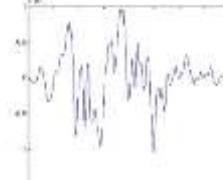
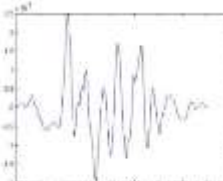
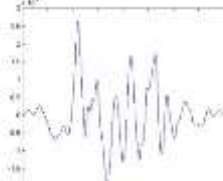
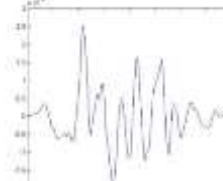
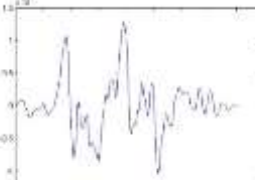
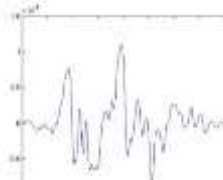
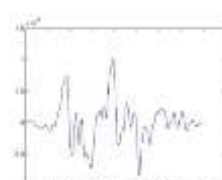
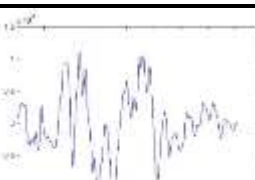
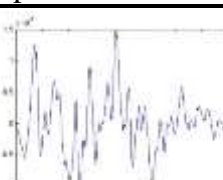

Topographical profiles obtained from the microscopic measurements for samples

Edgar Brother Model 35, LEA EK

		
	Second measurement, pellet number 490	Third measurement, pellet number 490
		
First measurement, pellet number 491	Second measurement, pellet number 491	Third measurement, pellet number 491
		
First measurement, pellet number 492	Second measurement, pellet number 492	Third measurement, pellet number 492
		
First measurement, pellet number 493	Second measurement, pellet number 493	Third measurement, pellet number 493
		
First measurement, pellet number 494	Second measurement, pellet number 494	Third measurement, pellet number 494

## Appendix 85

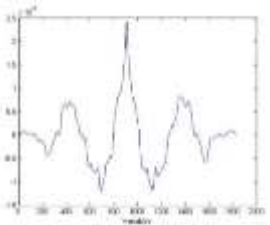
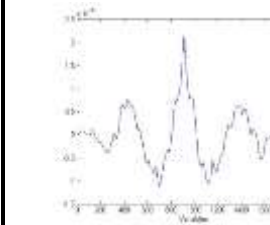
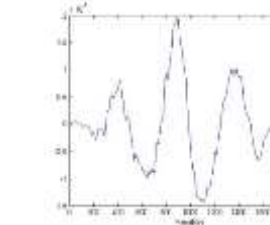
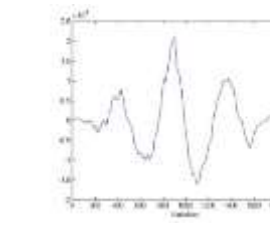
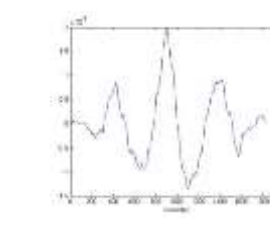
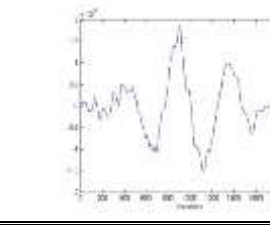
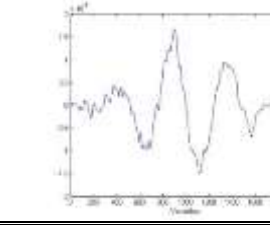
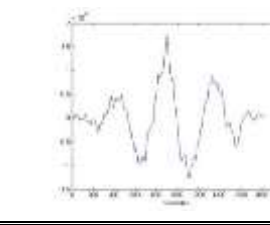
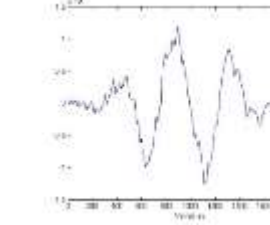
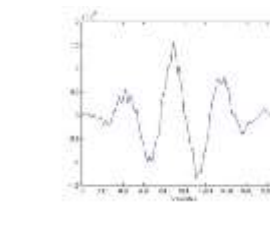
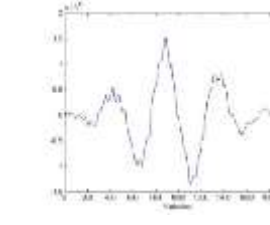
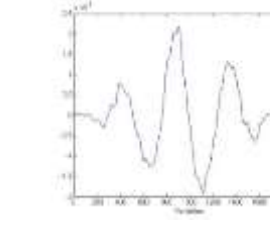
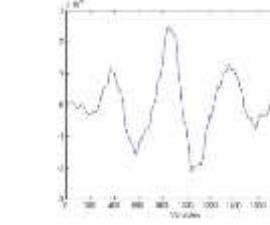
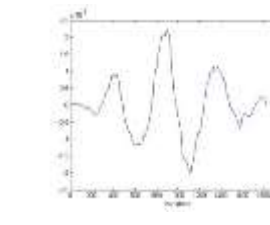
Topographical profiles obtained from the microscopic measurements for samples  
Edgar Brother Model 35, LEA EL

		
	Second measurement, pellet number 490	Third measurement, pellet number 490
		
First measurement, pellet number 491	Second measurement, pellet number 491	Third measurement, pellet number 491
		
First measurement, pellet number 492	Second measurement, pellet number 492	Third measurement, pellet number 492
		
First measurement, pellet number 493	Second measurement, pellet number 493	Third measurement, pellet number 493
		
First measurement, pellet number 494	Second measurement, pellet number 494	Third measurement, pellet number 494

## Appendix 86

Topographical profiles obtained from the microscopic measurements for samples

Baikal 90042234 ИЖ-35, LEA BB

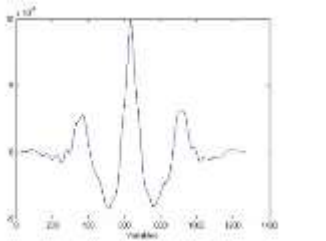
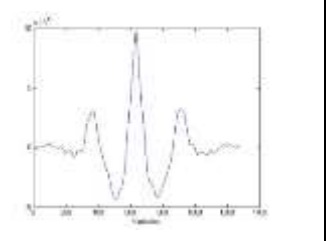
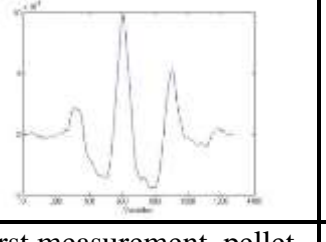
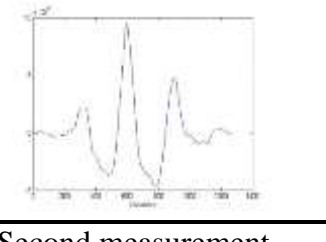
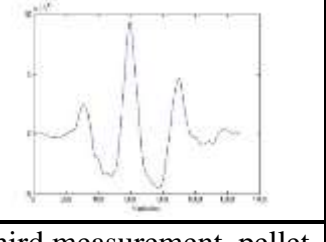
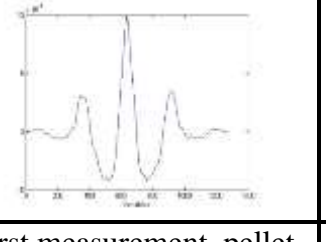
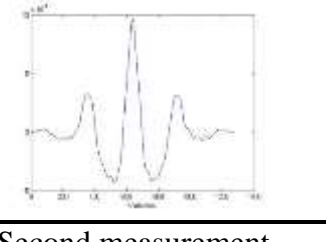
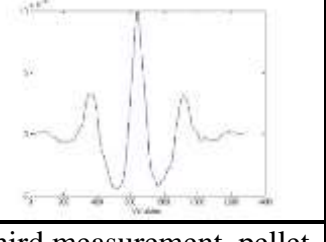
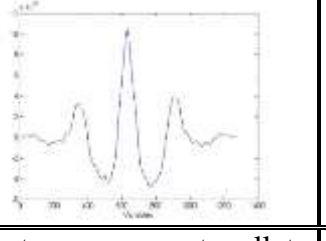
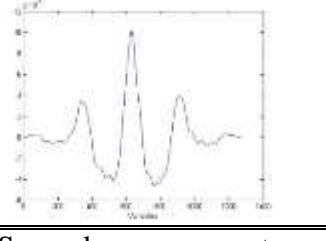
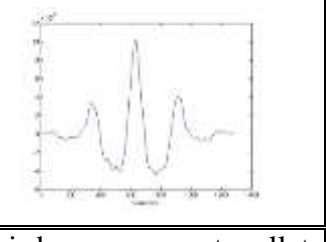
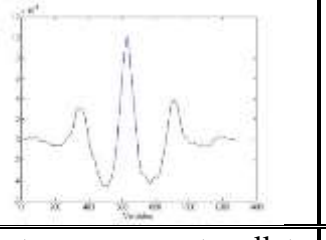
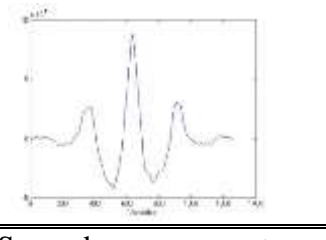
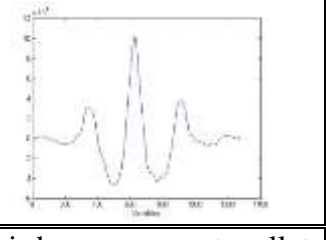
		
	Second measurement, pellet number 500	Third measurement, pellet number 500
		
First measurement, pellet number 501	Second measurement, pellet number 501	Third measurement, pellet number 501
		
First measurement, pellet number 502	Second measurement, pellet number 502	Third measurement, pellet number 502
		
First measurement, pellet number 503	Second measurement, pellet number 503	Third measurement, pellet number 503
		
First measurement, pellet number 504	Second measurement, pellet number 504	Third measurement, pellet number 504



## Appendix 87

Topographical profiles obtained from the microscopic measurements for samples

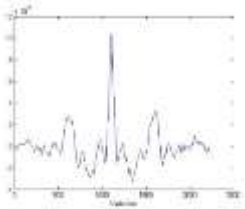
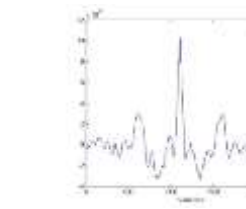
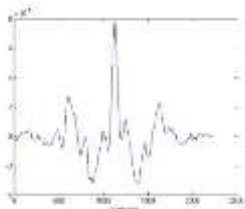
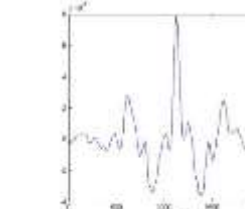
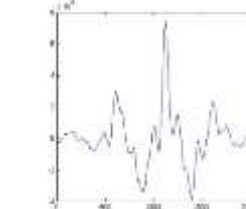
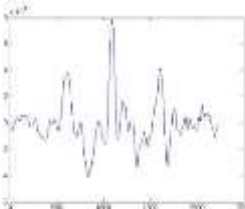
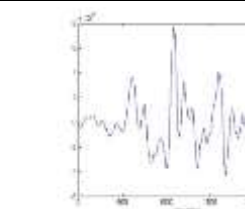
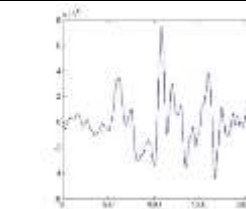
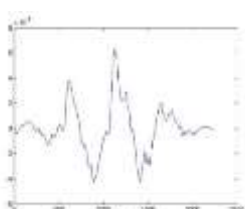
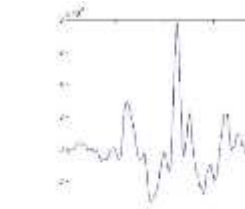
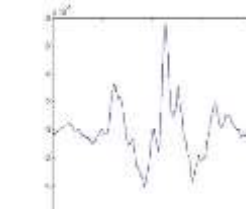
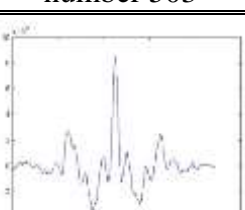
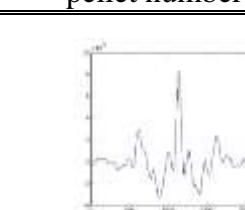
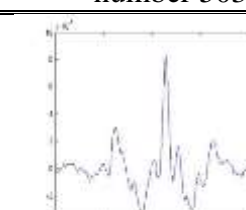
Baikal 90042234 ИЖ-35, LEA BC

		
	Second measurement, pellet number 500	Third measurement, pellet number 500
		
First measurement, pellet number 501	Second measurement, pellet number 501	Third measurement, pellet number 501
		
First measurement, pellet number 502	Second measurement, pellet number 502	Third measurement, pellet number 502
		
First measurement, pellet number 503	Second measurement, pellet number 503	Third measurement, pellet number 503
		
First measurement, pellet number 504	Second measurement, pellet number 504	Third measurement, pellet number 504

## Appendix 88

Topographical profiles obtained from the microscopic measurements for samples

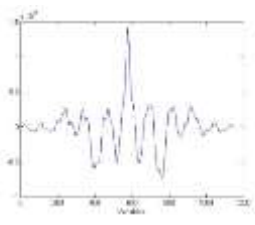
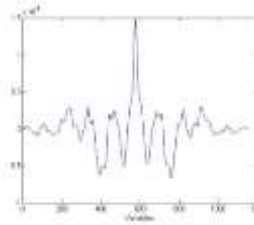
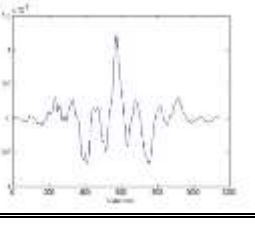
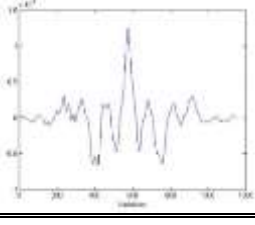
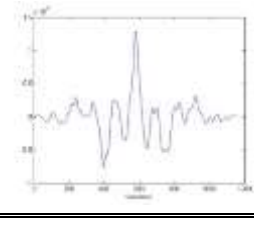
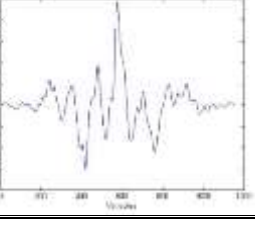
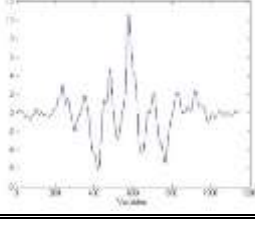
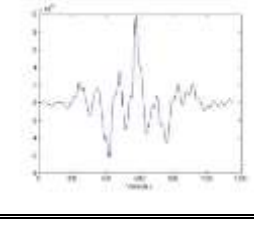
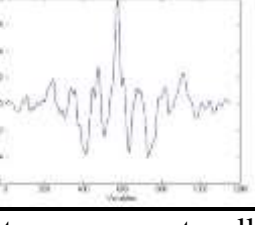
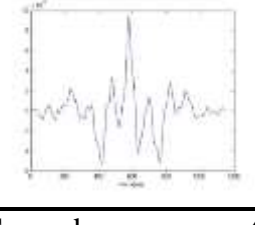
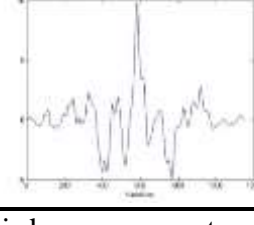
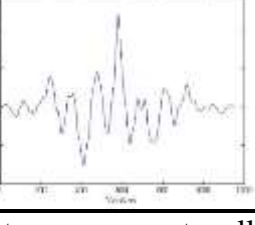
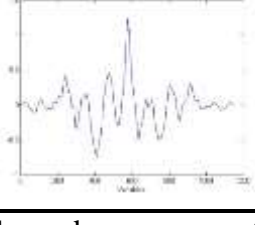
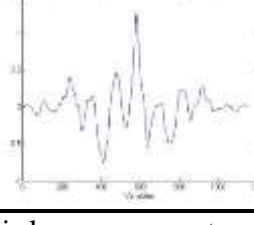
Baikal 90042234 ИЖ-35, LEA BD

		
	Second measurement, pellet number 500	Third measurement, pellet number 500
		
First measurement, pellet number 501	Second measurement, pellet number 501	Third measurement, pellet number 501
		
First measurement, pellet number 502	Second measurement, pellet number 502	Third measurement, pellet number 502
		
First measurement, pellet number 503	Second measurement, pellet number 503	Third measurement, pellet number 503
		
First measurement, pellet number 504	Second measurement, pellet number 504	Third measurement, pellet number 504

## Appendix 89

Topographical profiles obtained from the microscopic measurements for samples

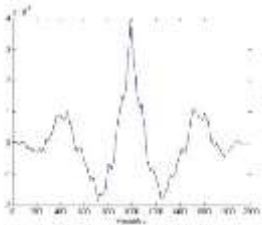
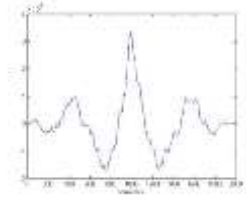
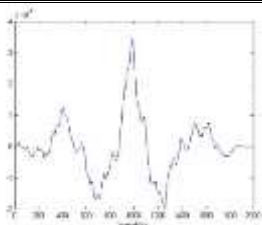
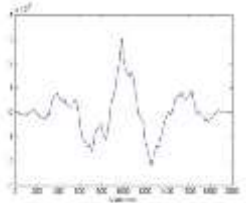
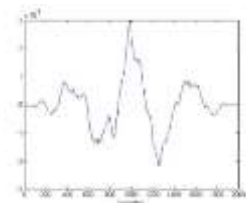
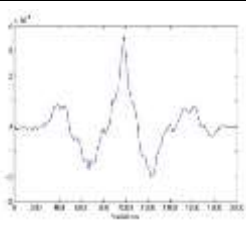
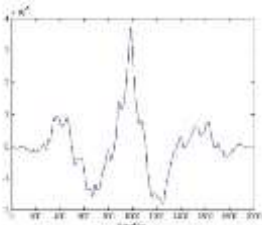
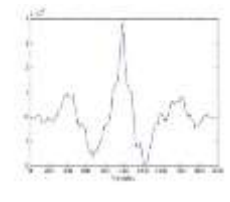
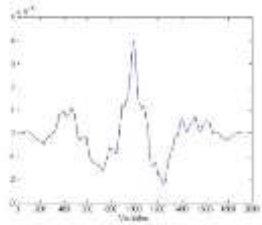
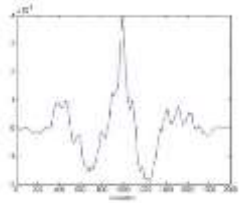
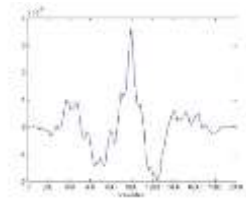
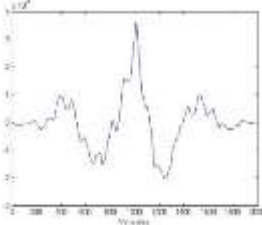
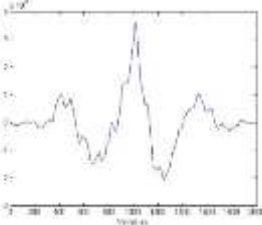
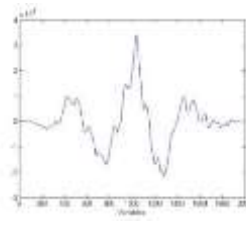
Baikal 90042234 ИЖ-35, LEA BE

		
	Second measurement, pellet number 500	Third measurement, pellet number 500
		
First measurement, pellet number 501	Second measurement, pellet number 501	Third measurement, pellet number 501
		
First measurement, pellet number 502	Second measurement, pellet number 502	Third measurement, pellet number 502
		
First measurement, pellet number 503	Second measurement, pellet number 503	Third measurement, pellet number 503
		
First measurement, pellet number 504	Second measurement, pellet number 504	Third measurement, pellet number 504

## Appendix 90

Topographical profiles obtained from the microscopic measurements for samples

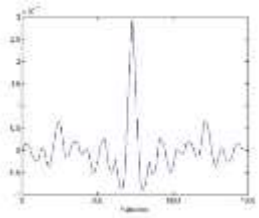
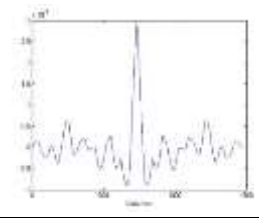
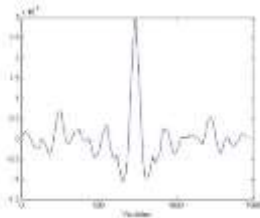
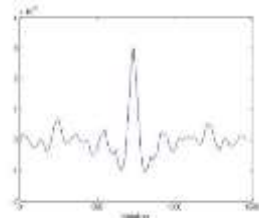
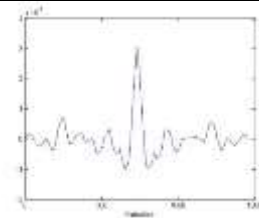
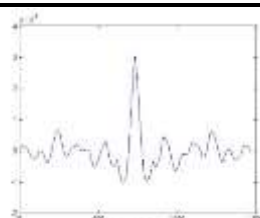
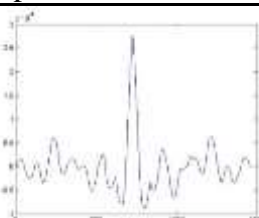
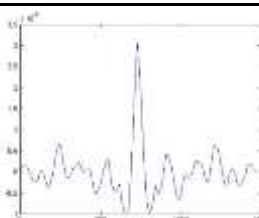

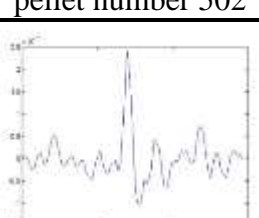


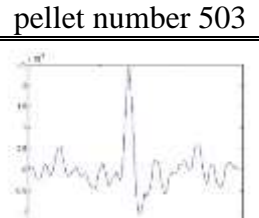

Baikal 90042234 ИЖ-35, LEA BF

		
	Second measurement, pellet number 500	Third measurement, pellet number 500
		
First measurement, pellet number 501	Second measurement, pellet number 501	Third measurement, pellet number 501
		
First measurement, pellet number 502	Second measurement, pellet number 502	Third measurement, pellet number 502
		
First measurement, pellet number 503	Second measurement, pellet number 503	Third measurement, pellet number 503
		
First measurement, pellet number 504	Second measurement, pellet number 504	Third measurement, pellet number 504

## Appendix 91

Topographical profiles obtained from the microscopic measurements for samples

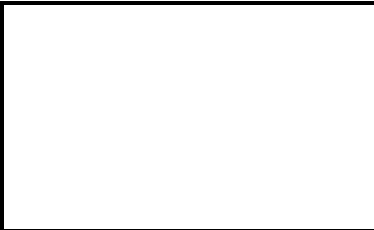
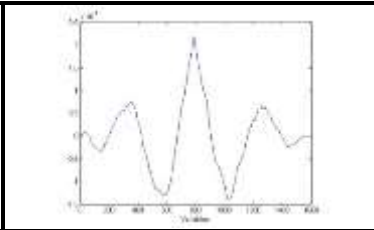
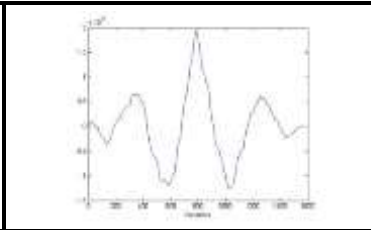
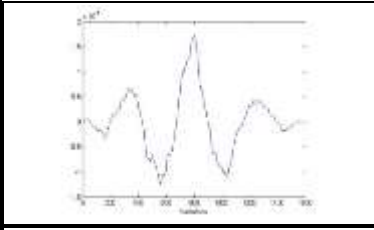
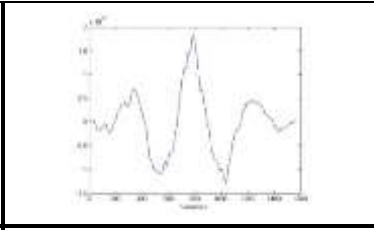
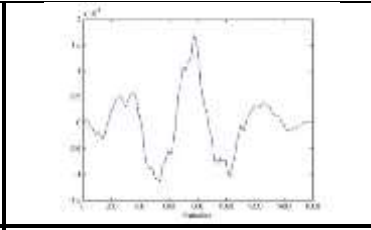
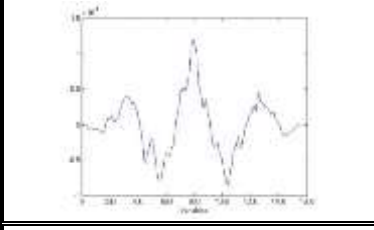
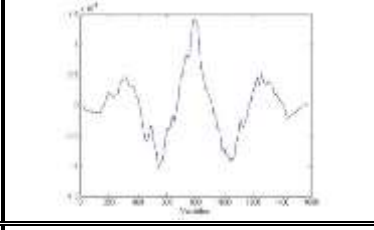
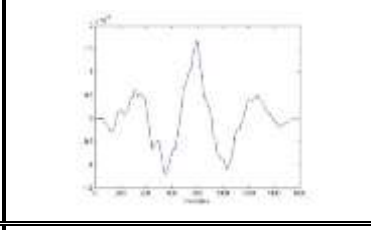
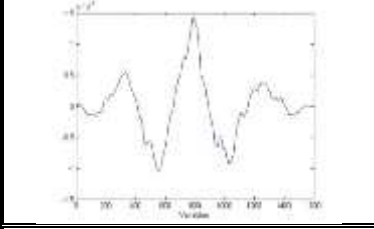
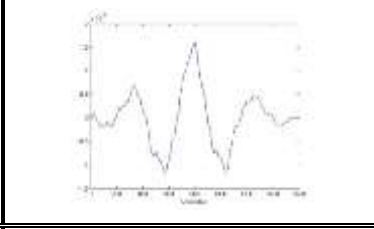
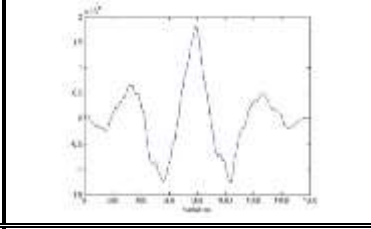
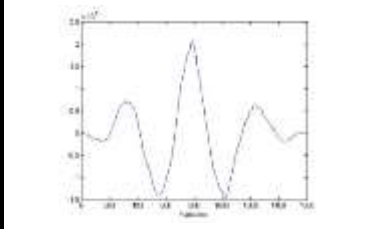
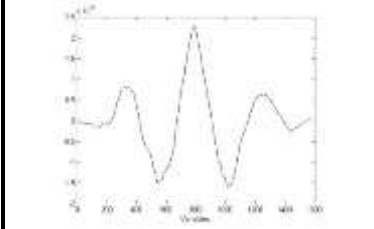
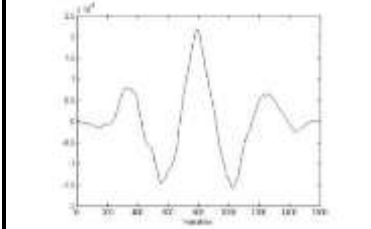
Baikal 90042234 ИЖ-35, LEA BG

		
	Second measurement, pellet number 500	Third measurement, pellet number 500
		
First measurement, pellet number 501	Second measurement, pellet number 501	Third measurement, pellet number 501
		
First measurement, pellet number 502	Second measurement, pellet number 502	Third measurement, pellet number 502
		
First measurement, pellet number 503	Second measurement, pellet number 503	Third measurement, pellet number 503
		
First measurement, pellet number 504	Second measurement, pellet number 504	Third measurement, pellet number 504

## Appendix 92

Topographical profiles obtained from the microscopic measurements for samples

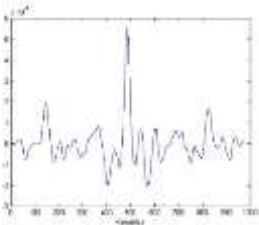
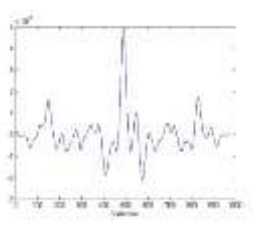
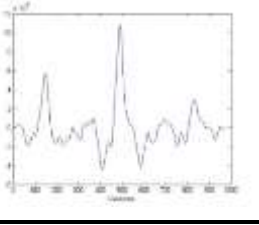
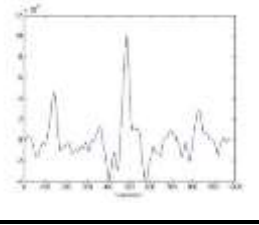
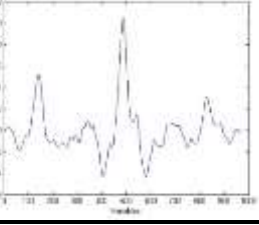
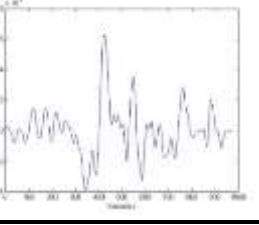
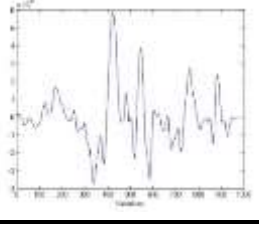
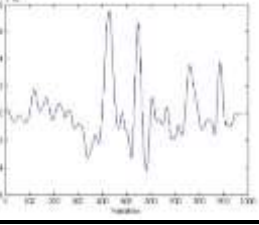
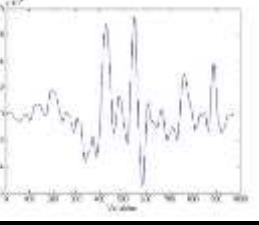
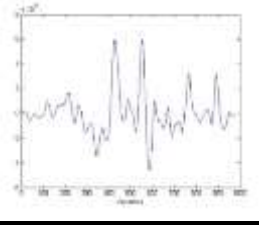
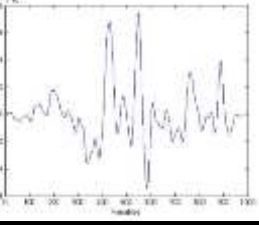
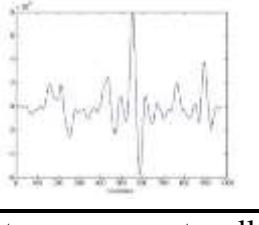
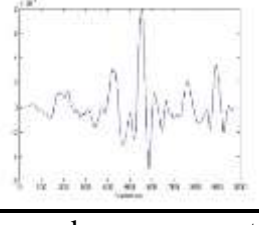
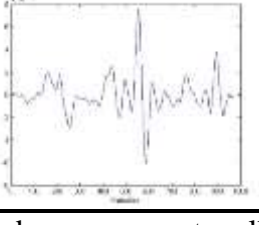
Baikal 90042234 ИЖ-35, LEA BH

		
	Second measurement, pellet number 500	Third measurement, pellet number 500
		
First measurement, pellet number 501	Second measurement, pellet number 501	Third measurement, pellet number 501
		
First measurement, pellet number 502	Second measurement, pellet number 502	Third measurement, pellet number 502
		
First measurement, pellet number 503	Second measurement, pellet number 503	Third measurement, pellet number 503
		
First measurement, pellet number 504	Second measurement, pellet number 504	Third measurement, pellet number 504

## Appendix 93

Topographical profiles obtained from the microscopic measurements for samples

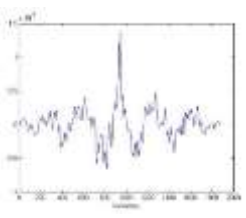
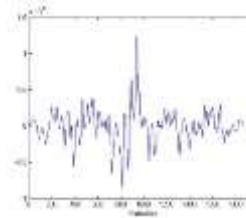
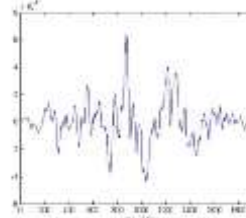
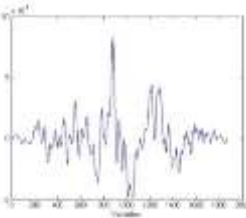
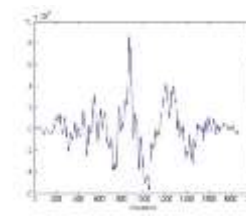
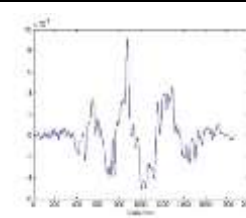
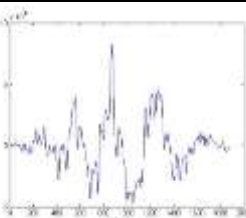
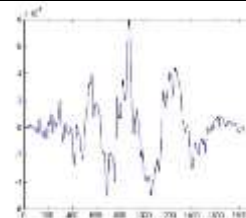
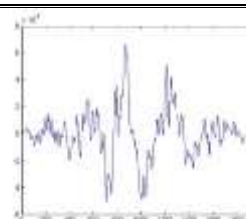
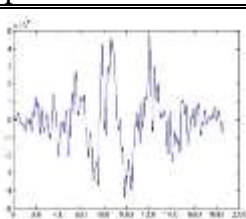
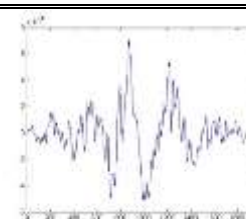
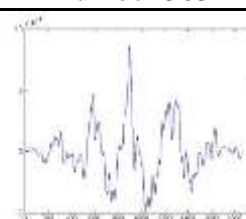
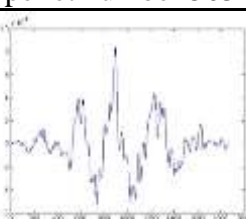
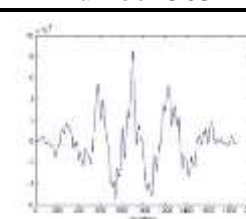
Baikal 90042234 ИЖ-35, LEA BI

		
	Second measurement, pellet number 500	Third measurement, pellet number 500
		
First measurement, pellet number 501	Second measurement, pellet number 501	Third measurement, pellet number 501
		
First measurement, pellet number 502	Second measurement, pellet number 502	Third measurement, pellet number 502
		
First measurement, pellet number 503	Second measurement, pellet number 503	Third measurement, pellet number 503
		
First measurement, pellet number 504	Second measurement, pellet number 504	Third measurement, pellet number 504

## Appendix 94

Topographical profiles obtained from the microscopic measurements for samples

Baikal 90042234 ИЖ-35, LEA BJ

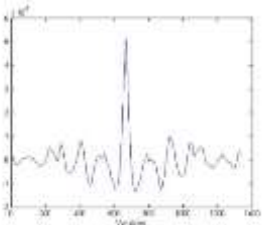
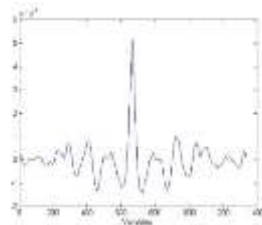
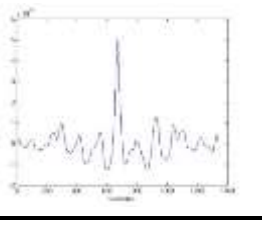
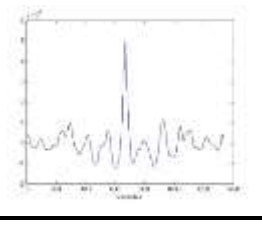
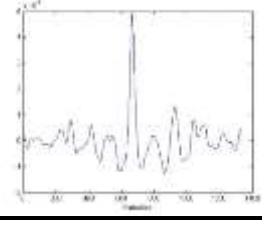
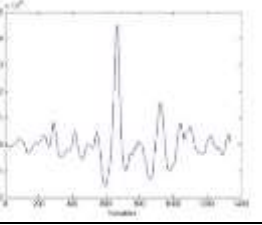
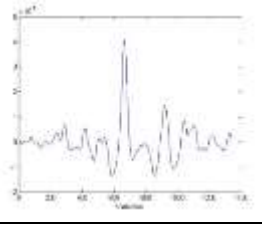
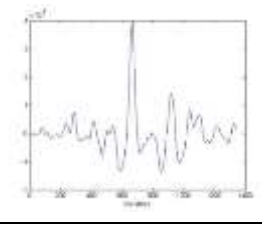
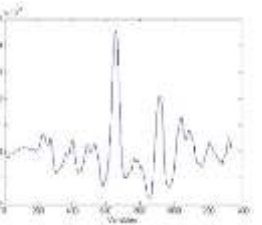
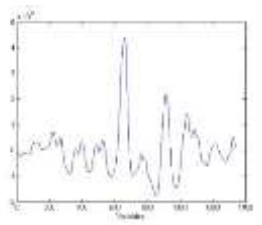
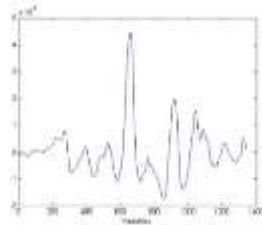
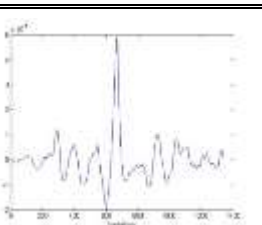
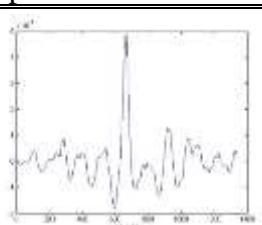
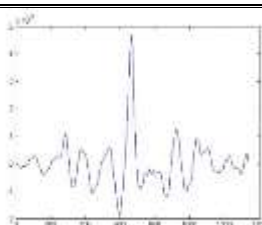
		
	Second measurement, pellet number 500	Third measurement, pellet number 500
		
First measurement, pellet number 501	Second measurement, pellet number 501	Third measurement, pellet number 501
		
First measurement, pellet number 502	Second measurement, pellet number 502	Third measurement, pellet number 502
		
First measurement, pellet number 503	Second measurement, pellet number 503	Third measurement, pellet number 503
		
First measurement, pellet number 504	Second measurement, pellet number 504	Third measurement, pellet number 504



## Appendix 95

Topographical profiles obtained from the microscopic measurements for samples

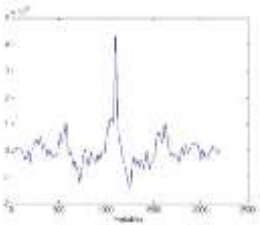
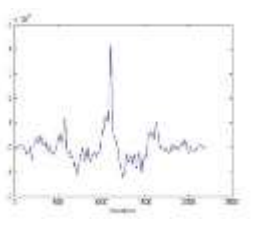
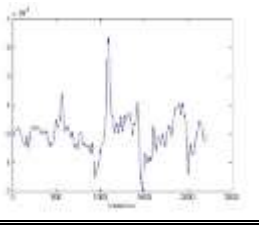
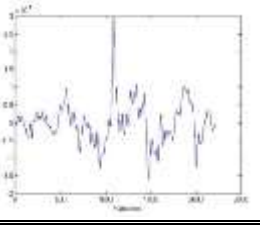
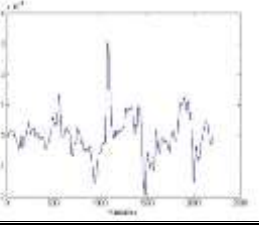
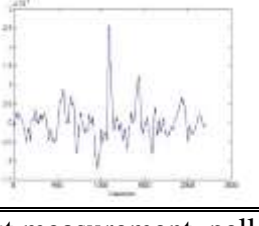
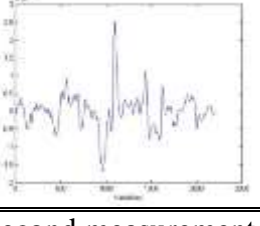
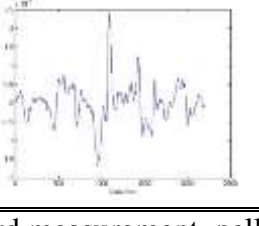
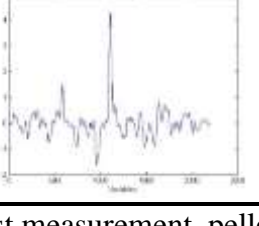
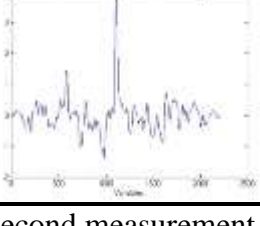
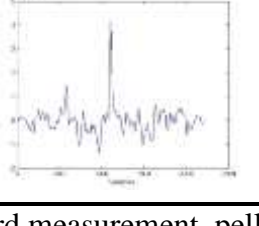
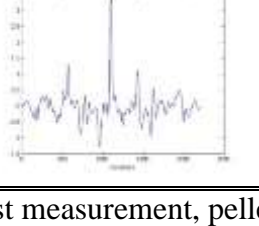
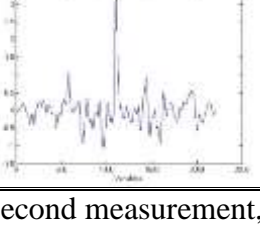
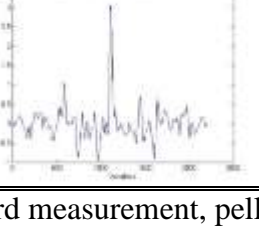
Baikal 90042234 ИЖ-35, LEA BK

		
	Second measurement, pellet number 500	Third measurement, pellet number 500
		
First measurement, pellet number 501	Second measurement, pellet number 501	Third measurement, pellet number 501
		
First measurement, pellet number 502	Second measurement, pellet number 502	Third measurement, pellet number 502
		
First measurement, pellet number 503	Second measurement, pellet number 503	Third measurement, pellet number 503
		
First measurement, pellet number 504	Second measurement, pellet number 504	Third measurement, pellet number 504

## Appendix 96

Topographical profiles obtained from the microscopic measurements for samples

Baikal 90042234 ИЖ-35, LEA BL

		
	Second measurement, pellet number 500	Third measurement, pellet number 500
		
First measurement, pellet number 501	Second measurement, pellet number 501	Third measurement, pellet number 501
		
First measurement, pellet number 502	Second measurement, pellet number 502	Third measurement, pellet number 502
		
First measurement, pellet number 503	Second measurement, pellet number 503	Third measurement, pellet number 503
		
First measurement, pellet number 504	Second measurement, pellet number 504	Third measurement, pellet number 504